EXPLORING IMMUNE VARIABILITY IN SUSCEPTIBILITY TO TUBERCULOSIS INFECTION IN HUMANS

EDITED BY: Julie G. Burel, Cecilia Lindestam Arlehamn, Chetan Seshadri and Jayne S. Sutherland

PUBLISHED IN: Frontiers in Immunology

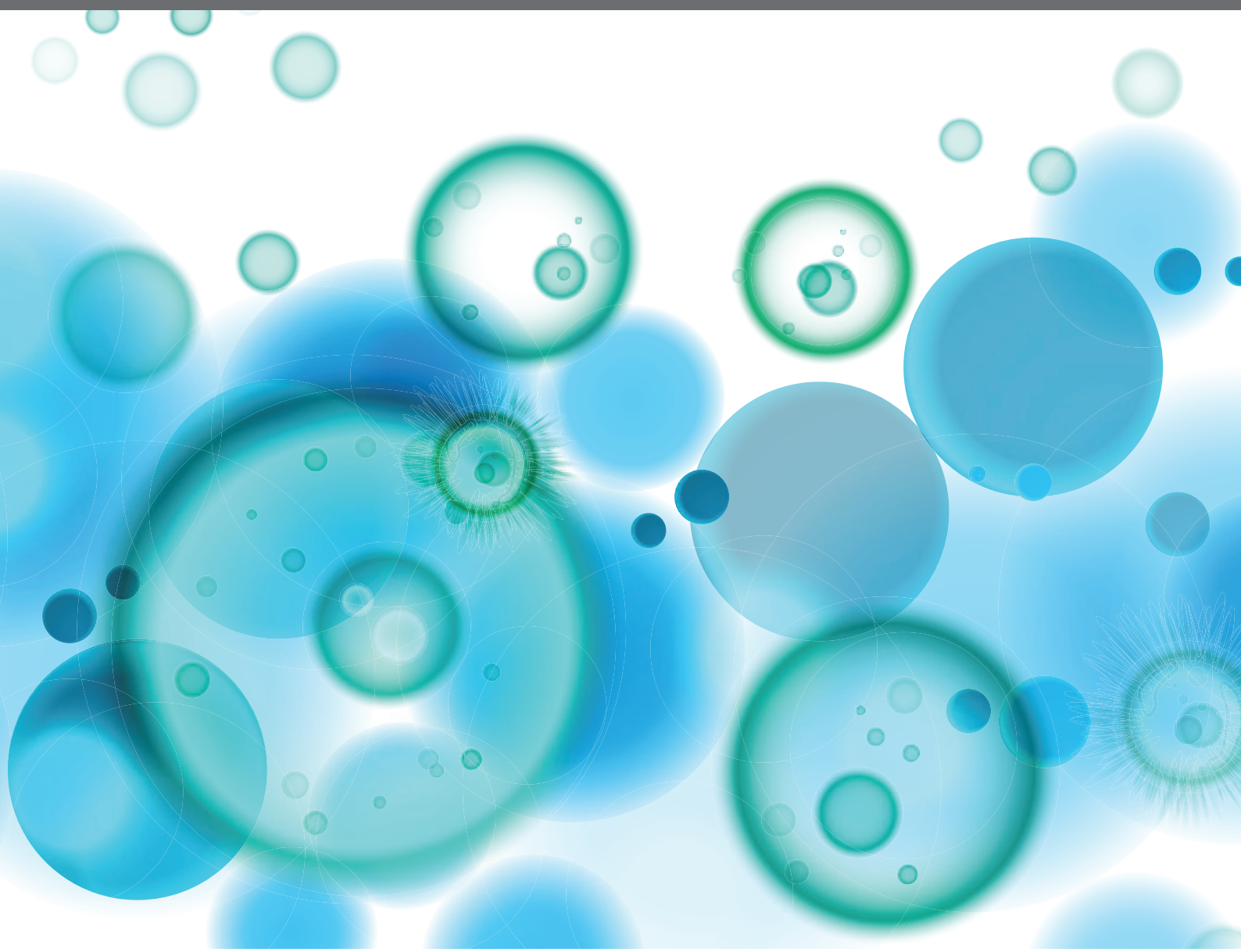

frontiers Research Topics

Frontiers eBook Copyright Statement

The copyright in the text of individual articles in this eBook is the property of their respective authors or their respective institutions or funders. The copyright in graphics and images within each article may be subject to copyright of other parties. In both cases this is subject to a license granted to Frontiers.

The compilation of articles constituting this eBook is the property of Frontiers.

Each article within this eBook, and the eBook itself, are published under the most recent version of the Creative Commons CC-BY licence. The version current at the date of publication of this eBook is CC-BY 4.0. If the CC-BY licence is updated, the licence granted by Frontiers is automatically updated to the new version.

When exercising any right under the CC-BY licence, Frontiers must be attributed as the original publisher of the article or eBook, as applicable.

Authors have the responsibility of ensuring that any graphics or other materials which are the property of others may be included in the CC-BY licence, but this should be checked before relying on the CC-BY licence to reproduce those materials. Any copyright notices relating to those materials must be complied with.

Copyright and source acknowledgement notices may not be removed and must be displayed in any copy, derivative work or partial copy which includes the elements in question.

All copyright, and all rights therein, are protected by national and international copyright laws. The above represents a summary only. For further information please read Frontiers' Conditions for Website Use and Copyright Statement, and the applicable CC-BY licence.

ISSN 1664-8714
ISBN 978-2-88974-405-3
DOI 10.3389/978-2-88974-405-3

About Frontiers

Frontiers is more than just an open-access publisher of scholarly articles: it is a pioneering approach to the world of academia, radically improving the way scholarly research is managed. The grand vision of Frontiers is a world where all people have an equal opportunity to seek, share and generate knowledge. Frontiers provides immediate and permanent online open access to all its publications, but this alone is not enough to realize our grand goals.

Frontiers Journal Series

The Frontiers Journal Series is a multi-tier and interdisciplinary set of open-access, online journals, promising a paradigm shift from the current review, selection and dissemination processes in academic publishing. All Frontiers journals are driven by researchers for researchers; therefore, they constitute a service to the scholarly community. At the same time, the Frontiers Journal Series operates on a revolutionary invention, the tiered publishing system, initially addressing specific communities of scholars, and gradually climbing up to broader public understanding, thus serving the interests of the lay society, too.

Dedication to Quality

Each Frontiers article is a landmark of the highest quality, thanks to genuinely collaborative interactions between authors and review editors, who include some of the world's best academicians. Research must be certified by peers before entering a stream of knowledge that may eventually reach the public - and shape society; therefore, Frontiers only applies the most rigorous and unbiased reviews.
Frontiers revolutionizes research publishing by freely delivering the most outstanding research, evaluated with no bias from both the academic and social point of view. By applying the most advanced information technologies, Frontiers is catapulting scholarly publishing into a new generation.

What are Frontiers Research Topics?

Frontiers Research Topics are very popular trademarks of the Frontiers Journals Series: they are collections of at least ten articles, all centered on a particular subject. With their unique mix of varied contributions from Original Research to Review Articles, Frontiers Research Topics unify the most influential researchers, the latest key findings and historical advances in a hot research area! Find out more on how to host your own Frontiers Research Topic or contribute to one as an author by contacting the Frontiers Editorial Office: frontiersin.org/about/contact

EXPLORING IMMUNE VARIABILITY IN SUSCEPTIBILITY TO TUBERCULOSIS INFECTION IN HUMANS

Topic Editors:
Julie G. Burel, La Jolla Institute for Immunology (LJI), United States
Cecilia Lindestam Arlehamn, La Jolla Institute for Immunology (LJI), United States
Chetan Seshadri, University of Washington, United States
Jayne S. Sutherland, Medical Research Council The Gambia Unit (MRC), Gambia

Citation: Burel, J. G., Arlehamn, C. L., Seshadri, C., Sutherland, J. S., eds. (2022). Exploring Immune Variability in Susceptibility to Tuberculosis Infection in Humans. Lausanne: Frontiers Media SA. doi: 10.3389/978-2-88974-405-3

Table of Contents

frontiers in Immunology

EDITORIAL
published: 07 January 2022
doi: 10.3389/fimmu.2021.830920

Editorial: Exploring Immune Variability in Susceptibility to Tuberculosis Infection in Humans

Chetan Seshadri[1,2*], *Jayne S. Sutherland*[3], *Cecilia S. Lindestam Arlehamn*[4] *and Julie G. Burel*[4]

[1] Department of Medicine, University of Washington School of Medicine, Seattle, WA, United States, [2] Tuberculosis Research and Training Center, University of Washington, Seattle, WA, United States, [3] Vaccines & Immunity Theme, Medical Research Council (MRC) Unit, The Gambia at the London School of Hygiene and Tropical Medicine, Banjul, The Gambia, [4] Center for Infectious Disease and Vaccine Research, La Jolla Institute for Immunology, La Jolla, CA, United States

Keywords: ***Mycobacterium tuberculosis*, infection, resistance, T cells, biomarkers, co-morbid illness, human immunity**

Editorial on the Research Topic

Exploring Immune Variability in Susceptibility to Tuberculosis Infection in Humans

INTRODUCTION

Tuberculosis (TB) occurs along a clinical and immunologic spectrum ranging from exposure and immune sensitization to the highly transmissible pulmonary form of the disease (1, 2). While active disease requires microbiologic confirmation, all other states derive from the use of immunodiagnostics to infer the presence or absence of a paucibacillary infection. The tuberculin skin test (TST) and interferon gamma release assays (IGRA) quantify T cells specific for *Mycobacterium tuberculosis* (M.tb) in the blood, and have been used to define 'resisters,' 'reverters,' and 'latent' infection in humans (3, 4). There is no gold standard for the diagnosis of clinically silent infection with M.tb, and there is limited correlation between immune reactivity and the presence of viable bacilli in humans and animal models (5, 6).

It is against this backdrop that we present the following Research Topic of eleven articles exploring immune variability in susceptibility to tuberculosis infection in humans. The Research Topic spans several themes, including the clinical spectrum of M.tb infection, T cell immunity and transcriptional biomarkers, and the influence of co-morbid illnesses. Together, they advance how we conceptualize and study immunophenotypes of M.tb infection, such as 'resisters,' 'reverters,' and even 'latency'.

EXPLORING THE SPECTRUM OF M.TB INFECTION IN HUMANS

Two review articles address our evolving understanding of the clinical spectrum of tuberculosis in humans. Guttierez et al. comprehensively review the varying definitions of 'resisters' through several household contact and community studies. Based on the heterogeneity in study designs, they argue that a single definition of 'resistance' may be inadequate and provide recommendations on how future studies might pursue a more standardized approach. Dubé et al. review the evidence linking human and murine genetic variation in pattern recognition receptors with both the immune response as well as 'resistance' to M.tb infection. While genetic variation in this class of genes is

OPEN ACCESS

Edited and reviewed by:
Scott N. Mueller,
The University of Melbourne, Australia

***Correspondence:**
Chetan Seshadri
seshadri@uw.edu

Specialty section:
This article was submitted to Immunological Memory, a section of the journal Frontiers in Immunology

Received: *07 December 2021*
Accepted: *17 December 2021*
Published: *07 January 2022*

Citation:
Seshadri C, Sutherland JS, Lindestam Arlehamn CS and Burel JG (2022) Editorial: Exploring Immune Variability in Susceptibility to Tuberculosis Infection in Humans. Front. Immunol. 12:830920. doi: 10.3389/fimmu.2021.830920

clearly associated with altered immunity, it is less clear whether it is associated with hard clinical definitions such as 'latency,' which mask the underlying phenotypic heterogeneity of TB. Instead, the authors argue that future studies should be designed to account for heterogeneity by looking for associations with endophenotypes.

CHARACTERIZING M.TB-SPECIFIC IMMUNITY

Using longitudinally collected samples, Mpande et al. identified a group of IGRA reverters and compared M.tb-specific CD4 T cell responses with IGRA converters or non-converters from the same cohort. Among IGRA reverters, M.tb-specific CD4 T cells showed a similar activation phenotype but presented an early differentiated phenotype compared to IGRA persistent individuals and more closely resembled phenotypes seen among non-converters. The authors conclude that the magnitude and differentiation status of M.tb-specific Th1 cells among some IGRA reverters may be consistent with well-controlled M.tb infection.

Sharan et al. performed a study of early (one week and three weeks) Mtb-specific T cell responses in the lungs of rhesus macaques after aerosol infection with either a low- or a high-dose of M.tb. The key finding was higher Mtb-specific CD4 +IFN-γ+ and TNF-α+ T cell responses in the bronchoalveolar lavage (BAL) after one week in the low dose group that was delayed to three weeks in the high dose group. These results provide insight into T cell priming events occurring very early after infection that depend on bacterial load.

Meier et al. performed a longitudinal assessment of M.tb-specific T cells from HIV-infected individuals up to the time of TB diagnosis. They found that Rv2031c-induced TNF-α was significantly higher in cases compared to controls up to two years prior to TB diagnosis. At time-points closer to diagnosis, they found increased Rv2431 induced IP10 and Rv2031 induced TNF-α in progressors compared to non-progressors. The data provide T cell correlates of risk that may complement blood transcriptional signatures that have been the focus of recent work (7).

Silva et al. investigated cytokine production by peripheral blood immune cells derived from subjects with active, 'latent,' or no infection with M.tb after *in vitro* stimulation with M.tb-derived glycolipids. Compared to stimulation with purified protein derivative (PPD), the authors found that glycolipid stimulation elicited diversity beyond canonical Th1 responses to include B cells and CD33+ cells producing several pro and anti-inflammatory cytokines. Further, the magnitude of the cytokine response to M.tb glycolipids was reduced in 'latent' or active infection compared to controls suggesting potential hyporesponsiveness upon M.tb exposure, or a mechanism of trained immunity (8).

TRANSCRIPTIONAL SIGNATURES AND BIOMARKERS

Three studies focused on blood transcriptional signatures and other soluble mediators associated with M.tb infection. Baguma et al. assessed a cohort of pre-adolescent children who are intrinsically at lower risk of developing TB disease than post-pubescent adolescents and young adults. They found pre-adolescent children had lower levels of myeloid-associated pro-inflammatory mediators than young adults *in vivo* and after *in vitro* M.tb infection. Wilkinson et al. performed a longitudinal analysis of whole blood and plasma derived from HIV-1 infected individuals during the first six months of antiretroviral therapy. They found a consistent decrease in immune activation and inflammation over this period that may contribute to the reduced incidence of TB after ART initiation. Domaszewska et al. performed a meta-analysis of published whole blood transcriptomes from humans and identified IFN-rich and IFN-low endotypes of TB that did not appear to correlate with the time after M.tb infection in cynomolgus macaques but could distinguish severity of disease.

CO-MORBID ILLNESSES

In addition to the studies of HIV co-infection noted above, two studies addressed the role of comorbid illnesses and Mtb infection. Petruccioli et al. examined subjects with immune-mediated inflammatory diseases, who have a high probability of developing active TB, and compared them to individuals with active TB and Mtb infection. They found that among patients with inflammatory diseases, anti-TB therapy did not affect the phenotypes or functions of M.tb-specific CD4 T cells. Diabetes is a major risk factor for progression to active TB and poly (ADP-ribose) polymerase (PARP) activation is mechanistically associated with the development of Type I diabetes. van Doorn et al. used an *in vitro* human macrophage model to investigate the role of PARP inhibitors as host-directed therapy for TB. They find that PARP inhibition decreased survival of both drug-sensitive and drug-resistant M.tb.

SUMMARY

The work presented in this Research Topic cover the spectrum of diversity of M.tb infection across a variety of human cohorts and illustrate just how far we still need to travel in order to unravel the immunology underlying this diversity. Operational definitions such as 'resistant' and 'latent' will hopefully give way to molecularly defined endophenotypes that will facilitate better treatments for this global scourge.

AUTHOR CONTRIBUTIONS

CS wrote the initial draft. All authors reviewed and edited the manuscript.

FUNDING

National Institutes of Health R01-AI146072 to CS.

REFERENCES

1. Drain PK, Bajema KL, Dowdy D, Dheda K, Naidoo K, Schumacher SG, et al. Incipient and Subclinical Tuberculosis: A Clinical Review of Early Stages and Progression of Infection. *Clin Microbiol Rev* (2018) 31(4):e00021–18. doi: 10.1128/CMR.00021-18
2. Simmons JD, Stein CM, Seshadri C, Campo M, Alter G, Fortune S, et al. Immunological Mechanisms of Human Resistance to Persistent *Mycobacterium Tuberculosis* Infection. *Nat Rev Immunol* (2018) 18(9):575–89. doi: 10.1038/s41577-018-0025-3
3. Stein CM, Nsereko M, Malone LL, Okware B, Kisingo H, Nalukwago S, et al. Long-Term Stability of Resistance to Latent M. Tuberculosis Infection in Highly Exposed TB Household Contacts in Kampala, Uganda. *Clin Infect Dis* (2018) 44106(Xx):1–8. doi: 10.1093/cid/ciy751/5085255
4. Andrews JR, Nemes E, Tameris M, Landry BS, Mahomed H, McClain JB, et al. Serial QuantiFERON Testing and Tuberculosis Disease Risk Among Young Children: An Observational Cohort Study. *Lancet Respir Med* (2017) 5(4):282–90. doi: 10.1016/S2213-2600(17)30060-7
5. Behr MA, Edelstein PH, Ramakrishnan L. Is Mycobacterium Tuberculosis Infection Life Long? *BMJ* (2019) 367:1–7. doi: 10.1136/bmj.l5770
6. Behr MA, Kaufmann E, Duffin J, Edelstein PH, Ramakrishnan L. Latent Tuberculosis: Two Centuries of Confusion. *Am J Respir Crit Care Med* (2021) 204(2):142–8. doi: 10.1164/rccm.202011-4239PP
7. Turner CT, Gupta RK, Tsaliki E, Roe JK, Mondal P, Nyawo GR, et al. Blood Transcriptional Biomarkers for Active Pulmonary Tuberculosis in a High-Burden Setting: A Prospective, Observational, Diagnostic Accuracy Study. *Lancet Respir Med* (2020) 8(4):407–19. doi: 10.1016/S2213-2600(19)30469-2
8. Khan N, Downey J, Sanz J, Kaufmann E, Blankenhaus B, Pacis A, et al. M. Tuberculosis Reprograms Hematopoietic Stem Cells to Limit Myelopoiesis and Impair Trained Immunity. *Cell* (2020) 183(3):752–70.e22. doi: 10.1016/j.cell.2020.09.062

Conflict of Interest: The authors declare that the research was conducted in the absence of any commercial or financial relationships that could be construed as a potential conflict of interest.

Publisher's Note: All claims expressed in this article are solely those of the authors and do not necessarily represent those of their affiliated organizations, or those of the publisher, the editors and the reviewers. Any product that may be evaluated in this article, or claim that may be made by its manufacturer, is not guaranteed or endorsed by the publisher.

Copyright © 2022 Seshadri, Sutherland, Lindestam Arlehamn and Burel. This is an open-access article distributed under the terms of the Creative Commons Attribution License (CC BY). The use, distribution or reproduction in other forums is permitted, provided the original author(s) and the copyright owner(s) are credited and that the original publication in this journal is cited, in accordance with accepted academic practice. No use, distribution or reproduction is permitted which does not comply with these terms.

frontiers in Immunology

REVIEW
published: 25 February 2021
doi: 10.3389/fimmu.2021.619988

Phenotype Definition for "Resisters" to *Mycobacterium tuberculosis* Infection in the Literature—A Review and Recommendations

Jesús Gutierrez[1*†], *Elouise E. Kroon*[2†], *Marlo Möller*[2] *and Catherine M. Stein*[1]

[1] Department of Population and Quantitative Health Science, Case Western Reserve University School of Medicine, Cleveland, OH, United States, [2] DSI-NRF Centre of Excellence for Biomedical Tuberculosis Research, South African Medical Research Council Centre for Tuberculosis Research, Division of Molecular Biology and Human Genetics, Faculty of Medicine and Health Sciences, Stellenbosch University, Cape Town, South Africa

OPEN ACCESS

Edited by:
Chetan Seshadri,
University of Washington,
United States

Reviewed by:
Reinout Van Crevel,
Radboud University Nijmegen Medical Centre, Netherlands
Carmen Judith Serrano,
Mexican Social Security Institute (IMSS), Mexico

***Correspondence:**
Jesús Gutierrez
jesus.gutierrez@case.edu

[†]These authors have contributed equally to this work

Specialty section:
This article was submitted to Microbial Immunology, a section of the journal Frontiers in Immunology

Received: 21 October 2020
Accepted: 14 January 2021
Published: 25 February 2021

Citation:
Gutierrez J, Kroon EE, Möller M and Stein CM (2021) Phenotype Definition for "Resisters" to Mycobacterium tuberculosis Infection in the Literature —A Review and Recommendations. Front. Immunol. 12:619988. doi: 10.3389/fimmu.2021.619988

Tuberculosis (TB) remains a worldwide problem. Despite the high disease rate, not all who are infected with *Mycobacterium Tuberculosis* (*Mtb*) develop disease. Interferon-γ (IFN-γ) specific T cell immune assays such as Quantiferon and Elispot, as well as a skin hypersensitivity test, known as a tuberculin skin test, are widely used to infer infection. These assays measure immune conversion in response to *Mtb*. Some individuals measure persistently negative to immune conversion, despite high and prolonged exposure to *Mtb*. Increasing interest into this phenotype has led to multiple publications describing various aspects of these responses. However, there is a lack of a unified "resister" definition. A universal definition will improve cross study data comparisons and assist with future study design and planning. We review the current literature describing this phenotype and make recommendations for future studies.

Keywords: tuberculosis, resister, phenotype, tuberculin skin test, interferon-γ release assay, review

INTRODUCTION

Tuberculosis (TB) remains a major public health problem globally. Since 2007, *Mycobacterium tuberculosis* (*Mtb*) has been responsible for the greatest number of deaths from a single infectious agent around the world. In 2018, 10.0 million people developed active disease and approximately 1.5 million people died (1). One of the challenges faced in developing effective TB preventative treatment strategies is understanding the underlying innate and adaptive responses to natural clearance of *Mtb*. We currently lack a gold standard to measure infection and can only infer it from a tuberculin skin test (TST) or *in vitro* based Interferon-γ (IFN-γ) release assays (IGRA). These assays are markers of immune conversion in response to *Mtb* exposure and do not capture the full spectrum of anti-*Mtb* immunity (2–4). Despite this inherent limitation, the study of persons who test persistently negative for these assays and do not develop TB provide unique and important epidemiological, genetic, and immunological insights into understanding the possible mechanisms of infection clearance (2, 5).

There are several historical case contact studies that point to the existence of a group of individuals who remain negative for reactivity to a TST despite heavy and repeated exposure to *Mtb*

(2, 5, 6). These individuals have been previously labeled as "resisters" or "early clearers" of infection. For example, two different studies described the cumulative prevalence of these individuals among nurses and nursing students (7–9). One study took place at the Boston City Hospital from 1932 to 1947 and revealed that 52 out of 362 nurses (14.4%) fit this phenotype over a three-year follow-up period (7). The other study was performed at Fairview Hospital in Minneapolis and found that 16 out of 184 nursing students (8.7%) did not show any evidence of reactivity to a TST during a three-year follow-up (8). Another study performed in 1966 aboard the U.S.S. Richard E. Byrd found that 7 crew members out of approximately 70 who shared the same berthing compartment as a symptomatic pulmonary TB sailor remained TST negative during a 6-month follow-up (10). As one of these studies points out, these individuals appeared to be "endowed with a very superior resistance to tuberculosis which destroyed the tubercle bacillus before it could establish a 'beach head' in the body" (7).

Although recent work suggests this phenotype may be best characterized immunologically (4), several longitudinal epidemiological studies have attempted to define this "resister" phenotype using IGRAs in addition to the TST. Unfortunately, due to the heterogeneity of these studies as well as the instability observed in TST and IGRA results, a unifying definition has been difficult to ascertain.

Perhaps the greatest obstacle in trying to define a unified phenotype of resistance to TB is the inability to define a singular state. Resistance to *Mtb* remains a spectrum and is dependent on host, environmental and bacterial factors. To date, both household contact studies as well as community studies have been used to facilitate the identification of the spectrum of phenotypes of interest and these studies include cross sectional, case-control, and cohort study designs.

The purpose of this review is to, according to study design, summarize how different studies in the literature describe individuals who test IGRA and TST negative after single or multiple *Mtb* exposure (**Tables 1** and **2**). Second, we compare the differences. Third, based on the differences, we argue why a single definition of a "resister" phenotype may be inadequate. Lastly, we aim to make recommendations on how future studies should approach their study design and definitions.

STUDY DESIGNS AND DEFINITIONS

Household Contact Studies

The past few years has seen increased interest in using household contact studies in order to understand the pathophysiology of *Mtb* infection—including the host immune response—and to define "resistance" or "early clearance" to infection. Some of the advantages of this particular study design include the ability to recruit a highly exposed group of individuals who can be followed prospectively while collecting extensive epidemiological data (11). All of these aspects ensure that all stages of *Mtb* infection and disease can be captured allowing a more defined and robust phenotypic examination (11).

Kampala, Uganda

The study by Stein et al. is unique among household contact (HHC) studies in that it revisited a cohort that had been originally recruited between 2002 and 2012 in order to assess the robustness of the "resister" phenotype several years later (12). This follow-up study retraced 407 HIV negative participants who were at least 15 years of age at the start of the retracing study and who had been initially classified as "persistent TST negative" (negative TST results for a minimum of 12 months and up to 24 months optimally) or "TST negative incomplete" (negative TST results for less than 12 months). The average time in between recruitment for these studies was approximately 9.5 years (12).

In addition to the TST used in the previous study, Stein et al. added the use of the QuantiFERON TB Gold In-Tube (QFT) test to further refine the "resister" phenotype. There were three QFT tests performed per participant. The first one was done at baseline followed by two others done in the 1 to 2-year period after baseline. A final TST (5 tuberculin units [TU], PPD-S2, Tubersol, Sanofi Pasteur Limited, USA) was performed following the last QFT test. Based on the additional testing, participants were further grouped into the following "resister" categories: "definite resister", "probable resister", and "possible resister" (see **Table 1**). The investigators defined certainty level using quantitative values of the QFT and TST such that if values were close to the positive/negative thresholds, they had a lower level of certainty. The levels of certainty also incorporated missed visits for both IGRA and TST data. Stein et al. also highlighted the presence of 32 TST/QFT "discordant" individuals who had consistent TST results but opposite QFT tests results. At the end of the study, most (82.7%) of the retraced "persistent TST negatives" remained QFT and repeat TST negative ("resisters") while 16.3% converted to LTBI and 1.0% were labelled as "discordant". In addition, 91.7% of these "resisters" had a TST of 0 mm (12).

Chennai and Pune, India

Mave et al. recruited a total of 799 children, adolescents and adults who had been living in the same household of an adult pulmonary TB index case from two different sites in India (15). Follow-up included three QFT tests and three TSTs (5 TU, PPD, SPAN/Arkray, India) at baseline, at 4 months and at 12 months. The cut offs used for the QFT tests were those suggested by the manufacturer and they used the more stringent 5 mm. cut off for the TST on all subjects. They also classified HHCs using a TB risk score and defined high exposure as those adults with a score > 6 and children with a score > 5 (13, 14). Using these tests, the authors defined the following phenotypes: "persistent LTBI negative" (pLTBI-), "resisters", and "resisters with a complete absence of response" (**Table 1**). By the end of the follow up period, 91.6% of all HHCs developed latent TB infection. Sixty-seven HHCs (8%) were classified as "pLTBI-" and 52 of these were further classified as "resisters". Although none of these "resisters" had a complete absence of response to both tests, approximately half of them had no response to at least one of the tests. Finally, the authors mentioned that the two tests only had a 60% agreement but did not reveal how they dealt with discordant results.

TABLE 1 | Summary of tests and definitions used by household contact studies.

Household contact study	Study location	Risk score used	Tests used	Cut-offs	Resister' definition	Other definitions	LTBI definition
Stein et al. (11, 12)	Kampala, Uganda	Validated TB risk score by Mandalakas et al. (13); Ma et al. (14)	TST (5 tuberculin units [TU], PPD-S2, Tubersol, Sanofi Pasteur Limited, USA) QFT Gold In-Tube (QFT-GIT)	TST: 10mm (HIV– contacts) and 5mm (HIV+ contacts) QFT: IFN-γ (TB Ag – Nil) at 0.35 IU/ml	*Initial houlsehold contact study*: TST negative after at least 12 months of follow-up. *Retracing study:* Three negative QFT tests (one at baseline and two others during the 1-2 year follow-up period) and a final negative TST following the last QFT test. *Average duration of time in between studies:* 9.5 years.	**Probable 'resister':** one 'low level positive' QFT that disagreed with the other 4 data points. A low level positive included values of 0.35 IU/ml < IFN-γ (TB Ag – Nil) < 0.5 IU/ml. **Possible 'resister'**: TST induration ≤ 8mm or one QFT positive plus all other negative tests or a TST negative incomplete with 2 negative QFTs but missing the last visit of the study.	**Definite LTBI:** All TST and QFT +. **Definite converters:** Persistently TST negative in initial study who converted to 3+ QFT and a +TST on retracing.
Mave et al. (15)	Chennai and Pune, India	Validated TB risk score by Mandalakas et al. (13); Ma et al. (14)	TST (5 TU, PPD, SPAN/ Arkray, India) QFT-GIT	TST: 5mm QFT: IFN-γ (TB Ag – Nil) at 0.35 IU/ml	HHCs with high TB exposure who were TST and QFT negative at baseline and up to 12 months following exposure (TST < 5mm and QFT IFN-γ (TB Ag – Nil) < 0.35 IU/mL).	**Persistent LTBI negative (pLTBI-):** TST and QFT negative at baseline and up to 12 months following exposure. **'Resisters' with complete absence of response**: TST = 0mm and IFN-γ (TB Ag – Nil) < 0.01 IU/ml.	**LTBI:** At least one positive TST or QFT test. TST ≥ 5mm or QFT IFN-γ (TB Ag – Nil) ≥ 0.35 IU/mL.
Verrall et al. (16, 17)	Bandung, Indonesia	Score, derived using regression methods, was based on the index TB case's sputum smear grade, the presence of cavities and the extent of the CXR disease	QFT- GIT	IFN-γ (TB Ag – Nil) at 0.35 IU/ml	**Persistently negative (Early clearers):** Persistently IFN-γ (TB Ag – Nil) < 0.35 IU/ml at baseline and at 14 weeks.		**Conversion:** IFN-γ (TB Ag – Nil) < 0.35 IU/ml at baseline to IFN-γ (TB Ag – Nil) > 0.35 IU/ml at 14 weeks.
Hill et al. (18)	Banjul, The Gambia	No risk score used	TST (2 TU, PPD RT23, Statens Serum Institut, Denmark) ELISPOT	TST: 10mm ELISPOT: For a positive ESAT-6/ CFP-10 result it was necessary for at least one of the two pools of overlapping peptides to be positive. Phytohaemagglutinin wells were set to at least 150 SFU/ well/2 x 10^5 above negative control wells. Negative control wells were required to have less than 20 SFU.	HHCs with high TB exposure: TST < 5mm at baseline and 18 months following exposure and negative ELISPOT at baseline, 3 months and 18 months following exposure.		**TST conversion**: Negative at baseline and ≥ 10 mm & an increase in induration ≥ 6 mm at 18 months. **Positive ELISPOT:** ESAT-6/CFP-10- at least one of the two pools of overlapping peptides positive. **ELISPOT conversion:** as a newly positive test, plus a change in the combined ESAT-6 and CFP-10 count (> negative control) ≥ 6 SFU/well/2x10^5 (30 SFU/million cells).
Coulter et al. (19)	The Gambia	Based on sleeping proximity to the index TB case and smear grade of the index TB case	in-house IGRA	Unknown	**Non-converters:** IGRA negative at baseline and at 6 months		**LTBI:** IGRA positive at baseline **IGRA converters:** IGRA negative at baseline and IGRA positive at 6 months
Medawar et al. (20)	The Gambia	HHCs sleeping in the same room as index TB case	QFT-GIT	Negative QFT: IFN-γ (TB Ag – Nil) ≤ 0.2 Positive QFT: IFN-γ (TB Ag – Nil) ≥ 0.7	**QFT nonconverters**: IGRA negative at baseline and at 6 months	**QFT reverters: IGRA positive at baseline and IGRA negative at 6 months**	**LTBI:** IGRA positive at baseline and at 6 months **IGRA converters:** IGRA negative at baseline and IGRA positive at 6 months
Weiner et al. (21)	The Gambia	Based on sleeping proximity to the index TB case and smear grade of the index TB case	*Cohort 1*: TST (2 TU, PPD RT23, Statens Serum Institut, Denmark) *Cohort 2:* QFT-GIT	TST: 10mm QFT: IFN-γ (TB Ag – Nil) at 0.35 IU/ml	*Cohort 1* **TST nonconverters:** TST = 0mm at baseline and at 3 months. *Cohort 2* **Nonconverters:** IFN-γ (TB Ag – Nil) < 0.35 IU/mL at baseline and at 6 months.		**Cohort 1: (TST converters)** 0 mm at baseline and converted to positive >10 mm by 3 months. **Cohort 2: (converters)** IFN-γ (TB Ag – Nil) < 0.35 IU/mL at baseline and IFN-γ (TB Ag – Nil) > 0.35 IU/ mL at 6 months.

(Continued)

TABLE 1 | Continued

Household contact study	Study location	Risk score used	Tests used	Cut-offs	Resister' definition	Other definitions	LTBI definition
Aissa et al. (22) and Cobat et al. (23)	Val de Merne, Paris, France	Exposure measures included daytime and nighttime proximity to the index case, duration of exposure to the index case in number of days during the 3 months prior to the index case's diagnosis, and the index case infectivity. Index case infectivity was assessed using the duration of cough before diagnosis, presence of cavitation and extent of disease on CXR, and bacillary density in sputum smears and culture	TST (2 TU, PPD RT23, Statens Serum Institut, Denmark)	Aissa et al.: 5mm Cobat et al.: 0mm	*Aissa et al.*: TST < 5mm at baseline (V1) and 8-12 weeks (V2) *Cobat et al.*: TST = 0mm at V2 and V2		**LTBI:** TST ≥ 10 mm (no prior BCG vaccination). TST ≥ 15 mm at V1 or V2 or converted from TST < 5mm (V1) to TST ≥ 10 mm at V2 (BCG-vaccinated contacts).
Quistrebert et al. (24)	Southern Vietnam	No risk score used	*Vienam cohort*: TST (5 TU, Tubertest, Sanofi Pasteur, France) and QFT-GIT *Val de Merne cohort*: in-house IGRA *South African cohort*: in-house IGRA	TST: 5mm QFT: IFN-γ (TB Ag – Nil) at 0.35 IU/ml	*Vietnam cohort* **Double negatives:** TST < 5mm and QFT-GIT IFN-γ (TB Ag – Nil) < 0.35 IU/mL *Val de Merne cohort (Aissa et al.)* **Negative**: (i) TST < 5 mm at both V1 and V2, ii) < 5 mm at V1, when only one visit was done **Uninfected subjects:** HHCs with a negative TST and a null IFN-γ production *South African cohort* **Uninfected**: TST < 5 mm and a null IFN-γ production		*Vietnam study* **Double positives:** TST ≥ 5mm and a positive QFT-GIT IFN-γ (TB Ag – Nil) ≥ 0.35 IU/mL. *French study* **Positive:** TST i) ≥ 5 mm at both V1 and V2, ii) < 5 mm at V1 and ≥ 10 mm at V2. **Infected subjects** as HHCs who presented both a positive TST and a positive IGRA result (IFN-γ production > 175 pg/mL) *South African cohort* **Infected:** Both positive TST and IGRA result (IFN-γ production > 20.9 pg/mL).
Chen et al. (25)	Shanghai, China	Based on shared air space with an individual with pulmonary TB in the household or other indoor setting for > 15 hr per week or > 180 hr total during an infectious period (an infectious period was defined as the interval from 3 months before collection of the first culture-positive sputum specimen or the date of onset of cough, whichever was longer, through 2 weeks after the initiation of appropriate anti-tuberculosis treatment)	ELISPOT (TS-SPOT; Beijing Jinhao, China)	Positive if either Panel Test (containing ESAT-6/CFP-10/Rv3615c peptides pool) showed at least six spot-forming cells (SFCs) more than the negative control when the negative control ≤5 SFCs; or if the number of spots in Panel Test was at least double the number in the negative control when the negative control >5 SFCs	**Resisters:** persons who were highly exposed to *Mtb* and were IGRA/TST negative without clinical syndromes of active TB infection at enrollment. However, no TST was performed		**LTBI:** persons who were highly exposed to Mtb and were IGRA/TST positive without clinical syndromes of active TB infection at enrollment. However, no TST was performed
Vorkas et al. (26)	Port-au-Prince, Haiti	Based on living in the same house as the active TB case for at least 1 month in the 6 months prior to diagnosis	QFT-GIT	Not specified	HHCs with IGRA negative result at enrollment		HHCs with IGRA positive result at enrollment

TABLE 2 | Summary of tests and definitions used by community-based studies.

Community-based study	Study location	Risk score used	Tests used	Cut-offs	Resister' definition	Other definitions	LTBI definition
Cobat et al. (27)	Cape Town, South Africa	None. Risk is inferred from community exposure in a high incidence environment.	TST (2 TU, PPD RT23, Statens Serum Institut, Denmark)	TST: 0mm	TST = 0mm at baseline only.		TST > 0mm at baseline only.
Gallant et al. (28)	Cape Town, South Africa	None. Risk is inferred from community exposure in a high incidence environment.	TST (2 TU, PPD RT23, Statens Serum Institut, Denmark) In-house IGRA	TST: 5mm In-house IGRA: 63 pg/mL	**Double negatives** at a single time point. TST < 5mm and IFN-γ response to BCG or PPD or ESAT-6 < 63 pg/mL.		TST ≥ 5mm, IFN-γ response to BCG or PPD or ESAT-6 > 63 pg/mL.
Kroon et al. (29)	Cape Town, South Africa	None. Risk is inferred from community exposure in a high incidence environment.	TST (2 TU, PPD RT23, Statens Serum Institut, Denmark; 5 TU, PPD-S2, Tubersol, Sanofi Pasteur Limited, USA) QFT Gold Plus (QFT-Plus)	TST: 5mm QFT-Plus: Criteria for negative QFT-plus result: 1) Nil ≤ 8.0, and 2) TB1 minus Nil <0.35 or ≥0.35 and <25% of Nil value, and 3) TB2 minus Nil <0.35 or 0.35 and <25% of Nil value, and 4) Mitogen minus Nil ≥ 0.5. Criteria for positive QFT-plus result either: 1) Nil ≤ 8.0, and 2) TB1 minus Nil ≥0.35 and ≥25% of Nil value, and 3) Any TB2 minus Nil 4) Any Mitogen minus Nil Or 1) Nil ≤ 8.0, and 2) Any TB1 minus Nil 3) TB2 minus Nil ≥0.35 and ≥25% of Nil value, 4) Any Mitogen minus Nil.	**HIV-1-infected persistently TB, tuberculin and IGRA negative (HITTIN)**: HIV+ persons who had experienced a period of very low CD4 counts, who had no symptoms or history of previous TB, had three consecutive negative IGRA readings, and a TST = 0mm.		**HIV-1-infected IGRA positive tuberculin positive (HIT)**: HIV +persons who had experienced a period of very low CD4 counts, who had no symptoms or history of previous TB with two consecutive positive IGRA results and a TST ≥ 5mm.
Mahomed et al. (30)	Worcester, South Africa	Risk was inferred from community exposure in a high incidence environment. A subset of participants reported current or prior household contact, mostly within three years of enrollment.	TST (2 TU, PPD RT23, Statens Serum Institut, Denmark) QFT-GIT	TST: 5mm QFT-GIT: IFN-γ (TB Ag – Nil) at 0.35 IU/ml	Focus of the study was on converters/incident TB cases. No definition of resister/nonconverter given.		**Converters**: IFN-γ (TB Ag – Nil) > 0.35 IU/ml and TST ≥ 5mm at baseline measurement. 50% had active follow-up (every 3 months), and 50% had passive follow-up (at 2 year visit).

(Continued)

TABLE 2 | Continued

Community-based study	Study location	Risk score used	Tests used	Cut-offs	Resister' definition	Other definitions	LTBI definition
Nemes et al. (31)	Worcester, South Africa	Risk was inferred from community exposure in a high incidence environment. A subset of participants reported current or prior household contact, mostly within three years of enrollment.	QFT-GIT	QFT-GIT: IFN-γ (TB Ag – Nil) at 0.2, 0.35 and 0.7 IU/ml	**Stringent nonconverters:** IFN-γ (TB Ag – Nil) < 0.2 IU/ml at baseline, day 360, and day 720.	**Stringent QFT persistent positives:** IFN-γ (TB Ag – Nil) > 0.7 IU/ml at baseline, day 360, and day 720. **"Uncertain" converters:** IFN-γ (TB Ag – Nil) < 0.35 IU/ml at baseline, and IFN-γ > 0.35 IU/ml at day 360, with at least one result within the uncertainty zone of 0.2-0.7 IU/ml.	**Stringent converters:** IFN-γ (TB Ag – Nil) < 0.2 at baseline and > 0.7 at day 360).
Andrews et al. (32)	Worcester, Ceres & Robertson, South Africa	None. Risk is inferred from community exposure in a high incidence environment.	QFT-GIT	QFT-GIT: IFN-γ (TB Ag – Nil) at 0.35 and 4.0 IU/ml	**Nonconverters:** IFN-γ (TB Ag – Nil) < 0.35 IU/ml at baseline, day 336 and end of study.		**Converters:** IFN-γ (TB Ag – Nil) >4.00 IU/ml at baseline, day 336 and end of study.
Simmons et al. (33)	North West Province, South Africa	None. Risk is inferred from work exposure in gold mines, a high incidence environment.	TST (2 TU, PPD RT23, Statens Serum Institut, Denmark) QFT-Plus	TST: 0mm and 5mm QFT-Plus: Both antigen tube readings of IFN-γ (TB Ag – Nil) at 0.35 IU/ml	**"Uninfected" :** Miners who had a negative QFT-Plus up to one year after baseline. A stricter definition was also used as those with a negative QFT-Plus and TST = 0 mm after one year of follow-up.		**"TB infected":** Miners who had a positive QFT-Plus up to one year after baseline. A stricter definition was also used as those with a postive QFT-Plus and a TST > 5mm after one year of follow up.
Li et al. (34)	Beijing, China	None. Risk inferred from working at Beijing Chest Hospital ≥3 years	ELISPOT (T.SPOTTB; Oxford Immunotec)	ELISPOT ≥24 spots for ESAT-6, CFP-10, or both	**"Highly exposed but uninfected" (HEBUI): Negative ELISPOT at baseline only**		**"Latent":** Positive ELISPOT at baseline only

Bandung, Indonesia

This HHC study by Verral et al. sought to outline characteristics and associated risk factors of "early clearers" of *Mtb* infection (16, 17, 35). The HHCs for this study were recruited as part of the TANDEM project and originated in Bandung, one of the largest urban centers in Indonesia (36). The authors enrolled 1,347 HHCs of pulmonary TB index cases who were at least 5 years of age. Unlike the previous HHC studies, the authors only used the QFT test and the follow-up period was much shorter. The authors also used a different measure to evaluate the extent of exposure of HHCs. This score, which they derived using regression methods, was based on the index case's sputum smear grade, the presence of cavities and the extent of the CXR disease (16, 17, 35). It also included the HHC's number of hours spent with the index case as well as the sleeping proximity. To categorize each HHC, Verral et al. used QFT tests at baseline and 14 weeks later. The cut offs used were those recommended by the manufacturer. The authors defined "early clearers" as those HHCs who had negative QFT results at the end of the follow-up period (**Table 1**) (16, 17, 35).

Of the 1347 HHCs enrolled in the study, 490 were QFT negative at baseline and qualified for a follow up test. Of these, 317 (64.7%) had a subsequent negative QFT result and were labeled "early clearers" and 116 (23.7%) had a positive QFT result and were labeled "converters". The rest could not be reached for a repeat test, had indeterminate results, had active disease or unevaluated symptoms of TB. The authors point out that the rate of "early clearers" in this particular study (~25%) was similar to those found in the cohorts from Uganda (14%) and The Gambia (45%) (6, 18). "Early clearers" had lower measures of exposures and, along with converters, were younger than those who had a positive QFT test at baseline.

The Gambia

There are four HHC studies from The Gambia that provide insight in the natural progression of *Mtb* infection. The first study by Hill et al. took place in Banjul and used the ELISPOT test and TST to define phenotypes while the study by Weiner et al. utilized the QFT and TST (18, 21). Coulter et al. and Medawar et al., utilized QFT only (19, 20).

Hill et al. analyzed the test results of 558 HHCs who were at least 15 years of age. These HHCs underwent 3 ELISPOTs at baseline, at 3 months and at 18 months (16). In addition, all HHCs also underwent a TST (2 TU, PPD RT23, Statens Serum Institut, Denmark) at baseline and a "subcohort" of 196 consecutively recruited HHCs also underwent a repeat TST at 18 months. The authors used a more stringent cut off for the ELISPOT than is recommended by the manufacturer. A positive TST required an induration of at least 10 mm plus an increase in such induration of at least 6 mm. Using the ELISPOT, the authors identified 97 (17%) HHCs who had three negative results during the 18-month follow-up. In the "subcohort" of 196 HHCs who underwent both ELISPOT and TST testing, 27 (14%) had consistently negative results after 18 months (**Table 1**).

Coulter et al. recruited 31 household TB contacts of 10 active TB index cases and classified them as LTBI, IGRA converters or non-converters, based on an in-house IGRA taken at baseline and 6 months later (19). Whole blood was stimulated by PPD, ESAT-6 and CFP-10. No details are provided on the threshold for IFN-γ positivity. Ten participants (32%) tested baseline IGRA positive and were defined as LTBI. Eleven (35%) participants who tested IGRA negative at baseline and remained negative at follow-up were defined as IGRA non-converters. Ten (32%) IGRA converters, who tested baseline negative and converted to positive at 6 months were also included. Exposure was measured by the smear grade of the index patient as well as sleeping proximity to the index patient (19). In a second study the group selected HHC from another longitudinal HHC cohort study (20). High exposure was defined by sleeping proximity and only persons sleeping in the same room as the index case was included. HHCs were seen at baseline and 6 months later. Seventeen (25%) were defined as "QFT nonconverters" based on 2 negative readings, 14 (21%) as "QFT converter" based on a negative at baseline and positive after 6 months, 18 (27%) as "QFT reverter" based on positive at baseline and negative after 6 months and lastly 18 (27%) as "LTBI" based on 2 positive readings. A QFT was considered negative if IFN-γ (TB Ag – Nil) < 0.2 IU/ml and positive if IFN-γ (TB Ag – Nil) > 0.7 IU/ml, which avoided what they referred to as the "grey zone" (20). It is not clear whether the participants represented in these two studies originated from the same cohort.

The fourth and most recent study by Weiner et al. was a case-control study nested within the larger study of HHCs at Medical Research Council Unit The Gambia (21). The authors used the same TB exposure score as Coulter et al. (19, 21). Weiner et al. aimed to characterize the host transcriptomic, metabolic, and antibody responses to *Mtb* in "nonconverters" when compared to "converters". To do so, they established two different cohorts. In cohort 1, "nonconverters" were defined as HHCs who had a TST (2 TU, PPD RT23, Statens Serum Institut, Denmark) result of 0 mm at baseline and at the 3-month follow-up. In cohort 2, "nonconverters" were defined as HHCs who had a negative QFT test result at baseline and at the 6-month follow-up (**Table 1**) (21). Unfortunately, the authors did not provide the cut-off values they used to determine a negative QFT test result, nor did they mention the number of "nonconverters" identified.

Val-de Marne, Paris, France

This cohort of HHCs was described in multiple substudies aimed at characterizing the genetics of a *Mtb* infection resistance phenotype. They lived with pulmonary TB index cases for 3 months prior to their TB diagnosis and were recruited between April 2004 and January 2009. Between April 2004 to December 2005, 325 index cases and 2009 HHCs were initially identified and described (22). Participants were seen for two visits. During the screening visit (V1) a TST (5 TU, Tubertest, Sanofi Pasteur, France) was administered and blood was taken for an in-house IGRA. A repeat TST was administered 8–12 weeks later during visit 2 (V2).

A negative TST was defined as a TST reading <5 mm at both V1 and V2 or a single reading < 5 mm if only one visit (V1) was completed. In contacts without prior BCG vaccination a positive TST reading was defined as ≥ 10 mm. A TST reading was

considered positive in BCG-vaccinated persons if it was ≥ 15 mm at both V1 or V2 or < 5 mm at V1 and converted to ≥ 10 mm at V2 (22). The authors also collected exposure measures of HHCs. These included daytime and nighttime proximity to the index case, duration of exposure to the index case in days during the 3 months prior to the index case's diagnosis, and the index case infectivity. Index case infectivity was assessed using the duration of cough before diagnosis, presence of cavitation and extent of disease on CXR, and bacillary density in sputum smears and culture (22, 24).

Aissa et al. identified 1575 contacts who completed the screening process. Of these contacts a total of 1,150/1,575 (73%) remained uninfected, 410 (26%) had latent infection and 15 (1%) had active TB. Later and by using more stringent TST definitions, a total of 84/540 (15.6%) HHCs with TST readings of 0 mm at both visits, were defined and was used to replicate findings in the Sequella cohort which was recruited in South Africa and is described under community-based studies (**Table 1**) (23).

An additional in-house IGRA was later described in the same cohort (24, 37). The in-house IGRA was defined to measure IFN-γ production after stimulating peripheral blood mononuclear cells (PBMCs) with ESAT-6 and null production of IFN-γ was defined as a negative IGRA. A positive IGRA result was defined as IFN-γ > 175 pg/mL (24). A negative TST was defined as a TST reading <5 mm at both V1 and V2 or a single reading <5 mm if only one visit (V1) was completed. A TST reading was considered positive if it was ≥ 5 mm at both V1 and V2 or < 5 mm at V1 and converted to ≥ 10 mm at V2 (24).

Contacts were defined as *Mtb* infection "resisters" if they had a negative TST and null IFN-γ production, irrespective of previous BCG status. In total, 33/664 (5%) were identified as *Mtb* uninfected (TST negative and IGRA null). There were 147/664 (22%) infected (TST positive and IGRA positive) persons and 484 HHC who had discordant results or missing information. This cohort was used to validate loci identified in the HHC study in Vietnam (22, 24).

Southern Vietnam

This study included 1,108 HHCs of 466 pulmonary TB cases from 2010 to 2015 in an endemic region of Southern Vietnam (24). The objective of the study was to characterize the genetics of a TST and QFT negative *Mtb* resister phenotype. However, participants were not followed or defined longitudinally. Participants were invited for a baseline TST (5 TU, Tubertest, Sanofi Pasteur, France) and QFT test. A negative TST was defined as a TST reading < 5mm. QFT results were defined according to the manufacturer's instruction (24). Although the authors defined the HHC subjects included in the study as being at high risk of infection, they did not provide information on any measures of exposure that they may have used to make this determination.

The study defined resistance to *Mtb* infection as a negative TST and IGRA reading at a single time point ("double negatives"). This group was compared to the group classified as *Mtb* infected i.e. a positive TST and IGRA reading ("double positives"). In total, 188 (17%) "double negatives" and 512 (46%) "double positives" were identified, as well as 408 participants with discordant results who were excluded (24).

Shanghai, China

The cross-sectional study by Chen et al. sought to identify the CD69 expression profiles of a number of different phenotypes, including "resisters" (25). The authors defined "resisters" as individuals who were close contacts to TB index cases with persistently negative TST/IGRA results despite prolonged exposure. Prolonged exposure was defined as sharing air space with an individual with pulmonary TB in the household or other indoor setting for > 15 h per week or > 180 h total during an infectious period. The infectious period was defined as the interval from 3 months before collection of the first culture-positive sputum specimen or the date of onset of cough, whichever was longer, through 2 weeks after the initiation of appropriate TB treatment. However, the authors only used the ELISPOT assay at baseline (according to the manufacturer's instructions) and did not confirm the persistence of this result with subsequent tests. Based on these definitions, Chen et al. identified 13 "resisters" (25).

Port-au-Prince, Haiti

A cross-sectional study design was utilized to recruit HHCs from high transmission risk households (26). High risk of exposure of the HHCs was defined as sleeping in the same house as the TB index case for at least one month during the six months prior to the index case diagnosis. HHCs were seen at baseline and 6 months later and were screened for LTBI using QFT. Unfortunately, the authors did not provide the QFT cut-offs used in their study. At baseline, 19 (61%) HHCs tested QFT positive and 12 (39%) tested QFT negative. All of the twelve (39%) initially negative HHC remained IGRA negative on both visits and they were labeled as "TB healthy household contacts" who had "resisted infection" (26).

Community Studies

In high TB burden settings, contact outside the household accounts for the majority of TB transmission in these settings. This occurs especially in cases of prolonged stay in low socio-economic communities with a high burden of TB and HIV (38, 39). Some activities associated with transmission include drinking in social groups, using public transportation, school and workplace exposures (38–46). Individuals who are severely immunocompromised, as with HIV-infection, are more susceptible to progress to TB (47–49).

Genotype and phenotypic drug susceptibility testing in the Western Cape, South Africa, show that considerable community transmission occurs in children <13 years with household TB transmission cases only contributing to around 8–19% (46, 50–53). Age can be used as a proxy for exposure frequency with at least 80% of individuals converting to positive TST reactions by the age of 30 (28, 45). High *Mtb* infection transmission rates in a high burden community show the importance of utilizing community-based research in these settings (45, 54, 55).

Sequella Study, Cape Town, South Africa

The Sequella study recruited 475 healthy, HIV-uninfected children and adolescents from 155 nuclear families from local clinics in two suburbs in Cape Town, South Africa (28). Blood was collected for an in-house IGRA and TST (2 TU, PPD RT23, Statens Serum Institut, Denmark) at baseline only. TST measurements were recorded as negative if TST < 5 mm. IFN-γ was measured after whole blood was stimulated with live BCG, PPD or ESAT-6 and positive responders were initially defined as IFN-γ responses of > 62 pg/mL (28).

The resister phenotype was defined as participants with double negative results at a single time point and were not longitudinally followed. A total of 164 (38%) were classified as TST negative or TST < 5 mm with 162 having TST readings of 0 mm and 260 with readings ≥ 5 mm. The double negatives identified were as follows: BCG negative (n=15), PPD negative (n=26) and ESAT-6 negative (n=81) (28).

More recently this cohort was used to validate findings in the aforementioned Vietnamese cohort (24). *Mtb* infection resisters were now defined as uninfected subjects with a negative TST (< 5 mm) and a null IFN-γ production [128/415 (31%)], and infected subjects as those with both positive TST and IGRA result (IFN-γ production > 20.9 pg/mL) [152/415 (37%)]. A third of the participants [135/415 (33%)] had discordant results.

Cape Town, South Africa

The ResisTB study is a community based case-control study conducted in Cape Town, South Africa (29). Participants were recruited from ART clubs at HIV clinics in Cape Town.

The "resistance" phenotype was defined as HIV-1-infected persistently TB, tuberculin and IGRA negative (HITTIN). All participants had to be HIV positive persons aged 35 to 60 years and living in an area of high transmission of *Mtb*, i.e., Cape Town. In addition, the criteria included a history of living with a low CD4+ count (either with two CD4+ < 350 cells/mm^3 counts at least 6 months apart or a single CD4+ count < 200 cells/mm^3) prior to initiating ART. During this period, these individuals would have been extremely susceptible to infection and disease. By the time of enrollment all participants were immune reconstituted on ART for at least one year with the most recent CD4+ count > 200 cells/mm^3 (29).

Participants were screened with a QuantiFERON-TB Gold Plus (QFT-Plus) in-tube test and were classified as IGRA positive or negative according to the manufacturer's instructions. Once identified participants were longitudinally followed-up. Individuals who tested IGRA negative were re-contacted on average 203 ± 151 days later for a second IGRA and TST administration (5 TU, PPD-S2, Tubersol, Sanofi Pasteur Limited, USA; 2 TU, Tuberculin PPD RT23, Statens Serum Institute, Denmark). The TST was read 3 days later and after this was done, a third IGRA was taken. Individuals in the final case group were designated HITTIN if they had three consecutive, negative IGRA tests and a negative TST reading (n=48) (**Table 2**). In parallel, a subset of control participants with an initial positive IGRA test were re-contacted for a second IGRA after an average of 292 ± 70 days. Those participants who tested IGRA positive in two consecutive tests (IGRA double+) and displayed a TST > 5 mm are defined as HIV-1-infected IGRA positive tuberculin positive (HIT, n=35) (29).

Worcester, South Africa

An adolescent youth cohort was recruited from local schools in Worcester, Western Cape, South Africa, during May 2005 until April 2007 (30, 31, 56–58). The TB notification rate in Worcester, was 1,400 cases per 100,000 in 1996. In total 6,363 adolescents aged 12–18 years (median 15yr, IQR:14–16) were enrolled into the cohort. The study included a majority younger participants ≤ 15 years old [56.5% (3603/6363)] and females [54.3% (3458/6363)] (58). Most of the participants, 1,055 of the 1,728 who had a current and prior household contact, reported the contact was within three years of the enrolment. Participants were screened with baseline TST (2 TU, Tuberculin PPD RT23, Statens Serum Institute, Denmark)) and QFT.

Nemes et al. investigated the consistency of serial QFT testing algorithms and included a more refined QFT conversion definition [a decrease from the manufacturer's guidelines of IFN-γ (TB Ag – Nil) < 0.35 IU/ml to < 0.2 IU/ml and an increase from IFN-γ (TB Ag – Nil) > 0.35 to >0.7 IU/ml] to control technical and immunological variability that may occur within the "uncertainty zone" of 0.2–0.7 IU/ml (31).

The QFT results for participants in cohort 1 were classified according to the more stringent cutoffs compared to the manufacturer's guidelines and were grouped into four categories. Stringent QFT nonconverters were defined as IFN-γ (TB Ag – Nil) < 0.2 IU/ml at baseline, day 360, and day 720. Stringent QFT persistent positives were defined as IFN-γ (TB Ag – Nil) > 0.7 IU/ml at baseline, day 360, and day 720. Stringent QFT converters were defined as IFN-γ (TB Ag – Nil) < 0.2 IU/ml at baseline and IFN-γ > 0.7 IU/ml at day 360. Lastly "uncertain" converters were defined as IFN-γ (TB Ag – Nil) < 0.35 IU/ml at baseline, and IFN-γ > 0.35 IU/ml at day 360, with at least one result within the uncertainty zone of 0.2–0.7 IU/ml (**Table 2**). A total of n=648/2,432 individuals were identified as stringent nonconverters and 989/2,432 were stringent persistent positives (31).

Applying a more stringent cutoff for a negative QFT result in cohort 1 improved concordance between TST and IGRA results. In the group with a negative QFT reading between 0.2–0.34 IU/ml, 53% had a discordant positive TST result, compared to 15% in the group with QFT IFN-γ values <0.2 IU/ml. In total 43% of those with QFT IFN-γ values between 0.2–0.7 IU/ml had discordant TST and QFT results, with 85% concordance in those with values < 0.2 IU/ml and > 0.7 IU/ml (31).

Importantly, stringent QFT nonconverters in cohort 1 had lower risk of developing TB disease (TB incidence 0.16 cases/100 Person-Years) than stringent QFT converters (TB incidence 1.60 cases/100 Person-Years, p=0.0003) and stringent persistent positives (TB incidence 0.97 cases/100 Person-Years, p=0.005). Due to immunological and technical assay variability "uncertain" QFT converters likely have a higher number of false positive converters since this group does not have a significantly different risk of TB disease compared to stringent nonconverters (TB incidence 0.66 cases/100 Person-Years, p=0.229) (31).

Rural Western Cape (Ceres, Robertson, Worcester), South Africa

Participants were recruited to a MVA85A tuberculosis vaccine trial during 2009 to 2011 in rural Western Cape, South Africa (32). The trial enrolled young children between 18–24 weeks old, with a median age of 20.4 weeks (IQR 19.3–22.0).

All children were screened with a baseline QFT. Similarly, to the previously described study stricter QFT cut-off values were applied (**Table 2**). A revised positive QFT test was defined as a IFN-γ (TB Ag – Nil) >4.00 IU/ml and a negative QFT as <0.35 IU/ml. Conversion was defined as a baseline negative QFT which was followed by a positive QFT. They defined an "uncertainty zone" of a QFT reading between 0.35–4.00 IU/ml. In total 2772/2797 of the children had a baseline negative QFT result. After 336 days, 2,512/2,772 (91%) had a repeat QFT and 2,327 (93%) remained QFT negative. QFT converters had higher risk of developing TB disease (TB incidence 28.0 cases/100 Person-Years) compared to those in the "uncertainty zone" (IRR 11.4; p=0.00047) and QFT non-converters (IRR 42·5; p<0.0001) (32).

This study did not use TST in conjunction with the QFT test. The generalizability is limited to young infants only, and because of young age, they likely have not been exposed to prolonged and sufficient *Mtb* exposure. Infants who developed active disease by day 336 were not included in the analysis and those who converted were given IPT. The authors suggest that QFT IFN-γ values ≥ 4.00 IU/ml in young children should prompt increased clinical diagnostic vigilance and potential interventions to prevent TB.

Gold Mines, South Africa

In South African gold mines, 13% of HIV-uninfected and 45.5% of HIV- infected gold miners tested TST = 0 mm (59). Due to a very high *Mtb* infection pressure and TB transmission in gold mines, transmission modelling assumes at least one lifetime infection in all gold miners (60). A study of goldminers, describes the long term follow up of some of these miners (33, 59, 61). Briefly, Simmons et al. analyzed a subset of 307 miners who were HIV-negative and had at least 15 years of mining experience in order to ascertain epidemiological factors associated with resistance to infection (**Table 2**). Both the QFT-Plus and TST (2 TU, PPD RT23, Statens Serum Institut, Denmark) were used during a one year follow up. The authors defined miners who were "uninfected" as those who had a negative QFT- Plus at baseline and one year later. They also used a stricter definition of "uninfected" as those miners who had a negative QFT- Plus and a TST = 0 mm. at baseline and one year later. Based on the stricter definition, the authors found that 18.7% of miners of Black/African ethnicity included in this analysis remained "uninfected" using the stricter definition. There is likely a spectrum of "resistance" to *Mtb* infection and given a high enough *Mtb* infection pressure, as in gold mines, most individuals are likely to become infected (2).

Beijing, China

A group of healthcare workers (HCW) in a TB hospital in Beijing, China were screened for Mtb infection with ELISPOT (T.SPOTTB; Oxford Immunotec) (34). A test was considered positive if ELISPOT ≥24 spots for ESAT-6, CFP-10, or both. HCW were only screened once at baseline. In total, 24 (50%) of HCW were defined as "latently" infected with a positive ELISPOT. The other half, 24 (50%) tested ELISPOT negative and were defined as "highly exposed but uninfected" (HEBUI). These HCW were enrolled if they had been working at the hospital for more than 3 years. Their work was considered high risk since standard infection control procedures such as wearing masks are not mandated, nor always followed (34).

DISCUSSION

Making comparisons across studies that have differing definitions of clinical groups of interest is a difficult proposition. A brief overview of the twenty studies presented in this review revealed seventeen different definitions for resistance to *Mtb* infection as measured by IGRA and TST. The definitions vary in a number of important categories, which include how the intensity and duration of exposure to *Mtb* was measured, the type of diagnostic tests and cut-offs used and the durability of the phenotype across different lengths of studies.

Extent of Exposure

One of the important aspects of a HHC study is the opportunity to characterize the extent of exposure to *Mtb*. Unfortunately, only a minority of the HHC studies reviewed provided a good measure of this important factor. Stein et al. and Mave et al. utilized the same epidemiological risk score (11, 12, 15). This score is composed of a number of questions that provides a good understanding of the extent of exposure (i.e. whether the HHC share the same room or bed as the index case, whether the index case is actively coughing, whether the index case has a smear-positive sputum, whether the index case see the HHC every day) (11, 12, 15). The score can be used in both adult and pediatric populations. The use of this risk score allowed Stein et al. to make sure the extent of exposure would not differ between "resisters" and "converters" while Mave et al. included the score itself in their definition of resistance. Verral et al. also used an epidemiological risk score created specifically for their analysis using a logistic regression of exposure variables against QFT results. The resulting variable took into account both the intensity and duration of exposure (35). Of the studies that took place in The Gambia, Hill et al. did not use a risk score. On the other hand, Weiner et al. and Coulter et al. used a basic score composed of two variables (smear grade of the index case and the sleeping proximity to the index case), which they used to identify "nonconverters" and "converters" with the highest level of exposure (19, 21). Medawar et al. included HHC who were highly exposed based on sleeping in the same bedroom as the TB index case only (20). In another study, Vorkas et al. defined risk as a HHC who was sleeping in the same house as the TB case for at least a month during the 6 months before the index case was diagnosed (26). Finally, Chen et al. defined prolonged exposure as sharing air space with an individual with pulmonary TB in the household or other indoor setting for > 15 h per week or > 180 h total during a specific infectious period (25). The rest of the HHC

studies, Cobalt et al., Jabot-Hanin et al., and Quistrebert et al., did not use a formal risk assessment of their participants as they concluded being a household contact living in the same residence as the index case would be enough to consider them at high risk of exposure. However, a household contact with a negative TST and/or QFT who qualifies for a study's definition of "resister" may simply be the result of an exposure which is low in intensity or short in duration (2). This is why it is important to establish a measure of exposure, such as a validated epidemiological risk score, that could be used across studies.

The intensity of *Mtb* exposure is difficult to define within the context of a community based study design. Participants are usually unknowingly exposed to TB cases in comparison to HHC studies where there are defined TB cases and contacts. In high TB burden communities, the intensity of *Mtb* exposure is therefore inferred from community based rather than household transmission.

The extent of *Mtb* exposure is mostly defined by the duration of exposure in the community based studies. Incorporating an epidemiological risk score could be useful to identify and quantify possible high risk activities participants could be involved with e.g. classifying the amount of time an individual works in a high risk environment as with the gold mine studies, time spent using public transport in high incidence settings, previous or current TB contact and living in overcrowded conditions. Assigning risk scores to these activities would be cumbersome and difficult to substantiate, since none of these factors operate independently. For community based studies cumulative exposure to *Mtb* occurs by working or living in a high TB incidence environment (62). Simmons et al. defined a group of HIV-uninfected miners who worked for a prolonged time (>15 years) in South African gold mines which are known to be high TB risk environments (33, 59, 61). They restricted their analysis to include African miners who were more at risk based on poor socioeconomic status, living in crowded hostels and working underground in more poorly ventilated areas. Li et al. included HCW who worked for more than 3 years in a TB hospital where mask wearing was not mandated (34). In comparison, the ResisTB, Sequella and the Worcester based studies recruited participants from known high TB incidence areas (28, 29, 58). In addition, the ResisTB study used age as a proxy for exposure frequency and duration with older age (ages 35–60 years) representing a group who would have prolonged exposure in a high TB incidence environment (29). The results obtained from these community based studies are specific to the community described and one should be wary of making generalized conclusions.

Diagnostic Tests

The "resister" definition should include both a negative TST and IGRA test result. The predictive value of using both tests is highlighted by the Mahomed et al. cohort which showed that TB incidence rates were higher for those participants with a baseline positive TST (≥ 5 mm) and IGRA (> 0.35 IU/ml) [0.6 cases per 100 person years (95% CI 0.43–0.82), 0.64 cases per 100 person years (0.45–0.87)], compared to participants who had baseline negative TST and IGRA results [0.22 cases per 100 person years (0.11–0.39), 0.22 cases per 100 person years (0.12–0.38)] (30). Of the studies reviewed, eight of them used both of these tests in their definitions of resistance (12, 15, 18, 24, 28–30, 57), eight of them only used an IGRA test (16, 17, 19, 20, 25, 26, 31, 32, 34, 35) and three of them only used a TST (23, 24, 27). Although Weiner et al. used both tests, they applied the TST to one cohort and the IGRA test to another cohort (21) (**Tables 1** and **2**).

A TST is a highly sensitive test and is a marker of TB immunoreactivity rather than a marker of infection (63). It is less specific than an IGRA and is known to have decreased specificity with false positives and cross-reactions to previous BCG vaccination and nontuberculous mycobacteria (NTM). Individuals with a negative TST may not have been sufficiently exposed to *Mtb*, or they were exposed but cleared infection. This could be either due to their own immunity or after receiving *Mtb* sterilizing prophylactic therapy such as Isoniazid. It is therefore imperative that documentation of *Mtb* exposure is maximized in the resistance phenotype as persons with prolonged exposure are less likely to revert and tend to remain TST positive after isoniazid preventive therapy, or even after completing TB treatment (63–66). However, application or reading errors, in addition to immunosuppressed states such as HIV-infection, immunosuppressive drug treatment and malnutrition could also account for false negatives.

Phenotypes defined as "resisters" or so-called persistently TST negative likely contain heterogeneous subgroups as discussed above. To improve the specificity of the phenotype, a TST is combined with an IGRA test. TST and *in vitro* IFN-γ assays do not measure similar aspects of host immunity and may depend on the host as well as the frequency and exposure setting of *Mtb* and NTM (28). In general, the proportion of individuals testing IGRA positive is lower than those having a positive TST and combining the two tests gives a stricter resistance definition (67).

There are two forms of commercially based IGRA tests available. One is based on an enzyme-linked immunosorbent assay (ELISA) and the other is an enzyme-linked immunosorbent spot (ELISPOT) assay. IGRA performs better as a marker of *Mtb* infection in a high compared to a low TB burden community and shows comparable reversion and conversion rates to TST (56). The studies covered in this review used different IGRA tests in their work. Galant et al. and the Val de Merne cohort described by Jabot-Hanin et al. and Quistrebert et al., as well as Coulter et al. described in-house IGRAs (19, 24, 28, 37). Hill et al., Chen et al. and Li et al. used an ELISPOT and the rest, except for Kroon et al. and Simmons et al. who used QFT-Plus, used QFT in their studies (18, 25, 29, 34). The latest QFT-Plus removed TB-7.7 from the assay and added a TB antigen tube with peptides which measure CD8+ cytotoxic T lymphocyte responses (68). This assay was developed to improve the lack of sensitivity of the QFT test, especially in HIV-infected persons. However, more studies are still needed to show that this is indeed the case (69). QFT-Plus shows good agreement with QFT (70–73) with mostly similar specificity and sensitivity (74–76). In addition, good concordance is seen between QFT, QFT-Plus and T.SPOT (73, 77).

IGRA results should be interpreted within the scope of performing the tests in low vs high TB burden settings, the immunocompetency of the patient and the range of output

values from the tests (75, 78, 79). Output values often fall within a zone of uncertainty, defined as the total IFN-γ reading between 0.2–0.7 IU/ml after subtracting nil from TB Ag readings (31). Most participants with reversions tend to fall in this zone (31). This has been seen in QFT as well as QFT-Plus (73). Values falling in this zone are usually related to host immunological or technical variability (56, 80). This could also be indicative of participants who were recently infected and then possibly cleared infection. More reliable cut-offs for IGRA negativity set as values less than 0.2 IU/ml and > 0.7 IU/ml for a positive IGRA have been suggested (20, 31). Using these stricter definitions, they show that stringent nonconverters are less likely to develop TB over 2 years compared to recently converted or persistently QFT positive persons (31, 56). This would need to be evaluated within the context of the QFT-Plus assay which requires a value 25% greater than the nil value and a reading greater than the current standard cutoff of 0.35 IU/ml in either the TBAg1 or TBAg2 tube to be considered positive. Except for Nemes et al., all of the definitions for resistance in the literature use the established standard cutoffs when using IGRAs.

Finally, when using TST and IGRA tests, it is important to consider and collect information on factors that are associated with a positive result. For example, associations with smoking and diabetes have been established with positive TST and IGRA (81–84). Socio-economic factors such as low income and education, male sex, race, older age and HHC were identified as predictive factors for positive TST and IGRA results by Mahomed et al. (30). No significant differences were seen for socio-economic factors nor other factors such as smoking, BMI, and diabetes between HIT and HITTIN in the study by Kroon et al. (29). Mave et al. and Vorkas et al. also report no significant differences in demographic factors or clinical characteristics between converters and nonconverters (85). Simmons et al. report a BMI > 30 to be a risk factor for testing IGRA or TST positive (36). Similarly, Igo et al. found an association between a persistently TST negative result and a lower prevalence of lean mass wasting in the Uganda cohort. This is also in line with what some other studies have found (73, 86). Verrall et al. highlighted important evidence that BCG-vaccination provides dose dependent protection against IGRA conversion in HHC (16, 17). This protection effect is not seen in cases of high TB exposure and decreases with older age (16, 17, 87). In studies which show documented previous BCG vaccination or scars, no significant differences were seen between converters and nonconverters (12, 21), nor did a previous BCG show increased risk of conversion in Hill et al. (18). In addition, it would be of important for HHC studies to report the *Mtb* genotype as different strains are linked to TB clustering and variation in transmission (88). Verrall et al. reports an increased risk of conversion based on *Mtb* lineage, compared to Stein et al. who reported no difference in conversion based on *Mtb* lineage (12, 16, 17, 89).

Durability of Responses

Based on previous epidemiological studies, and as suggested by Stein et al., resistance to *Mtb* does not appear to be absolute (12, 90, 91). In fact, there appears to be a threshold above which infection will be acquired due to a high enough intensity of exposure (2). Considering the shortcomings aforementioned of both the TST and IGRA tests, long term follow-up composed of multiple testing is imperative to evaluate the durability of the results. With an average follow up time of close to 10 years, Stein et al. provides sufficient time to evaluate their definition of resistance. This study also showed that the majority of conversions happened by month 3 of follow-up (9.8%), with 2.2% converting between 3–6 months and even still some (0.7%) converted after 6–12 months. Most of the individuals in this study remained both TST and QFT negative despite the long follow-up. Although it is not clear how the HHCs' exposure varied in between the original and the follow-up study, since the participants continued living in a highly endemic area, we can presume that this did not change much. Based on these results, Stein et al. concluded that the "resister" phenotype is robust (12).

Similarly, the studies performed by Mave et al., Kroon et al., and Simmons et al. used both tests serially throughout a follow-up period of approximately year, which is an appropriate amount of time to capture conversions to LTBI or active disease (6, 15, 29). Of note, Mave et al. concluded that "pLTBI-" are rare and "resisters" are even rarer among HHCs. However, they attributed the low prevalence of these phenotypes partly to the more stringent cut-off use for the TST (15). Although not statistically significant, prevalence of the "pLTBI-" phenotype among children declined as age increased, which could certainly be the result of increased extent of exposure. Andrews et al. also had a sufficiently long follow-up of at least 336 days, however, the subjects were toddlers who were less than 2 years of age at enrollment (32). Both Nemes et al. and Mahomed et al. provided data on at least 2 years of either passive or active follow-up of adolescents with a maximum total time of 3.8 years (30, 31). A few studies followed participants between three to six months, a time when the majority of conversions would occur (23, 24, 26, 35, 37). The rest of the studies were cross-sectional in nature and only examined participants at a single time point (27, 28, 34). Despite their limitations, cross-sectional studies such as Cobat et al., Gallant et al., and Quistrebert et al., are appropriate to generate hypotheses and continue to contribute to our growing understanding of this phenotype. However, the durability and robustness of that which is measured remains unknown, since only a single time point is taken into account. Further follow-up to confirm robustness of the phenotype is needed to fully understand the implications of these biologic findings.

Can a Unified "Resister" Definition Exist?

Differences based on extent of exposure, diagnostic tests and durability of responses orders different studies according to a spectrum of host resistance (**Figure 1**). Early clearance is hypothesized to involve innate clearance of *Mtb* prior to an adaptive immune response (35). Theoretically, early clearance captures early response in a phenotype exposed to *Mtb* in an environment where *Mtb* exposure can be measured. "Early clearance" may not be achieved with each exposure and depends on the index case infectivity, TB severity and duration of contact (16, 17). In comparison, longitudinal studies with a longer follow-up, capture a more extreme and robust phenotype (12). The more extreme cases might only be captured by a smaller and high TB risk group, e.g persons living with HIV, who are able to remain TB free despite persistent or high

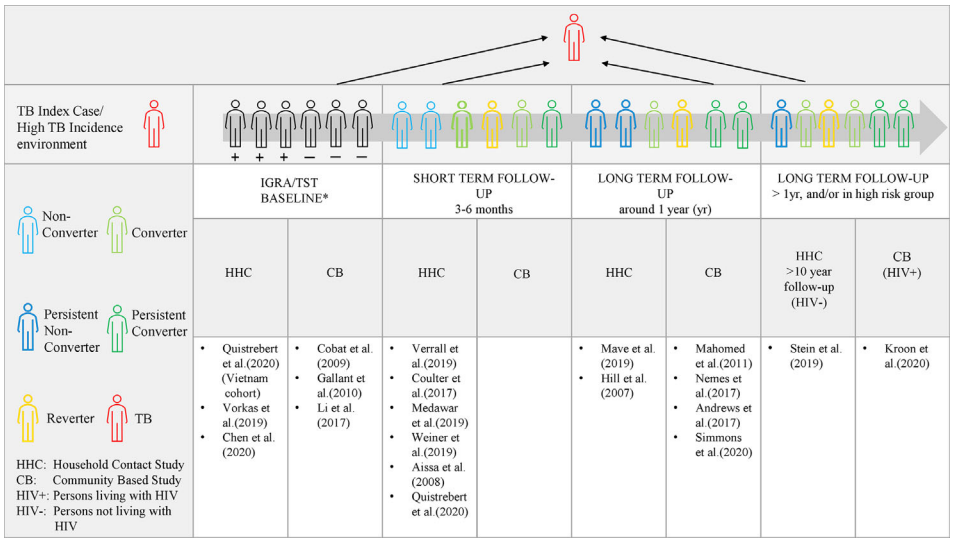

FIGURE 1 | The spectrum of IGRA/TST nonconverters. Evidence of protection to *Mtb* at a shorter time period in relation to the index case, allows the study of correlates of protection which may be overcome by exposure intensity and frequency (represented by the grey arrow). Long term follow-up allows for a more robust and extreme phenotype definition as in Stein et al. (followed for 10 years) and Kroon et al. (in persons living with HIV). Persistent non-conversion is not absolute and may eventually be overcome by time and very high levels of exposure or continuous exposure. *At baseline, individuals may test either TST/IGRA positive, negative or be discordant.

intensity exposure (29). The entire spectrum is of value and contributes to our understanding host protection against *Mtb*.

Studies investigating adaptive response using additional immunological assays show IFN-γ independent T-cell responses, differences in T-cell receptors, as well as the presence of antibodies in many of the studies (4, 20, 21, 25, 29, 34). This highlights the significance of avoiding terms such as innate or adaptive resistance until both mechanisms have been further illustrated. Similarly, terms such as early clearance or resistance to *Mtb* infection are imprecise. Both assume infection but are unable to unequivocally prove it. Crucially, the description of what was measured should be given preference rather than using terminology inferring underlying immunological or biological events (92).

As has been previously proposed, descriptions of the observed states of outcome should rather be used (92). Based on Lalvani et al.'s suggestion and by using the easily accessible TST as well as IGRA at the baseline and follow-up visits, a phenotype can be defined as 'persistently IGRA/TST negative (nonconverters), transiently IGRA/TST positive (reverters or conversion), or sustained IGRA/TST conversion (92)'. With prolonged follow-up and at least 2 visits, those who remain TST/IGRA negative are termed persistent nonconverters and those who remain positive would be termed persistent converters. For further definition, detailed innate and adaptive immunological assays are required (**Figures 1**).

CONCLUSION

Based on our review, the lack of a unifying definition of the "resister" phenotype in the literature is apparent. As described above, we found differences in how some key components were assessed and incorporated into the definition of this phenotype. Moving forward, we propose the following recommendations when trying to identify "resisters" in household contact studies or community based studies: First, the extent of exposure must be measured and considered when defining resistance. This would be ideally done using an epidemiological risk score that has been validated across different types of studies and settings such as those used by Stein et al., Mave et al. and Verrall et al. Second, both IGRA and TST must be used when evaluating an individual's response to *Mtb* and a stricter cut-off criteria should be considered for both tests. Third, the durability of the phenotype must be tested across multiple time points, ideally during at least a year of follow-up. Lastly, we propose that studies avoid terms which make assumptions about pathophysiological states which can only be inferred, such as infection. In addition, a review of both the innate and adaptive responses should be conducted before deciding on the final phenotype definition.

AUTHOR CONTRIBUTIONS

CS and MM conceived of the idea for the manuscript. JG and EK drafted the manuscript. All authors contributed to the article and approved the submitted version.

FUNDING

This work was supported by the National Institutes of Health [1R01AI124349-01]. This research was partially funded by the

South African government through the South African Medical Research Council (SAMRC) and supported by the National Research Foundation of South Africa. The content is solely the responsibility of the authors and does not necessarily represent the official views of the SAMRC. EK is supported through funding by the SAMRC through its Division of Research Capacity Development under the Clinician Researcher Development PHD Scholarship Programme. EK is also supported by a Career Development Fellowship [TMA2018CDF-2353-NeutroTB] awarded by The European and Developing Countries Clinical Trials Partnership. JG was supported by NIH training grant HL007567 and CS was supported by NIH grants R01AI124348, UO1-AI-09-001, and RO1AI147319. Funders were not involved in the writing of the manuscript or the decision to submit it for publication.

ACKNOWLEDGMENTS

The work herein was made possible through funding by the South African Medical Research Council through its Division of Research Capacity Development under the SAMRC Clinician Researcher MD PhD Development program. The content of any Publications from any studies during this Degree are solely the responsibility of the authors and do not necessarily represent the official views of the South African Medical Research Council. This publication is supported by NeutroTB which is part of the EDCTP2 program supported by the European Union (grant number TMA2018CDF-2353-NeutroTB). The views and opinions of authors expressed herein do not necessarily state or reflect those of EDCTP. The authors would also like to thank Drs. W. Henry Boom, Thomas Hawn, and Chetan Seshadri for helpful discussion.

REFERENCES

1. WHO. Global tuberculosis report 2019, in: *WHO*. Available at: http://www.who.int/tb/publications/global_report/en/ (Accessed October 31, 2019).
2. Simmons JD, Stein CM, Seshadri C, Campo M, Alter G, Fortune S, et al. Immunological mechanisms of human resistance to persistent Mycobacterium tuberculosis infection. *Nat Rev Immunol* (2018) 18:575–89. doi: 10.1038/s41577-018-0025-3
3. Lu LL, Chung AW, Rosebrock TR, Ghebremichael M, Yu WH, Grace PS, et al. A Functional Role for Antibodies in Tuberculosis. *Cell* (2016) 167:433–443.e14. doi: 10.1016/j.cell.2016.08.072
4. Lu LL, Smith MT, Yu KKQ, Luedemann C, Suscovich TJ, Grace PS, et al. IFN-γ-independent immune markers of Mycobacterium tuberculosis exposure. *Nat Med* (2019) 25:977–87. doi: 10.1038/s41591-019-0441-3
5. McHenry ML, Williams SM, Stein CM. Genetics and evolution of tuberculosis pathogenesis: New perspectives and approaches. *Infect Genet Evol* (2020) 81:104204. doi: 10.1016/j.meegid.2020.104204
6. Stein CM, Zalwango S, Malone LL, Thiel B, Mupere E, Nsereko M, et al. Resistance and Susceptibility to Mycobacterium tuberculosis Infection and Disease in Tuberculosis Households in Kampala, Uganda. *Am J Epidemiol* (2018) 187:1477–89. doi: 10.1093/aje/kwx380
7. Badger TL, Ayrazian LF. Clinical Observations on the Pathogenesis of Tuberculosis: From a 15 Year Follow-up of 745 Nurses. *Trans Am Clin Climatol Assoc* (1948) 60:12–28.
8. Badger TL, Ayvazian LF. Tuberculosis in nurses; clinical observations on its pathogenesis as seen in a 15 year follow-up of 745 nurses. *Am Rev Tuberc* (1949) 60:305–31. doi: 10.1164/art.1949.60.3.305
9. Myers JA, Boynton RE, Diehl HS. Prevention of Tuberculosis among Students of Nursing. *Am J Nurs* (1947) 47:661–6. doi: 10.2307/3457892
10. Hardy MA, Schmidek HH. Epidemiology of tuberculosis aboard a ship. *JAMA* (1968) 203:175–9.
11. Stein CM, Hall NB, Malone LL, Mupere E. The household contact study design for genetic epidemiological studies of infectious diseases. *Front Genet* (2013) 4:61:61. doi: 10.3389/fgene.2013.00061
12. Stein CM, Nsereko M, Malone LL, Okware B, Kisingo H, Nalukwago S, et al. Long-term Stability of Resistance to Latent Mycobacterium tuberculosis Infection in Highly Exposed Tuberculosis Household Contacts in Kampala, Uganda. *Clin Infect Dis* (2019) 68:1705–12. doi: 10.1093/cid/ciy751
13. Mandalakas AM, Detjen AK, Hesseling AC, Benedetti A, Menzies D. Interferon-gamma release assays and childhood tuberculosis: systematic review and meta-analysis. *Int J Tuberc Lung Dis* (2011) 15:1018–32. doi: 10.5588/ijtld.10.0631
14. Ma N, Zalwango S, Malone LL, Nsereko M, Wampande EM, Thiel BA, et al. Clinical and epidemiological characteristics of individuals resistant to M. tuberculosis infection in a longitudinal TB household contact study in Kampala, Uganda. *BMC Infect Dis* (2014) 14:352. doi: 10.1186/1471-2334-14-352
15. Mave V, Chandrasekaran P, Chavan A, Shivakumar SVBY, Danasekaran K, Paradkar M, et al. Infection free "resisters" among household contacts of adult pulmonary tuberculosis. *PloS One* (2019) 14:e0218034. doi: 10.1371/journal.pone.0218034
16. Verrall AJ, Alisjahbana B, Apriani L, Novianty N, Nurani AC, van Laarhoven A, et al. Early Clearance of Mycobacterium tuberculosis: The INFECT Case Contact Cohort Study in Indonesia. *J Infect Dis* (2020) 221:1351–60. doi: 10.1093/infdis/jiz168
17. Verrall AJ, Schneider M, Alisjahbana B, Apriani L, van Laarhoven A, Koeken VACM, et al. Early Clearance of Mycobacterium tuberculosis Is Associated With Increased Innate Immune Responses. *J Infect Dis* (2020) 221:1342–50. doi: 10.1093/infdis/jiz147
18. Hill PC, Brookes RH, Fox A, Jackson-Sillah D, Jeffries DJ, Lugos MD, et al. Longitudinal assessment of an ELISPOT test for Mycobacterium tuberculosis infection. *PloS Med* (2007) 4:e192. doi: 10.1371/journal.pmed.0040192
19. Coulter F, Parrish A, Manning D, Kampmann B, Mendy J, Garand M, et al. IL-17 Production from T Helper 17, Mucosal-Associated Invariant T, and γδ Cells in Tuberculosis Infection and Disease. *Front Immunol* (2017) 8:1252. doi: 10.3389/fimmu.2017.01252
20. Medawar L, Tukiman HM, Mbayo G, Donkor S, Owolabi O, Sutherland JS. Analysis of cellular and soluble profiles in QuantiFERON nonconverters, converters, and reverters in the Gambia. *Immun Inflammation Dis* (2019) 7:260–70. doi: 10.1002/iid3.269
21. Weiner J, Domaszewska T, Donkor S, Kaufmann SHE, Hill PC, Sutherland JS. Changes in transcript, metabolite and antibody reactivity during the early protective immune response in humans to Mycobacterium tuberculosis infection. *Clin Infect Dis* (2019) 71(1):30–40. doi: 10.1093/cid/ciz785
22. Aissa K, Madhi F, Ronsin N, Delarocque F, Lecuyer A, Decludt B, et al. Evaluation of a model for efficient screening of tuberculosis contact subjects. *Am J Respir Crit Care Med* (2008) 177:1041–7. doi: 10.1164/rccm.200711-1756OC
23. Cobat A, Poirier C, Hoal E, Boland-Auge A, de La Rocque F, Corrard F, et al. Tuberculin skin test negativity is under tight genetic control of chromosomal region 11p14-15 in settings with different tuberculosis endemicities. *J Infect Dis* (2015) 211:317–21. doi: 10.1093/infdis/jiu446
24. Quistrebert J, Orlova M, Kerner G, Ton LT, Luong NT, Danh NT, et al. Genome-wide association study of resistance to Mycobacterium tuberculosis infection identifies a locus at 10q26.2 in three distinct populations. *medRxiv* (2020). doi: 10.1101/2020.07.14.20152801
25. Chen Z-Y, Wang L, Gu L, Qu R, Lowrie DB, Hu Z, et al. Decreased Expression of CD69 on T Cells in Tuberculosis Infection Resisters. *Front Microbiol* (2020) 11:1901:1901. doi: 10.3389/fmicb.2020.01901
26. Vorkas CK, Wipperman MF, Li K, Bean J, Bhattarai SK, Adamow M, et al. Mucosal-associated invariant and γδ T cell subsets respond to initial Mycobacterium tuberculosis infection. *JCI Insight* (2018) 3(19):e121899. doi: 10.1172/jci.insight.121899

27. Cobat A, Gallant CJ, Simkin L, Black GF, Stanley K, Hughes J, et al. Two loci control tuberculin skin test reactivity in an area hyperendemic for tuberculosis. *J Exp Med* (2009) 206:2583–91. doi: 10.1084/jem.20090892
28. Gallant CJ, Cobat A, Simkin L, Black GF, Stanley K, Hughes J, et al. Impact of age and sex on mycobacterial immunity in an area of high tuberculosis incidence. *Int J Tuberc Lung Dis* (2010) 14:952–9.
29. Kroon EE, Kinnear CJ, Orlova M, Fischinger S, Shin S, Boolay S, et al. An observational study identifying highly tuberculosis-exposed, HIV-1-positive but persistently TB, tuberculin and IGRA negative persons with M. tuberculosis specific antibodies in Cape Town, South Africa. *EBioMedicine* (2020) 61:103053. doi: 10.1016/j.ebiom.2020.103053
30. Mahomed H, Hawkridge T, Verver S, Geiter L, Hatherill M, Abrahams D-A, et al. Predictive factors for latent tuberculosis infection among adolescents in a high-burden area in South Africa. *Int J Tuberc Lung Dis* (2011) 15:331–6.
31. Nemes E, Rozot V, Geldenhuys H, Bilek N, Mabwe S, Abrahams D, et al. Optimization and Interpretation of Serial QuantiFERON Testing to Measure Acquisition of Mycobacterium tuberculosis Infection. *Am J Respir Crit Care Med* (2017) 196:638–48. doi: 10.1164/rccm.201704-0817OC
32. Andrews JR, Nemes E, Tameris M, Landry BS, Mahomed H, McClain JB, et al. Serial QuantiFERON testing and tuberculosis disease risk among young children: an observational cohort study. *Lancet Respir Med* (2017) 5:282–90. doi: 10.1016/S2213-2600(17)30060-7
33. Simmons J, Van PT, Stein CM, Chihota V, Ntshiqa T, Maenetje P, et al. *Monocyte fatty acid transcriptional programs and AMPK polymorphisms associate with resistance to TST/IGRA conversion. in (Keystone Virtual 2020 Abstract)*. Available at: https://virtual.keystonesymposia.org/ks/live/551/page/3981/7236.
34. Li H, Wang X-X, Wang B, Fu L, Liu G, Lu Y, et al. Latently and uninfected healthcare workers exposed to TB make protective antibodies against Mycobacterium tuberculosis. *Proc Natl Acad Sci USA* (2017) 114:5023–8. doi: 10.1073/pnas.1611776114
35. Verrall AJ, Netea MG, Alisjahbana B, Hill PC, van Crevel R. Early clearance of Mycobacterium tuberculosis: a new frontier in prevention. *Immunology* (2014) 141:506–13. doi: 10.1111/imm.12223
36. Ugarte-Gil C, Alisjahbana B, Ronacher K, Riza AL, Koesoemadinata RC, Malherbe ST, et al. Diabetes Mellitus Among Pulmonary Tuberculosis Patients From 4 Tuberculosis-endemic Countries: The TANDEM Study. *Clin Infect Dis* (2020) 70:780–8. doi: 10.1093/cid/ciz284
37. Jabot-Hanin F, Cobat A, Feinberg J, Grange G, Remus N, Poirier C, et al. Major Loci on Chromosomes 8q and 3q Control Interferon γ Production Triggered by Bacillus Calmette-Guerin and 6-kDa Early Secretory Antigen Target, Respectively, in Various Populations. *J Infect Dis* (2015) 213(7):1173–9. doi: 10.1093/infdis/jiv757
38. Tadokera R, Bekker L-G, Kreiswirth BN, Mathema B, Middelkoop K. TB transmission is associated with prolonged stay in a low socio-economic, high burdened TB and HIV community in Cape Town, South Africa. *BMC Infect Dis* (2020) 20:1–9. doi: 10.1186/s12879-020-4828-z
39. Verver S, Warren RM, Munch Z, Richardson M, van der Spuy GD, Borgdorff MW, et al. Proportion of tuberculosis transmission that takes place in households in a high-incidence area. *Lancet* (2004) 363:212–4. doi: 10.1016/S0140-6736(03)15332-9
40. Andrews JR, Morrow C, Wood R. Modeling the role of public transportation in sustaining tuberculosis transmission in South Africa. *Am J Epidemiol* (2013) 177:556–61. doi: 10.1093/aje/kws331
41. Classen C, Warren R, Richardson M, Hauman J, Gie R, Ellis J, et al. Impact of social interactions in the community on the transmission of tuberculosis in a high incidence area. *Thorax* (1999) 54:136–40. doi: 10.1136/thx.54.2.136
42. Escombe AR, Huaroto L, Ticona E, Burgos M, Sanchez I, Carrasco L, et al. Tuberculosis transmission risk and infection control in a hospital emergency department in Lima, Peru. *Int J Tuberc Lung Dis* (2010) 14:1120–6.
43. Uys PW, van Helden PD, Hargrove JW. Tuberculosis reinfection rate as a proportion of total infection rate correlates with the logarithm of the incidence rate: a mathematical model. *J R Soc Interface* (2009) 6:11–5. doi: 10.1098/rsif.2008.0184
44. Van Rie A, Warren R, Richardson M, Victor TC, Gie RP, Enarson DA, et al. Exogenous reinfection as a cause of recurrent tuberculosis after curative treatment. *NEnglJMed* (1999) 341:1174–9. doi: 10.1056/NEJM199910143411602
45. Wood R, Liang H, Wu H, Middelkoop K, Oni T, Rangaka MX, et al. Changing prevalence of TB infection with increasing age in high TB burden townships in South Africa. *Int J Tuberc Lung Dis* (2010) 14:406–12.
46. Yates TA, Khan PY, Knight GM, Taylor JG, McHugh TD, Lipman M, et al. The transmission of Mycobacterium tuberculosis in high burden settings. *Lancet Infect Dis* (2016) 16:227–38. doi: 10.1016/S1473-3099(15)00499-5
47. Crampin AC, Mwaungulu JN, Mwaungulu FD, Mwafulirwa DT, Munthali K, Floyd S, et al. Recurrent TB: relapse or reinfection? The effect of HIV in a general population cohort in Malawi. *AIDS* (2010) 24:417–26. doi: 10.1097/QAD.0b013e32832f51cf
48. Houben RMGJ, Crampin AC, Ndhlovu R, Sonnenberg P, Godfrey-Faussett P, Haas WH, et al. Human immunodeficiency virus associated tuberculosis more often due to recent infection than reactivation of latent infection [Review article]. *Int J Tuberc Lung Dis* (2011) 15:24–31.
49. Sonnenberg P, Murray J, Glynn JR, Shearer S, Kambashi B, Godfrey-Faussett P. HIV-1 and recurrence, relapse, and reinfection of tuberculosis after cure: a cohort study in South African mineworkers. *Lancet* (2001) 358:1687–93. doi: 10.1016/S0140-6736(01)06712-5
50. Andrews JR, Morrow C, Walensky RP, Wood R. Integrating social contact and environmental data in evaluating tuberculosis transmission in a South African township. *J Infect Dis* (2014) 210:597–603. doi: 10.1093/infdis/jiu138
51. Marais BJ, Hesseling AC, Schaaf HS, Gie RP, van Helden PD, Warren RM. Mycobacterium tuberculosis Transmission Is Not Related to Household Genotype in a Setting of High Endemicity. *J Clin Microbiol* (2009) 47:1338–43. doi: 10.1128/JCM.02490-08
52. Marais BJ, Victor TC, Hesseling AC, Barnard M, Jordaan A, Brittle W, et al. Beijing and Haarlem Genotypes Are Overrepresented among Children with Drug-Resistant Tuberculosis in the Western Cape Province of South Africa. *J Clin Microbiol* (2006) 44:3539–43. doi: 10.1128/JCM.01291-06
53. Zelner JL, Murray MB, Becerra MC, Galea J, Lecca L, Calderon R, et al. Age-specific risks of tuberculosis infection from household and community exposures and opportunities for interventions in a high-burden setting. *Am J Epidemiol* (2014) 180(8):853–61. doi: 10.1093/aje/kwu192
54. Middelkoop K, Mathema B, Myer L, Shashkina E, Whitelaw A, Kaplan G, et al. Transmission of Tuberculosis in a South African Community With a High Prevalence of HIV Infection. *J Infect Dis* (2015) 211:53–61. doi: 10.1093/infdis/jiu403
55. Middelkoop K, Bekker L-G, Myer L, Dawson R, Wood R. Rates of tuberculosis transmission to children and adolescents in a community with a high prevalence of HIV infection among adults. *Clin Infect Dis* (2008) 47(3):349–55. doi: 10.1086/589750
56. Andrews JR, Hatherill M, Mahomed H, Hanekom WA, Campo M, Hawn TR, et al. The Dynamics of QuantiFERON-TB Gold In-Tube Conversion and Reversion in a Cohort of South African Adolescents. *Am J Respir Crit Care Med* (2015) 191:584–91. doi: 10.1164/rccm.201409-1704OC
57. Mahomed H, Hawkridge T, Verver S, Abrahams D, Geiter L, Hatherill M, et al. The tuberculin skin test versus QuantiFERON TB Gold® in predicting tuberculosis disease in an adolescent cohort study in South Africa. *PloS One* (2011) 6:e17984. doi: 10.1371/journal.pone.0017984
58. Mahomed H, Ehrlich R, Hawkridge T, Hatherill M, Geiter L, Kafaar F, et al. Screening for TB in high school adolescents in a high burden setting in South Africa. *Tuberc (Edinb)* (2013) 93:357–62. doi: 10.1016/j.tube.2013.02.007
59. Hanifa Y, Grant AD, Lewis J, Corbett EL, Fielding K, Churchyard G. Prevalence of latent tuberculosis infection among gold miners in South Africa. *Int J Tuberc Lung Dis* (2009) 13:39–46.
60. Vynnycky E, Sumner T, Fielding KL, Lewis JJ, Cox AP, Hayes RJ, et al. Tuberculosis Control in South African Gold Mines: Mathematical Modeling of a Trial of Community-Wide Isoniazid Preventive Therapy. *Am J Epidemiol* (2015) 181:619–32. doi: 10.1093/aje/kwu320
61. Wallis RS. Mathematical Models of Tuberculosis Reactivation and Relapse. *Front Microbiol* (2016) 7:669. doi: 10.3389/fmicb.2016.00669
62. Morrison J, Pai M, Hopewell PC. Tuberculosis and latent tuberculosis infection in close contacts of people with pulmonary tuberculosis in low-income and middle-income countries: a systematic review and meta-analysis. *Lancet Infect Dis* (2008) 8:359–68. doi: 10.1016/S1473-3099(08)70071-9
63. Behr MA, Edelstein PH, Ramakrishnan L. Is Mycobacterium tuberculosis infection life long? *BMJ* (2019) 367:l5770. doi: 10.1136/bmj.l5770

64. Houk VN, Kent DC, Sorensen K, Baker JH. The eradication of tuberculosis infection by isoniazid chemoprophylaxis. *Arch Environ Health* (1968) 16:46–50. doi: 10.1080/00039896.1968.10665013
65. Menzies D. Interpretation of repeated tuberculin tests. Boosting, conversion, and reversion. *Am J Respir Crit Care Med* (1999) 159:15–21. doi: 10.1164/ajrccm.159.1.9801120
66. Sepulveda RL, Araya D, Ferrer X, Sorensen RU. Repeated tuberculin testing in patients with active pulmonary tuberculosis. *Chest* (1993) 103:359–63. doi: 10.1378/chest.103.2.359
67. Rangaka MX, Wilkinson KA, Glynn JR, Ling D, Menzies D, Mwansa-Kambafwile J, et al. Predictive value of interferon-γ release assays for incident active tuberculosis: a systematic review and meta-analysis. *Lancet Infect Dis* (2012) 12:45–55. doi: 10.1016/S1473-3099(11)70210-9
68. Package Inserts QFT-Plus – QuantiFERON. Available at: https://www.quantiferon.com/products/quantiferon-tb-gold-plus-qft-plus/package-inserts/ (Accessed January 29, 2020).
69. Shafeque A, Bigio J, Hogan CA, Pai M, Banaei N. Fourth generation QuantiFERON-TB Gold-Plus: What is the evidence? *J Clin Microbiol* (2020) 58(9):e01950–19. doi: 10.1128/JCM.01950-19
70. Barcellini L, Borroni E, Brown J, Brunetti E, Campisi D, Castellotti PF, et al. First evaluation of QuantiFERON-TB Gold Plus performance in contact screening. *Eur Respir J* (2016) 48:1411–9. doi: 10.1183/13993003.00510-2016
71. Takasaki J, Manabe T, Morino E, Muto Y, Hashimoto M, Iikura M, et al. Sensitivity and specificity of QuantiFERON-TB Gold Plus compared with QuantiFERON-TB Gold In-Tube and T-SPOT.TB on active tuberculosis in Japan. *J Infect Chemother* (2018) 24:188–92. doi: 10.1016/j.jiac.2017.10.009
72. Venkatappa TK, Punnoose R, Katz DJ, Higgins MP, Banaei N, Graviss EA, et al. Comparing QuantiFERON-TB Gold Plus with Other Tests To Diagnose Mycobacterium tuberculosis Infection. *J Clin Microbiol* (2019) 57:e00985–19. doi: 10.1128/JCM.00985-19
73. Zhang H, Xin H, Wang D, Pan S, Liu Z, Cao X, et al. Serial testing of Mycobacterium tuberculosis infection in Chinese village doctors by QuantiFERON-TB Gold Plus, QuantiFERON-TB Gold in-Tube and T-SPOT.TB. *J Infect* (2019) 78:305–10. doi: 10.1016/j.jinf.2019.01.008
74. Hoffmann H, Avsar K, Göres R, Mavi S-C, Hofmann-Thiel S. Equal sensitivity of the new generation QuantiFERON-TB Gold plus in direct comparison with the previous test version QuantiFERON-TB Gold IT. *Clin Microbiol Infect* (2016) 22:701–3. doi: 10.1016/j.cmi.2016.05.006
75. Petruccioli E, Chiacchio T, Pepponi I, Vanini V, Urso R, Cuzzi G, et al. First characterization of the CD4 and CD8 T-cell responses to QuantiFERON-TB Plus. *J Infect* (2016) 73:588–97. doi: 10.1016/j.jinf.2016.09.008
76. Siegel SAR, Cavanaugh M, Ku JH, Kawamura LM, Winthrop KL. Specificity of QuantiFERON-TB Plus, a New-Generation Interferon Gamma Release Assay. *J Clin Microbiol* (2018) 56(12):e00629–18. doi: 10.1128/JCM.00629-18
77. Wang L, Tian X-D, Yu Y, Chen W. Evaluation of the performance of two tuberculosis interferon gamma release assays (IGRA-ELISA and T-SPOT.TB) for diagnosing Mycobacterium tuberculosis infection. *Clin Chim Acta* (2018) 479:74–8. doi: 10.1016/j.cca.2018.01.014
78. Telisinghe L, Amofa-Sekyi M, Maluzi K, Kaluba-Milimo D, Cheeba-Lengwe M, Chiwele K, et al. The sensitivity of the QuantiFERON®-TB Gold Plus assay in Zambian adults with active tuberculosis. *Int J Tuberc Lung Dis* (2017) 21:690–6. doi: 10.5588/ijtld.16.0764
79. König Walles J, Tesfaye F, Jansson M, Tolera Balcha T, Winqvist N, Kefeni M, et al. Performance of QuantiFERON-TB Gold Plus for detection of latent tuberculosis infection in pregnant women living in a tuberculosis- and HIV-endemic setting. *PloS One* (2018) 13:e0193589. doi: 10.1371/journal.pone.0193589
80. van Zyl-Smit RN, Zwerling A, Dheda K, Pai M. Within-Subject Variability of Interferon-g Assay Results for Tuberculosis and Boosting Effect of Tuberculin Skin Testing: A Systematic Review. *PloS One* (2009) 4:e8517. doi: 10.1371/journal.pone.0008517
81. Lindsay RP, Shin SS, Garfein RS, Rusch MLA, Novotny TE. The Association between active and passive smoking and latent tuberculosis infection in adults and children in the united states: results from NHANES. *PloS One* (2014) 9:e93137. doi: 10.1371/journal.pone.0093137
82. Lee M-R, Huang Y-P, Kuo Y-T, Luo C-H, Shih Y-J, Shu C-C, et al. Diabetes Mellitus and Latent Tuberculosis Infection: A Systematic Review and Metaanalysis. *Clin Infect Dis* (2017) 64:719–27. doi: 10.1093/cid/ciw836
83. Lin H-H, Wu C-Y, Wang C-H, Fu H, Lönnroth K, Chang Y-C, et al. Association of Obesity, Diabetes, and Risk of Tuberculosis: Two Population-Based Cohorts. *Clin Infect Dis* (2018) 66:699–705. doi: 10.1093/cid/cix852
84. Lin C-H, Kuo S-C, Hsieh M-C, Ho S-Y, Su I-J, Lin S-H, et al. Effect of diabetes mellitus on risk of latent TB infection in a high TB incidence area: a community-based study in Taiwan. *BMJ Open* (2019) 9:e029948. doi: 10.1136/bmjopen-2019-029948
85. Igo RP, Hall NB, Malone LL, Hall JB, Truitt B, Qiu F, et al. Fine-mapping Analysis of a Chromosome 2 Region Linked to Resistance to Mycobacterium tuberculosis Infection in Uganda Reveals Potential Regulatory Variants. *Genes Immun* (2019) 20:473–83. doi: 10.1038/s41435-018-0040-1
86. Cubilla-Batista I, Ruiz N, Sambrano D, Castillo J, de Quinzada MO, Gasteluiturri B, et al. Overweight, Obesity, and Older Age Favor Latent Tuberculosis Infection among Household Contacts in Low Tuberculosis-Incidence Settings within Panama. *Am J Trop Med Hyg* (2019) 100:1141–4. doi: 10.4269/ajtmh.18-0927
87. Ewer K, Millington KA, Deeks JJ, Alvarez L, Bryant G, Lalvani A. Dynamic antigen-specific T-cell responses after point-source exposure to Mycobacterium tuberculosis. *Am J Respir Crit Care Med* (2006) 174:831–9. doi: 10.1164/rccm.200511-1783OC
88. Wiens KE, Woyczynski LP, Ledesma JR, Ross JM, Zenteno-Cuevas R, Goodridge A, et al. Global variation in bacterial strains that cause tuberculosis disease: a systematic review and meta-analysis. *BMC Med* (2018) 16:196. doi: 10.1186/s12916-018-1180-x
89. Verrall AJ. *Innate Factors in Early Clearance of Mycobacterium tuberculosis* (2018). Available at: https://ourarchive.otago.ac.nz/handle/10523/7999 (Accessed December 10, 2020).
90. Heimbeck J. Incidence of tuberculosis in young adult women, with special reference to employment. *Br J Tuberc* (1938) 32:154–66. doi: 10.1016/S0366-0850(38)80144-7
91. Israel HL, Hetherington HW. Ord JG. A study of tuberculosis among students of nursing. *JAMA* (1941) 117:839–44. doi: 10.1001/jama.1941.02820360021007
92. Lalvani A, Seshadri C. Understanding How BCG Vaccine Protects Against Mycobacterium tuberculosis Infection: Lessons From Household Contact Studies. *J Infect Dis* (2020) 221:1229–31. doi: 10.1093/infdis/jiz261

Conflict of Interest: The authors declare that the research was conducted in the absence of any commercial or financial relationships that could be construed as a potential conflict of interest.

Copyright © 2021 Gutierrez, Kroon, Möller and Stein. This is an open-access article distributed under the terms of the Creative Commons Attribution License (CC BY). The use, distribution or reproduction in other forums is permitted, provided the original author(s) and the copyright owner(s) are credited and that the original publication in this journal is cited, in accordance with accepted academic practice. No use, distribution or reproduction is permitted which does not comply with these terms.

frontiers in Immunology

ORIGINAL RESEARCH
published: 25 February 2021
doi: 10.3389/fimmu.2021.639965

Inflammatory Determinants of Differential Tuberculosis Risk in Pre-Adolescent Children and Young Adults

Richard Baguma[1†], Stanley Kimbung Mbandi[1†], Miguel J. Rodo[1], Mzwandile Erasmus[1], Jonathan Day[1], Lebohang Makhethe[1], Marwou de Kock[1], Michele van Rooyen[1], Lynnett Stone[1], Nicole Bilek[1], Marcia Steyn[1], Hadn Africa[1], Fatoumatta Darboe[1], Novel N. Chegou[2], Gerard Tromp[2], Gerhard Walzl[2], Mark Hatherill[1], Adam Penn-Nicholson[1] and Thomas J. Scriba[1]*

[1] South African Tuberculosis Vaccine Initiative (SATVI), Department of Pathology, Institute of Infectious Disease and Molecular Medicine and Division of Immunology, University of Cape Town, Cape Town, South Africa, [2] DST-NRF Centre of Excellence for Biomedical Tuberculosis Research, South African Medical Research Council Centre for Tuberculosis Research, Division of Molecular Biology and Human Genetics, Department of Biomedical Sciences, Faculty of Medicine and Health Sciences, Stellenbosch University, Cape Town, South Africa

OPEN ACCESS

Edited by:
Cecilia Lindestam Arlehamn, La Jolla Institute for Immunology (LJI), United States

Reviewed by:
Keith Kauffman, National Institutes of Health (NIH), United States
Paul Ogongo, Institute of Primate Research, Kenya

***Correspondence:**
Thomas J. Scriba
thomas.scriba@uct.ac.za

[†]These authors have contributed equally to this work

Specialty section:
This article was submitted to Microbial Immunology, a section of the journal Frontiers in Immunology

Received: 10 December 2020
Accepted: 14 January 2021
Published: 25 February 2021

Citation:
Baguma R, Mbandi SK, Rodo MJ, Erasmus M, Day J, Makhethe L, de Kock M, van Rooyen M, Stone L, Bilek N, Steyn M, Africa H, Darboe F, Chegou NN, Tromp G, Walzl G, Hatherill M, Penn-Nicholson A and Scriba TJ (2021) Inflammatory Determinants of Differential Tuberculosis Risk in Pre-Adolescent Children and Young Adults. Front. Immunol. 12:639965. doi: 10.3389/fimmu.2021.639965

The risk of progression from *Mycobacterium tuberculosis* (*M.tb*) infection to active tuberculosis (TB) disease varies markedly with age. TB disease is significantly less likely in pre-adolescent children above 4 years of age than in very young children or post-pubescent adolescents and young adults. We hypothesized that pro-inflammatory responses to *M.tb* in pre-adolescent children are either less pronounced or more regulated, than in young adults. Inflammatory and antimicrobial mediators, measured by microfluidic RT-qPCR and protein bead arrays, or by analyzing published microarray data from TB patients and controls, were compared in pre-adolescent children and adults. Multivariate analysis revealed that *M.tb*-uninfected 8-year-old children had lower levels of myeloid-associated pro-inflammatory mediators than uninfected 18-year-old young adults. Relative to uninfected children, those with *M.tb*-infection had higher levels of similar myeloid inflammatory responses. These inflammatory mediators were also expressed after *in vitro* stimulation of whole blood from uninfected children with live *M.tb*. Our findings suggest that myeloid inflammation is intrinsically lower in pre-pubescent children than in young adults. The lower or more regulated pro-inflammatory responses may play a role in the lower risk of TB disease in this age group.

Keywords: inflammation, tuberculosis, anti-mycobacterial immunity, age, pediatric

INTRODUCTION

Infection with *Mycobacterium tuberculosis (M.tb)* predisposes to pulmonary tuberculosis (TB) disease, which kills more people than any other infectious agent (1). The risk of progression from infection to disease varies markedly with age. Infants and young children are at very high risk of TB disease following infection. However, pre-adolescent children above 4 years of age, in the so-called

"Golden Age" or "Wonder Years" (2), are curiously at significantly lower risk of active TB disease compared with post-pubescent adolescents and young adults (3–5). Upon first thought this pattern may be interpreted to follow the prevalence of underlying *M.tb* infection, which increases with age during childhood in settings endemic for TB (6). However, the dramatic increase in TB disease risk during puberty cannot be sufficiently explained by changes in *M.tb* infection incidence, which appears to increase only marginally during the same period (2). The clinical presentation of TB is also different by age. TB typically manifests as mild and/or pauci-bacillary lymph node disease in pre-adolescent children of the Golden Age (3–5). By contrast, post-pubescent adolescents and adults more commonly present with multi-bacillary, "adult-type" pulmonary disease with more pronounced immunopathology, including cavitary disease (2–5). These phenomena have led us (7) and others (2) to surmise that pre-pubescent children have more effective or successful immunity against *M.tb* and that the onset of puberty coincides with or brings about immunological changes that result in less successful control of the infection.

The determinants of effective immune control of *M.tb* in humans are thought to be dependent on a complex collaboration of multiple adaptive and innate immune responses that must be maintained in a manner that balances pro- and anti-inflammatory responses (8, 9). Although intact antigen-specific T cell responses of the Th1 lineage are necessary for host resistance against TB, based on current evidence from humans the magnitude or functional characteristics of such Th1 responses are not associated with clinical outcome of *M.tb* infection [reviewed in (10)]. However, mounting evidence suggests that excessive skewing of the inflammatory milieu towards either a pro-inflammatory or an anti-inflammatory response can lead to a loss of immunological control of *M.tb* and TB disease progression (11). For example, dysregulated TNF responses in mycobacterial infection have been associated with detrimental outcome of TB in zebrafish and humans (12). Furthermore, upregulation of Type I IFN responses during murine influenza infection impairs control of subsequent *M.tb* challenge (13). Elevated Type I/II IFN is also measured as a blood biomarker of incipient or subclinical TB disease in *M.tb*-infected humans, and blood transcriptomic signatures that detect such Type I/II IFN responses can be used to identify individuals at high risk of incident TB (14–17). Conversely, peripheral blood neutrophil count has been inversely associated with risk of TB and this neutrophil-mediated bacterial control was dependent on the neutrophil peptides, cathelicidin LL-37 and lipocalin-2 (18).

The low risk of TB in pre-adolescent children presents an opportunity to study natural resistance and/or characteristics of successful immunity to *M.tb* in humans. We previously characterized frequencies and functions of antigen-specific T cell responses in pre-adolescent children and young adults and observed no differences (7). We also measured mycobacterial growth inhibition in whole blood from pre-adolescent children and young adults as an *in vitro* surrogate of differential immunological control of *M.tb*, but also observed no significant differences between these age groups (7).

Here, we hypothesized that pro-inflammatory responses to *M.tb* in pre-adolescent children are either less pronounced or more regulated, than in young adults.

We compared blood gene expression of antimicrobial effector molecules, pro- and anti-inflammatory and other immune mediators as well as soluble host-derived inflammatory molecules in healthy *M.tb*-infected or uninfected 8-year-old children and 18-year-old young adults. Our analyses reveal that uninfected 8-year-old children had lower levels of myeloid-associated pro-inflammatory mediators than uninfected 18-year-old young adults. Relative to uninfected children, those with *M.tb*-infection had higher levels of similar myeloid inflammatory responses. These inflammatory mediators were also expressed after *in vitro* stimulation of whole blood from uninfected 8-year-old children with live *M.tb*.

MATERIALS AND METHODS

Ethics Statement

Participants were recruited under protocols approved by the University of Cape Town Human Research Ethics Committee. Written informed consent was obtained from adults prior to enrolment. Children provided written informed assent while their legal guardians provided written informed consent prior to enrollment.

Study Design and Participants

This was a cross-sectional study comprising two cohorts of healthy, HIV-negative participants from the Worcester region in the Western Cape Province of South Africa, a setting with high burden of TB. Individuals with any acute or chronic disease, those taking immunosuppressive medication, with a previous diagnosis of active TB disease or who currently or previously participated in a TB vaccine trial, were excluded. Women who were pregnant or lactating were also excluded from participation. We aimed to enroll young adults aged 18 years and 8-year-old children with equal numbers of *M.tb*-infected and uninfected participants in each age group. *M.tb*-infection status was assessed with the QuantiFERON-TB Gold In-Tube Assay (QFT) (Qiagen), according to the manufacturer's instructions. HIV infection was diagnosed by rapid HIV-antibody test. Some aspects of these cohorts have been described before (7).

Venous blood was collected from participants directly into QFT tubes, into sodium heparin tubes for whole blood stimulation assays and into Cell Preparation Tubes (CPT) for isolation of peripheral blood mononuclear cells (PBMC).

We also analyzed two whole blood microarray datasets from children and adults with microbiologically-confirmed TB or latent *M.tb* infection (LTBI controls), published previously (19, 20). Datasets were sourced from the NCBI database Gene Expression Omnibus (GEO); analyses are described further below.

Mycobacterial Strains and Whole Blood Stimulations

Three mycobacterial strains (*M.tb* H37Rv, *M.tb* HN878 and *M.tb* CDC1551), selected to encompass a range of virulence and

inflammation-inducing *M.tb* strains, with HN878 known to be more virulent than *M.tb* H37Rv and *M.tb* CDC1551 (21, 22), were separately added to Sarstedt tubes containing 300 µl RPMI at volumes equating to 5 x 10^5 colony forming units [CFU]/ml inocula. 300 µl fresh heparinized whole blood was added and the tubes were incubated for 12 h at 37°C with slow constant rotation. Bacilli were sedimented at 208 x g for 10 min. The supernatants were aspirated and filtered through a 0.22 µm (pore-size) Costar® Spin-X® centrifuge tube filter (Corning, USA) for 2 min at 14,000 x g before storing at -80°C for later measurement of soluble host marker levels.

Peripheral Blood Mononuclear Cells Culture

Cryopreserved PBMC were thawed into medium containing DNase (50 IU/ml, Sigma-Aldrich), cell viability assessed, counted and plated out at 1 x 10^6 cells/well in RPMI 1640 media with 10% human AB serum (Sigma-Aldrich). Following overnight rest at 37°C, 5% CO_2, PBMC were then lysed and homogenized with 350 µl/well of Buffer RLT Plus (Qiagen, USA) and stored at -80°C for later RNA isolation.

RNA Extraction, Reverse transcription, and Specific Target/Transcript Amplification

RNA was extracted from PBMC lysates using the RNeasy Plus Micro kit for purification of total RNA from animal cells (Qiagen, Valencia, CA) according to the manufacturer's instructions. RNA yield and purity were determined using a Nano Drop ND 2000 spectrophotometer (Thermo Scientific, Waltham, MA).

Reverse transcription was performed using 100 ng of purified total RNA in a 20 µl reaction volume containing 1 µl 10mM dNTP (Sigma-Aldrich, USA), 1 µl Oligo$(dT)_{12-18}$ (Sigma-Aldrich, USA), 4 µl 5X First-Strand Buffer (Invitrogen, USA), 2 µl 0.1M DTT (Invitrogen, USA), 0.5 µl RNaseOUT™ (40 U/µl) (Invitrogen, USA), 0.5 µl sterile endotoxin free water (dH_20) and 1 µl SuperScript™ III Reverse Transcriptase (200 units) (Invitrogen, USA), according to the manufacturer's instructions. cDNA was then diluted 1:5 with dH_20.

The protocol for microfluidic RT-qPCR has been previously described (16, 23). In order to increase the number of cDNA templates for downstream microfluidic RT-qPCR where the cDNA is dispensed into 96 nanowells, a pre-amplification PCR was performed at 10 µl containing 5 µl of 2X TaqMan PreAmp Master Mix (Thermo Fisher Scientific, USA), 2.5 µl of 0.2X 96-pooled TaqMan Gene Expression (GE) assay (Thermo Fisher Scientific, USA) mix and 2.5 µl of 1:5 diluted cDNA using the following thermal profile: one cycle at 95°C for 10 min, followed by 16 cycles of 95°C for 15 s and 60°C for 4 min. Pre-amplification products were diluted 1:25 with dH_20 and stored at -80°C until needed.

Confirmation of successful pre-amplification was done on a Rotor-Gene 6000 RT-PCR

instrument (Corbett Life Science) in a 20 µl reaction volume consisting of 10 µl of 2X TaqMan Universal PCR Master Mix, 1 µl of 20X select TaqMan GE assay and 4 µl of 1:25 diluted pre-amplified cDNA made up to a final volume of 20 µl with dH_20. The cycling program consisted of a 2 min incubation at 50°C, a 10 min incubation at 95°C, followed by 40 cycles of 95°C for 15 s and 60°C for 1 min.

High-Throughput Microfluidic RT-qPCR

We selected a total of 87 genes based on broad relevance to inflammation, immunopathology, antimycobacterial response, type I IFN response, immune regulation as well as risk for TB (see **Table S1** in **Supplementary Material**). Expression levels of these genes were measured using the previously described high-throughput microfluidic 96.96 Dynamic Array and BioMark™ HD instrument (Fluidigm, USA) (24). Specifically, a 5 µl sample mix was prepared for each sample containing 2.5 µl of 2X TaqMan Universal PCR Master Mix (Applied Biosystems, PN 4304437), 0.25 µl of 20X GE Sample Loading Reagent (Fluidigm PN 85000746) and 2.25 µl of pre-amplified cDNA (diluted 1:25). 5 µl of assay mix was prepared with 2.5 µl of each 20X TaqMan GE Assay (Thermo Fisher Scientific, USA) and 2.5 µl of 2X Assay Loading Reagent (Fluidigm PN 85000736). An IFC Controller HX (Fluidigm, USA) was used to prime the Dynamic Array™ (chip) with control line fluid and before loading the sample and assay mixes into their appropriate inlets. The chip was subsequently returned to the IFC Controller HX for loading and mixing. After approximately 60 min, the chip was transferred to the BioMark™ HD instrument for RT-qPCR according to the manufacturer's protocol.

Luminex Multiplex Immunoassay

The concentrations of 24 soluble host-derived markers were considered for measurement in supernatants from the 12 h cultures (*see above*) using MILLIPLEX® MAP kits (Millipore, Billerica, MA). These markers were selected for potential relevance as essential role players in the inflammatory processes likely to be affiliated with age-associated differential risk of TB. These markers were analyzed in 15-plex (TNF-α, MIP-1α, MIP-1β, MCP-1, IL-10, IL-1α, IL-1RA, sCD40L, Fractalkine, IFN-γ, IFN-α2, IP-10, IL-4, IL-15 and VEGF), 5-plex (MMP-1, MMP-2, MMP-7, MMP-9, and MMP-10), 1-plex (D-dimer), and 3-plex (CRP, Fibrinogen, and SAP) assays in 1:2, 1:100, 1:100, and 1:20,000 dilutions, respectively. IL-4, IL-15, MMP-7, and MMP-10 were not detectable and were thus omitted from further evaluation. For samples in which marker concentrations were extrapolated and/or were above the Upper Limit of Quantitation (ULOQ) or below the Lower Limit of Quantitation (LLOQ), readings were assigned values calculated as follows:

i. <OOR (reading below LLOQ) = {value of lowest standard X dilution factor}
ii. OOR> (reading above ULOQ) = {highest standard X dilution factor} + 50

Internal controls were included throughout each run. In summary, following pre-wetting of the filter plates with 200 µl of wash buffer, 25 µl of standards, controls and diluted samples

were added to each well containing 25 µl of assay buffer. Pre-combined beads of all the 24 individual markers were added to all wells before incubating sealed plates with agitation for 1 h in the dark at room temperature. The plates were washed twice and 25 µl of detection antibody was added, and the sealed plates incubated with agitation for 30 min. Streptavidin-Phycoerythrin (25 µl per well) was added and incubated for 10 min. Plates were washed twice and 150 µl of sheath fluid was added to each well. The beads were re-suspended by agitation for 5 min before running the plates on a Bio Plex 200 instrument (Bio Rad Laboratories, Hercules, CA, USA). Data were acquired and analyzed using the Bio Plex Manager 6.1 Software (Bio Rad).

Statistical Analysis

All appropriate descriptive statistics applied to RT-qPCR and Luminex data were performed using R for statistical computing (25) or PRISM (GraphPad Software v8, San Diego, Calif.).

Previously published microarray data from children aged 4–12 years and adults with microbiologically-confirmed TB or LTBI controls were processed in the same facility and run on Illumina HT12 beadarrays: GSE39940 and GSE37250 (19, 20). Each array was separately renormalized *via* normal-exponential background correction followed by quantile normalization and $\log_2$-transformation. In order to reduce the potential influence of batch effects, we applied surrogate variable analysis implemented in the R package sva (26). The demographic and phenotypic annotation reported by the original authors were used to subset the samples into HIV negative children aged 4 to 12 years and adults, sensitized to *M.tb* (*M.tb* infected controls) and those with microbiologically-confirmed TB disease (see **Table S2** in **Supplementary Material**). Discrimination between TB and *M.tb* infected controls by the Sweeney3 and RISK6 signatures was done using signature scores generated as previously described (16, 27, 28). For the Sweeney3 signature (27), scores were computed for each sample by subtracting the geometric mean of GBP5 and DUSP3 from the geometric mean of KLF2 in R as implemented in MetaIntegrator package (29) on the gene-level expression data. Changes in cell subset proportions were performed with immunoStates (30).

Linear models were fitted with R/Bioconductor *limma* package (31) to extract the age effect on genes differentially expressed in TB disease between pre-adolescents and adults. Genes were considered differentially expressed with false discovery rate (FDR)-adjusted at 1% with at least an absolute $\log_2$-fold change of 0.5. Genes were tested for enrichment using blood transcriptional modules (BTMs) developed by Chaussabel and co-workers (32) within the tmod R package (33) and the CERNO statistical test was applied on the genes ordered by minimum significant difference that uses combination of effect size and statistical significance.

Microfluidic RT-qPCR data were analyzed using the BioMark™ Real-Time PCR Analysis Software in the BioMark™ HD instrument (Fluidigm, CA) to obtain threshold cycle (Ct) values. Analysis settings were as follows: amplification curve quality threshold was set to 0.65, baseline correction to linear (derivative) and Ct threshold method to auto (global). For ease of interpretation, Ct values were transformed to Et values (40 − Ct), because a higher Et value indicates higher mRNA levels. Results were presented as changes in relative mRNA transcript expression normalized with the geometric mean of the Et values of the reference genes (34). TB risk signature scores were calculated as previously described (28). P values were adjusted to account for multiple comparisons. The method for each analysis is indicated in the *Figure Legends*.

Comparison of soluble host-derived markers was assessed using the non-parametric Mann-Whitney U and Wilcoxon matched-pairs signed-rank tests to determine differences between groups (18 compared to 8 year olds and *M.tb*-infected (QFT+) compared to uninfected (QFT-) individuals) and within groups (*M.tb* H37Rv, *M.tb* HN878 and *M.tb* CDC1551-stimulated samples) respectively. Unstimulated values were considered as background and subtracted from the *M.tb* stimulated values before further analysis. Soluble host-derived marker median concentration point estimates and 95% confidence intervals of the differences between groups were calculated using the rank inversion method and bootstrapping 2000X using the quantreg package in R (35). To visualize the groups of participants and groups of markers with similar expression profiles, unsupervised hierarchical clustering (i.e. heatmaps) was performed using factoextra (36), FactoMineR (37) and ComplexHeatmap (38) packages, respectively in R (25). P values were adjusted to account for multiple comparisons. The method for each analysis is indicated in the *Figure Legends*.

Data from all enrolled participants including microfluidic RT-qPCR and soluble host-derived markers are available on FigShare (https://doi.org/10.25375/uct.13351466.v1).

RESULTS

Study Participants

In total, 117 healthy participants were enrolled into the two cohorts of this study: 53 children aged 8 years, and 64 young adults aged 18 years. Participants in each age group were approximately equally stratified according to *M.tb* infection status by QFT, which shows excellent agreement with tuberculin skin test (TST) in this setting (39, 40). The demographic characteristics of the study participants are summarized in **Table 1**.

Performance of Blood Transcriptomic TB Signatures in Pre-Adolescent Children and Adults

We first sought to compare the diagnostic performance of Sweeney3, a concise and well-validated blood transcriptomic signature of TB disease (41), that was shown to correlate with the severity of lung inflammation in TB patients (42), in pre-adolescent children and adults. Re-analysis of public whole blood microarray datasets from culture-confirmed TB cases and asymptomatic *M.tb*-infected controls showed that discrimination between TB and controls by Sweeney3 was significantly poorer in pre-adolescent children (AUC 0.84, 95%CI 0.74–0.95), than in adults (AUC 0.97, 95%CI 0.94–0.99, p = 0.03, **Figure 1A**). These data suggest that pre-adolescent children with TB may present with

TABLE 1 | Summary of demographic characteristics of study participants.

	Children		Young adults	
	QFT+	QFT-	QFT+	QFT-
Participants, n	25	28	39	25
Female, n (%)	11 (44)	15 (54)	22 (56)	13 (52)
Ethnicity, n (%)				
Black African	0 (0)	3 (11)	18 (46)	6 (24)
Mixed race	25 (100)	25 (89)	21 (54)	18 (72)
Caucasian	0 (0)	0 (0)	0 (0)	1 (4)

less pronounced inflammation than adult TB cases and motivated further investigation of inflammation as a determinant of age-associated differential risk for TB in healthy individuals. We therefore determined whether signature scores of a recently described parsimonious blood transcriptomic signature of TB risk, RISK6 (28), were different in healthy pre-adolescent vs young adults. We previously showed that RISK6 scores were associated with *in vivo* pulmonary inflammation measured by ^{18}F-labeled fluorodeoxyglucose (^{18}F FDG) PET-CT in TB patients (28). RISK6 scores, measured by microfluidic RT-qPCR, were significantly higher in 18-year-old young adults than in 8-year-old children (**Figure 1B**). This difference seemed to be primarily driven by persons with underlying *M.tb* infection, since RISK6 scores were only significantly higher in QFT+ adults than in QFT+ children; no difference was observed in the corresponding QFT- groups (**Figure 1C**).

Expression of Neutrophil Antimicrobial Effectors in Pre-Adolescent Children and Adults

Higher expression of RISK6 in QFT+ adults prompted us to investigate if other mediators of inflammation or antimicrobial responses with a known role in immunity to *M.tb* may also be elevated in this group; we therefore quantified transcript expression by microfluidic RT-qPCR in PBMC from the different participant groups. mRNA expression of the antimicrobial mediators, cathelicidin (CAMP), defensin A1 (DEFA1), human neutrophil peptide 3 (HNP3) and the IFN-inducible immunity-related p47 GTPase IRGM1, were significantly elevated in QFT+ young adults, compared with QFT+ children (**Figure 1D**). A similar picture was observed for the chemokine, CCL5 (encoding RANTES) and the chemokine receptor, CXCR3 (**Figure 1E**). We also compared mRNA expression of these and other genes in QFT- young adults and children, but did not observe such differences (**Supplementary Figure 1**).

Elevated Myeloid Inflammation in Adults Relative to Pre-Adolescent Children

To determine if the inflammatory signals observed by blood mRNA expression profiling were also detectable at the protein level, we measured concentrations of myeloid inflammatory mediators, acute phase proteins and matrix metalloproteinases in plasma from unstimulated blood by Luminex assay. Unsupervised hierarchical clustering of plasma samples based on levels of 20 soluble markers revealed two major sample clusters. The cluster with higher expression of many markers, relative to the other cluster, was significantly enriched for adult samples (Fisher exact, p = 0.0005, **Figure 2A**). When analyzed on a univariate level, concentrations of the myeloid inflammatory mediators, TNF, MIP-1α, MIP-1β, MCP-1, and IL-10, as well as the angiogenic factor, vascular endothelial growth factor (VEGF), were significantly elevated in plasma from QFT- 18-year-old young adults compared with QFT- 8-year-old children (**Figure 2A**). By contrast, MMP-2 was lower whereas IFN-γ, IFN-α2, acute phase proteins D-dimer, serum amyloid protein (SAP) and C-reactive protein (CRP) and the matrix metalloproteinases MMP-1 and MMP-9 were not different. A similar assessment performed for QFT+ 18-year-old adults compared with QFT+ 8-year-old children revealed far fewer differences (**Supplementary Figure 2A**). In light of observing elevated myeloid inflammatory mediators in QFT- adults, we again turned to the public microarray datasets from TB cases and asymptomatic *M.tb*-infected controls to assess whether differential expression of gene modules associated with TB may reveal further biological differences between 4–12-year-old pre-adolescent children and adults. As previously reported (44), many gene modules were differentially expressed between TB cases and LTBI controls, including elevated expression of inflammation, interferon response and myeloid cell subset modules, and lower expression of lymphoid cell (T, B and NK) subset modules in TB (**Figure 2B**). By analyzing age as an interaction term, we detected age-associated differences within the TB vs control comparison. Genes within the mitochondrial respiration, monocyte and interferon modules were more elevated in adults than in pre-adolescent children (**Figure 2B**), again suggesting that myeloid inflammatory mediators were more pronounced in adult TB than in pediatric TB. This difference in the myeloid cell subset was confirmed with the recently published immunoStates computational approach (30) to infer leukocyte representations from gene expression profiles, which also showed that monocytes were significantly elevated in TB cases relative to LTBI controls in adults, but not in pre-adolescent children (**Figure 2C**).

In Vitro and *In Vivo Mycobacterium tuberculosis* Infection Induces Myeloid Inflammation

To address if the observed patterns of age-associated myeloid inflammatory responses can be induced by *in vivo M.tb* infection, we compared plasma levels of inflammatory proteins in QFT+ and QFT- 8-year-old children. Unsupervised hierarchical clustering based on the 20 soluble markers investigated in **Figure 2A** showed that samples segregated into two clusters with higher expression of many markers in the cluster significantly enriched for QFT+ individuals (Fisher exact, p = 0.001, **Figure 2D**). On univariate analysis, myeloid inflammatory mediators including TNF, MIP-1α, MIP-1β, IL-10, IL-1α, IL-1RA, IFN-α2, and IP-10 were significantly higher in QFT+ 8-year-old children than in QFT- 8-year-old children (**Figure 2D**), suggesting that *in vivo* infection with *M.tb*, detected by QFT assay, can induce myeloid inflammatory responses. MMP-9 and

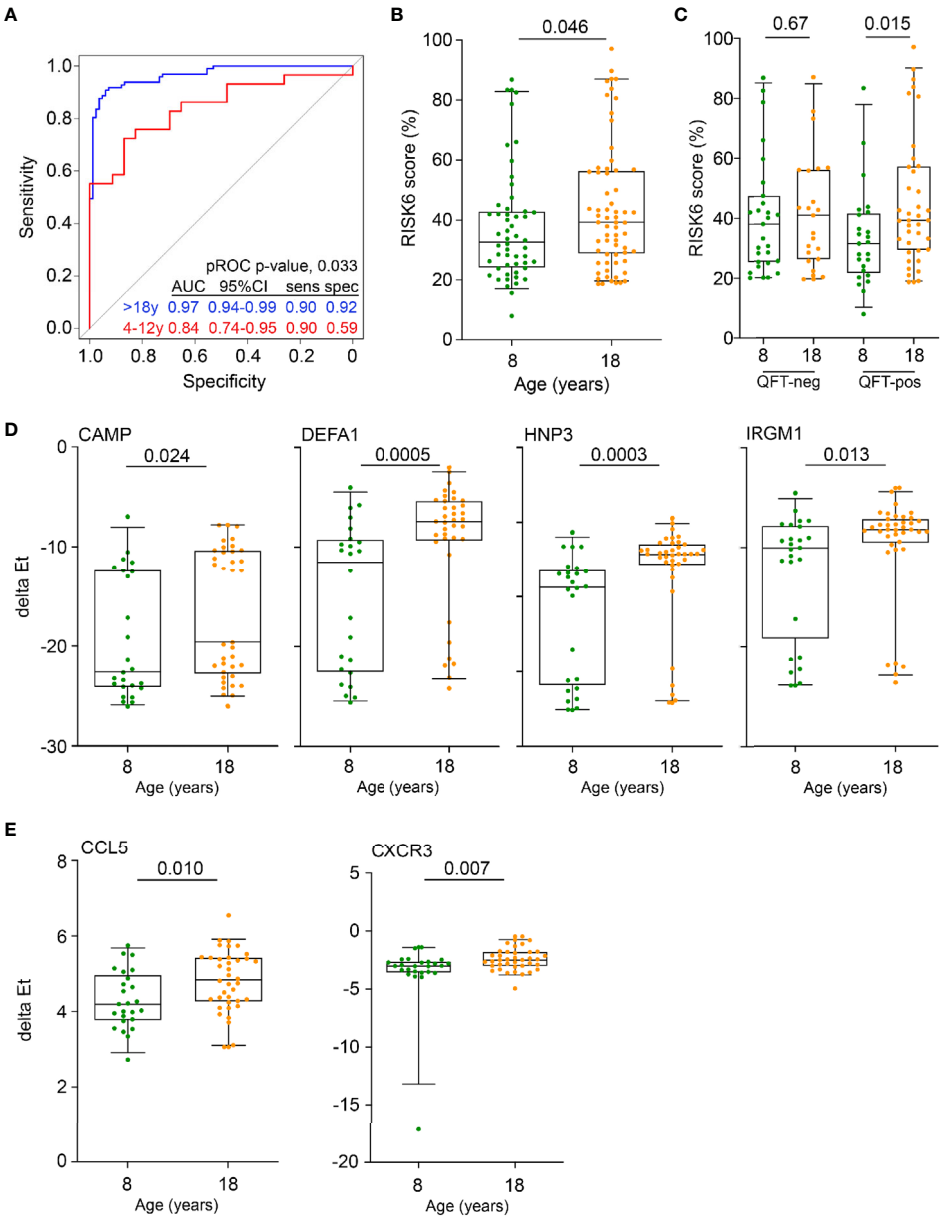

FIGURE 1 | Inflammation and antimicrobial mediators are more abundant in adolescents and adults than in pre-adolescent children. **(A)** Diagnostic performance of the Sweeney3 transcriptomic signature, by analysis of published whole blood microarray data, in differentiating between culture-confirmed TB and LTBI controls in adults (blue) and pre-adolescent children (red). Specificities (spec) are reported at the corresponding sensitivities (sens) of 0.90. The p value for comparing ROC curves in adults and pre-adolescent children was computed using pROC. **(B)** Comparison of RISK6 signature scores, measured by RT-qPCR, between 8- and 18-year-old participants. **(C)** RISK6 signature scores, measured by RT-qPCR, in 8- and 18-year-old participants stratified by QFT status. P values <0.05 were considered significant. **(D)** Expression levels of anti-mycobacterial genes, measured by RT-qPCR, in 8- and 18-year-old QFT+ participants. P values <0.0024 (after adjustment for 21 comparisons using the Bonferroni method) were considered statistically significant. **(E)** Expression levels of myeloid inflammatory genes in 8- and 18-year-old QFT+ participants. P values <0.0023 (after adjustment for 22 comparisons using the Bonferroni method) were considered statistically significant. Horizontal lines depict the median, boxes the interquartile range and whiskers the 95th percentiles. P values were computed with the Mann-Whitney U test.

VEGF were also higher in QFT+ 8-year-old children, while MMP-1 was lower (**Figure 2D**). However, no differences in soluble marker levels were observed between QFT+ and QFT- 18-year-old young adults (**Supplementary Figure 2B**). To confirm whether *M.tb* can directly induce expression of these inflammatory mediators in blood leukocytes, we analyzed the same markers after *in vitro* stimulation of whole blood with 3 different strains of live *M.tb*. In QFT- 8-year-old children, soluble levels of TNF, MIP-1α, MIP-1β, IL-10, and IL-1α were higher after stimulation of blood with H37Rv and HN878; whereas H37Rv, but not HN878, also induced IL-1RA, IFN-γ and MMP-9 secretion (**Figure 2E**). Stimulation with the *M.tb* strain

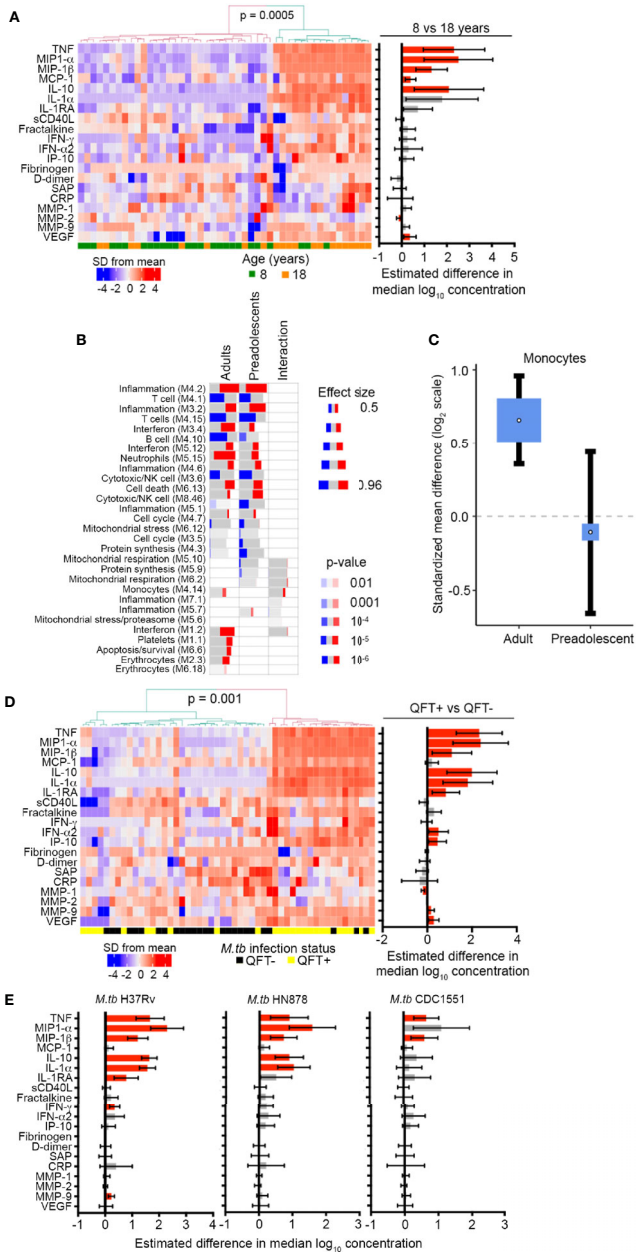

FIGURE 2 | Inflammation and pro-inflammatory, myeloid mediators are more abundant in adolescents and adults than pre-adolescent children and are induced by *in vivo* and *in vitro M.tb* infection. **(A)** Heatmap depicting concentrations of host-derived soluble inflammatory markers in unstimulated blood in QFT- 8- and 18-year-old individuals. The bar graph on the right represents estimated median differences in concentrations of host-derived soluble inflammatory markers between QFT- 8- and 18-year-old individuals. Error bars depict 95% confidence intervals. P values were adjusted using the Benjamini-Hochberg method (by controlling the false discovery rate at 5%) (43). **(B)** Analysis of gene modules, performed using gene set enrichment analysis (GSEA), differentially expressed between TB cases and LTBI controls in adults or pre-adolescent children, as well as the age-associated interaction term between the differentially expressed genes within each module. P values were adjusted using the Benjamini-Hochberg method (by controlling the false discovery rate at 1%). **(C)** Forest plot depicting differences in monocyte abundance between TB cases and LTBI controls in adults or pre-adolescent children, estimated from whole blood gene expression using cell mixture deconvolution. Positive and negative effect sizes indicate higher and lower levels of monocytes in TB versus healthy LTBI controls, respectively. The y axis represents standardized mean difference between TB and LTBI, computed as Hedges' g, on a $\log_2$ scale. The size of the blue rectangles is proportional to the SEM difference in the study. Whiskers represent the 95% confidence interval. The white point represents the magnitude of the effect size. **(D)** Heatmap depicting concentrations of host-derived soluble inflammatory markers in unstimulated blood in QFT+ 8-year-old children relative to QFT- 8-year-old children. The bar graph on the right represents estimated median differences in concentrations of host-derived soluble inflammatory markers. **(E)** Estimated median differences and 95% CI (error bars) in concentrations of host-derived soluble inflammatory markers in whole blood from QFT- 8-year-old children in response to *in vitro* stimulation with different strains of live *M.tb*, relative to unstimulated blood. P values were adjusted using the Benjamini-Hochberg method (by controlling the false discovery rate at 5%).

CDC1551, only induced significant increases in TNF and MIP-1β (**Figure 2E**).

mRNA Transcripts That Are Higher in 8-Year-Old Children

These results show that healthy young adults have greater myeloid inflammatory responses than healthy, pre-adolescent children and that monocytes, Type I IFN responses and mitochondrial respiration were more elevated in adult TB than in pediatric TB. We also detected elevated expression of a number of genes in blood from pre-adolescent children relative to young adults, including the IFNGR1 and intracellular pattern recognition receptor, NOD2 (**Figure 3A**) and the Type I IFN stimulated genes IFNAR2, MX2, OAS1 as well as STAT2 (**Figure 3B**). Cellular deconvolution of whole blood gene expression by immunoStates also showed that pre-adolescent children with TB had elevated proportions of B cells and macrophages of the M2 phenotype than LTBI controls, whereas in adults, this difference in B cells was not observed and M2 macrophages were significantly lower in TB cases (**Figure 3C**).

DISCUSSION

The risk of progression from *Mycobacterium tuberculosis* infection to active disease is significantly lower in pre-adolescent children above 4 years of age than in post-pubescent adolescents and young adults (3–5). Further, the typical clinical presentation of TB manifests as mild and/or pauci-bacillary lymph node disease in pre-adolescent children, whereas post-pubescent adolescents and adults more commonly present with multi-bacillary, "adult-type" pulmonary disease (3–5). To investigate possible immunological underpinnings of these age-associated characteristics of TB, we compared blood gene expression of antimicrobial effector molecules, pro- and anti-inflammatory and other immune mediators as well as soluble host-derived inflammatory molecules in pre-adolescent children and young adults.

In light of the well-described links between excessive innate inflammation and risk of TB progression as well as the role of inflammation as a cause of immunopathology and tissue destruction (12, 45, 46), we hypothesized that pro-inflammatory responses to *M.tb* in pre-adolescent children are either less pronounced or more regulated, than in young adults.

Three main findings emerged from our analyses: 1) diagnostic performance of transcriptomic signatures of TB for differentiating between culture-confirmed TB and LTBI controls was poorer in pre-adolescent children than in adults. 2) Pre-adolescent children had lower levels of myeloid-associated pro-inflammatory mediators than young adults. These mediators were induced by *in vivo* and *in vitro M.tb* infection, as supported by higher expression in QFT+ than QFT- 8-year-old children and significantly higher expression after *in vitro* stimulation of blood with live *M.tb*. 3) Compared with young adults, pre-adolescent children had higher levels of IFN stimulated genes IFNAR2, MX2, OAS1 and STAT2, as well as B cells and M2 macrophages than adults.

The "Golden Age" associated poorer performance of the previously published Sweeney3 signature of TB in differentiating between TB and LTBI controls, the lower RISK6 signature scores and the lower levels of myeloid-associated pro-inflammatory mediators all support our hypothesis that children have lower inflammation than young adults. Importantly, we observed this difference in both healthy individuals and in those with TB disease, suggesting that this finding did not only reflect differences in TB disease manifestation, but that these age-associated outcomes may reflect intrinsic differences that are not only restricted to mycobacterial immune responses. This is also supported by the results from our previous study of mycobacteria-specific T cell responses and mycobacterial growth inhibition in the same 8- and 18-year-old cohort; no age-associated differences in these common measures of mycobacteria-associated immune outcomes were observed (7). The observation that M2 macrophages, which are typically anti-inflammatory, were more abundant in pre-adolescent children than adults, further supports this. We were not able to definitively interpret the higher abundance of B cells in pre-adolescent children, since this designation includes many subclasses of B cells with different functions. Ultimately, this finding may simply reflect greater lymphocyte proportions in pre-adolescent children than adults.

Our observations are consistent with the hypothesis that pro- and anti-inflammatory responses must be balanced to avoid bias towards an excessive response (8, 9) and suggest that pre-adolescent children may be more likely to maintain an optimal balance. If this is true, then similar age-associated differences must exist for other infections and diseases, including autoimmune and inflammatory conditions. Indeed, sarcoidosis, a granulomatous disease associated with dysregulated IFN responses (47, 48), is not commonly reported in young, pre-adolescent children and increases after puberty (49). Among other infectious diseases, cutaneous leishmaniasis, schistosomiasis and leptospirosis follow the same curve that is observed for TB (50), with lowest incidences in pre-adolescent children above 4 years of age. While many factors affect the risk for these diseases, as is also true for TB, we hypothesize that the age-associated balance of inflammatory responses plays a role.

It was interesting that we observed higher expression of multiple Type I IFN mRNAs in pre-adolescent children compared with young adults. Our integrated analyses of differences in global gene expression between *M.tb* infection and TB disease, also revealed modest, but interesting age-associated differences in transcriptional programs typically associated with human TB, namely interferon signaling and myeloid inflammation (51, 52). To our knowledge, no study has hitherto teased apart the transcriptional program within each age stratum in the context of the observed epidemiological difference in TB disease incidence and pathophysiology, which we reveal in our analyses. We observed more exacerbated transcriptional dysregulation in interferon signaling in adults when compared to pre-adolescent children. Notably, pathways associated with mitochondrial stress/proteasome and mitochondrial respiration, suggestive of impaired mitochondrial function, which may be linked to necrotizing granulomatous lesions often observed in adult TB disease or,

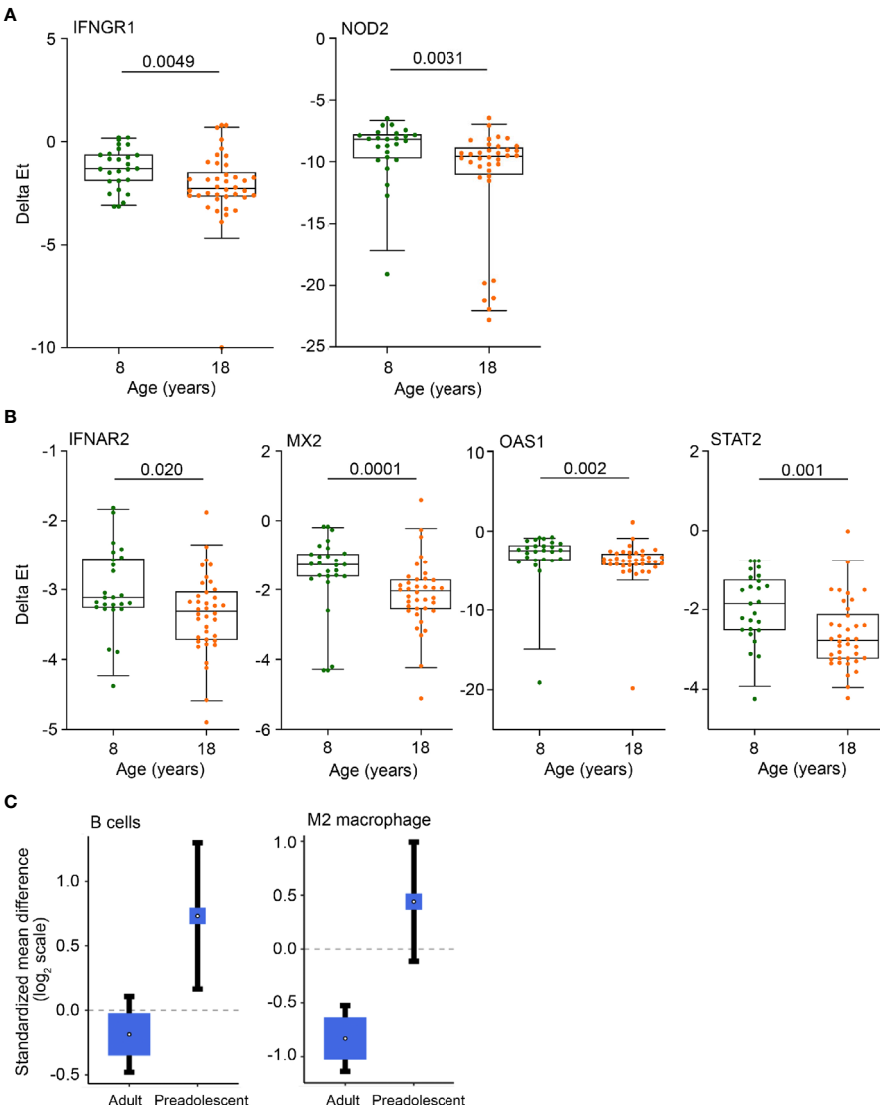

FIGURE 3 | Anti-mycobacterial response and Type I IFN genes, B cells and M2 macrophages are more abundant in pre-adolescent children than adults. **(A, B)** Expression levels of anti-mycobacterial response genes **(A)** and Type 1 IFN response genes **(B)**, measured by RT-qPCR, in 8- and 18-year-old QFT+ participants. Horizontal lines depict the median, boxes the interquartile range and whiskers the 95th percentiles. P values were computed with the Mann-Whitney U test. For **(A)**, p values <0.0024 (after adjustment for 21 comparisons using the Bonferroni method), and for **(B)**, p values <0.0045 (11 comparisons) were considered statistically significant. **(C)** Forest plots depicting differences in B cell and M2 macrophage abundance between TB cases and LTBI controls in adults or pre-adolescent children, estimated from whole blood gene expression using cell mixture deconvolution. Positive and negative effect sizes indicate higher and lower levels of that cell type in TB versus healthy LTBI controls, respectively. The y axes represent standardized mean differences between TB and LTBI, computed as Hedges' g, on a $\log_2$ scale. The size of the blue rectangles is proportional to the SEM difference in the study. Whiskers represent the 95% confidence interval. The white point represents the magnitude of the effect size.

alternatively, may be related to dysregulated inflammatory processes. Mitochondria mass, size, number, and fragmentation is known to be affected by virulent *M.tb* after macrophage infection (53) and recent findings by Pajuelo and colleagues provided evidence that *M.tb* hijacks a host cell death pathway involving the mitochondrion (54). Our results may at first appear to contradict the hypothesized higher inflammation in adults, especially in light of reports that Type I IFN responses predispose to TB disease progression (13, 55, 56). However, the biology of Type I IFN mRNAs is known to be particularly influenced by immunological changes during sexual maturation during and after puberty, which lead to divergence in immune and inflammatory responses between males and females. For example, females have higher expression of Type I IFN upon TLR7 stimulation than males (57), and the effects of oestrogens typically lead to higher levels of inflammation in females, while progesterone and androgens, such as testosterone,

generally mediate immunosuppressive activities (58, 59). Since TB notification rates in males are typically double those in females (1), and Type I IFN responses are typically higher in females, we propose that it may be too simplistic to expect a direct association between risk of TB and Type I IFN responses.

We acknowledge that our results reflect peripheral blood and not the site of disease, which limits our ability to directly establish a link between mitochondrial function and events at the site of disease. Our work is also subject to other limitations. The relatively small sample size limited statistical power to definitively address the influence of covariates, such as sex and ethnicity, on immunological outcomes and also did not allow analyses using age as a continuous variable. The restriction of our enrolled cohort of children and young adults to very specific ages (8 and 18 years of age) also limits the generalizability of our conclusions. Furthermore, analysis of the influence of underlying *M.tb* infection on age-associated immunological outcomes is limited by the absence of a true measure of *in vivo M.tb* in humans. It is well known that IFN-γ release assays, including the QFT assay we used to infer *M.tb* infection, are at best imperfect tests for infection (60). Finally, we note that the age-associated immunological differences observed in our study are modest in magnitude. In light of the many well-known risk factors for TB (61), independent replication of our findings is necessary.

In summary, our results suggest that myeloid inflammation is intrinsically lower in pre-pubescent children than in young adults and that this may play a role in age-associated differential risk of TB and/or the differences in clinical presentation of this disease. Further dissection of these age-associated differences may reveal opportunities to develop interventions that aim to optimize the balance between pro- and anti-inflammatory responses.

DATA AVAILABILITY STATEMENT

New data was generated and analysed in this study and can be found in the following online repository: https://doi.org/10.25375/uct.13351466.v1. Publicly available datasets were also analysed in this study. This data can be found here: Gene Expression Omnibus, https://www.ncbi.nlm.nih.gov/geo/, GSE39940 and GSE37250.

ETHICS STATEMENT

Participants were recruited under protocols approved by the University of Cape Town Human Research Ethics Committee. Written informed consent was obtained from adults prior to enrolment. Children provided written informed assent while their legal guardians provided written informed consent prior to enrollment.

AUTHOR CONTRIBUTIONS

MH, APN and TJS designed the study. MdK, MvR, LS and MH performed clinical investigations. RB, ME, JD, LM, MdK, NB, MS, HA, FD and NC processed samples or performed assays. RB, SKM, MR, JD, FD, NC, GT, GW, APN and TJS analysed and interpreted the data. RB, SKM, APN and TJS wrote the manuscript. All authors contributed to the article and approved the submitted version.

FUNDING

This work was supported by grants from the European and Developing Countries Clinical Trials Partnership (TA.2011.40200.010) and from the European Commission funded TBVAC2020 Consortium (H2020-PHC-643381). The funders were not involved in the research.

SUPPLEMENTARY MATERIAL

The Supplementary Material for this article can be found online at: https://www.frontiersin.org/articles/10.3389/fimmu.2021.639965/full#supplementary-material

REFERENCES

1. WHO. *Global tuberculosis report 2020*. Geneva, Switzerland: WHO (2020). Available at: http://www.who.int/tb/publications/global_report/en/.
2. Seddon JA, Chiang SS, Esmail H, Coussens AK. The Wonder Years: What Can Primary School Children Teach Us About Immunity to Mycobacterium tuberculosis? *Front Immunol* (2018) 9:2946/full:2946. doi: 10.3389/fimmu.2018.02946/full
3. Marais BJ, Gie RP, Schaaf HS, Beyers N, Donald PR, Starke JR. Childhood Pulmonary Tuberculosis. *Am J Respir Crit Care Med* (2006) 173(10):1078–90. doi: 10.1164/rccm.200511-1809SO
4. Marais BJ, Gie RP, Schaaf HS, Hesseling AC, Obihara CC, Starke JJ, et al. The natural history of childhood intra-thoracic tuberculosis: A critical review of literature from the pre-chemotherapy era. *Int J Tuberc Lung Dis* (2004) 8 (4):392–402.
5. Perez-Velez CM, Marais BJ. Tuberculosis in children. *New Engl J Med* (2012) 367:348–61. doi: 10.1056/NEJMra1008049
6. Andrews JR, Morrow C, Walensky RP, Wood R. Integrating Social Contact and Environmental Data in Evaluating Tuberculosis Transmission in a South African Township. *J Infect Dis* (2014) 210(4):597–603. doi: 10.1093/infdis/jiu138
7. Baguma R, Penn-Nicholson A, Smit E, Erasmus M, Day J, Makhethe L, et al. Application of a whole blood mycobacterial growth inhibition assay to study immunity against Mycobacterium tuberculosis in a high tuberculosis burden population. Cardona P-J, editor. *PloS One* (2017) 12(9):e0184563. doi: 10.1371/journal.pone.0184563
8. Sable SB, Posey JE, Scriba TJ. Tuberculosis vaccine development: Progress in clinical evaluation. *Clin Microbiol Rev Am Soc Microbiol* (2020) 33(1):e00100-19. doi: 10.1128/CMR.00100-19
9. Scriba TJ, Coussens AK, Fletcher HA. Human Immunology of Tuberculosis. *Microbiol Spectr* (2017) 5(1):213–37. doi: 10.1128/9781555819569.ch11
10. Andersen P, Scriba TJ. Moving tuberculosis vaccines from theory to practice. *Nat Rev Immunol* (2019) 19(9):550–62. doi: 10.1038/s41577-019-0174-z
11. Mayer-Barber KD, Sher A. Cytokine and lipid mediator networks in tuberculosis. *Immunol Rev* (2015) 264(1):264–75. doi: 10.1111/imr.12249

12. Tobin DM, Roca FJ, Oh SF, McFarland R, Vickery TW, Ray JP, et al. Host genotype-specific therapies can optimize the inflammatory response to mycobacterial infections. *Cell* (2012) 148(3):434–46. doi: 10.1016/j.cell.2011.12.023
13. Redford PS, Mayer-Barber KD, McNab FW, Stavropoulos E, Wack A, Sher A, et al. Influenza A virus impairs control of mycobacterium tuberculosis coinfection through a type i interferon receptor-dependent pathway. *J Infect Dis* (2014) 209(2):270–4. doi: 10.1093/infdis/jit424
14. Scriba TJ, Penn-Nicholson A, Shankar S, Hraha T, Thompson EG, Sterling D, et al. Sequential inflammatory processes define human progression from M. tuberculosis infection to tuberculosis disease. Sassetti CM, editor. *PloS Pathog* (2017) 13(11):e1006687. doi: 10.1371/journal.ppat.1006687
15. Suliman S, Thompson EG, Sutherland J, Weiner J, Ota MOC, Shankar S, et al. Four-Gene Pan-African Blood Signature Predicts Progression to Tuberculosis. *Am J Respir Crit Care Med* (2018) 197:1198–208. doi: 10.1164/rccm.201711-2340OC
16. Zak DE, Penn-Nicholson A, Scriba TJ, Thompson E, Suliman S, Amon LM, et al. A blood RNA signature for tuberculosis disease risk: a prospective cohort study. *Lancet* (2016) 387(10035):2312–22. doi: 10.1016/S0140-6736(15)01316-1
17. Drain PK, Bajema KL, Dowdy D, Dheda K, Naidoo K, Schumacher SG, et al. Incipient and subclinical tuberculosis: A clinical review of early stages and progression of infection. *Clin Microbiol Rev* (2018) 31(4):e00021-18. doi: 10.1128/CMR.00021-18
18. Martineau AR, Newton SM, Wilkinson KA, Kampmann B, Hall BM, Nawroly N, et al. Neutrophil-mediated innate immune resistance to mycobacteria. *J Clin Invest* (2007) 117(7):1988–94. doi: 10.1172/JCI31097
19. Anderson ST, Kaforou M, Brent AJ, Wright VJ, Banwell CM, Chagaluka G, et al. Diagnosis of childhood tuberculosis and host RNA expression in Africa. *N Engl J Med* (2014) 370(18):1712–23. doi: 10.1056/NEJMoa1303657
20. Kaforou M, Wright VJ, Oni T, French N, Anderson ST, Bangani N, et al. Detection of Tuberculosis in HIV-Infected and -Uninfected African Adults Using Whole Blood RNA Expression Signatures: A Case-Control Study. *PloS Med* (2013) 10(10):e1001538. doi: 10.1371/journal.pmed.1001538
21. Subbian S, Tsenova L, Yang G, O'Brien P, Parsons S, Peixoto B, et al. Chronic pulmonary cavitary tuberculosis in rabbits: a failed host immune response. *Open Biol* (2011) 1(4):110016. doi: 10.1098/rsob.110016
22. Subbian S, Tsenova L, O'Brien P, Yang G, Kushner NL, Parsons S, et al. Spontaneous latency in a rabbit model of pulmonary tuberculosis. *Am J Pathol* (2012) 181(5):1711–24. doi: 10.1016/j.ajpath.2012.07.019
23. Darboe F, Mbandi SK, Naidoo K, Yende-Zuma N, Lewis L, Thompson EG, et al. Detection of tuberculosis recurrence, diagnosis and treatment response by a blood transcriptomic risk signature in HIV-infected persons on antiretroviral therapy. *Front Microbiol* (2019) 10(JUN):1441. doi: 10.3389/fmicb.2019.01441
24. Spurgeon SL, Jones RC, Ramakrishnan R. High Throughput Gene Expression Measurement with Real Time PCR in a Microfluidic Dynamic Array. Seoighe C, editor. *PloS One* (2008) 3(2):e1662. doi: 10.1371/journal.pone.0001662
25. R Core Team. *R: A language and environment for statistical computing*. Austria: R Found Stat Comput Vienna (2019). Available at: http://www.r-project.org/.
26. Leek JT, Storey JD. Capturing heterogeneity in gene expression studies by surrogate variable analysis. *PloS Genet* (2007) 3(9):1724–35. doi: 10.1371/journal.pgen.0030161
27. Sweeney TE, Braviak L, Tato CM, Khatri P. Genome-wide expression for diagnosis of pulmonary tuberculosis: A multicohort analysis. *Lancet Respir Med* (2016) 4(3):213–24. doi: 10.1016/S2213-2600(16)00048-5
28. Penn-Nicholson A, Mbandi SK, Thompson E, Mendelsohn SC, Suliman S, Chegou NN, et al. RISK6, a 6-gene transcriptomic signature of TB disease risk, diagnosis and treatment response. *Sci Rep* (2020) 10(1):1–21. doi: 10.1038/s41598-020-65043-8
29. Haynes WA, Vallania F, Liu C, Bongen E, Tomczak A, Andres-Terrè M, et al. Empowering multi-cohort gene expression analysis to increase reproducibility. *Pac Symp Biocomput* (2017) 22:144–53. doi: 10.1101/071514
30. Vallania F, Tam A, Lofgren S, Schaffert S, Azad TD, Bongen E, et al. Leveraging heterogeneity across multiple datasets increases cell-mixture deconvolution accuracy and reduces biological and technical biases. *Nat Commun* (2018) 9(1):4735. doi: 10.1038/s41467-018-07242-6
31. Ritchie ME, Phipson B, Wu D, Hu Y, Law CW, Shi W, et al. Limma powers differential expression analyses for RNA-sequencing and microarray studies. *Nucleic Acids Res* (2015) 43(7):e47. doi: 10.1093/nar/gkv007
32. Obermoser G, Presnell S, Domico K, Xu H, Wang Y, Anguiano E, et al. Systems scale interactive exploration reveals quantitative and qualitative differences in response to influenza and pneumococcal vaccines. *Immunity* (2013) 38(4):831–44. doi: 10.1016/j.immuni.2012.12.008
33. Weiner 3rd J, Domaszewska T. tmod: an R package for general and multivariate enrichment analysis. *PeerJ* (2016) 4. doi: 10.7287/peerj.preprints.2420v1
34. Vandesompele J, De Preter K, Pattyn F, Poppe B, Van Roy N, De Paepe A, et al. Accurate normalization of real-time quantitative RT-PCR data by geometric averaging of multiple internal control genes. *Genome Biol* (2002) 3(7):research0034.1. doi: 10.1186/gb-2002-3-7-research0034
35. Koenker R. *Quantile regression*. Cambridge, United Kingdom: Cambridge University Press (2005). 349 p. Available at: https://books.google.co.za/books/about/Quantile_Regression.html?id=hdkt7V4NXsgC&redir_esc=y.
36. Kassambara A, Mundt F. *Factoextra: extract and visualize the results of multivariate data analyses*. Available at: http://www.sthda.com/english/rpkgs/factoextrahttps://rdrr.io/github/kassambara/factoextra/%0Ahttps://github.com/kassambara/factoextra/issues%0Ahttp://www.sthda.com/english/rpkgs/factoextra%0ABugReports.
37. Lê S, Josse J, Husson F. FactoMineR: An R package for multivariate analysis. *J Stat Softw* (2008) 25. doi: 10.18637/jss.v025.i01
38. Gu Z, Eils R, Schlesner M. Complex heatmaps reveal patterns and correlations in multidimensional genomic data. *Bioinformatics* (2016) 32(18):2847–9. doi: 10.1093/bioinformatics/btw313
39. Mahomed H, Hawkridge T, Verver S, Geiter L, Hatherill M, Abrahams D, et al. Predictive factors for latent tuberculosis infection among adolescents in a high-burden area in South Africa. *Int J Tuberc Lung Dis* (2011) 15(3):331–6.
40. Andrews JR, Hatherill M, Mahomed H, Hanekom WA, Campo M, Hawn TR, et al. The dynamics of QuantiFERON-TB Gold in-Tube conversion and reversion in a cohort of South African adolescents. *Am J Respir Crit Care Med* (2015) 191(5):584–91. doi: 10.1164/rccm.201409-1704OC
41. Sweeney TE, Khatri P. Blood transcriptional signatures for tuberculosis diagnosis: A glass half-empty perspective - Authors' reply. *Lancet Respir Med* (2016) 4:e29. doi: 10.1016/S2213-2600(16)30039-X
42. Warsinske HC, Rao AM, Moreira FMF, Santos PCP, Liu AB, Scott M, et al. Assessment of Validity of a Blood-Based 3-Gene Signature Score for Progression and Diagnosis of Tuberculosis, Disease Severity, and Treatment Response. *JAMA Netw Open* (2018) 1(6):e183779. doi: 10.1001/jamanetworkopen.2018.3779
43. Benjamini Y, Hochberg Y. Controlling the False Discovery Rate: A Practical and Powerful Approach to Multiple Testing. *J R Stat Soc Ser B* (1995) 57(1):289–300. doi: 10.1111/j.2517-6161.1995.tb02031.x
44. Berry MPR, Graham CM, McNab FW, Xu Z, Bloch SAA, Oni T, et al. An interferon-inducible neutrophil-driven blood transcriptional signature in human tuberculosis. *Nature* (2010) 466(7309):973–7. doi: 10.1038/nature09247
45. Elkington P, Shiomi T, Breen R, Nuttall RK, Ugarte-Gil CA, Walker NF, et al. MMP-1 drives immunopathology in human tuberculosis and transgenic mice. *J Clin Invest* (2011) 121(5):1827–33. doi: 10.1172/JCI45666
46. Walker NF, Clark SO, Oni T, Andreu N, Tezera L, Singh S, et al. Doxycycline and HIV infection suppress tuberculosis-induced matrix metalloproteinases. *Am J Respir Crit Care Med* (2012) 185(9):989–97. doi: 10.1164/rccm.201110-1769OC
47. Koth LL, Solberg OD, Peng JC, Bhakta NR, Nguyen CP, Woodruff PG. Sarcoidosis blood transcriptome reflects lung inflammation and overlaps with tuberculosis. *Am J Respir Crit Care Med* (2011) 184(10):1153–63. doi: 10.1164/rccm.201106-1143OC
48. Maertzdorf J, Weiner J, Mollenkopf HJNetwork TbT, , Bauer T, Prasse A, et al. Common patterns and disease-related signatures in tuberculosis and sarcoidosis. *Proc Natl Acad Sci U.S.A.* (2012) 109(20):7853–8. doi: 10.1073/pnas.1121072109
49. Hoffmann AL, Milman N, Byg KE. Childhood sarcoidosis in Denmark 1979-1994: Incidence, clinical features and laboratory results at presentation in 48 children. *Acta Paediatr Int J Paediatr* (2004) 93(1):30–6. doi: 10.1080/08035250310007213
50. Guerra-Silveira F, Abad-Franch F. Sex Bias in Infectious Disease Epidemiology: Patterns and Processes. *PloS One* (2013) 8(4):e62390. doi: 10.1371/journal.pone.0062390

51. Weiner J, Kaufmann SHE. High-throughput and computational approaches for diagnostic and prognostic host tuberculosis biomarkers. *Int J Infect Dis* (2017) 56:258–62. doi: 10.1016/j.ijid.2016.10.017. Elsevier B.V.
52. Singhania A, Verma R, Graham CM, Lee J, Tran T, Richardson M, et al. A modular transcriptional signature identifies phenotypic heterogeneity of human tuberculosis infection. *Nat Commun* (2018) 9(1):1–17. doi: 10.1038/s41467-018-04579-w
53. Fine-Coulson K, Giguère S, Quinn FD, Reaves BJ. Infection of A549 human type II epithelial cells with Mycobacterium tuberculosis induces changes in mitochondrial morphology, distribution and mass that are dependent on the early secreted antigen, ESAT-6. *Microbes Infect* (2015) 17(10):689–97. doi: 10.1016/j.micinf.2015.06.003
54. Pajuelo D, Gonzalez-Juarbe N, Tak U, Sun J, Orihuela CJ, Niederweis M. NAD + Depletion Triggers Macrophage Necroptosis, a Cell Death Pathway Exploited by Mycobacterium tuberculosis. *Cell Rep* (2018) 24(2):429–40. doi: 10.1016/j.celrep.2018.06.042
55. Mayer-Barber KD, Andrade BB, Oland SD, Amaral EP, Barber DL, Gonzales J, et al. Host-directed therapy of tuberculosis based on interleukin-1 and type i interferon crosstalk. *Nature* (2014) 511(7507):99–103. doi: 10.1038/nature13489
56. O'Garra A, Redford PS, McNab FW, Bloom CI, Wilkinson RJ, Berry MPR. The immune response in tuberculosis. *Annu Rev Immunol* (2013) 31:475–527. doi: 10.1146/annurev-immunol-032712-095939
57. Webb K, Peckham H, Radziszewska A, Menon M, Oliveri P, Simpson F, et al. Sex and Pubertal Differences in the Type 1 Interferon Pathway Associate With Both X Chromosome Number and Serum Sex Hormone Concentration. *Front Immunol* (2019) 9:3167/full:3167. doi: 10.3389/fimmu.2018.03167/full
58. Lahita RG. Sex Hormones as Immunomodulators of Disease. *Ann N Y Acad Sci* (1993) 685(1):278–87. doi: 10.1111/j.1749-6632.1993.tb35876.x
59. Giefing-Kröll C, Berger P, Lepperdinger G, Grubeck-Loebenstein B. How sex and age affect immune responses, susceptibility to infections, and response to vaccination. *Aging Cell* (2015) 14:309–21. doi: 10.1111/acel.12326
60. Pai M, Denkinger CM, Kik SV, Rangaka MX, Zwerling A, Oxlade O, et al. Gamma interferon release assays for detection of Mycobacterium tuberculosis infection. *Clin Microbiol Rev* (2014) 27(1):3–20. doi: 10.1128/CMR.00034-13
61. Lawn SD, Zumla AI. Tuberculosis. *Lancet* (2011) 378(9785):57–72. doi: 10.1016/S0140-6736(10)62173-3

Conflict of Interest: AP-N and TS have a patent of the RISK6 signature pending.

The remaining authors declare that the research was conducted in the absence of any commercial or financial relationships that could be construed as a potential conflict of interest.

The handling editor declared a past co-authorship with several of the authors, TS and MH.

Copyright © 2021 Baguma, Mbandi, Rodo, Erasmus, Day, Makhethe, de Kock, van Rooyen, Stone, Bilek, Steyn, Africa, Darboe, Chegou, Tromp, Walzl, Hatherill, Penn-Nicholson and Scriba. This is an open-access article distributed under the terms of the Creative Commons Attribution License (CC BY). The use, distribution or reproduction in other forums is permitted, provided the original author(s) and the copyright owner(s) are credited and that the original publication in this journal is cited, in accordance with accepted academic practice. No use, distribution or reproduction is permitted which does not comply with these terms.

frontiers in Immunology

ORIGINAL RESEARCH
published: 05 March 2021
doi: 10.3389/fimmu.2021.645446

Antiretroviral Treatment-Induced Decrease in Immune Activation Contributes to Reduced Susceptibility to Tuberculosis in HIV-1/Mtb Co-infected Persons

Katalin A. Wilkinson[1,2]*, *Deborah Schneider-Luftman*[3], *Rachel Lai*[4], *Christopher Barrington*[3], *Nishtha Jhilmeet*[2], *David M. Lowe*[2,5], *Gavin Kelly*[3] and *Robert J. Wilkinson*[1,2,4]

[1] Tuberculosis Laboratory, The Francis Crick Institute, London, United Kingdom, [2] Wellcome Centre for Infectious Diseases Research in Africa, Institute of Infectious Diseases and Molecular Medicine, University of Cape Town, Cape Town, South Africa, [3] Bioinformatics and Biostatistics, The Francis Crick Institute, London, United Kingdom, [4] Department of Infectious Disease, Imperial College London, London, United Kingdom, [5] Institute of Immunity and Transplantation, University College London, London, United Kingdom

OPEN ACCESS

Edited by:
Cecilia Lindestam Arlehamn, La Jolla Institute for Immunology (LJI), United States

Reviewed by:
Shibali Das, Washington University School of Medicine in St. Louis, United States
Robert Blomgran, Linköping University, Sweden

***Correspondence:**
Katalin A. Wilkinson
katalin.wilkinson@crick.ac.uk

Specialty section:
This article was submitted to Immunological Memory, a section of the journal Frontiers in Immunology

Received: 23 December 2020
Accepted: 10 February 2021
Published: 05 March 2021

Citation:
Wilkinson KA, Schneider-Luftman D, Lai R, Barrington C, Jhilmeet N, Lowe DM, Kelly G and Wilkinson RJ (2021) Antiretroviral Treatment-Induced Decrease in Immune Activation Contributes to Reduced Susceptibility to Tuberculosis in HIV-1/Mtb Co-infected Persons. Front. Immunol. 12:645446. doi: 10.3389/fimmu.2021.645446

Antiretroviral treatment (ART) reduces the risk of developing active tuberculosis (TB) in HIV-1 co-infected persons. In order to understand host immune responses during ART in the context of *Mycobacterium tuberculosis* (Mtb) sensitization, we performed RNAseq analysis of whole blood-derived RNA from individuals with latent TB infection coinfected with HIV-1, during the first 6 months of ART. A significant fall in RNA sequence abundance of the Hallmark IFN-alpha, IFN-gamma, IL-6/JAK/STAT3 signaling, and inflammatory response pathway genes indicated reduced immune activation and inflammation at 6 months of ART compared to day 0. Further exploratory evaluation of 65 soluble analytes in plasma confirmed the significant decrease of inflammatory markers after 6 months of ART. Next, we evaluated 30 soluble analytes in QuantiFERON Gold in-tube (QFT) samples from the Ag stimulated and Nil tubes, during the first 6 months of ART in 30 patients. There was a significant decrease in IL-1alpha and IL-1beta (Ag-Nil) concentrations as well as MCP-1 (Nil), supporting decreased immune activation and inflammation. At the same time, IP-10 (Ag-nil) concentrations significantly increased, together with chemokine receptor-expressing CD4 T cell numbers. Our data indicate that ART-induced decrease in immune activation combined with improved antigen responsiveness may contribute to reduced susceptibility to tuberculosis in HIV-1/Mtb co-infected persons.

Keywords: antiretroviral treatment, tuberculosis, plasma biomarker, RNAseq, QuantiFERON

INTRODUCTION

Tuberculosis (TB) remains the leading bacterial cause of death worldwide (1). The biggest recognized risk factor for developing TB disease is Human immunodeficiency virus (HIV-1) infection (2). Antiretroviral treatment (ART) is an effective way to reduce the risk of TB in HIV-1 co-infected persons, reducing TB incidence between 54 and 92% at the individual level (3). More broadly, ART was shown to be associated with the decline of TB in sub-Saharan Africa

between 2003 and 2016, preventing an estimated 1.88 million cases (4). In order to understand how ART reduces susceptibility to TB in HIV-1 infected persons, we longitudinally analyzed a group of individuals with latent TB infection, co-infected with HIV-1, over 6 months from starting ART (day 0). Our hypothesis was that this highly susceptible group who undergo immune reconstitution through ART, and thereby become less susceptible to TB, will yield insight into protective mechanisms against TB in humans.

Before the commencement of ART, the risk of TB is increased at all stages of HIV-1 infection. This could be due to depletion of *Mycobacterium tuberculosis* (Mtb) specific T cells early during HIV-1 infection (5) as well as impairment of function of these antigen-specific CD4 T cells (6). We and others have shown that increased ART-mediated immunity broadly correlates with the expansion of early differentiated (central memory) T-cell responses and overall reduction in cellular activation (7–9). More specifically, we recently demonstrated that the numbers of Mtb-antigen specific CD4 T cells increase during the first 6 months of ART, together with proportionally expanded polyfunctionality (cells co-producing TNF, IFN-gamma, and IL-2), and a concomitant decrease in their activation profile (10).

As the risk and incidence of active TB remains much higher in individuals with latent TB infection co-infected with HIV-1 (termed HIV-1/Mtb co-infected persons), compared to those not infected with HIV-1, despite widespread implementation of ART regimes globally and even during long-term ART (11), it is important to understand the host immune response in the context of Mtb infection and ART. Therefore, we performed exploratory RNAseq analysis of whole blood derived RNA from HIV-1/Mtb co-infected individuals during the first 6 months of ART, followed by evaluation of multiple soluble analytes in plasma. For more precise assessment of the change in soluble plasma biomarkers in the context of Mtb sensitization (latent TB infection) during ART, we used QuantiFERON® Gold in-tube (QFT) plasma samples. These samples have been shown to be useful in evaluating host biomarkers other than IFN-gamma, regardless of HIV-1 status (12, 13). Moreover, we recently used similar QFT plasma samples to evaluate the predictive performance of 13 plasma biomarkers in HIV-1 infected individuals likely to progress to active TB and found that unstimulated plasma analyte concentrations better identified TB risk in these HIV-1 co-infected patients, demonstrating that underlying inflammatory processes, and higher overall background immune activation might render them more susceptible to progress to TB (14). However, no studies so far evaluated QFT plasma analyte concentrations longitudinally, during ART. Here we present data suggesting that the ART-induced decrease in immune activation combined with improved antigen responsiveness may contribute to reduced susceptibility to tuberculosis in HIV-1/Mtb co-infected persons.

MATERIALS AND METHODS

Study Cohort

HIV-1 infected persons starting ART were recruited from the Ubuntu Clinic in Khayelitsha, South Africa, during 2 longitudinal studies in 2011–2012. The University of Cape Town Faculty of Health Sciences Human Research Ethics Committee approved these studies (HREC 245/2009 and 545/2010). All participants gave written informed consent prior to inclusion in the study, in accordance with the Declaration of Helsinki. Blood for plasma separation, Quantiferon Gold In-tube (QFT) assay and RNA extraction (Tempus^{TM} tubes) was collected at baseline (Day 0) and after one (1 M), three (3 M), and six months (6 M) of receiving ART. All samples were stored at −80°C for future use. The University of Cape Town Faculty of Health Sciences Human Research Ethics Committee approved these studies (HREC 245/2009 and 545/2010). All participants gave written informed consent in accordance with the Declaration of Helsinki. The 2 cohorts have previously been described (15–17). At the time of recruitment, the following exclusion criteria applied: evidence or clinical concern of active tuberculosis (TB), current INH or TB chemotherapy, grade III-IV peripheral neuropathy, pregnancy, abnormal liver function, age <18 years. Development of active TB during longitudinal follow up was determined by induced sputum culture at 1, 3, or 6 months of receiving ART. These individuals were referred to the TB services for treatment and were excluded from our analyses with sample collection terminated. All remaining participants experienced an increase in CD4 counts and a decrease in HIV viral load during the first 6 months of ART. They were all sensitized by Mtb, as determined by positivity in at least one interferon gamma release assay, QFT and/or ELISpot, at least one timepoint during the longitudinal follow up, as previously shown (17). We therefore infer latent TB infection in these individuals and term them HIV-1/Mtb co-infected persons throughout this manuscript.

RNA Sequencing Library Preparation

Total RNA was extracted from whole blood using the Tempus Spin RNA Isolation kit (Thermofisher) according to the manufacturer's recommendations as described (17). The quantity and quality of the extracted RNA were measured by the Qubit fluorometer and the Caliper LabChip system, respectively. RNA libraries for whole blood RNA were constructed using the Ovation Human Blood RNAseq Library Systems (Tecan, Mannedorf, Switzerland) where ribosomal and globin RNA were removed according to the manufacturer's protocol. The final libraries were assessed using TapeStation 2200 System (Agilent, Santa Clara, CA). All libraries were sequenced on Illumina Hi-Seq 4000 instrument with paired-end 100 cycle reactions and 40 million reads per sample.

RNAseq Data Analysis

Indexed libraries were pooled and sequenced on an Illumina HiSeq 4000 configured to generate 101 cycles of paired-end data. Raw data was demultiplexed and FastQ files created using bcl2fastq (2.20.0). Datasets were analyzed using the BABS-RNASeq Nextflow (18) pipeline developed at the Francis Crick Institute. The GRCh38 human reference genome was used with the Ensembl release-86 (19) gene annotations. Dataset quality and replication was validated using FastQC (0.11.7, Andrews, link), RSeQC (20), RNAseqC (21) and Picard (2.10.1, link). Reads were then aligned to the genome and expression

quantified using STAR (22) and RSEM (23). Estimates of gene expression were loaded into R version 3.5.1 using the tximport package. DEseq2 (24) was used to test for significant differences between day 0 and 6 months of ART. Default parameters were applied and false discovery rate was set to 0.1. Gene set enrichment analysis was performed using fgsea (25). Hallmark pathways ("h.all.v6.2.symbols.gmt") were downloaded (http://software.broadinstitute.org/gsea) and used to test for enrichment genes ranked by their stat value calculated by DESeq2. The data was deposited to Gene Expression Omnibus (GEO) under accession number GSE158208.

Multiplex Immune Assays for Cytokines and Chemokines

The preconfigured multiplex Human Immune Monitoring 65-plex ProcartaPlex immunoassay kit (Thermo Fisher Scientific, UK) was used to measure 65 protein targets in plasma. Bio-Plex Pro Human Cytokine 27-Plex Immunoassay (Bio-Rad Laboratories, Hercules, CA, USA) and customized MilliplexTM kits (Millipore, St Charles, MO, USA) were used to measure 30 analytes in the QFT plasma samples from unstimulated (Nil) and TB specific antigen stimulated (Ag) samples. All assays were conducted on the Bio-Plex platform (Bio-Rad Laboratories, Hercules, CA, USA), using Luminex xMAP technology. Additional confirmatory experiments were run on the Meso Scale Discovery Inc (Rockville, MD) platform, using the plasma samples only (not QFT). All assays were conducted as per the manufacturer's recommendation and all analytes measured are listed in **Supplementary Table 1**.

Flow Cytometry Analysis

Cryopreserved peripheral blood mononuclear cells were thawed, counted, rested in 5 ml RPMI supplemented with 10% FCS at 37°C for 4 h in a 50 ml Falcon tube, washed again and stained with LIVE/DEAD® Fixable Near-IR Stain as well as the following surface markers: CD14 and CD19 (APC-AF750), CD4 (FITC), CD45RA (BV570), CD27 (BV711), CXCR3 (PE-Cy7), CCR4 (BV510), CCR6 (BV605). Cells were acquired on a BD-Fortessa flow cytometer and analyzed using FlowJo as previously described (10).

Data Cleaning and Analysis for QFT Plasma Samples

After removal of missing data 30 analytes measured at 4 time-points over the course of 6 months were evaluated: baseline (D0), after one (1 M), three (3 M) and six months (6 M) of receiving ART. Subjects with more than 50% of data missing (due to undetectable concentration values) across all the time points for the analytes of interest were removed. One missing data point (0.8% of all data) was imputed using KNN imputation (k = 15). All analytes were sampled in Nil and Ag (antigen stimulated) assays. As some analytes resulted in no change or negative values upon antigen stimulation compared to the unstimulated sample (Ag-Nil), only analytes with Ag stimulated values found to be significantly different than their Nil counterparts were retained for the main analysis, after transformation into (Ag-Nil). These selected analytes in the form of (Ag-Nil) and all unstimulated analytes (Nil-only values) were considered for the remaining part of the analysis.

Statistical Analyses for QFT Plasma Samples

All analyses were carried out in R version 3.6.1, using the analytical framework provided in the Limma package (26). Limma follows a parametric empirical Bayes model within multiple linear regressions. A linear regression model is fitted for each molecule of interest, the resulting estimates are then linked to global hyper-parameters in order to share information between the molecules. This allows to calculate correlations between analytes of interest, together with correlations between related samples, but also helps correct for unequal quality / unequal variance between time points. Limma is also equipped with mixed effect modeling with unconditional growth and constant intra-block correlation, which allows us to adjust for the potential batch effect of data collection at each time point.

Using Limma with mixed effect for each biomarker n∈[1, N], $N = 43$, we have:

- $Yn, i, j = \beta 0, n, j + \beta 1, n, jti, j + \epsilon n, i, j,$
- $\beta 0, n, j = \gamma 0, n + U0, n, j$
- $\beta 1, n, j = \gamma 1, n + U1, n, j$

Where j represents subjects–j∈[1, Npeople], Npeople = 30, and i represents time points–i∈[0, 1, 3, 6].

Time (here being the follow-up rounds) is treated as a discrete categorical variable. This allows us to model the effect of time on analyte progression without imposing parametric specifications on the shape of the relationship between time and analytes. Results for each biomarker are combined, and those with fixed effects with $p \leq \alpha = 0.05$ are considered significant, after false discovery rate (FDR) adjustment. While, traditionally, FDR adjustment is made via Bonferroni correction–$\alpha' = \alpha/N$–we opt here for the Benjamini & Hochberg (BH) FDR correction procedure (27) as it is more robust to false negatives and still adequately controls for family-wise error rate. This procedure is repeated for all time points, as well as for each time point in order to evaluate change between baseline and specific time points (D0 vs. M1, D0 vs. M3, and D0 vs. M6). Results are quoted in log-fold changes, which is equal to the log-2 transform of the ratio between 2 elements [$\log_2$(A/B)].

Clustering Analysis for QFT Plasma Samples

In order to further understand the structure of the biomarker data, we subjected the samples to an unsupervised clustering analysis as well as principal components analysis (PCA). The cytokines and biomarkers data were aggregated across all time points and all subjects, and analyzed through K-means clustering. In both K-means and in PCA, we used the log-fold change in biomarker concentrations across all the follow-up timepoints to evaluate groupings and similarity between analytes. K-means clustering is an unsupervised learning algorithm that clusters data based on their similarity. It is carried out by evaluating the sum of squares distance between each analyte and the centroid

of the K clusters, in terms of their log-fold change across the 6 months observation period of the study. At first, a number of clusters K is set. Each analyte is randomly assigned to one of the K clusters, then reassigned to the cluster that has the smallest distance from its centroid to that point. This process is reiterated until no further cluster reassignment occurs. K is chosen as the smallest integer which minimizes the within-cluster sum of squares—a measure of within-cluster similarity.

RESULTS

RNA Sequencing Analysis

Exploratory analysis performed in 6 samples from D0 and 6 samples from 6 M (not paired) revealed 155 differentially expressed genes (**Figure 1A**, **Supplementary Figure 1A** and **Supplementary Table 2**). Gene Set Enrichment Analysis (GSEA) using Reactome identified a significant fall in the Interferon-alpha, Interferon-gamma, IL-6/JAK/STAT3 signaling and overall inflammatory response pathway genes (**Figure 1B**). These results were replicated by similar findings using Hallmark pathway analysis as well (**Supplementary Figure 1B**). While interestingly there was an increase in Heme metabolism as shown by GSEA (**Figure 1B**), overall the data points toward reduced immune activation and inflammation at 6 months of ART compared to day 0.

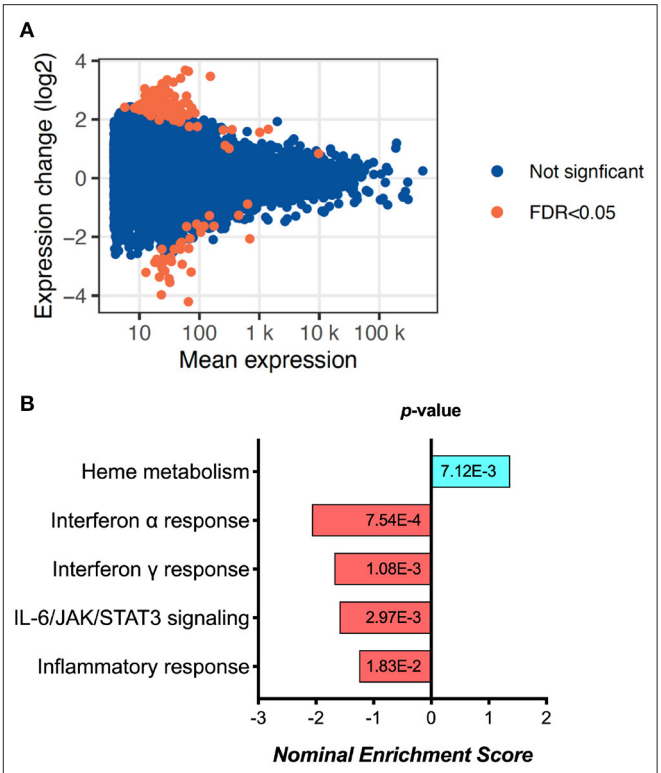

FIGURE 1 | RNA sequencing analysis results, showing **(A)** the MA plot visualizing the statistically different genes by transforming the data onto M (log ratio) and A (mean average) scales; and **(B)** the pathways significantly changed between day 0 and 6 months of ART based on Gene set enrichment analysis (GSEA).

Multiplex Analysis Using Plasma

Next we used plasma collected at day 0 and 6 months of ART ($n = 39$, paired samples) in further exploratory analysis of soluble markers using the Immune Monitoring 65-Plex Human ProcartaPlex™ Panel (Invitrogen, Thermo Fischer). Twenty nine analytes were excluded from analysis due to (1) being undetectable in all samples (FGF-2, IL-5, IL-31, MCSF, MIF, TNF-beta), 99% of samples (MCP-3, IL-23), 96% of samples (IL-7); (2) the median concentration being 0 pg/ml at both timepoints (bNGF, G-CSF, GM-CSF, GRO-alpha, IL-1alpha, IL-1beta, IL-3, IL-4, IL-6, IL-8, IL-9, IL-10, IL-12p70, IL-15, IL-20, IL-22, IL-27, LIF); (3) the median concentration being 1 pg/ml at both timepoints, although there was a trend showing decrease over time (IFN-alpha, IL-13). The remaining results are summarized in **Table 1**, demonstrating a significant decrease in soluble plasma analytes overall. Since these plasma analyte determinations were exploratory, we did not perform correction for multiple comparisons. However, we did utilize an alternative immune marker monitoring platform, Meso Scale Discovery system, to further confirm the trends seen in selected markers from all groups (highlighted by italics in **Table 1**). Results are summarized in **Supplementary Table 3**. While there were notable differences in the range of concentrations detected by the 2 different platforms, as shown previously by others (28–31), overall the data confirm the significant decrease in HIV-1 induced immune activation and inflammation over the first 6 months of ART. Since the MSD Angiogenesis panel allows individual evaluation of VEGF-A, C, and D, it was interesting to find an increase over time in VEGF-D plasma concentrations (from median of 851–1,046 pg/ml, $p = 0.0002$, **Supplementary Table 3**).

Multiplex Analysis Using QFT Plasma

In order to assess more precisely the change in soluble plasma biomarkers in the context of Mtb sensitization during ART, we next used QuantiFERON® Gold in-tube (QFT) plasma samples. Here we longitudinally analyzed 30 soluble analytes in 30 HIV-1-infected individuals (9 male, 21 female; mean age 34.3 years) at baseline (D0) and after one (1 M), three (3 M), and six months (6 M) of receiving ART, using the Nil and selected Antigen-stimulated (Ag-Nil) QFT plasma samples. The HIV-1 viral load (VL) and CD4 counts of the 30 participants during ART are summarized in **Supplementary Table 4**.

First, we assessed the effect of antigen stimulation at each timepoint by comparing Ag stimulated samples to unstimulated (Nil) samples. The QFT assay was optimized to assess an IFN-gamma response in the form of (Ag-Nil), however, here we intended to assess the effect of antigen stimulation on other analytes as well and in order to be able to compare the effects we opted to assess the ratio, or fold change in analyte concentration between Ag stimulated and Nil assays. The analytes that showed a significant response difference over time are summarized in **Table 2** and were selected to be included in further analysis in the form of (Ag-Nil). All data related to the analysis are summarized in **Supplementary Table 5**.

TABLE 1 | Multiplex analysis of plasma.

No	Analyte[a]	Day 0 median	Day 0 (IQR)	6M median	6M (IQR)	*p*-value[b]
T cell response related						
1	*IFN-gamma*	53	34.1–80.3	27	19.8–37.7	<0.0001
2	IL-18	116	30.5–187.6	51	18.5–104.3	<0.0001
3	CD40-Ligand	236	0–305	0	0–245	<0.0001
4	*IP-10*	240	109–375	67	24–148	<0.0001
5	MIG	968	707–1256	526	0–715.5	<0.0001
6	IL-16	1,637	1,107–1,840	1,119	743–1,610	<0.0001
7	IL-2R	25,084	15,178–40,542	7,953	4,746–13,525	<0.0001
8	TSLP	19	9.9–30.5	4	0–15	0.0006
9	I-TAC	314	0–735	0	0–326	0.0014
10	IL-2	32	11.5–91.1	18	11.5–106.7	0.19
11	IL-21	98	0–222.3	62	0–200.4	0.1
12	*IL-17A*	348	56–690	309	135.7–674.5	0.26
TNF superfamily related						
13	TNF-RII	662	585–717	569	521–633	<0.0001
14	Tweak/TNFSF12	2,266	1,286–3,432	1,306	909–1,779	<0.0001
15	CD30	10,436	7,935–14,690	4,673	3,001–6,851	<0.0001
16	ENA-78(LIX)	859	407–1,973	603	323–1,425	0.004
17	APRIL	4,274	3,390–5,268	3,836	2,893–4,846	0.005
18	*TNF-alpha*	3	1.48–7.6	3	0.35–4.06	0.027
19	TRAIL	682	0–966	0	0–804	0.034
20	BAFF	49	0–96.7	0	0–126.6	0.427
Monocyte/macrophage related						
21	MCP-2	25	12.9–38.9	11	6.6–15.7	<0.0001
22	*MIP-1alpha*	17	13–24	10	6.1–15	<0.0001
23	BLC	1,113	593.5–2,170	422	155.7–755.8	<0.0001
24	Eotaxin-3	72	0–102.8	0	0–36.7	0.0002
25	MDC/CCL22	4,374	1,529–10,229	1,515	446–4,264	0.0004
26	MIP-3alpha	26	9.7–55.9	10	2.7–35.1	0.0016
27	*MIP-1beta*	61	30.2–92.2	42	14.1–63.4	0.008
28	Eotaxin-2	6	0.9–20.3	2	0–12.3	0.071
29	Fractalkine	16	9.5–29.9	12	5.5–23	0.074
30	*MCP-1*	253	121.7–388.2	211	104.6–319.7	0.22
31	Eotaxin-1	14	7.3–38.7	11	5.6–47.9	0.78
Growth factors						
32	*VEGF-A*	815	512.7–1,055	425	223.2–658.8	<0.0001
33	HGF	565	427.7–714	456	329–502.6	0.0005
34	MMP-1	1,879	1,065–4,429	1,649	764–2,731	0.049
35	SDF-1alpha	7,690	6,142–8,754	6,940	5,496–8,884	0.085
36	SCF	38	23.1–48.8	34	17.4–48.8	0.59

[a]*analyte concentrations expressed as median (IQR) pg/ml;* [b]*Wilcoxon matched pairs (n = 39).*

The change in analytes at 1, 3, and 6 months of ART, compared to day 0 is shown in **Supplementary Figure 2**, while the consistent change in analytes across all time points is summarized in **Figure 2**. There was a consistent decrease in IL-1alpha and IL-1beta concentrations in the (Ag-Nil) samples, as well as MCP-1 concentration in the Nil samples (as already seen in the plasma analyte evaluation above using MSD). Interestingly, there was an increase in antigen specific (Ag-Nil) IP-10 concentrations, especially at 6 months of ART. The fold change in these analyte concentrations at each timepoint is shown in **Table 3**.

IL-1beta and IL-1alpha (Ag-Nil) were also found to be strongly correlated (corr = 0.55, p = 4.14e-06) at 6 months, but not correlated to IP10 (corr = −0.075, p = 0.56 for IL-1alpha, corr = −0.130, p = 0.33 for IL-1beta). This is also reflected in the principal components analysis (PCA) loading plot

TABLE 2 | Analytes found to be significantly changed by Ag stimulation, that were retained for further analysis.

	Analyte	*P*-value[a]	Ratio[b]
1	MCP-1	1.22E-11	2.9
2	IP-10	4.30E-10	6.15
3	IL-1beta	3.57E-07	3.45
4	IL-6	1.57E-06	4.99
5	FGF-BASIC	1.57E-06	2.89
6	IL1-alpha	5.27E-05	1,278.39
7	MIP-1beta	1.43E-04	436.93
8	IL-2	5.73E-04	20.84
9	MIP-1alpha	1.49E-03	1,321.72
10	IFN-alpha2	5.98E-03	5.3
11	IFN-gamma	1.64E-02	4.81
12	IL-9	4.69E-02	3.39

[a] *P-value: p-value from paired Wilcoxon signed rank test and adjusted for FDR via BH procedure.*
[b] *Ratio: fold change in analyte concentration between Ag stimulated and Nil assays, calculated across all time points and all samples.*

(**Figure 3A** showing the first 2 principal components), where IL-1alpha and IL-1beta strongly influence PC1 (53% of variance), while IP-10 almost solely, drives PC2 (32% of variance). This was supported by clustering analysis using K-means, that found $K = 3$ clusters to be optimal for the data (**Figure 3B**); with IL-6 (Ag-Nil), MIP-1alpha (Ag-Nil), and IL-8 (Nil) grouped together, IP-10 (Ag-Nil) in its own cluster, and all other compounds grouped in the third cluster (PC1, first principal component, variance explained: 77.4% and PC2, second principal component, variance explained: 18.6%).

Chemokine Receptor Analysis Using Flow Cytometry

Overall, the above data support a decrease in HIV-1 induced immune activation and inflammation over the first 6 months of ART, even in the context of Mtb sensitization. However, to better understand the increase in antigen specific IP-10 (Ag-Nil) concentrations, we evaluated the expression of chemokine receptors CXCR3, CCR4, and CCR6 on the surface of CD4 T cells, using PBMC in a subset of 25 patients from the same cohort, as previously described (10). We found expanding numbers of CD4 T cells expressing CXCR3 (the receptor for IP-10), as well as CCR4 and CCR6 between day 0 and 6 months or ART. Thus, the number of $CD4^+CXCR3^+$ T cells increased from median 20 (IQR 12–41) cells/μL at day 0 to 23 (IQR 12–68) at 6 months of ART ($p = 0.009$). Similarly, the number of $CD4^+CCR4^+$ T cells increased from median 31 (IQR 6–40) to 52 (IQR 33–58, $p = 0.0001$) and the number of $CD4^+CCR6^+$ T cells increased from median 27 (IQR 18–35) to 36 (IQR 22–44, $p = 0.045$), respectively, all Wilcoxon matched pairs comparisons for $n = 25$ at day 0 and 6 months of ART, with data shown in **Supplementary Figure 3**. These results indicate expanding numbers of CD4 T cells that are capable to respond to chemokine signaling over the first 6 months of ART.

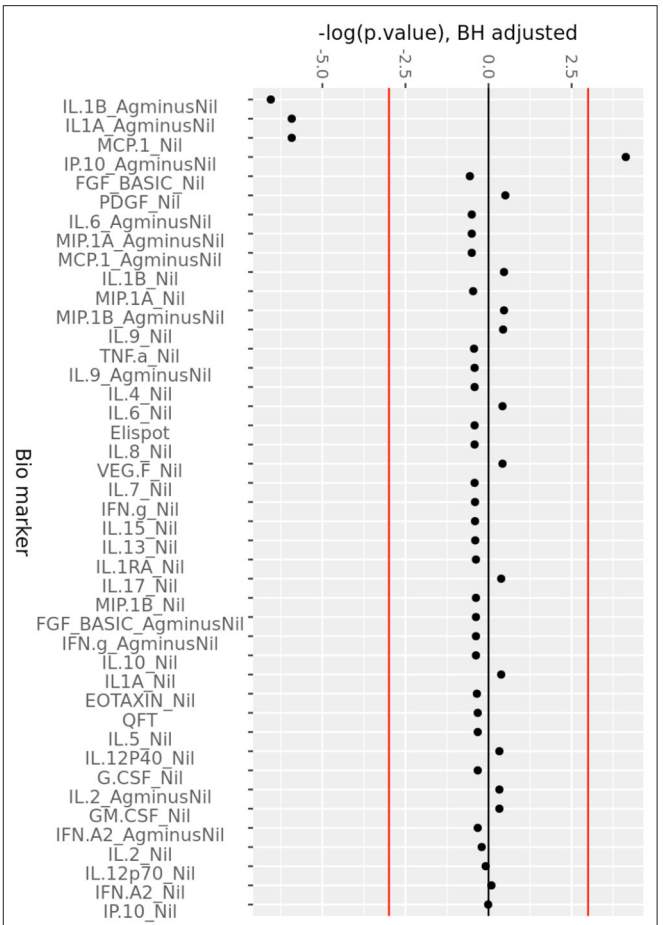

FIGURE 2 | Consistent change in QFT plasma analytes over 6 months of ART. Minus log-transformed *p*-values for each analyte, resulting from the Limma analysis framework, after BH FDR correction, considering all timepoints. Sign represents direction of effect size (negative: decrease from D0 level, positive: increase from D0 level). Red lines: α significance thresholds.

TABLE 3 | Analytes with significant changes from baseline, over the follow up period.

Analyte (condition)	Month 1[a]	Month 3[a]	Month 6[a]	Adj. P-Val[b]
IL-1beta (Ag-Nil)	−3,240.28	−4,086.82	−3,047.68	1.43E-03
IL-1alpha (Ag-Nil)	−2,053.01	−2,791	−2,283.65	2.68E-03
MCP-1 (Nil)	−1,152.4	−1,263.36	−791.29	2.68E-03
IP-10 (Ag-Nil)	22,221.56	929.38	47,674.16	1.61E-02

[a] *log-fold change between the concentration at baseline (day 0) and concentrations at 1, 3, and 6 months of ART respectively (negative value mean decrease and positive value means increase).*
[b] *Adj. P-Val: P-value from Limma analysis, after adjustment for FDR.*

DISCUSSION

The aim of this study was to better understand host immune responses during ART. Our exploratory RNAseq analysis

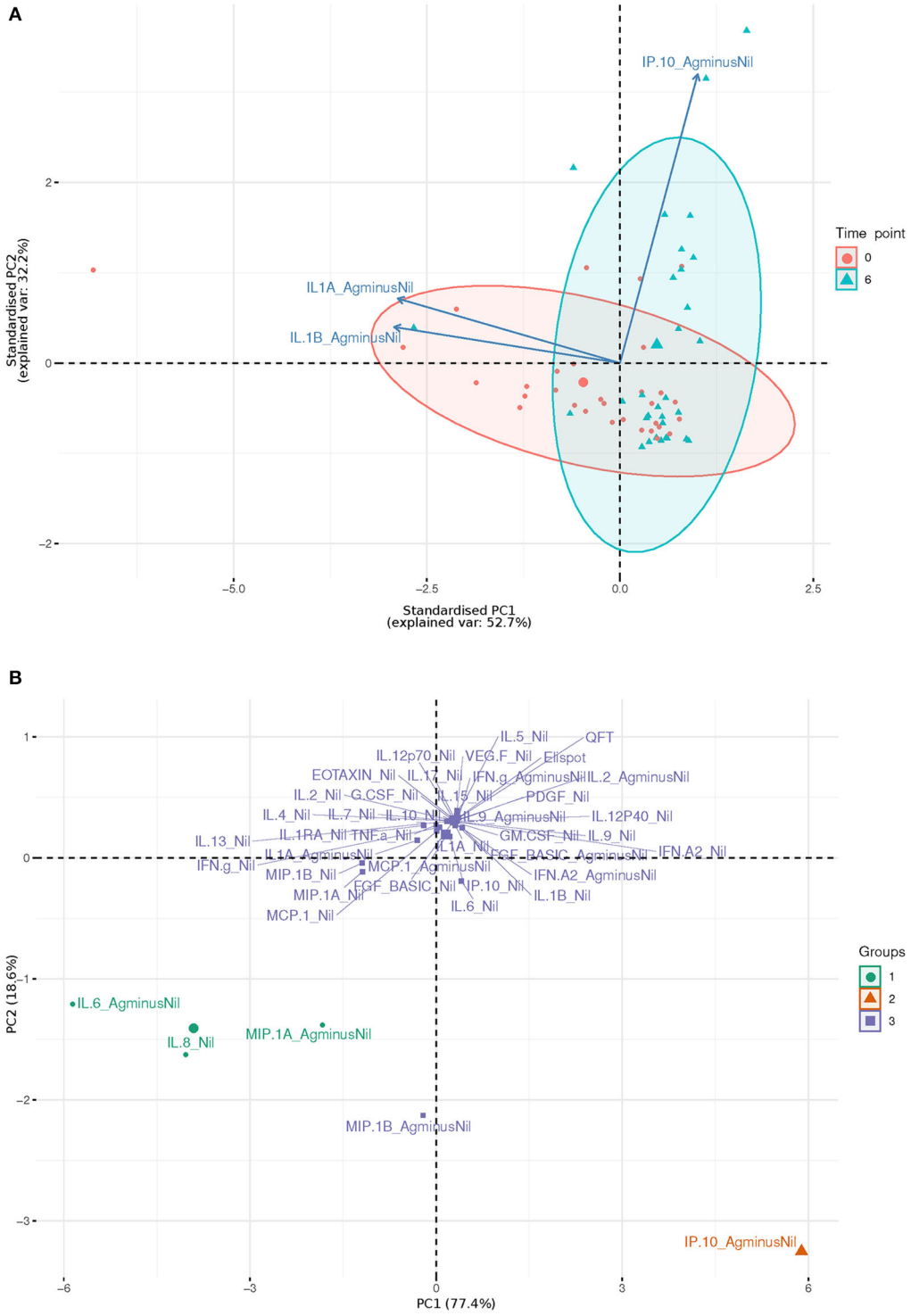

FIGURE 3 | First two principal components plots: **(A)** Over three most significantly changing analytes (arrows) between day 0 (red) and 6 months (blue), each dot representing a patient sample. **(B)** Over each analyte of interest and all time points, grouped by K-means clustering, using $K = 3$, each dot representing a compound.

indicates a significant fall in the Hallmark Interferon alpha, Interferon gamma and IL-6-JAK-STAT-signaling, together with overall inflammatory response pathway genes between day 0 and 6 months of ART, suggesting reduced immune activation and inflammation at 6 months of ART compared to day 0. This trend is supported by decreasing concentrations of soluble markers in plasma from the same cohort, indicating an overall decline in HIV-1 induced immune activation and

inflammation during the first 6 months of ART. Our more targeted analysis of soluble plasma biomarkers in the context of Mtb sensitization during ART, using QFT supernatants, shows a decrease in antigen specific IL-beta and IL-1alpha as well as MCP-1, in line with decreased HIV-1 induced immune activation and inflammation. At the same time, antigen specific IP-10 (Ag-nil) concentrations significantly increased, together with chemokine expressing CD4 T cells, in keeping with memory T cell expansion as we demonstrated previously (7, 10). Overall, our data indicates that the ART- induced decrease in immune activation combined with improved antigen responsiveness may contribute to reduced susceptibility to tuberculosis in HIV-1/Mtb co-infected persons.

The increase in antigen specific IP-10 (Ag-Nil) coincides with increasing numbers of CXCR3+CD4+ T cells. CXCR3, the receptor for IP-10 (also known as IFN-gamma inducible protein 10 or CXCL10), is a chemokine receptor highly expressed on effector T cells and plays an important role in T cell trafficking, effector T cell recruitment from the lymphoid tissue to the peripheral sites and an important role in memory CD4 T cell function throughout the activation and differentiation pathway (32). Our data showing a decrease in plasma IP-10 but an increase in antigen specific IP-10, together with expanding numbers of CD4 T cells expressing various chemokine receptors, are in line with the overall memory CD4 T cell expansion (10) and point toward broadly improved capacity to respond to new infections through better responsiveness to antigen, as a result of ART.

The increase in Heme metabolism as indicated by RNAseq, together with increasing concentrations of VEGF-D in plasma, may reflect reversal of the endothelial dysfunction associated with both HIV-1 infection and ART (33). The heme oxygenase system acts as a potent antioxidant, protects endothelial cells from apoptosis, is involved in regulating vascular tone, attenuates inflammatory response in the vessel wall, and participates in angiogenesis and vasculogenesis (34). Vascular endothelial growth factor-D (VEGF-D) is a secreted protein that can promote the remodeling of blood vessels and lymphatics in development and disease (35). While their increase could indicate normalization of endothelial integrity and activity on ART, recent evidence suggests that HIV-1 associated endothelial activation persists despite ART (36). Due to increased rates of cardiovascular disease among people living with HIV-1, this is an important area to explore in further studies.

Multiple studies have used QFT plasma samples mainly to differentiate between active and latent TB (37). Our previous analysis of similar samples to identify TB risk in HIV-1 co-infected patients indicated that unstimulated plasma (Nil) analyte concentrations may reflect underlying inflammatory processes and this higher overall background activation might render these co-infected individuals more susceptible to progress to TB (14). Indeed, excessive inflammation leading to tissue damage are pathological hallmarks of TB and HIV-associated TB immune reconstitution inflammatory syndrome (38) and excessive IL-1beta production is associated with dissemination to extrapulmonary sites and poor treatment outcome (39). We also showed that the activation profile of Mtb-specific CD4 T cells in terms of HLA-DR expression identifies TB disease activity irrespective of HIV-1 status (40). Recent data using the macaque model of SIV/Mtb co-infection indicates that SIV induces chronic immune activation, leading to dysregulated T cell homeostasis which is associated with reactivation of LTBI (41, 42). This may imply that HIV-1 induced chronic immune activation leads to LTBI reactivation and therefore increased susceptibility to TB in HIV-1 co-infected individuals. Taken together, our data supports that ART reduces chronic immune activation, thereby leading to reduced susceptibility to TB, through an overall decrease in HIV-1 induced immune activation and inflammation, including decreased T cell activation, increased numbers of polyfunctional antigen specific T cells (10), with improved capacity to respond to new infections through better responsiveness to antigen.

DATA AVAILABILITY STATEMENT

The datasets presented in this study can be found in online repositories. The names of the repository/repositories and accession number(s) can be found in the article/**Supplementary Material**.

ETHICS STATEMENT

The studies involving human participants were reviewed and approved by the University of Cape Town Faculty of Health Sciences Human Research Ethics Committee (HREC 245/2009 and 545/2010). The patients/participants provided their written informed consent to participate in this study.

AUTHOR CONTRIBUTIONS

KW, RL, and RW conceived the experiments. RW contributed resources. DL recruited participants and contributed samples. KW, RL, and NJ performed the experiments. DS-L, CB, RL, GK, and KW performed data analysis. KW and DS-L wrote the draft manuscript. All authors contributed to manuscript revision, read, and approved the submitted version.

FUNDING

Research supported by Wellcome (104803, 087754, and 203135), The South African National Research Foundation (443386), the European Union Horizon 2020 research and innovation programme under grant agreement no 643381 and The Francis Crick Institute which receives support from UKRI (FC001218), Cancer Research UK (FC001218), and Wellcome (FC001218).

ACKNOWLEDGMENTS

We acknowledge Robert Goldstone and Philip East for helpful discussions related to the RNAseq experiments. The Advanced Sequencing STP of the Francis Crick Institute performed the RNA sequencing experiments.

SUPPLEMENTARY MATERIAL

The Supplementary Material for this article can be found online at: https://www.frontiersin.org/articles/10.3389/fimmu.2021.645446/full#supplementary-material

Supplementary Figure 1 | RNA sequencing analysis results, showing **(A)** Volcano plot visualizing the differentially expressed genes identified in RNA sequencing analysis; and **(B)** Hallmark pathway analysis results.

Supplementary Figure 2 | Change in QFT plasma analytes compared to day 0, at 1, 3, and 6 M of ART. Minus log-transformed *p*-values for each analyte, resulting from the Limma analysis framework, after BH FDR correction at 1, 3, and 6 Months of ART, compared to day 0. Sign represents direction of effect size (negative: decrease from D0 level, positive: increase from D0 level). Red lines: α significance thresholds.

Supplementary Figure 3 | Change in CD4 T cells expressing the chemokine receptors CXCR3, CCR4, and CCR6, determined by flow cytometry analysis in peripheral blood mononuclear cells in a subset of 25 patients from the same cohort, at day 0 and 6 months of ART.

Supplementary Table 1 | Analytes evaluated in the study.

Supplementary Table 2 | Differentially expressed genes revealed by RNA sequencing. This list is provided in an Excel spreadsheet.

Supplementary Table 3 | MSD analysis results.

Supplementary Table 4 | HIV-1 viral load (VL) and CD4 T-cell counts (CD4) at each time point of the study in $n = 30$ patients included in the QFT plasma analysis.

Supplementary Table 5 | Mean (standard deviation, SD) in pg/ml for all analytes of interest in the study, across each time point in the n=30 patients included in the final analysis. *P*-value: *p*-value from group means test for each analyte, where H0 = no change in means across time point.

REFERENCES

1. WHO. *Global Tuberculosis Report 2020*. WHO (2020). Available online at: https://wwwwhoint/tb/publications/global_report/en/
2. Maartens G, Wilkinson RJ. Tuberculosis. *Lancet.* (2007) 370:2030–43. doi: 10.1016/S0140-6736(07)61262-8
3. Lawn SD, Wood R, De Cock KM, Kranzer K, Lewis JJ, Churchyard GJ. Antiretrovirals and isoniazid preventive therapy in the prevention of HIV-associated tuberculosis in settings with limited health-care resources. *Lancet Infect Dis.* (2010) 10:489–98. doi: 10.1016/S1473-3099(10)70078-5
4. Dye C, Williams BG. Tuberculosis decline in populations affected by HIV: a retrospective study of 12 countries in the WHO African Region. *Bull World Health Organ.* (2019) 97:405–14. doi: 10.2471/BLT.18.228577
5. Geldmacher C, Ngwenyama N, Schuetz A, Petrovas C, Reither K, Heeregrave EJ, et al. Preferential infection and depletion of *Mycobacterium tuberculosis*-specific CD4 T cells after HIV-1 infection. *J Exp Med.* (2010) 207:2869–81. doi: 10.1084/jem.20100090
6. Singh SK, Larsson M, Schon T, Stendahl O, Blomgran R. HIV interferes with the dendritic cell-T cell axis of macrophage activation by shifting *Mycobacterium tuberculosis*-specific CD4 t cells into a dysfunctional phenotype. *J Immunol.* (2019) 202:816–26. doi: 10.4049/jimmunol.1800523
7. Wilkinson KA, Seldon R, Meintjes G, Rangaka MX, Hanekom WA, Maartens G, et al. Dissection of regenerating T cell responses against tuberculosis in HIV infected adults with latent tuberculosis. *Am J Respir Crit Care Med.* (2009) 180:674–83. doi: 10.1164/rccm.200904-0568OC
8. Mahnke YD, Fletez-Brant K, Sereti I, Roederer M. Reconstitution of peripheral T cells by tissue-derived CCR4+ central memory cells following HIV-1 antiretroviral therapy. *Pathog Immun.* (2016) 1:260–90. doi: 10.20411/pai.v1i2.129
9. Riou C, Tanko RF, Soares AP, Masson L, Werner L, Garrett NJ, et al. Restoration of CD4+ responses to copathogens in HIV-infected individuals on antiretroviral therapy is dependent on T cell memory phenotype. *J Immunol.* (2015) 195:2273–81. doi: 10.4049/jimmunol.1500803
10. Riou C, Jhilmeet N, Rangaka MX, Wilkinson RJ, Wilkinson KA. Tuberculosis Antigen-specific T-cell responses during the first 6 months of antiretroviral treatment. *J Infect Dis.* (2020) 221:162–7. doi: 10.1093/infdis/jiz417
11. Lawn SD, Wilkinson RJ. ART and prevention of HIV-associated tuberculosis. *Lancet HIV.* (2015) 2:e221–2. doi: 10.1016/S2352-3018(15)00081-8
12. Manngo PM, Gutschmidt A, Snyders CI, Mutavhatsindi H, Manyelo CM, Makhoba NS, et al. Prospective evaluation of host biomarkers other than interferon gamma in QuantiFERON Plus supernatants as candidates for the diagnosis of tuberculosis in symptomatic individuals. *J Infect.* (2019) 79:228–35. doi: 10.1016/j.jinf.2019.07.007
13. Chegou NN, Sutherland JS, Namuganga AR, Corstjens PL, Geluk A, Gebremichael G, et al. Africa-wide evaluation of host biomarkers in QuantiFERON supernatants for the diagnosis of pulmonary tuberculosis. *Sci Rep.* (2018) 8:2675. doi: 10.1038/s41598-018-20855-7
14. Lesosky M, Rangaka MX, Pienaar C, Coussens AK, Goliath R, Mathee S, et al. Plasma biomarkers to detect prevalent or predict progressive tuberculosis associated with human immunodeficiency virus-1. *Clin Infect Dis.* (2019) 69:295–305. doi: 10.1093/cid/ciy823
15. Lowe DM, Bangani N, Goliath R, Kampmann B, Wilkinson KA, Wilkinson RJ, et al. Effect of antiretroviral therapy on HIV-mediated impairment of the neutrophil antimycobacterial response. *Ann Am Thorac Soc.* (2015) 12:1627–37. doi: 10.1513/AnnalsATS.201507-463OC
16. Horvati K, Bosze S, Gideon HP, Bacsa B, Szabo TG, Goliath R, et al. Population tailored modification of tuberculosis specific interferon-gamma release assay. *J Infect.* (2016) 72:179–88. doi: 10.1016/j.jinf.2015.10.012
17. Jhilmeet N, Lowe DM, Riou C, Scriba TJ, Coussens A, Goliath R, et al. The effect of antiretroviral treatment on selected genes in whole blood from HIV-infected adults sensitised by *Mycobacterium tuberculosis*. *PLoS ONE.* (2018) 13:e0209516. doi: 10.1371/journal.pone.0209516
18. Di Tommaso P, Chatzou M, Floden EW, Barja PP, Palumbo E, Notredame C. Nextflow enables reproducible computational workflows. *Nat Biotechnol.* (2017) 35:316–9. doi: 10.1038/nbt.3820
19. Aken BL, Achuthan P, Akanni W, Amode MR, Bernsdorff F, Bhai J, et al. Ensembl 2017. *Nucleic Acids Res.* (2017) 45:D635–42. doi: 10.1093/nar/gkw1104
20. Wang L, Wang S, Li W. RSeQC: quality control of RNA-seq experiments. *Bioinformatics.* (2012) 28:2184–5. doi: 10.1093/bioinformatics/bts356
21. DeLuca DS, Levin JZ, Sivachenko A, Fennell T, Nazaire MD, Williams C, et al. RNA-SeQC: RNA-seq metrics for quality control and process optimization. *Bioinformatics.* (2012) 28:1530–2. doi: 10.1093/bioinformatics/bts196
22. Dobin A, Davis CA, Schlesinger F, Drenkow J, Zaleski C, Jha S, et al. STAR: ultrafast universal RNA-seq aligner. *Bioinformatics.* (2013) 29:15–21. doi: 10.1093/bioinformatics/bts635
23. Li B, Dewey CN. RSEM: accurate transcript quantification from RNA-Seq data with or without a reference genome. *BMC Bioinformatics.* (2011) 12:323. doi: 10.1186/1471-2105-12-323
24. Love MI, Huber W, Anders S. Moderated estimation of fold change and dispersion for RNA-seq data with DESeq2. *Genome Biol.* (2014) 15:550. doi: 10.1186/s13059-014-0550-8
25. Korotkevich G, Sukhov V, Sergushichev A. Fast gene set enrichment analysis. *bioRxiv.* (2019). doi: 10.1101/060012
26. Ritchie ME, Phipson B, Wu D, Hu Y, Law CW, Shi W, et al. limma powers differential expression analyses for RNA-sequencing and microarray studies. *Nucleic Acids Res.* (2015) 43:e47. doi: 10.1093/nar/gkv007
27. Hochberg YBaY. Controlling the false discovery rate: a practical and powerful approach to multiple testing. *J R Stat Soc Ser B.* (1995) 57:289–300. doi: 10.1111/j.2517-6161.1995.tb02031.x
28. Christiansson L, Mustjoki S, Simonsson B, Olsson-Strömberg U, Loskog ASI, Mangsbo SM. The use of multiplex platforms for absolute and relative protein quantification of clinical material. *EuPA Open Proteom.* (2014) 3:37–47. doi: 10.1016/j.euprot.2014.02.002

29. Akyüz L, Wilhelm A, Butke F, Su-Jin P, Kuckuck A, Volk HD, et al. Validation of novel multiplex technologies. *Adv Prec Med*. (2017) 2:1–9. doi: 10.18063/APM.2017.02.001
30. Breen EC, Reynolds SM, Cox C, Jacobson LP, Magpantay L, Mulder CB, et al. Multisite comparison of high-sensitivity multiplex cytokine assays. *Clin Vaccine Immunol.* (2011) 18:1229–42. doi: 10.1128/CVI.05032-11
31. Chowdhury F, Williams A, Johnson P. Validation and comparison of two multiplex technologies, luminex and mesoscale discovery, for human cytokine profiling. *J Immunol Methods.* (2009) 340:55–64. doi: 10.1016/j.jim.2008.10.002
32. Groom JR, Luster AD. CXCR3 in T cell function. *Exp Cell Res.* (2011) 317:620–31. doi: 10.1016/j.yexcr.2010.12.017
33. Marincowitz C, Genis A, Goswami N, De Boever P, Nawrot TS, Strijdom H. Vascular endothelial dysfunction in the wake of HIV and ART. *FEBS J.* (2019) 286:1256–70. doi: 10.1111/febs.14657
34. Kim YM, Pae HO, Park JE, Lee YC, Woo JM, Kim NH, et al. Heme oxygenase in the regulation of vascular biology: from molecular mechanisms to therapeutic opportunities. *Antioxid Redox Signal.* (2011) 14:137–67. doi: 10.1089/ars.2010.3153
35. Stacker SA, Achen MG. Emerging roles for VEGF-D in human disease. *Biomolecules.* (2018) 8:1. doi: 10.3390/biom8010001
36. Kamtchum-Tatuene J, Mwandumba H, Al-Bayati Z, Flatley J, Griffiths M, Solomon T, et al. HIV is associated with endothelial activation despite ART, in a sub-Saharan African setting. *Neurol Neuroimmunol Neuroinflamm.* (2019) 6:e531. doi: 10.1212/NXI.0000000000000531
37. Sudbury EL, Clifford V, Messina NL, Song R, Curtis N. Mycobacterium tuberculosis-specific cytokine biomarkers to differentiate active TB and LTBI: A systematic review. *J Infect.* (2020) 81:873–81. doi: 10.1016/j.jinf.2020.09.032
38. Lai RP, Meintjes G, Wilkinson KA, Graham CM, Marais S, Van der Plas H, et al. HIV-tuberculosis-associated immune reconstitution inflammatory syndrome is characterized by toll-like receptor and inflammasome signalling. *Nat Commun.* (2015) 6:8451. doi: 10.1038/ncomms9451
39. Abate E, Blomgran R, Verma D, Lerm M, Fredrikson M, Belayneh M, et al. Polymorphisms in CARD8 and NLRP3 are associated with extrapulmonary TB and poor clinical outcome in active TB in ethiopia. *Sci Rep.* (2019) 9:3126. doi: 10.1038/s41598-019-40121-8
40. Wilkinson KA, Oni T, Gideon HP, Goliath R, Wilkinson RJ, Riou C. Activation profile of *Mycobacterium tuberculosis*-specific CD4(+) T cells reflects disease activity irrespective of HIV status. *Am J Respir Crit Care Med.* (2016) 193:1307–10. doi: 10.1164/rccm.201601-0116LE
41. Bucsan AN, Chatterjee A, Singh DK, Foreman TW, Lee TH, Threeton B, et al. Mechanisms of reactivation of latent tuberculosis infection due to SIV coinfection. *J Clin Invest.* (2019) 129:5254–60. doi: 10.1172/JCI125810
42. Sharan R, Bucsan AN, Ganatra S, Paiardini M, Mohan M, Mehra S, et al. Chronic immune activation in TB/HIV co-infection. *Trends Microbiol.* (2020) 28:619–32. doi: 10.1016/j.tim.2020.03.015

Conflict of Interest: The authors declare that the research was conducted in the absence of any commercial or financial relationships that could be construed as a potential conflict of interest.

Copyright © 2021 Wilkinson, Schneider-Luftman, Lai, Barrington, Jhilmeet, Lowe, Kelly and Wilkinson. This is an open-access article distributed under the terms of the Creative Commons Attribution License (CC BY). The use, distribution or reproduction in other forums is permitted, provided the original author(s) and the copyright owner(s) are credited and that the original publication in this journal is cited, in accordance with accepted academic practice. No use, distribution or reproduction is permitted which does not comply with these terms.

frontiers in Immunology

ORIGINAL RESEARCH
published: 12 March 2021
doi: 10.3389/fimmu.2021.620622

HIV-Infected Patients Developing Tuberculosis Disease Show Early Changes in the Immune Response to Novel *Mycobacterium tuberculosis* Antigens

Noemi Rebecca Meier[1,2] *Manuel Battegay*[2,3], *Tom H. M. Ottenhoff*[4], *Hansjakob Furrer*[5], *Johannes Nemeth*[6] *and Nicole Ritz*[1,2,7,8]* *on behalf of the Swiss HIV Cohort Study*

[1] University of Basel Children's Hospital, Mycobacterial Research Laboratory, Basel, Switzerland, [2] University of Basel, Faculty of Medicine, Basel, Switzerland, [3] Division of Infectious Diseases and Hospital Epidemiology, University Hospital Basel, University of Basel, Basel, Switzerland, [4] Leiden University Medical Center, Department of Infectious Diseases, Leiden, Netherlands, [5] Department of Infectious Diseases, Bern University Hospital, University of Bern, Bern, Switzerland, [6] Division of Infectious Diseases, Zürich University Hospital, University of Zürich, Zurich, Switzerland, [7] University of Basel Children's Hospital, Paediatric Infectious Diseases and Vaccinology Unit, Basel, Switzerland, [8] Royal Children's Hospital Melbourne, Department of Paediatrics, University of Melbourne, Parkville, VIC, Australia

OPEN ACCESS

Edited by:
Jayne S. Sutherland, Medical Research Council the Gambia Unit (MRC), Gambia

Reviewed by:
Delia Goletti, Istituto Nazionale per le Malattie Infettive Lazzaro Spallanzani (IRCCS), Italy
Katalin A. Wilkinson, Francis Crick Institute, United Kingdom
Virginie Rozot, South African Tuberculosis Vaccine Initiative SATVI, South Africa

***Correspondence:**
Nicole Ritz
nicole.ritz@unibas.ch

Specialty section:
This article was submitted to Microbial Immunology, a section of the journal Frontiers in Immunology

Received: 23 October 2020
Accepted: 09 February 2021
Published: 12 March 2021

Citation:
Meier NR, Battegay M, Ottenhoff THM, Furrer H, Nemeth J and Ritz N (2021) HIV-Infected Patients Developing Tuberculosis Disease Show Early Changes in the Immune Response to Novel Mycobacterium tuberculosis Antigens. Front. Immunol. 12:620622. doi: 10.3389/fimmu.2021.620622

Background: In individuals living with HIV infection the development of tuberculosis (TB) is associated with rapid progression from asymptomatic TB infection to active TB disease. Sputum-based diagnostic tests for TB have low sensitivity in minimal and subclinical TB precluding early diagnosis. The immune response to novel *Mycobacterium tuberculosis in-vivo* expressed and latency associated antigens may help to measure the early stages of infection and disease progression and thereby improve early diagnosis of active TB disease.

Methods: Serial prospectively sampled cryopreserved lymphocytes from patients of the Swiss HIV Cohort Study developing TB disease ("cases") and matched patients with no TB disease ("controls") were stimulated with 10 novel *Mycobacterium tuberculosis* antigens. Cytokine concentrations were measured in cases and controls at four time points prior to diagnosis of TB: T1-T4 with T4 being the closest time point to diagnosis.

Results: 50 samples from nine cases and nine controls were included. Median CD4 cell count at T4 was 289/ul for the TB-group and 456/ul for the control group. Viral loads were suppressed in both groups. At T4 Rv2431c-induced and Rv3614/15c-induced interferon gamma-induced protein (IP)-10 responses and Rv2031c-induced and Rv2346/Rv2347c-induced tumor necrosis factor (TNF)-α responses were significantly higher in cases compared to controls ($p < 0.004$). At T3 - being up to 2 years prior to TB diagnosis - Rv2031c-induced TNF-α was significantly higher in cases compared to controls ($p < 0.004$). Area under the receiver operating characteristics (AUROC) curves resulted in an AUC > 0.92 for all four antigen-cytokine pairs.

Conclusion: The *in vitro Mycobacterium tuberculosis*-specific immune response in HIV-infected individuals that progress toward developing TB disease is different from those in HIV-infected individuals that do not progress to developing TB. These differences precede the clinical diagnosis of active TB up to 2 years, paving the way for the development of immune based diagnostics to predict TB disease at an early stage.

Keywords: T cell response, IGRA, RV, IP-10, TNF-alpha, Mycobacterium tuberculosis, TB, LTBI

BACKGROUND

Tuberculosis (TB) remains a major global health topic with an estimated quarter of the world's population being latently infected with *Mycobacterium tuberculosis* (1, 2). In 2019, an estimated 10 million people developed TB disease, killing 1.4 million people worldwide. Of those ∼208,000 were co-infected with HIV (3). HIV-infected individuals are at particular risk of rapid progression from TB infection to subclinical and active TB disease (4, 5). Early detection, prediction of TB progression and treatment of TB infection and disease in these high-risk groups is therefore crucial to prevent disease progression and further transmission (6–9).

In the recent years, the binary perception of active versus latent TB has been replaced with the concept that TB is a spectrum of disease. After infection by *Mycobacterium tuberculosis* the pathogen may be cleared, persist, progress to disease in a slow or rapid fashion, or cycle through subclinical stages before developing into symptomatic TB disease (10, 11). Understanding of these dynamics is inherently difficult because clinical samples are typically collected only once disease has already developed. In this regard, the Swiss HIV Cohort Study, a systematic longitudinal study enrolling HIV-infected individuals in Switzerland, offers a unique opportunity to monitor the development of disease prior to the development of clinically apparent symptoms. We hypothesized that the analysis of the *Mycobacterium tuberculosis*-specific immune response during the time preceding clinical disease may inform on kinetics and pathophysiology involved in this process and may help to develop improved early diagnostic assays.

Currently, detection of TB relies almost entirely on sputum-based diagnostic assays which are likely to have lower sensitivity in minimal and subclinical TB disease (12). The most developed non-sputum-based assay used in HIV-infected individuals detects urine lipoarabinomannan but has a very limited sensitivity of 42% in patients with symptoms which further decreases in those with subclinical TB disease and higher CD4 counts (13). Blood-based diagnostic tests such as interferon-γ release assays (IGRA) using the RD1-*Mycobacterium tuberculosis* antigens early secretory antigen target (ESAT)-6, and culture filtrate protein (CFP)-10 have also a limited sensitivity of ∼69% for detection of TB disease in HIV-infected individuals [pooled analysis from (14)]. In some studies the sensitivity of blood-based assays is even lower, as shown in a study within the framework of the Swiss HIV Cohort Study with 39% having a positive T-SPOT.TB within 6 months before culture-confirmed TB diagnosis (15).

Recent research suggest novel antigens may help to delineate the immune response preceding clinical disease as *Mycobacterium tuberculosis* changes its gene expression during infection and preceding clinical disease (16, 17). For example *Mycobacterium tuberculosis* antigens belonging to the group of latency associated antigens from the *Mycobacterium tuberculosis* dormancy of survival regulon (DosR) are of interest in the early and latent phases of infection (18). These genes are activated during the dormant non-replicative state and several studies show immune responses induced by these antigens to be more pronounced in latent TB infection compared to TB disease [reviewed in (16)]. Other antigens including heparin-binding haemagglutinin (HBHA) have also been used in blood tests for TB diagnosis (19, 20). In addition, the recently described *in-vivo* expressed *Mycobacterium tuberculosis* antigens, expressed in patients with pulmonary TB, have been found to elicit significant T cell responses (21). However, no study so far has been able to longitudinally investigate the immune response to these novel *Mycobacterium tuberculosis* antigens before the development of symptomatic TB disease.

The aim of this study was therefore to compare cytokine production after *in-vitro* stimulation with novel *Mycobacterium tuberculosis* antigens in HIV-infected patients up to 4 years prior to TB diagnosis. For this we used the prospectively collected and cryopreserved lymphocytes of the biobank of the Swiss HIV Cohort Study that allow longitudinal testing of the immune response prior to development of TB disease.

METHODS

Study Design and Population

This case-control study was done within the framework of the Swiss HIV Cohort study which is a large cohort study in Switzerland which prospectively enrolls adult HIV-infected individuals. Demographic and clinical data including CD4 count, HIV viral load, antiretroviral treatment and screening and treatment of opportunistic infections are routinely collected, and blood samples for biobanking are taken at least annually (15).

The database of the Swiss HIV Cohort study was searched for TB cases confirmed by culture or polymerase chain reaction

Abbreviations: AUROC, area under the receiver operating characteristics; BCG, Bacille Calmette-Guérin; CFP-10, culture filtrate protein 10; CI, confidence interval; DosR, dormancy of survival regulon; ESAT-6, early secretory antigen target 6; GM-CSF, granulocyte-macrophage colony-stimulating factor; IFN-γ, interferon-gamma; IGRA, interferon-γ release assay; IL, interleukin; IP-10, INF-γ-inducible protein 10; ROC, receiver operating characteristics; TB, tuberculosis; TNF-α, tumor necrosis factor α; TST, Tuberculin skin test.

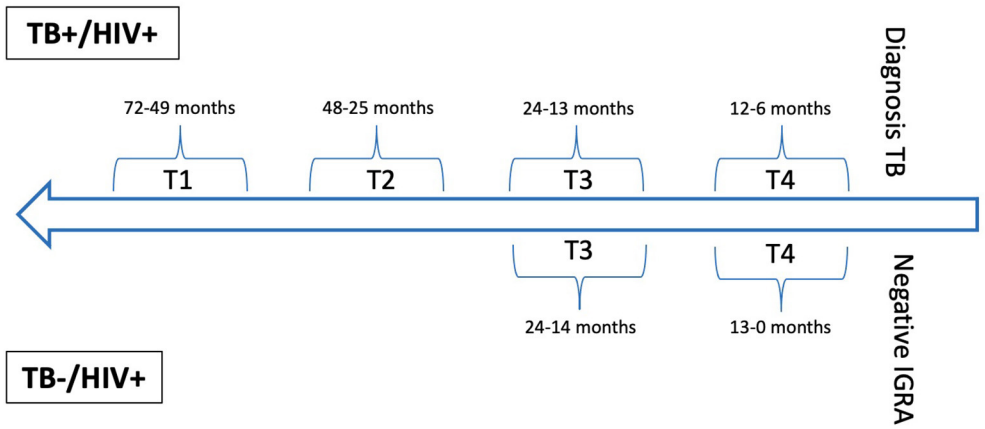

FIGURE 1 | Study sampling timeline for TB and control group.

and matched controls without a suspicion of TB and a negative IGRA. For cases annual or biennial blood samples (T1-T4), taken prior the diagnosis of TB disease were included. For controls two sequential annual blood samples (T3 and T4) were included, with T4 taken as close as possible to the negative IGRA (**Figure 1**, **Supplementary Table 1**). Matching was done for age, sex, body mass index, CD4 cell count, and HIV viral load.

Viability of Frozen Lymphocytes, Sample Preparation, and Stimulation

For best possible conditions using frozen isolated peripheral blood mononuclear cells (PBMC) the following precautions were taken to ensure test performance: (i) sample processing in study centers according to harmonized protocol [as described in (15)] (ii) quality control of frozen samples in the framework of different studies [as described in (15)] and viability check of samples before the start of the assay (minimum of 70% recovery rate) (iii) sample selection from three study centers only (Basel, Berne, Zurich) to assure optimal cryopreservation and shipment and (iv) exclusion of samples that were stored before 2001.

Thawed lymphocytes (100,000 cells/condition) were stimulated overnight for 17 h at 37°C with the positive controls phytohemagglutinin (Merck chemicals LTD., Beeston, Nottingham, UK) at a concentration of 5 µg/ml and staphylococcus enterotoxin B (Sigma Aldrich GmbH, Schnelldorf, Germany) at a concentration of 10 µg/ml, novel *Mycobacterium tuberculosis* antigens (Rv0081, Rv1733c, Rv2031c, Rv0867c, Rv2389c, Rv3407, Rv2346/47c, Rv2431c, Rv3614/15c, and Rv3865) and a fusion protein of ESAT-6 and CFP-10 [all recombinant proteins expressed from *Escherichia coli* BL21 were produced by Kees L.M.C. Franken from the Ottenhoff lab at Leiden University Medical Center in the Netherlands (22)] at a concentration of 5 µg/ml and left unstimulated in the presence of CD28 and CD49d antibodies (Biolegend Inc., San Diego, Ca 92121, USA) at a concentration of 2 µg/ml each. The addition of costimulatory antibodies CD28 and CD49d has been done according to previously published protocols (23–25). After stimulation supernatants were stored at −20°C until further analysis. Experiments were done in a biosafety level 3* facility.

Cytokine Measurement

Granulocyte-macrophage colony-stimulating factor (GM-CSF), interferon gamma (IFN-γ), IFN-γ -inducible protein (IP)-10, interleukin (IL)-1RA, IL-6, and tumor necrosis factor (TNF)-α were measured using a human cytokine / chemokine magnetic bead panel (Milliplex MAP kit, Merck Millipore, Billerica, MA, USA), a Magpix Luminex instrument and Xponent software (version 4.2 Luminex Corp, Austin, Texas, USA) according to manufacturer's instructions. Standard curves using a 5-parameter logistic regression were applied to calculate concentrations of cytokines. Antigen- and mitogen-induced cytokine production was calculated by subtraction of non-stimulated background concentrations from sample concentrations. Measurements below the limit of quantification were set to 0.1 pg/ml, measurements above the limit of quantification were set to 10,000 pg/ml (calibration range: 3.2–10,000 pg/ml). A valid positive control was defined as an uncorrected cytokine concentration > 20 pg/ml (26). A valid negative control was defined as uncorrected cytokine concentration < 20 pg/ml. In cases where the nil concentration was higher than 20 pg/ml, the positive control had to be higher than the nil concentration.

Statistical Analysis

Results from patients with invalid positive and negative control values were excluded from analysis for the specific time point and cytokine. If more than 25% of measurements from all patients for any cytokine were below the limit of quantification, the results from this cytokine were excluded from analysis. A Mann-Whitney *U*-test was used to compare differences in cytokine concentrations between the two groups at T3 and T4. Differences were considered significant if the *p*-value was < 0.004 (Bonferroni correction for multiple testing). Receiver operating characteristics (ROC) analyses were performed using area under the receiver operating characteristics (AUROC) where *p*-values were significant and optimal cut-off values determined.

Differences in cytokine production between time points were calculated as absolute difference between T3 and T4 for controls and between T1, T2, and T3 to T4 for cases. All plots and statistical analyses were performed using R-studio software (version 1.1.463).

Ethical Approval

The Swiss HIV Cohort Study was approved by the ethics committees of the different study centers and written consent was obtained from all participants.

RESULTS

Study Population

A total of 50 samples from 18 individuals were included in the final analysis. Seven cases were male, median age was 45 (IQR 38–51) years, median CD4 cell count was 289 cells/μl, median RNA viral load was 16 copies/ml at T4 (**Table 1**). The median (range) time between TB diagnosis and T4 lymphocyte collection was 117 (29–312) days. In the controls seven were male, median age was 52 (IQR 41.5–56.5) years, median CD4 count was 456 cells/μl, median RNA viral load was 0 copies/ml at T4. The median (range) time between negative IGRA and T4 lymphocyte collection was 0 (0–420) days (**Table 1**). Age, sex, body mass index, CD4 count and RNA viral load were not significantly different between cases and controls. At T4 seven cases and eight controls were on antiretroviral treatment.

TABLE 1 | Characteristics of study population.

Variable		Tuberculosis group (T4) N = 9		Control group (T4) N = 9	
		n	%	*n*	%
Median age, IQR (years)		45 (38–51)	-	52 (41.5–56.5)	-
Males		7	77.8	7	77.8
Median body mass index, IQR (kg/m^2)		21.7 (20.5–23.2)	-	25.8 (24.1–27.7)	-
White ethnicity		6	66.7	9	100
TB disease	Pulmonary	4	44.4	-	-
	Extrapulmonary	4	44.4	-	-
	Pulmonary and extrapulmonary	1	11.1	-	-
Median CD4 cell count at TB diagnosis, IQR (cells/μl)		289 (152–422.5)	-	456 (258.5–601)	-
Median HIV-RNA at TB diagnosis, IQR (copies/ml)		16 (0–121,500)	-	0 (0–10,030)	-
Median time between cell sampling at T4 and TB diagnosis, range (days)		117 (29–312)	-	0 (0–420)	-
Median time between cell sampling at T3 and TB diagnosis, range (days)		440 (68–846)	-	392 (0–938)	-
Antiretroviral therapy at TB diagnosis		7	77.8	8	88.9
TST*	Negative	5	55.6	2	22.2
	>5–9 mm	0	0	0	0
	10–14 mm	0	0	1	11.1
	>15 mm	1	11.1	0	0
	Not done	3	33.3	6	66.7
IGRA	Negative	0	0	9	100
	Positive	1	11.1	0	0
	Indeterminate	0	0	0	0
	Not done	8	88.8	0	0
TB diagnosis**	Culture positive	3	33.3	-	-
	Sputum positive	4	44.4	-	-
	FNP PCR positive	1	11.1	-	-
	Lymphnode biopsy positive	1	11.1	-	-

**TST, tuberculin skin test.*
***One TB patient had a positive IGRA with clinical suspicion of but had no microbiological confirmation.*

Antigen-Induced Cytokine Concentrations in Cases and Controls at T3 and T4

For the final analysis at T4 results from eight individuals were included for both study groups. At T3 results from seven individuals in the TB group and nine in the control group were included (**Supplementary Table 2**). GM-CSF, IFN-γ IL-6, IP-10, and TNF-α were detectable in most individuals in both study groups. Measurements for IL-1RA were commonly below the limit of quantification and therefore excluded from analysis (**Supplementary Table 3**).

Comparison of Results in TB Patients and Controls at Time Point Closest to Diagnosis (T4)

Median cytokine concentrations in response to *Mycobacterium tuberculosis* antigens were generally higher in cases compared to controls at T4. These differences were most pronounced for IFN-γ, IP-10, and TNF-α and reached statistical significance for Rv2031c-induced TNF-α and Rv2346/47c-induced TNF-α ($p < 0.002$ for both) as well as for Rv2431c-induced IP-10 and Rv3614/15c-induced IP-10 ($p < 0.004$, $p < 0.002$, respectively) (**Figure 2**). Importantly, cytokine concentrations for the ESAT-6/CFP-10-induced IFN-γ were not significantly different in cases and controls at T4 (**Supplementary Table 4**).

Comparison of Results in TB Patients and Controls at Time Point 3 (T3)

Median cytokine concentrations in response to *Mycobacterium tuberculosis* antigens at T3 were generally higher in TB patients compared to controls (**Figure 2**). These trends were most pronounced for GM-CSF and TNF-α and reached significance for Rv2031c-induced TNF-α ($p < 0.004$). Median cytokine concentrations for the ESAT-6/CFP-10 -induced IFN-γ were also not significantly different in cases and controls at T3 (**Supplementary Table 4**).

Area Under the Receiver Operating Characteristics

AUROC curves resulted in high AUC for the four antigen-cytokine pairs with significant differences between cases and

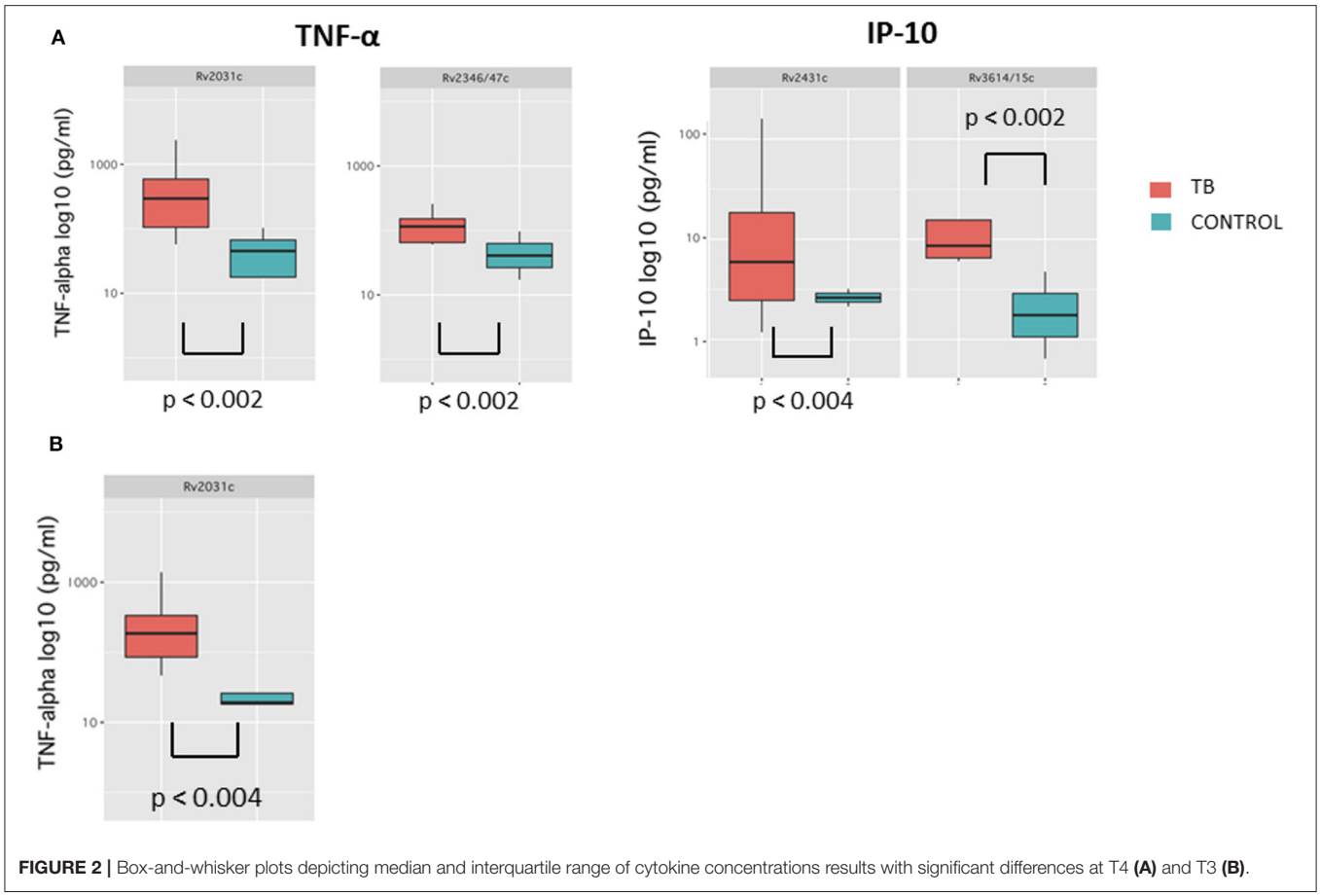

FIGURE 2 | Box-and-whisker plots depicting median and interquartile range of cytokine concentrations results with significant differences at T4 **(A)** and T3 **(B)**.

TABLE 2 | Discriminatory potential of antigen-cytokine in cases and controls at T3 and T4.

Antigen	Cytokine	TP	TB	*n*	Controls	*n*	*p*-value	AUROC	Cut-off	Sensitivity (%)	Specificity (%)
Rv2431c	IP-10	T4	6.0 (1.2–159.8)	8	−9.2 (−6.8-3.2)	7	<0.004	0.929 (95% CI = 0.800–1)	2.2	0.87	1
Rv3614/15c	IP-10	T4	8.6 (0.6–238.8)	8	−0.7 (−9.3-4.7)	7	<0.002	0.964 (95% CI = 0.881–1)	5.4	0.87	1
Rv2031c	TNF-α	T4	304.1 (57.3-2381.0)	8	9.2 (-72.9-103.1)	8	< 0.002	0.953 (95% CI= 0.862-1)	72.9	0.87	1
Rv2346/47c	TNF-α	T4	115.5 (6.6–1004.0)	8	−38.4 (-389.9-96.6)	8	<0.002	0.937 (95% CI = 0.824–1)	25.3	0.87	1
Rv2031c	TNF-α	T3	185.6 (46.5–1390.6)	7	2.6 (−814.1-447.7)	9	<0.004	0.921 (95% CI = 0.76–1)	36.3	1.0	0.89

Median concentrations of cytokines (pg/ml) and ranges (in parenthesis) induced by stimulation of lymphocytes overnight and ability to discriminate between TB group and control group. AUROC, Area under the receiver operating characteristics.

controls: Rv2431c-induced IP-10 AUC 0.929 (95% CI = 0.800–1; T4); Rv3614/15c-induced IP-10 AUC 0.964 (95% CI = 0.881–1: T4); Rv2031c-induced TNF-α AUC 0.953 (95% CI = 0.862–1; T4) and 0.921 (95% CI = 0.76–1; T3); Rv2346/47c-induced TNF-α AUC 0.937 (95% CI = 0.824–1; T4). Cut-off concentrations were 2.2 pg/ml for Rv2431c-induced IP-10, 5.4 pg/ml for Rv3614/15c-induced IP-10, 72.9 pg/ml for Rv2031c-induced TNF-α, 25.3 pg/ml for Rv2346/47c-induced and 36.3 pg/ml for Rv2031c-induced TNF-α (**Table 2** and **Figure 3**).

Antigen-Induced Cytokine Concentrations Over Time

Differences in median cytokine concentrations between T3 and T4 in the controls were variable. Differences in GM-CSF, IFN-γ, and IP-10 concentrations were small for most stimulatory antigens except for ESAT-6/CFP-10 and Rv1733c. Larger differences in cytokine concentrations were observed for IL-6 and TNF-α. For IL-6 these differences were most pronounced following the with ESAT-6/CFP-10, Rv1733c, and Rv2389c

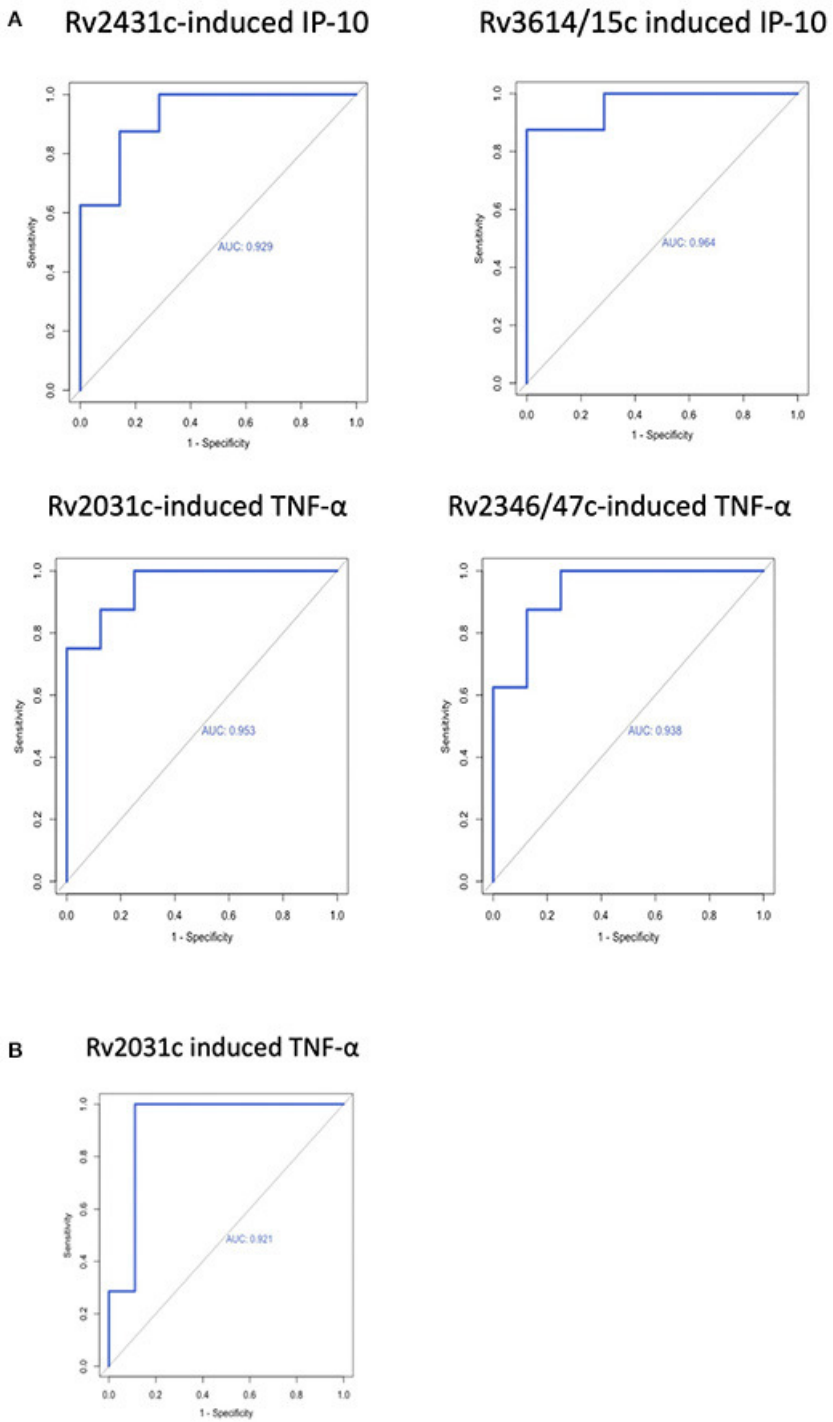

FIGURE 3 | Receiver operating characteristic curves of antigen-cytokine pairs with significant difference between cases and controls at **(A)** T4 and **(B)** T3.

(**Supplementary Figure 1**, **Figure 5** show all data in normal scale for all cytokines).

Differences in median cytokine concentrations varied between T1, T2, T3, and T4 in the TB group and no clear pattern was detected (**Figure 4**). Generally, changes over time were more pronounced for IL-6 and TNF-α. Induced cytokine concentrations varied substantially for ESAT-6/CFP-10, Rv1733c, Rv2389c, and Rv3865 specifically for GM-CSF, IL-6, and TNF-α. Smaller differences in concentrations were seen in response to Rv0081, Rv0867c, Rv3407, Rv2346/47c, Rv2431c, and

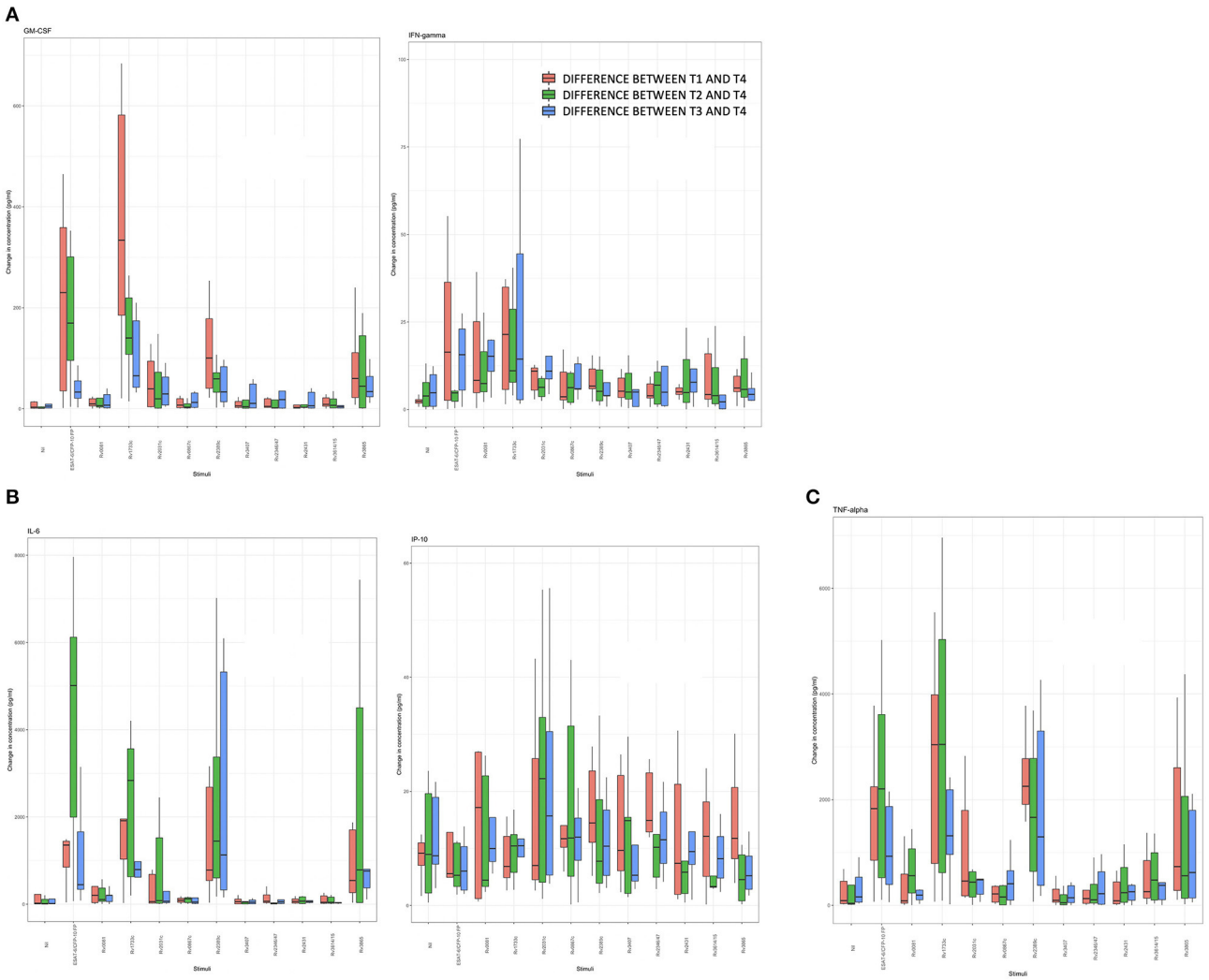

FIGURE 4 | Difference of cytokine concentrations between T1, T2, T3, and T4 for the cases **(A–C)**.

Rv3614/15c. Interestingly, differences in cytokine concentrations for the three *in-vivo* expressed antigens (Rv2346/47c, Rv2431c, and Rv3614/15c) over time were small among all cytokines (**Figures 4**, **5A–F** showing all data in normal scale for all cytokines).

DISCUSSION

HIV-infected patients are at high risk of rapid progression from TB infection to TB disease. This study provides the first results in a unique setting of HIV-infected individuals with confirmed TB diagnosis in which their immune-response can be investigated prospectively during the stages developing TB disease prior to clinical diagnosis. The routine annual biobanking of lymphocytes allows analysis of potential early markers for minimal and subclinical TB disease. In the present study we show that several antigen-cytokine combinations clearly differentiate HIV-infected patients developing TB from those that do not develop TB up to 2 years prior to clinical diagnosis.

The three *in vivo*-expressed *Mycobacterium tuberculosis* antigens, Rv2346/47c, Rv2431c, and Rv3614/15c and the DosR antigen Rv2031c induced significantly higher TNF-α and IP-10 responses in TB patients shortly before clinical diagnosis compared to controls. Further to this our study found, that differences between patients developing TB and controls were already observed more than 12 months prior to diagnosis. Significantly different concentrations of TNF-α induced by Rv2031c were found between 1 and 2 years prior to clinical diagnosis of TB. Thus, this antigen-cytokine pair may serve as an early and antigen specifically induced correlate for TB infection and/or subclinical TB disease.

The potential of novel *Mycobacterium tuberculosis* antigens has mainly been studied for diagnostic purposes [summarized in (16)] or as novel vaccine candidates (21). So far, no study has assessed those antigens

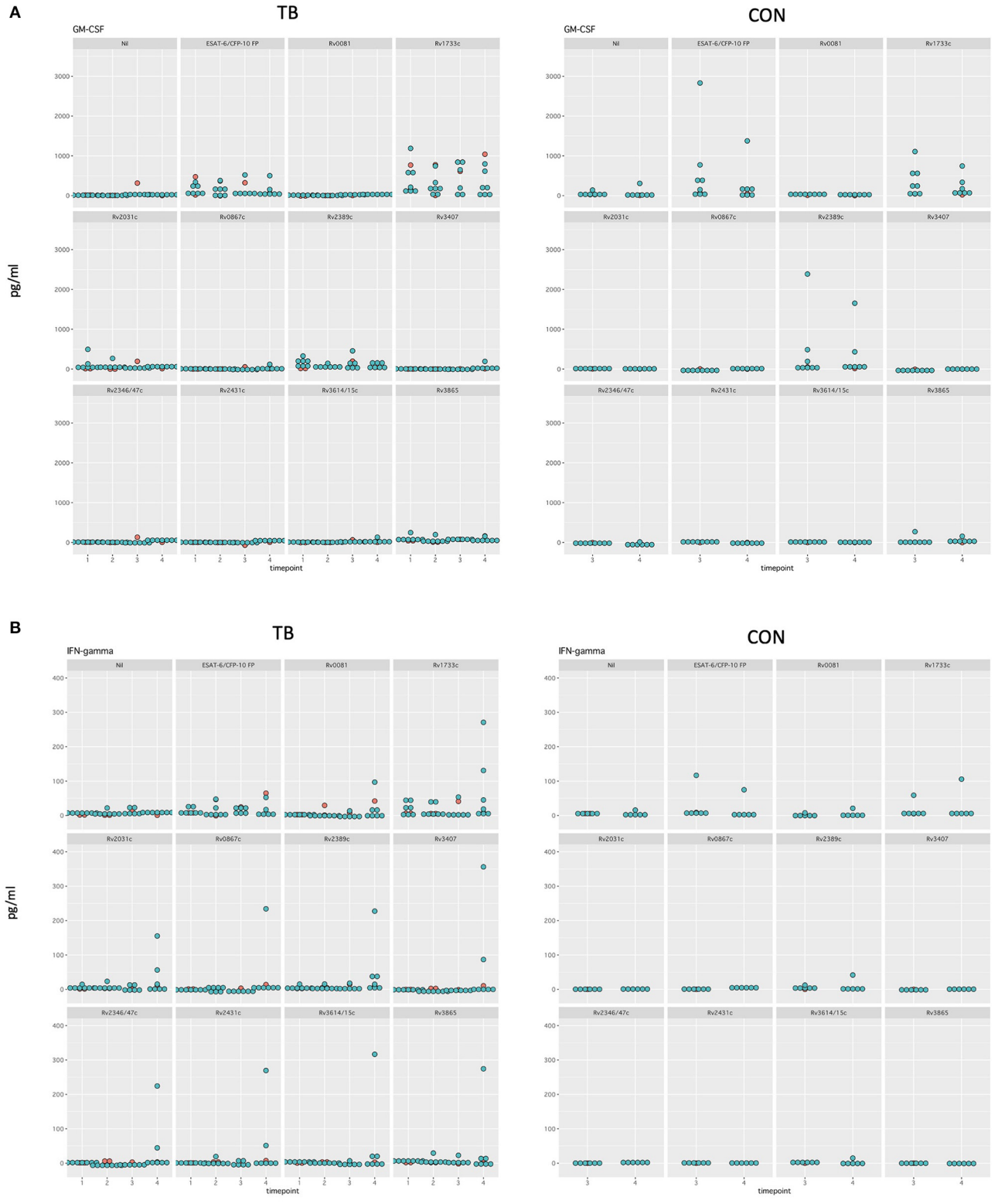

FIGURE 5 | (Continued)

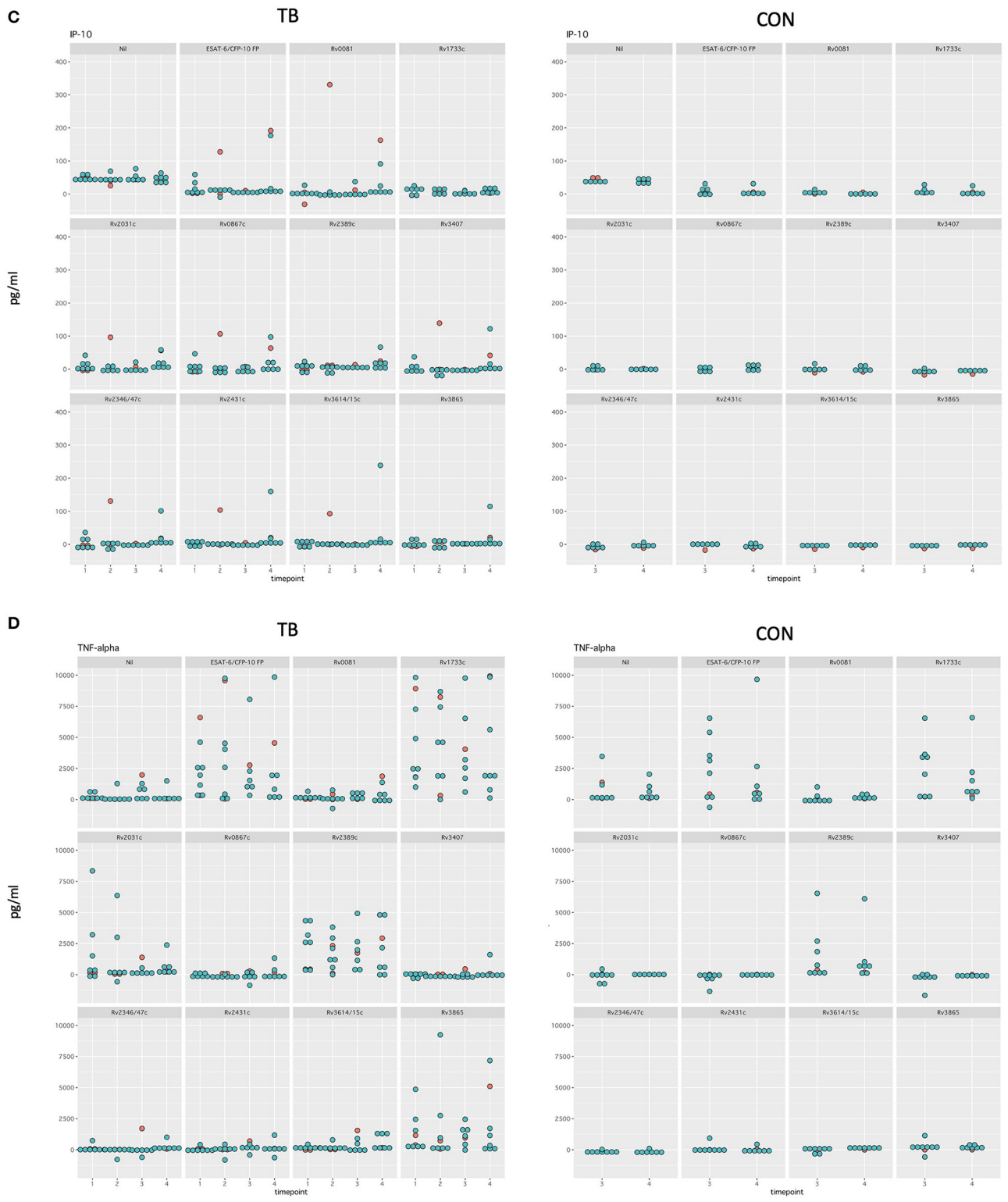

FIGURE 5 | (Continued)

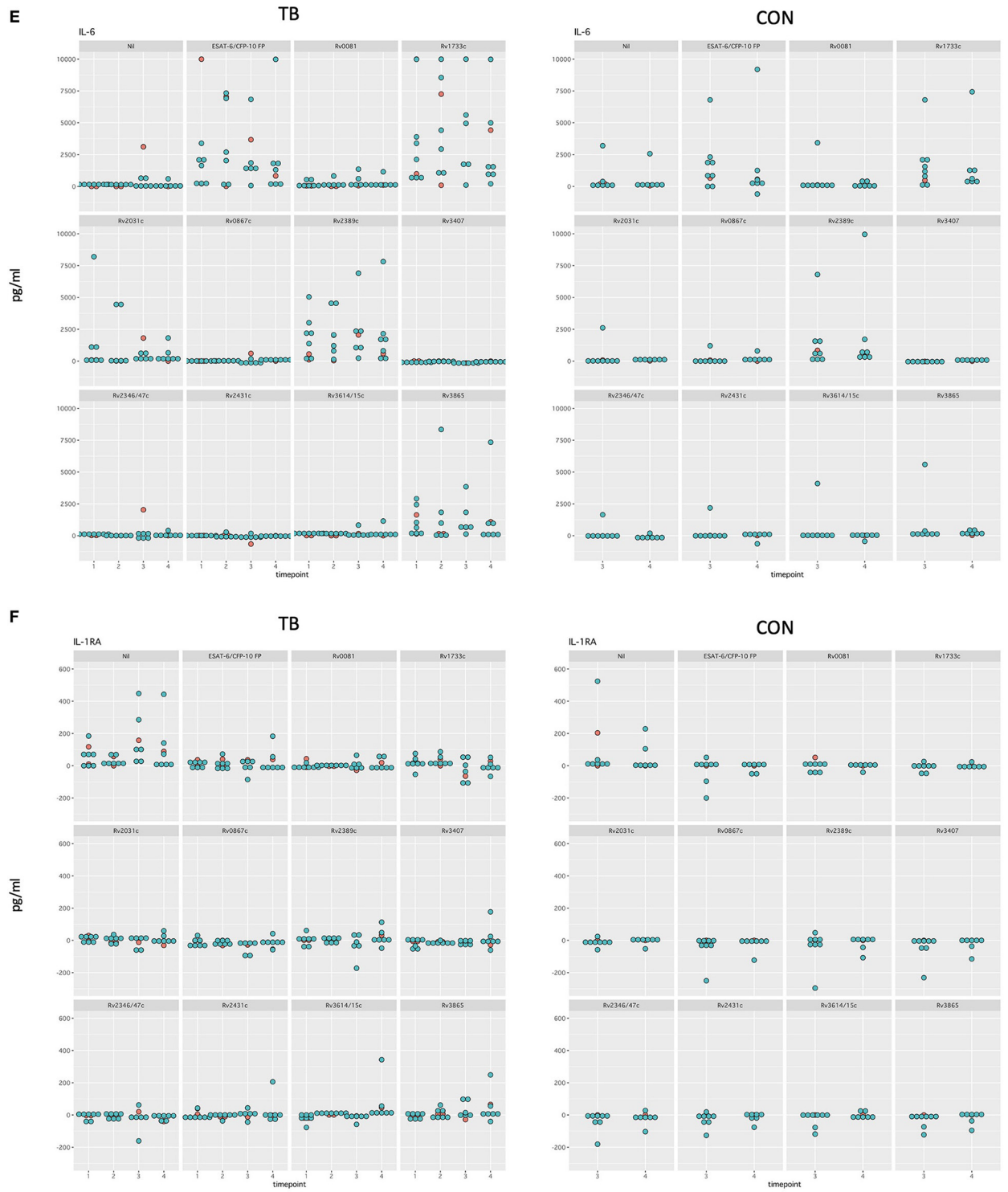

FIGURE 5 | Dotplot of all cytokines in normal scale comparing TB and control group for all timepoints included **(A–F)**. Patients receiving antiretroviral treatment are color coded in red and patients not receiving antiretroviral treatment are color coded in blue.

during development of TB disease. We included the latency associated antigens from the *Mycobacterium tuberculosis* DosR regulon which encodes for ∼50 genes that are activated during the dormant non-replicative stage of TB (18). The DosR encoded antigens Rv0081, Rv1733c, and Rv2031c were used in this study based

on evidence of previous studies that these are highly immunogenic (27–30).

Our results are in line with the few previous studies investigating this antigen. A study in a high TB-endemic setting with non-HIV-infected individuals described increased TNF-α concentrations induced by Rv2031c in patients with TB infection compared to controls (30). Important for this antigen is the role of measuring cytokines other than IFN-γ, as two other studies measuring IFN-γ only did not find significant differences in patients with TB disease, TB infection and controls (28, 31). A further study including a subgroup of four HIV-infected individuals also did not find noteworthy responses of IFN-γ induced by Rv2031c and two cytokines that were not measured in our study (IL-2, IL-17) (32).

The *in vivo*-expressed *Mycobacterium tuberculosis* antigens included in our study have not been studied in detail in humans. Research suggests that they are associated with virulence (Rv2346/47c, Rv2431c, Rv3614/15c, and Rv3865) (33), in particular Rv2346/47c, Rv3614/15c, and Rv3865 are all associated with the ESAT-6 secretion system. Since their absence in the Bacille Calmette-Guérin (BCG) vaccine strain, some of these antigens are of special interest in the diagnosis of previously immunized individuals (34). Data from our own study in children also showed the discriminatory potential of Rv2346/47c-induced IP-10 response in a population of HIV-negative children for TB infection and disease compared to exposed non-infected children (25). Further to this animal data showed the added value of Rv2346c when pooled with ESAT-6, CFP-10 and Rv3615c in a skin test in TB infected cattle (35).

Our study highlights the importance of antigen-induced TNF-α and IP-10 in the immune response during TB infection and developing disease. TNF-α seems to be key in HIV-TB coinfection with concentrations detected in this setting (36). Similar findings were seen in a South-African study using Quantiferon supernatants of HIV-infected individuals with TB and controls which showed that IP-10 was significantly different in stimulated and unstimulated samples between the groups (37). Generally, TNF-α is key for granuloma formation and recruitment of immune cells to the site of infection (38). We found TNF-α concentration to be significantly elevated in the TB group compared to the control group for two antigens. Several studies also show the discriminatory potential of TNF-α in diagnosing different stages of TB (23, 24, 39). IP-10 has been investigated in several studies (40, 41) also including HIV-infected individuals (42–45). In the current study and in our study using the same assays in children (25), *ex vivo* IP-10 responses significantly increased diagnostic accuracy if compared to the current standard testing.

Importantly, the current standard immunodiagnostic test—being IFN-γ-induced by ESAT-6/CFP-10—was unable to differentiate cases from controls at any time point. This suggests that the use of novel antigen-cytokine pairs is clearly needed to improve sensitivity to detect TB infection and disease in HIV-infected individuals. Due to its exploratory character this study included a limited set of samples. Despite this, clear trends in cytokine production induced by novel *Mycobacterium tuberculosis* antigens between cases and controls could be observed. The study setting prevented us from using fresh blood for the stimulation assays. To account for cryopreservation precautions were taken to minimize impact on assay performance. Some cytokines showed a high range of values and considerable variation over time. In our study setting we are unable to determine if this is true variation due to disease progression or variability.

CONCLUSIONS

The *ex vivo Mycobacterium tuberculosis*-specific immune response of HIV-infected individuals developing TB disease is different form HIV-infected individuals without signs of TB infection. In line with our hypothesis, antigen specific responses were different prior to the clinical development of TB. These differences precede the clinical diagnosis of active TB up to 2 years, paving the way for the development of immune based diagnostics to predict early TB disease.

DATA AVAILABILITY STATEMENT

The raw data supporting the conclusions of this article will be made available by the authors, without undue reservation.

ETHICS STATEMENT

The studies involving human participants were reviewed and approved by Ethikkommission beider Basel, Kantonale Ethikkommission Bern (21/88); Comité départemental d'éthique des spécialités médicales et de médecine communautaire et de premier recours, Hôpitaux Universitaires de Genève (01–142); Commission cantonale d'éthique de la recherche sur l'être humain, Canton de Vaud (131/01); Comitato etico cantonale, Repubblica e Cantone Ticino (CE 813); Ethikkommission des Kantons St. Gallen (EKSG 12/003); Kantonale Ethikkommission Zürich (KEK-ZH-NR: EK-793). The patients/participants provided their written informed consent to participate in this study.

MEMBERS OF THE SWISS HIV COHORT STUDY

Aebi-Popp K, Anagnostopoulos A, Battegay M, Bernasconi E, Böni J, Braun DL, Bucher HC, Calmy A, Cavassini M, Ciuffi A, Dollenmaier G, Egger M, Elzi L, Fehr J, Fellay J, Furrer H, Fux CA, Günthard HF (President of the SHCS), Haerry D (deputy of "Positive Council"), Hasse B, Hirsch HH, Hoffmann M, Hösli I, Huber M, Kahlert CR (Chairman of the Mother & Child Substudy), Kaiser L, Keiser O, Klimkait T, Kouyos RD, Kovari H, Ledergerber B, Martinetti G, Martinez de Tejada B, Marzolini C, Metzner KJ, Müller N, Nicca D, Paioni P, Pantaleo G, Perreau M, Rauch A (Chairman of the Scientific Board), Rudin C, Scherrer AU (Head of Data Center), Schmid P, Speck R, Stöckle

M (Chairman of the Clinical and Laboratory Committee), Tarr P, Trkola A, Vernazza P, Wandeler G, Weber R, Yerly S.

AUTHOR CONTRIBUTIONS

NM, NR, and MB developed the research question and the study design. TO provided the antigens. NM performed the experiments. NM and NR performed the data analysis. MB, TO, HF, and JN critically revised the analysis and the draft manuscript written by NM and NR. All authors reviewed and approved the final manuscript.

FUNDING

This study has been financed within the framework of the Swiss HIV Cohort Study, supported by the Swiss National Science Foundation (grant #177499), by SHCS project 813 and by the SHCS research foundation. The data are gathered by the Five Swiss University Hospitals, two Cantonal Hospitals, 15 affiliated hospitals and 36 private physicians (listed in http://www.shcs.ch/180-health-care-providers).

ACKNOWLEDGMENTS

We thank the patients from the Swiss HIV cohort study, the nurses, physicians, and the lab personnel for their excellent work. A special thank goes to Alexandra Scherrer from the data center for her support. We also want to thank Kees LMC Franken for producing all the mycobacterial antigens used in our study.

SUPPLEMENTARY MATERIAL

The Supplementary Material for this article can be found online at: https://www.frontiersin.org/articles/10.3389/fimmu.2021.620622/full#supplementary-material

REFERENCES

1. Houben RM, Dodd PJ. The global burden of latent tuberculosis infection: a re-estimation using mathematical modelling. *PLoS Med*. (2016) 13:e1002152. doi: 10.1371/journal.pmed.1002152
2. Cohen A, Mathiasen VD, Schon T, Wejse C. The global prevalence of latent tuberculosis: a systematic review and meta-analysis. *Eur Respiratory J*. (2019) 54:655. doi: 10.1183/13993003.00655-2019
3. World Health Organization. *Global Tuberculosis Report 2020* Geneva. (2020).
4. Kwan CK, Ernst JD. HIV and tuberculosis: a deadly human syndemic. *Clin Microbiol Rev*. (2011) 24:351–76. doi: 10.1128/CMR.00042-10
5. Havlir DV, Barnes PF. Tuberculosis in patients with human immunodeficiency virus infection. *N Engl J Med*. (1999) 340:367–73. doi: 10.1056/NEJM199902043400507
6. Menzies D, Pai M, Comstock G. Meta-analysis: new tests for the diagnosis of latent tuberculosis infection: areas of uncertainty and recommendations for research. *Ann Internal Med*. (2007) 146:340–54. doi: 10.7326/0003-4819-146-5-200703060-00006
7. Sauzullo I, Vullo V, Mastroianni CM. Detecting latent tuberculosis in compromised patients. *Curr Opin Infect Dis*. (2015) 28:275–82. doi: 10.1097/QCO.0000000000000158
8. Elzi L, Schlegel M, Weber R, Hirschel B, Cavassini M, Schmid P, et al. Reducing tuberculosis incidence by tuberculin skin testing, preventive treatment, and antiretroviral therapy in an area of low tuberculosis transmission. *Clin Infect Dis*. (2007) 44:94–102. doi: 10.1086/510080
9. Esmail H, Cobelens F, Goletti D. Transcriptional biomarkers for predicting development of tuberculosis: progress and clinical considerations. *Eur Respiratory J*. (2020) 55:1957. doi: 10.1183/13993003.01957-2019
10. Ritz N, Curtis N. Novel concepts in the epidemiology, diagnosis and prevention of childhood tuberculosis. *Swiss Med Wkly*. (2014) 144:w14000. doi: 10.4414/smw.2014.14000
11. Drain PK, Bajema KL, Dowdy D, Dheda K, Naidoo K, Schumacher SG, et al. Incipient and subclinical tuberculosis: a clinical review of early stages and progression of infection. *Clin Microbiol Rev*. (2018) 31:18. doi: 10.1128/CMR.00021-18
12. Sohn H, Aero AD, Menzies D, Behr M, Schwartzman K, Alvarez GG, et al. Xpert MTB/RIF testing in a low tuberculosis incidence, high-resource setting: limitations in accuracy and clinical impact. *Clin Infect Dis*. (2014) 58:970–6. doi: 10.1093/cid/ciu022
13. Bjerrum S, Schiller I, Dendukuri N, Kohli M, Nathavitharana RR, Zwerling AA, et al. Lateral flow urine lipoarabinomannan assay for detecting active tuberculosis in people living with HIV. *Cochrane Database Syst Rev*. (2019) 10:CD011420. doi: 10.1002/14651858.CD011420.pub3
14. Huo ZY, Peng L. Accuracy of the interferon-gamma release assay for the diagnosis of active tuberculosis among HIV-seropositive individuals: a systematic review and meta-analysis. *BMC Infect Dis*. (2016) 16:8. doi: 10.1186/s12879-016-1687-8
15. Elzi L, Steffen I, Furrer H, Fehr J, Cavassini M, Hirschel B, et al. Improved sensitivity of an interferon-gamma release assay [T-SPOT.TB (TM)] in combination with tuberculin skin test for the diagnosis of latent tuberculosis in the presence of HIV co-Infection. *BMC Infect Dis*. (2011) 11:319. doi: 10.1186/1471-2334-11-319
16. Meier NR, Jacobsen M, Ottenhoff THM, Ritz N. A systematic review on novel *Mycobacterium tuberculosis* antigens and their discriminatory potential for the diagnosis of latent and active tuberculosis. *Front Immunol*. (2018) 9:2476. doi: 10.3389/fimmu.2018.02476
17. Ernst JD. The immunological life cycle of tuberculosis. *Nat Rev Immunol*. (2012) 12:581–91. doi: 10.1038/nri3259
18. Voskuil MI, Schnappinger D, Visconti KC, Harrell MI, Dolganov GM, Sherman DR, et al. Inhibition of respiration by nitric oxide induces a *Mycobacterium tuberculosis* dormancy program. *J Exp Med*. (2003) 198:705–13. doi: 10.1084/jem.20030205
19. Chiacchio T, Delogu G, Vanini V, Cuzzi G, De Maio F, Pinnetti C, et al. Immune characterization of the HBHA-specific response in *Mycobacterium tuberculosis*-infected patients with or without HIV infection. *PLoS ONE*. (2017) 12:e0183846. doi: 10.1371/journal.pone.0183846
20. Delogu G, Vanini V, Cuzzi G, Chiacchio T, De Maio F, Battah B, et al. Lack of response to HBHA in HIV-infected patients with latent tuberculosis infection. *Scand J Immunol*. (2016) 84:344–52. doi: 10.1111/sji.12493
21. Coppola M, van Meijgaarden KE, Franken KL, Commandeur S, Dolganov G, Kramnik I, et al. New genome-wide algorithm identifies novel *in-vivo* expressed mycobacterium tuberculosis antigens inducing human T-cell responses with classical and unconventional cytokine profiles. *Sci Rep*. (2016) 6:37793. doi: 10.1038/srep37793
22. Franken KL, Hiemstra HS, van Meijgaarden KE, Subronto Y, den Hartigh J, Ottenhoff TH, et al. Purification of his-tagged proteins by immobilized chelate affinity chromatography: the benefits from the use of organic solvent. *Protein Expression Purification*. (2000) 18:95–9. doi: 10.1006/prep.1999.1162
23. Tebruegge M, Dutta B, Donath S, Ritz N, Forbes B, Camacho-Badilla K, et al. Mycobacteria-specific cytokine responses detect tuberculosis infection and distinguish latent from active tuberculosis. *Am J Respiratory Crit Care Med*. (2015) 192:485–99. doi: 10.1164/rccm.201501-0059OC
24. Tebruegge M, Ritz N, Donath S, Dutta B, Forbes B, Clifford V, et al. Mycobacteria-specific mono- and polyfunctional CD4+ T cell profiles in children with latent and active tuberculosis: a prospective proof-of-concept study. *Front Immunol*. (2019) 10:431. doi: 10.3389/fimmu.2019.00431

25. Meier NR, Sutter T, Vogt JE, Ottenhoff THM, Jacobsen M, Ritz N. Machine learning algorithms evaluate immune response to novel *Mycobacterium tuberculosis* antigens for diagnosis of tuberculosis. *Front Cell Infect Microbiol*. (2020) 10:594030. doi: 10.3389/fcimb.2020.594030
26. Rangaka MX, Wilkinson KA, Glynn JR, Ling D, Menzies D, Mwansa-Kambafwile J, et al. Predictive value of interferon-gamma release assays for incident active tuberculosis: a systematic review and meta-analysis. *Lancet Infect Dis*. (2012) 12:45–55. doi: 10.1016/S1473-3099(11)70210-9
27. Chegou NN, Essone PN, Loxton AG, Stanley K, Black GF, van der Spuy GD, et al. Potential of host markers produced by infection phase-dependent antigen-stimulated cells for the diagnosis of tuberculosis in a highly endemic area. *PLoS ONE*. (2012) 7:e38501. doi: 10.1371/journal.pone.0038501
28. Hozumi H, Tsujimura K, Yamamura Y, Seto S, Uchijima M, Nagata T, et al. Immunogenicity of dormancy-related antigens in individuals infected with *Mycobacterium tuberculosis* in Japan. *Int J Tuberculosis Lung Dis*. (2013) 17:818–24. doi: 10.5588/ijtld.12.0695
29. Serra-Vidal MM, Latorre I, Franken KL, Diaz J, de Souza-Galvao ML, Casas I, et al. Immunogenicity of 60 novel latency-related antigens of *Mycobacterium tuberculosis*. *Front Microbiol*. (2014) 5:517. doi: 10.3389/fmicb.2014.00517
30. Belay M, Legesse M, Mihret A, Bekele Y, Ottenhoff TH, Franken KL, et al. Pro- and anti-inflammatory cytokines against Rv2031 are elevated during latent tuberculosis: a study in cohorts of tuberculosis patients, household contacts and community controls in an endemic setting. *PLoS ONE*. (2015) 10:e0124134. doi: 10.1371/journal.pone.0124134
31. Goletti D, Butera O, Vanini V, Lauria FN, Lange C, Franken KL, et al. Response to Rv2628 latency antigen associates with cured tuberculosis and remote infection. *Eur Respiratory J*. (2010) 36:135–42. doi: 10.1183/09031936.00140009
32. Loxton AG, Black GF, Stanley K, Walzl G. Heparin-binding hemagglutinin induces IFN-gamma(+) IL-2(+) IL-17(+) multifunctional CD4(+) T cells during latent but not active tuberculosis disease. *Clin Vaccine Immunol*. (2012) 19:746–51. doi: 10.1128/CVI.00047-12
33. Commandeur S, van Meijgaarden KE, Prins C, Pichugin AV, Dijkman K, van den Eeden SJ, et al. An unbiased genome-wide *Mycobacterium tuberculosis* gene expression approach to discover antigens targeted by human T cells expressed during pulmonary infection. *J Immunol*. (2013) 190:1659–71. doi: 10.4049/jimmunol.1201593
34. Mahairas GG, Sabo PJ, Hickey MJ, Singh DC, Stover CK. Molecular analysis of genetic differences between *Mycobacterium bovis* BCG and virulent M-bovis. *J Bacteriol*. (1996) 178:1274–82. doi: 10.1128/JB.178.5.1274-1282.1996
35. Jones GJ, Whelan A, Clifford D, Coad M, Vordermeier HM. Improved skin test for differential diagnosis of bovine tuberculosis by the addition of Rv3020c-derived peptides. *Clin Vaccine Immunol*. (2012) 19:620–2. doi: 10.1128/CVI.00024-12
36. Whalen C, Horsburgh CR, Hom D, Lahart C, Simberkoff M, Ellner J. Accelerated course of human-immunodeficiency-virus infection after tuberculosis. *Am J Respiratory Crit Care Med*. (1995) 151:129–35. doi: 10.1164/ajrccm.151.1.7812542
37. Lesosky M, Rangaka MX, Pienaar C, Coussens AK, Goliath R, Mathee S, et al. Plasma biomarkers to detect prevalent or predict progressive tuberculosis associated with human immunodeficiency virus-1. *Clin Infect Dis*. (2019) 69:295–305. doi: 10.1093/cid/ciy823
38. Algood HM, Lin PL, Flynn JL. Tumor necrosis factor and chemokine interactions in the formation and maintenance of granulomas in tuberculosis. *Clin Infect Dis*. (2005) 41(Suppl.3):S189–93. doi: 10.1086/429994
39. Wang F, Hou H, Xu L, Jane M, Peng J, Lu Y, et al. *Mycobacterium tuberculosis*-specific TNF-alpha is a potential biomarker for the rapid diagnosis of active tuberculosis disease in Chinese population. *PLoS ONE*. (2013) 8:e79431. doi: 10.1371/journal.pone.0079431
40. Ruhwald M, Bjerregaard-Andersen M, Rabna P, Kofoed K, Eugen-Olsen J, Ravn P. CXCL10/IP-10 release is induced by incubation of whole blood from tuberculosis patients with ESAT-6, CFP10 and TB7.7. *Microbes Infection*. (2007) 9:806–12. doi: 10.1016/j.micinf.2007.02.021
41. Aabye MG, Ravn P, Johansen IS, Eugen-Olsen J, Ruhwald M. Incubation of whole blood at 39°C augments gamma interferon (IFN-gamma)-induced protein 10 and IFN-gamma responses to *Mycobacterium tuberculosis* antigens. *Clin Vaccine Immunol*. (2011) 18:1150–6. doi: 10.1128/CVI.00051-11
42. Vanini V, Petruccioli E, Gioia C, Cuzzi G, Orchi N, Rianda A, et al. IP-10 is an additional marker for tuberculosis (TB) detection in HIV-infected persons in a low-TB endemic country. *J Infection*. (2012) 65:49–59. doi: 10.1016/j.jinf.2012.03.017
43. Goletti D, Raja A, Syed Ahamed Kabeer B, Rodrigues C, Sodha A, Carrara S, et al. Is IP-10 an accurate marker for detecting *M. tuberculosis*-specific response in HIV-infected persons? *PLoS ONE*. (2010) 5:e12577. doi: 10.1371/journal.pone.0012577
44. Kabeer BS, Sikhamani R, Raja A. Comparison of interferon gamma and interferon gamma-inducible protein-10 secretion in HIV-tuberculosis patients. *Aids*. (2010) 24:323–5. doi: 10.1097/QAD.0b013e32833 4895e
45. Aabye MG, Ruhwald M, Praygod G, Jeremiah K, Faurholt-Jepsen M, Faurholt-Jepsen D, et al. Potential of interferon-gamma-inducible protein 10 in improving tuberculosis diagnosis in HIV-infected patients. *Eur Respiratory J*. (2010) 36:1488–90. doi: 10.1183/09031936.000 39010

Conflict of Interest: The authors declare that the research was conducted in the absence of any commercial or financial relationships that could be construed as a potential conflict of interest.

Copyright © 2021 Meier, Battegay, Ottenhoff, Furrer, Nemeth and Ritz. This is an open-access article distributed under the terms of the Creative Commons Attribution License (CC BY). The use, distribution or reproduction in other forums is permitted, provided the original author(s) and the copyright owner(s) are credited and that the original publication in this journal is cited, in accordance with accepted academic practice. No use, distribution or reproduction is permitted which does not comply with these terms.

frontiers in Immunology

REVIEW
published: 30 June 2021
doi: 10.3389/fimmu.2021.714808

Underwhelming or Misunderstood? Genetic Variability of Pattern Recognition Receptors in Immune Responses and Resistance to *Mycobacterium tuberculosis*

Jean-Yves Dubé[1,2,3]*, *Vinicius M. Fava*[2,3], *Erwin Schurr*[1,2,3,4,5] *and Marcel A. Behr*[1,2,3,5]*

[1] Department of Microbiology and Immunology, McGill University, Montreal, QC, Canada, [2] Program in Infectious Diseases and Immunity in Global Health, The Research Institute of the McGill University Health Centre, Montreal, QC, Canada, [3] McGill International TB Centre, McGill University, Montreal, QC, Canada, [4] Department of Human Genetics, Faculty of Medicine, McGill University, Montreal, QC, Canada, [5] Department of Medicine, Faculty of Medicine, McGill University, Montreal, QC, Canada

OPEN ACCESS

Edited by:
Chetan Seshadri,
University of Washington,
United States

Reviewed by:
Sarah Dunstan,
The University of Melbourne, Australia
Thomas Richard Hawn,
University of Washington,
United States

***Correspondence:**
Jean-Yves Dubé
jean-yves.dube@mail.mcgill.ca
Marcel A. Behr
marcel.behr@mcgill.ca

Specialty section:
This article was submitted to Microbial Immunology, a section of the journal Frontiers in Immunology

Received: 25 May 2021
Accepted: 17 June 2021
Published: 30 June 2021

Citation:
Dubé J-Y, Fava VM, Schurr E and Behr MA (2021) Underwhelming or Misunderstood? Genetic Variability of Pattern Recognition Receptors in Immune Responses and Resistance to Mycobacterium tuberculosis. Front. Immunol. 12:714808. doi: 10.3389/fimmu.2021.714808

Human genetic control is thought to affect a considerable part of the outcome of infection with *Mycobacterium tuberculosis* (*Mtb*). Most of us deal with the pathogen by containment (associated with clinical "latency") or sterilization, but tragically millions each year do not. After decades of studies on host genetic susceptibility to *Mtb* infection, genetic variation has been discovered to play a role in tuberculous immunoreactivity and tuberculosis (TB) disease. Genes encoding pattern recognition receptors (PRRs) enable a consistent, molecularly direct interaction between humans and *Mtb* which suggests the potential for co-evolution. In this review, we explore the roles ascribed to PRRs during *Mtb* infection and ask whether such a longstanding and intimate interface between our immune system and this pathogen plays a critical role in determining the outcome of *Mtb* infection. The scientific evidence to date suggests that PRR variation is clearly implicated in altered immunity to *Mtb* but has a more subtle role in limiting the pathogen and pathogenesis. In contrast to 'effectors' like IFN-γ, IL-12, Nitric Oxide and TNF that are critical for *Mtb* control, 'sensors' like PRRs are less critical for the outcome of *Mtb* infection. This is potentially due to redundancy of the numerous PRRs in the innate arsenal, such that *Mtb* rarely goes unnoticed. Genetic association studies investigating PRRs during *Mtb* infection should therefore be designed to investigate endophenotypes of infection – such as immunological or clinical variation – rather than just TB disease, if we hope to understand the molecular interface between innate immunity and *Mtb*.

Keywords: mycobacterium tuberculosis, tuberculosis, pattern recognition receptor (PRR), genetic association studies (GAS), C-type lectin receptors (CLRs), NOD-like receptors (NLRs), toll-like receptors (TLR), microbe associated molecular pattern (MAMP)

INTRODUCTION

Tuberculosis (TB) was the number one cause of death due to a single infectious agent, *Mycobacterium tuberculosis* (*Mtb*), in the year 2019 according to the WHO. SARS-CoV-2 has surpassed *Mtb* in the last year; however, deployment of vaccines and experience with containment measures should blunt the death rate from COVID-19 in the years to come, such that TB may reprise its role as the most important cause of infectious mortality. Near 40 million people have died from TB in the last 20 years while treatment has saved 60 million (WHO). Yet, in the same interval, an estimated 10- to 20-fold more people were infected but did not progress to disease (1, 2). Together, this suggests broad host control or tolerance of this pathogen, despite the important minority who progress to disease each year.

Our time together with *Mtb* has potentially spurred human adaptation to allow us as a population to subsist with this obligate pathogen. *Mtb* has been evolving to parasitize humans for millennia and within that time the relationship has possibly changed us too, when and where *Mtb* was endemic (3–5). Current and past abundance of human genetic diversity allows researchers to test the importance of genetic variation in *Mtb* infection outcomes and infer an evolutionary response by our species to survive the *Mtb* pandemic. One example where *Mtb* has potentially exerted a purifying selection on humans is that of the *TYK2* P1104A variant, which was calculated to have decreased in western Europeans concomitant with endemic TB over the last two millennia (6, 7). The *TYK2* P1104A variant is known to disrupt IL-23-dependent IFN-γ production (6) and was associated with a 5-fold increased risk for developing TB in the contemporary UK biobank (8). We are not aware of any evidence of positive selection of a TB resistance gene to date.

Is every case of TB a situation where the host genetic combination is vulnerable to *Mtb*? We can hypothesize a genetic combination impervious to *Mtb*. We may not have to extend our imagination very far, as there are documented cases of people who remain TST negative in high-burden settings, such that it is statistically unlikely that they have never inhaled *Mtb* [recently reviewed in (9)]. Therefore, developing TB is, in part, a result of genetics, and not just being a human exposed to *Mtb*, a postulate supported by the 21% heritability estimate for household contacts in Peru progressing from TST positivity to TB (10). Environmental parameters can also have an effect (e.g. level of exposure, lung damage, HIV co-infection) and thus in theory identical twins could have different outcomes with *Mtb* infection. *Mtb* also has variation which might contribute to a different outcome for the bacterium and the host: there are 9 lineages described to date (11–13) with some being deemed more virulent in experimental models (14).

Genetic variation creates differences that can fine tune a host-pathogen interaction, or abrogate it completely, resulting in altered immunity. One modality where there is a direct opportunity for co-evolution is in physical interactions between host molecules and *Mtb* molecules. These interactions can be placed into a few camps including: 1) between classical T-cell receptors and MHC molecules presenting microbial epitopes (15); 2) between antibodies and cognate microbial ligands (16); 3) between donor-unrestricted T cells and their respective mycobacterial epitopes presented on invariant host molecules operating analogously to MHC (17, 18); 4) between inborn sensors of microbial products, otherwise known as pattern-recognition receptors (PRRs), and their cognate microbe-associated molecular patterns (MAMPs). By their nature as structural molecules, MAMPs are subjected to a stronger purifying selection than many proteins. Unlike T-cell receptors, PRRs cannot generate diversity within an individual, yet there is variability amongst human population PRR gene pools as discussed further below. Most of all, should we even expect strong selective pressure on host PRRs to recognize *Mtb* MAMPs? In this paper, we sought to review what is known about the relative importance of the MAMP-PRR interaction for the mammalian host during *Mtb* infection primarily through two sources of data: 1) controlled animal experiments using engineered genetic knockouts (KOs) of PRRs; 2) natural experiments in humans where genetic diversity permits us to seek associations between polymorphisms and the course of *Mtb* infection. We later place this in perspective with genes known to have strong effects on animal outcomes and lastly discuss how to approach human genetic studies of PRRs in the years to come.

Abbreviations: BCG, Bacille Calmette-Guérin, attenuated *M. bovis* vaccine against *Mtb*; CFUs, Colony-forming units, a measure of the amount of bacteria; CLR, C-type lectin receptor; Collectins, Soluble CLR; KO, Knockout, removal of a gene from a genome; LAM, Lipoarabinomannan, mannosylated = ManLAM, uncapped = araLAM; LPS, Lipopolysaccharide, a.k.a. endotoxin, MAMP from Gram negative bacteria; MAMP, Microbe-associated molecular pattern, recognized by host PRR(s); MDP, Muramyl dipeptide; MHC, Major histocompatibility complex; *Mtb, Mycobacterium tuberculosis*, causative agent of TB; NLR, NOD-like receptor; NOD, Nucleotide-binding oligomerization domain-containing; PIMs, phosphatidylinositol mannosides; PRR, Pattern recognition receptor, recognize MAMP(s); TB, Tuberculosis, the disease caused by *Mtb*; TDM, Trehalose dimycolate; TLR, Toll-like receptor; TST, Tuberculin skin test, indicates adaptive T-cell response to mycobacterial antigens.

PRRS AND THEIR FUNCTIONS AGAINST *MTB* AT THE CELLULAR LEVEL

The interactions between many PRRs, *Mtb* and *Mtb* MAMPs have been described over the last few decades and are summarized in **Figure 1**. Various mechanisms have been uncovered by which PRR recognition of *Mtb* leads to a cellular effect. Immediately below, we briefly review the molecular functionality of the PRRs which have been demonstrated to mediate an immune response to mycobacteria. Whether these molecular and/or cellular effects translate to protection or pathology in the whole animal is examined in the subsequent section.

Toll-Like Receptors

Toll-like receptors (TLRs) were the prototypical PRR fitting the hypothesis proposed earlier by Janeway Jr (19) that there existed inborn sensors in animals for products common among groups of microbes but absent from the host, allowing host recognition of non-self invading microbes – a form of antibody or T-cell receptor for innate immunity. The discoveries in the 1990s on the Toll gene

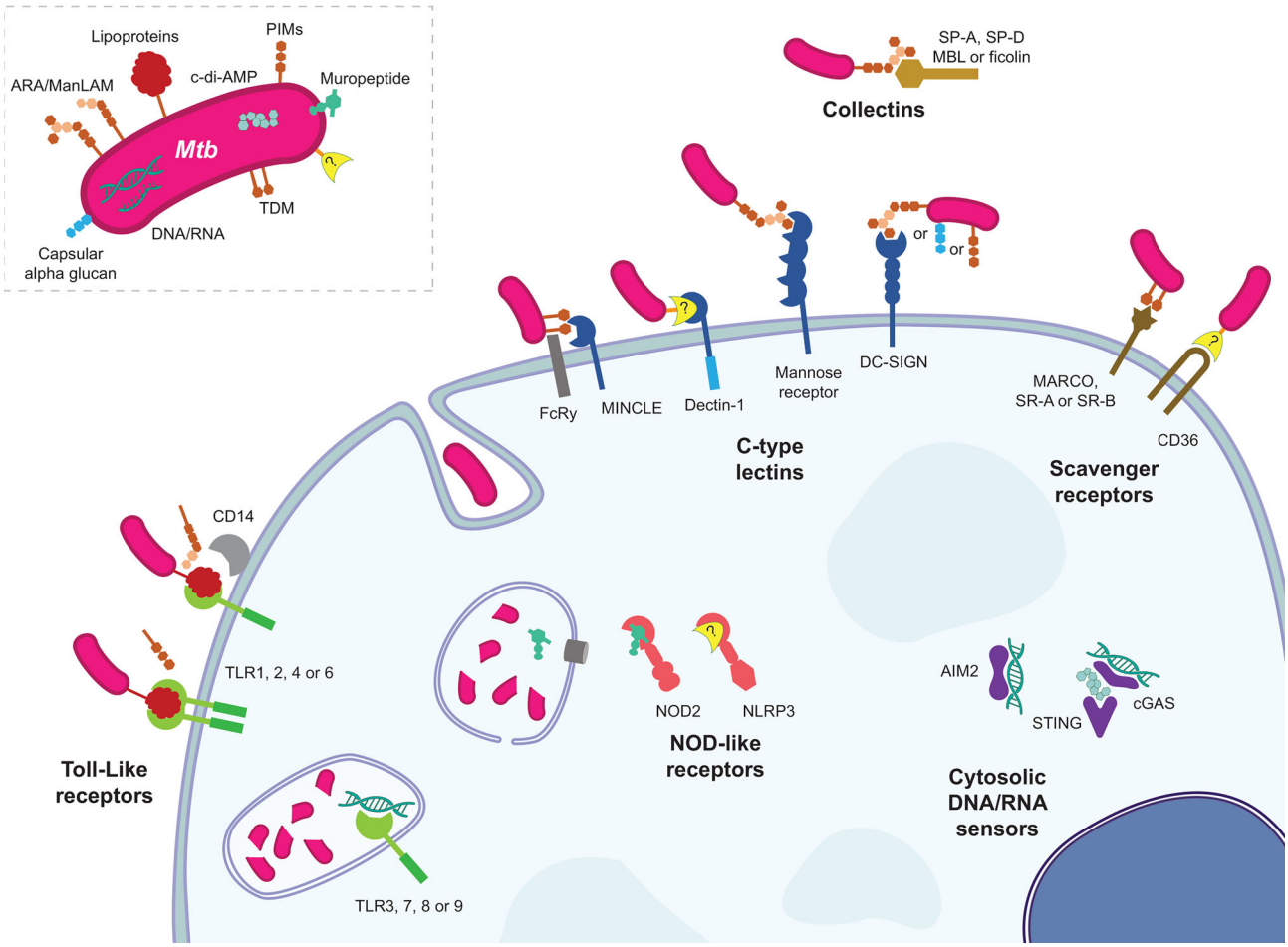

FIGURE 1 | The various host PRR and *Mtb* MAMP interactions. Representative MAMP-PRR interaction are depicted in their approximate cellular locations highlighting the numerous ways in which *Mtb* announces its arrival to a phagocyte.

of *Drosophila*, followed by work exploiting mutant forms of TLR4 in human cells and mice demonstrated that mammalian TLR4 was a sensor of Gram-negative endotoxin (a.k.a. lipopolysaccharide, LPS) (20–23). In total there are 10 TLRs in humans (13 in mice), each with different microbial ligands and slightly varying effects. TLR2 cooperates with TLR1 or TLR6, as well as other PRRs like CD14, to sense mycobacterial lipoproteins and lipoglycans. Identified mycobacterial TLR2 ligands include LAM (non-capped araLAM and not ManLAM) (24, 25), 19 kDa lipoprotein (LpqH), 38 kDa lipoprotein (PstS1) (26), PIMs (with differing activities) (27, 28), 27 kDa lipoprotein (LprG) (29), and LprA (30) to name a few (31). Mycobacteria including *Mtb* shed membrane vesicles containing TLR2 ligands that are sufficient to generate a TLR2-dependent immune response (32). More recently *Mtb* sulfoglycolipids have been shown to be competitive TLR2 antagonists (33). TLR4's mycobacterial ligands are less clear, but *Mtb* extracts have TLR4-dependent stimulatory activity; many proteins have been proposed as TLR4 agonists, with GroEL1 and 2 being examples (34). TLR5, which recognizes flagellin, does not have a known mycobacterial ligand (mycobacteria do not swim – they float). TLR3, TLR7 and TLR8 recognize RNA, and recent reports revealed that they may respond to host and/or mycobacterial RNA during infection (35–37). TLR9 recognizes CG-rich DNA (i.e. CpG motifs) and has been shown to contribute to the cellular response to *Mtb*'s CG-rich genomic DNA (38, 39). TLR10 has no known ligands, mycobacterial or otherwise. Murine TLR11, 12, and 13 are not reviewed here because they have no direct relevance to human health.

A complete review of TLR signalling, not specific to mycobacteria, has been recently published elsewhere (40). Briefly, when TLRs are engaged and oligomerize on the membrane, adaptor proteins MyD88 or TRIF are recruited to the cytoplasmic side to form 'myddosomes' or 'triffosomes', respectively. These supramolecular platforms direct signalling events that lead to activation of MAPK and NF-κB pathways, for example. Such signalling begins an inflammatory response by the cell which includes upregulation of costimulatory molecules and antigen presentation by MHC molecules, plus secretion of soluble factors like cytokines, in the cases of macrophages and dendritic cells (DCs).

C-Type Lectin Receptors

C-type lectin receptors (CLRs) are a large, diverse category of receptors of which some members function as PRRs by binding to MAMPs; other CLRs bind endogenous ligands or non-microbial exogenous ligands. The etymology of the name originates from some members requiring calcium (Ca^{++}, hence "C") to bind their respective carbohydrate ligands (hence "lectin"). There are both membrane-bound and soluble forms of CLRs. A full review of this complex category of PRRs has recently been published and provides more mechanistic detail than is presented here (41).

The mannose receptor (CD206) expressed on macrophages was shown to assist these phagocytes in uptake of the tubercule bacillus (42) with ManLAM being the mycobacterial ligand for CD206 (43). The ManLAM-CD206 interaction was later demonstrated to uniquely induce IL-8 and cyclooxengenase expression *via* PPARγ, while PPARγ knockdown was associated with reduced bacterial growth and increased TNF production during monocyte-derived macrophage infection (44). *Pparg*-KO mice had about half the pulmonary bacterial burden and reduced lung pathology than WT counterparts when aerosol infected with *Mtb* (45).

The CLR called DC-SIGN (Dendritic Cell-Specific Intercellular adhesion molecule-3-Grabbing Non-integrin, a.k.a. CD209) is a main receptor on DCs for binding to *Mtb* (46). DC-SIGN expressed on dendritic cells has been show to interact with ManLAM (47), PIM6 (48) and capsular alpha-glucan (49). The DC-SIGN homologues L-SIGN (human) and SIGNR1 (mouse, one of five homologues), have been shown to interact with ManLAM too (50). DC-SIGN ManLAM ligation modulated TLR-induced signalling (e.g. NF-κB pathway) *via* Raf-1 (51, 52).

MINCLE (Macrophage inducible Ca^{++}-dependent lectin receptor, encoded by *CLEC4E*) associates with FcRγ to bind mycobacterial cord factor trehalose-6,6'-dimycolate (TDM) and TDM is sufficient to induce granuloma formation in murine lungs if functional MINCLE and FcRγ are present (53). MINCLE signals *via* the SYK-CARD9 pathway to lead to the production of proinflammatory cytokines (54). *Card9*-KO mice succumb more quickly to *Mtb* than WT, associated with defective anti-inflammatory signalling presumably leading to lethal immunopathology (55). MINCLE expression is low in resting macrophages, and first requires induction *via* signalling through MCL (encoded by *Clec4d* and not to be confused with MCL-1). MCL is also a FcRγ-coupled and TDM CLR but cannot mediate the same pro-inflammatory response on its own (56). MINCLE and MCL expression are co-dependent (57, 58).

Dectin-1 was shown to mediate part of the immune response of splenic DCs to *Mtb* (59). *Mif*-KO mice have impaired survival and immunity compared to WT during aerosol infection with *Mtb* HN878 strain, while bacterial killing and cytokine production were nearly restored when *Mif*-KO cells were complemented with Dectin-1 (overexpressed). These results suggest the MIF defect mostly manifests in defective Dectin-1 signalling (60). The mycobacterial ligand for Dectin-1 remains unknown. Dectin-2 was reported to recognize ManLAM (61, 62), but pathogenesis studies have yet to be done with this CLR.

Recently, DCAR (dendritic cell immunoactivating receptor; encoded by *Clec4b1*), also a FcRγ-coupled CLR, was demonstrated to be a receptor of PIMs. DCAR is expressed on monocytes and macrophages. *Clec4b1*-KO mice had partially defective immune responses and bacterial control during BCG infection (63).

Soluble CLRs

Collectins are soluble, non-cell-bound proteins; they are CLRs in that they specifically associate with sugars on the surface of microbes to mediate an effect. Surfactant proteins (SP) are collectins that exist in pulmonary surfactant. SP-A promoted attachment and phagocytosis of *Mtb* by alveolar macrophages by a mechanism that required mannose receptor but not SP-A contacting *Mtb* (64, 65). SP-A supressed nitrite production from AMs preventing *Mtb* killing and controlling bacterial growth (66). SP-A was shown to bind to ManLAM (67) and APA, the alanine- and proline-rich antigenic glycoprotein (68). SP-D binds to ManLAM and agglutinates *Mtb*, but in contrast to SP-A, SP-D reduced *Mtb* binding to macrophages (69). Reduced uptake occurred without agglutination using a modified SP-D (70). However, SP-D increased phagosome-lysosome fusion, but did not alter the respiratory burst (71).

The collectin mannan-binding lectin (MBL) and ficolins are serum-borne receptors that bind to microbes to initiate the complement cascade. MBL was first demonstrated to interact with *Mtb* and *M. leprae* sonicate (72). Ficolins, of which there are at least three in humans and two in mice, are also part of the lectin-complement system. Ficolin-2 was shown to bind to *Mtb* to play a protective role involving opsonization and inflammatory signalling in macrophages (73). Another group suggested ficolin-3 was important for agglutination and phagocytosis of *Mtb* (74). MBL and ficolins were suggested to bind to ManLAM and/or Ag85 (75, 76).

NOD-Like Receptors

Nucleotide-binding Oligomerization Domain-containing (NOD)-like receptors (NLRs) are a group of cytoplasmic sensors. Reviews with more detail on their mechanisms of action than presented here have been published, for example (77). Its members NOD1 and NOD2 are essential in the detection of peptidoglycan fragments D-glutamyl-meso-diaminopimelic acid (iE-DAP) and muramyl dipeptide (MDP), respectively (78–81). Both NOD1 and NOD2 signal through the adaptor protein RIPK2 to reach NF-κB and MAPK pathways. Few reports have been published on an important role for NOD1 during *Mtb* infection, one showing NOD1 plays a role in cytokine production only in the absence of NOD2 or after LPS-pretreatment of BMDMs (82). Mycobacteria do possess the iE-DAP moiety in their peptidoglycan (83). In contrast, NOD2 has been well-studied in *Mtb* infection [Pubmed searches of "Mycobacterium tuberculosis AND NOD1" or "…NOD2" yielded 7 and 57 hits, respectively, at the time of writing (15-2-2021)].

Mycobacteria produce a distinct NOD2 ligand, *N*-glycolyl MDP, while most other bacteria produce *N*-acetyl MDP (84, 85). *N*-glycolylated peptidoglycan and MDP were shown to be better inducers of immune responses compared to the *N*-acetylated forms by comparing with mycobacterial KOs and synthetic MDPs (86–88). The absence of NOD2 during *Mtb* infection

was accompanied by reduced nitric oxide and cytokine production from mouse macrophages (89, 90) and reduced iNOS from human macrophages (91). NOD2 signalling has been called "non-redundant" in that although there are shared pathways with TLR and CLR signalling (e.g. NF-κB), NOD2 signalling appears to work synergistically with other MAMPs and little immune response is produced with MDP stimulation alone (86, 88, 92).

Only one other NLR has been significantly studied in the context of *Mtb* infection: NLRP3 (NLR family pyrin domain containing 3). There is no known mycobacterial ligand for this NLR – it has been suggested that NLRP3 can sense specific host products in the context of infection (77). Recently, ESX-1-mediated membrane damage has been tied to caspase-1 activation, NLRP3 oligomerization, inflammasome formation and finally IL-1β release (93).

Nucleic Acid Cytosolic Surveillance Receptors

AIM2 (absent in melanoma 2) appears to play a role in *Mtb* infection. This cytosolic DNA receptor was necessary for full caspase-1 cleavage/activation and IL-1β release during *Mtb* infection and *Mtb* DNA transfection (94). STING (Stimulator of interferon genes), part of a cytosolic DNA sensing system, was essential for autophagy targeting of ESAT-6-producing mycobacteria in mouse bone marrow-derived macrophages (95) and zebrafish embryos (96). cGAS (cyclic guanosine monophosphate–adenosine monophosphate (cGAMP) synthase), a DNA sensor that works with STING, was required for *Mtb* autophagy in addition to STING (97). Type I IFN production during *Mtb* infection elicited by cGAS-produced, STING-sensed cGAMP was dependent on RD-1 (98, 99). *Mtb*-produced c-di-AMP was also shown to contribute to type I IFN production through STING (100). It has been suggested that *Mtb* DNA engagement of the AIM2 inflammasome leads to the inhibition of host cell-protective STING functions (101).

Scavenger Receptors and Complement

Scavenger receptors (SR) are a diverse and poorly defined group of cell surface receptors that interact with endogenous and microbial ligands. Details of these receptors have been recently reviewed elsewhere (102, 103). Inhibitors of scavenger receptors reduced *Mtb* binding to macrophages (104).

MARCO is a scavenger receptor that was suggested to bind and "tether" *Mtb* to a macrophage's surface by interacting with TDM (105), and zebrafish lacking MARCO expression had reduced macrophage uptake of *M. marinum* (106). Similarly, blocking MARCO on human mesenchymal stems cells reduced *Mtb* uptake (107).

KO of the gene encoding scavenger receptor A (SR-A) did not affect inflammatory gene transcription during *Mtb* infection (108). The KO increased TNF and MIP-1α production from AMs treated with TDM (109). Overexpression of Scavenger receptor B1 (SR-B1) in immortal cells was associated with increased BCG and *Mtb* binding to the cells, but the corresponding KO in murine macrophages had no effect on BCG binding (110). SR-B1 was essential for EsxA-mediated transcytosis of *Mtb* across M cells (111). A related SR-B family member, CD36, was identified with a *Drosophila* RNAi screen to be essential for uptake of *M. fortuitum* (112). CD36 knockdown in human monocyte-derived macrophages reduced surfactant lipid uptake as well as intracellular growth of *Mtb*, suggesting CD36 normally promotes intracellular *Mtb* growth or survival (113). Another group showed *Cd36* KO macrophages control *Mtb*, BCG and *M. marinum* infections better, independent of phagocytosis rate, nitric oxide and ROS production. Similarly, mice receiving BCG i.p. had lower bacterial loads with *Cd36* KO *vs* WT (114). Homologues of SR-BII and CD36 in *Dictyostelium discoideum* (a social amoeba) are similarly involved in phagocytosis of *M. marinum* (115).

CONSEQUENCES OF PRR KOs IN MICE

The overall importance of individual genes during *Mtb* infection is best addressed in two ways: observing what happens to individuals with diverse expression or functionality of the gene of interest who perchance become infected with *Mtb* (the natural experiment); alternatively, individuals of known or controlled gene status can be intentionally infected with *Mtb* – unethical in humans and therefore animal models are necessary. As mentioned above, many PRRs are important for specific cellular processes relevant to *Mtb* infection. It is therefore hypothesized that in the absence of a PRR, certain aspects of the host-*Mtb* interaction are lost, which should result in a phenotype in the whole animal. We have also assumed that the animal would suffer most from the aberrant immune response. This assumption is perhaps too simplistic: *Mtb* is a professional, obligate pathogen, and although it is perceived as hard-to-kill, it might also suffer from a host environment that does not behave as *Mtb* has evolved to 'expect'. Additionally, we have suggested that the potential coevolution of humans and *Mtb* has shaped the PRR-MAMP interaction, which clearly would not apply in infections of animals like mice, which are not natural hosts for *Mtb*. However, one can still use mice to generate testable hypothesis for human studies and validate genetic effects observed first in humans. Numerous KO mouse studies of *Mtb* infection have been performed over the years with hypotheses of defective immunity in the animal that should manifest as decreased survival, increased bacterial burden and/or detectable differences in the immune response (e.g. bronchoalveolar lavage cytokines or T-cell defects).

Systematic Literature Search of *Mtb* and PRRs

To non-biasedly form a conclusion as to the importance of PRRs during *Mtb* infection in animal models, we used the Medline database *via* Pubmed to repeatedly search every known PRR and its role in *Mtb* infection in a living animal with the term below (where "[PRR]" was changed in each search):

"Mycobacterium tuberculosis AND [PRR]"

Where PRR names were ambiguous, we searched multiple times using the different names. After removing duplicates, this search produced over 1100 papers, which were screened for data using KO animals during *Mtb* infection. The results of this *in silico* exercise are summarized in **Table 1**. We have added a few studies of which we were aware but that were missed by the screen (noted in **Table 1**). It is possible that other appropriate data are absent; however the non-biased approach reinforces the validity of our subsequent conclusions.

In **Table 1**, we summarized the results of individual experiments presented in the literature on murine *Mtb* infections comparing a PRR KO to the 'WT' control animal. All data found were exclusive to the mouse. We have included the dose, *Mtb* strain and route of infection per experiment. *Mtb* can establish an infection *via* the lungs with just a few bacilli (156, 157), and therefore models using large doses and atypical routes may represent different aspects of *Mtb* disease but not necessarily follow the normal mode of infection. The magnitude of disease in mice also changes with the strain of *Mtb*, where for example the H37Rv strain is expected to be less virulent than the related Erdman strain and the HN878 strain. It is possible that some of the different outcomes across different studies addressing the same PRR knockout were due to differences in the infection model. However, our review of the data did not reveal an obvious effect of dose, strain nor route (**Table 1**).

Where survival data were present, it was clear that PRRs can have an effect on survival, although in most cases there was either no significant difference in survival from WT to KO, or it was quantitatively small. There were two instances where KO mice survived longer than WT [CD14 (135) and SR-A (152)], demonstrating that some host systems are detrimental to *Mtb* tolerance.

TLR KOs Resulted in Small and Inconsistent Effects on Survival and *Mtb* Burden

For TLR2, two of four experiments showed reduced survival in KOs. A single *Tlr6*-KO study did not show a difference in bacterial burden nor immune response (117). For TLR4, two of seven experiments showed reduced survival in KOs. Note that many TLR4 studies took advantage of the C3H/HeJ mouse (having a spontaneous *Tlr4* loss-of-function mutation) employing other only somewhat related C3H strains as wildtype control. The maximum difference in pulmonary bacterial burden observed in most of these papers was approximately one log more in *Tlr2* or *Tlr4* KOs *vs* WT. Defects in immune responses were observed in a majority of *Tlr2* KO experiments and a minority of *Tlr4* KO experiments. Two experiments with *Tlr9* KO from one study showed more rapid death with high dose infection compared to low dose, and only the high-dose resulted in a statistically significant increase in pulmonary bacterial burden (158). No survival data for other TLRs have been published. Interestingly, most experiments with combination KOs of *Tlr2*, *4* and/or *9* resulted in no differences in bacterial burden nor immunologic responses. Two of seven experiments (*Tlr2/9* double KOs) resulted in shortened survival times, but with small or unreported differences in bacterial burden. Together, mutations in TLRs, even multiple, had only modest or negligible effects on the host's survival and bacterial control but were frequently associated with altered immune responses. In particular, TLR2 and 9 stood out.

Of note, *Myd88*-KO mice succumbed rapidly (all dead within 1-2 months) to *Mtb* infection, despite TLRs seeming to be largely dispensable. This was attributed to the necessity of MyD88 for IL-1R signalling (*Il1r1* KO mice are equally susceptible) and intrinsic macrophage function requiring MyD88 (121, 159, 160). An earlier report with *Myd88*-KO mice showed a nearly 2-log increase in pulmonary colony-forming units (CFU) compared to WT but mice survived at least 12 weeks with limited immunological changes; no survival was presented (161).

Few CLR KOs Resulted in Small Reductions in Survival and Bacterial Control

For CLRs, only MCL and Dectin-1 were found by us to have been disrupted in *Mtb* survival challenges. In one report, MCL (*Clec4d*)-KO caused a significant difference in survival, but specifically this was 20% mortality by 6 weeks, after which no *Clec4d*-KO mice died to week 10 (when the experiment was ended) (143). However, in the same study, pulmonary bacterial burden was less than half a log higher in the KO at four months (no significant difference at 2 months). Proinflammatory immunologic responses were elevated in the KO. Thus, MCL might play a role early in infection to control the immune response, but not so much for bacterial control.

Another lone report showed Dectin-1 (*Clec7a*)-KO mice did not have changed mortality after infection with *Mtb*, and in fact had slightly lower bacterial burdens compared to WT at 2 and 4 months post infection (144). Therefore, Dectin-1 is likely not required by the host during *Mtb* infection. No survival data was found for murine DC-SIGN homologues, mannose receptor, nor MINCLE. Only one of three studies reported a difference in bacterial burden with SIGNR1 (*Cd209b*)-KO at one- and nine-months post infection, but by scoring Ziehl-Neelsen-stained lung sections rather than directly counting CFUs (140). When assessed, altered immunity was consistently observed with this KO. A single study found a difference in bacterial burden and immunological response with a SIGNR3 (*CD209d*)-KO but not a SIGNR5 (*Cd209a*)-KO (139). Another lone study addressing the mannose receptor showed no bacterial or immunologic effect with KO (140). Two studies on MINCLE presented opposing data on pulmonary bacterial burden (more or less a half log compared to WT) and only one identified significant immunological changes with KO. Double KO of the genes encoding mannose receptor plus SIGNR1 showed no bacterial or immunologic differences. KOs of other membrane-bound CLRs have not been tested during *in vivo Mtb* infection.

KOs of genes encoding collectins SP-A and SP-D had no long-term effect on bacterial burden during *Mtb* infection – survival was not tested/presented. Immunologic responses were similar to WT but with decreased neutrophil numbers in the lung. Double KO for SP-A and SP-D genes was similar to the

TABLE 1 | Results of KO mouse studies in *Mtb* infection.

PRR KO(S)	DOSE, CFU	STRAIN	ROUTE	Δ SURVIVAL[A]	Δ MTB[B]	Δ IMM[C]	NOTES[D]	SOURCE
TLR2	100	H37Rv	aero	-	N	N		Reiling et al. (116)
	2,000	H37Rv	aero	Y (60/150)	–	Y		Reiling et al. (116)
	100	Kurono	aero	-	Y (1)	Y		Sugawara et al. (117)
	100	H37Rv	aero	N	Y (1)	–		Drennan et al. (118)
	500	H37Rv	aero	Y (100/>155)	Y (1)	Y		Drennan et al. (118)
	75	H37Rv	aero	N	N	N	manual	Bafica et al. (119)
	20	H37Rv	aero	-	Y (<1)	Y		Tjärnlund et al. (120)
	100	H37Rv	aero	–	N	–		Hölscher et al. (121)
	100,000	H37Rv	i.t.	-	Y (1)	Y		Carlos et al. (122)
	150	H37Rv	i.n.	–	–	Y		Teixeira-Coelho et al. (123)
	10,000,000	H37Rv	i.v.	-	-	Y		Choi et al. (124)
	75	Erdman	aero	–	Y (1)	–		McBride et al. (125)
	10	Erdman	aero	-	Y (2)	-		McBride et al. (126)
	100	Erdman	aero	–	Y (2)	Y		McBride et al. (126)
	150	Erdman	aero	-	Y (1)	-		McBride et al. (126)
	100	Erdman	aero	–	Y (<1)	Y	chimera	Konowich et al. (127)
	20	HN878	aero		Y (3)	Y		Gopalakrishnan et al. (128)
RP105	200	H37Rv	aero	–	Y (<1)	Y		Blumenthal et al. (129)
TLR4	100	H37Rv	aero	Y (180/>250)	Y (1)	Y	HeJ/HeN	Abel et al. (130)
	100	H37Rv	aero	–	N	N	HeJ/HeN	Reiling et al. (116)
	2,000	H37Rv	aero	N	-	N	HeJ/HeN	Reiling et al. (116)
	144	Erdman	aero	N	N	–	HeJ/other C3H	Kamath et al. (131)
	472	Erdman	aero	N	N	N	HeJ/other C3H	Kamath et al. (131)
	75	H37Rv	aero	N	Y (-1)	N	HeJ/OuJ	Shim et al. (132)
	100,000	H37Rv	i.n.	Y (90/>110)	Y (<1)	Y	HeJ/HeN	Branger et al. (133)
	500,000	H37Rv	i.n.	N	–	–	HeJ/HeN	Branger et al. (133)
	20	H37Rv	aero	-	Y (<1)	Y		Tjärnlund et al. (120)
	100	H37Rv	aero	–	N	–		Hölscher et al. (121)
	150	K strain	aero	-	Y (2)	Y	HeJ/HeN and B6	Park et al. (134)
CD14	100	H37Rv	aero	–	N	N		Reiling et al. (116)
	100,000	H37Rv	i.n.	Y (>224/210)	N	Y		Wieland et al. (135)
LBP	100,000	H37Rv	i.n.	N	N	Y		Branger et al. (136)
TLR6	100	Kurono	aero	-	N	N		Sugawara et al. (117)
TLR9	75	H37Rv	aero	Y (90/>150)	N	Y	manual	Bafica et al. (119)
	500	H37Rv	aero	Y (45/>90)	Y (<1)	Y (not shown)	manual	Bafica et al. (119)
	100	H37Rv	aero	–	N	–		Hölscher et al. (121)
	75	Erdman	aero	-	N	N		Gopalakrishnan et al. (137)
SIGNR1	100,000	H37Rv	i.n.	–	N	Y		Wieland et al. (138)
	1,000	H37Rv	i.n.	-	N	-		Tanne et al. (139)
	200	H37Rv	i.n.	–	Y (score)	Y		Court et al. (140)
SIGNR3	1,000	H37Rv	i.n.	-	Y (1)	Y		Tanne et al. (139)
SIGNR5	1,000	H37Rv	i.n.	–	N	–		Tanne et al. (139)
CD206(MR)	200	H37Rv	i.n.	-	N	N		Court et al. (140)
MINCLE	100	H37Rv	aero	–	Y (>-1)	N		Heitmann et al. (141)
	100	Erdman	aero	-	Y (<1)	Y		Lee et al. (142)
MCL	100	H37Rv	aero	Y	Y (<1)	Y	N>30 for survival	Wilson et al. (143)
DECTIN-1	100	H37Rv	aero	N	Y, (>-1)	N		Marakalala et al. (144)
FICOLIN-A/2	1,000,000	H37Rv	i.v.	Y (10/22)	–	–		Luo et al. (73)
SP-A	50	Erdman	aero	-	N	Y		Lemos et al. (145)
	6,000	Erdman	aero	–	Y (<1)	–		Lemos et al. (145)
SP-D	50	Erdman	aero	-	N	Y		Lemos et al. (145)
	6,000	Erdman	aero	–	Y (<1)	–		Lemos et al. (145)
NOD2	35	1254	aero	-	N	N		Gandotra et al. (89)
	1,500	H37Rv	aero	–	N	N		Gandotra et al. (89)
	400	H37Rv	aero	Y (200/>230)	Y (<1)	Y		Divangahi et al. (90)
NLRP3	300	H37Rv	aero	N	N	Y		McElvania TeKippe et al. (146)
	100	H37Rv	aero	-	N	Y		Walter et al. (147)
	300	H37Rv	aero	–	N	N		Dorhoi et al. (148)
NLRP12	300	H37Rv	aero	N	N	N	manual	Allen et al. (149)
NLRC3	200	H37Rv	aero	–	Y (-1)	Y	manual	Hu et al. (150)
NLRC4	300	H37Rv	aero	N	-	-		McElvania TeKippe et al. (146)

(Continued)

TABLE 1 | Continued

PRR KO(S)	DOSE, CFU	STRAIN	ROUTE	Δ SURVIVAL[A]	Δ MTB[B]	Δ IMM[C]	NOTES[D]	SOURCE
cGAS	200	Erdman	aero	Y (150/210)	N	–		Collins et al. (97)
	100	Erdman	aero	N (100)	N	Y	manual	Watson et al. (99)
	1,000	H37Rv	i.n.	N	N	N		Marinho et al. (151)
STING	200	Erdman	aero	N	N	-	gt/gt STING	Collins et al. (97)
	1,000	H37Rv	i.n.	N	N	N		Marinho et al. (151)
AIM2	1,000,000	H37Rv	i.t.	Y (45/>56)	Y (1)	Y		Saiga et al. (94)
Marco	200	H37Rv	i.n.	–	Y (score)	Y		Court et al. (140)
SR-A	200	H37Rv	i.n.	-	N	N		Court et al. (140)
	75	H37Rv	aero	Y (>430/230)	Y (-1, ns)	Y		Sever-Chroneos et al. (152)
SR-B1	100	H37Rv	aero	-	N	N		Schafer et al. (110)
	1,000	H37Rv	aero	–	N	Y		Schafer et al. (110)
CD11b(CR3)	200,000	Erdman	i.v.	N	N	-	3 backgrounds	Hu et al. (153)
	100,000	Erdman	i.v.	–	Y (<1, ns)	–		Melo et al. (154)
TLR-2/4	60	H37Rv	aero	-	N	N		Shi et al. (108)
	600	H37Rv	aero	–	N	N		Shi et al. (108)
	100	H37Rv	aero	-	N	-		Hölscher et al. (121)
TLR2/4/9	100	H37Rv	aero	–	N	N		Hölscher et al. (121)
TLR2/9	75	H37Rv	aero	Y (90/>150)	Y (<1)	Y	manual	Bafica et al. (119)
	75	H37Rv	aero	Y (120/>280)	–	–	manual	Mayer-Barber et al. (155)
	75	Erdman	aero	-	N	N		Gopalakrishnan et al. (137)
NOD2/TLR2	100	H37Rv	aero	–	N	–		Gandotra et al. (89)
CD206/SIGNR1	200	H37Rv	i.n.	-	N	N		Court et al. (140)
SR-A/CD36	200	H37Rv	i.n.	–	N	N		Court et al. (140)
SP-A/D	50	Erdman	aero	-	N	Y		Lemos et al. (145)
	6000	Erdman	aero	–	Y (<1)	–		Lemos et al. (145)

A, change in survival (Yes/No) (median survival KO/median survival control). B, change in pulmonary Mtb CFU burden (Yes/No) (maximum log KO/control). C, change in immune response observed (Yes/No). D, any irregularities from other studies (manual means source was not found in systematic search and was added manually afterwards).

SP-A single KO (145). KO of the gene encoding ficolin-A (homologue of human ficolin-2 and/or 3) decreased the survival of mice given one million CFU H37Rv strain i.v. compared to WT, but survival was enhanced compared to WT when KO mice were given a plasmid containing ficolin-A or ficolin-2 by i.m. electroporation on the day of infection (73). This suggests ficolins might help control systemic or bloodborne *Mtb*. Thus, as with TLRs, CLRs are generally dispensable for *Mtb* immunity. The few exceptions seem to suggest an early, minor role in *Mtb* infection for CLRs like MCL and SP-A/D.

KOs of Certain Cytosolic PRRs Worsened *Mtb* Infection Outcome

NOD2 disruption produced a late survival phenotype: KO mice died faster than WT near 6 months post *Mtb* infection. Bacterial burden was slightly higher and immunological responses were also reduced in KO mice in this study (90). A separate study did not find significant differences in bacterial burden nor immunological responses with *Nod2*-KO nor *Nod2-Tlr2*-double KO, but survival was not evaluated (89). In contrast, *Nlrp3*-KO had no effect on bacterial burden in three studies. Immunological responses with *Nlrp3*-KO can be altered, but survival did not change.

Aim2-KO mice succumbed rapidly to infection with one million CFU H37Rv strain delivered i.t. compared to WT. The KO had greater bacterial burden and pathology and altered immunity (94). However, no other independent studies were found besides this one, and the high dose delivery makes the result difficult to compare to other PRR-KO survival studies with the more physiological low-dose aerosol infection. The importance of AIM2 during mycobacterial infection is supported by data with BCG, where repeated infection of WT and *Aim2*-KO mice vial the tail vein showed KO mice were defective in controlling bacterial burden which was associated with altered immunity (enhance type I IFN, reduced type II IFN) (101). Additionally, the adaptor protein ASC (a.k.a. PYCARD) was also shown to be important for survival in at least two separate studies (146, 155). This supports the importance of AIM2 and/or another inflammasome sensor for *Mtb* infection, with NLRP3 seemingly dispensable.

Pulmonary burden of *Mtb* in *Cgas*-KO and *Sting1*$^{gt/gt}$ mice was unchanged from WT at 3 and 6 weeks post aerosol infection of 200 CFU of the Erdman strain, although *Cgas*-KO mice had late reduced survival (deaths between 100 and 200 days p.i.) while the STING mutant did not differ from WT (97). In another study, an Erdman-strain aerosol experiment running 100 days did not reveal a difference between WT and *Cgas*-KO mice in terms of survival and bacterial burden, but less type I IFN was present in the lungs and serum (99). In a third study with i.n. infection with 1000 CFU H37Rv strain, cGAS and STING mutations did not affect survival past 250 days (no mice died as with WT), although *Cgas*-KO mice did not maintain weight as well. Bacterial burden and immunology were the same as WT too (151). Together, these studies suggest cGAS plays a minor role during *Mtb* infection (that emerged as a death phenotype late in one study), while STING is dispensable. These findings are difficult to reconcile with the proposed model where cGAS functions upstream of STING as the mycobacterial DNA

sensor; accordingly a STING mutant should be defective for cGAS functions. Furthermore, *Mtb* CDC1551 mutants that either lack their own c-di-AMP production, or overexpress it, significantly decreased and increased survival relative to WT, respectively (100), contributing further confusion regarding the importance of STING. It is possible that the importance of cGAS during mouse survival of *Mtb* infection is related to a STING-independent function of cGAS, and that the STING phenotype with mutant *Mtb* is more valuable as a mechanistic lesson than a biologically relevant one.

No Other PRR KOs Were Detrimental to the Host During *Mtb* Infection

No data was found showing scavenger receptor KOs were detrimental to *Mtb* control. A difference in bacterial burden during *Mtb* infection of *Marco*-KO mice was only detected by scoring Ziehl-Neelsen-stained lungs, not by CFU enumeration, at 6 and 9 months post infection (140). KOs for SR-A and SR-B genes did not result in increased bacterial burdens nor were they consistently associated with immunological changes. Two independent studies examining the complement receptor CR3/*Cd11b* KO during *Mtb* infection found no evidence that they play a role in *Mtb* control nor survival (153, 154).

In summary, most PRR KO experiments presented did not show reduced survival compared to WT. Control of bacterial burden was either unaffected or just slightly increased by PRR KOs in most experiments. We suspect that publication bias against negative data would also mean that PRR KO effects are, if anything, over-represented in the literature. In contrast, altered immunity was found often in PRR KOs during *Mtb* infection. It is possible that the effects on immunity with some PRR KOs are not large or relevant enough to result in changes in survival and bacterial burden that are sufficiently robust to be statistically detectable with a practical number of animals.

PRR DIVERSITY IN HUMANS AND OUTCOMES OF *MTB* INFECTION

Selective pressure caused by human-microbe interactions coupled with population admixture has helped shape the response of modern humans to pathogens (162). A recent example is a locus controlling COVID-19 severity in modern humans that can be traced to Neanderthal introgression (163). *Mtb* and humans have coexisted for an estimated 2,000 – 6,000 years (3, 4) and purifying selection of human genes by *Mtb* was traced to the bronze age for the *TYK2* P1104A mutation. Similarly, as members of the first line of host innate immune defense PRRs have been subjected to purifying selection (164). PRR diversity in humans may explain, at least in part, the variable susceptibility to *Mtb* across populations.

For example, humans express 10 functional TLRs which are subdivided in two categories: cell surface (TLR1, 2, 4 – 6 and 10) and intracellular endolysosomal (TLR3, 7 – 9). The intracellular TLRs underwent strong purifying selection and have poor tolerance to loss of function mutations (165). Conversely, cell surface TLRs are more permissive to genetic variation across human populations (166). This difference may be attributed to the nature of ligands. Bacterial antigens detected by cell surface TLRs are clearly distinct from host molecules while nucleic acids detected by intracellular TLRs (RNA or DNA with CpGs) can resemble host endogenous factors. It has been proposed that mutations in intracellular TLRs are less tolerated to prevent "autoimmunity" (167–169). *Mtb* is detected by heterodimers of TLR1, 2 and 6, therefore presenting redundancy in the host response. Interestingly, mutations in the *TLR1* (S248N, I602S), *TLR6* (P249S) and *TLR10* (I775V) genes clustered on chromosome 4p14 have shown signs of recent positive selection in Europeans (165). It has been suggested, although not confirmed, that tuberculosis and leprosy epidemics in Europe have played a role in this selective pressure (170). Of particular interest is the TLR1 I602S mutation which has been associated with both TB and leprosy (171–175). The TLR1 602S amino acid was shown to impair NF-κB activity in response to *Mtb* and decrease IL-6 production (174). Studies evaluating TLR2 mutations in TB have provided inconsistent results, which limited the interpretation of its role in TB pathogenesis (176, 177). Moreover, TLR4 and TLR9 have also been suggested to contribute to TB susceptibility (178–180).

NLR is another group of PRRs that shows signs of diversity between populations. NLRs encompass three families of cytosolic PRRs (NOD receptors, NLRPs and IPAFs) involved in viral and intracellular bacterial pathogen recognition. An excess of rare *NOD1* non-synonymous variants segregating in the human population provided evidence for weak negative selection against these variants (181). In contrast, there was evidence among Asians and Europeans of positive selection for rare variants in *NOD2* (181). In a meta-analysis, the NOD2 R702W amino acid change was associated with protection from TB (182, 183). Curiously, the same NOD2 R702W mutation is one of the strongest known genetic risk factors for Crohn's disease, suggesting a pivotal role for NOD2 in balancing host inflammatory responses (184). Most NLRPs shows signs of strong selective constrains emphasizing their essential function in the human innate immune response (181). Macrophages challenged with *Mtb* or *M. marinum in vitro* showed a NLRP3-dependent increase in IL1β production (176). In a small population of cases with HIV/*Mtb* co-infection a non-coding variant in NLRP3 had a weak association with early mortality (185).

DC-SIGN (CD209), a member of CLR family, is a major dendritic cell receptor of *Mtb* (46). In ancient humans a duplication of *CD209* gave origin to the *CD209L* gene. Interestingly, natural selection has prevented accumulation of amino acid changes in CD209 while the closely related *CD209L* gene was permissive (186). This discrepancy in selective pressures highlights the importance of function for CD209 while diversity in CD209L might have benefitted human adaptation to pathogens. Two promoter variants in CD209 are associated with TB in multiple African populations (187–189), South Asians (190) and Brazilians (191). Other PRRs, such as ficolins, have been evaluated for association with TB (192, 193),

while studies with genes encoding proteins of the complement and PRRs for the RIG-1 family have not yet been reported.

HOW SOME NON-PRR KOs COMPARE

Through animal experimentation, certain genes and associated pathways have been shown to be major determinants of the host outcome upon *Mtb* infection. Here, we define how some of these pathways compare to PRR pathways at the molecular level, and the level of importance to *Mtb* infection, as internal positive controls to our review.

For the sake of controls, similar systems to the PRR-MAMP interaction would include endogenous receptor-ligand systems. Receptor-cytokine interactions are an example which includes mechanisms that are even functionally related to PRR signalling pathways (e.g. the IL-1R/IL-1 system, which uses MyD88 like the TLRs as mentioned above).

IL-1R deficient mice were more susceptible to *Mtb* after intranasal infection with 10^5 CFU H37Rv strain, with a median survival of around 110 days, while no WT had died by 140 days; the remaining KO mice had 4 logs more pulmonary CFU than WT at 140 days post infection (194). Another study by a different group showed that with 100 CFU Kurono strain aerosol infection *Il1r1* KO mice had died after 45 days (KO mice had 3 logs more pulmonary CFU than WT at 35 days) (195). During another H37Rv strain infection (200 CFU i.n.), *Il1r1* KO mice phenocopied *Myd88* KO mice (died around 4 weeks post infection) (159). There have been variable phenotypes with IL-1α and IL-1β deficiency: in one study *Il1b* KO was sufficient to phenocopy *Il1r1* KO (155); in another study the double cytokine KO only reduced pulmonary *Mtb* CFU control (196); in a third study only double cytokine KO, not single, shortened survival like *Il1r1* KO (197). Lastly, heterozygous deficiency of IL-1R antagonist, overexpressed in mice carrying the *Sst1* (super susceptibility to tuberculosis 1) locus, almost completely rescued these mice from their type-I IFN driven early mortality and excessive pulmonary CFU burden during *Mtb* Erdman strain infection, again highlighting the protective effect of IL-1R signalling (198). Thus, MyD88-dependent cytokine-receptor systems can be critical for *Mtb* control in mice.

In mice lacking TNF receptor, or treated with anti-TNF antibodies, mice succumbed to uncontrolled *Mtb* Erdman strain i.v. infection in about a month while WT controls all survived past 125 days (199). This result has been replicated in *Tnf* KO mice in numerous studies over the years (118, 160, 197). TNF receptor deficient mice died approximately as rapidly as *Tnf* KO, even if the receptor KO was only on myeloid cells; lymphoid cell receptor KO did not differ from WT (200). Thus, the TNF pathway is critical for *Mtb* control in mice to prevent rapid death. The importance of TNF with *Mtb* infection in humans was demonstrated when anti-TNF treatment was associated with the emergence of TB in patients receiving this treatment for other reasons (201).

Similarly, IFN-γ signalling has been known to be critical for control of *Mtb* in animal models for decades (202, 203). IFN-γ from CD4+ T cells in particular is necessary for survival, and animals lacking IFN-γ from just CD4+ T cells succumb after two months post aerosol infection; however IFN-γ's role was mostly extrapulmonary with a limited role in the lungs (204). IL-12p40, upon which IFN-γ is partly dependent, has also been knocked-out in mice and resulted in uncontrolled replication of *Mtb* (Erdman strain, administered i.v.) and mortality within 1.5 months compared to WT mice which lived "to old age" (205). Human mutations in IFN-γ or IL-12 pathway genes causing impaired IFN-γ-mediated immunity result in Mendelian Susceptibility to Mycobacterial Disease, which manifests as childhood BCG dissemination or non-tuberculous mycobacterial infection, and occasionally *Mtb* infection later in those who live (206).

Cytokine and PRR signalling on their own do not have direct bactericidal effects – they are thought to modulate innate defense mechanisms and instruct adaptive immunity. The endgame of bacteriologic control are the host's killing mechanisms, which in macrophages include low phagosomal pH, digestive enzymes like lysozymes, and reactive oxygen species. As an example, the well-studied nitric oxide is produced by NOS2 to attack *Mtb*. Mice lacking NOS2 all died within 50 days of i.v. infection with 10^5 CFU Erdman strain while WT median survival was about 150 days (207). In a separate study, aerosol infection with 100 CFU H37Rv strain similarly resulted in death before day 50 associated with increased *Mtb* burden (208). Thus, effectors like nitric oxide are irreplaceable for control of *Mtb* and host survival.

WHY HAVE GENETIC STUDIES OF TB IN HUMANS BEEN UNDERWHELMING?

Genetic epidemiology studies have provided only a handful of PRR and non-PRR genes as global risk factors for TB. This lack of success is in striking contrast to leprosy, the second most common mycobacterial disease in humans (209). Strain diversity of *Mtb* compared to *M. leprae* might have played a role; however, the most likely cause for the lack of consistent results is phenotypic heterogeneity among TB cases. Most studies define TB as a single entity combining cases regardless of their clinical and biological characteristics. While this approach has worked for leprosy (210, 211), in other instances combining all leprosy cases has proven troublesome due to the presence of well-defined endophenotypes (212, 213). Common endophenotypes in leprosy are excessive host inflammatory responses, so-called lepra reactions, that sub-divide the overall group of patients. Endophenotypes can result in misclassification of genetic effects (213, 214). Indeed, the genetic associations can be in opposite direction between endophenotype and disease *per se* (212, 215).

Genetic modulators with opposing effects on unrecognized endophenotypes and clinically defined TB might be difficult to detect even in studies with very large sample sizes. This raises the question if similar, perhaps more complex endophenotypes, underlie the disappointing results from TB genetic studies. Specifically, considering the impact of PPR genes on intermediary immune phenotypes in the mouse, it is

conceivable that PPR polymorphism may yet have a role to play in the genetics of TB pathogenesis. Heterogeneity among cases appears to be predominant in large scale genetic studies in TB and the existence of TB endotypes has been proposed (216). Recent advances in molecular and analytical techniques have allowed the identification of at least two TB endotypes through unbiased clustering of transcriptional changes in distinct molecular pathways (217). One endophenotype presented immune exhaustion resulting in poor prognosis compared to the second endophenotype.

What remains unclear is to what extent TB endophenotypes represent the continued progression of TB pathogenesis or if they are distinct forms of the same disease. More studies will be necessary to settle this question. Such future studies need to focus on defining endophenotypes with the full weight of omics approaches, keeping in mind that these better-resolution phenotypes may represent kinetic entities. Such a 'systems-medicine' definition of TB, in excess of clinical and microbiological data, is expected to improve power for efficient mapping of endophenotypes. Molecular (RNA, proteins and metabolites) and immune (cellular) phenotyping using blood can provide information for dissociating TB cases into endophenotypes. This is a two-step approach, where first identification of interindividual molecular/cellular similarities is done prior to the genetic study. How to deal with the genetic study in the second step would depend on the groups, but could be either a continuous phenotype or stratified by endophenotype. Using an omics signature would overcome the limitations where patients are clinically similar but the genetic cause of TB is not the same. Clinical heterogeneity with *Mtb* infection that is ambiguous (e.g. placement on a spectrum from TST positive to active TB) can be better-defined or bypassed with non-biased omics data. However, independently of the nature of TB endotypes, it is now clear that heterogeneity may impact on genetic studies of TB and perhaps shed new light on the role of PPR polymorphisms.

FINAL THOUGHTS AND CONCLUSION

PRRs appear to be important for immunologic responses but have a more subtle role in control of *Mtb* and the course of TB. We hypothesize that this is partly due to the redundancy of many PRRs sensing different *Mtb* MAMPs. Amongst this redundancy, however, there may be unique immunological adjustments performed by specific PRRs. In contrast, genes that produce products mediating distinct effects, like IFN-γ, IL-12, nitric oxide and TNF are clearly essential to the host's survival. Although we can consider PRRs 'less important' than effectors, this prompts an interesting question: Is this a situation of reduced selective pressure, which explains human PRR diversity? It is imaginable that the immunological outcome performed by an orchestra of PRRs can be quite varied as individual PRR activities are tuned differently by genetics. By contrast, altering the potency of an effector like IFN-γ would directly correlate with *Mtb* control, and therefore selection would be purifying.

Human genetic association studies of TB have yielded but a few promising leads. Animal and cellular human data clearly demonstrate that PRRs affect immunity during *Mtb* infection, despite small and/or delayed survival and bacteriologic phenotypes in PRR KO mice. Thus, PRR mutation in humans might manifest in endophenotypes of *Mtb* infection – states of altered immunity wherein the progression of TB may possess subtly different parameters. Defining such endophenotypes of *Mtb* infection through molecular and immunological profiling of patients may provide a roadmap on which to trace the effects of PRR variation on the course of TB.

AUTHOR'S NOTE

Literature searches were performed on the Medline database with Pubmed and results were collected and curated using Endnote X9 (Clarivate Analytics, USA). The text, table and figure were created with Microsoft Word, Excel and PowerPoint, respectively.

AUTHOR CONTRIBUTIONS

All authors listed have made a substantial, direct, and intellectual contribution to the work, and approved it for publication.

FUNDING

J-YD is supported by a Canadian Institutes of Health Research (CIHR) Canada Graduate Scholarship – Master's Program, Fonds de Recherche du Québec – Santé (FRQ-S) Doctoral Training Award, RI-MUHC studentships and scholarships from the McGill Department of Microbiology and Immunology. MB: CIHR foundation grant (FDN-148362). ES CIHR foundation grant (FDN-143332) grant by NIH (1R01AI124349).

REFERENCES

1. Houben RM, Dodd PJ. The Global Burden of Latent Tuberculosis Infection: A Re-Estimation Using Mathematical Modelling. *PloS Med* (2016) 13(10): e1002152. doi: 10.1371/journal.pmed.1002152
2. Behr MA, Edelstein PH, Ramakrishnan L. Revisiting the Timetable of Tuberculosis. *BMJ* (2018) 362:k2738. doi: 10.1136/bmj.k2738
3. Bos KI, Harkins KM, Herbig A, Coscolla M, Weber N, Comas I, et al. Pre-Columbian Mycobacterial Genomes Reveal Seals as a Source of New World Human Tuberculosis. *Nature* (2014) 514(7523):494–7. doi: 10.1038/nature13591
4. Menardo F, Duchêne S, Brites D, Gagneux S. The Molecular Clock of Mycobacterium Tuberculosis. *PloS Pathog* (2019) 15(9):e1008067. doi: 10.1371/journal.ppat.1008067

5. Gagneux S. Host-Pathogen Coevolution in Human Tuberculosis. *Philos Trans R Soc Lond B Biol Sci* (2012) 367(1590):850–9. doi: 10.1098/rstb.2011.0316
6. Boisson-Dupuis S, Ramirez-Alejo N, Li Z, Patin E, Rao G, Kerner G, et al. Tuberculosis and Impaired IL-23-Dependent IFN-γ Immunity in Humans Homozygous for a Common TYK2 Missense Variant. *Sci Immunol* (2018) 3 (30):eaau8714. doi: 10.1126/sciimmunol.aau8714
7. Kerner G, Laval G, Patin E, Boisson-Dupuis S, Abel L, Casanova JL, et al. Human Ancient DNA Analyses Reveal the High Burden of Tuberculosis in Europeans Over the Last 2,000 Years. *Am J Hum Genet* (2021) 108(3):517–24. doi: 10.1016/j.ajhg.2021.02.009
8. Kerner G, Ramirez-Alejo N, Seeleuthner Y, Yang R, Ogishi M, Cobat A, et al. Homozygosity for TYK2 P1104A Underlies Tuberculosis in About 1% of Patients in a Cohort of European Ancestry. *Proc Natl Acad Sci USA* (2019) 116(21):10430–4. doi: 10.1073/pnas.1903561116
9. Möller M, Kinnear CJ, Orlova M, Kroon EE, van Helden PD, Schurr E, et al. Genetic Resistance to Mycobacterium Tuberculosis Infection and Disease. *Front Immunol* (2018) 9:2219(2219). doi: 10.3389/fimmu.2018.02219
10. Luo Y, Suliman S, Asgari S, Amariuta T, Baglaenko Y, Martínez-Bonet M, et al. Early Progression to Active Tuberculosis is a Highly Heritable Trait Driven by 3q23 in Peruvians. *Nat Commun* (2019) 10(1):3765. doi: 10.1038/s41467-019-11664-1
11. Napier G, Campino S, Merid Y, Abebe M, Woldeamanuel Y, Aseffa A, et al. Robust Barcoding and Identification of Mycobacterium Tuberculosis Lineages for Epidemiological and Clinical Studies. *Genome Med* (2020) 12 (1):114. doi: 10.1186/s13073-020-00817-3
12. Ngabonziza JCS, Loiseau C, Marceau M, Jouet A, Menardo F, Tzfadia O, et al. A Sister Lineage of the Mycobacterium Tuberculosis Complex Discovered in the African Great Lakes Region. *Nat Commun* (2020) 11 (1):2917. doi: 10.1038/s41467-020-16626-6
13. Coscolla M, Gagneux S, Menardo F, Loiseau C, Ruiz-Rodriguez P, Borrell S, et al. Phylogenomics of Mycobacterium Africanum Reveals a New Lineage and a Complex Evolutionary History. *Microb Genom* (2021) 7(2):000477. doi: 10.1099/mgen.0.000477
14. Bottai D, Frigui W, Sayes F, Di Luca M, Spadoni D, Pawlik A, et al. TbD1 Deletion as a Driver of the Evolutionary Success of Modern Epidemic Mycobacterium Tuberculosis Lineages. *Nat Commun* (2020) 11(1):684. doi: 10.1038/s41467-020-14508-5
15. Ernst JD. Antigenic Variation and Immune Escape in the MTBC. *Adv Exp Med Biol* (2017) 1019:171–90. doi: 10.1007/978-3-319-64371-7_9
16. Kroon EE, Kinnear CJ, Orlova M, Fischinger S, Shin S, Boolay S, et al. An Observational Study Identifying Highly Tuberculosis-Exposed, HIV-1-Positive But Persistently TB, Tuberculin and IGRA Negative Persons With M. tuberculosis specific antibodies in Cape Town, South Africa. *EBioMedicine* (2020) 61:103053. doi: 10.1016/j.ebiom.2020.103053
17. Joosten SA, Ottenhoff THM, Lewinsohn DM, Hoft DF, Moody DB, Seshadri C. Harnessing Donor Unrestricted T-Cells for New Vaccines Against Tuberculosis. *Vaccine* (2019) 37(23):3022–30. doi: 10.1016/j.vaccine.2019.04.050
18. Ruibal P, Voogd L, Joosten SA, Ottenhoff THM. The Role of Donor-Unrestricted T-Cells, Innate Lymphoid Cells, and NK Cells in Anti-Mycobacterial Immunity. *Immunol Rev* (2021) 301(1):30–47. doi: 10.1111/imr.12948
19. Janeway CA. Approaching the Asymptote? Evolution and Revolution in Immunology. *Cold Spring Harb Symp Quant Biol* (1989) 54:1–13. doi: 10.1101/SQB.1989.054.01.003
20. Lemaitre B, Nicolas E, Michaut L, Reichhart JM, Hoffmann JA. The Dorsoventral Regulatory Gene Cassette Spätzle/Toll/cactus Controls the Potent Antifungal Response in Drosophila Adults. *Cell* (1996) 86(6):973–83. doi: 10.1016/s0092-8674(00)80172-5
21. Medzhitov R, Preston-Hurlburt P, Janeway CAJr. A Human Homologue of the Drosophila Toll Protein Signals Activation of Adaptive Immunity. *Nature* (1997) 388(6640):394–7. doi: 10.1038/41131
22. Poltorak A, He X, Smirnova I, Liu MY, Van Huffel C, Du X, et al. Defective LPS Signaling in C3H/HeJ and C57BL/10ScCr Mice: Mutations in Tlr4 Gene. *Science* (1998) 282(5396):2085–8. doi: 10.1126/science.282.5396.2085
23. Qureshi ST, Larivière L, Leveque G, Clermont S, Moore KJ, Gros P, et al. Endotoxin-Tolerant Mice Have Mutations in Toll-Like Receptor 4 (Tlr4). *J Exp Med* (1999) 189(4):615–25. doi: 10.1084/jem.189.4.615
24. Means TK, Lien E, Yoshimura A, Wang S, Golenbock DT, Fenton MJ. The CD14 Ligands Lipoarabinomannan and Lipopolysaccharide Differ in Their Requirement for Toll-Like Receptors. *J Immunol* (1999) 163(12):6748–55.
25. Means TK, Wang S, Lien E, Yoshimura A, Golenbock DT, Fenton MJ. Human Toll-Like Receptors Mediate Cellular Activation by Mycobacterium Tuberculosis. *J Immunol* (1999) 163(7):3920–7.
26. Brightbill HD, Libraty DH, Krutzik SR, Yang RB, Belisle JT, Bleharski JR, et al. Host Defense Mechanisms Triggered by Microbial Lipoproteins Through Toll-Like Receptors. *Science* (1999) 285(5428):732–6. doi: 10.1126/science.285.5428.732
27. Jones BW, Means TK, Heldwein KA, Keen MA, Hill PJ, Belisle JT, et al. Different Toll-Like Receptor Agonists Induce Distinct Macrophage Responses. *J Leukoc Biol* (2001) 69(6):1036–44.
28. Gilleron M, Quesniaux VF, Puzo G. Acylation State of the Phosphatidylinositol Hexamannosides From Mycobacterium Bovis Bacillus Calmette Guerin and Mycobacterium Tuberculosis H37Rv and its Implication in Toll-Like Receptor Response. *J Biol Chem* (2003) 278 (32):29880–9. doi: 10.1074/jbc.M303446200
29. Gehring AJ, Dobos KM, Belisle JT, Harding CV, Boom WH. Mycobacterium Tuberculosis LprG (Rv1411c): A Novel TLR-2 Ligand That Inhibits Human Macrophage Class II MHC Antigen Processing. *J Immunol* (2004) 173 (4):2660–8. doi: 10.4049/jimmunol.173.4.2660
30. Pecora ND, Gehring AJ, Canaday DH, Boom WH, Harding CV. Mycobacterium Tuberculosis LprA is a Lipoprotein Agonist of TLR2 That Regulates Innate Immunity and APC Function. *J Immunol* (2006) 177 (1):422–9. doi: 10.4049/jimmunol.177.1.422
31. Drage MG, Pecora ND, Hise AG, Febbraio M, Silverstein RL, Golenbock DT, et al. TLR2 and its Co-Receptors Determine Responses of Macrophages and Dendritic Cells to Lipoproteins of Mycobacterium Tuberculosis. *Cell Immunol* (2009) 258(1):29–37. doi: 10.1016/j.cellimm.2009.03.008
32. Prados-Rosales R, Baena A, Martinez LR, Luque-Garcia J, Kalscheuer R, Veeraraghavan U, et al. Mycobacteria Release Active Membrane Vesicles That Modulate Immune Responses in a TLR2-Dependent Manner in Mice. *J Clin Invest* (2011) 121(4):1471–83. doi: 10.1172/jci44261
33. Blanc L, Gilleron M, Prandi J, Song OR, Jang MS, Gicquel B, et al. Mycobacterium Tuberculosis Inhibits Human Innate Immune Responses *via* the Production of TLR2 Antagonist Glycolipids. *Proc Natl Acad Sci USA* (2017) 114(42):11205–10. doi: 10.1073/pnas.1707840114
34. Cehovin A, Coates AR, Hu Y, Riffo-Vasquez Y, Tormay P, Botanch C, et al. Comparison of the Moonlighting Actions of the Two Highly Homologous Chaperonin 60 Proteins of Mycobacterium Tuberculosis. *Infect Immun* (2010) 78(7):3196–206. doi: 10.1128/iai.01379-09
35. Bai W, Liu H, Ji Q, Zhou Y, Liang L, Zheng R, et al. TLR3 Regulates Mycobacterial RNA-Induced IL-10 Production Through the PI3K/AKT Signaling Pathway. *Cell Signal* (2014) 26(5):942–50. doi: 10.1016/j.cellsig.2014.01.015
36. Keegan C, Krutzik S, Schenk M, Scumpia PO, Lu J, Pang YLJ, et al. Mycobacterium Tuberculosis Transfer RNA Induces IL-12p70 *via* Synergistic Activation of Pattern Recognition Receptors Within a Cell Network. *J Immunol* (2018) 200(9):3244–58. doi: 10.4049/jimmunol.1701733
37. Pawar K, Shigematsu M, Sharbati S, Kirino Y. Infection-Induced 5'-Half Molecules of Trnahisgug Activate Toll-Like Receptor 7. *PloS Biol* (2020) 18 (12):e3000982. doi: 10.1371/journal.pbio.3000982
38. Matsumoto S, Matsumoto M, Umemori K, Ozeki Y, Furugen M, Tatsuo T, et al. DNA Augments Antigenicity of Mycobacterial DNA-Binding Protein 1 and Confers Protection Against Mycobacterium Tuberculosis Infection in Mice. *J Immunol* (2005) 175(1):441–9. doi: 10.4049/jimmunol.175.1.441
39. Ruiz A, Guzmán-Beltrán S, Carreto-Binaghi LE, Gonzalez Y, Juárez E. DNA From Virulent M. Tuberculosis Induces TNF-α Production and Autophagy in M1 Polarized Macrophages. *Microb Pathog* (2019) 132:166–77. doi: 10.1016/j.micpath.2019.04.041
40. Fitzgerald KA, Kagan JC. Toll-Like Receptors and the Control of Immunity. *Cell* (2020) 180(6):1044–66. doi: 10.1016/j.cell.2020.02.041
41. Brown GD, Willment JA, Whitehead L. C-Type Lectins in Immunity and Homeostasis. *Nat Rev Immunol* (2018) 18(6):374–89. doi: 10.1038/s41577-018-0004-8

42. Schlesinger LS. Macrophage Phagocytosis of Virulent But Not Attenuated Strains of Mycobacterium Tuberculosis is Mediated by Mannose Receptors in Addition to Complement Receptors. *J Immunol* (1993) 150(7):2920–30.
43. Schlesinger LS, Hull SR, Kaufman TM. Binding of the Terminal Mannosyl Units of Lipoarabinomannan From a Virulent Strain of Mycobacterium Tuberculosis to Human Macrophages. *J Immunol* (1994) 152(8):4070–9.
44. Rajaram MV, Brooks MN, Morris JD, Torrelles JB, Azad AK, Schlesinger LS. Mycobacterium Tuberculosis Activates Human Macrophage Peroxisome Proliferator-Activated Receptor Gamma Linking Mannose Receptor Recognition to Regulation of Immune Responses. *J Immunol* (2010) 185 (2):929–42. doi: 10.4049/jimmunol.1000866
45. Guirado E, Rajaram MV, Chawla A, Daigle J, La Perle KM, Arnett E, et al. Deletion of Pparγ in Lung Macrophages Provides an Immunoprotective Response Against M. tuberculosis infection in mice. *Tuberculosis (Edinb)* (2018) 111:170–7. doi: 10.1016/j.tube.2018.06.012
46. Tailleux L, Schwartz O, Herrmann JL, Pivert E, Jackson M, Amara A, et al. DC-SIGN is the Major Mycobacterium Tuberculosis Receptor on Human Dendritic Cells. *J Exp Med* (2003) 197(1):121–7. doi: 10.1084/jem.20021468
47. Maeda N, Nigou J, Herrmann JL, Jackson M, Amara A, Lagrange PH, et al. The Cell Surface Receptor DC-SIGN Discriminates Between Mycobacterium Species Through Selective Recognition of the Mannose Caps on Lipoarabinomannan. *J Biol Chem* (2003) 278(8):5513–6. doi: 10.1074/jbc.C200586200
48. Driessen NN, Ummels R, Maaskant JJ, Gurcha SS, Besra GS, Ainge GD, et al. Role of Phosphatidylinositol Mannosides in the Interaction Between Mycobacteria and DC-SIGN. *Infect Immun* (2009) 77(10):4538–47. doi: 10.1128/iai.01256-08
49. Geurtsen J, Chedammi S, Mesters J, Cot M, Driessen NN, Sambou T, et al. Identification of Mycobacterial Alpha-Glucan as a Novel Ligand for DC-SIGN: Involvement of Mycobacterial Capsular Polysaccharides in Host Immune Modulation. *J Immunol* (2009) 183(8):5221–31. doi: 10.4049/jimmunol.0900768
50. Koppel EA, Ludwig IS, Hernandez MS, Lowary TL, Gadikota RR, Tuzikov AB, et al. Identification of the Mycobacterial Carbohydrate Structure That Binds the C-Type Lectins DC-SIGN, L-SIGN and SIGNR1. *Immunobiology* (2004) 209(1-2):117–27. doi: 10.1016/j.imbio.2004.03.003
51. Gringhuis SI, den Dunnen J, Litjens M, van Het Hof B, van Kooyk Y, Geijtenbeek TB. C-Type Lectin DC-SIGN Modulates Toll-Like Receptor Signaling *via* Raf-1 Kinase-Dependent Acetylation of Transcription Factor NF-Kappab. *Immunity* (2007) 26(5):605–16. doi: 10.1016/j.immuni.2007.03.012
52. Gringhuis SI, den Dunnen J, Litjens M, van der Vlist M, Geijtenbeek TB. Carbohydrate-Specific Signaling Through the DC-SIGN Signalosome Tailors Immunity to Mycobacterium Tuberculosis, HIV-1 and Helicobacter Pylori. *Nat Immunol* (2009) 10(10):1081–8. doi: 10.1038/ni.1778
53. Ishikawa E, Ishikawa T, Morita YS, Toyonaga K, Yamada H, Takeuchi O, et al. Direct Recognition of the Mycobacterial Glycolipid, Trehalose Dimycolate, by C-Type Lectin Mincle. *J Exp Med* (2009) 206(13):2879–88. doi: 10.1084/jem.20091750
54. Ostrop J, Jozefowski K, Zimmermann S, Hofmann K, Strasser E, Lepenies B, et al. Contribution of MINCLE-SYK Signaling to Activation of Primary Human APCs by Mycobacterial Cord Factor and the Novel Adjuvant TDB. *J Immunol* (2015) 195(5):2417–28. doi: 10.4049/jimmunol.1500102
55. Dorhoi A, Desel C, Yeremeev V, Pradl L, Brinkmann V, Mollenkopf HJ, et al. The Adaptor Molecule CARD9 is Essential for Tuberculosis Control. *J Exp Med* (2010) 207(4):777–92. doi: 10.1084/jem.20090067
56. Miyake Y, Toyonaga K, Mori D, Kakuta S, Hoshino Y, Oyamada A, et al. C-Type Lectin MCL is an Fcrγ-Coupled Receptor That Mediates the Adjuvanticity of Mycobacterial Cord Factor. *Immunity* (2013) 38(5):1050–62. doi: 10.1016/j.immuni.2013.03.010
57. Miyake Y, Oh-hora M, Yamasaki S. C-Type Lectin Receptor MCL Facilitates Mincle Expression and Signaling Through Complex Formation. *J Immunol* (2015) 194(11):5366–74. doi: 10.4049/jimmunol.1402429
58. Kerscher B, Wilson GJ, Reid DM, Mori D, Taylor JA, Besra GS, et al. Mycobacterial Receptor, Clec4d (CLECSF8, MCL), is Coregulated With Mincle and Upregulated on Mouse Myeloid Cells Following Microbial Challenge. *Eur J Immunol* (2016) 46(2):381–9. doi: 10.1002/eji.201545858
59. Rothfuchs AG, Bafica A, Feng CG, Egen JG, Williams DL, Brown GD, et al. Dectin-1 Interaction With Mycobacterium Tuberculosis Leads to Enhanced IL-12p40 Production by Splenic Dendritic Cells. *J Immunol* (2007) 179 (6):3463–71. doi: 10.4049/jimmunol.179.6.3463
60. Das R, Koo MS, Kim BH, Jacob ST, Subbian S, Yao J, et al. Macrophage Migration Inhibitory Factor (MIF) is a Critical Mediator of the Innate Immune Response to Mycobacterium Tuberculosis. *Proc Natl Acad Sci U.S.A.* (2013) 110(32):E2997–3006. doi: 10.1073/pnas.1301128110
61. Yonekawa A, Saijo S, Hoshino Y, Miyake Y, Ishikawa E, Suzukawa M, et al. Dectin-2 is a Direct Receptor for Mannose-Capped Lipoarabinomannan of Mycobacteria. *Immunity* (2014) 41(3):402–13. doi: 10.1016/j.immuni.2014.08.005
62. Decout A, Silva-Gomes S, Drocourt D, Blattes E, Rivière M, Prandi J, et al. Deciphering the Molecular Basis of Mycobacteria and Lipoglycan Recognition by the C-Type Lectin Dectin-2. *Sci Rep* (2018) 8(1):16840. doi: 10.1038/s41598-018-35393-5
63. Toyonaga K, Torigoe S, Motomura Y, Kamichi T, Hayashi JM, Morita YS, et al. C-Type Lectin Receptor DCAR Recognizes Mycobacterial Phosphatidyl-Inositol Mannosides to Promote a Th1 Response During Infection. *Immunity* (2016) 45(6):1245–57. doi: 10.1016/j.immuni.2016.10.012
64. Downing JF, Pasula R, Wright JR, Twigg HL3rd, Martin WJ2nd. Surfactant Protein a Promotes Attachment of Mycobacterium Tuberculosis to Alveolar Macrophages During Infection With Human Immunodeficiency Virus. *Proc Natl Acad Sci U.S.A.* (1995) 92(11):4848–52. doi: 10.1073/pnas.92.11.4848
65. Gaynor CD, McCormack FX, Voelker DR, McGowan SE, Schlesinger LS. Pulmonary Surfactant Protein A Mediates Enhanced Phagocytosis of Mycobacterium Tuberculosis by a Direct Interaction With Human Macrophages. *J Immunol* (1995) 155(11):5343–51.
66. Pasula R, Wright JR, Kachel DL, Martin WJ2nd. Surfactant Protein A Suppresses Reactive Nitrogen Intermediates by Alveolar Macrophages in Response to Mycobacterium Tuberculosis. *J Clin Invest* (1999) 103(4):483–90. doi: 10.1172/jci2991
67. Sidobre S, Nigou J, Puzo G, Rivière M. Lipoglycans are Putative Ligands for the Human Pulmonary Surfactant Protein A Attachment to Mycobacteria. *Crit role Lipids Lectin Carbohydrate Recognit J Biol Chem* (2000) 275 (4):2415–22. doi: 10.1074/jbc.275.4.2415
68. Ragas A, Roussel L, Puzo G, Rivière M. The Mycobacterium Tuberculosis Cell-Surface Glycoprotein Apa as a Potential Adhesin to Colonize Target Cells *via* the Innate Immune System Pulmonary C-Type Lectin Surfactant Protein a. *J Biol Chem* (2007) 282(8):5133–42. doi: 10.1074/jbc.M610183200
69. Ferguson JS, Voelker DR, McCormack FX, Schlesinger LS. Surfactant Protein D Binds to Mycobacterium Tuberculosis Bacilli and Lipoarabinomannan *via* Carbohydrate-Lectin Interactions Resulting in Reduced Phagocytosis of the Bacteria by Macrophages. *J Immunol* (1999) 163(1):312–21.
70. Ferguson JS, Voelker DR, Ufnar JA, Dawson AJ, Schlesinger LS. Surfactant Protein D Inhibition of Human Macrophage Uptake of Mycobacterium Tuberculosis is Independent of Bacterial Agglutination. *J Immunol* (2002) 168(3):1309–14. doi: 10.4049/jimmunol.168.3.1309
71. Ferguson JS, Martin JL, Azad AK, McCarthy TR, Kang PB, Voelker DR, et al. Surfactant Protein D Increases Fusion of Mycobacterium Tuberculosis-Containing Phagosomes With Lysosomes in Human Macrophages. *Infect Immun* (2006) 74(12):7005–9. doi: 10.1128/iai.01402-06
72. Garred P, Harboe M, Oettinger T, Koch C, Svejgaard A. Dual Role of Mannan-Binding Protein in Infections: Another Case of Heterosis? *Eur J Immunogenet* (1994) 21(2):125–31. doi: 10.1111/j.1744-313x.1994.tb00183.x
73. Luo F, Sun X, Wang Y, Wang Q, Wu Y, Pan Q, et al. Ficolin-2 Defends Against Virulent Mycobacteria Tuberculosis Infection *In Vivo*, and its Insufficiency is Associated With Infection in Humans. *PloS One* (2013) 8 (9):e73859. doi: 10.1371/journal.pone.0073859
74. Bartlomiejczyk MA, Swierzko AS, Brzostek A, Dziadek J, Cedzynski M. Interaction of Lectin Pathway of Complement-Activating Pattern Recognition Molecules With Mycobacteria. *Clin Exp Immunol* (2014) 178 (2):310–9. doi: 10.1111/cei.12416
75. Polotsky VY, Belisle JT, Mikusova K, Ezekowitz RA, Joiner KA. Interaction of Human Mannose-Binding Protein With Mycobacterium Avium. *J Infect Dis* (1997) 175(5):1159–68. doi: 10.1086/520354
76. Świerzko AS, Bartłomiejczyk MA, Brzostek A, Łukasiewicz J, Michalski M, Dziadek J, et al. Mycobacterial Antigen 85 Complex (Ag85) as a Target for

Ficolins and Mannose-Binding Lectin. *Int J Med Microbiol* (2016) 306 (4):212–21. doi: 10.1016/j.ijmm.2016.04.004
77. Zhong Y, Kinio A, Saleh M. Functions of NOD-Like Receptors in Human Diseases. *Front Immunol* (2013) 4:333. doi: 10.3389/fimmu.2013.00333
78. Girardin SE, Boneca IG, Viala J, Chamaillard M, Labigne A, Thomas G, et al. Nod2 is a General Sensor of Peptidoglycan Through Muramyl Dipeptide (MDP) Detection. *J Biol Chem* (2003) 278(11):8869–72. doi: 10.1074/jbc.C200651200
79. Inohara N, Ogura Y, Fontalba A, Gutierrez O, Pons F, Crespo J, et al. Host Recognition of Bacterial Muramyl Dipeptide Mediated Through NOD2. *Implications Crohn's Disease J Biol Chem* (2003) 278(8):5509–12. doi: 10.1074/jbc.C200673200
80. Chamaillard M, Hashimoto M, Horie Y, Masumoto J, Qiu S, Saab L, et al. An Essential Role for NOD1 in Host Recognition of Bacterial Peptidoglycan Containing Diaminopimelic Acid. *Nat Immunol* (2003) 4(7):702–7. doi: 10.1038/ni945
81. Girardin SE, Boneca IG, Carneiro LA, Antignac A, Jéhanno M, Viala J, et al. Nod1 Detects a Unique Muropeptide From Gram-Negative Bacterial Peptidoglycan. *Science* (2003) 300(5625):1584–7. doi: 10.1126/science.1084677
82. Lee JY, Hwang EH, Kim DJ, Oh SM, Lee KB, Shin SJ, et al. The Role of Nucleotide-Binding Oligomerization Domain 1 During Cytokine Production by Macrophages in Response to Mycobacterium Tuberculosis Infection. *Immunobiology* (2016) 221(1):70–5. doi: 10.1016/j.imbio.2015.07.020
83. Mahapatra S, Crick DC, McNeil MR, Brennan PJ. Unique Structural Features of the Peptidoglycan of Mycobacterium Leprae. *J Bacteriol* (2008) 190(2):655–61. doi: 10.1128/JB.00982-07
84. Essers L, Schoop HJ. Evidence for the Incorporation of Molecular Oxygen, a Pathway in Biosynthesis of *N*-Glycolylmuramic Acid in *Mycobacterium Phlei*. *Biochim Biophys Acta* (1978) 544:180–4. doi: 10.1016/0304-4165(78)90221-0
85. Raymond JB, Mahapatra S, Crick DC, Pavelka MSJr. Identification of the namH Gene, Encoding the Hydroxylase Responsible for the N-Glycolylation of the Mycobacterial Peptidoglycan. *J Biol Chem* (2005) 280(1):326–33. doi: 10.1074/jbc.M411006200
86. Coulombe F, Divangahi M, Veyrier F, de Leseleuc L, Gleason JL, Yang Y, et al. Increased NOD2-Mediated Recognition of *N*-Glycolyl Muramyl Dipeptide. *J Exp Med* (2009) 206(8):1709–16. doi: 10.1084/jem.20081779
87. Hansen JM, Golchin SA, Veyrier FJ, Domenech P, Boneca IG, Azad AK, et al. *N*-Glycolylated Peptidoglycan Contributes to the Immunogenicity But Not Pathogenicity of Mycobacterium Tuberculosis. *J Infect Dis* (2014) 209 (7):1045–54. doi: 10.1093/infdis/jit622
88. Dubé J-Y, McIntosh F, Zarruk JG, David S, Nigou J, Behr MA. Synthetic Mycobacterial Molecular Patterns Partially Complete Freund's Adjuvant. *Sci Rep* (2020) 10(1):5874. doi: 10.1038/s41598-020-62543-5
89. Gandotra S, Jang S, Murray PJ, Salgame P, Ehrt S. Nucleotide-Binding Oligomerization Domain Protein 2-Deficient Mice Control Infection With Mycobacterium Tuberculosis. *Infect Immun* (2007) 75(11):5127–34. doi: 10.1128/IAI.00458-07
90. Divangahi M, Mostowy S, Coulombe F, Kozak R, Guillot L, Veyrier F, et al. NOD2-Deficient Mice Have Impaired Resistance to Mycobacterium Tuberculosis Infection Through Defective Innate and Adaptive Immunity. *J Immunol* (2008) 181(10):7157–65. doi: 10.4049/jimmunol.181.10.7157
91. Landes MB, Rajaram MV, Nguyen H, Schlesinger LS. Role for NOD2 in Mycobacterium Tuberculosis-Induced iNOS Expression and NO Production in Human Macrophages. *J Leukoc Biol* (2015) 97(6):1111–9. doi: 10.1189/jlb.3A1114-557R
92. Ferwerda G, Girardin SE, Kullberg BJ, Le Bourhis L, de Jong DJ, Langenberg DM, et al. NOD2 and Toll-Like Receptors are Nonredundant Recognition Systems of Mycobacterium Tuberculosis. *PloS Pathog* (2005) 1(3):279–85. doi: 10.1371/journal.ppat.0010034
93. Beckwith KS, Beckwith MS, Ullmann S, Sætra RS, Kim H, Marstad A, et al. Plasma Membrane Damage Causes NLRP3 Activation and Pyroptosis During Mycobacterium Tuberculosis Infection. *Nat Commun* (2020) 11 (1):2270. doi: 10.1038/s41467-020-16143-6
94. Saiga H, Kitada S, Shimada Y, Kamiyama N, Okuyama M, Makino M, et al. Critical Role of AIM2 in Mycobacterium Tuberculosis Infection. *Int Immunol* (2012) 24(10):637–44. doi: 10.1093/intimm/dxs062
95. Watson RO, Manzanillo PS, Cox JS. Extracellular M. Tuberculosis DNA Targets Bacteria for Autophagy by Activating the Host DNA-Sensing Pathway. *Cell* (2012) 150(4):803–15. doi: 10.1016/j.cell.2012.06.040
96. van der Vaart M, Korbee CJ, Lamers GE, Tengeler AC, Hosseini R, Haks MC, et al. The DNA Damage-Regulated Autophagy Modulator DRAM1 Links Mycobacterial Recognition *via* TLR-MYD88 to Autophagic Defense [Corrected]. *Cell Host Microbe* (2014) 15(6):753–67. doi: 10.1016/j.chom.2014.05.005
97. Collins AC, Cai H, Li T, Franco LH, Li XD, Nair VR, et al. Cyclic GMP-AMP Synthase Is an Innate Immune DNA Sensor for Mycobacterium Tuberculosis. *Cell Host Microbe* (2015) 17(6):820–8. doi: 10.1016/j.chom.2015.05.005
98. Wassermann R, Gulen MF, Sala C, Perin SG, Lou Y, Rybniker J, et al. Mycobacterium Tuberculosis Differentially Activates cGAS- and Inflammasome-Dependent Intracellular Immune Responses Through ESX-1. *Cell Host Microbe* (2015) 17(6):799–810. doi: 10.1016/j.chom.2015.05.003
99. Watson RO, Bell SL, MacDuff DA, Kimmey JM, Diner EJ, Olivas J, et al. The Cytosolic Sensor cGAS Detects Mycobacterium Tuberculosis DNA to Induce Type I Interferons and Activate Autophagy. *Cell Host Microbe* (2015) 17(6):811–9. doi: 10.1016/j.chom.2015.05.004
100. Dey B, Dey RJ, Cheung LS, Pokkali S, Guo H, Lee JH, et al. A Bacterial Cyclic Dinucleotide Activates the Cytosolic Surveillance Pathway and Mediates Innate Resistance to Tuberculosis. *Nat Med* (2015) 21(4):401–6. doi: 10.1038/nm.3813
101. Yan S, Shen H, Lian Q, Jin W, Zhang R, Lin X, et al. Deficiency of the AIM2-ASC Signal Uncovers the STING-Driven Overreactive Response of Type I IFN and Reciprocal Depression of Protective IFN-γ Immunity in Mycobacterial Infection. *J Immunol* (2018) 200(3):1016–26. doi: 10.4049/jimmunol.1701177
102. Patten DA , Shetty S. More Than Just a Removal Service: Scavenger Receptors in Leukocyte Trafficking. *Front Immunol* (2018) 9:2904. doi: 10.3389/fimmu.2018.02904
103. Pombinho R, Sousa S, Cabanes D. Scavenger Receptors: Promiscuous Players During Microbial Pathogenesis. *Crit Rev Microbiol* (2018) 44(6):685–700. doi: 10.1080/1040841X.2018.1493716
104. Zimmerli S, Edwards S, Ernst JD. Selective Receptor Blockade During Phagocytosis Does Not Alter the Survival and Growth of Mycobacterium Tuberculosis in Human Macrophages. *Am J Respir Cell Mol Biol* (1996) 15 (6):760–70. doi: 10.1165/ajrcmb.15.6.8969271
105. Bowdish DM, Sakamoto K, Kim MJ, Kroos M, Mukhopadhyay S, Leifer CA, et al. MARCO, TLR2, and CD14 are Required for Macrophage Cytokine Responses to Mycobacterial Trehalose Dimycolate and Mycobacterium Tuberculosis. *PloS Pathog* (2009) 5(6):e1000474. doi: 10.1371/journal.ppat.1000474
106. Benard EL, Roobol SJ, Spaink HP, Meijer AH. Phagocytosis of Mycobacteria by Zebrafish Macrophages is Dependent on the Scavenger Receptor Marco, a Key Control Factor of Pro-Inflammatory Signalling. *Dev Comp Immunol* (2014) 47(2):223–33. doi: 10.1016/j.dci.2014.07.022
107. Khan A, Mann L, Papanna R, Lyu MA, Singh CR, Olson S, et al. Mesenchymal Stem Cells Internalize Mycobacterium Tuberculosis Through Scavenger Receptors and Restrict Bacterial Growth Through Autophagy. *Sci Rep* (2017) 7(1):15010. doi: 10.1038/s41598-017-15290-z
108. Shi S, Blumenthal A, Hickey CM, Gandotra S, Levy D, Ehrt S. Expression of Many Immunologically Important Genes in Mycobacterium Tuberculosis-Infected Macrophages is Independent of Both TLR2 and TLR4 But Dependent on IFN-Alphabeta Receptor and STAT1. *J Immunol* (2005) 175 (5):3318–28. doi: 10.4049/jimmunol.175.5.3318
109. Ozeki Y, Tsutsui H, Kawada N, Suzuki H, Kataoka M, Kodama T, et al. Macrophage Scavenger Receptor Down-Regulates Mycobacterial Cord Factor-Induced Proinflammatory Cytokine Production by Alveolar and Hepatic Macrophages. *Microb Pathog* (2006) 40(4):171–6. doi: 10.1016/j.micpath.2005.12.006
110. Schäfer G, Guler R, Murray G, Brombacher F, Brown GD. The Role of Scavenger Receptor B1 in Infection With Mycobacterium Tuberculosis in a Murine Model. *PloS One* (2009) 4(12):e8448. doi: 10.1371/journal.pone.0008448
111. Khan HS, Nair VR, Ruhl CR, Alvarez-Arguedas S, Galvan Rendiz JL, Franco LH, et al. Identification of Scavenger Receptor B1 as the Airway Microfold

Cell Receptor for Mycobacterium Tuberculosis. *Elife* (2020) 9:e52551. doi: 10.7554/eLife.52551
112. Philips JA, Rubin EJ, Perrimon N. Drosophila RNAi Screen Reveals CD36 Family Member Required for Mycobacterial Infection. *Science* (2005) 309 (5738):1251–3. doi: 10.1126/science.1116006
113. Dodd CE, Pyle CJ, Glowinski R, Rajaram MV, Schlesinger LS. CD36-Mediated Uptake of Surfactant Lipids by Human Macrophages Promotes Intracellular Growth of Mycobacterium Tuberculosis. *J Immunol* (2016) 197 (12):4727–35. doi: 10.4049/jimmunol.1600856
114. Hawkes M, Li X, Crockett M, Diassiti A, Finney C, Min-Oo G, et al. CD36 Deficiency Attenuates Experimental Mycobacterial Infection. *BMC Infect Dis* (2010) 10:299. doi: 10.1186/1471-2334-10-299
115. Sattler N, Bosmani C, Barisch C, Guého A, Gopaldass N, Dias M, et al. Functions of the Dictyostelium LIMP-2 and CD36 Homologues in Bacteria Uptake, Phagolysosome Biogenesis and Host Cell Defence. *J Cell Sci* (2018) 131(17):jcs218040. doi: 10.1242/jcs.218040
116. Reiling N, Hölscher C, Fehrenbach A, Kröger S, Kirschning CJ, Goyert S, et al. Cutting Edge: Toll-Like Receptor (TLR)2- and TLR4-Mediated Pathogen Recognition in Resistance to Airborne Infection With Mycobacterium Tuberculosis. *J Immunol* (2002) 169(7):3480–4. doi: 10.4049/jimmunol.169.7.3480
117. Sugawara I, Yamada H, Li C, Mizuno S, Takeuchi O, Akira S. Mycobacterial Infection in TLR2 and TLR6 Knockout Mice. *Microbiol Immunol* (2003) 47 (5):327–36. doi: 10.1111/j.1348-0421.2003.tb03404.x
118. Drennan MB, Nicolle D, Quesniaux VJ, Jacobs M, Allie N, Mpagi J, et al. Toll-Like Receptor 2-Deficient Mice Succumb to Mycobacterium Tuberculosis Infection. *Am J Pathol* (2004) 164(1):49–57. doi: 10.1016/s0002-9440(10)63095-7
119. Báfica A, Scanga CA, Schito ML, Hieny S, Sher A. Cutting Edge: *In Vivo* Induction of Integrated HIV-1 Expression by Mycobacteria is Critically Dependent on Toll-Like Receptor 2. *J Immunol* (2003) 171(3):1123–7. doi: 10.4049/jimmunol.171.3.1123
120. Tjärnlund A, Guirado E, Julián E, Cardona PJ, Fernández C. Determinant Role for Toll-Like Receptor Signalling in Acute Mycobacterial Infection in the Respiratory Tract. *Microbes Infect* (2006) 8(7):1790–800. doi: 10.1016/j.micinf.2006.02.017
121. Hölscher C, Reiling N, Schaible UE, Hölscher A, Bathmann C, Korbel D, et al. Containment of Aerogenic Mycobacterium Tuberculosis Infection in Mice Does Not Require MyD88 Adaptor Function for TLR2, -4 and -9. *Eur J Immunol* (2008) 38(3):680–94. doi: 10.1002/eji.200736458
122. Carlos D, Frantz FG, Souza-Júnior DA, Jamur MC, Oliver C, Ramos SG, et al. TLR2-Dependent Mast Cell Activation Contributes to the Control of Mycobacterium Tuberculosis Infection. *Microbes Infect* (2009) 11(8-9):770–8. doi: 10.1016/j.micinf.2009.04.025
123. Teixeira-Coelho M, Cruz A, Carmona J, Sousa C, Ramos-Pereira D, Saraiva AL, et al. TLR2 Deficiency by Compromising P19 (IL-23) Expression Limits Th 17 Cell Responses to Mycobacterium Tuberculosis. *Int Immunol* (2011) 23(2):89–96. doi: 10.1093/intimm/dxq459
124. Choi HH, Kim KK, Kim KD, Kim HJ, Jo EK, Song CH. Effects of Mycobacterial Infection on Proliferation of Hematopoietic Precursor Cells. *Microbes Infect* (2011) 13(14-15):1252–60. doi: 10.1016/j.micinf.2011.08.001
125. McBride A, Bhatt K, Salgame P. Development of a Secondary Immune Response to Mycobacterium Tuberculosis is Independent of Toll-Like Receptor 2. *Infect Immun* (2011) 79(3):1118–23. doi: 10.1128/iai.01076-10
126. McBride A, Konowich J, Salgame P. Host Defense and Recruitment of Foxp3$^+$ T Regulatory Cells to the Lungs in Chronic Mycobacterium Tuberculosis Infection Requires Toll-Like Receptor 2. *PloS Pathog* (2013) 9 (6):e1003397. doi: 10.1371/journal.ppat.1003397
127. Konowich J, Gopalakrishnan A, Dietzold J, Verma S, Bhatt K, Rafi W, et al. Divergent Functions of TLR2 on Hematopoietic and Nonhematopoietic Cells During Chronic Mycobacterium Tuberculosis Infection. *J Immunol* (2017) 198(2):741–8. doi: 10.4049/jimmunol.1601651
128. Gopalakrishnan A, Dietzold J, Verma S, Bhagavathula M, Salgame P. Toll-Like Receptor 2 Prevents Neutrophil-Driven Immunopathology During Infection With Mycobacterium Tuberculosis by Curtailing CXCL5 Production. *Infect Immun* (2019) 87(3):e00760-18. doi: 10.1128/iai.00760-18
129. Blumenthal A, Kobayashi T, Pierini LM, Banaei N, Ernst JD, Miyake K, et al. RP105 Facilitates Macrophage Activation by Mycobacterium Tuberculosis Lipoproteins. *Cell Host Microbe* (2009) 5(1):35–46. doi: 10.1016/j.chom.2008.12.002
130. Abel B, Thieblemont N, Quesniaux VJ, Brown N, Mpagi J, Miyake K, et al. Toll-Like Receptor 4 Expression is Required to Control Chronic Mycobacterium Tuberculosis Infection in Mice. *J Immunol* (2002) 169 (6):3155–62. doi: 10.4049/jimmunol.169.6.3155
131. Kamath AB, Alt J, Debbabi H, Behar SM. Toll-Like Receptor 4-Defective C3H/HeJ Mice are Not More Susceptible Than Other C3H Substrains to Infection With Mycobacterium Tuberculosis. *Infect Immun* (2003) 71 (7):4112–8. doi: 10.1128/iai.71.7.4112-4118.2003
132. Shim TS, Turner OC, Orme IM. Toll-Like Receptor 4 Plays No Role in Susceptibility of Mice to Mycobacterium Tuberculosis Infection. *Tuberculosis (Edinb)* (2003) 83(6):367–71. doi: 10.1016/s1472-9792(03)00071-4
133. Branger J, Leemans JC, Florquin S, Weijer S, Speelman P, van der Poll T. Toll-Like Receptor 4 Plays a Protective Role in Pulmonary Tuberculosis in Mice. *Int Immunol* (2004) 16(3):509–16. doi: 10.1093/intimm/dxh052
134. Park J, Kim H, Kwon KW, Choi HH, Kang SM, Hong JJ, et al. Toll-Like Receptor 4 Signaling-Mediated Responses are Critically Engaged in Optimal Host Protection Against Highly Virulent Mycobacterium Tuberculosis K Infection. *Virulence* (2020) 11(1):430–45. doi: 10.1080/21505594.2020.1766401
135. Wieland CW, van der Windt GJ, Wiersinga WJ, Florquin S, van der Poll T. CD14 Contributes to Pulmonary Inflammation and Mortality During Murine Tuberculosis. *Immunology* (2008) 125(2):272–9. doi: 10.1111/j.1365-2567.2008.02840.x
136. Branger J, Leemans JC, Florquin S, Speelman P, Golenbock DT, van der Poll T. Lipopolysaccharide Binding Protein-Deficient Mice Have a Normal Defense Against Pulmonary Mycobacterial Infection. *Clin Immunol* (2005) 116(2):174–81. doi: 10.1016/j.clim.2005.03.014
137. Gopalakrishnan A, Dietzold J, Salgame P. Vaccine-Mediated Immunity to Experimental Mycobacterium Tuberculosis is Not Impaired in the Absence of Toll-Like Receptor 9. *Cell Immunol* (2016) 302:11–8. doi: 10.1016/j.cellimm.2015.12.009
138. Wieland CW, Koppel EA, den Dunnen J, Florquin S, McKenzie AN, van Kooyk Y, et al. Mice Lacking SIGNR1 Have Stronger T Helper 1 Responses to Mycobacterium Tuberculosis. *Microbes Infect* (2007) 9(2):134–41. doi: 10.1016/j.micinf.2006.10.018
139. Tanne A, Ma B, Boudou F, Tailleux L, Botella H, Badell E, et al. A Murine DC-SIGN Homologue Contributes to Early Host Defense Against Mycobacterium Tuberculosis. *J Exp Med* (2009) 206(10):2205–20. doi: 10.1084/jem.20090188
140. Court N, Vasseur V, Vacher R, Frémond C, Shebzukhov Y, Yeremeev VV, et al. Partial Redundancy of the Pattern Recognition Receptors, Scavenger Receptors, and C-Type Lectins for the Long-Term Control of Mycobacterium Tuberculosis Infection. *J Immunol* (2010) 184(12):7057–70. doi: 10.4049/jimmunol.1000164
141. Heitmann L, Schoenen H, Ehlers S, Lang R, Holscher C. Mincle is Not Essential for Controlling Mycobacterium Tuberculosis Infection. *Immunobiology* (2013) 218(4):506–16. doi: 10.1016/j.imbio.2012.06.005
142. Lee WB, Kang JS, Yan JJ, Lee MS, Jeon BY, Cho SN, et al. Neutrophils Promote Mycobacterial Trehalose Dimycolate-Induced Lung Inflammation *via* the Mincle Pathway. *PloS Pathog* (2012) 8(4):e1002614. doi: 10.1371/journal.ppat.1002614
143. Wilson GJ, Marakalala MJ, Hoving JC, van Laarhoven A, Drummond RA, Kerscher B, et al. The C-Type Lectin Receptor CLECSF8/CLEC4D is a Key Component of Anti-Mycobacterial Immunity. *Cell Host Microbe* (2015) 17 (2):252–9. doi: 10.1016/j.chom.2015.01.004
144. Marakalala MJ, Guler R, Matika L, Murray G, Jacobs M, Brombacher F, et al. The Syk/CARD9-Coupled Receptor Dectin-1 is Not Required for Host Resistance to Mycobacterium Tuberculosis in Mice. *Microbes Infect* (2011) 13(2):198–201. doi: 10.1016/j.micinf.2010.10.013
145. Lemos MP, McKinney J, Rhee KY. Dispensability of Surfactant Proteins A and D in Immune Control of Mycobacterium Tuberculosis Infection Following Aerosol Challenge of Mice. *Infect Immun* (2011) 79(3):1077–85. doi: 10.1128/iai.00286-10
146. McElvania Tekippe E, Allen IC, Hulseberg PD, Sullivan JT, McCann JR, Sandor M, et al. Granuloma Formation and Host Defense in Chronic Mycobacterium Tuberculosis Infection Requires PYCARD/ASC But Not NLRP3 or Caspase-1. *PloS One* (2010) 5(8):e12320. doi: 10.1371/journal.pone.0012320
147. Walter K, Hölscher C, Tschopp J, Ehlers S. NALP3 is Not Necessary for Early Protection Against Experimental Tuberculosis. *Immunobiology* (2010) 215 (9-10):804–11. doi: 10.1016/j.imbio.2010.05.015

148. Dorhoi A, Nouailles G, Jörg S, Hagens K, Heinemann E, Pradl L, et al. Activation of the NLRP3 Inflammasome by Mycobacterium Tuberculosis is Uncoupled From Susceptibility to Active Tuberculosis. *Eur J Immunol* (2012) 42(2):374–84. doi: 10.1002/eji.201141548
149. Allen IC, McElvania-TeKippe E, Wilson JE, Lich JD, Arthur JC, Sullivan JT, et al. Characterization of NLRP12 During the In Vivo Host Immune Response to Klebsiella Pneumoniae and Mycobacterium Tuberculosis. *PloS One* (2013) 8(4):e60842. doi: 10.1371/journal.pone.0060842
150. Hu S, Du X, Huang Y, Fu Y, Yang Y, Zhan X, et al. NLRC3 Negatively Regulates CD4+ T Cells and Impacts Protective Immunity During Mycobacterium Tuberculosis Infection. *PloS Pathog* (2018) 14(8): e1007266. doi: 10.1371/journal.ppat.1007266
151. Marinho FV, Benmerzoug S, Rose S, Campos PC, Marques JT, Báfica A, et al. The cGAS/STING Pathway Is Important for Dendritic Cell Activation But Is Not Essential to Induce Protective Immunity Against Mycobacterium Tuberculosis Infection. *J Innate Immun* (2018) 10(3):239–52. doi: 10.1159/000488952
152. Sever-Chroneos Z, Tvinnereim A, Hunter RL, Chroneos ZC. Prolonged Survival of Scavenger Receptor Class A-Deficient Mice From Pulmonary Mycobacterium Tuberculosis Infection. *Tuberculosis (Edinb)* (2011) 91 Suppl 1(Suppl 1):S69–74. doi: 10.1016/j.tube.2011.10.014
153. Hu C, Mayadas-Norton T, Tanaka K, Chan J, Salgame P. Mycobacterium Tuberculosis Infection in Complement Receptor 3-Deficient Mice. *J Immunol* (2000) 165(5):2596–602. doi: 10.4049/jimmunol.165.5.2596
154. Melo MD, Catchpole IR, Haggar G, Stokes RW. Utilization of CD11b Knockout Mice to Characterize the Role of Complement Receptor 3 (CR3, CD11b/CD18) in the Growth of Mycobacterium Tuberculosis in Macrophages. *Cell Immunol* (2000) 205(1):13–23. doi: 10.1006/cimm.2000.1710
155. Mayer-Barber KD, Barber DL, Shenderov K, White SD, Wilson MS, Cheever A, et al. Cutting Edge: Caspase-1 Independent IL-1β Production Is Critical for Host Resistance to Mycobacterium Tuberculosis and Does Not Require TLR Signaling In Vivo. *J Immunol* (2010) 184(7):3326–30. doi: 10.4049/jimmunol.0904189
156. Flynn JL, Gideon HP, Mattila JT, Lin PL. Immunology Studies in non-Human Primate Models of Tuberculosis. *Immunol Rev* (2015) 264(1):60–73. doi: 10.1111/imr.12258
157. Plumlee CR, Duffy FJ, Gern BH, Delahaye JL, Cohen SB, Stoltzfus CR, et al. Ultra-Low Dose Aerosol Infection of Mice With Mycobacterium Tuberculosis More Closely Models Human Tuberculosis. *Cell Host Microbe* (2021) 29(1):68–82.e5. doi: 10.1016/j.chom.2020.10.003
158. Bafica A, Scanga CA, Feng CG, Leifer C, Cheever A, Sher A. TLR9 Regulates Th1 Responses and Cooperates With TLR2 in Mediating Optimal Resistance to Mycobacterium Tuberculosis. *J Exp Med* (2005) 202(12):1715–24. doi: 10.1084/jem.20051782
159. Fremond CM, Togbe D, Doz E, Rose S, Vasseur V, Maillet I, et al. IL-1 Receptor-Mediated Signal is an Essential Component of MyD88-Dependent Innate Response to Mycobacterium Tuberculosis Infection. *J Immunol* (2007) 179(2):1178–89. doi: 10.4049/jimmunol.179.2.1178
160. Fremond CM, Yeremeev V, Nicolle DM, Jacobs M, Quesniaux VF, Ryffel B. Fatal Mycobacterium Tuberculosis Infection Despite Adaptive Immune Response in the Absence of Myd88. *J Clin Invest* (2004) 114(12):1790–9. doi: 10.1172/jci21027
161. Sugawara I, Yamada H, Mizuno S, Takeda K, Akira S. Mycobacterial Infection in MyD88-Deficient Mice. *Microbiol Immunol* (2003) 47 (11):841–7. doi: 10.1111/j.1348-0421.2003.tb03450.x
162. Quintana-Murci L. Human Immunology Through the Lens of Evolutionary Genetics. *Cell* (2019) 177(1):184–99. doi: 10.1016/j.cell.2019.02.033
163. Zeberg H, Paabo S. The Major Genetic Risk Factor for Severe COVID-19 is Inherited From Neanderthals. *Nature* (2020) 587(7835):610–2. doi: 10.1038/s41586-020-2818-3
164. Barreiro LB, Quintana-Murci L. From Evolutionary Genetics to Human Immunology: How Selection Shapes Host Defence Genes. *Nat Rev Genet* (2010) 11(1):17–30. doi: 10.1038/nrg2698
165. Barreiro LB, Ben-Ali M, Quach H, Laval G, Patin E, Pickrell JK, et al. Evolutionary Dynamics of Human Toll-Like Receptors and Their Different Contributions to Host Defense. *PloS Genet* (2009) 5(7):e1000562. doi: 10.1371/journal.pgen.1000562
166. Ferwerda B, McCall MB, Alonso S, Giamarellos-Bourboulis EJ, Mouktaroudi M, Izagirre N, et al. TLR4 Polymorphisms, Infectious Diseases, and Evolutionary Pressure During Migration of Modern Humans. *Proc Natl Acad Sci USA* (2007) 104(42):16645–50. doi: 10.1073/pnas.0704828104
167. Pisitkun P, Deane JA, Difilippantonio MJ, Tarasenko T, Satterthwaite AB, Bolland S. Autoreactive B Cell Responses to RNA-Related Antigens Due to TLR7 Gene Duplication. *Science* (2006) 312(5780):1669–72. doi: 10.1126/science.1124978
168. Krieg AM, Vollmer J. Toll-Like Receptors 7, 8, and 9: Linking Innate Immunity to Autoimmunity. *Immunol Rev* (2007) 220:251–69. doi: 10.1111/j.1600-065X.2007.00572.x
169. Celhar T, Magalhaes R, Fairhurst AM. TLR7 and TLR9 in SLE: When Sensing Self Goes Wrong. *Immunol Res* (2012) 53(1-3):58–77. doi: 10.1007/s12026-012-8270-1
170. Mathieson I, Lazaridis I, Rohland N, Mallick S, Patterson N, Roodenberg SA, et al. Genome-Wide Patterns of Selection in 230 Ancient Eurasians. *Nature* (2015) 528(7583):499–503. doi: 10.1038/nature16152
171. Wong SH, Gochhait S, Malhotra D, Pettersson FH, Teo YY, Khor CC, et al. Leprosy and the Adaptation of Human Toll-Like Receptor 1. *PloS Pathog* (2010) 6:e1000979. doi: 10.1371/journal.ppat.1000979
172. Ma X, Liu Y, Gowen BB, Graviss EA, Clark AG, Musser JM. Full-Exon Resequencing Reveals Toll-Like Receptor Variants Contribute to Human Susceptibility to Tuberculosis Disease. *PloS One* (2007) 2(12):e1318. doi: 10.1371/journal.pone.0001318
173. Uciechowski P, Imhoff H, Lange C, Meyer CG, Browne EN, Kirsten DK, et al. Susceptibility to Tuberculosis is Associated With TLR1 Polymorphisms Resulting in a Lack of TLR1 Cell Surface Expression. *J Leukoc Biol* (2011) 90(2):377–88. doi: 10.1189/jlb.0409233
174. Hawn TR, Misch EA, Dunstan SJ, Thwaites GE, Lan NT, Quy HT, et al. A Common Human TLR1 Polymorphism Regulates the Innate Immune Response to Lipopeptides. *Eur J Immunol* (2007) 37(8):2280–9. doi: 10.1002/eji.200737034
175. Marques Cde S, Brito-de-Souza VN, Guerreiro LT, Martins JH, Amaral EP, Cardoso CC, et al. Toll-Like Receptor 1 N248S Single-Nucleotide Polymorphism is Associated With Leprosy Risk and Regulates Immune Activation During Mycobacterial Infection. *J Infect Dis* (2013) 208(1):120–9. doi: 10.1093/infdis/jit133
176. Mortaz E, Adcock IM, Tabarsi P, Masjedi MR, Mansouri D, Velayati AA, et al. Interaction of Pattern Recognition Receptors With Mycobacterium Tuberculosis. *J Clin Immunol* (2015) 35(1):1–10. doi: 10.1007/s10875-014-0103-7
177. Jin X, Yin S, Zhang Y, Chen X. Association Between TLR2 Arg677Trp Polymorphism and Tuberculosis Susceptibility: A Meta-Analysis. *Microb Pathog* (2020) 144:104173. doi: 10.1016/j.micpath.2020.104173
178. Cubillos-Angulo JM, Arriaga MB, Silva EC, Müller BLA, Ramalho DMP, Fukutani KF, et al. Polymorphisms in TLR4 and TNFA and Risk of Mycobacterium Tuberculosis Infection and Development of Active Disease in Contacts of Tuberculosis Cases in Brazil: A Prospective Cohort Study. *Clin Infect Dis* (2019) 69(6):1027–35. doi: 10.1093/cid/ciy1001
179. Graustein AD, Horne DJ, Arentz M, Bang ND, Chau TT, Thwaites GE, et al. TLR9 Gene Region Polymorphisms and Susceptibility to Tuberculosis in Vietnam. *Tuberculosis (Edinb)* (2015) 95(2):190–6. doi: 10.1016/j.tube.2014.12.009
180. Velez DR, Wejse C, Stryjewski ME, Abbate E, Hulme WF, Myers JL, et al. Variants in Toll-Like Receptors 2 and 9 Influence Susceptibility to Pulmonary Tuberculosis in Caucasians, African-Americans, and West Africans. *Hum Genet* (2010) 127(1):65–73. doi: 10.1007/s00439-009-0741-7
181. Vasseur E, Boniotto M, Patin E, Laval G, Quach H, Manry J, et al. The Evolutionary Landscape of Cytosolic Microbial Sensors in Humans. *Am J Hum Genet* (2012) 91(1):27–37. doi: 10.1016/j.ajhg.2012.05.008
182. Wang C, Chen ZL, Pan ZF, Wei LL, Xu DD, Jiang TT, et al. NOD2 Polymorphisms and Pulmonary Tuberculosis Susceptibility: A Systematic Review and Meta-Analysis. *Int J Biol Sci* (2013) 10(1):103–8. doi: 10.7150/ijbs.7585
183. Austin CM, Ma X, Graviss EA. Common Nonsynonymous Polymorphisms in the NOD2 Gene are Associated With Resistance or Susceptibility to Tuberculosis Disease in African Americans. *J Infect Dis* (2008) 197 (12):1713–6. doi: 10.1086/588384
184. Hui KY, Fernandez-Hernandez H, Hu J, Schaffner A, Pankratz N, Hsu NY, et al. Functional Variants in the LRRK2 Gene Confer Shared Effects on Risk

for Crohn's Disease and Parkinson's Disease. *Sci Transl Med* (2018) 10(423): eaai7795. doi: 10.1126/scitranslmed.aai7795
185. Ravimohan S, Nfanyana K, Tamuhla N, Tiemessen CT, Weissman D, Bisson GP. Common Variation in NLRP3 Is Associated With Early Death and Elevated Inflammasome Biomarkers Among Advanced HIV/TB Co-Infected Patients in Botswana. *Open Forum Infect Dis* (2018) 5(5):ofy075. doi: 10.1093/ofid/ofy075
186. Barreiro LB, Patin E, Neyrolles O, Cann HM, Gicquel B, Quintana-Murci L. The Heritage of Pathogen Pressures and Ancient Demography in the Human Innate-Immunity CD209/CD209L Region. *Am J Hum Genet* (2005) 77 (5):869–86. doi: 10.1086/497613
187. Barreiro LB, Neyrolles O, Babb CL, Tailleux L, Quach H, McElreavey K, et al. Promoter Variation in the DC-SIGN-Encoding Gene CD209 is Associated With Tuberculosis. *PloS Med* (2006) 3(2):e20. doi: 10.1371/journal.pmed.0030020
188. Vannberg FO, Chapman SJ, Khor CC, Tosh K, Floyd S, Jackson-Sillah D, et al. CD209 Genetic Polymorphism and Tuberculosis Disease. *PloS One* (2008) 3(1):e1388. doi: 10.1371/journal.pone.0001388
189. Ben-Ali M, Barreiro LB, Chabbou A, Haltiti R, Braham E, Neyrolles O, et al. Promoter and Neck Region Length Variation of DC-SIGN is Not Associated With Susceptibility to Tuberculosis in Tunisian Patients. *Hum Immunol* (2007) 68(11):908–12. doi: 10.1016/j.humimm.2007.09.003
190. Kobayashi K, Yuliwulandari R, Yanai H, Lien LT, Hang NT, Hijikata M, et al. Association of CD209 Polymorphisms With Tuberculosis in an Indonesian Population. *Hum Immunol* (2011) 72(9):741–5. doi: 10.1016/j.humimm.2011.04.004
191. da Silva RC, Segat L, da Cruz HL, Schindler HC, Montenegro LM, Crovella S, et al. Association of CD209 and CD209L Polymorphisms With Tuberculosis Infection in a Northeastern Brazilian Population. *Mol Biol Rep* (2014) 41 (8):5449–57. doi: 10.1007/s11033-014-3416-y
192. Xu DD, Wang C, Jiang F, Wei LL, Shi LY, Yu XM, et al. Association of the FCN2 Gene Single Nucleotide Polymorphisms With Susceptibility to Pulmonary Tuberculosis. *PloS One* (2015) 10(9):e0138356. doi: 10.1371/journal.pone.0138356
193. Li Y, You EQ, Lin WH, Liu XN, Shen DP, Zhang XL, et al. Association of Ficolin-1 and Ficolin-3 Gene Variation and Pulmonary Tuberculosis Susceptibility in a Chinese Population. *J Clin Lab Anal* (2021) 35(4): e23732. doi: 10.1002/jcla.23732
194. Juffermans NP, Florquin S, Camoglio L, Verbon A, Kolk AH, Speelman P, et al. Interleukin-1 Signaling is Essential for Host Defense During Murine Pulmonary Tuberculosis. *J Infect Dis* (2000) 182(3):902–8. doi: 10.1086/315771
195. Sugawara I, Yamada H, Hua S, Mizuno S. Role of Interleukin (IL)-1 Type 1 Receptor in Mycobacterial Infection. *Microbiol Immunol* (2001) 45(11):743–50. doi: 10.1111/j.1348-0421.2001.tb01310.x
196. Yamada H, Mizumo S, Horai R, Iwakura Y, Sugawara I. Protective Role of Interleukin-1 in Mycobacterial Infection in IL-1 α/β Double-Knockout Mice. *Lab Invest* (2000) 80(5):759–67. doi: 10.1038/labinvest.3780079
197. Bourigault ML, Segueni N, Rose S, Court N, Vacher R, Vasseur V, et al. Relative Contribution of IL-1α, IL-1β and TNF to the Host Response to Mycobacterium Tuberculosis and Attenuated M. *bovis BCG Immun Inflammation Dis* (2013) 1(1):47–62. doi: 10.1002/iid3.9
198. Ji DX, Yamashiro LH, Chen KJ, Mukaida N, Kramnik I, Darwin KH, et al. Type I Interferon-Driven Susceptibility to Mycobacterium Tuberculosis is Mediated by IL-1ra. *Nat Microbiol* (2019) 4(12):2128–35. doi: 10.1038/s41564-019-0578-3
199. Flynn JL, Goldstein MM, Chan J, Triebold KJ, Pfeffer K, Lowenstein CJ, et al. Tumor Necrosis Factor-Alpha is Required in the Protective Immune Response Against Mycobacterium Tuberculosis in Mice. *Immunity* (1995) 2(6):561–72. doi: 10.1016/1074-7613(95)90001-2
200. Segueni N, Benmerzoug S, Rose S, Gauthier A, Bourigault ML, Reverchon F, et al. Innate Myeloid Cell TNFR1 Mediates First Line Defence Against Primary Mycobacterium Tuberculosis Infection. *Sci Rep* (2016) 6:22454. doi: 10.1038/srep22454
201. Keane J, Gershon S, Wise RP, Mirabile-Levens E, Kasznica J, Schwieterman WD, et al. Tuberculosis Associated With Infliximab, a Tumor Necrosis Factor Alpha-Neutralizing Agent. *N Engl J Med* (2001) 345(15):1098–104. doi: 10.1056/NEJMoa011110
202. Cooper AM, Dalton DK, Stewart TA, Griffin JP, Russell DG, Orme IM. Disseminated Tuberculosis in Interferon Gamma Gene-Disrupted Mice. *J Exp Med* (1993) 178(6):2243–7. doi: 10.1084/jem.178.6.2243
203. Flynn JL, Chan J, Triebold KJ, Dalton DK, Stewart TA, Bloom BR. An Essential Role for Interferon Gamma in Resistance to Mycobacterium Tuberculosis Infection. *J Exp Med* (1993) 178(6):2249–54. doi: 10.1084/jem.178.6.2249
204. Sakai S, Kauffman KD, Sallin MA, Sharpe AH, Young HA, Ganusov VV, et al. CD4 T Cell-Derived IFN-Gamma Plays a Minimal Role in Control of Pulmonary Mycobacterium Tuberculosis Infection and Must Be Actively Repressed by PD-1 to Prevent Lethal Disease. *PloS Pathog* (2016) 12(5): e1005667. doi: 10.1371/journal.ppat.1005667
205. Cooper AM, Magram J, Ferrante J, Orme IM. Interleukin 12 (IL-12) is Crucial to the Development of Protective Immunity in Mice Intravenously Infected With Mycobacterium Tuberculosis. *J Exp Med* (1997) 186(1):39–45. doi: 10.1084/jem.186.1.39
206. Döffinger R, Dupuis S, Picard C, Fieschi C, Feinberg J, Barcenas-Morales G, et al. Inherited Disorders of IL-12- and IFNgamma-Mediated Immunity: A Molecular Genetics Update. *Mol Immunol* (2002) 38(12-13):903–9. doi: 10.1016/s0161-5890(02)00017-2
207. MacMicking JD, North RJ, LaCourse R, Mudgett JS, Shah SK, Nathan CF. Identification of Nitric Oxide Synthase as a Protective Locus Against Tuberculosis. *Proc Natl Acad Sci* (1997) 94(10):5243–8. doi: 10.1073/pnas.94.10.5243
208. Jung YJ, LaCourse R, Ryan L, North RJ. Virulent But Not Avirulent Mycobacterium Tuberculosis can Evade the Growth Inhibitory Action of a T Helper 1-Dependent, Nitric Oxide Synthase 2-Independent Defense in Mice. *J Exp Med* (2002) 196(7):991–8. doi: 10.1084/jem.20021186
209. Fava VM, Dallmann-Sauer M, Schurr E. Genetics of Leprosy: Today and Beyond. *Hum Genet* (2020) 139(6-7):835–46. doi: 10.1007/s00439-019-02087-5
210. Zhang F, Liu H, Chen S, Low H, Sun L, Cui Y, et al. Identification of Two New Loci at IL23R and RAB32 That Influence Susceptibility to Leprosy. *Nat Genet* (2011) 43(12):1247–51. doi: 10.1038/ng.973
211. Zhang FR, Huang W, Chen SM, Sun LD, Liu H, Li Y, et al. Genomewide Association Study of Leprosy. *N Engl J Med* (2009) 361(27):2609–18. doi: 10.1056/NEJMoa0903753
212. Fava VM, Cobat A, Gzara C, Alcais A, Abel L, Schurr E. Reply to Zhang et al.: The Differential Role of LRRK2 Variants in Nested Leprosy Phenotypes. *Proc Natl Acad Sci USA* (2020) 117(19):10124–5. doi: 10.1073/pnas.2002654117
213. Fava VM, Cobat A, Van Thuc N, Latini AC, Stefani MM, Belone AF, et al. Association of TNFSF8 Regulatory Variants With Excessive Inflammatory Responses But Not Leprosy Per Se. *J Infect Dis* (2015) 211(6):968–77. doi: 10.1093/infdis/jiu566
214. Fava VM, Sales-Marques C, Alcais A, Moraes MO, Schurr E. Age-Dependent Association of TNFSF15/TNFSF8 Variants and Leprosy Type 1 Reaction. *Front Immunol* (2017) 8:155. doi: 10.3389/fimmu.2017.00155
215. Fava VM, Xu YZ, Lettre G, Van Thuc N, Orlova M, Thai VH, et al. Pleiotropic Effects for Parkin and LRRK2 in Leprosy Type-1 Reactions and Parkinson's Disease. *Proc Natl Acad Sci USA* (2019) 116(31):15616–24. doi: 10.1073/pnas.1901805116
216. Lange C, Aarnoutse R, Chesov D, van Crevel R, Gillespie SH, Grobbel HP, et al. Perspective for Precision Medicine for Tuberculosis. *Front Immunol* (2020) 11:566608. doi: 10.3389/fimmu.2020.566608
217. DiNardo AR, Gandhi T, Heyckendorf J, Grimm SL, Rajapakshe K, Nishiguchi T, et al. Gene Expression Signatures Identify Biologically and Clinically Distinct Tuberculosis Endotypes. *medRxiv* (2021) 2020:5.13.20100776. doi: 10.1101/2020.05.13.20100776

Conflict of Interest: The authors declare that the research was conducted in the absence of any commercial or financial relationships that could be construed as a potential conflict of interest.

Copyright © 2021 Dubé, Fava, Schurr and Behr. This is an open-access article distributed under the terms of the Creative Commons Attribution License (CC BY). The use, distribution or reproduction in other forums is permitted, provided the original author(s) and the copyright owner(s) are credited and that the original publication in this journal is cited, in accordance with accepted academic practice. No use, distribution or reproduction is permitted which does not comply with these terms.

frontiers in Immunology

ORIGINAL RESEARCH
published: 04 August 2021
doi: 10.3389/fimmu.2021.694680

Gene Set Enrichment Analysis Reveals Individual Variability in Host Responses in Tuberculosis Patients

Teresa Domaszewska[1,2], *Joanna Zyla*[3], *Raik Otto*[4], *Stefan H. E. Kaufmann*[1,5,6] *and January Weiner*[1*]

[1] Department of Immunology, Max Planck Institute for Infection Biology, Berlin, Germany, [2] Department for Infectious Disease Epidemiology, Robert Koch Institute, Berlin, Germany, [3] Department of Data Science and Engineering, Silesian University of Technology, Gliwice, Poland, [4] Knowledge Management in Bioinformatics, Institute for Computer Science, Humboldt-Universität zu Berlin, Berlin, Germany, [5] Max Planck Institute for Biophysical Chemistry, Emeritus Group Systems Immunology, Göttingen, Germany, [6] Hagler Institute for Advanced Study, Texas A&M University, College Station, TX, United States

OPEN ACCESS

Edited by:
Jayne S. Sutherland, Medical Research Council The Gambia Unit (MRC), Gambia

Reviewed by:
Hannah Priyadarshini Gideon, University of Pittsburgh, United States
Nicola Ivan Lorè, Division of Immunology, Transplantation and Infectious Diseases, San Raffaele Scientific Institute (IRCCS), Italy

***Correspondence:**
January Weiner
january.weiner@bihealth.de

Specialty section:
This article was submitted to Microbial Immunology, a section of the journal Frontiers in Immunology

Received: 13 April 2021
Accepted: 19 July 2021
Published: 04 August 2021

Citation:
Domaszewska T, Zyla J, Otto R, Kaufmann SHE and Weiner J (2021) Gene Set Enrichment Analysis Reveals Individual Variability in Host Responses in Tuberculosis Patients. Front. Immunol. 12:694680. doi: 10.3389/fimmu.2021.694680

Group-aggregated responses to tuberculosis (TB) have been well characterized on a molecular level. However, human beings differ and individual responses to infection vary. We have combined a novel approach to individual gene set analysis (GSA) with the clustering of transcriptomic profiles of TB patients from seven datasets in order to identify individual molecular endotypes of transcriptomic responses to TB. We found that TB patients differ with respect to the intensity of their hallmark interferon (IFN) responses, but they also show variability in their complement system, metabolic responses and multiple other pathways. This variability cannot be sufficiently explained with covariates such as gender or age, and the molecular endotypes are found across studies and populations. Using datasets from a *Cynomolgus* macaque model of TB, we revealed that transcriptional signatures of different molecular TB endotypes did not depend on TB progression post-infection. Moreover, we provide evidence that patients with molecular endotypes characterized by high levels of IFN responses (IFN-rich), suffered from more severe lung pathology than those with lower levels of IFN responses (IFN-low). Harnessing machine learning (ML) models, we derived gene signatures classifying IFN-rich and IFN-low TB endotypes and revealed that the IFN-low signature allowed slightly more reliable overall classification of TB patients from non-TB patients than the IFN-rich one. Using the paradigm of molecular endotypes and the ML-based predictions allows more precisely tailored treatment regimens, predicting treatment-outcome with higher accuracy and therefore bridging the gap between conventional treatment and precision medicine.

Keywords: tuberculosis, endotypes, individual variability in host response, interferon, immune response, gene set enrichment analysis

INTRODUCTION

Tuberculosis (TB) remains a major threat to human health with 10 million new cases and 1.4 million deaths in 2019 (1). Only a small proportion of the estimated 1.7 billion individuals infected with *Mycobacterium tuberculosis* (Mtb) fall sick with active TB (1). The vast majority of infected individuals contain Mtb in a dormant status resulting in latent TB infection (LTBI), making it difficult to identify the individuals who require treatment (2).

The disparity between progression to TB and continued LTBI constitutes the most obvious kind of variability among Mtb infected individuals. This individual variability exists also on more subtle levels as revealed by gene expression analyses (3–7). Moreover, prospective cohort studies harnessed transcriptomic signatures to predict the risk of TB progression (8, 9). Multiple signatures of TB have been proposed and cross-validated on independent datasets leading to the identification of common motives that were identified in TB patients by most studies with respect to the interferon (IFN) response (3, 4, 7, 10, 11). Patterns of TB-related gene expression regulation however, are heterogeneous and vary within and between studies. Gene-expression trends observed in the majority of TB patients were frequently contradicted by individual TB patients, independently of the applied technology (3). This raises the question whether active TB induces a unique host response pattern or alternatively whether there are multiple, individual host-dependent patterns and whether these are distinct or overlap.

In 2010 Berry et al. proposed a 393- transcript signature of TB which was dominated by IFN-signaling genes (3). The authors investigated transcriptional profiles of TB patients and healthy individuals, and observed that some of the profiles of healthy individuals with LTBI clustered with those of TB patients. Reciprocally, a subgroup of TB patients presented transcriptional profiles that clustered with healthy LTBI and were thus misclassified by their transcriptional signature.

Comparison of the transcriptomes of TB patients to those of healthy individuals gave rise to assumptions regarding the immune response of TB patients, in particular the stronger IFN response as compared to healthy controls. In clinical practice, the most widely used test for Mtb infection is the Interferon Gamma Release Assay (IGRA) which determines the release of IFN γ *in vitro* after stimulation of whole blood (WB) samples with Mtb-specific antigens. The false negative rate of IGRA among Mtb infected individuals is in the order of 15% (12). Thus, blood cells of 15% of the patients do not produce detectable IFN-γ levels in response to antigen-specific stimulation. The majority of cohort studies report differentially expressed IFN signaling pathways in TB patients *versus* healthy individuals. Yet, the multiple published 'TB *vs* healthy' and 'TB *vs* LTBI' signatures only show a limited abundance of shared transcripts. Arguably, this can be explained by different assumptions: (1) expression of different genes may be highly correlated and thus, selecting one or another gene does not influence the performance of the model; (2) different molecular mechanisms dominate the response to TB in different cohorts; (3) various cohorts contain varying numbers of individuals with a certain type of dominant response which influences outcome of comparison of 'all TB patients' to 'all healthy subjects'. For example, the study of Maertzdorf et al. identified JAK-STAT signaling and TLR signaling pathways next to IFN response as dominant in TB (7). In contrast, a study by Verhagen et al. suggested the importance of calcium signaling pathway in TB (13). Studies by Cliff et al. and Cai et al. identified complement system signaling as important correlates of TB (14, 15). It is tempting to speculate that these studies detected different modi in the response to TB: while some cohorts presented dominant regulation of IFN signaling in response to Mtb infection, other presented stronger regulation of calcium or complement signaling. However, a cohort-level analysis cannot determine whether the cohorts comprise patients with cohort-specific responses to TB or alternatively different proportions of patients with specific responses.

We postulated various patterns of host responses to TB, and reasoned that the published WB transcriptomic studies of TB patients are averaged representations of multiple different responses to TB. To test this hypothesis, it is necessary to analyze individual transcriptional profiles between and within independent studies. To address data heterogeneity, we conducted a Gene Set Analysis (GSA) on the integrated transcriptome data with various gene set collections, including pre-defined blood transcriptional modules (BTMs) (16, 17) to reliably identify variability on the level of individual patients. We observed various patterns of gene set enrichment in individuals within single studies, which were reproduced on the level of the meta dataset (MDS) and identified expression patterns within individuals that were significantly correlated with the severity of pathology in the patients' lungs and characterized by strong enrichment in IFN-response-related modules. Using Random Forest (RF) machine learning (ML) we revealed gene signatures which distinguished between TB patients with different transcriptional response patterns. We then detected additional immune responses, including complement system response, as strongly correlated with the IFN response and therefore contributing to what we defined as "IFN-rich" and "IFN-low" endotypes of TB. To determine whether these two endotypes were a function of time post infection (p.i.), we analyzed data from *Cynomolgus* macaques (18) and observed that even though the IFN response peaked between 20 and 42 days p.i., in various animals the onset of IFN response started at various time points p.i. and lasted for variable periods of time. We further investigated whether additional elements of the host response to TB presenting variable activation in the individual patients can be detected independently of the IFN response. We identified such patterns in the enrichment of metabolic pathways of D-arginine and D-ornithine, as well as in the modules related to insulin and calcium metabolism, using KEGG (19) and MSigDB (20) based GSA followed by principal component analysis (PCA) and eigenvector analysis. Based on these findings, we hypothesize that progression to and severity of TB depend on the variability between individual host responses. Not only does the susceptibility to active disease but also kinetics of the crosstalk between Mtb and the human host differ. Hence, subgroups of TB patients represent different endotypes who would benefit from a personalized host-directed therapy in adjunct to canonical TB drug treatment (2, 21).

METHODS

The overview of the workflow of the study and the used statistical methods can be found in the **Supplementary Figure 1**.

Data Acquisition and Preprocessing

All utilized datasets are publicly available in Gene Expression Omnibus (GEO) data repository (22). Study-normalized datasets were acquired from GEO *via* the R-package *GEOquery* (23).

Included studies met the following criteria: (i) they contained WB data from untreated TB patients and healthy controls (including LTBI) each; (ii) they contained at least eight samples from TB patients and healthy controls each; (iii) they were performed using platforms which measured expression of at least 16,000 overlapping genes; (iv) they were performed using platforms with annotations available in *BiomaRt* R package (24, 25). Seven datasets were used to create MDS and two independent datasets were used for validation. Additionally, three datasets from sepsis patients who also present strong IFN responses were acquired to validate the presented method.

Data analysis was performed with R (26). The analysis script including all analytical steps is available on the website: (https://github.com/terkaterka/immune-response-to-TB). Datasets were analyzed with R package *limma* for differential expression analysis (27). Microarray data was quantile normalized within single studies to assure comparability. During pre-processing HGNC and ENSEMBL identifiers were mapped to mRNA-array probe names using biomaRt 'mapIds' function (*biomaRt* version 2.24.1 (24, 25). Figures were created with the packages *ggplot2* and *UMAP* (28, 29).

We utilized the processed data provided by the respective studies for the integrative meta-analysis. Each dataset was randomly split into 80%/20% partitions with the 80% being used to train the ML algorithm and the 20% being selected for the test set. Only samples classified by the studies as either healthy, LTBI, affected by other diseases (OD) and samples of untreated TB patients were included. MDS was created out of the training sets from each study using only common genes. Nonparametric standardization based on median and interquartile range (IQR) values (Equation 1) was used to standardize the expression values measured in each study, in order to minimize batch effects and heterogeneity between the experiments.

$$e'_{i,j} = \frac{e_{i,j} - mediane_{.j}}{IQR_{.j}} \quad (1)$$

Where:

$e'_{i,j}$ – normalized expression value for gene i,

$e_{i,j}$ – expression measurement of gene i,

$IQR_{.,j}$ – IQR for expression measurement of gene i across all samples.

All utilized data underwent initial quality controls which comprised outliers and artifact-detection and quality-assurance. We ascertained that case and control cohorts clustered according to TB and IFN status and not by their study of origin. Umap-algorithm (29) derived figures depicting the clustering pattern are found in the **Supplementary Figure 2**. To test whether the transformation caused a bias in the GSA (for example significantly changing the findings), we have compared, for each data set, whether the outcome of the GSA changed after applying the transformation. (**Supplementary Method 1**, **Supplementary Figure 3**).

GSA for Individual Patients

To perform GSA for individual patients, row-wise z-transformation of gene expression values was applied. For each gene, mean expression and standard deviation of its expression were calculated for healthy individuals from every cohort. Subsequently, the mean gene expression of healthy individuals was subtracted from the expression measurements of every individual present in the MDS and the result was divided by standard deviation of gene expression for healthy individuals. The z-score was calculated based on all samples from healthy individuals. Thus, for each patient and gene, the expression z-score is the number of standard deviations below or above the average for healthy individuals. The larger the absolute value of the z-score, the higher the deviation of the expression of that gene from the average in the healthy population.

GSA with CERNO test (30) was performed for every donor on the list of genes ordered by decreasing absolute z-score using tmodCERNOtest function from the R-package *tmod* (31, 32) and BTMs (16, 17).

Definition of IFN I and IFN II Modules

Two previously published sets of BTMs were utilized (16, 17). A third custom set was generated, based on the classification of genes as IFN I stimulated genes, as IFN II stimulated genes and as genes activated by both IFN I and IFN II signaling pathways according to Interferome v2.0 database (33). The sets consisted of genes which overlapped between originally defined BTMs and genes from the MDS classified by the Interferome v2.0 database either as IFN I inducible genes (IFN I gene sets), IFN II inducible genes (IFN II gene sets) or IFN I and II inducible genes (IFN I and II gene sets). Two additional modules contained (i) all genes classified as IFN I genes and (ii) all genes classified as IFN II genes. The defined module sets are available on the website: (https://github.com/terkaterka/immune-response-to-TB).

Identification of IFN+ and IFN- TB Patient Groups

GSA was performed on the list of genes from every individual included in MDS sorted by increasing z-score using the three created module sets. Individuals presenting no significant enrichment in any of the IFN I modules were defined as IFN-low and are represented graphically as 'IFN I-'. Individuals presenting enrichment in at least one IFN I module were defined as IFN-rich and are further represented graphically as 'IFN I+'. Similarly, the 'IFN II-' and 'IFN I and II-' individuals presented no enrichment in the IFN II or IFN I and II module set, respectively. Those presenting respective enrichments were defined as 'IFN II+ or 'IFN I+ and II+'. Ultimately, the overlaps between study participants classified as IFN I+, IFN II+, and IFN I+ and II+ were analyzed and their classification was compared to IFN+ and IFN- participant groups based on the original BTMs (16, 17).

Analysis of the Influence of Clinical Factors on IFN Status

To investigate the influence of discrete features (sex, diabetes, HIV, smoking status) on the IFN status the chi-square test was performed and Cramér's V effect size was calculated. Moreover, the odds ratio (OR) was calculated with 95% CI and the test for OR was conducted (H0: OR=1). For continuous variables (age), the Mann-Whitney test was performed and rank biserial correlation was calculated as effect size.

Principal Component Analysis

PCA was performed on the MDS as well as on the subset of MDS containing only samples from active TB patients using R-packages *stats*, *pca3d* and *tmod* (26, 31, 34, 35). The fraction of variance (loading) explained by each factorial predictor (TB status, IFN status, study, ethnicity, residence, HIV, OD, mRNA-array technology) was calculated for each principal component (PC; **Supplementary Figure 4**).

Correlation Between IFN Status and Disease Severity

The dataset GSE19491 (3) was used to compare the IFN status with the disease severity assessed by lung X-Ray studies of TB patients and healthy individuals. The IFN status was determined by transcriptome analysis and a GSA of all participants contained in the study (61 TB patients, 105 healthy individuals including 69 LTBI and 36 non-LTBI, and 274 OD patients). 72 individuals from the study underwent lung X-Ray investigation and were diagnosed as 'healthy' (n = 34), 'minimal disease (n = 14), 'moderate disease' (n = 13), or 'advanced disease' (n = 11) by physicians blinded to the transcriptome analysis and the clinical diagnosis of the patients (3). The X-Ray based diagnosis was compared with the IFN status assigned on the basis of GSA.

Machine Learning

Random Forest Models With 10-Fold Cross Validation

Random Forest (RF) models were generated using R package *randomForest* (36, 37) to classify TB patients with or without IFN-rich immune response and non-TB individuals including uninfected, LTBI and OD. Class balancing was used to retain the proportion of one case to three control individuals by down-sampling of the majority class. 10-fold cross-validation using R package *caret* was implemented to test the models and their performance was evaluated by creating receiver-operator characteristic (ROC) curves using R package *pROC* (38).

Determination of the Signature Size

We ranked the transcripts found in either model according to the amount of statistical importance in the RF model to identify a cut-off for the number of transcripts required to effectively discriminate TB patients from non-TB samples. TB IFN+ and TB IFN- signatures were defined consisting of top (i) 5, (ii) 7, (iii) 10, (iv) 20, (v) 50 or (vi) 200 ranked transcripts, and new models which were trained only on the transcripts that surpassed the cut-off threshold were created. The new models were tested using 10-fold cross validation within the training MDS and their performance was evaluated using ROC plot. The optimal signature size was chosen when the increase of the number of selected transcripts ranked by highest statistical importance did not cause further significant improvement of signature's area under curve (AUC) in classification of TB patients and non-TB disease controls.

Determination of the TB IFN+ and TB IFN- Transcriptional Signatures

For the identification of TB IFN+ and TB IFN- signatures two new class balanced RF models retaining the proportion of one TB to three non-TB cases were trained using the subsets of the complete training MDS subsets containing (i) all TB IFN+ and non-TB (Signature Model 1), (ii) all TB IFN- and non-TB (Signature Model 2). A signature consisting of the 20 top ranking transcripts from the Signature Model 1 was defined as IFN+ signature. A signature of 50 top ranking transcripts from the Signature Model 2 was defined as IFN- signature. Obtained TB IFN+ and TB IFN- signatures were tested on the test MDS and their performance was evaluated by a ROC curve analysis.

Validation of the TB IFN+ and TB IFN- Signatures

The obtained TB IFN+ and TB IFN- signatures were tested on the external dataset from Cai et al. (15) and Blankley et al. (39) and their performance was evaluated by a ROC curve analysis. The performances of IFN+ and IFN- TB signatures in detection of sepsis patients were tested to assure that the signatures were disease and not only IFN-response specific.

Influence of Time Post Infection of *Cynomolgus* Macaques on IFN Status

To determine whether the IFN status in individuals with active TB is the result of time p.i., a longitudinal dataset was procured to assess the changes in the WB gene expression after Mtb infection in *Cynomolgus* macaques (GSE84152 (18);, acquired from the GEO database. The dataset contained mRNA-array data collected from 38 macaques at two time points before Mtb infection and at days 3, 7, 10, 20, 30, 42, 56, 90, 120, 150, 180 p.i., when the diagnosis of TB *vs* LTBI was made. The samples were normalized and z-scores were calculated using the above-described method. GSA using BTMs was performed on samples from individual macaques. The samples were assigned IFN I+/IFN I- status which was compared with their binary clinical diagnosis and severity of lung inflammation.

Identification of Other TB Endotypes

To determine other endotypes of TB the KEGG (19, 40) and Hallmark (20) gene set collections were investigated by CERNO enrichment method. At first, the results of AUC values from enrichment of each pathway for each patient were extracted. Then, a PCA was performed on a matrix of AUC values and the previously defined IFN+ group was labeled on 2D projection (**Supplementary Figure 5**). To extract other endotypes the eigenvalues of the first PCA component were calculated for all KEGG pathways as well as for all Hallmark MSigDB gene sets and IFN modules across active TB patients. Next, the Spearman

rank correlation coefficient was calculated between each KEGG or Hallmark pathway and previously defined IFN modules. Pathways not showing a statistically significant correlation with IFN modules were considered as new TB endotypes. Additionally, we tested whether the proportion of individuals presenting enrichment (adjusted p-value<0.05, Benjamini-Hochberg correction (41); in given enriched gene set and in the IFN gene set was independent using chi square test.

RESULTS

GSA Reveals Individual Variability in Transcriptional Profiles Among TB Patients Within and Between Cohorts

The MDS was generated from seven publicly available datasets using IQR based standardization (Equation 1) for successful integration (**Supplementary Figures 2, 3**). We conducted a GSA for every donor in the MDS on the list of genes sorted by z-score-transformed expression values. Despite visible trends including strong enrichment in T-cell, IFN response and inflammation modules, the enrichment profiles differed between individual TB patients within cohorts which was reproduced between cohorts (**Figure 1**). The group of modules presenting substantial variability between the samples in the enrichment included IFN related modules, generally considered characteristic for TB patients.

Enrichment of IFN Signaling Gene Sets in the Majority of TB Patients

Given the critical role of IFN type I in the pathogenesis of TB, we focused on the variability of the enrichment of the IFN I-related modules among TB patients since numerous studies have identified IFN I signaling as dominant mechanism in TB (3, 4, 7). The roles of IFN I and IFN II responses in TB differ markedly: IFN I pathways are generally considered detrimental while IFN II is generally assumed beneficial (42). Since many of the IFN stimulated genes (ISGs) can be stimulated by both IFN I and IFN II signaling, we compared the IFN I and IFN II responses in TB patients. We created novel module sets based on the BTMs (16, 17) as well as on the assignment of genes as 'IFN I inducible', 'IFN II inducible', and 'IFN I and II inducible' by Interferome v2.0 database (33). We conducted a GSA with the modules containing genes whose activity was inducible by IFN I signaling and assigned an IFN I status to TB patients based on the following enrichment results: TB patients presenting no significant enrichment in IFN I modules were termed 'IFN-low' ('IFN I-' for the purpose of graphical representation in this manuscript) and those presenting enrichment were designated as IFN-rich ('IFN I+'). Out of 457 TB patients, 70% were classified as IFN I+, and 30% as IFN I-. In a similar way we constructed IFN II modules and determined their enrichment in individual TB patients. Intriguingly, enrichment for the modules related to IFN I and IFN II signaling were frequently shared by the same TB patients. Out of 319 TB patients presenting enrichment in IFN I modules (IFN I+ patients), 267 (84%) also showed enrichment in IFN II modules resulting in substantial overlap between IFN I and IFN II induction.

In the following, we use the terms 'IFN+ patient group' and 'IFN- patient group' based on the enrichment defined using IFN I modules since we focus on IFN I responses, however the high redundancy within the enrichment in IFN II modules implied that that they refer to TB patients with both IFN I and IFN II

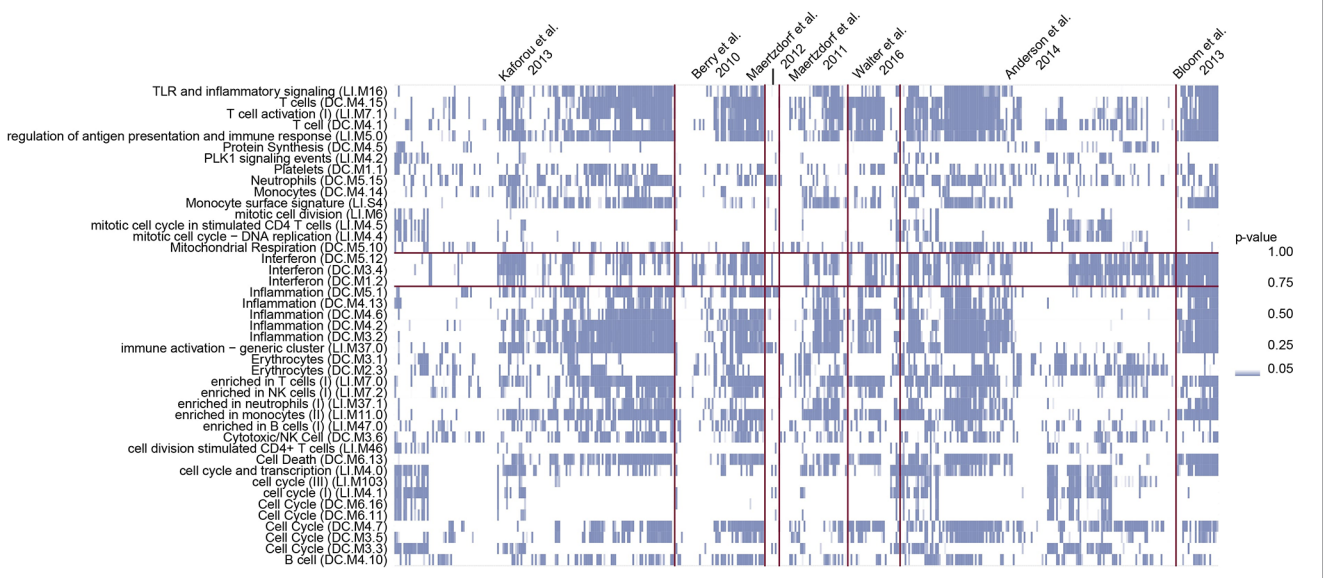

FIGURE 1 | GSA identifies substantial variability among TB patients. Columns show the transcriptional profiles of individual patients and blue squares represent p-values from CERNO test in modules described by the row names. The intensity of the color is proportional to the p-value of enrichment. Study cohorts are separated by vertical purple lines. The horizontal purple lines mark IFN modules. Clearly, in every studied cohort there are individuals presenting enrichment in IFN gene sets as well as presenting no significant enrichment in those sets.

signaling enrichment in 84% of the cases. Our terminology of 'IFN+' status is not to be confused with the abundance of IFN I signaling molecules in blood cells since abundance of ISGs in blood could be related to events at the sites of infection and should be interpreted only as prevalence of IFN inducible transcripts among the significantly regulated genes in TB patients compared to healthy individuals. Similarly, 'IFN-' status does not imply a lack of upregulated IFN or ISGs in blood of TB patients but a lack of significant enrichment of IFN modules in an individual sample.

To benchmark the modules, we conducted a GSA on the MDS and compared the enrichment status with the differences in the expression levels of several ISGs, among others the BATF2 gene, described as an important ISG (43, 44) which were significantly higher in the IFN+ compared to IFN- patient groups (**Figure 2A**). This indicates that genes identified as crucial for classification of TB patients had different activities in IFN+ and IFN- individuals.

Finally, we tested whether other factors influence predictors of IFN+ status among TB patients. Categorical variables, i.e., sex, diabetes, HIV and smoking status were tested using a chi-square test. Possible association with age was tested using a Mann-Whitney test. For all these investigated factors we did not observe differences and dependencies regarding IFN status (p-value>0.05).

PCA Supplemented by GSA Indicates Influence of T-Cell and NK-Cell Activity on IFN Status

To further benchmark the implemented division into IFN+ and IFN- groups we tested the differences between the TB patients categorized into the two groups using PCA. The results indicated that although the clusters of IFN+ and IFN- TB patient groups overlapped, the two centers of the clusters were geometrically shifted in regards to each other as best shown by PC2 and PC7 (**Figure 2B**, **Supplementary Figure 6**). GSA applied on genes sorted by their weights in these PCs resulted in a list of significantly enriched BTMs which were dominated by modules related to inflammatory response, induced by IFN type I signaling, and T cells, the main producers of IFN type II (**Figures 2C, D**). This result based on unsupervised analysis strengthens the proposed distinction between gene expression profiles of IFN+ and IFN- TB patient groups.

IFNR and ISG, but Not IFNα, IFNβ or IFNγ Genes Proper Are More Abundant in the IFN+ Than in IFN- TB Patient Groups

Enrichment of ISGs in WB does not imply elevated abundance of IFN transcripts in the same tissue but could be related to increased transcription of IFN e.g., at the site of infection. We tested whether the observed enrichment was related to increased expression of the actual IFN α, β or γ genes, IFN receptor genes (IFNR), or ISGs. To avoid using the genes on which the division into IFN+ and IFN- patient groups was based, we identified genes described in IFN signaling pathways, but not included in the original BTMs (16, 17), and determined whether their expression levels varied significantly between IFN+ and IFN- TB patient groups. There were no significant differences of mRNA-transcript levels of the actual IFN α, β or γ genes (IFNA2, IFNB1 or IFNG) between IFN+ and IFN- TB patient groups. In contrast, differences were observed in several of the IFNR (e.g., IFNAR2, IFNGR2) and ISGs (e.g., CXCL10) between IFN+ and IFN- TB patient groups (**Figure 3**, **Supplementary Figures 7A–C**). Hence, differences in IFN+ and IFN- TB patient groups were not a result of increased expression of the actual IFN genes in the WB. Additionally, the differential expression of the IFNR genes and ISGs outside of the defined gene sets confirmed that the transcriptional activation of IFN signaling pathways differed between the patient groups and was not an artifact of the method used for the division.

Interestingly, despite IFN type I and type II signaling pathways being the most studied in the immune response to TB, we found that also IFN λ receptor gene (IFNLR1), but not IFN λ gene (IFNL) itself, which both belong to type III IFN signaling pathway was significantly overexpressed in IFN+ compared to IFN- TB patients or healthy (**Supplementary Figures 7D, E**). IFN λ has been described to have largely overlapping expression and function to IFN type I and to be ubiquitously expressed on epithelial surfaces such as in respiratory tract (45).

IFN+ Status Correlates With Severe Lung Pathology in TB Patients

Based on X-Ray images of their lungs, Berry et al. (3) assigned 80 of their study participants to one out of four groups: (i) no pathology, (ii) minimal pathology, (iii) moderate pathology, and (iv) advanced pathology by three independent physicians blinded to mRNA-array data and clinical diagnosis of the donors. We defined the IFN+/IFN- status of these 80 individuals based on GSA and compared them with the X-Ray based on pathologic classifications. 21% of donors classified into 'no disease' category presented IFN+ status (**Figure 4**). Among patients with 'minimal disease' 46% were IFN+ TB patients, in 'moderate disease' category 85% and in 'advanced disease' category 100% patients were IFN+. Pairwise comparisons of IFN+ patients in the four categories indicated a correlation between the enrichment in IFN I gene set and the severity of pulmonary pathology of TB patients. This agrees with and extends previous findings of Berry et al. (3) showing that the transcriptional signature of blood cells correlates with extent of pathology in TB patients.

Gene Signatures in IFN+ and IFN- TB Patient Groups Are Distinct

Gene signatures are frequently used to differentiate between TB patients and healthy individuals (8, 9, 46). We created random forests (RF) models trained on subsets of IFN- and IFN+ TB patients and non-TB controls and tested performances of five different sizes of gene signatures derived from these models to determine whether IFN- and IFN+ TB patient groups' signatures differed. The optimal balance between signature size and model performance was 20 transcripts in case of the IFN+ and 50 transcripts in case of the IFN- signature (**Supplementary Figure 8** and **Supplementary Table 1**). We then derived the two signatures from the training MDS and tested their performances

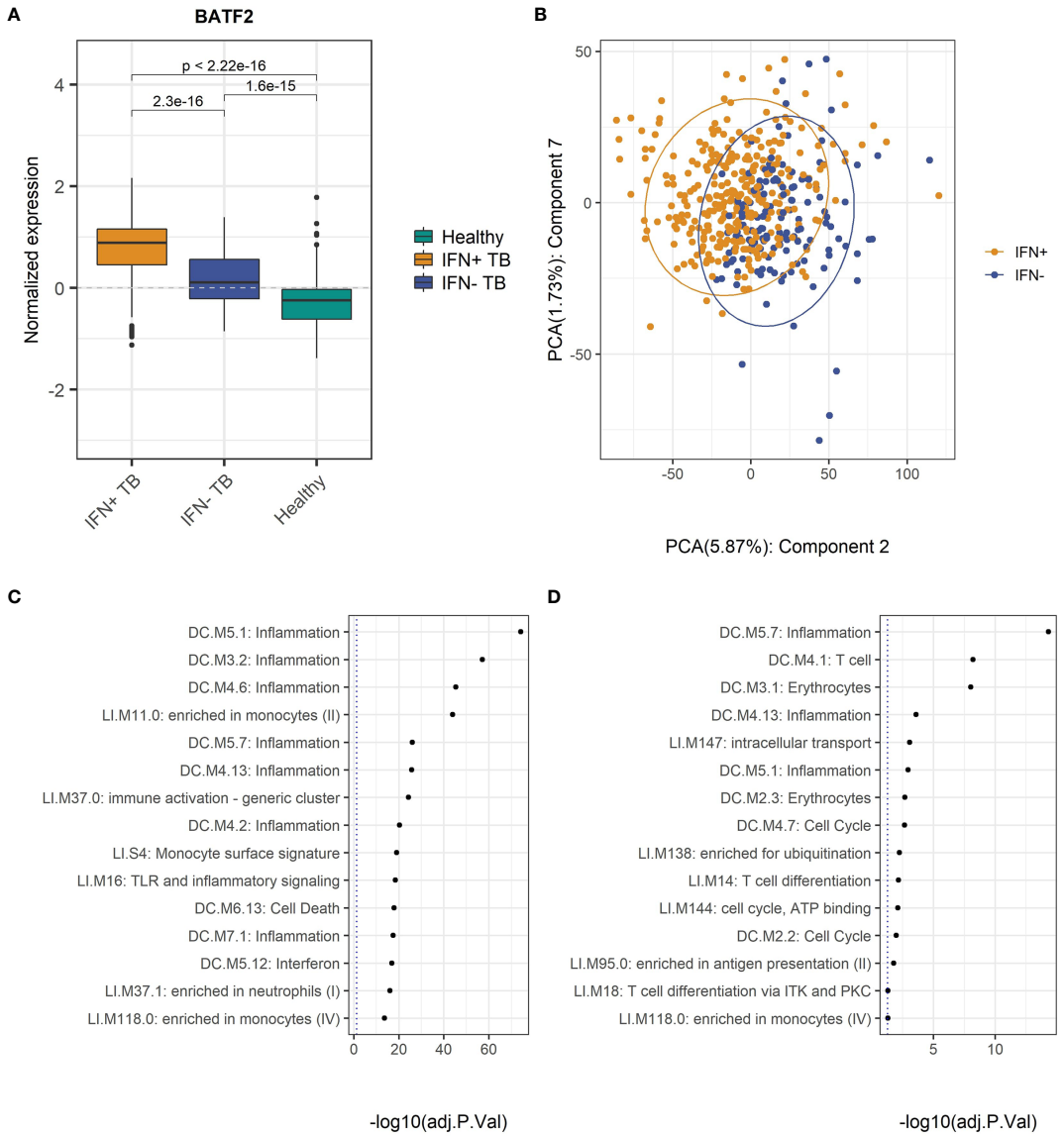

FIGURE 2 | Differences in the gene expression patterns of IFN- and IFN+ TB patients. **(A)** Normalized expression of the BATF2 gene is significantly higher in IFN+ than IFN- TB patient or healthy groups. The p-values were calculated for pairwise comparisons using Wilcoxon test. **(B)** PC2 and PC7 present the difference in the gene expression data of IFN+ and IFN- TB patient groups from the training MDS. **(C)** GSA performed on the list of genes from TB patients from training MDS sorted by decreasing weights in PC2. **(D)** GSA performed on the list of genes from TB patients from MDS sorted by decreasing weights in PC7. GSA indicates that modules related to T cells and inflammation are responsible for differences in IFN status of the TB patients.

with respect to identification of TB patient groups in the test MDS and two independent TB validation data sets, as well as in the identification of sepsis patients who also present IFN responses. This strategy allowed us to determine whether the signatures were TB-specific and not only IFN-specific. The study scheme is presented in the **Figure 5A** and the performance of the IFN+ and IFN- TB signatures in cross-validation in the **Figure 5B**.

The IFN- signature showed a slightly better overall performance in the identification of TB patients (AUC = 0.86, 95% CI = 0.82-0.90; **Figure 5C**) in the validation set over the IFN+ TB signature (AUC = 0.84, 95% CI = 0.80-0.89; **Figure 5C**). Even though greatest sensitivity and specificity were obtained by the IFN+ signature in the classification of IFN+ TB patients, this model had lower specificity when discerning between IFN- and IFN+ TB patients against OD patients as well as the between the IFN- TB patient groups *versus* healthy individuals.

Performance of IFN+ and IFN- Signatures on Validation Datasets

We next validated the IFN- and IFN+ RF models on two independent datasets [(15, 47); **Table 1**]. In the first validation

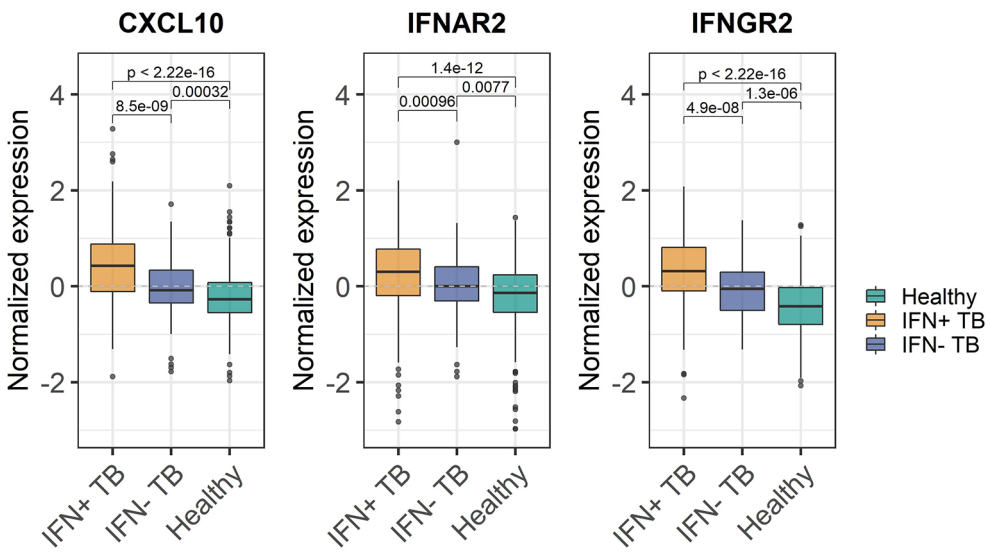

FIGURE 3 | Expression of IFN inducible CXCL10 gene, IFNAR2 and IFNGR2 receptor genes in IFN+ and IFN- TB patient groups and healthy controls. Significant differences have been observed between the expression of IFN-inducible genes between IFN- and IFN+ TB patients. The p-values were calculated for pairwise comparisons using Wilcoxon test.

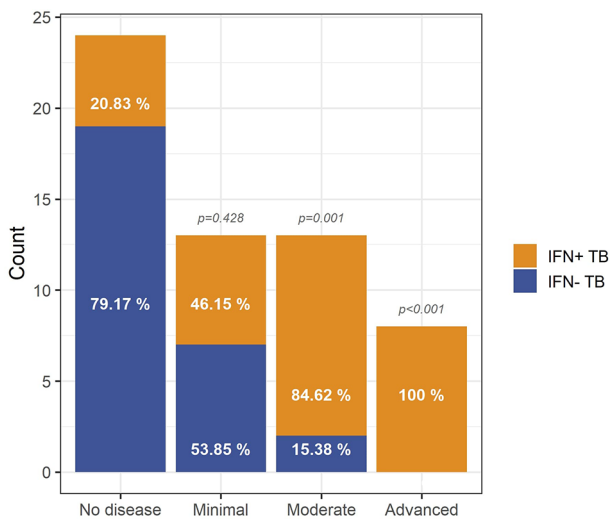

FIGURE 4 | Relationship between IFN status and lung pathology of TB patients. The vast majority of TB patients with moderate ($p = 10^{-3}$) and advanced ($p = 4{\cdot}10^{-4}$) pathology is IFN+ whereas absence of pathology is most prevalent in the IFN- TB patient group, indicating that the IFN endotype is associated with a higher level of pathology in TB patients. The p-values were calculated for pairwise comparisons using Fisher's exact test for count data with Bonferroni correction.

set of 21 samples from China containing IFN+ TB patient group and healthy individuals, both models achieved robust discrimination between TB patients and healthy individuals (**Figure 5D**). In contrast, on the set of 202 samples containing a mixed population of IFN+ TB patient group, sarcoidosis patients and healthy individuals of different ethnicities from London, the IFN- TB signature failed to correctly discriminate the IFN- TB patient group from patients with sarcoidosis (**Figure 5E**). Even though the IFN- signature was more universal and stable in discriminating TB patients against healthy and OD controls, it was insufficient for discrimination of TB from sarcoidosis.

Additionally, we used the TB IFN+ and TB IFN- signatures on datasets from sepsis patients to test whether our signatures did not only detect the IFN responses but also were specific for TB. Both IFN+ and IFN- TB signatures were not sensitive to sepsis (**Supplementary Figure 9**).

Influence of Time After Infection on IFN Status

We embarked on clarifying whether the IFN status of TB patients was influenced by time p.i. TB patients are diagnosed at various time periods of unknown lengths p.i. Therefore, we interrogated the impact of time p.i. between infection and diagnosis on IFN status. To this end, we harnessed a data set from a controlled Mtb infection experiment of 38 Cynomolgus macaques (18). In this study, animals were infected with Mtb at a fixed time point and blood samples were collected at 11 time points within 6 months p.i. The WB transcriptome had been profiled by mRNA-array at each time point and diagnosis of infection outcome was based on clinical definitions of active TB and LTBI, as well as on the basis of total lung inflammation measured by positron emission tomography - computed tomography (PET-CT) as abundances of [^{18}F] fluorodeoxyglucose (FDG) as surrogate marker of severity of pulmonary pathology (18). Sixteen out of the 38 infected macaques developed active TB while 22 remained with LTBI during the time frame of the study (18).

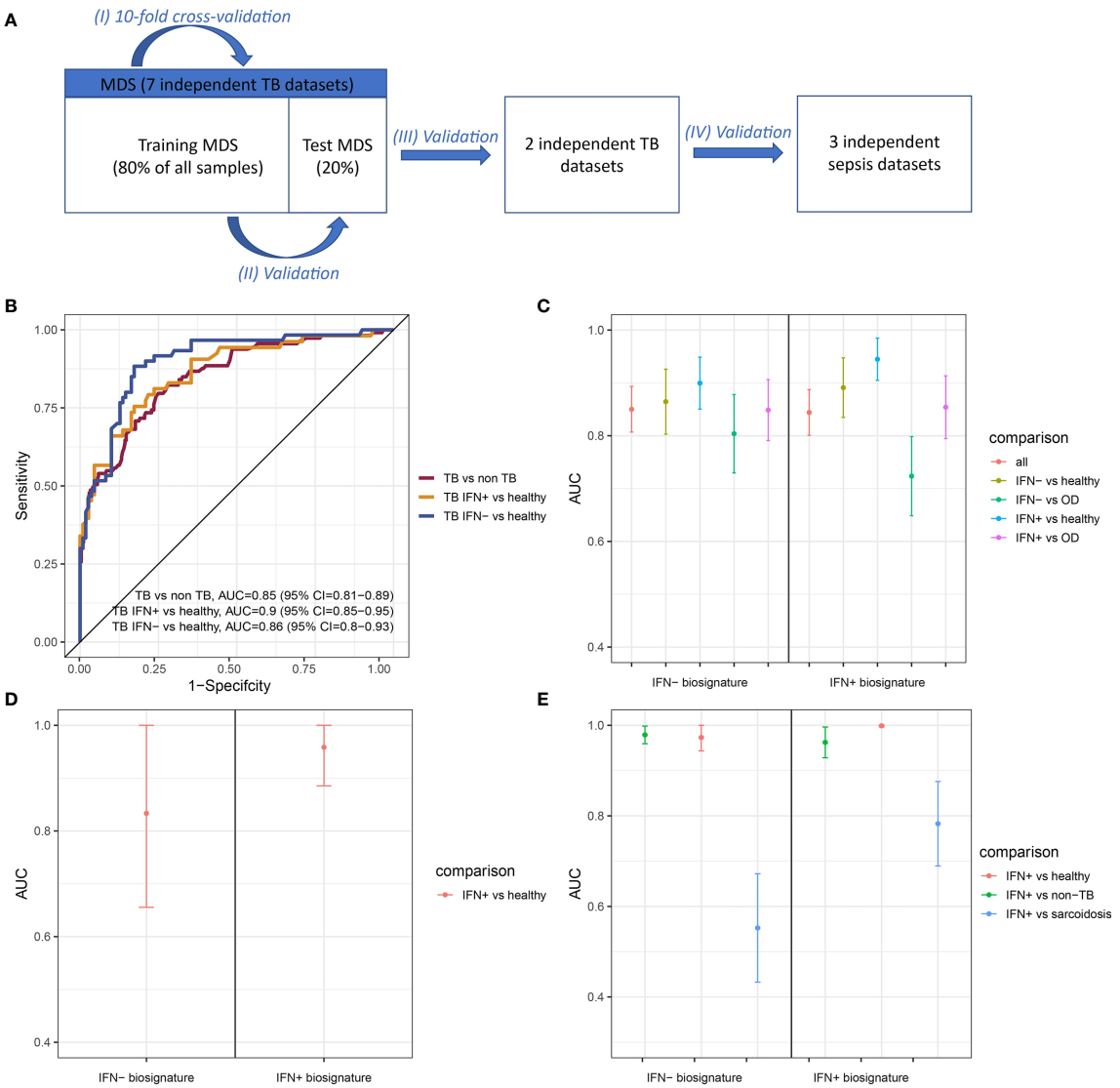

FIGURE 5 | Performance of IFN+ and IFN- signatures on test and validation datasets. **(A)** The validation scheme. To assure the performance of the method four types of validation were used. **(B)** ROC curve presenting the trade-off between sensitivity and specificity of the signature derived from training set consisting of transcriptomic profiles from IFN- TB patients and non-TB controls (healthy, LTBI and OD) and tested on the test set. **(C)** Signatures' performance in classifying TB patients in the test MDS containing IFN+ TB, IFN- TB, healthy and OD controls. **(D)** Signatures' performance in classifying TB patients in the validation dataset from China containing only IFN+ TB patient group and healthy controls. **(E)** Signatures' performance in classifying TB patients in the validation dataset derived from the samples of individuals from London, including IFN+ TB patient group, sarcoidosis patients and healthy individuals. Error bars represent 95% confidence intervals for mean value.

At each time point of the study, we assigned these animals either the IFN+ or IFN- status based on the GSA. We observed the peak of the type I IFN response between the 20th and 42nd day p.i. Intriguingly, enrichment in IFN modules was independent from the disease status: between days 20 and 42 p.i., the majority of animals which developed active TB disease as well as those which remained asymptomatic presented strong enrichment in IFN gene sets (**Figure 6**, **Supplementary Figure 10**). Animals progressing to active TB had a prolonged activation of IFN type I response in comparison to animals with LTBI: 75% of them presented enrichment with p-value < 0.0001 at day 56 p.i. compared to 27% with LTBI. Average numbers of time points in which animals with active TB presented enrichment in "IFN type I" gene set with p-value < 0.0001 were 5.9 compared to 4.6 time points in which LTBI animals presented the enrichment in the same module. Additionally, the animals with active TB which had to be at certain time point excluded from the study due to high pathology presented peak of the "IFN type I" gene set enrichment in the last measurement before the exclusion from the experiment, which indicates that the strong IFN enrichment corresponded with heavy disease manifestation. We conclude that the strong regulation of IFN

TABLE 1 | List of publicly available studies acquired for the analysis.

MDS			
Accession number	**Citation**	**Study location**	**Number of cases**
GSE19491	(3)	London, South Africa	54 TB 96 OD 93 CTRL
GSE47673	(6)	Malawi, South Africa	215 TB 194 OD 175 CTRL
GSE28623	(7)	The Gambia	46 TB 62 CTRL
GSE34608	(10)	Germany	8 TB 18 sarcoidosis 18 CTRL
GSE42834	(4)	London	35 TB 91 OD 113 CTRL
GSE39941	(48)	South Africa, Malawi, Kenya	114 TB 175 OD 57 CTRL
GSE73408	(49)	USA	35 TB 39 pneumonia 35 CTRL
Validation data sets			
Accession number	**Citation**	**Study location**	**Number of cases**
		TB	
GSE54992	(15)	China	9 TB 12 CTRL
GSE83456	(39)	London	45 TB 47 EPTB 49 OD 61 CTRL
		Sepsis	
GSE13904	(50)	USA	32 sepsis 67 septic shock 22 SIRS 18 CTRL
GSE9960	(51)	Australia	70 sepsis
GSE28750	(52)	Australia	27 sepsis 30 post-surgical sepsis 20 CTRL

OD, patients with disease other than TB; CTRL, healthy control patients; EPTB, extrapulmonary TB patients; SIRS, systemic inflammatory response syndrome.

signaling genes is not specific for active TB, yet, it was present for a longer time in animals with active TB. The enrichment in IFN modules was not correlated with time p.i. In fact, in the LTBI animals the IFN response decreased after a peak between days 20 and 30 p.i. (**Figure 6** and **Supplementary Figure 10**) while in animals with active TB the enrichment remained on a high level after the peak between the days 20 and 42 p.i.

Gene Set Analysis Suggests Additional Potential Endotypes in TB Patients

Given the differences between groups of TB patients classified as IFN+ and IFN- using GSA we hypothesized that the IFN+ TB endotype can be characterized by additional properties other than intensities of IFN responses, and that potentially also other endotypes of TB patients may exist, which are not correlated with the IFN responses. To this end, we performed an explorative analysis targeted at discovering gene sets which differ in their enrichment between individual patients, accounting for their correlation to IFN responses. We calculated the correlation between eigengenes of the KEGG and MSigDB Hallmark gene set collections and IFN gene set (first PCA components). These databases have a broader (although less specific) scope than the BTMs. Next, we performed GSA using those gene set collections and tested the independence from IFN gene set enrichment in individual proportions. For several of them, the enrichment in individual patients strongly correlated (positively or negatively) with the IFN status. This was the case among others for "Hallmark p53 pathway" module (correlation coefficient of the eigengenes r=0.98), "NF-kappa B signaling pathway" (r=0.96), "Hallmark complement" (r=0.96), "T cell receptor signaling

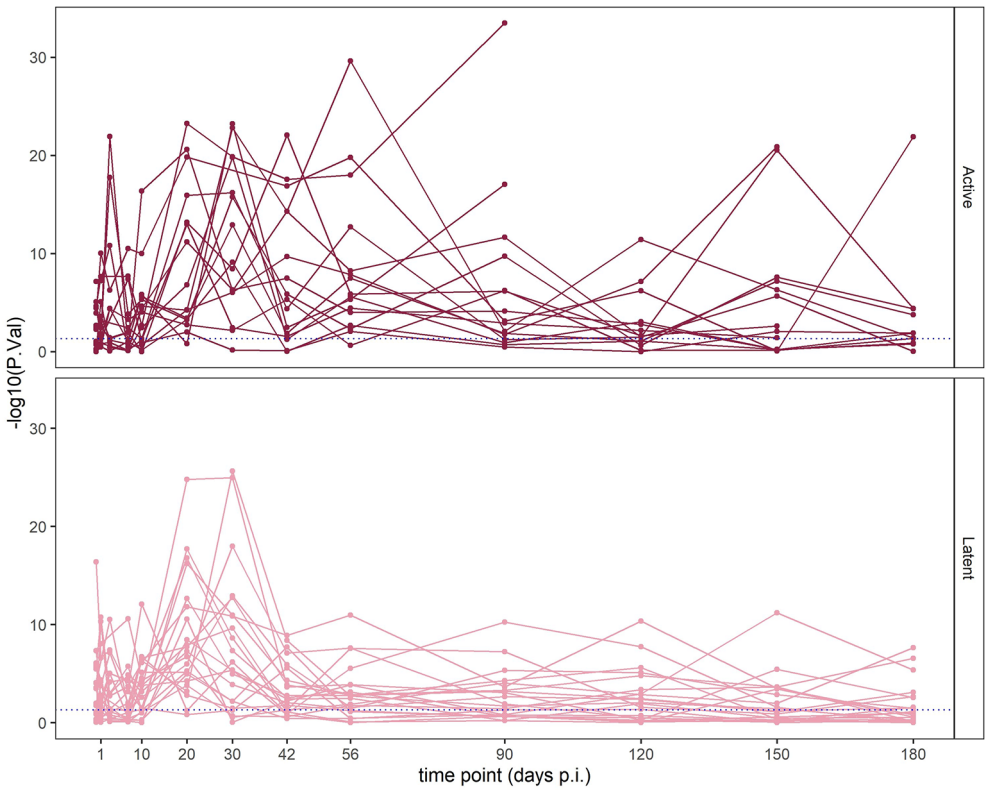

FIGURE 6 | Enrichment of the "IFN I" module in individual macaques over time p.i. Horizontal axis corresponds to time p.i.; vertical axis shows the $-\log_{10}$ of FDR in the enrichment (higher values mean lower adjusted p-values; values above the blue line are significant at $p < 0.05$). Each line corresponds to one animal. Top panel shows macaques which developed active TB disease; lower panel shows macaques which did not develop disease.

pathway" (r=-0.94), "Th17 cell differentiation" (r=-0.94). Likewise, the proportion of patients presenting enrichment in those modules significantly overlapped with the enrichment in the IFN gene set (p-value from chi^2 test <0.05). This suggests that the "IFN-rich" endotype is distinguished not only by its pronounced IFN response but also by pronounced NF-kappa B signaling and complement system signaling, while the genes belonging to T cell receptor signaling pathway and Th17 cell differentiation are strongly down-regulated in this endotype (**Figure 7A** and **Supplementary Table 2**). This allowed us to additionally characterize the IFN+ TB endotype not only based on its IFN response but also on other characteristic gene expression features presented by the TB patients with a pronounced IFN response.

We also identified several gene sets which were not correlated with IFN responses, but which nonetheless showed a significant variability in individual patients while at the same time showing differences in enrichment between patients and healthy controls. The enrichment in those modules was much weaker (p-value <0.05 before Benjamini-Hochberg adjustment; p-value >0.05 after the adjustment) and occurred far less commonly among TB patients from different cohorts than the enrichment in the IFN modules. To unravel these, for each given gene set, we tested the correlation of enrichments across all TB patients between the given gene set and the IFN response. This yielded 16 gene sets (out of 388 analyzed in total) which showed enrichment (p-value <0.05 before Benjamini-Hochberg adjustment) in at least 10% of TB patients in the MDS and with no enrichment in the remaining TB patients and, at the same time, no significant correlation with the IFN response (p-value ≥ 0.05; **Figure 7C**). The collection of those 16 gene sets could be grouped into 4 TB endotypes within which the enrichment of the gene sets among the TB patients was correlated (**Figure 7C**). Since such defined endotypes were characterized by correlated, weak enrichment in gene sets with unclear biological connection that we could identify, we named them "Weak TB endotype I-IV" ("WTBE I", "WTBE II", "WTBE III", and "WTBE IV"). The WTBE I, WTBE II, and WTBE III each included at least one gene set which is related to mechanisms that have been previously described as important in TB disease and could lead to diverse clinical characteristics of TB among patients: (1) calcium reabsorption, (2) insulin secretion, and (3) amino acid (D-Arginine and D-ornithine)-metabolism (53–55).

We also observed a spectrum of responses presenting strong enrichment in various subgroups of patients, which only partially overlapped with the IFN endotype. To narrow down the results, we focused only on the responses which were present in more

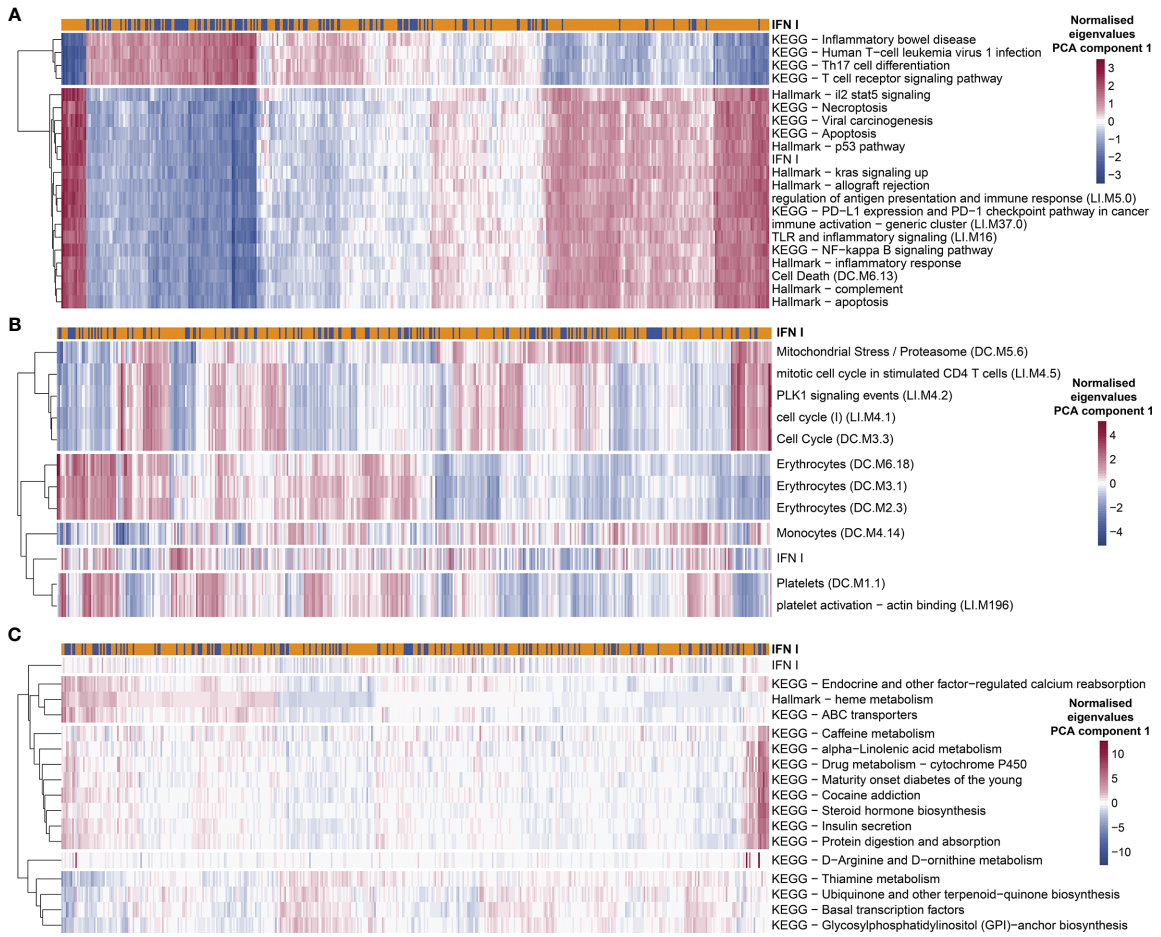

FIGURE 7 | Exploratory analysis suggests additional potential endotypes of TB. The enrichment in KEGG and Hallmark MSigDB gene collections presented variability among individual TB patients which was strongly correlated **(A)**, completely uncorrelated **(C)** or moderately correlated but occurring only in a not-significant proportion of patients with IFN+ status **(B)**. Red color in each plot represents high eigen value from PC1 for particular gene set and patient, while blue shows low eigen value. Colors are normalized row-wise within panels.

than 10% of the TB patients in MDS, where the 10% consisted of TB patients from at least 6 out of 7 investigated cohorts. Furthermore, to exclude gene sets linked strongly to the IFN endotype, we considered only gene sets which were enriched independent of IFN gene set enrichment. Nine modules presented strong enrichment correlated with $r<0.5$ and chi^2 p-value > 0.05: "platelet activation - actin binding", "PLK1 signaling events", "Mitochondrial Stress/Proteasome", "Platelets", "cell cycle", "Erythrocytes", "Monocytes", "mitotic cell cycle in stimulated CD4 T cells", "Hallmark heme metabolism" (**Figure 7B** and **Supplementary Table 2**). The role of platelets has been previously described as detrimental in primary progressive TB (56).

DISCUSSION

Using a novel approach to transcriptome analysis, we discovered individual variability among TB patients across seven cohorts, in particular with respect to IFN responses. Principally, IFN responses are induced by IFN type I or IFN type II which cause harmful or beneficial sequelae, respectively, in TB. We found that IFN responses were not equally distributed amongst TB patients. Rather, in a subgroup of TB patients, IFN responses were the dominant immune responses, which we defined as IFN+ group of TB patients while they were less pronounced in the group defined as IFN- group of TB patients. The distinct population of TB patients who did not develop IFN responses detectable by GSA presented less severe lung pathology. The findings were complemented by non-human primate studies which revealed that enrichment in IFN gene sets is not a result of time p.i. Finally, we determined that the gene signature from the IFN- TB patient group provided comparable, slightly higher sensitivity and specificity for overall diagnosis of TB, primarily because of better classification of IFN- TB patients from OD patients, and analyzed further mechanisms differentially regulated between subgroups of TB patients which should be further explored as new potential TB endotypes with different underlying host

immune responses. Our results revealed various enrichment patterns among TB patients within cohorts, which could be reproduced between cohorts. The dominant patterns included enrichment of modules including T cells, B cells, innate immunity, IFN signaling, monocytes and erythropoiesis. However, 30% of the TB patients did not present enrichment in IFN related modules.

Two types of IFN signaling are considered crucial for the outcome of TB: (i) the IFN I signaling pathway is thought to be mostly detrimental and (ii) the IFN II pathway is considered to play a major role in protection (42). Yet, our analyses revealed that the majority of TB cases shared IFN I and IFN II response enrichments indicating that detrimental and beneficial mechanisms coexist in active TB disease in a fine-tuned way. Consistently, lung pathology was far more prevalent in the IFN+ than IFN- TB patient groups. Possibly, the balance between both types of IFN determines the outcome of the infection.

Unsupervised analysis identified that samples collected from IFN- and IFN+ TB patient groups cluster together but are shifted with regard to each other. GSE on the weights of genes revealed contribution of T cells, which are potent producers of IFN γ and IFN α cytokines (42). PCA of samples from TB patients showed that even though the data had been normalized, differences between datasets from different studies still stratified the data (**Supplementary Figure 4D**).

Our analysis demonstrates that differences in the enrichment of IFN related modules is not a consequence of varying abundances of IFN α, IFN β or IFN γ in WB since the IFN+ and IFN- patient groups presented similar expression of IFN α, IFN β and IFN γ genes. Rather, significant differences in the expression of IFN α and IFN γ receptors and ISGs such as CXCL10 between the IFN+ and IFN- TB patient groups were critical. We conclude that regulation of gene expression in IFN+ and IFN- TB patient groups was not caused by differential expression of IFN α, β or γ, but by differential expression of IFNR genes and ISGs.

The abundance of the transcript BATF2 contributed to the differences in enrichment observed between IFN+ and IFN- TB patient groups. The BATF2 levels were significantly higher in IFN+ than IFN- TB patient groups. This leucine zipper transcription factor has been shown to exacerbate lung pathology in an experimental mouse model (43) and has been suggested as a single biomarker for TB (44). We conclude that BATF2 is regulated by IFN and primarily detrimental in TB.

We defined diagnostic signatures of IFN+ and IFN- TB patient groups using ML methods. The selected IFN+ signature comprised 20 transcripts, while the optimal IFN- signature consisted of 50 transcripts. 7 transcripts were present in both IFN+ and IFN- TB signatures: GBP5, AIM2, GBP2, POLB, WARS1, LHFPL2, DUSP3. Several of these genes are related to IFN-signaling which emphasizes the important role of IFN in TB even in patients in whom IFN signaling is enriched marginally.

The IFN+ and IFN- signatures were assessed on the test MDS and validated on two independent datasets, one including healthy controls and TB patients from China (15) and one including healthy controls as well as TB and sarcoidosis patients from an ethnically diverse population in London (47). The signature derived from the IFN+ TB patient group was highly sensitive and specific towards IFN+ TB patient groups, however its performance was unsatisfactory with respect to discriminating between the IFN- TB patient group from healthy, and in particular against patients with OD. The IFN- TB signature presented slightly higher AUC values for identification of TB patients in the test set, but lower ones in the two validation sets. To the advantage of the IFN- TB signature, its classification was characterized by similar sensitivity and specificity for discriminating IFN- and IFN+ patient groups against healthy, OD and all non-TB controls. The exception was the discrimination of TB *versus* sarcoidosis patients, which was only satisfactory for the IFN+ TB signature. TB and sarcoidosis have been shown to present a remarkably high overlap between biomarkers that discriminate *versus* healthy controls (10). In summary, our results demonstrate that: (i) the IFN+ and IFN- TB patient groups were characterized by different signatures; (ii) the IFN- TB signature identified the IFN+ TB patient group whereas the IFN+ signature failed to diagnose the IFN- TB patient group; (iii) even though the TB IFN- signature was more stable in detecting TB patients, it failed to differentiate between IFN+ TB patient group and sarcoidosis patients.

Using datasets from the macaque TB model from Gideon et al. (18) we probed whether the IFN status in TB can be explained by the time p.i. The heterogeneity in IFN responses was observed in the animals independent of the severity of TB disease and did not correlate with the time p.i. We observed a slight overall increase of IFN responses between 20- and 40-day p.i. corresponding with the findings of Gideon et al. (18). During this time period adaptive immunity kicks in (57). The effect size and p-value of enrichment in IFN gene sets in given animals did not correspond with the establishment of active TB or LTBI and varied among diseased as well as LTBI animals. Thus, a strong IFN response upon Mtb infection did not correlate with a particular stage of infection and progression to active disease, and its dynamics was highly individual.

In the study of Berry et al. (2010) the transcriptomes of eight out of 52 LTBI patients clustered with profiles of TB patients and four out of 21 TB patients presented transcriptional profiles resembling those of LTBI. Similar observations were reported by Blankley et al. (47) who determined transcriptional profiles of 61 healthy donors, 47 patients with extrapulmonary TB, 45 patients with pulmonary TB and 49 donors with sarcoidosis. They found that a subset of patients with TB clustered with the healthy donors. The GSA enrichment scores of modules related to IFN responses reflected the extent of symptoms presented by the study participants (47). As suggested by the recent studies of Zak et al. (8), Suliman et al. (9) and Singhania et al. (58), classification as 'TB' and 'non-TB' by clinical assessment and transcriptomic profiling can be confounded by subclinical incipient TB and early stages of progression to active TB disease. Transcriptomic profiling, but not clinical diagnosis, identifies subclinical TB and risk of progression to active TB within 12 months (8, 9). Our study further emphasizes the need to better define the continuum from LTBI to subclinical TB to active TB disease and also to distinguish between different endotypes of active TB.

To this end, we next explored the possibility of further novel, molecular endotypes of TB, which are not directly linked to IFN responses. We found that TB patients differ in the activity of genes associated with calcium signaling, insulin signaling and amino acid metabolism. These findings introduce an exciting new avenue of exploring pathways linked to TB. We are aware that our results are based on lack of an observed correlation with the IFN response – and thus might indicate lack of evidence for association with IFN rather than evidence of lack. However, given the large number of patients on which we based our study, we feel reasonably confident that if such effect exists, its magnitude must be small. Clearly, as these findings are based on an exploratory analysis, a further validation targeted directly at our hypotheses will be essential. The concept of endotypes to describe subgroups of patients on the basis of distinct transcriptomic, epigenetic or metabolic features has been applied to several diseases, most recently also to TB (21). A combination of a specific endotype and certain environmental factors has important impact on the disease phenotype. It is likely that different endotypes require distinct types of host-directed therapy (2). Our data support the definition of molecular endotypes of TB with the IFN subtypes described here as major but not exclusive contributors.

Although our study provides deeper insight into individual variability among TB patients at the level of gene expression, there are limitations: first, human cohorts are highly variable due to numerous factors including genetic variability, conditions of life and circumstances of infections (such as coinfections, the frequency of reinfection with Mtb, and time to and reason of diagnosis). Additional confounders include varying study designs and conduct, as well as technical variation. To partly account for these confounders, we validated our results in several ways including cross-validation and leaving 20% of the acquired studies unprocessed for independent testing, acquisition of independent validation datasets and testing the gene signatures of IFN+ and IFN- TB on a different disease - sepsis. Application of our data collection, normalization and analytical methods in numerous external datasets revealed that the proposed analytical framework is robust and can be used in other multi-cohort studies. Our dataset collection selected out of published TB datasets and newly defined sets of IFN I, IFN II as well as IFN I and II inducible genes can be accessed on the website: (https://github.com/terkaterka/immune-response-to-TB).

An important conclusion from our study is that TB disease signatures are confounded and biased if they do not account for individual variability between study participants. The complexity of human TB presenting a continuum from LTBI to subclinical TB to different forms of active TB disease implies that the assignment of TB patients into one of the two general classes: 'diseased' or 'healthy' is insufficient. Future focus should lie on detection and exploration of other than IFN determinants of the course of TB in individual patients. It is thus most likely that active TB manifests as different endotypes which may need personalized treatment regimens as alternative or in adjunct to canonical treatment regimens. Notably, host-directed therapy will most likely differ in these two endotypes of active TB described here with the IFN+ group likely benefiting from IFN dampening and the IFN- group likely from IFN promoting therapy.

DATA AVAILABILITY STATEMENT

Publicly available datasets were analyzed in this study. This data can be found here: All of the used, publicly available datasets are referenced in the manuscript. The datasets are found in the Gene Expression Omnibus (GEO; https://www.ncbi.nlm.nih.gov/geo/) data repository.

AUTHOR CONTRIBUTIONS

TD collected the data sets, performed data analysis, and wrote the main manuscript file. JZ was incorporated into calculations and algorithm development that could be described as the performance of tasks in the technical informatics discipline defined by the Polish Ministry of Science and Higher Education. TD and JZ prepared the figures. RO performed Umap analysis of the datasets. JW designed and supervised the study with additional input from SK. All authors contributed to the article and approved the submitted version.

FUNDING

This work received intramural funding from the Max Planck Society to SK. This work was partially supported by the Silesian University of Technology grant for Support and Development of Research Potential (JZ).

SUPPLEMENTARY MATERIAL

The Supplementary Material for this article can be found online at: https://www.frontiersin.org/articles/10.3389/fimmu.2021.694680/full#supplementary-material

REFERENCES

1. World Health Organization. *Global Tuberculosis Report 2020*. Geneva: World Health Organization (2020).
2. Kaufmann SHE, Dorhoi A, Hotchkiss RS, Bartenschlager R. Host-Directed Therapies for Bacterial and Viral Infections. *Nat Rev Drug Discov Nat Publishing Group* (2018) 17:35–56. doi: 10.1038/nrd.2017.162
3. Berry MPR, Graham CM, McNab FW, Xu Z, Bloch SAA, Oni T, et al. An Interferon-Inducible Neutrophil-Driven Blood Transcriptional Signature in Human Tuberculosis. *Nature* (2010) 466(7309):973–7. doi: 10.1038/nature09247
4. Bloom CI, Graham CM, Berry MPR, Rozakeas F, Redford PS, Wang Y, et al. Transcriptional Blood Signatures Distinguish Pulmonary Tuberculosis, Pulmonary Sarcoidosis, Pneumonias and Lung Cancers. *PloS One* (2013) 8 (8):e70630. doi: 10.1371/journal.pone.0070630

5. Dawany N, Showe LC, v. KA, Chang C, Ive P, Conradie F, et al. Identification of a 251 Gene Expression Signature That Can Accurately Detect M. Tuberculosis in Patients With and Without HIV Co-Infection. Torrelles JB, Editor. *PloS One* (2014) 9(2):e89925. doi: 10.1371/journal.pone.0089925
6. Kaforou M, Wright VJ, Oni T, French N, Anderson ST, Bangani N, et al. Detection of Tuberculosis in HIV-Infected and -Uninfected African Adults Using Whole Blood RNA Expression Signatures: A Case-Control Study. *PloS Med* (2013) 10(10):e1001538. doi: 10.1371/journal.pmed.1001538
7. Maertzdorf J, Ota M, Repsilber D, Mollenkopf HJ, Weiner J, Hill PC, et al. Functional Correlations of Pathogenesis-Driven Gene Expression Signatures in Tuberculosis. Doherty TM, Editor. *PloS One* (2011) 6(10):e26938. doi: 10.1371/journal.pone.0026938
8. Zak DE, Penn-Nicholson A, Scriba TJ, Thompson E, Suliman S, Amon LM, et al. A Blood RNA Signature for Tuberculosis Disease Risk: A Prospective Cohort Study. *Lancet* (2016) 387(10035):2312–22. doi: 10.1016/S0140-6736(15)01316-1
9. Suliman S, Thompson EG, Sutherland J, Weiner J, Ota MOC, Shankar S, et al. Four-Gene Pan-African Blood Signature Predicts Progression to Tuberculosis. *Am J Respir Crit Care Med* (2018) 197(9):1198–208. doi: 10.1164/rccm.201711-2340OC
10. Maertzdorf J, Weiner J, Mollenkopf H-J, Bauer T, Prasse A, Müller-Quernheim J, et al. Common Patterns and Disease-Related Signatures in Tuberculosis and Sarcoidosis. *Proc Natl Acad Sci USA* (2012) 109(20):7853–8. doi: 10.1073/pnas.1121072109
11. Cliff JM, Kaufmann SHE, McShane H, van Helden P, O'Garra A. The Human Immune Response to Tuberculosis and Its Treatment: A View From the Blood. *Immunol Rev* (2015) Mar264(1):88–102. doi: 10.1111/imr.12269
12. Diel R, Loddenkemper R, Nienhaus A. Evidence-Based Comparison of Commercial Interferon-γ Release Assays for Detecting Active TB: A Metaanalysis. *Chest* (2010) 137(4):952–68. doi: 10.1378/chest.09-2350
13. Verhagen LM, Zomer A, Maes M, Villalba JA, del Nogal B, Eleveld M, et al. A Predictive Signature Gene Set for Discriminating Active From Latent Tuberculosis in Warao Amerindian Children. *BMC Genomics* (2013) 14 (1):74. doi: 10.1186/1471-2164-14-74
14. Cliff JM, Lee J-S, Constantinou N, Cho J-E, Clark TG, Ronacher K, et al. Distinct Phases of Blood Gene Expression Pattern Through Tuberculosis Treatment Reflect Modulation of the Humoral Immune Response. *J Infect Dis* (2013) 207(1):18–29. doi: 10.1093/infdis/jis499
15. Cai Y, Yang Q, Tang Y, Zhang M, Liu H, Zhang G, et al. Increased Complement C1q Level Marks Active Disease in Human Tuberculosis. Herrmann JL, Editor. *PloS One* (2014) 9(3):e92340. doi: 10.1371/journal.pone.0092340
16. Chaussabel D, Quinn C, Shen J, Patel P, Glaser C, Baldwin N, et al. A Modular Analysis Framework for Blood Genomics Studies: Application to Systemic Lupus Erythematosus. *Immunity* (2008) 29(1):150–64. doi: 10.1016/j.immuni.2008.05.012
17. Li S, Rouphael N, Duraisingham S, Romero-Steiner S, Presnell S, Davis C, et al. Molecular Signatures of Antibody Responses Derived From a Systems Biology Study of Five Human Vaccines. *Nat Immunol* (2014) 15(2):195–204. doi: 10.1038/ni.2789
18. Gideon HP, Skinner JA, Baldwin N, Flynn JL, Lin PL. Early Whole Blood Transcriptional Signatures Are Associated With Severity of Lung Inflammation in Cynomolgus Macaques With Mycobacterium Tuberculosis Infection. *J Immunol* (2016) 197(12):4817–28. doi: 10.4049/jimmunol.1601138
19. Kanehisa M, Furumichi M, Tanabe M, Sato Y, Morishima K. KEGG: New Perspectives on Genomes, Pathways, Diseases and Drugs. *Nucleic Acids Res* (2017) 45(D1):D353–61. doi: 10.1093/nar/gkw1092
20. Liberzon A, Birger C, Thorvaldsdóttir H, Ghandi M, Mesirov JP, Tamayo P. The Molecular Signatures Database Hallmark Gene Set Collection. *Cell Syst* (2015) 1(6):417–25. doi: 10.1016/j.cels.2015.12.004
21. DiNardo AR, Nishiguchi T, Grimm SL, Schlesinger LS, Graviss EA, Cirillo JD, et al. Tuberculosis Endotypes to Guide Stratified Host-Directed Therapy. *Med* (2021) 2(3):217–32. doi: 10.1016/j.medj.2020.11.003
22. Edgar R, Domrachev M, Lash AE. Gene Expression Omnibus: NCBI Gene Expression and Hybridization Array Data Repository. *Nucleic Acids Res* (2002) 30(1):207–10. doi: 10.1093/nar/30.1.207
23. Davis S, Meltzer PS. GEOquery: A Bridge Between the Gene Expression Omnibus (GEO) and BioConductor. *Bioinf (Oxford England)* (2007) 23 (14):1846–7. doi: 10.1093/bioinformatics/btm254
24. Durinck S, Moreau Y, Kasprzyk A, Davis S, De Moor B, Brazma A, et al. BioMart and Bioconductor: A Powerful Link Between Biological Databases and Microarray Data Analysis. *Bioinf (Oxford England)* (2005) 21(16):3439–40. doi: 10.1093/bioinformatics/bti525
25. Durinck S, Spellman PT, Birney E, Huber W. Mapping Identifiers for the Integration of Genomic Datasets With the R/Bioconductor Package biomaRt. *Nat Protoc* (2009) 4(8):1184–91. doi: 10.1038/nprot.2009.97
26. R Core Team R. R: A Language and Environment for Statistical Computing. In: RDC Team, editor. *R Foundation for Statistical Computing*, vol. 1. Vienna, Austria: R Foundation for Statistical Computing (2018). p. 409.
27. Ritchie ME, Phipson B, Wu D, Hu Y, Law CW, Shi W, et al. Limma Powers Differential Expression Analyses for RNA-Sequencing and Microarray Studies. *Nucleic Acids Res* (2015) 43(7):e47. doi: 10.1093/nar/gkv007
28. Wickham H. *Ggplot2: Elegant Graphics for Data Analysis*. New York: Springer-Verlag (2009).
29. McInnes L, Healy J. UMAP: Uniform Manifold Approximation and Projection for Dimension Reduction. *arXiv* (2018) 1802.03426. doi: 10.21105/joss.00861
30. Yamaguchi KD, Ruderman DL, Croze E, Wagner TC, Velichko S, Reder AT, et al. IFN-Beta-Regulated Genes Show Abnormal Expression in Therapy-Naïve Relapsing-Remitting MS Mononuclear Cells: Gene Expression Analysis Employing All Reported Protein-Protein Interactions. *J Neuroimmunol* (2008) Mar195(1–2):116–20. doi: 10.1016/j.jneuroim.2007.12.007
31. Zyla J, Marczyk M, Domaszewska T, Kaufmann SHE, Polanska J, Weiner J. Gene Set Enrichment for Reproducible Science: Comparison of CERNO and Eight Other Algorithms. *Bioinformatics* (2019) 35(24):5146–54. doi: 10.1093/bioinformatics/btz447
32. Weiner J 3rd, Domaszewska T. Tmod: An R Package for General and Multivariate Enrichment Analysis. *PeerJ Preprints* (2016) e2420v.
33. Rusinova I, Forster S, Yu S, Kannan A, Masse M, Cumming H, et al. INTERFEROME V2.0: An Updated Database of Annotated Interferon-Regulated Genes. *Nucleic Acids Res* (2012) 41(D1):D1040–6. doi: 10.1093/nar/gks1215
34. Weiner J. *Tmod: Module Enrichment Tool* (2017). Available at: http://bioinfo.mpiib-berlin.mpg.de/tmod/.
35. Weiner J 3rd. *Pca3d: Three Dimensional PCA Plots*. CRAN.r-project.org (2020). Available at: https://rdrr.io/cran/pca3d/man/pca3d-package.html.
36. Kuhn M. Building Predictive Models in R Using the Caret Package. *J Stat Software* (2008) 28(5):1–26. doi: 10.18637/jss.v028.i05
37. Liaw A, Wiener M. Classification and Regression by Randomforest. *R News* (2002) 2(3).
38. Robin X, Turck N, Hainard A, Tiberti N, Lisacek F, Sanchez J-C, et al. pROC: An Open-Source Package for R and S+ to Analyze and Compare ROC Curves. *BMC Bioinf* (2011) 12(1):77. doi: 10.1186/1471-2105-12-77
39. Blankley S, Graham CM, Levin J, Turner J, Berry MPR, Bloom CI, et al. A 380-Gene Meta-Signature of Active Tuberculosis Compared With Healthy Controls. *Eur Respir J* (2016) 47(6):1873–6. doi: 10.1183/13993003.02121-2015
40. Kanehisa M, Sato Y, Kawashima M, Furumichi M, Tanabe M. KEGG as a Reference Resource for Gene and Protein Annotation. *Nucleic Acids Res* (2016) 44(D1):D457–62. doi: 10.1093/nar/gkv1070
41. Benjamini Y, Hochberg Y. Controlling the False Discovery Rate: A Practical and Powerful Approach to Multiple Testing. *J R Stat Soc Ser B* (1995) 57 (1):289–300. doi: 10.1111/j.2517-6161.1995.tb02031.x
42. O'Garra A, Redford PS, McNab FW, Bloom CI, Wilkinson RJ, Berry MPR. The Immune Response in Tuberculosis. *Annu Rev Immunol* (2013) 31 (1):475–527. doi: 10.1146/annurev-immunol-032712-095939
43. Guler R, Mpotje T, Ozturk M, Nono JK, Parihar SP, Chia JE, et al. Batf2 Differentially Regulates Tissue Immunopathology in Type 1 and Type 2 Diseases. *Mucosal Immunol* (2019) 12(2):390–402. doi: 10.1038/s41385-018-0108-2
44. Roe JK, Thomas N, Gil E, Best K, Tsaliki E, Morris Jones S, et al. Blood Transcriptomic Diagnosis of Pulmonary and Extrapulmonary Tuberculosis. *JCI Insight* (2016) 1(16):e87238. doi: 10.1172/jci.insight.87238
45. Hemann EA, Gale M, Savan R. Interferon Lambda Genetics and Biology in Regulation of Viral Control. *Front Immunol* (2017) 8(DEC):1707. doi: 10.3389/fimmu.2017.01707
46. Maertzdorf J, McEwen G, Weiner J, Tian S, Lader E, Schriek U, et al. Concise Gene Signature for Point-of-Care Classification of Tuberculosis. *EMBO Mol Med* (2016) 8(2):86–95. doi: 10.15252/emmm.201505790
47. Blankley S, Graham CM, Turner J, Berry MPR, Bloom CI, Xu Z, et al. The Transcriptional Signature of Active Tuberculosis Reflects Symptom Status in

Extra-Pulmonary and Pulmonary Tuberculosis. Neyrolles O, Editor. *PloS One* (2016) 11(10):e0162220. doi: 10.1371/journal.pone.0162220
48. Anderson ST, Kaforou M, Brent AJ, Wright VJ, Banwell CM, Chagaluka G, et al. Diagnosis of Childhood Tuberculosis and Host RNA Expression in Africa. *N Engl J Med* (2014) 370(18):1712–23. doi: 10.1056/NEJMoa 1303657
49. Walter ND, Miller MA, Vasquez J, Weiner M, Chapman A, Engle M, et al. Blood Transcriptional Biomarkers for Active Tuberculosis Among Patients in the United States: A Case-Control Study With Systematic Cross-Classifier Evaluation. *J Clin Microbiol* (2016) 54(2):274–82. doi: 10.1128/JCM.01990-15
50. Wong HR, Cvijanovich N, Allen GL, Lin R, Anas N, Meyer K, et al. Genomic Expression Profiling Across the Pediatric Systemic Inflammatory Response Syndrome, Sepsis, and Septic Shock Spectrum. *Crit Care Med* (2009) 37 (5):1558–66. doi: 10.1097/CCM.0b013e31819fcc08
51. Tang BMP, McLean AS, Dawes IW, Huang SJ, Lin RCY. Gene-Expression Profiling of Peripheral Blood Mononuclear Cells in Sepsis. *Crit Care Med* (2009) 37(3):882–8. doi: 10.1097/CCM.0b013e31819b52fd
52. Sutherland A, Thomas M, Brandon RA, Brandon RB, Lipman J, Tang B, et al. Development and Validation of a Novel Molecular Biomarker Diagnostic Test for the Early Detection of Sepsis. *Crit Care* (2011) 15(3):R149. doi: 10.1186/cc10274
53. Borah K, Beyß M, Theorell A, Wu H, Basu P, Mendum TA, et al. Intracellular Mycobacterium Tuberculosis Exploits Multiple Host Nitrogen Sources During Growth in Human Macrophages. *Cell Rep* (2019) 29(11):3580–3591.e4. doi: 10.1016/j.celrep.2019.11.037
54. Philips L, Visser J, Nel D, Blaauw R. The Association Between Tuberculosis and the Development of Insulin Resistance in Adults With Pulmonary Tuberculosis in the Western Sub-District of the Cape Metropole Region, South Africa: A Combined Cross-Sectional, Cohort Study. *BMC Infect Dis* (2017) 17(1). doi: 10.1186/s12879-017-2657-5
55. Trimble WS, Grinstein S. TB or Not TB: Calcium Regulation in Mycobacterial Survival. *Cell Elsevier* (2007) 130:12–4. doi: 10.1016/j.cell.2007.06.039
56. Scheuermann L, Pei G, Domaszewska T, Zyla J, Oberbeck-Müller D, Bandermann S, et al. Platelets Restrict the Oxidative Burst in Phagocytes and Facilitate Primary Progressive Tuberculosis. *Am J Respir Crit Care Med* (2020) 202(5):730–44. doi: 10.1164/rccm.201910-2063OC
57. Coleman MT, Maiello P, Tomko J, Frye LJ, Fillmore D, Janssen C, et al. Early Changes by 18Fluorodeoxyglucose Positron Emission Tomography Coregistered With Computed Tomography Predict Outcome After Mycobacterium Tuberculosis Infection in Cynomolgus Macaques. *Infect Immun* (2014) 82(6):2400–4. doi: 10.1128/IAI.01599-13
58. Singhania A, Verma R, Graham CM, Lee J, Tran T, Richardson M, et al. A Modular Transcriptional Signature Identifies Phenotypic Heterogeneity of Human Tuberculosis Infection. *Nat Commun* (2018) 9(1):2308. doi: 10.1038/s41467-018-04579-w

Conflict of Interest: The authors declare that the research was conducted in the absence of any commercial or financial relationships that could be construed as a potential conflict of interest.

Publisher's Note: All claims expressed in this article are solely those of the authors and do not necessarily represent those of their affiliated organizations, or those of the publisher, the editors and the reviewers. Any product that may be evaluated in this article, or claim that may be made by its manufacturer, is not guaranteed or endorsed by the publisher.

Copyright © 2021 Domaszewska, Zyla, Otto, Kaufmann and Weiner. This is an open-access article distributed under the terms of the Creative Commons Attribution License (CC BY). The use, distribution or reproduction in other forums is permitted, provided the original author(s) and the copyright owner(s) are credited and that the original publication in this journal is cited, in accordance with accepted academic practice. No use, distribution or reproduction is permitted which does not comply with these terms.

frontiers in Immunology

ORIGINAL RESEARCH
published: 10 August 2021
doi: 10.3389/fimmu.2021.716857

Mycobacterium tuberculosis Immune Response in Patients With Immune-Mediated Inflammatory Disease

*Elisa Petruccioli[1], Linda Petrone[1], Teresa Chiacchio[1], Chiara Farroni[1], Gilda Cuzzi[1], Assunta Navarra[2], Valentina Vanini[1,3], Umberto Massafra[4], Marianna Lo Pizzo[5], Giuliana Guggino[5], Nadia Caccamo[6,7], Fabrizio Cantini[8], Fabrizio Palmieri[9] and Delia Goletti[1]**

[1] Translational Research Unit, National Institute for Infectious Diseases Lazzaro Spallanzani-IRCCS, Rome, Italy, [2] Clinical Epidemiology Unit, National Institute for Infectious Diseases Lazzaro Spallanzani-IRCCS, Rome, Italy, [3] UOS Professioni Sanitarie Tecniche, National Institute for Infectious Diseases Lazzaro Spallanzani-IRCCS, Rome, Italy, [4] Department of Internal Medicine, S. Pietro Fatebenefratelli Hospital, Rome, Italy, [5] Department of Health Promotion, Mother and Child Care, Internal Medicine and Medical Specialties, Rheumatology Section-University of Palermo, Palermo, Italy, [6] Central Laboratory of Advanced Diagnosis and Biomedical Research, University of Palermo, Palermo, Italy, [7] Department of Biomedicine, Neurosciences and Advanced Diagnostic, University of Palermo, Palermo, Italy, [8] Rheumatology Department, Hospital of Prato, Azienda USL Toscana Centro, Prato, Italy, [9] Respiratory Infectious Diseases Unit, National Institute for Infectious Diseases Lazzaro Spallanzani-IRCCS, Rome, Italy

OPEN ACCESS

Edited by:
Cecilia Lindestam Arlehamn, La Jolla Institute for Immunology (LJI), United States

Reviewed by:
Katalin A. Wilkinson, Francis Crick Institute, United Kingdom
Taylor Foreman, National Institutes of Health (NIH), United States

***Correspondence:**
Delia Goletti
delia.goletti@inmi.it

Specialty section:
This article was submitted to Immunological Memory, a section of the journal Frontiers in Immunology

Received: *29 May 2021*
Accepted: *20 July 2021*
Published: *10 August 2021*

Citation:
Petruccioli E, Petrone L, Chiacchio T, Farroni C, Cuzzi G, Navarra A, Vanini V, Massafra U, Lo Pizzo M, Guggino G, Caccamo N, Cantini F, Palmieri F and Goletti D (2021) Mycobacterium tuberculosis Immune Response in Patients With Immune-Mediated Inflammatory Disease. Front. Immunol. 12:716857. doi: 10.3389/fimmu.2021.716857

Subjects with immune-mediated inflammatory diseases (IMID), such as rheumatoid arthritis (RA), have an intrinsic higher probability to develop active-tuberculosis (TB) compared to the general population. The risk ranges from 2.0 to 8.9 in RA patients not receiving therapies. According to the WHO, the RA prevalence varies between 0.3% and 1% and is more common in women and in developed countries. Therefore, the identification and treatment of TB infection (TBI) in this fragile population is important to propose the TB preventive therapy. We aimed to study the M. tuberculosis (Mtb) specific T-cell response to find immune biomarkers of Mtb burden or Mtb clearance in patients with different TB status and different risk to develop active-TB disease. We enrolled TBI subjects as example of Mtb-containment, the active-TB as example of a replicating Mtb status, and the TBI-IMID as fragile population. To study the Mtb-specific response in a condition of possible Mtb sterilization, we longitudinally enrolled TBI subjects and active-TB patients before and after TB therapy. Peripheral blood mononuclear cells were stimulated overnight with Mtb peptides contained in TB1- and TB2-tubes of the Quantiferon-Plus kit. Then, we characterized by cytometry the Mtb-specific CD4 and CD8 T cells. In TBI-IMID, the TB therapy did not affect the ability of CD4 T cells to produce interferon-γ, tumor necrosis factor-α, and interleukin-2, their functional status, and their phenotype. The TB therapy determined a contraction of the triple functional CD4 T cells of the TBI subjects and active-TB patients. The $CD45RA^{-}$ $CD27^{+}$ T cells stood out as a main subset of the Mtb-specific response in all groups. Before the TB-preventive therapy, the TBI subjects had higher proportion of Mtb-specific $CD45RA^{-}CD27^{+}CD4^{+}$ T cells and the active-TB subjects had higher proportion of Mtb-specific $CD45RA^{-}CD27^{-}CD4^{+}$ T cells compared to other groups. The TBI-IMID patients showed a phenotype similar to TBI,

suggesting that the type of IMID and the IMID therapy did not affect the activation status of Mtb-specific CD4 T cells. Future studies on a larger and better-stratified TBI-IMID population will help to understand the change of the Mtb-specific immune response over time and to identify possible immune biomarkers of Mtb-containment or active replication.

Keywords: tuberculosis, immune-mediated inflammatory disease, *M. tuberculosis*, IFN-γ, CD27

INTRODUCTION

M. tuberculosis (Mtb) was estimated to be responsible for 10 million of new active tuberculosis (TB) disease cases and about 1.4 million TB deaths in 2019 (1). Almost a quarter of the world population is estimated to have TB infection (TBI) (2). However, only 5–10% of individuals with TBI will progress to active-TB disease during their lifetime (3). TB disease risk progression is higher within the first 2 years after Mtb exposure (3–6) and is strictly dependent on the efficiency of the immune system to control Mtb.

Indeed, among patients with the dysregulation of the immune system, subjects with immune-mediated inflammatory diseases (IMID), such as rheumatoid arthritis (RA), psoriatic arthritis (PsA), and ankylosing spondylitis (AS), have an intrinsic higher probability to develop active-TB compared to the general population (7–10). The risk ranges from 2.0 to 8.9 in RA patients not receiving therapies, and is lower in PsA and AS patients (7–11). The therapeutic strategy for IMID deeply changed thanks to the introduction of biologics drugs inhibiting specific pathway of the immune response. Briefly, we distinguish two main categories of biological drugs based on their action on tumor necrosis factor (TNF)-α: anti-TNF-α agents and non-anti-TNF-α agents. The anti-TNF-α agents, mainly but not exclusively monoclonal antibodies, include infliximab, adalimumab, golimumab, certolizumab pegol, and etanercept. The non-anti-TNF-α biologics include anti-Interleukin (IL)-1 anakinra, IL-6 inhibitor tocilizumab, anti-CD20 rituximab, anti-CD28 abatacept, anti-IL-12-23 Ustekinumab, anti-IL-17 secukinumab, and ixekizumab (10).

Recently, tofacitinib, baricitinib, upadacitinib, and filgotinib, a new class of synthetic drugs targeting the Janus kinases (JAKs) system, have been licensed for the treatment of rheumatoid arthritis (12). TB-reactivation risk associated with the JAK inhibitors seems negligible (13). However, since their recent marketing in Europe, these drugs were not investigated in the present study.

Among the different biologic agents, the anti-TNF-α increases the risk to develop TB disease up to 10 times (10). Indeed, TNF-α is fundamental for the Mtb-containment, inducing the construction and maintenance of the granuloma and stimulating the phagocytic ability of macrophages (10). Moreover, *in vitro* studies on Mtb-infected cells demonstrated that anti-TNF antibodies such as infliximab and adalimumab inhibit T-cell activation and IFN-γ production (14). Therefore, the risk related to Mtb-reactivation is associated with the direct effect of TNF-α blocking and to the indirect inhibition of other immune mediators. Differently, biologic drugs based on inhibition of IL-1, IL-6, IL-12-IL-23, IL-17, and CD28 lymphocytes act with less consequences on the granuloma integrity (11).

Therefore, the Mtb reactivation of IMID patients is due to both immune dysregulations related to the specific IMID and to the current therapeutic strategy.

Before starting the biologic therapy, based on these evidences, it is necessary to diagnose TBI among IMID patients and offer them the TB preventive therapy, preferably (11). Currently, the tuberculin skin test (TST) and the interferon-γ release assays (IGRAs), such as the QuantiFERON-TB Gold Plus (QFT-Plus) (Qiagen) and the T-Spot-TB (Oxford Immunotec), are the available commercial tests for detecting TBI (3, 15–18). Unfortunately, they have a poor predictive value for TB developing (3, 5, 15, 16, 18, 19). A recent meta-analysis reported that anti-TNF-α drugs significantly reduce the rate of positive score to IGRAs (20) and it has been demonstrated that IGRAs are falsely negative scored in RA patients with CD4 T-cell counts <650/μl and/or CD8 T-cell counts <400/μl (21). Moreover, we have recently demonstrated that that TBI-IMID had a lower IFN-γ response to QFT-Plus, with a higher proportion of results in the "uncertainty zone" (22) of QTF-plus assay compared to TBI individuals (23).

Several studies demonstrated that the TBI subjects with remote Mtb exposure, re-exposed to Mtb, had a lower probability to progress to active-TB disease compared to recently Mtb-infected subjects (4, 24), suggesting that the remote TBI achieved a sort of immune control of Mtb-infection. Probably in remote TBI individuals, Mtb remains in a low replication status continuously stimulating at low grade the immune system and favouring its containment. Indeed, several studies showed a decline of IFN-γ response levels during successful therapy, a condition of low or absent bacterial load (25–27). Due to the adult age of the manifestations of IMID, the majority of TBI-IMID subjects have a remote infection usually discovered during the TBI screening proposed before starting the biologics (28). Although a remote Mtb exposure, the TBI-IMID have an intrinsic higher risk to develop the active-TB disease (7, 10). In the last decade, several reports proposed that the differentiation status and functional ability of CD4 T cells depended on the degree and length of Mtb exposure (29, 30). Therefore, the different states of Mtb-infection could be identified by the differentiation status and functional ability of T cells (31, 32). Recently, it has been demonstrated that highly activated and moderately differentiated functional Mtb-specific T cells are potential immune biomarkers to discriminate recent and

remote TBI individuals (29). Active-TB status has been associated to high level of cell-activation markers such as HLA-DR (33–37) or to the loss of CD27 (38–42).

In the last few years, several studies focused on the role of CD8 T cells in the Mtb-infection (32, 43–45). The CD8 T-cell response has been associated to Mtb load, showing that patients with active-TB and recent Mtb-infection have an increased Mtb-specific CD8 T-cell response (23, 25, 46–50). Moreover, decreased CD8 T-cell response during anti-TB treatment has been shown in longitudinal studies (25).

Currently, few reports are available on Mtb-specific immune response characterization in TBI-IMID. In this regard, Mtb-specific T cells producing IFN-γ, TNF-α, and IL-2 have been described in TBI-IMID patients under TNF-α antagonist therapy (51). Moreover, IFN-γ, IL-17, and IL-4 cytokines, which characterize three categories of differentiated CD4 T cells, may help distinguish the active-TB status from TBI-IMID with high specificity but low sensitivity (52).

Based on these findings, we aimed to study the Mtb-specific T-cell response to find immune biomarkers of Mtb burden or Mtb clearance in patients with different TB status and different risk to develop active-TB disease, such as the TBI-IMID individuals. We enrolled TBI subjects as a model for Mtb-containment, the active-TB as a model for replicating Mtb status, and the TBI-IMID as fragile population to contextualize it in the spectrum of TB. Moreover, to study the Mtb-specific response in a condition of possible Mtb sterilization, we longitudinally enrolled TBI subjects and active-TB patients before and after TB therapy.

MATERIAL AND METHODS

Population Characteristics

This study was approved by the Ethical Committee of "L. Spallanzani" National Institute of Infectious Diseases (INMI)-IRCCS, approval number 72/2015. Written informed consent was required to participate in the study conducted at INMI. We prospectively enrolled HIV-uninfected subjects with TBI with and without IMID and patients with pulmonary active-TB. Microbiologically diagnosed active-TB was defined based on the Mtb isolation from sputum culture. Active-TB patients were enrolled within 7 days of starting the specific TB treatment (T0) and at the end of therapy (T1).

In the absence of clinical, microbiological, and radiological signs of active-TB, TBI was defined based on a positive score to QFT-Plus (Qiagen, Hilden, Germany). The TBI cohort included subjects with a remote infection (contact with a smear-positive pulmonary TB patient at least 3 years before the enrolment) and subjects reporting a recent contact (within 3 months). TBI subjects reporting a time of exposure between 4 months and 3 years were not enrolled (38). TBI subjects and TBI-IMID patients were enrolled before starting the specific TB preventive therapy (T0) and at the end of treatment (T1). Demographic and epidemiological information were collected at enrolment and are reported in **Table 1**. The information relative to the type of IMID and IMID-therapy are reported in **Table 2**.

QFT-Plus Evaluation

QFT-Plus assay was performed for each patient at T0 and T1. Two TBI-IMID and one active-TB patients did not perform the T1 evaluation. QFT-Plus kits were used according to manufacturer's instructions (53). The QFT-Plus Analysis Software (available from www.quantiFERON.com) was used to analyze raw data and to calculate the IFN-γ results in international units per milliliter (IU/ml). The software performs a quality control assessment of the assay, generates a standard curve, and provides a test result for each subject. Test results were interpreted according to manufacturer's criteria (53). TB1 tube contained peptides designed to induce mainly a CD4 T-cell response, whereas TB2 tube contained peptides to induce both a CD4 and CD8 T-cell response (48, 49).

Intracellular Staining Assay

Intracellular staining (ICS) was performed for each patient at T0 and T1. Peripheral blood mononuclear cells (PBMCs) were isolated using Ficoll density gradient centrifugation with the SepMate™ tubes (StemCell) and resuspended in complete RPMI-16-40 medium (Gibco, CA, USA) with 10% fetal bovine serum (PAA Laboratories GmbH, Pasching, Austria). To characterize by flow cytometry the Mtb-specific T-cell response, 1×10^6 PBMC resuspended in 1 ml of medium were dispensed in TB1, TB2, Mitogen, and Nil tubes of the QFT-Plus kit. After a 1 h incubation, PBMCs were transferred in polystyrene round-bottom tubes, and 1 µl/ml of Golgi plug (BD Biosciences, San Josè, USA) was added to inhibit cytokine secretion. Anti-CD28 and anti-CD49d monoclonal antibodies (mAb) at 2 µg/ml each were added to co-stimulate cells.

Following an incubation of 16–24 h, the ICS was performed. As previously described (46), PBMCs were stained with anti-CD4 peridinin chlorophylprotein (PerCp)-Cy5.5 conjugate, anti-CD8 allophycocyanin (APC)-H7, anti-CD3 conjugate PE-cyanine 7 (Cy7), anti-IFN-γ Pacific Blue (PB) conjugate, anti-TNF-α fluorescein isothiocyanate (FITC), anti-IL-2 R-phycoerythrin (PE), anti-CD45RA APC, anti-CD27 Horizon V500 (all from BD Biosciences).

Flow Cytometry Data Analysis

The Mtb-specific T-cell response was characterized evaluating the frequencies of CD4 and CD8 T cells producing IFN-γ, TNF-α, and IL-2 (**Figure 1**). At least 100,000 lymphocytes were acquired with a FACS CANTO II (BD Biosciences). Cytometry data were analyzed using FlowJo software (Version 9.3). Background cytokine production in the Nil tube was subtracted from each stimulated condition. If the background was higher than half of the antigen-specific response, the results were scored as negative. A frequency of IFN-γ-producing T cells of at least 0.03% was considered as positive response. The cytokine profile has been evaluated only in patients with a positive total response to the Mtb stimulation using the Boolean gate function of FlowJo software. For responders, we also calculated the functional differentiation

TABLE 1 | Clinical characteristics of enrolled patients.

	TBI-IMID	TBI	Active-TB	TOTAL	p
N	14	12	13	39	
Timing of TBI infection N (%):					
Recent	2 (14)	8 (67)	NA	–	0.006*
Remote	12 (86)	4 (33)	NA	–	
Age median (IQR)	63 (54–75)	37 (22–53)	38 (26–42)	45 (29–56)	0.0002*
Sex: Female N (%)	6 (43)	9 (75)	6 (46)	21 (53)	0.2070**
Origin N (%)					
West Europe	10 (71.4)	6 (50)	6 (46)	22 (56)	
East Europe	2 (14.3)	5 (42)	5 (38)	12 (31)	
Africa	1 (7.1)	1 (8)	0 (0)	2 (5)	0.5295**
Asia	1 (7.1)	0 (0)	1 (8)	2 (5)	
South America	0 (0)	0 (0)	1 (8)	1 (3)	
BCG vaccinated N (%)	4 (28.5)	6 (50)	8 (61.5)	18 (46)	0.2175**
Therapy N (%)	14 (100) ±	12 (100)	13 (100) §	39 (100)	NA
H	11 (78.6)	8 (66.7)	–	18 (46.2)	
H+R	3 (21.4)	4 (33.3)	–	7 (17.9)	
H+R+Z+E	–	–	12 (92.3)	12 (30.7)	
H+R+E+quinolone	–	–	1 (7.7)	1 (2.6)	
Therapy duration median (IQR)	6 (4.6–6)	6 (3–6)	6 (6–9)	NA	NA
QTF Plus N (%) at the time of enrolment§					0.4299**
Positive	12 (86)	11 (92)	12 (92)	34 (87)	
Negative	2 (14)	0 (8)	1 (8)	3 (77)	
Number of lymphocytes x10^3/μl at T0 median (IQR) §§#	1.9 (1.5–2.2)	2 (1.6–2.3)	1.7 (1–1.9)	1.8 (1.4–2.1)	0.13*
Number of lymphocytes x10^3/μl at T1 median (IQR) §§§#	1.6 (1.5–2.1)	1.9 (1.8–2.4)	2 (1.7–2.8)	1.9 (1.6–2.2)	0.051*
P values of the comparison of the number of lymphocytes x10^3/μl at T1 *vs* the number of lymphocytes x10^3/μl at T0 #	0.75	0.73	0.002		

*N, Number; TB, tuberculosis; TBI, TB infection; BCG, bacillus Calmette-Guérin; IQR, interquartile range; H, Isionazid; R, Rifampicin; Z, Pyrazinamide; E, Ethambutol; NA, not applicable *Kruskal- Wallis test; **Chi Square test; §All TBI and TBI-IMID patients have a QTF-Plus positive results in the past; ±One subject performed 2 weeks preventive therapy with H+R then continued with only H and therefore was included in the H-therapy group; §One patient discontinued and repeated the therapy.§§Data available at T0 (or within a month) in 14 TBI-IMID, 11 TBI, 13 Active-TB; §§§Data available at T1 (or within a month) in 14 TBI-IMID, 9 TBI and 12 Active-TB; #Wilcoxon matched-pairs signed rank test applied to compare T0 vs T1: TBI-IMID patients p = 0.75; TBI subjects p = 0.73; Active TB p = 0.002.*

score (FDS) as previously described (29, 30) by applying the following equation:

$$\mathrm{FDS} = \frac{\mathrm{IFN}-\gamma^{+} \quad \mathrm{IL}-2^{+/-} \quad \mathrm{TNF}-\alpha^{+/-}}{\mathrm{IFN}-\gamma^{-} \quad \mathrm{IL}-2^{+/-} \quad \mathrm{TFN}-\alpha^{+/-}}$$

The phenotype as well has been evaluated only in responders, assessing the proportion of CD45RA and CD27 on the gate of CD4 T cells able to produce IFN-γ, IL-2, or TNF-α (total CD4 T-cell response).

The number of CD4 and CD8 responders to TB1 and TB2 stimulation is reported in detail in **Table 3**.

Statistical Analysis

Data were analyzed using Graph Pad Prism (Version 8.2.1 for Windows) and Stata (Stata 15, StataCorp. 2017. Stata Statistical

TABLE 2 | Type of disease and type of therapy of TBI-IMID patients, enrolled before and after TB treatment.

Type of therapy	Psoriasis(2)		Psoriasic arthritis(2)		Rheumatoid arthritis(4)		Ankylosing spondylitis(6)		Total(14)	
	T0	T1	T0	T1	T0	T1	T0	T1	T0	T1
Biologic, N	0	0	0	0	0	1**	0	2§,#	0	3
Biologic + CS, N	0	0	0	0	0	1+	0	0	0	1
Biologic +NSAID + ID, N	0	0	0	1*	0	0	0	0	0	1
Biologic + NSAID, N	0	0	0	0	0	0	1§	0	1	0
ID, N	1	1	0	0	0	0	1	0	2	1
NSAID, N	0	0	1	1	1	1	1	1	3	3
ID + CS + NSAID, N	0	0	1	0	0	0	0	0	1	0
ID + CS, N	0	0	0	0	2	0	1	1	3	1
ID + NSAID, N	1	1	0	0	0	0	0	0	1	1
No therapy, N	0	0	0	0	1	1	2	2	3	3

*T0, before TB therapy; T1, after TB therapy; N, Number; ID, Immunosuppressive Drug; CS, corticosteroids; NSAID, Nonsteroidal Anti-Inflammatory Drug; before *Ustekinumab (anti IL-12/IL-23),**Tocilizumab (anti-IL6); +Abatacept (anti CTLA4); §Golimumab (anti TNF-α), #Etanercept (soluble receptor blocking the TNFα interaction with cell surface receptors).*

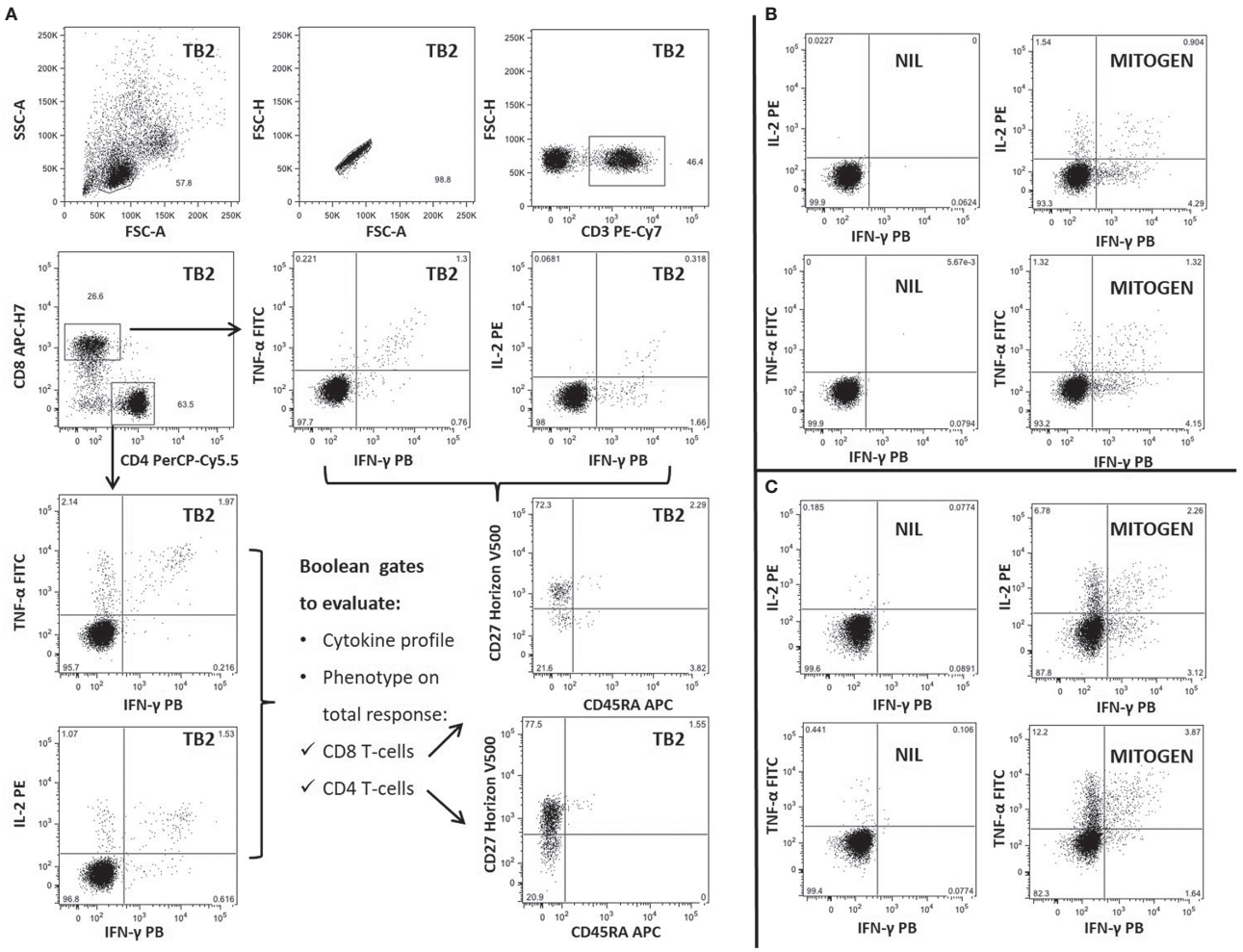

FIGURE 1 | Gating strategy and representative panel of Mtb-specific CD4 and CD8 T-cell response in one patient with TBI-IMID. Briefly, lymphocytes were gated according to FSC and SSC parameters, doublets were excluded (FSC-A/FSC-H), and CD4 and CD8 T cells were gated inside the CD3-T cells subset. Frequency of IFN-γ, IL-2, and TNF-α producing T cells was evaluated inside CD4 and CD8 subsets. CD45RA and CD27 proportion on Mtb-specific T cells was evaluated inside the total cytokine response. The CD45RA and CD27 gating position was decided on bulk CD4 and CD8 T-cell subsets. **(A)** TB2-specific CD4 and CD8 T cells; **(B)** Cytokine panels of CD8 T cells stimulated with NIL and MITOGEN; **(C)** Cytokine panels of CD4 T cells stimulated with NIL and MITOGEN. FSC, forward scatter; SSC, side scatter; TB2, peptides of TB2 tube of QFT-plus kit; MITOGEN, positive control stimulation of QFT-plus kit; NIL, unstimulated tube of QFT-plus kit.

Software: Release 15. College Station, TX: StataCorp LLC). The median and interquartile ranges (IQRs) were calculated for continuous measures. Kruskal–Wallis test was used for comparison among several groups. The Chi-Square and Fisher tests were used for proportions. The Wilcoxon matched-pairs signed rank test was used to compare the different time points. Bonferroni correction was applied when appropriate.

RESULTS

Characteristics of the Population

Thirty-nine subjects at different TB stages were enrolled. The TB-IMID patients had the higher age compared to the other groups (p = 0.0002), they included a higher proportion of remote Mtb exposed subjects compared to TBI (p=0.006), and they have a similar number of lymphocytes before and after TB therapy completion (p = 0.75, **Table 1**). One TBI-IMID patient was taking biologic drugs at T0 and at T1, and four TBI-IMID patients were taking biologics at T1 (**Tables 2**, **4**). Regarding the TB therapy, the majority of TBI-IMID patients received isionazid, whereas only three received isoniazid and rifampicin for 3 months; one subject received for 2 weeks isionazid and rifampicine then continued with isoniazid only. The duration of the preventive therapy regimen had a median of 6 months (**Table 1**). The TBI subjects showed similar lymphocyte counts before and after therapy (p = 0.73, **Table 1**) and received mainly isoniazid. Finally, as expected, patients with active-TB showed a significant increase of the lymphocyte counts after TB therapy completion (p = 0.002, **Table 1**) and received the standard TB regimen.

TABLE 3 | Number of CD4 and CD8 T-cell responders among IMID-TBI, TBI subjects, and active-TB patients, enrolled before and after TB treatment.

Stimulation and type of T-cell response	Type of cytokines produced	TBI-IMID(14)		TBI(12)		Active-TB(13)		p*	
		T0 N	T1 N	T0 N	T1 N	T0 N	T1 N	T0	T1
TB1 specific CD4 T cells	**Any cytokines**	13 (93)	12 (86)	11 (92)	10 (83)	10 (77)	10 (77)	0.493	0.878
	IFN-γ	12 (86)	10 (71)	9 (75)	8 (67)	9 (69)	8 (61)	0.641	0.913
	TNF-α	11 (78)	11 (78)	11 (92)	8 (67)	10 (77)	9 (69)	0.665	0.822
	IL-2	10 (71)	11 (78)	10 (83)	8 (67)	7 (54)	7 (54)	0.290	0.436
TB2 specific CD4 T cells	**Any cytokines**	11 (78)	12 (86)	12 (100)	11 (92)	11 (85)	11 (85)	0.340	1.000
	CD4 IFN-γ	11 (78)	12 (86)	10 (83)	10 (83)	10 (77)	9 (69)	1.000	0.610
	TNF-α	10 (71)	12 (86)	12 (100)	9 (75)	9 (69)	9 (69)	0.094	0.641
	IL-2	9 (64)	9 (64)	10 (83)	7 (58)	6 (46)	8 (61)	0.198	1.000
TB1 specific CD8 T cells	**Any cytokines**	3 (21)	4 (28)	4 (33)	6 (50)	3 (23)	5 (38)	0.811	0.552
	IFN-γ	3 (21)	4 (28)	4 (33)	6 (50)	3 (23)	5 (38)	0.811	0.552
	TNF-α	0 (0)	0 (0)	1 (8)	0 (0)	0 (0)	2 (15)	0.308	0.194
	IL-2	0 (0)	1 (7)	1 (8)	2 (17)	1 (8)	2 (15)	0.528	0.716
TB2 specific CD8 T cells	**Any cytokines**	2 (14)	4 (28)	4 (33)	8 (67)	4 (30)	6 (46)	0.481	0.160
	CD4 IFN-γ	2 (14)	4 (28)	4 (33)	8 (67)	4 (31)	5 (38)	0.481	0.145
	TNF-α	0 (0)	1 (7)	1 (8)	2 (17)	2 (15)	4 (31)	0.393	0.291
	IL-2	0 (0)	1 (7)	0 (0)	2 (17)	1 (8)	1 (8)	0.641	0.668

T0*, before TB therapy; T1, after TB therapy; N, Number; *Fisher Test.*

QFT-Plus Trend Before and After TB Treatment

In this study, the diagnosis of TBI is based on a positive IGRA and clinical and radiological parameters; therefore, the TBI-IMID and the TBI subjects have for definition a positive IGRA result. However, among the TBI-IMID patients, two patients had a negative QFT-Plus at T0 and a previously positive IGRA: one patient had a remote Mtb-infection, whereas the other one had a recent Mtb-infection and was taking an immunosuppressive drug. Among the subjects with TBI, one patient with a remote Mtb-infection had a negative QFT-Plus at T0 and a previously positive IGRA.

Differently, the assumption of a positive IGRA is not a criterion for the diagnosis of active-TB disease. Evaluating the QFT-Plus response at T0 and T1, we did not observe any significant differences in any groups (**Supplementary Figure 1**), and remarkably, all patients responded to Mitogen stimulation (data not shown).

TABLE 4 | Comparison of CD4 T-cells cytokine production according to the use of biologic drugs at T0 and T1.

Biologic agents	N	Any cytokine in response to TB1			Any cytokine in response to TB2		
		T0 mean (IQR)	T1 mean (IQR)	P*	T0 mean (IQR)	T1 mean (IQR)	P*
Never	9	0.31 (0.10–0.74)	0.41 (0.14–0.50)	0.722	0.17 (0–0.38)	0.43 (0.21–0.68)	0.094
Only T0	0	–	–	–	–	–	–
Only T1	4	0.35 (0.24–0.50)	0.26 (0.19–0.74)	0.715	0.39 (0.18–0.55)	0.50 (0.18–0.82)	0.273
T0 and T1	1	0.17 (na)	0.30 (na)	(na)	0.12 (na)	0.14 (na)	(na)
Overall	14	0.29 (0.17–0.54)	0.31 (0.18–0.50)	0.850	0.20 (0.9–0.55)	0.43 (0.15–0.80)	0.032

*T0, before TB therapy; T1, after TB therapy; N, Number; *Wilcoxon matched-pairs signed rank test; na, not available.*

Frequency of Mtb-Specific T Cells Is Similar in Patients Enrolled Before and After TB Treatment

We evaluated the ability of CD4 and CD8 T cells to produce IFN-γ, IL-2, and TNF-α in response to TB1 or TB2 stimulation (**Figures 2**, **3** and **Table 3**). In **Figure 1**, we showed a representative flow-cytometry analysis of Mtb-specific T cells for each studied group. Regarding the Mtb-specific CD4 T-cell response, we did not observe significant differences in terms of number of responders before and after TB treatment in any groups (**Table 3**). The frequency of Mtb-specific CD4 T cells, producing IFN-γ, IL-2, and TNF-α, was similar among TBI-IMID (**Figures 2A, B**), TBI subjects (**Figures 2C, D**), and active-TB patients (**Figures 2E, F**) at T0 and T1 with the exception of a lower frequency of TB2-specific TNF-α^+ CD4 T cells at T0 compared to T1 in TBI-IMID group (**Figure 2B**) and a higher frequency of TB1- and TB2-specific IL-2^+ CD4 T cells at T0 compared to T1 in TBI group (**Figures 2C, D**). Moreover, all groups of patients produced IFN-γ, IL-2, and TNF-α in response to TB1 or TB2 stimulations (**Figure 2** and **Table 3**). Considering the different IMID therapy of TBI-IMID (**Table 2**), we indicated in the graph the presence or not of an undergoing therapy with biologic drugs at each time point (**Figures 2A, B**). Stratifying for the presence of the undergoing biologic therapy (**Table 4**), we found that four patients were taking biologics only at T1, one patient at both T0 and T1, and nine patients neither at T0 nor at T1. We did not find any significant differences among TBI-IMID comparing T0 and T1 in terms of total response (production of any cytokines by CD4 T cells) (**Table 4**). Due to sample size, we could not stratify for type of biologic agents used and for the others IMID therapies.

Regarding the Mtb-specific CD8 T-cell response, we observed a not significant higher number of responders at T1 compared to T0 in response to TB2 stimulation (**Table 3**). Moreover, the number of CD8 T-cell responders was lower than the number of CD4 T-cell responders (**Table 3**). The frequency of Mtb-specific CD8 T cells was similar among TBI-IMID (**Figures 3A, B**), TBI subjects (**Figures 3C, D**), and active-TB (**Figures 3E, F**) patients at T0 and T1 and the responders produced mainly IFN-γ in response to TB1 or TB2 stimulations. Due to the low number of CD8 T-cell responders, we did not analyze the data according to the presence or not of biologic drugs.

Patients of all studied groups responded to the *in vitro* mitogen stimulation (**Supplementary Figure 2**). Regarding the CD4 T-cell response, the TBI-IMID patients showed a higher frequency of T cells producing IFN-γ or TNF-α or IL-2 at T1 compared to T0, whereas no significant differences were observed in TBI subjects and active-TB patients (**Supplementary Figure 2A–E**). Regarding the CD8 T-cell response, the TBI subjects showed a higher frequency of T cells producing IL-2 at T0 compared to T1, whereas no significant differences were observed in TBI-IMID and active-TB patients (**Supplementary Figure 2B–F**).

We next compared the cytokine production of Mtb-specific CD4 T cells among the different groups at each time point (**Figure 4**); we focused on CD4 T cells since the number of CD8 T cells responders was too low to allow a robust statistical analysis (**Table 3**). The frequency of Mtb-specific CD4 T cells producing IFN-γ, IL-2, or TNF-α was similar in TB, TBI subjects, and TBI-IMID patients enrolled at T0 (**Figures 4A, C**) and at T1 (**Figures 4B, D**). Differently, in response to mitogen stimulation, we reported a higher level of TNF-α ($p = 0.0013$) and IL-2 in TBI-IMID compared to TBI (**Supplementary Figure 3**).

TB-IMID Patients Had a Similar Cytokine Profile Before and After TB Preventive Therapy

We further investigated the functional cytokine profile of Mtb-specific T cells (**Figure 5**). We focused on CD4 T cells since the number of CD8 T cells responders was too low to allow a robust statistical analysis (**Table 3**).

In TBI-IMID group, we did not observe any significant changes comparing CD4 cytokine profile at T0 and T1 (**Figures 5A, B**) with the exception of a decrease of the IFN-γ^+ IL-2^+ CD4 T-cell subset at T1 compared to T0 in response to TB2 stimulation (**Figure 5B**). The CD4 T-cell response to TB1 and TB2 was mainly characterized by polyfunctional IFN-γ^+ IL-2^+ TNF-α^+ CD4 T cells; among the monofunctional T cells, the IFN-γ^+ IL-2^- TNF-α^- CD4 T cells were the most representative subset (**Figures 5A, B**).

In TBI group, we observed significant changes comparing CD4 T-cell cytokine profile at T0 and T1 (**Figures 5C, D**): the proportion of polyfunctional IFN-γ^+ IL-2^+ TNF-α^+ CD4 T cells was significantly higher at T0 than at T1 in response to TB1 ($p = 0.0039$) and to TB2 ($p = 0.0195$). Differently, we reported a higher but not significant proportion of monofunctional IFN-γ^+ IL-2^- TNF-α^- CD4 T cells at T1 compared to T0 in response to both stimuli. The proportion of the monofunctional IFN-γ^+ IL-2^- TNF-α^- T cells in TBI subjects after TB treatment was quite higher compared to TBI-IMID at the same time point (see below for the details).

In the active-TB group, we did not observe any significant change comparing CD4 cytokine profile at T0 and T1 (**Figures 5E, F**). In this case, the CD4 response to TB1 and TB2 was not similar. The TB1 response was mainly characterized by polyfunctional IFN-γ^+ IL-2^+ TNF-α^+ CD4 T cells; among the monofunctional T cells, the IFN-γ^- IL-2^- TNF-α^+ CD4 T cells and the IFN-γ^+ IL-2^- TNF-α^- CD4 T cells were the most representative subsets (**Figure 5E**). In contrast, the TB2 response showed a low proportion of polyfunctional IFN-γ^+ IL-2^+ TNF-α^+ CD4 T cells and an increased proportion of monofunctional IFN-γ^+ IL-2^- TNF-α^- CD4 T cells at both time points (**Figure 5F**).

It is known that Mtb-specific T cells change their functional capacity depending on antigen and bacterial load (25, 30, 31, 33). Based on these evidences, it has been proposed a single measurement of functional differentiation, FDS, of responders that describes the different type of Mtb-infection and Mtb burden (30). This analysis led us to synthetize the functional changes of T cells before and after therapy reported in **Figure 5**. The FDS of Mtb-specific CD4 T cells before and after therapy was not significantly different between T0 and T1 in any groups

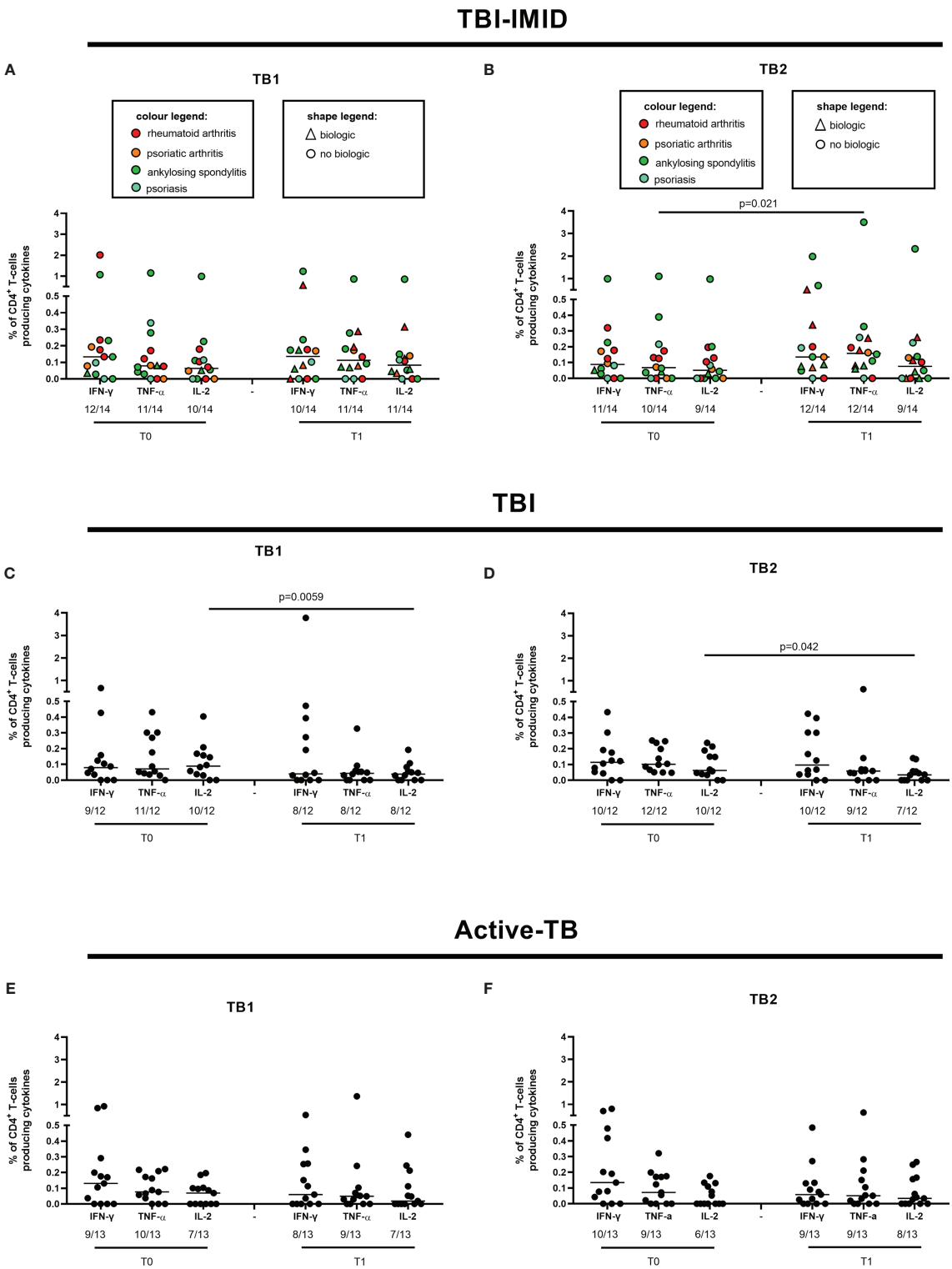

FIGURE 2 | CD4 T cells producing IFN-γ, IL-2, and TNF-α in response to Mtb antigen stimulation before and after TB therapy completion. PBMC of patients enrolled before (T0) and after TB therapy (T1) were stimulated overnight with TB1 and TB2 peptides. **(A, B)** TBI-IMID; **(C, D)** TBI subjects; **(E, F)** Active-TB patients. Number of responders over total enrolled patients is reported below each panel. Horizontal lines indicate the median. Statistical analysis was performed using the Wilcoxon matched-pairs signed rank test and the p value was considered significant if ≤0.05. TB, tuberculosis; TBI, tuberculosis infection; IMID, immune mediated inflammatory disease; TB1, peptides of TB1 tube of QFT-plus kit; TB2, peptides of TB2 tube of QFT-plus kit.

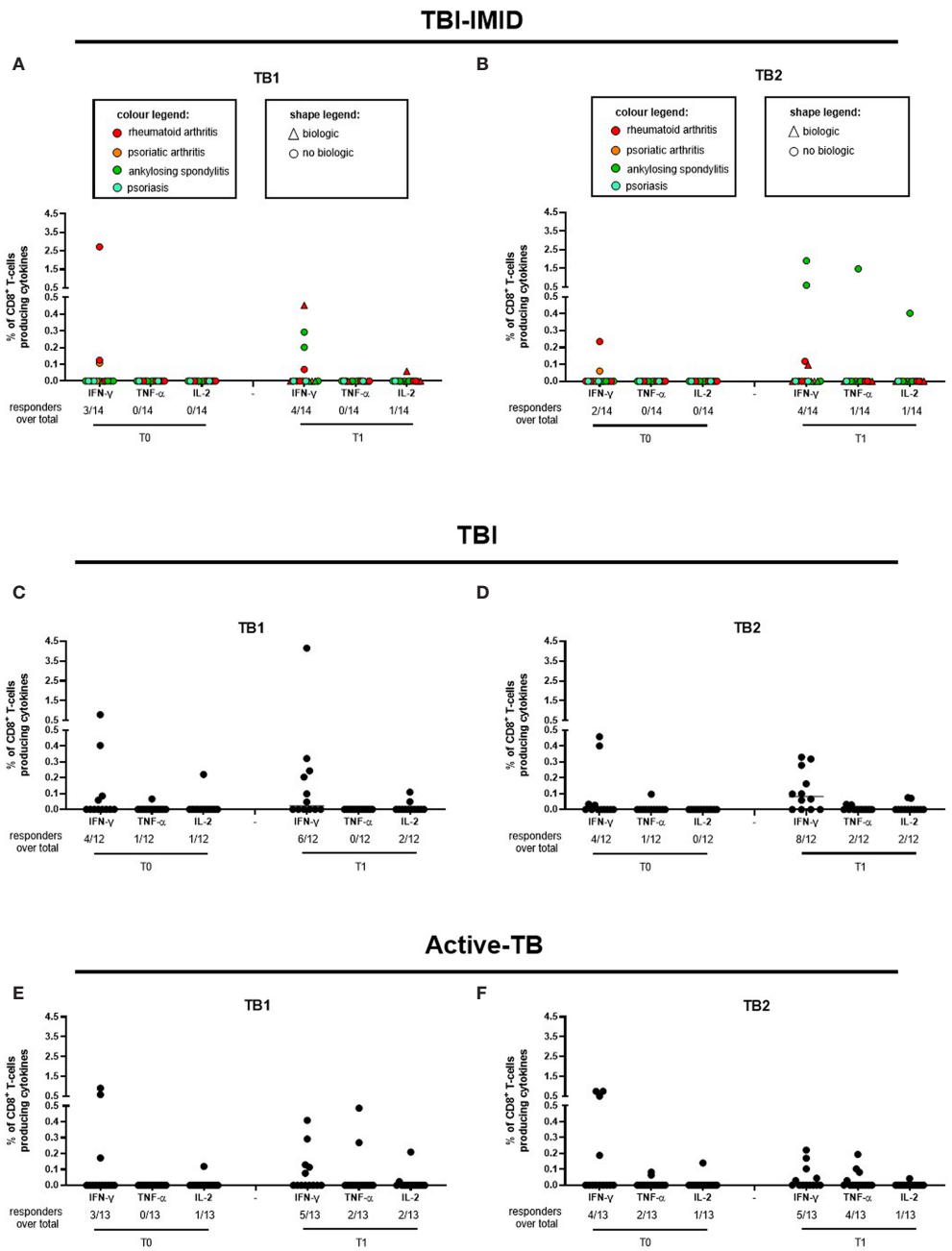

FIGURE 3 | CD8 T cells producing IFN-γ, IL-2, and TNF-α in response to Mtb antigen stimulation. PBMC of patients enrolled before (T0) and after TB therapy (T1) were stimulated overnight with TB1 and TB2 peptides. **(A, B)** TBI-IMID; **(C, D)** TBI patients; **(E, F)** Active-TB patients. Number of responders over total enrolled patients is reported below each panel. Horizontal lines indicate the median. Statistical analysis was performed using the Wilcoxon matched-pairs signed rank test and the p value was considered significant if ≤0.05. TB, tuberculosis; TBI, tuberculosis infection; IMID, immune mediated inflammatory disease; TB1, peptides of TB1 tube of QFT-plus kit; TB2, peptides of TB2 tube of QFT-plus kit.

of patients (**Supplementary Figure 4**). The FDS comparison at the baseline did not show any significant differences among groups (data not shown). To note that, we could not include in the FDS calculation the patients without the IFN-γ IL-$2^{+/-}$ TNF-$\alpha^{+/-}$ $CD4^+$ T-cell subset (TBI-IMID T0 in response to TB1: two patients, TBI-IMID T1 in response to TB1: one patient; TBI-IMID T0 in response to TB2: one patient; TBI T1 in response to TB2: one patient; active-TB T0 in response to TB2: two patients).

Since the TBI-IMID and the TBI included both recent and remote Mtb-infection, we choose to analyze again the FDS including the most represented category: remote TBI-IMID (12 patients over 14 enrolled) and recent TBI (8 patients over 12

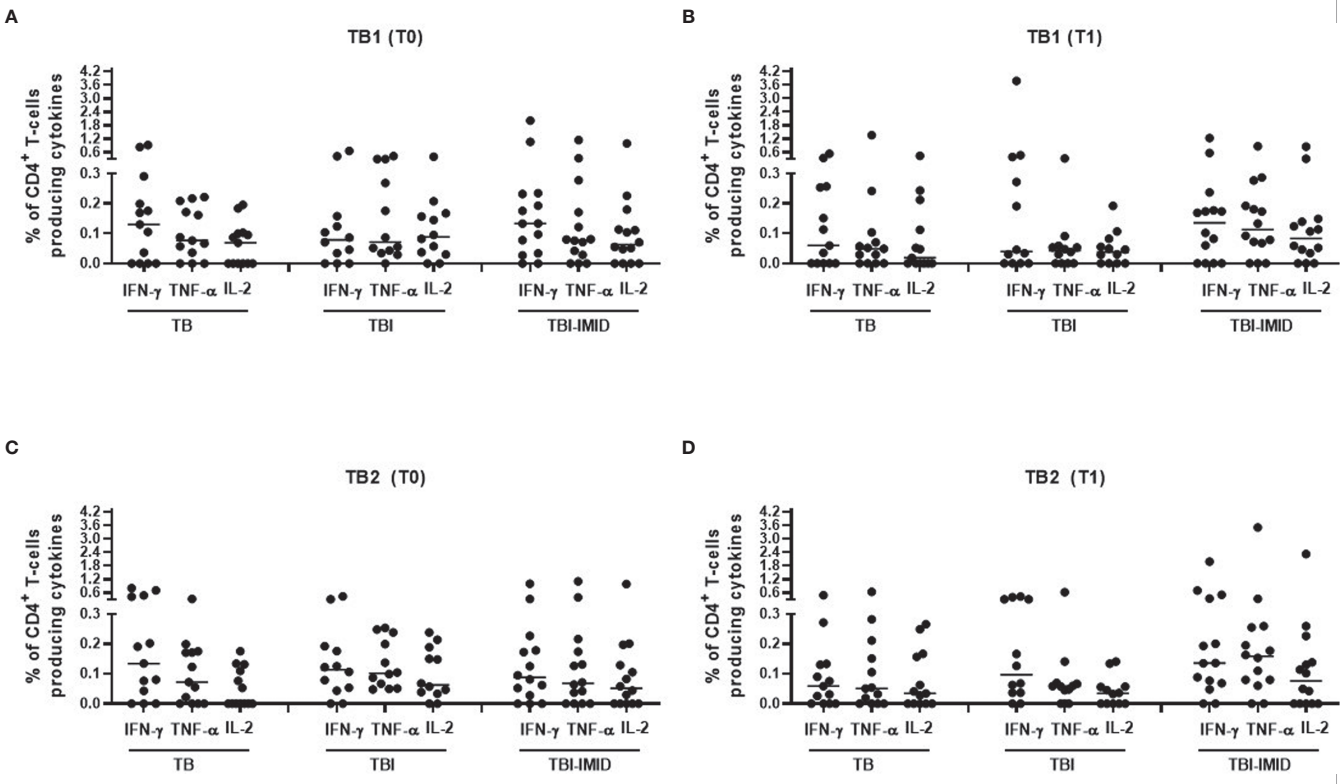

FIGURE 4 | Comparison of CD4 T cells producing IFN-γ, IL-2, and TNF-α in response to Mtb antigen stimulation at each time point. PBMC of patients enrolled before (T0) and after TB therapy (T1) were stimulated overnight with TB1 and TB2 peptides. **(A, B)** TB1 response at T0 and T1; **(C, D)** TB2 response at T0 and T1. Horizontal lines indicate the median. Statistical analysis was performed using the Mann–Whitney unmatched test, Bonferroni correction was applied, and the p value was considered significant if ≤0.017. TB, tuberculosis; TBI, tuberculosis infection; IMID, immune mediated inflammatory disease; TB1, peptides of TB1 tube of QFT-plus kit; TB2, peptides of TB2 tube of QFT-plus kit.

enrolled) (**Supplementary Figure 5**). Even with this stratification, we did no observe significant differences before and after TB therapy in any studied groups.

Collectively, these data suggested that the TB treatment did not deeply affect the CD4 cytokine profile of the TBI-IMID patients. Differently, the TBI subjects showed a significant decrease of triple functional T cells after treatment and the active-TB a not significant but evident increase of the proportion of monofunctional IFN-γ^+ IL-2^- TNF-α^- $CD4^+$ T cells (**Figure 5**).

Then, we compared the cytokine profile of Mtb-specific CD4 T cells among the different groups at each time point (**Figures 6** and **7**). In response to TB1 stimulation at T0, we did not observe any significant differences (**Figure 6A**). However, the main involved subset was constituted by the triple functional IFN-γ^+ IL-2^+ TNF-α^+ $CD4^+$ T cells in all groups; in active-TB and TBI-IMID, the contribution of monofunctional IFN-γ^+ IL-2^- TNF-α^- $CD4^+$ T cells was also evident (**Figure 6A**). Similarly, in response to TB1 stimulation at T1, we did not observe any significant differences (**Figure 6B**). In particular, we observed: in active-TB a high proportion of monofunctional IFN-$\gamma^{+/-}$ IL-2^- TNF-$\alpha^{+/-}$ $CD4^+$ T cells and triple functional IFN-γ^+ IL-2^+ TNF-α^+ $CD4^+$ T cells; in TBI, a great contribution of monofunctional IFN-γ^+ IL-2^- TNF-α^- $CD4^+$ T cells; in TBI-IMID, a high proportion of monofunctional IFN-γ^+ IL-2^- TNF-α^- $CD4^+$ T cells and triple functional IFN-γ^+ IL-2^+ TNF-α^+ $CD4^+$ T cells (**Figure 6B**).

In response to TB2 stimulation at T0, we did not observe any significant differences (**Figure 7A**). However, in active-TB, the monofunctional IFN-γ^+ IL-2^- TNF-α^- $CD4^+$ T cells constituted the main involved subset, whereas in TBI and TBI-IMID the triple functional IFN-γ^+ IL-2^+ TNF-α^+ $CD4^+$ T cells was the major represented subset (**Figure 7A**). In response to TB2 stimulation at T1 (**Figure 7B**), we observed a high contribution of the monofunctional IFN-γ^+ IL-2^- TNF-α^- $CD4^+$ T cells in active-TB and TBI. In TBI-IMID, we reported a high and significant percentage of double functional IFN-γ^+ IL-2^- TNF-α^+ $CD4^+$ T cells compared to TBI ($p = 0.0161$) and a high contribution of triple functional IFN-γ^+ IL-2^+ TNF-α^+ $CD4^+$ T cells in TBI-IMID (**Figure 7B**).

Collectively, these data indicated at T0 a predominant TB1-induced polyfunctional profile and at T1 an increase of TB1-induced monofunctional IFN-γ^+ IL-2^- TNF-α^- $CD4^+$ T cells in all groups (**Figure 6**). The TB2 cytokine profile was more heterogeneous, showing that triple functional IFN-γ^+ IL-2^+ TNF-α^+ $CD4^+$ T cells were mainly represented in TBI-IMID patients at both T0 and T1 (**Figure 7**).

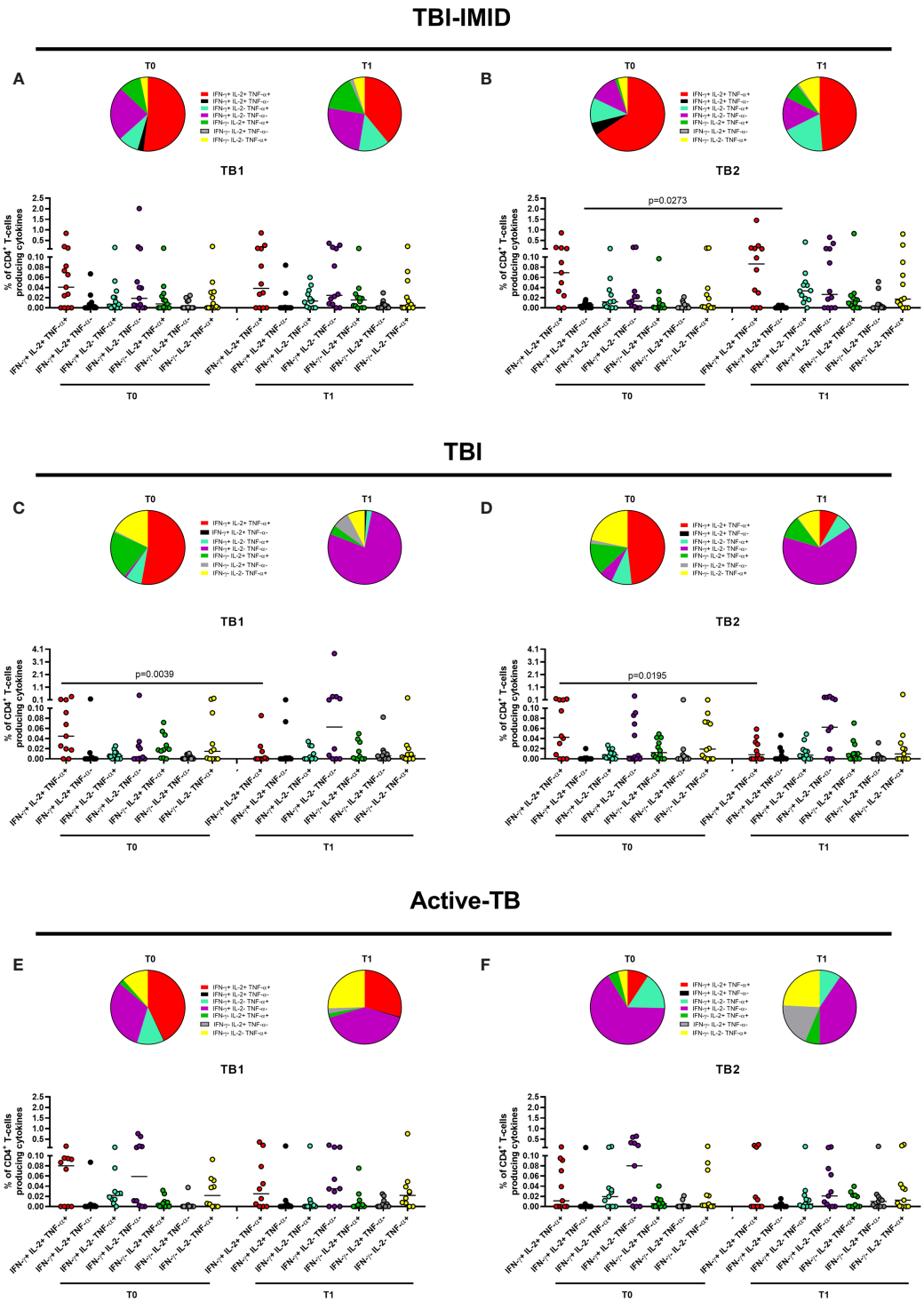

FIGURE 5 | Functional profile of Mtb-specific CD4 T cells before and after TB therapy completion. PBMC of patients enrolled before (T0) and after TB therapy (T1) were stimulated overnight with TB1 and TB2 peptides. **(A, B)** TBI-IMID patients; **(C, D)** TBI subjects; **(E, F)** Active-TB patients. Cytokine profile was evaluated only on responders using Boolean gate combination. The number of CD4 and CD8 responders to TB1 and TB2 stimulation is reported in detail in **Table 3**. Horizontal lines indicate the median. Statistical analysis was performed using the Wilcoxon matched-pairs signed rank test, and the p value was considered significant if ≤0.05. TB, tuberculosis; TBI, tuberculosis infection; IMID, immune mediated inflammatory disease; TB1, peptides of TB1 tube of QFT-plus kit; TB2, peptides of TB2 tube of QFT-plus kit.

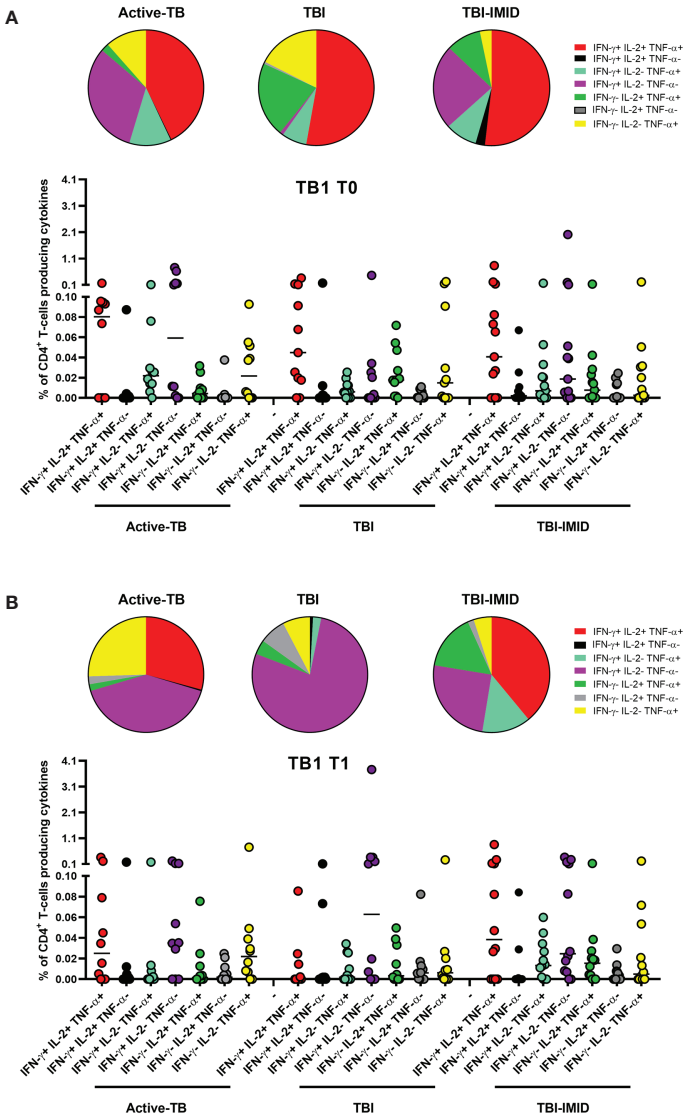

FIGURE 6 | Comparison of functional profile of TB1 specific CD4 T cells at each time point. PBMC of patients enrolled before (T0) and after TB therapy (T1) were stimulated overnight with TB1 peptides. **(A)** T0; **(B)** T1. Cytokine profile was evaluated only on responders using Boolean gate combination. The number of CD4 and CD8 responders to TB1 and TB2 stimulation is reported in detail in **Table 3**. Horizontal lines indicate the median. Statistical analysis was performed using the Mann–Whitney unmatched test, Bonferroni correction was applied, and the p value was considered significant if ≤0.017. TB, tuberculosis; TBI, tuberculosis infection; IMID, immune mediated inflammatory disease; TB1, peptides of TB1 tube of QFT-plus kit; TB2, peptides of TB2 tube of QFT-plus kit.

TB Treatment Did Not Affect the Phenotype of Mtb-Specific T Cells

Next, we investigated if the TB treatment had or not an impact on the phenotype of Mtb-specific T cells, evaluating the proportion of CD45RA and CD27 (**Figure 8**). Even in this case, we focused on CD4 T cells since the number of CD8 T cells responders was too low to perform a robust statistical analysis (**Table 3**).

Since we did not observe differences in term of FDS and considering the low frequency of the Mtb-specific T cells, we decided to analyze the phenotype of Mtb-specific CD4 T cells able to produce any cytokines (total response based on IFN-γ, TNF-α, or IL-2 production). In this way, we had the maximum number of events available for the phenotype description, and we avoided as much as possible the interference of the background that could not be subtracted in the phenotype evaluation.

In TBI-IMID and TBI subjects, the Mtb-specific CD4 T-cell response was mainly represented by the $CD45RA^{-}CD27^{+}$ subset both at T0 and T1 (with a frequency ranging from 55% to 79%) (**Figures 8A–D**). In TBI-IMID patients, we did not observe significant differences in response to TB1 and TB2 antigens and any evident trend (**Figures 8A, B**). In TBI subjects, we observed a lower proportion of Mtb-specific $CD45RA^{-}$ $CD27^{+}$ CD4 T cells at T1 compared to T0 ($p = 0.0098$) in response to TB2 and a similar trend in response to TB1 (**Figures 8C, D**).

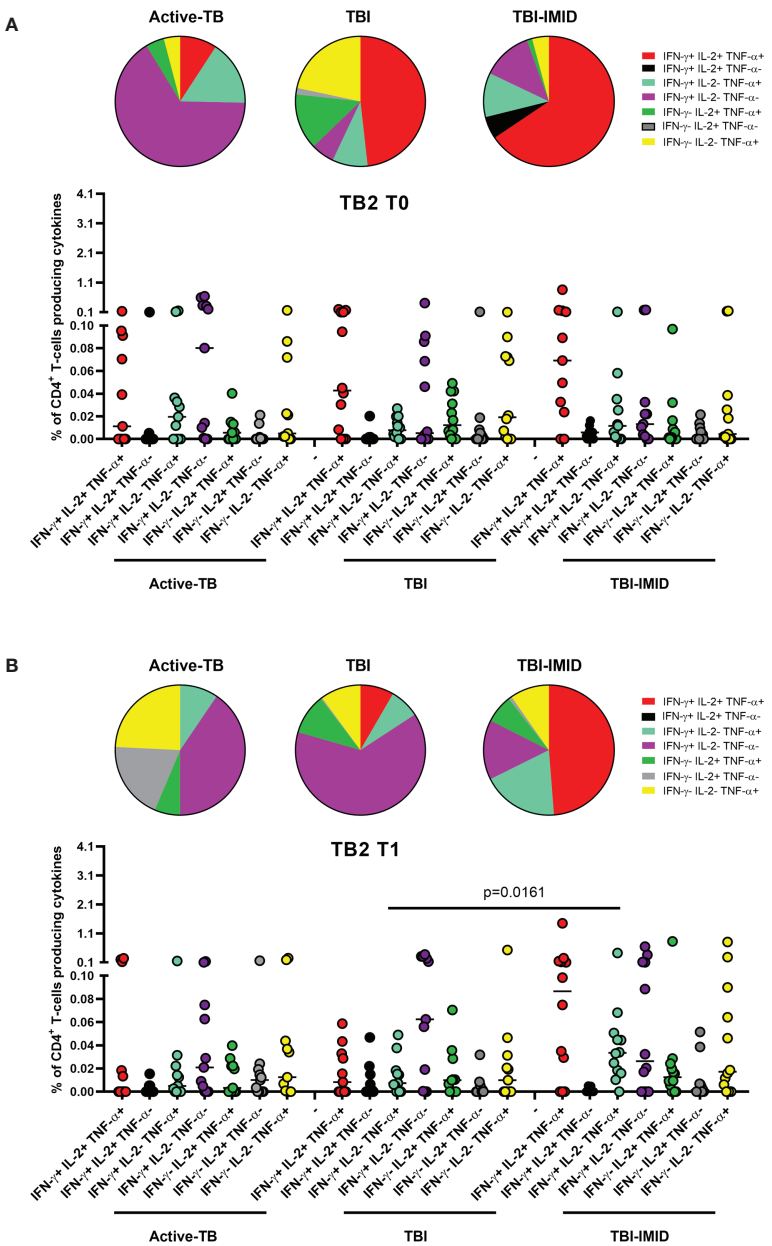

FIGURE 7 | Comparison of functional profile of TB2 specific CD4 T cells at each time point. PBMC of patients enrolled before (T0) and after TB therapy (T1) were stimulated overnight with TB2 peptides. **(A)** T0; **(B)** T1. Cytokine profile was evaluated only on responders using Boolean gate combination. The number of CD4 and CD8 responders to TB1 and TB2 stimulation is reported in detail in **Table 3**. Horizontal lines indicate the median. Statistical analysis was performed using the Mann–Whitney unmatched test, Bonferroni correction was applied, and the p value was considered significant if ≤0.017. TB, tuberculosis; TBI, tuberculosis infection; IMID, immune mediated inflammatory disease; TB1, peptides of TB1 tube of QFT-plus kit; TB2, peptides of TB2 tube of QFT-plus kit.

In active-TB, the Mtb-specific CD4 T-cell response was mainly represented by the CD45RA$^-$ CD27$^+$ subset both a T0 and T1 (with a frequency ranging from 46% to 67%) (**Figures 8E, F**). We observed an increased Mtb-specific CD4$^+$ CD45RA$^-$ CD27$^+$ subset and a contraction of the CD45RA$^-$ CD27$^-$ subset after therapy completion in response to TB1 and TB2 antigens (**Figures 8E, F**). The frequency of the CD45RA$^-$ CD27$^+$ subset was significantly increased in response to TB2 (p = 0.0195, **Figure 8F**), whereas the frequency of the CD45RA$^-$ CD27$^-$ subset was significantly decreased in response to TB1 (p = 0.0195, **Figure 8E**).

Then, we compared the phenotype profile of Mtb-specific CD4 T cells among the different groups at each time point (**Figure 9**). In response to TB1 stimulation at T0, we found that the CD45RA$^-$CD27$^+$ subset was significantly lower in active-TB compared to TBI and TBI-IMID (p = 0.0021; p = 0.0027) and the

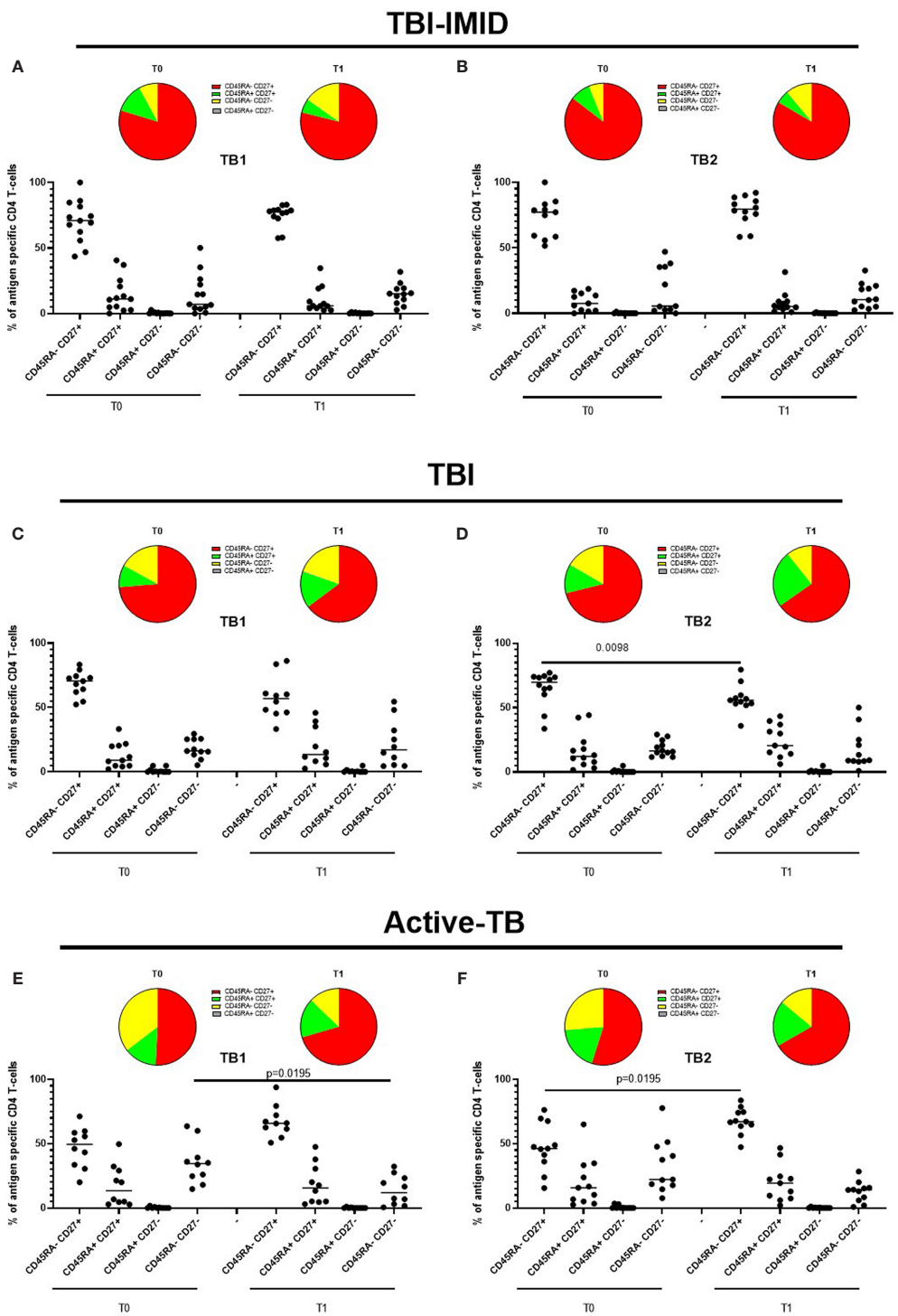

FIGURE 8 | Phenotype of Mtb-specific CD4 T cells before and after TB therapy completion. PBMC of patients enrolled before (T0) and after TB therapy (T1) were stimulated overnight with TB1 and TB2 peptides, and CD45RA and CD27 proportions were evaluated on total cytokine response and T cells producing IFN-γ, IL-2, and TNF-α. **(A, B)** TBI-IMID patients; **(C, D)** TBI subjects; **(E, F)** Active-TB patients. Phenotype was evaluated only on responders. The number of CD4 and CD8 responders to TB1 and TB2 stimulation is reported in detail in **Table 3**. Horizontal lines indicate the median. Statistical analysis was performed using the Wilcoxon matched-pairs signed rank test, and the p value was considered significant if ≤0.05. TB, tuberculosis; TBI, tuberculosis infection; IMID, immune mediated inflammatory disease; TB1, peptides of TB1 tube of QFT-plus kit; TB2, peptides of TB2 tube of QFT-plus kit.

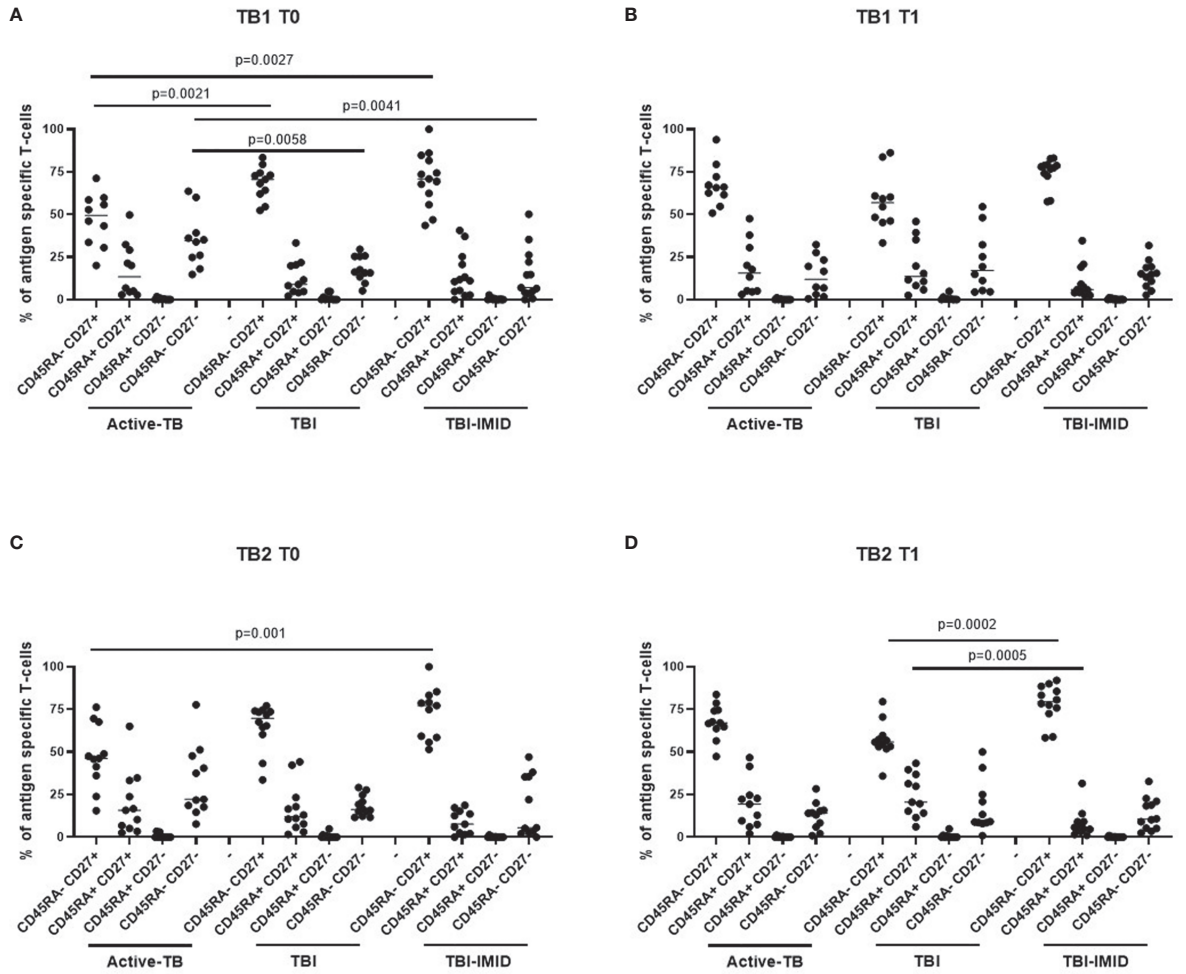

FIGURE 9 | Comparison of phenotype of Mtb-specific CD4 T cells at each time point. PBMC of patients enrolled before (T0) and after TB therapy (T1) were stimulated overnight with TB1 and TB2 peptides, and CD45RA and CD27 proportions were evaluated on total cytokine response and T cells producing IFN-γ, IL-2, and TNF-α. **(A, B)** TB1 stimulation at T0 and T1; **(C, D)** TB2 stimulation at T0 and T1. Phenotype was evaluated only on responders. The number of CD4 and CD8 responders to TB1 and TB2 stimulation is reported in detail in **Table 3**. Horizontal lines indicate the median. Statistical analysis was performed using the Mann–Whitney unmatched test, Bonferroni correction was applied, and the p value was considered significant if ≤0.017. TB, tuberculosis; TBI, tuberculosis infection; IMID, immune mediated inflammatory disease; TB1, peptides of TB1 tube of QFT-plus kit; TB2, peptides of TB2 tube of QFT-plus kit.

$CD45RA^-CD27^-$ subset was significantly higher in active-TB compared to TBI and TBI-IMID ($p = 0.0058$; $p = 0.0041$) (**Figure 9A**). Differently, at T1, we did not find any significant differences (**Figure 9B**).

In response to TB2 stimulation at T0, we found a phenotype profile similar to TB1 stimulation for all groups; however, only the $CD45RA^-CD27^+$ subset was significantly lower in active-TB compared to TBI-IMID ($p = 0.001$) (**Figure 9C**). At T1, we observed that the TBI subjects had lower proportion of the $CD45RA^-CD27^+$ subset ($p = 0.0002$) and a higher proportion of $CD45RA^+CD27^+$ ($p = 0.0005$) compared to TBI-IMID (**Figure 9D**).

Collectively, these data highlighted a loss of $CD27^+$ CD4 T cells in active-TB patients and this profile was more evident at T0.

DISCUSSION

Among patients with dysregulation of the immune system, subjects with IMID, such as RA, PsA, and AS, have an intrinsic higher probability to develop active-TB compared to the general population (7, 10). The risk of Mtb reactivation in the general population of TBI subjects usually is the highest during the first 2 years after Mtb exposure (3, 4, 6).

According to the WHO, the prevalence of RA varies between 0.3% and 1% and is more common in women and in developed countries (7–10). Therefore, the identification and treatment of TBI in this fragile population is important to propose the TB preventive therapy (7–10).

In this study, we explored the Mtb-specific immunity of TBI-IMID patients at the baseline and after TB therapy completion.

The main finding of this study regards the CD4 T-cell response. We demonstrate in TBI-IMID that TB therapy did not affect the ability of CD4 T cells to produce IFN-γ, TNF-α, and IL-2, their functional status, and their phenotype. Moreover, we demonstrated that at the baseline TBI subjects and TBI-IMID patients had a similar phenotype that instead was different from active-TB patients. We enrolled two different categories of controls: the TBI without IMID to study the Mtb-specific immune response in a population controlling the Mtb replication and the active-TB group as a positive control of the ongoing Mtb replication. TB treatment did not significantly affect the CD4 cytokine production neither in the TBI nor in the active-TB group. As previously demonstrated, the CD8 T-cell response was detected in lower proportion compared to the CD4 T-cell response (48, 50). The CD4 functional status in TBI subjects showed a significant decrease of triple functional T cells after treatment and in active-TB a not significant increase of the proportion of monofunctional IFN-γ^+ IL-2^- TNF-α^-. The baseline level of polyfunctional IFN-γ^+ IL-2^+ TNF-α^+ CD4 T cells in both TBI-IMID and TBI was similar to the results reported in other TBI population (29, 31, 47).

The comparison among groups at each time point confirmed as shown by the pair-wise comparison that at T0 all the studied groups had a similar cytokine profile mainly constituted by the triple functional IFN-γ^+ IL-2^+ TNF-α^+ CD4 T-cell subset and at T1 all groups had a notable proportion of monofunctional IFN-γ^+ IL-2^- TNF-α^- CD4 T cells.

Since it has been demonstrated that recent and remote TBI subjects, naïve for TB therapy, had a similar CD4 cytokine profile (29), the functional differences after TB therapy between TBI and TBI-IMID individuals were not ascribable to their remote or recent Mtb exposure but probably to the IMID status itself. TB therapy did not affect neither the functional differentiation status of CD4 T cells in the TBI, TBI-IMID, and active-TB groups. Considering that the majority of TBI had a recent infection and the majority of TBI-IMID had a remote exposure, our data were in line with recent findings on recent subsets and persistent QFT$^+$ individuals (29).

In active-TB, the baseline functional status of TB1 CD4-specific T cells was in agreement with previous reports reporting a high proportion of the IFN-γ^+ IL-2^+ TNF-α^+ CD4 T-cell subset in response to ESAT-6 CFP-10 stimulation (25, 31, 54). For the TB2 stimulation, the functional status skewed towards the IFN-γ^+ IL-2^- TNF-α^- CD4 T cells, maybe as a consequence of the ability of TB2 peptides to stimulate also the CD8 T cells (48).

T-cell expression of surface molecules such as CD45RA, CD27, and CCR7 identifies different T-cell subsets that reflect different stages of cell differentiation (55). The effector T cells are expanded during active-Mtb replication, whereas the memory cells associate with control and eradication of Mtb-infection (31, 47, 56). The phenotype characterization demonstrated a great contribution of the CD45RA$^-$ CD27$^+$ subset to the Mtb-specific immune response in all groups. The presence of CD27 could be associated to both central memory (CD45RA$^-$ CD27$^+$ CCR7$^+$) and effector memory subsets (CD45RA$^-$ CD27$^+$ CCR7$^-$) (29, 55). Since we did not evaluate the CCR7 expression, we could not assign a precise memory status to the different subsets evaluated. However, as previously demonstrated (31), at the baseline, the Mtb-specific CD45RA$^-$ CD27$^+$ CD4 T cells were more represented in the TBI individuals, whereas the active-TB patients had a higher proportion of Mtb-specific CD45RA$^-$ CD27$^-$ CD4 T cells compared to TBI subjects. These findings reflect the loss of CD27 during active-TB disease, already documented in several studies (38–41, 57). Interestingly, after therapy completion, the active-TB patients had a phenotype more similar to TBI groups, with an increased proportion of the CD45RA$^-$ CD27$^+$ subset and a contraction of the CD45RA$^-$ CD27$^-$ CD4 T cells. These data suggest that the high Mtb load in active-TB patients induces the differentiation of Mtb-specific CD45RA$^-$ CD27$^-$ CD4 T cells, whereas the low Mtb load of TBI individuals favours the CD45RA$^-$ CD27$^+$ subset.

The phenotype comparison among groups at each time point confirmed previous study on CD27 expression in patients with different TB status (31, 38, 40). Indeed, at the baseline, the TBI subjects had a higher proportion of Mtb-specific CD45RA$^-$ CD27$^+$ CD4 T cells compared to active-TB and the active-TB a higher proportion of Mtb-specific CD45RA$^-$ CD27$^-$ CD4 T cells compared to TBI subjects. These data reflected the modulation of CD27 according to the Mtb bacterial load (39, 41). Interestingly, the TBI-IMID patients showed a phenotype profile similar to TBI subjects, suggesting that the type of IMID and the concomitant IMID therapy did not affect the activation status of Mtb-specific CD4 T cells. After TB therapy completion, the differences among Mtb-specific CD45RA$^-$ CD27$^+$ CD4 T cells and CD45RA$^-$ CD27$^-$ CD4 T cells were less evident, suggesting that TB therapy, decreasing the Mtb load, led to an increased CD27 expression.

Moreover, lately, recent and remote TBI have been shown to have a similar phenotype according to the expression of CD45RA CD27 CCR7 markers (29). Therefore, the phenotype of TBI-IMID individuals was not even due to their remote Mtb exposure. Larger studies are needed to better understand the modulation of the phenotype in these IMID patients.

Considering that the IMID therapies were mostly based on the modulation of the immune system, indirectly we could suppose that the type of IMID therapy did not affect the immune response. Stratifying for the presence or not of biologic drugs, we did not find any significant differences among TBI-IMID before and after therapy completion. Although the sample size did not permit a deeper analysis, in support of these findings, we have previously demonstrated that neither the number of lymphocytes nor the type of IMID therapy influenced the IFN-γ response to QFT-Plus in TBI-IMID patients (28). Due to the adult age of the IMID manifestations, the TBI-IMID were older compared to TBI subjects. As lymphocyte counts decline with age (58) and potentially contribute to the immune impairment, we evaluated the lymphocyte counts in this study. No significant differences were found nor comparing all the three groups at each time points, neither comparing the two time points within each group. An exception was found considering those with active-TB in which a restore of the lymphocyte counts was observed after therapy completion (59). Moreover, the similar cytokine profile and phenotype of TBI subjects and TBI-IMID patients seem to

support the presence of a comparable immune response to Mtb antigens. Therefore, as the immunity status at the different time points was comparable, the data reported could be considered reliable. Although these data are preliminary, we highlighted differences between the CD4 T-cell cytokine response over time of TBI-IMID compared to TBI and active-TB. Surprisingly, the monofunctional IFN-γ^+ IL-2$^-$ TNF-α^- CD4 T cells characterized the TBI and active-TB after therapy completion, whereas the TBI-IMID patients maintain a cytokine profile similar to the baseline. It is not possible to state if TB therapy induced a protective cytokine profile in TBI-IMID; however, these patients have been followed for 6 years and none of them developed until now active-TB disease. Since the phenotype studied based on CD45RA and CD27 did not allow to define a particular profile over time, we may need to better characterize the response using also other activation markers such as HLA-DR (29, 60).

Limitations of this longitudinally study are the relatively low number of patients enrolled, the variety of the IMID considered, and the different regimens of IMID therapy. However, since only few studies are available on Mtb immune response in this fragile population of TBI subjects, we retain this is a good controlled study including two types of control populations (TBI and active-TB). More importantly, besides the reported caveats, we answered to opened important questions on Mtb-specific response in this particular understudied category of fragile TBI subjects at high risk to progress to active-TB disease.

In conclusions, we evaluated over time the modulation of Mtb-specific immune response in patients at different stages of TB: a low-replicating Mtb status in TBI, a low-replicating Mtb status in TBI-IMID patients with high risk to develop the active-TB disease, and a high-replicating Mtb status in active-TB patients. The TB therapy did not modify the CD4 T-cell cytokine profile of TBI-IMID patients but determined a contraction of the triple functional CD4 T cells of the TBI subjects and active-TB patients. The CD45RA$^-$ CD27$^+$ T cells stood out as a main subset of the Mtb-specific response in all groups of patients. Before the TB-preventive therapy, the TBI subjects had higher proportion of Mtb-specific CD45RA$^-$CD27$^+$CD4$^+$ T cells and the active-TB higher proportion of Mtb-specific CD45RA$^-$CD27$^-$CD4$^+$ T cells compared to other groups. The TBI-IMID patients showed a phenotype similar to TBI, suggesting that the type of IMID and the IMID therapy did not affect the activation status of Mtb-specific CD4 T cells.

Future studies on a larger and better-stratified TBI-IMID population will help to understand the change of the Mtb-specific immune response over time and to identify possible immune biomarkers of Mtb-containment or active replication.

DATA AVAILABILITY STATEMENT

The datasets presented in this study can be found in online repositories. The names of the repository/repositories and accession number(s) can be found below: The data sets generated during and/or analyzed during the current study are available in our institutional repository after request at rawdata.inmi.it.

ETHICS STATEMENT

The study involving human participants were approved by the Ethical Committee of "L. Spallanzani" National Institute of Infectious Diseases (INMI)-IRCCS, approval number 72/2015. The study was performed following the guidelines of the Declaration of Helsinki. The patients/participants provided their written informed consent to participate in this study.

AUTHOR CONTRIBUTIONS

EP performed the experiments, analyzed and interpreted data, and wrote the manuscript. LP analyzed and interpreted data and revised the manuscript. TC performed the experiments. CF analyzed and interpreted data and revised the manuscript. GC enrolled patients and collected clinical data. AN performed the statistical analysis and interpreted data. VV processed blood samples. UM enrolled patients and revised the manuscript. ML, GG, NC, and FC revised the manuscript and participated in the interpretation of data. FP enrolled patients and revised the manuscript. DG designed and wrote the study, coordinated and supervised the project, contributed to the interpretation of the results, and revised the manuscript. All authors contributed to the article and approved the submitted version.

FUNDING

This study was funded by GR-2018-12367178 and Ricerca Corrente by Line four, all funded by Italian Ministry of Health.

ACKNOWLEDGMENTS

The authors thank all patients and nurses that helped to conduct this study.

SUPPLEMENTARY MATERIAL

The Supplementary Material for this article can be found online at: https://www.frontiersin.org/articles/10.3389/fimmu.2021.716857/full#supplementary-material

Supplementary Figure 1 | IFN-γ response to antigens present in QFT-Plus test, TB1 and TB2, before and at the end of TB treatment. **(A, B)** TBI-IMID patients; **(C, D)** TBI subjects; **(E, F)** Active-TB patients. Statistical analysis was performed using the Wilcoxon matched-pairs signed rank test, and the p value was considered significant if ≤0.05. Two TB-IMID and one active-TB patients did not perform the test at T1. Number of responders over total enrolled patients is reported below each panel. TB, tuberculosis; TBI, tuberculosis infection; IMID, immune mediated inflammatory disease; TB1, peptides of TB1 tube of QFT-plus kit; TB2, peptides of TB2 tube of QFT-plus kit; IU/ml, international unit at millilitre; T0, before TB therapy, T1, after TB therapy completion.

Supplementary Figure 2 | Cytokine production CD4 and CD8 T cells in response to mitogen stimulation before and after TB therapy completion: PBMC of

patients enrolled before (T0) and after TB therapy (T1) were stimulated overnight with Mitogen reagent of QFT-Plus kit. **(A, B)** TBI-IMID patients; **(C, D)** TBI subjects; **(E, F)** Active-TB patients. Number of responders over total enrolled patients is reported below each graph. Horizontal lines indicate the median. Statistical analysis was performed using the Wilcoxon matched-pairs signed rank test, and the p value was considered significant if ≤0.05 for cytokine production. TB, tuberculosis; TBI, tuberculosis infection; IMID, immune mediated inflammatory disease.

Supplementary Figure 3 | Comparison of cytokine production CD4 and CD8 T cells in response to mitogen stimulation: PBMC of patients enrolled before (T0) and after TB therapy (T1) were stimulated overnight with Mitogen reagent of QFT-Plus kit. **(A)** T0; **(B)** T1. Number of responders over total enrolled patients is reported below each graph. Horizontal lines indicate the median. Statistical analysis was performed using the Mann–Whitney unmatched test, Bonferroni correction was applied, and the p value was considered significant if ≤0.017 for cytokine production. TB, tuberculosis; TBI, tuberculosis infection; IMID, immune mediated inflammatory disease.

Supplementary Figure 4 | Functional differentiation score (FDS) of Mtb-specific CD4 T cells is similar before and after TB therapy in TBI-IMID, TBI subjects, and active-TB patients. FDS has been calculated as previously described (28, 29) only on CD4 T-cell responders to Mtb antigen stimulation. **(A, B)** TBI-IMID patients; **(C, D)** TBI subjects; **(E, F)** Active-TB patients. Horizontal lines indicate the median. The number of CD4 and CD8 responders to TB1 and TB2 stimulation is reported in detail in **Table 3**. Statistical analysis was performed using the Wilcoxon matched-pairs signed rank test, and the p value was considered significant if ≤0.05. TB, tuberculosis; TBI, tuberculosis infection; IMID, immune mediated inflammatory disease; TB1, peptides of TB1 tube of QFT-plus kit; TB2, peptides of TB2 tube of QFT-plus kit; T0, before TB therapy; T1, after TB therapy completion.

Supplementary Figure 5 | Functional differentiation score (FDS) of Mtb-specific CD4 T cells is similar before and after TB therapy in TBI-IMID remote and TBI recent subjects. FDS has been calculated as previously described (28, 29) only on CD4 T-cell responders to Mtb antigen stimulation. **(A, B)** TBI-IMID remote patients, n = 12; **(C, D)** TBI recent subjects, N = 8. Horizontal lines indicate the median. Statistical analysis was performed using the Wilcoxon matched-pairs signed rank test, and the p value was considered significant if ≤0.05. TB, tuberculosis; TBI, tuberculosis infection; IMID, immune mediated inflammatory disease; TB1, peptides of TB1 tube of QFT-plus kit; TB2, peptides of TB2 tube of QFT-plus kit; T0, before TB therapy; T1, after TB therapy completion.

REFERENCES

1. WHO. *TB REPORT 2020*. (2020). Available at: https://www.who.int/publications/i/item/9789240013131.
2. Houben RM, Dodd PJ. The Global Burden of Latent Tuberculosis Infection: A Re-Estimation Using Mathematical Modelling. *PloS Med* (2016) 13:e1002152. doi: 10.1371/journal.pmed.1002152
3. Goletti D, Lee MR, Wang JY, Walter N, Ottenhoff THM. Update on Tuberculosis Biomarkers: From Correlates of Risk, to Correlates of Active Disease and of Cure From Disease. *Respirology* (2018) 23:455–66. doi: 10.1111/resp.13272
4. Behr MA, Edelstein PH, Ramakrishnan L. Revisiting the Timetable of Tuberculosis. *BMJ* (2018) 362:k2738. doi: 10.1136/bmj.k2738
5. Petruccioli E, Scriba TJ, Petrone L, Hatherill M, Cirillo DM, Joosten SA, et al. Correlates of Tuberculosis Risk: Predictive Biomarkers for Progression to Active Tuberculosis. *Eur Respir J* (2016) 48:1751–63. doi: 10.1183/13993003.01012-2016
6. Trauer JM, Moyo N, Tay EL, Dale K, Ragonnet R, McBryde ES, et al. Risk of Active Tuberculosis in the Five Years Following Infection . . 15%? *Chest* (2016) 149:516–25. doi: 10.1016/j.chest.2015.11.017
7. Cantini F, Nannini C, Niccoli L, Iannone F, Delogu G, Garlaschi G, et al. Guidance for the Management of Patients With Latent Tuberculosis Infection Requiring Biologic Therapy in Rheumatology and Dermatology Clinical Practice. *Autoimmun Rev* (2015) 14:503–9. doi: 10.1016/j.autrev.2015.01.011
8. Cantini F, Nannini C, Niccoli L, Petrone L, Ippolito G, Goletti D. Risk of Tuberculosis Reactivation in Patients With Rheumatoid Arthritis, Ankylosing Spondylitis, and Psoriatic Arthritis Receiving Non-Anti-TNF-Targeted Biologics. *Mediators Inflamm* (2017) 2017:8909834. doi: 10.1155/2017/8909834
9. Cantini F, Niccoli L, Goletti D. Tuberculosis Risk in Patients Treated With Non-Anti-Tumor Necrosis Factor-α (TNF-α) Targeted Biologics and Recently Licensed TNF-α Inhibitors: Data From Clinical Trials and National Registries. *J Rheumatol Suppl* (2014) 91:56–64. doi: 10.3899/jrheum.140103
10. Goletti D, Petrone L, Ippolito G, Niccoli L, Nannini C, Cantini F. Preventive Therapy for Tuberculosis in Rheumatological Patients Undergoing Therapy With Biological Drugs. *Expert Rev Anti Infect Ther* (2018) 16:501–12. doi: 10.1080/14787210.2018.1483238
11. Cantini F, Niccoli L, Capone A, Petrone L, Goletti D. Risk of Tuberculosis Reactivation Associated With Traditional Disease Modifying Anti-Rheumatic Drugs and Non-Anti-Tumor Necrosis Factor Biologics in Patients With Rheumatic Disorders and Suggestion for Clinical Practice. *Expert Opin Drug Saf* (2019) 18:415–25. doi: 10.1080/14740338.2019.1612872
12. Nash P, Kerschbaumer A, Dörner T, Dougados M, Fleischmann RM, Geissler K, et al. Points to Consider for the Treatment of Immune-Mediated Inflammatory Diseases With Janus Kinase Inhibitors: A Consensus Statement. *Ann Rheum Dis* (2021) 80:71–87. doi: 10.1136/annrheumdis-2020-218398
13. Cantini F, Blandizzi C, Niccoli L, Petrone L, Goletti D. Systematic Review on Tuberculosis Risk in Patients With Rheumatoid Arthritis Receiving Inhibitors of Janus Kinases. *Expert Opin Drug Saf* (2020) 19:861–72. doi: 10.1080/14740338.2020.1774550
14. Saliu OY, Sofer C, Stein DS, Schwander SK, Wallis RS. Tumor-Necrosis-Factor Blockers: Differential Effects on Mycobacterial Immunity. *J Infect Dis* (2006) 194:486–92. doi: 10.1086/505430
15. Goletti D, Carrara S, Butera O, Amicosante M, Ernst M, Sauzullo I, et al. Accuracy of Immunodiagnostic Tests for Active Tuberculosis Using Single and Combined Results: A Multicenter TBNET-Study. *PloS One* (2008) 3:e3417. doi: 10.1371/journal.pone.0003417
16. Goletti D, Carrara S, Vincenti D, Saltini C, Rizzi EB, Schininà V, et al. Accuracy of an Immune Diagnostic Assay Based on RD1 Selected Epitopes for Active Tuberculosis in a Clinical Setting: A Pilot Study. *Clin Microbiol Infect* (2006) 12:544–50. doi: 10.1111/j.1469-0691.2006.01391.x
17. Goletti D, Navarra A, Petruccioli E, Cimaglia C, Compagno M, Cuzzi G, et al. Latent Tuberculosis Infection Screening in Persons Newly-Diagnosed With HIV Infection in Italy: A Multicentre Study Promoted by the Italian Society of Infectious and Tropical Diseases. *Int J Infect Dis* (2020) 92:62–8. doi: 10.1016/j.ijid.2019.12.031
18. Kik SV, Schumacher S, Cirillo DM, Churchyard G, Boehme C, Goletti D, et al. An Evaluation Framework for New Tests That Predict Progression From Tuberculosis Infection to Clinical Disease. *Eur Respir J* (2018) 52:1800946. doi: 10.1183/13993003.00946-2018
19. Abubakar I, Drobniewski F, Southern J, Sitch AJ, Jackson C, Lipman M, et al. Prognostic Value of Interferon-γ Release Assays and Tuberculin Skin Test in Predicting the Development of Active Tuberculosis (UK PREDICT TB): A Prospective Cohort Study. *Lancet Infect Dis* (2018) 18:1077–87. doi: 10.1016/S1473-3099(18)30355-4
20. Wong SH, Gao Q, Tsoi KK, Wu WK, Tam LS, Lee N, et al. Effect of Immunosuppressive Therapy on Interferon γ Release Assay for Latent Tuberculosis Screening in Patients With Autoimmune Diseases: A Systematic Review and Meta-Analysis. *Thorax* (2016) 71:64–72. doi: 10.1136/thoraxjnl-2015-207811
21. Igari H, Ishikawa S, Nakazawa T, Oya Y, Futami H, Tsuyuzaki M, et al. Lymphocyte Subset Analysis in QuantiFERON-TB Gold Plus and T-Spot.TB for Latent Tuberculosis Infection in Rheumatoid Arthritis. *J Infect Chemother* (2018) 24:110–6. doi: 10.1016/j.jiac.2017.09.012
22. Nemes E, Rozot V, Geldenhuys H, Bilek N, Mabwe S, Abrahams D, et al. Optimization and Interpretation of Serial QuantiFERON Testing to Measure Acquisition of Mycobacterium Tuberculosis Infection. *Am J Respir Crit Care Med* (2017) 196:638–48. doi: 10.1164/rccm.201704-0817OC
23. Chiacchio T, Petruccioli E, Vanini V, Cuzzi G, La Manna MP, Orlando V, et al. Impact of Antiretroviral and Tuberculosis Therapies on CD4(+) and

CD8(+) HIV/M. Tuberculosis-Specific T-Cell in Co-Infected Subjects. *Immunol Lett* (2018) 198:33–43. doi: 10.1016/j.imlet.2018.04.001
24. Andrews JR, Noubary F, Walensky RP, Cerda R, Losina E, Horsburgh CR. Risk of Progression to Active Tuberculosis Following Reinfection With Mycobacterium Tuberculosis. *Clin Infect Dis* (2012) 54:784–91. doi: 10.1093/cid/cir951
25. Day CL, Abrahams DA, Lerumo L, Janse van Rensburg E, Stone L, O'rie T, et al. Functional Capacity of Mycobacterium Tuberculosis-Specific T Cell Responses in Humans Is Associated With Mycobacterial Load. *J Immunol* (2011) 187:2222–32. doi: 10.4049/jimmunol.1101122
26. Goletti D, Parracino MP, Butera O, Bizzoni F, Casetti R, Dainotto D, et al. Isoniazid Prophylaxis Differently Modulates T-Cell Responses to RD1-Epitopes in Contacts Recently Exposed to Mycobacterium Tuberculosis: A Pilot Study. *Respir Res* (2007) 8(1):5. doi: 10.1186/1465-9921-8-5
27. Petruccioli E, Chiacchio T, Vanini V, Cuzzi G, Codecasa LR, Ferrarese M, et al. Effect of Therapy on Quantiferon-Plus Response in Patients With Active and Latent Tuberculosis Infection. *Sci Rep* (2018) 8:15626. doi: 10.1038/s41598-018-33825-w
28. Chiacchio T, Petruccioli E, Vanini V, Cuzzi G, Massafra U, Baldi G, et al. Characterization of QuantiFERON-TB-Plus Results in Latent Tuberculosis Infected Patients With or Without Immune-Mediated Inflammatory Diseases. *J Infect* (2019) 79:15–23. doi: 10.1016/j.jinf.2019.04.010
29. Mpande CAM, Rozot V, Mosito B, Musvosvi M, Dintwe OB, Bilek N, et al. Immune Profiling of Mycobacterium Tuberculosis-Specific T Cells in Recent and Remote Infection. *EBioMedicine* (2021) 64:103233. doi: 10.1016/j.ebiom.2021.103233
30. Moguche AO, Musvosvi M, Penn-Nicholson A, Plumlee CR, Mearns H, Geldenhuys H, et al. Antigen Availability Shapes T Cell Differentiation and Function During Tuberculosis. *Cell Host Microbe* (2017) 21:695–706.e5. doi: 10.1016/j.chom.2017.05.012
31. Petruccioli E, Petrone L, Vanini V, Sampaolesi A, Gualano G, Girardi E, et al. Ifnγ/Tnfα Specific-Cells and Effector Memory Phenotype Associate With Active Tuberculosis. *J Infect* (2013) 66:475–86. doi: 10.1016/j.jinf.2013.02.004
32. Prezzemolo T, Guggino G, La Manna MP, Di Liberto D, Dieli F, Caccamo N. Functional Signatures of Human CD4 and CD8 T Cell Responses to Mycobacterium Tuberculosis. *Front Immunol* (2014) 5:180. doi: 10.3389/fimmu.2014.00180
33. Sallin MA, Kauffman KD, Riou C, Du Bruyn E, Foreman TW, Sakai S, et al. Host Resistance to Pulmonary Mycobacterium Tuberculosis Infection Requires CD153 Expression. *Nat Microbiol* (2018) 3:1198–205. doi: 10.1038/s41564-018-0231-6
34. Du Bruyn E, Ruzive S, Lindestam Arlehamn CS, Sette A, Sher A, Barber DL, et al. Mycobacterium Tuberculosis-Specific CD4 T Cells Expressing CD153 Inversely Associate With Bacterial Load and Disease Severity in Human Tuberculosis. *Mucosal Immunol* (2021) 14:491–9. doi: 10.1038/s41385-020-0322-6
35. Adekambi T, Ibegbu CC, Cagle S, Kalokhe AS, Wang YF, Hu Y, et al. Biomarkers on Patient T Cells Diagnose Active Tuberculosis and Monitor Treatment Response. *J Clin Invest* (2015) 125:1827–38. doi: 10.1172/JCI77990
36. Riou C, Du Bruyn E, Ruzive S, Goliath RT, Lindestam Arlehamn CS, Sette A, et al. Disease Extent and Anti-Tubercular Treatment Response Correlates With Mycobacterium Tuberculosis-Specific CD4 T-Cell Phenotype Regardless of HIV-1 Status. *Clin Transl Immunol* (2020) 9:e1176. doi: 10.1002/cti2.1176
37. Musvosvi M, Duffy D, Filander E, Africa H, Mabwe S, Jaxa L, et al. T-Cell Biomarkers for Diagnosis of Tuberculosis: Candidate Evaluation by a Simple Whole Blood Assay for Clinical Translation. *Eur Respir J* (2018) 51:1800153. doi: 10.1183/13993003.00153-2018
38. Petruccioli E, Navarra A, Petrone L, Vanini V, Cuzzi G, Gualano G, et al. Use of Several Immunological Markers to Model the Probability of Active Tuberculosis. *Diagn Microbiol Infect Dis* (2016) 86:169–71. doi: 10.1016/j.diagmicrobio.2016.06.007
39. Nikitina IY, Kondratuk NA, Kosmiadi GA, Amansahedov RB, Vasilyeva IA, Ganusov VV, et al. Mtb-Specific CD27low CD4 T Cells as Markers of Lung Tissue Destruction During Pulmonary Tuberculosis in Humans. *PloS One* (2012) 7:e43733. doi: 10.1371/journal.pone.0043733
40. Petruccioli E, Petrone L, Vanini V, Cuzzi G, Navarra A, Gualano G, et al. Assessment of CD27 Expression as a Tool for Active and Latent Tuberculosis Diagnosis. *J Infect* (2015) 71:526–33. doi: 10.1016/j.jinf.2015.07.009
41. Portevin D, Moukambi F, Clowes P, Bauer A, Chachage M, Ntinginya NE, et al. Assessment of the Novel T-Cell Activation Marker-Tuberculosis Assay for Diagnosis of Active Tuberculosis in Children: A Prospective Proof-of-Concept Study. *Lancet Infect Dis* (2014) 14:931–8. doi: 10.1016/S1473-3099(14)70884-9
42. Lyadova I, Nikitina I. Cell Differentiation Degree as a Factor Determining the Role for Different T-Helper Populations in Tuberculosis Protection. *Front Immunol* (2019) 10:972. doi: 10.3389/fimmu.2019.00972
43. Prezzemolo T, van Meijgaarden KE, Franken KLMC, Caccamo N, Dieli F, Ottenhoff THM, et al. Detailed Characterization of Human Mycobacterium Tuberculosis Specific HLA-E Restricted CD8(+) T Cells. *Eur J Immunol* (2018) 48:293–305. doi: 10.1002/eji.201747184
44. Caccamo N, Pietra G, Sullivan LC, Brooks AG, Prezzemolo T, La Manna MP, et al. Human CD8 T Lymphocytes Recognize Mycobacterium Tuberculosis Antigens Presented by HLA-E During Active Tuberculosis and Express Type 2 Cytokines. *Eur J Immunol* (2015) 45:1069–81. doi: 10.1002/eji.201445193
45. La Manna MP, Orlando V, Prezzemolo T, Di Carlo P, Cascio A, Delogu G, et al. HLA-E-Restricted CD8(+) T Lymphocytes Efficiently Control Mycobacterium Tuberculosis and HIV-1 Coinfection. *Am J Respir Cell Mol Biol* (2020) 62:430–9. doi: 10.1165/rcmb.2019-0261OC
46. Riou C, Tanko RF, Soares AP, Masson L, Werner L, Garrett NJ, et al. Restoration of CD4+ Responses to Copathogens in HIV-Infected Individuals on Antiretroviral Therapy Is Dependent on T Cell Memory Phenotype. *J Immunol* (2015) 195:2273–81. doi: 10.4049/jimmunol.1500803
47. Chiacchio T, Petruccioli E, Vanini V, Cuzzi G, Pinnetti C, Sampaolesi A, et al. Polyfunctional T-Cells and Effector Memory Phenotype Are Associated With Active TB in HIV-Infected Patients. *J Infect* (2014) 69:533–45. doi: 10.1016/j.jinf.2014.06.009
48. Petruccioli E, Chiacchio T, Pepponi I, Vanini V, Urso R, Cuzzi G, et al. First Characterization of the CD4 and CD8 T-Cell Responses to QuantiFERON-TB Plus. *J Infect* (2016) 73:588–97. doi: 10.1016/j.jinf.2016.09.008
49. Petruccioli E, Vanini V, Chiacchio T, Cuzzi G, Cirillo DM, Palmieri F, et al. Analytical Evaluation of QuantiFERON- Plus and QuantiFERON- Gold In-Tube Assays in Subjects With or Without Tuberculosis. *Tuberculosis (Edinb)* (2017) 106:38–43. doi: 10.1016/j.tube.2017.06.002
50. Rozot V, Vigano S, Mazza-Stalder J, Idrizi E, Day CL, Perreau M, et al. Mycobacterium Tuberculosis-Specific CD8+ T Cells Are Functionally and Phenotypically Different Between Latent Infection and Active Disease. *Eur J Immunol* (2013) 43:1568–77. doi: 10.1002/eji.201243262
51. Sauzullo I, Scrivo R, Mengoni F, Ermocida A, Coppola M, Valesini G, et al. Multi-Functional Flow Cytometry Analysis of CD4+ T Cells as an Immune Biomarker for Latent Tuberculosis Status in Patients Treated With Tumour Necrosis Factor (TNF) Antagonists. *Clin Exp Immunol* (2014) 176:410–7. doi: 10.1111/cei.12290
52. Savolainen LE, Kantele A, Knuuttila A, Pusa L, Karttunen R, Valleala H, et al. Combined Expression of IFN-γ, IL-17, and IL-4 mRNA by Recall PBMCs Moderately Discriminates Active Tuberculosis From Latent Mycobacterium Tuberculosis Infection in Patients With Miscellaneous Inflammatory Underlying Conditions. *Front Immunol* (2016) 7:239. doi: 10.3389/fimmu.2016.00239
53. QIAGEN. What Is QuantiFERON-TB Gold Plus? In: *QTF-Plus*. (2021). Available at: https://www.quantiferon.com/products/quantiferon-tb-gold-plus-qft-plus/.
54. Riou C, Berkowitz N, Goliath R, Burgers WA, Wilkinson RJ. Analysis of the Phenotype of Mycobacterium Tuberculosis-Specific CD4+ T Cells to Discriminate Latent From Active Tuberculosis in HIV-Uninfected and HIV-Infected Individuals. *Front Immunol* (2017) 8:968. doi: 10.3389/fimmu.2017.00968
55. Caccamo N, Joosten SA, Ottenhoff THM, Dieli F. Atypical Human Effector/Memory CD4(+) T Cells With a Naive-Like Phenotype. *Front Immunol* (2018) 9:2832. doi: 10.3389/fimmu.2018.02832
56. Wang X, Cao Z, Jiang J, Niu H, Dong M, Tong A, et al. Association of Mycobacterial Antigen-Specific CD4(+) Memory T Cell Subsets With Outcome of Pulmonary Tuberculosis. *J Infect* (2010) 60:133–9. doi: 10.1016/j.jinf.2009.10.048

57. Geldmacher C, Ngwenyama N, Schuetz A, Petrovas C, Reither K, Heeregrave EJ, et al. Preferential Infection and Depletion of Mycobacterium Tuberculosis-Specific CD4 T Cells After HIV-1 Infection. *J Exp Med* (2010) 207:2869–81. doi: 10.1084/jem.20100090
58. Sansoni P, Cossarizza A, Brianti V, Fagnoni F, Snelli G, Monti D, et al. Lymphocyte Subsets and Natural Killer Cell Activity in Healthy Old People and Centenarians. *Blood* (1993) 82:2767–73. doi: 10.1182/blood.V82.9.2767.2767
59. La Manna MP, Orlando V, Dieli F, Di Carlo P, Cascio A, Cuzzi G, et al. Quantitative and Qualitative Profiles of Circulating Monocytes may Help Identifying Tuberculosis Infection and Disease Stages. *PloS One* (2017) 12: e0171358. doi: 10.1371/journal.pone.0171358
60. Mpande CAM, Musvosvi M, Rozot V, Mosito B, Reid TD, Schreuder C, et al. Antigen-Specific T Cell Activation Distinguishes Between Recent and Remote Tuberculosis Infection. *Am J Respir Crit Care Med* (2021) 203:1556–65. doi: 10.1164/rccm.202007-2686OC
61. wma. *Declaration of Helsinki Ethical Principles for Medical Research Involving Human Subjects*. Available at: https://www.wma.net/policies-post/wma-declaration-of-helsinki-ethical-principles-for-medical-research-involving-human-subjects.

Conflict of Interest: The authors declare that the research was conducted in the absence of any commercial or financial relationships that could be construed as a potential conflict of interest.

Publisher's Note: All claims expressed in this article are solely those of the authors and do not necessarily represent those of their affiliated organizations, or those of the publisher, the editors and the reviewers. Any product that may be evaluated in this article, or claim that may be made by its manufacturer, is not guaranteed or endorsed by the publisher.

Copyright © 2021 Petruccioli, Petrone, Chiacchio, Farroni, Cuzzi, Navarra, Vanini, Massafra, Lo Pizzo, Guggino, Caccamo, Cantini, Palmieri and Goletti. This is an open-access article distributed under the terms of the Creative Commons Attribution License (CC BY). The use, distribution or reproduction in other forums is permitted, provided the original author(s) and the copyright owner(s) are credited and that the original publication in this journal is cited, in accordance with accepted academic practice. No use, distribution or reproduction is permitted which does not comply with these terms.

frontiers in Immunology

ORIGINAL RESEARCH
published: 17 August 2021
doi: 10.3389/fimmu.2021.706723

Characterizing Early T Cell Responses in Nonhuman Primate Model of Tuberculosis

Riti Sharan[1], *Dhiraj Kumar Singh*[1], *Jyothi Rengarajan*[2] *and Deepak Kaushal*[1]*

[1] Southwest National Primate Research Center, Texas Biomedical Research Institute, San Antonio, TX, United States, [2] Emory Vaccine Center and Yerkes National Primate Research Center (YNPRC), Emory University School of Medicine, Atlanta, GA, United States

OPEN ACCESS

Edited by:
Jayne S. Sutherland, Medical Research Council The Gambia Unit (MRC), Gambia

Reviewed by:
Hannah Priyadarshini Gideon, University of Pittsburgh, United States
Munyaradzi Musvosvi, South African Tuberculosis Vaccine Initiative SATVI, South Africa
Anneliese Sophie Ashhurst, The University of Sydney, Australia

***Correspondence:**
Deepak Kaushal
dkaushal@txbiomed.org

Specialty section:
This article was submitted to Immunological Memory, a section of the journal Frontiers in Immunology

Received: 07 May 2021
Accepted: 28 July 2021
Published: 17 August 2021

Citation:
Sharan R, Singh DK, Rengarajan J and Kaushal D (2021) Characterizing Early T Cell Responses in Nonhuman Primate Model of Tuberculosis. Front. Immunol. 12:706723. doi: 10.3389/fimmu.2021.706723

Tuberculosis (TB), caused by *Mycobacterium tuberculosis (Mtb)*, remains a leading infectious disease killer worldwide with 1.4 million TB deaths in 2019. While the majority of infected population maintain an active control of the bacteria, a subset develops active disease leading to mortality. Effective T cell responses are critical to TB immunity with $CD4^+$ and $CD8^+$ T cells being key players of defense. These early cellular responses to TB infection have not yet been studied in-depth in either humans or preclinical animal models. Characterizing early T cell responses in a physiologically relevant preclinical model can provide valuable understanding of the factors that control disease development. We studied *Mtb*-specific T cell responses in the lung compartment of rhesus macaques infected with either a low- or a high-dose of *Mtb* CDC1551 *via* aerosol. Relative to baseline, significantly higher *Mtb*-specific $CD4^+IFN\text{-}\gamma^+$ and TNF-α^+ T cell responses were observed in the BAL of low dose infected macaques as early as week 1 post TB infection. The IFN-γ and TNF-*a* response was delayed to week 3 post infection in *Mtb*-specific $CD4^+$ and $CD8^+$T cells in the high dose group. The manifestation of earlier T cell responses in the group exposed to the lower *Mtb* dose suggested a critical role of these cytokines in the antimycobacterial immune cascade, and specifically in the granuloma formation to contain the bacteria. However, a similar increase was not reflected in the $CD4^+$ and $CD8^+IL\text{-}17^+$ T cells at week 1 post infection in the low dose group. This could be attributed to either a suppression of the IL-17 response or a lack of induction at this early stage of infection. On the contrary, there was a significantly higher $IL\text{-}17^+$ response in *Mtb*-specific $CD4^+$ and $CD8^+$T cells at week 3 in the high dose group. The results clearly demonstrate an early differentiation in the immunity following low dose and high dose infection, largely represented by differences in the IFN-γ and TNF-α response by *Mtb*-specific T cells in the BAL. This early response to antigen expression by the bacteria could be critical for both bacterial growth control and bacterial containment.

Keywords: ESAT-6/CFP-10, T cell responses, IFN-γ, TNF-α, LTBI

INTRODUCTION

Tuberculosis (TB) remains the leading cause of human death from a single infectious agent with a total of 1.4 million deaths in 2019 (1). The outcome of a pulmonary TB infection can either be complete clearance of the pathogen to active tuberculosis (ATB) disease. The percentage of the infected population developing the clinical symptoms of TB remains small with a much higher percentage being able to control the naturally acquired infections (2, 3). This latently infected population largely remains asymptomatic and in some cases even clear the infections (4). Generation of robust T cell responses is critical in the immunity to TB and are responsible for a dynamic balance between the host and pathogen in a latent TB infection (LTBI) (5). While co-morbidities, such as, with HIV is a known factor for the reactivation of LTBI (6), the underlying causes for the susceptibility to the active disease remains unknown. Antigen specific responses to TB infection, including novel features of T cell differentiation have revealed pathways that facilitate the immune control of infection (7). The production of inflammatory cytokines such as gamma interferon (IFN-γ) and tumor necrosis factor alpha (TNF-α) are critical in the protection against long-term rampant *Mtb* growth and loss of these factors leads to heightened *Mycobacterium tuberculosis* (*Mtb)* replication and death (8, 9). Indeed, stimulation with *Mtb* antigens Early Secretory Antigenic Target (ESAT)-6 and Culture Filtrate Protein (CFP)-10 induces IFN-γ and TNF-α production by the $CD4^+$ and $CD8^+$T cells that may provide tools to study the role of these early responses in protection from a fatal infection.

Characterizing the phenotype and function of these early T cell responses could provide a critical tool to distinguishing latent from active TB disease in future experiments wherein, the macaques would be followed for a longer duration of time (10). The aim of this study is to characterize the early T cell responses in a nonhuman primate (NHP) model of TB. The model recapitulates humans, wherein, the infectious doses differ between individuals. There have been reports of differential impact on functional $CD4^+$ and $CD8^+$ T cell responses by the disease stage and bacterial burden (11–13). However, there is a paucity of data on the distinguished early adaptive response signatures in a biologically and physiologically relevant animal model. The NHP model of TB serves as an excellent model recapitulating the spectrum of immune responses observed in humans, including the pathology (14, 15). Manipulating the bacteria in a macaque model of TB infection presents a valuable tool to dissect the local immune responses in a TB predominant microenvironment that is not possible in any other animal model (16–18). We hypothesized that measuring the TB-specific T cell responses early in a rhesus macaque model of TB infection could provide a better understanding of the early responses and their potential role in disease progression. Hence, we performed high parameter flow cytometry on stimulated bronchoalveolar lavage (BAL) cells from macaques infected *via* aerosol, with a low dose and high dose of *Mtb*, to measure key cytokines in TB infection, IFN-γ, TNF-α and IL-17 produced by $CD4^+$ and $CD8^+$ T cells in response to ESAT-6/CFP-10 and *Mtb* Cell Wall Fraction (*Mtb* CW). This enabled a comprehensive elucidation of the differences in the early responses and provided a potential tool to delineate the disease progression in long-term studies.

MATERIALS AND METHODS

Study Approval

All infected animals were housed under Animal Biosafety Level 3 facilities at the Southwest National Primate Research Center, where they were treated according to the standards recommended by AAALAC International and the NIH guide for the Care and Use of Laboratory Animals. The study procedures were approved by the Animal Care and Use Committee of the Texas Biomedical Research Institute.

Animal Infections

The study design is outlined in **Figure 1**. We infected 2 groups of specific pathogen free adult Indian rhesus macaques from the SNPRC colony with *Mtb* CDC1551 *via* aerosol. The first group (n=12) had a low dose of approximately 10 CFU deposited in the lungs while the second group (n=6) had a higher dose of 50 CFU deposited in the lungs. All higher dose infected animals had a positive tuberculin skin test 3 weeks after exposure, while the low dose infected group were TST positive at 5 weeks, confirming infection. The animals were monitored for C-Reactive Protein (CRP) values (an acute phase protein and inflammatory marker), body temperatures and body weights.

Antigen Stimulations and Flow Cytometry

The freshly collected BAL cells were stimulated *ex vivo* with *Mtb*-specific antigens, ESAT-6/CFP-10 and *Mtb* Cell Wall Fraction (BEI Resources, 10 μg/mL) for a total of 16 h. Brefeldin A (0.5 μg/mL, SIGMA) was added 2 h after the onset of stimulation. After stimulation, the cells were stained with LIVE/DEAD fixable Near-IR stain (ThermoFisher) and stained subsequently with the surface antibodies: CD4-PerCP-Cy5.5 (L200, BD Biosciences), CD8-APC (RPA, T8, BD Biosciences), CD3-AlexaFlour 700 (SP34 2, BD Biosciences), CD95-BV421 (DX2, BD Biosciences), CD28-PECy7 (CD28.2, BD Biosciences) and CD45-BUV395 (D058 1283, BD Biosciences). Cells were then fixed, permeabilized and stained with intracellular antibodies: IFNγ-APC-Cy7 (B27, Biolegend), IL-17-BV605 (BL168, Biolegend) and TNF-α-BV650 (MAb11, Biolegend). Cells were washed, suspended in BD stabilizing fixative buffer and acquired on BD Symphony flow cytometer. Analysis was performed using FlowJo (v10.6.1) using previously published gating strategy (18–20) (**Figures S1–S3**).

Statistical Analysis

Statistical analysis was performed using GraphPad Prism (version 8.4.1). Significance was determined using Mann Whitney U test in GraphPad Prism v8.4.1. A P value of <0.05 was considered as statistically significant. $^*P < 0.05$; $^{**}P < 0.01$; $^{***}P < 0.001$; $^{****}P < 0.0001$. Data are represented as median with interquartile range.

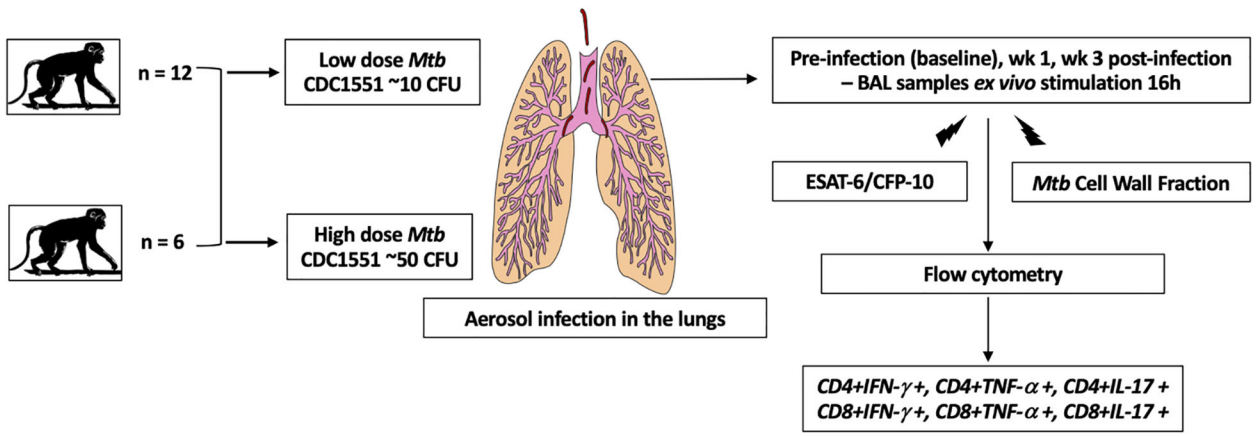

FIGURE 1 | Schematic of the study design. We infected 2 groups of adult Indian rhesus macaques with *Mtb* CDC1551 *via* aerosol. The first group (n = 12) had a low dose of approximately 10 CFU deposited in the lungs while the second group (n = 6) had a higher dose of 50 CFU deposited in the lungs. The BAL cells were collected at pre-infection, wk 1 and 3 post-infection. They were stimulated *ex vivo* with *Mtb*-specific antigens, ESAT-6/CFP-10 and *Mtb* Cell Wall Fraction. After stimulation, the cells were stained with the surface antibodies for flow cytometry and acquired on BD Symphony. Analysis was performed using FlowJo (v10.6.1).

RESULTS

Clinical Parameters

Upon infection with the low dose of *Mtb*, did not demonstrate the clinical signs of disease. These animals maintained low CRP values with not more than 5-7% body weight loss or fever (**Figure 2A**). Viable bacilli were not readily detected in the BAL of these animals (data not shown). On the contrary, the animals that received a high dose of 50 CFU, displayed higher than baseline CRP values (> 5 μg/mL) as early as 3 weeks post infection. No significant changes were observed in the body weight (**Figure 2B**) and temperature (**Figure 2C**) of this group up till week 3 of infection.

Early Mtb-Specific CD4$^+$ IFN-γ and TNF-α Response in Low Dose Infected Macaques

BAL samples were collected from study macaques at pre-infection, week 1 and week 3 post infection using standard operating procedures by the veterinarian. The single cells were prepared as per the lab standardized protocol (21). All *Mtb*-specific responses are background corrected. Upon stimulation with ESAT-6/CFP-10, there was a delayed IFN-γ response in the *Mtb*-specific CD4$^+$T cells in the high dose compared to the low dose group (**Figure 3A**). This difference was however, not observed in the *Mtb*-specific CD8$^+$T cells (**Figure 3B**). While the low dose infection resulted in a significant increase in the percentage of *Mtb*-specific CD4$^+$IFN-γ$^+$T cells as early as week 1 post-infection, this response was not observed in the high dose group till 3 weeks post infection (**Figure 3A**). The early response observed in the low dose infection decreased from week 1 to week 3 post-infection whereas the response spiked in the high dose infection group at week 3 post-infection (**Figure 3A**).

Similarly, there was a delayed increase in the percentage of *Mtb*-specific CD4$^+$TNF-α$^+$T cells in the high dose infection group with a higher percentage of this subset observed at week 3 post-infection (**Figure 3C**). On the contrary, the low dose infected macaques demonstrated an early TNF-α response in the *Mtb*-specific CD4$^+$ T cells at weeks 1 which decreased at

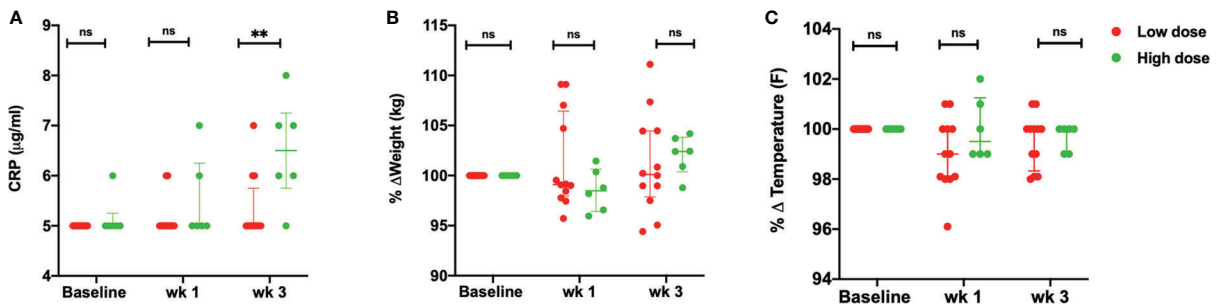

FIGURE 2 | Clinical parameters. **(A)** Serum CRP values (μg/mL) **(B)** percentage weight change (kg) and **(C)** percentage body temperature change (°F) of low dose (n = 12) and high dose (n = 6) *Mtb* infected rhesus macaques at baseline, wk 1 and 3 post-infection. The data are expressed as median with interquartile range. $^{**}P < 0.01$; ns, non significant. Significance was determined using Mann Whitney U test in GraphPad Prism v8.4.1.

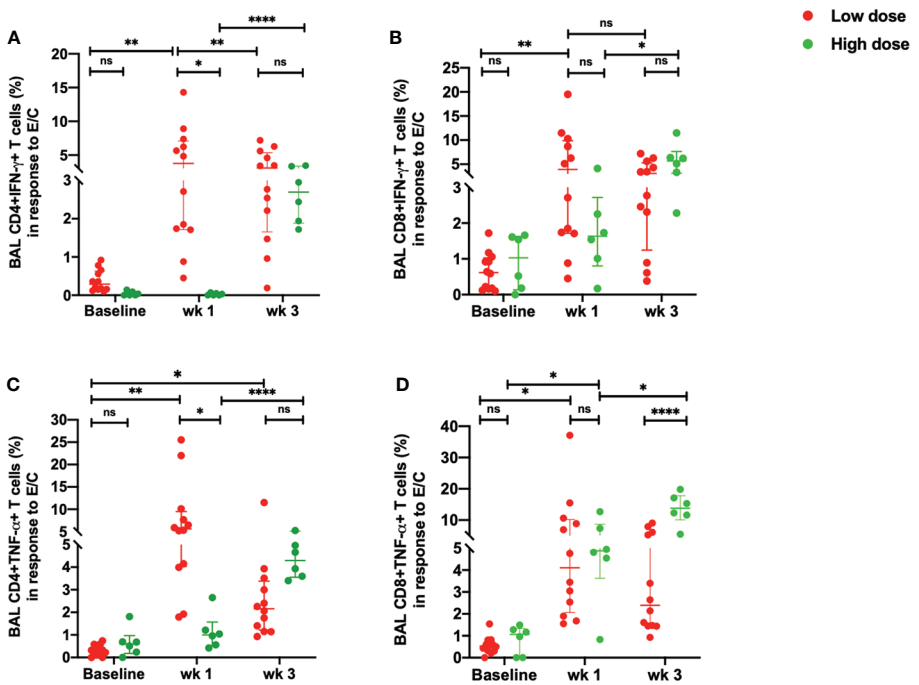

FIGURE 3 | Early ESAT-6/CFP-10-specific responses in the BAL. **(A)** percentage of CD4+IFN-γ+ T cells, **(B)** percentage of CD8+IFN-γ+ T cells, **(C)** percentage of CD4+TNF-α+ T cells and **(D)** percentage of CD8+ TNF-α+ T cells in response to ESAT/6/CFP-10 stimulation in low dose (n = 12) and high dose (n = 6) infection. The data are expressed as median with interquartile range. *P < 0.05; **P < 0.01; ****P < 0.0001; ns, non significant. Significance was determined using Mann Whitney U test in GraphPad Prism v8.4.1.

week 3 post-infection (**Figure 3C**). $CD4^+TNF\text{-}\alpha^+T$ cells were significantly higher in the low dose group than the high dose group at week 1 post-infection. Similarly, *Mtb*-specific $CD8^+TNF\text{-}\alpha^+T$ cells exhibited a significant increase in the high dose group at 3 weeks post-infection compared to the low dose infection group (**Figure 3D**). The low dose infection group maintained a consistent increase in the $CD8^+TNF\text{-}\alpha^+T$ cells at 1- and 3-weeks post-infection compared to the pre-infection levels (**Figure 3D**).

When BAL cells were stimulated with *Mtb* CW, the differences observed between low dose and high dose were similar to those elicited with ESAT-6/CFP-10. Thus, the percentages of CD4+IFN-γ+ (**Figure 4A**) and $CD4^+$ $TNF\text{-}\alpha^+T$ cells (**Figure 4B**) were significantly lower in the high dose group compared to the low dose group at week 1 post-infection. No significant difference was seen in the IFN-γ response in the *Mtb* CW-specific $CD4^+T$ cells between high dose and low dose infection group at week 3 post-infection (**Figure 4A**). Similarly, a delayed IFN-γ response in the $CD8^+T$ cells in response to the *Mtb* CW was observed with a significant increase in the high dose infection group compared to the low dose group at 3 weeks post-infection (**Figure 4C**). As with the gamma response, the *Mtb*-specific $CD4^+TNF\text{-}$ α^+T cells (**Figure 4B**) and $CD8^+$ $TNF\text{-}\alpha^+T$ cells (**Figure 4D**) elicited by *Mtb* CW stimulation at 3 weeks post-infection was significantly higher in the high dose group compared to the low dose group. Thus, an early and consistent TNF-α response was observed in the low dose group while a delayed but a more robust TNF-α response in both *Mtb*-specific $CD4^+$ and $CD8^+T$ cells was observed in the high infection dose. No significant changes were observed in the unstimulated samples between the two doses (**Figures S4A, B, D, E**).

In addition to the percentage of $CD4^+$ and $CD8^+$ T cells positive for cytokine production, we also gated for the percentage of *Mtb*-specific T cells expressing surface phenotypic markers consistent with central memory T cells (Tcm $CD28^+CD95^+$) and effector memory T cells (Tem $CD28^-CD95^+$) in the total *Mtb*-specific CD4 and CD8 population in low dose infected animals (**Figure S5**). We observed a higher central memory (>75%) $CD4^+$ T cells in response to stimulation, both in the low dose (**Figures S5A, B**) and high dose (**Figure S6**) infection. In comparison, the effector memory response was less than 20% at pre-infection, wks 1 and 3 post-infection in both the doses (**Figures S5A, B** and **S6A, B**). There were no significant differences in the percentages of Tcm and Tem from baseline to wk 1 and from wk 1 to wk 3 post-infection in response to stimulation with ESAT-6/CFP-10 and *Mtb CW* in the both the doses (**Figures S5A, B** and **S6A, B**). Comparable *Mtb*-specific central (~40%) and effector memory (~50%) $CD8^+$ T cells were observed in both the doses with no significant changes from pre-infection to wk 1 and from wk 1 to wk 3 post-infection (**Figures S5C, D** and **S6C, D**).

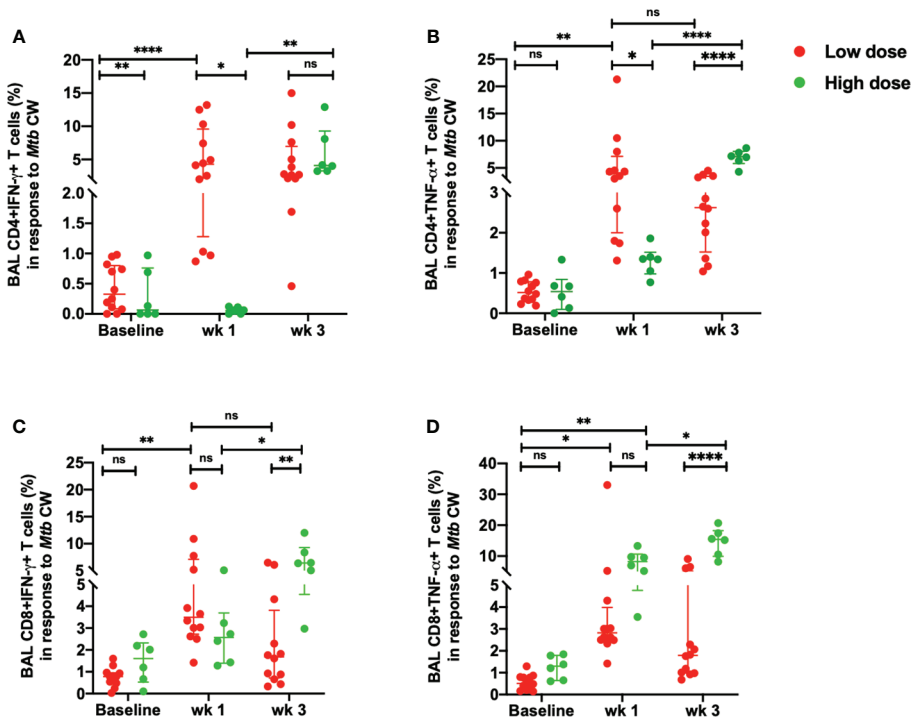

FIGURE 4 | Early *Mtb* CW-specific responses in the BAL. **(A)** percentage of CD4+IFN-γ+ T cells, **(B)** percentage of CD4+TNF-α+ T cells, **(C)** percentage of CD8+ IFN-γ+ T cells and **(D)** percentage of CD8+ TNF-α+ T cells in response to *Mtb* CW stimulation in low dose (n = 12) and high dose (n = 6) infection. The data are expressed as median with interquartile range. *P < 0.05; **P < 0.01; ****P < 0.0001; ns, non significant. Significance was determined using Mann Whitney U test in GraphPad Prism v8.4.1.

Controlled Early Inflammatory Response in Low Dose Mtb Infection

There was a significant increase in the percentage of *Mtb*-specific $CD4^+$ IL-17^+T cells in the high dose infected group at week 3 compared to the low dose infected group in response to both, ESAT-6/CFP-10 and *Mtb* CW antigens (**Figures 5A, B**). The low dose infected group demonstrated a consistent measure of the $CD4^+$ IL-17^+T cells from week 1 to week 3 post-infection with no significant changes compared to the pre-infection levels (**Figures 5A, B**). Similarly, the percentage of IL-17^+ $CD8^+$T cells in response to *Mtb* CW stimulation was significantly higher in the high dose infection group compared to the low dose infection group at 3 weeks post-infection (**Figures 5C, D**). No significant changes were observed in the unstimulated samples between the two doses (**Figures S4C, F**).

DISCUSSION

Our results clearly outline the differences in the early *Mtb*-specific T cells responses in a low dose *versus* higher dose infection in a rhesus macaque model of TB. The macaques exposed to a low-dose controlled *Mtb* infection were associated with an early IFN-γ and TNF-α response in *Mtb*-specific CD4+ T cells. A high dose infection caused a significantly higher TNF-α response in the $CD8^+$ T cells at 3 weeks post-infection but no noticeable changes in the IFN-γ response this early in infection. TNF-α secreting *Mtb*-specific $CD4^+$ T cells are a promising candidate to differentiate between active and latent TB infections (10, 22). In the study by Harari et al. (22), significant increase in the proportions of *Mtb*-specific $CD4^+$T cells expressing TNF-α was seen in patients with active disease and proposed to be the strongest predictor of diagnosis of active disease. Indeed, commensurate with these findings, we observed a significantly higher TNF-α response in the *Mtb*-specific $CD8^+$ T cells in the group infected with a higher number of bacilli. The difference in our study was that here we compared two different doses of infection of *Mtb* in a biologically relevant animal model. Though the difference between TNF-α expression by $CD4^+$ T cells was not significantly different between low dose and high dose infection groups at week 3, there was a consistent increase in the TNF-α expression from pre-infection to week 3 in the high dose group. Hence, while the low dose elicits an earlier TNF-α response that then remains at similar levels up till 3 weeks post infection, the same response is slower to develop in the higher dose but more robust as the infection progresses. Previous studies have shown the detection of *Mtb*-specific effector $CD4^+$ T cells expressing IFN-γ and/or TNF-α can distinguish between a latent TB and active TB infection (12, 23). A recent study demonstrated that increased amounts of TNF-α in an active TB infection subverted the immune-surveillance by perturbing dendritic cell mediated antigen transportation to the lymph node allowing bacterial reserve (24). Further studies on phenotyping the

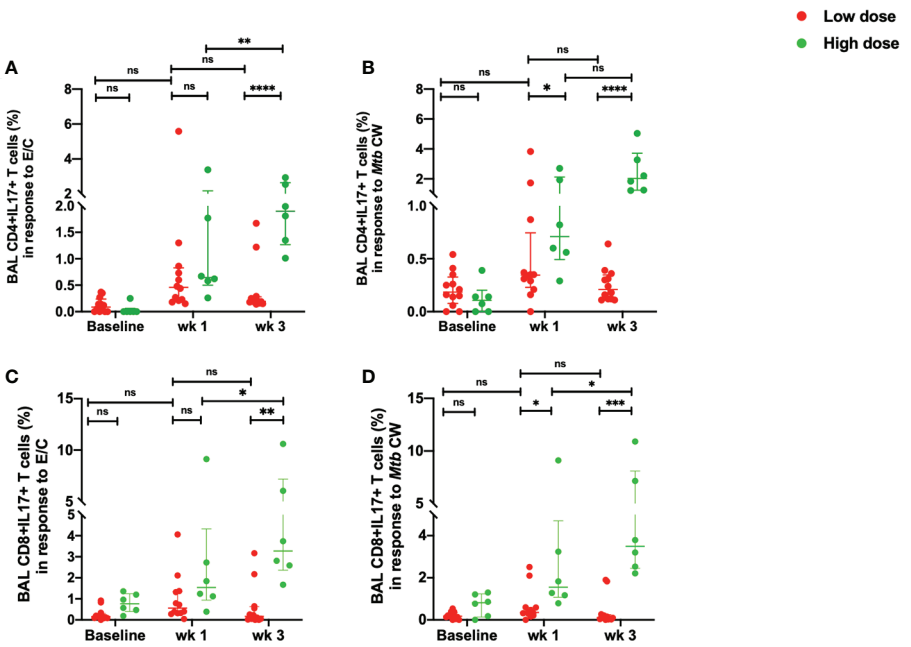

FIGURE 5 | Early *Mtb*-specific IL-17 responses in the BAL. **(A)** percentage of CD4+IL-17+ T cells in response to ESAT/6/CFP-10 stimulation, **(B)** percentage of CD4+IL-17+ T cells in response to *Mtb* CW stimulation, **(C)** percentage of CD8+ IL-17+ T cells in response to ESAT/6/CFP-10 stimulation and **(D)** percentage of CD8+ IL-17+ T cells in response to *Mtb* CW stimulation in low dose (n = 12) and high dose (n = 6) infection. The data are expressed as median with interquartile range. *P < 0.05; **P <0.01; ***P < 0.001; ****P < 0.0001; ns, non significant. Significance was determined using Mann Whitney U test in GraphPad Prism v8.4.1.

subsets in our study to distinguish the effector and memory functions could provide a highly discriminatory readout.

IFN-γ producing $CD4^+$T cells are the cornerstone of protective immunity in pulmonary *Mtb* infections (25). In the two doses studied here, the difference in the $CD4^+$IFN-γ^+ response to *Mtb* antigens, ESAT-6/CFP-10 and *Mtb* CW, was the highest at 1-week post-infection and diminished by week 3 post-infection. IFN-γ deficient mice studies have demonstrated a lack of survival even in low-dose *Mtb* infections with progression to active disease (26, 27). This early gamma response in the low dose infection alone could be representative of the protective role of $CD4^+$ T lymphocytes in mediating macrophage activation *via* iNOS expression (27, 28). IFN-γ is known to promote iNOS expression in macrophages that in turn serves to recruit other reactive nitrogen intermediates (RNI) (29). Not only is this early gamma response critical for TB control, it also plays a role in the long-term survival of the host by working synergistically with the early TNF-α responses and thus contributing to the granuloma formation that controls the disease progression (30). Interestingly, we observed a significantly higher $CD8^+$IFN-γ^+ T cells in the high dose group in response to stimulation with *Mtb* CW at 3 weeks post-infection, but did not see a similar response to ESAT-6/CFP-10 stimulation. While the role of $CD4^+$T cells in IFN-γ production in TB is well documented, the role of $CD8^+$ T cells in the IFN-γ production in human TB is less well studied. A part of the role of the $CD8^+$ T cells has been elucidated in mice experiments, wherein, mice deficient in $CD8^+$ T cells were unable to control *Mtb* infection (31). Additionally, $CD8^+$ T cells have been shown to undergo phenotypic and functional changes, comparable to $CD4^+$ T cells during pulmonary *Mtb* infection (32). *Mtb*-specific $CD8^+$ T cells have demonstrated differences in prevalence, frequency, phenotypic and functional profiles in latent *versus* active TB disease (33). Similar to our findings, a higher *Mtb*-specific $CD8^+$ T cells frequency (60%) was observed in the TB patients compared to 15% in LTBI patients. These $CD8^+$ T cell responses were directed against ESAT-6/CFP-10 *in vitro* stimulation comparable to our study in NHP model. Also, the IFN-γ response in the *Mtb*-specific $CD8^+$ T cells was not very different between active and LTBI cases like our study, in which we did not observe a significant difference in the $CD8^+$IFN-γ^+ T cells in the low dose and high dose when stimulated with ESAT-6/CFP-10.

While Th1 cells plays a distinct role in rendering protection in TB *via* production of IFN-γ and activating antimicrobial action in macrophages (34), Th17 cells implements neutrophilic inflammation, tissue damage and TB pathology (35). The data on the role of Th17 cells in TB remains controversial with some groups reporting a higher frequency correlating with TB protection in latent patients (36) while others reported lower expression in latent patients and increased frequencies in active or multi-drug resistant patients (37–39). Some are of the verdict that Th17 cells are minimally expressed in TB and do not have a significant role to play in the protection and/or pathology of TB in humans (40, 41). In our study, we observed a significant increase in the IL-17 expressing *Mtb*-specific $CD4^+$ and $CD8^+$ T cells in the high dose infection compared to the low dose at

3 weeks post-infection. *Mtb* infection in humans induces IFN-γ and IL-17 and the main source is the $CD4^+IFN\text{-}\gamma^+IL\text{-}17^+$ T cells (38). Moreover, the antigen-expanded $CD4^+IL\text{-}17^+$ T cells correlates with the clinical parameters associated with disease severity. Given these findings, the expansion of *Mtb*-specific $CD4^+IFN\text{-}\gamma^+IL\text{-}17^+$ T cells has been proposed as a biomarker for prediction of clinical outcome in active TB patients (38). T cells from MDR-TB patients has been shown to express high levels of IL-17 *via* the strong TLR-2 dependent TGFβ production by antigen-presenting cells (37). Mouse studies mimicking human vaccination post *Mtb*-exposure verified the presence of increased IL-17 which correlated to lung tissue damage (42). Conversely, protective role of Th17 responses have also been reported in the lung tissue following BCG vaccination (43, 44). However, it is to be noted that it is feasible to observe an increased bacterial burden with a higher initial inoculum that could impact the disease kinetics. While this study aims to identify the very early differences in the adaptive response to *Mtb*, it will be critical to follow the kinetics over a longer duration in future studies to ascertain the true role of IL-17 in this model. Overall, we have demonstrated a distinct phenotype of *Mtb*-specific $CD4^+$ and $CD8^+$T cells following *in vitro* stimulation with ESAT-6/CFP-10 and *Mtb* CW early in TB infection in a biologically and physiologically relevant animal model. Further, in depth phenotyping of these subsets into tissue resident memory cells at later time point in future studies would prove instrumental in improving our understanding of these early T cells responses and their correlation to disease progression.

DATA AVAILABILITY STATEMENT

The original contributions presented in the study are included in the article/**Supplementary Material**. Further inquiries can be directed to the corresponding author.

ETHICS STATEMENT

The animal study was reviewed and approved by Texas Biomedical Research Institute IACUC.

AUTHOR CONTRIBUTIONS

RS, DS, JR, and DK designed the study. RS and DS executed the experiments and analyzed the data. RS and DK wrote the manuscript. All authors contributed to the article and approved the submitted version.

FUNDING

This work was primarily supported by NIH grants R01AI111943 and R01AI123047 (to DK and JR), 1 K01 OD031898-01 (to RS) with additional support from NIH grants R01AI111914, R01AI134240, R01AI138587, and U19AI111211 and institutional grants from the Office of the Director, NIH P51OD011133 (to SNPRC), P30 RR00165 and P51OD011132 (to YNPRC), and P30 AI050409 [Emory University Center for AIDS Research (CFAR)].

SUPPLEMENTARY MATERIAL

The Supplementary Material for this article can be found online at: https://www.frontiersin.org/articles/10.3389/fimmu.2021.706723/full#supplementary-material

Supplementary Figure 1 | Gating strategy for *Mtb*-specific responses. The cells are gated on CD45 and Live/Dead to select live cells and perform red blood cell (RBC) discrimination. This is followed by singlet gating on SSC and FSC -Area, width and Height. Total CD4 and CD8 is then gated on total CD3 population. IFN-γ+, TNF-α+ and IL-17+ CD4+ and CD8+ T cells are then gated on total CD4 and CD8 population.

Supplementary Figure 2 | Gating strategy for *Mtb*-specific central memory and effector memory T cell responses. The cells are gated on CD45 and Live/Dead to select live cells and perform red blood cell (RBC) discrimination. This is followed by singlet gating on SSC and FSC -Area, width and Height. Total CD4 and CD8 is then gated on total CD3 population. Central (CD28+CD95+) and effector (CD28-CD95+) memory T cells are then gated on total CD4 and CD8 population in BAL and PBMCs.

Supplementary Figure 3 | Gating strategy for *Mtb*-specific cytokine positive cells in unstimulated, ESAT-6/CFP-10 stimulated and Mtb CW stimulated BAL samples. **(A)** CD4+IFN-γ+ T cells **(B)** CD8+ IFN-γ+ T cells **(C)** CD4+IL-17+T cells **(D)** CD8+ IL-17+T cells **(E)** CD4+TNF-α+T cells and **(F)** CD8+TNF-α+T cells.

Supplementary Figure 4 | Unstimulated responses in BAL of low dose (n = 12) and high dose (n = 6) infected macaques. **(A)** percentage of CD4+IFN-γ+ T cells, **(B)** percentage of CD4+TNF-α+ T cells, **(C)** percentage of CD4+IL-17+ T cells, **(D)** percentage of CD8+ IFN-γ+ T cells, **(E)** percentage of CD8+TNF-α+ T cells, **(F)** percentage of CD8+IL-17+ T cells. The data are expressed as median with interquartile range. $^*P < 0.05$; $^{**}P < 0.01$; $^{***}P < 0.001$; $^{****}P < 0.0001$. Significance was determined using Mann Whitney U test in GraphPad Prism v8.4.1.

Supplementary Figure 5 | Total CD4+ central and Effector memory T cell response in BAL of low dose infection (*n* = 12). **(A)** CD4+Tcm and Tem in response to ESAT-6/CFP-10 stimulation, **(B)** CD4+Tcm and Tem in response to *Mtb* CW stimulation, **(C)** CD8+ Tcm and Tem in response to ESAT-6/CFP-10 stimulation. The data are expressed as median with interquartile range. $^*P < 0.05$; $^{**}P < 0.01$; $^{***}P < 0.001$; $^{****}P < 0.0001$. Significance was determined using Mann Whitney U test in GraphPad Prism v8.4.1.

Supplementary Figure 6 | Total CD4+ central and Effector memory T cell response in BAL of high dose infection (*n* = 12). **(A)** CD4+Tcm and Tem in response to ESAT-6/CFP-10 stimulation, **(B)** CD4+Tcm and Tem in response to *Mtb* CW stimulation, **(C)** CD8+ Tcm and Tem in response to ESAT-6/CFP-10 stimulation and **(D)** CD8+ Tcm and Tem in response to *Mtb* CW stimulation. The data are expressed as median with interquartile range. $^*P < 0.05$; $^{**}P < 0.01$; $^{***}P < 0.001$; $^{****}P < 0.0001$. Significance was determined using Mann Whitney U test in GraphPad Prism v8.4.1.

REFERENCES

1. WHO. *Global Tuberculosis Report 2020*. Geneva: World Health Organization (2020). Licence: CC BY-NC-SA 3.0 IGO.
2. Shanmugasundaram U, Bucsan AN, Ganatra SR, Ibegbu C, Quezada M, Blair RV, et al. Pulmonary Mycobacterium Tuberculosis Control Associates With CXCR3- and CCR6-Expressing Antigen-Specific Th1 and Th17 Cell Recruitment. *JCI Insight* (2020) 5(14):e137858. doi: 10.1172/jci.insight.137858
3. Esaulova E, Das S, Singh DK, Choreño-Parra JA, Swain A, Arthur L, et al. The Immune Landscape in Tuberculosis Reveals Populations Linked to Disease and Latency. *Cell Host Microbe* (2020) 29(2):165–78.
4. Boom WH, Schaible UE, Achkar JM. The Knowns and Unknowns of Latent Mycobacterium Tuberculosis Infection. *J Clin Invest* (2021) 131(3):e136222. doi: 10.1172/JCI136222
5. Winslow GM, Cooper A, Reiley W, Chatterjee M, Woodland DL. Early T-Cell Responses in Tuberculosis Immunity. *Immunol Rev* (2008) 225:284–99. doi: 10.1111/j.1600-065X.2008.00693.x
6. Sharan R, Bucşan AN, Ganatra S, Paiardini M, Mohan M, Mehra S, et al. Chronic Immune Activation in TB/HIV Co-Infection. *Trends Microbiol* (2020) 28(8):619–32. doi: 10.1016/j.tim.2020.03.015
7. Moguche AO, Musvosvi M, Penn-Nicholson A, Plumlee CR, Mearns H, Geldenhuys H, et al. Antigen Availability Shapes T Cell Differentiation and Function During Tuberculosis. *Cell Host Microbe* (2017) 21(6):695–706.e5. doi: 10.1016/j.chom.2017.05.012
8. Choi HG, Kwon KW, Choi S, Back YW, Park HS, Kang SM, et al. Antigen-Specific IFN-γ/IL-17-Co-Producing CD4(+) T-Cells Are the Determinants for Protective Efficacy of Tuberculosis Subunit Vaccine. *Vaccines (Basel)* (2020) 8 (2):300. doi: 10.3390/vaccines8020300
9. Yuan J, Tenant J, Pacatte T, Eickhoff C, Blazevic A, Hoft DF, et al. A Subset of Mycobacteria-Specific CD4(+) IFN-γ(+) T Cell Expressing Naive Phenotype Confers Protection Against Tuberculosis Infection in the Lung. *J Immunol* (2019) 203(4):972–80. doi: 10.4049/jimmunol.1900209
10. Pollock KM, Whitworth HS, Montamat-Sicotte DJ, Grass L, Cooke GS, Kapembwa MS, et al. T-Cell Immunophenotyping Distinguishes Active From Latent Tuberculosis. *J Infect Dis* (2013) 208(6):952–68. doi: 10.1093/infdis/jit265
11. Casey R, Blumenkrantz D, Millington K, Montamat-Sicotte D, Kon OM, Wickremasinghe M, et al. Enumeration of Functional T-Cell Subsets by Fluorescence-Immunospot Defines Signatures of Pathogen Burden in Tuberculosis. *PloS One* (2010) 5(12):e15619. doi: 10.1371/journal.pone.0015619
12. Day CL, Abrahams DA, Lerumo L, Janse van Rensburg E, Stone L, O'Rie T, et al. Functional Capacity of Mycobacterium Tuberculosis-Specific T Cell Responses in Humans Is Associated With Mycobacterial Load. *J Immunol* (2011) 187(5):2222–32. doi: 10.4049/jimmunol.1101122
13. Millington KA, Innes JA, Hackforth S, Hinks TS, Deeks JJ, Dosanjh DP, et al. Dynamic Relationship Between IFN-Gamma and IL-2 Profile of Mycobacterium Tuberculosis-Specific T Cells and Antigen Load. *J Immunol* (2007) 178(8):5217–26. doi: 10.4049/jimmunol.178.8.5217
14. Scanga CA, Flynn JL. Modeling Tuberculosis in Nonhuman Primates. *Cold Spring Harb Perspect Med* (2014) 4(12):a018564. doi: 10.1101/cshperspect.a018564
15. Kaushal D, Mehra S, Didier PJ, Lackner AA. The Non-Human Primate Model of Tuberculosis. *J Med Primatol* (2012) 41(3):191–201. doi: 10.1111/j.1600-0684.2012.00536.x
16. Mehra S, Pahar B, Dutta NK, Conerly CN, Philippi-Falkenstein K, Alvarez X, et al. Transcriptional Reprogramming in Nonhuman Primate (Rhesus Macaque) Tuberculosis Granulomas. *PloS One* (2010) 5(8):e12266. doi: 10.1371/journal.pone.0012266
17. Mehra S, Alvarez X, Didier PJ, Doyle LA, Blanchard JL, Lackner AA, et al. Granuloma Correlates of Protection Against Tuberculosis and Mechanisms of Immune Modulation by Mycobacterium Tuberculosis. *J Infect Dis* (2013) 207 (7):1115–27. doi: 10.1093/infdis/jis778
18. Kaushal D, Foreman TW, Gautam US, Alvarez X, Adekambi T, Rangel-Moreno J, et al. Mucosal Vaccination With Attenuated Mycobacterium Tuberculosis Induces Strong Central Memory Responses and Protects Against Tuberculosis. *Nat Commun* (2015) 6:8533. doi: 10.1038/ncomms9533
19. Ganatra SR, Bucsan AN, Alvarez X, Kumar S, Chatterjee A, Quezada M, et al. Anti-Retroviral Therapy Does Not Reduce Tuberculosis Reactivation in a Tuberculosis-HIV Co-Infection Model. *J Clin Invest* (2020) 130(10):5171–9. doi: 10.1172/JCI136502
20. Foreman TW, Mehra S, LoBato DN, Malek A, Alvarez X, Golden NA, et al. CD4+ T-Cell-Independent Mechanisms Suppress Reactivation of Latent Tuberculosis in a Macaque Model of HIV Coinfection. *Proc Natl Acad Sci USA* (2016) 113(38):E5636–44. doi: 10.1073/pnas.1611987113
21. Mehra S, Golden NA, Dutta NK, Midkiff CC, Alvarez X, Doyle LA, et al. Reactivation of Latent Tuberculosis in Rhesus Macaques by Coinfection With Simian Immunodeficiency Virus. *J Med Primatol* (2011) 40(4):233–43. doi: 10.1111/j.1600-0684.2011.00485.x
22. Harari A, Rozot V, Bellutti Enders F, Perreau M, Stalder JM, Nicod LP, et al. Dominant TNF-α+ Mycobacterium Tuberculosis-Specific CD4+ T Cell Responses Discriminate Between Latent Infection and Active Disease. *Nat Med* (2011) 17(3):372–6. doi: 10.1038/nm.2299
23. Caccamo N, Guggino G, Joosten SA, Gelsomino G, Di Carlo P, Titone L, et al. Multifunctional CD4(+) T Cells Correlate With Active Mycobacterium Tuberculosis Infection. *Eur J Immunol* (2010) 40(8):2211–20. doi: 10.1002/eji.201040455
24. Xu W, Snell LM, Guo M, Boukhaled G, Macleod BL, Li M, et al. Early Innate and Adaptive Immune Perturbations Determine Long-Term Severity of Chronic Virus and Mycobacterium Tuberculosis Coinfection. *Immunity* (2021) 54(3):526–41.e7. doi: 10.1016/j.immuni.2021.01.003
25. Kumar P. Ifnγ-Producing CD4(+) T Lymphocytes: The Double-Edged Swords in Tuberculosis. *Clin Transl Med* (2017) 6(1):21. doi: 10.1186/s40169-017-0151-8
26. Cooper AM, Dalton DK, Stewart TA, Griffin JP, Russell DG, Orme IM. Disseminated Tuberculosis in Interferon Gamma Gene-Disrupted Mice. *J Exp Med* (1993) 178(6):2243–7. doi: 10.1084/jem.178.6.2243
27. Green AM, Difazio R, Flynn JL. IFN-γ From CD4 T Cells Is Essential for Host Survival and Enhances CD8 T Cell Function During Mycobacterium Tuberculosis Infection. *J Immunol* (2013) 190(1):270–7. doi: 10.4049/jimmunol.1200061
28. O'Garra A, Redford PS, McNab FW, Bloom CI, Wilkinson RJ, Berry MP. The Immune Response in Tuberculosis. *Annu Rev Immunol* (2013) 31:475–527. doi: 10.1146/annurev-immunol-032712-095939
29. Herbst S, Schaible UE, Schneider BE. Interferon Gamma Activated Macrophages Kill Mycobacteria by Nitric Oxide Induced Apoptosis. *PloS One* (2011) 6(5):e19105. doi: 10.1371/journal.pone.0019105
30. Cavalcanti YV, Brelaz MC, Neves JK, Ferraz JC, Pereira VR. Role of TNF-Alpha, IFN-Gamma, and IL-10 in the Development of Pulmonary Tuberculosis. *Pulm Med* (2012) 2012:745483. doi: 10.1155/2012/745483
31. Flynn JL, Goldstein MM, Triebold KJ, Koller B, Bloom BR. Major Histocompatibility Complex Class I-Restricted T Cells Are Required for Resistance to Mycobacterium Tuberculosis Infection. *Proc Natl Acad Sci USA* (1992) 89(24):12013–7. doi: 10.1073/pnas.89.24.12013
32. Feng CG, Bean AG, Hooi H, Briscoe H, Britton WJ. Increase in Gamma Interferon-Secreting CD8(+), as Well as CD4(+), T Cells in Lungs Following Aerosol Infection With Mycobacterium Tuberculosis. *Infect Immun* (1999) 67 (7):3242–7. doi: 10.1128/IAI.67.7.3242-3247.1999
33. Rozot V, Vigano S, Mazza-Stalder J, Idrizi E, Day CL, Perreau M, et al. Mycobacterium Tuberculosis-Specific CD8+ T Cells Are Functionally and Phenotypically Different Between Latent Infection and Active Disease. *Eur J Immunol* (2013) 43(6):1568–77. doi: 10.1002/eji.201243262
34. Nikitina IY, Panteleev AV, Kosmiadi GA, Serdyuk YV, Nenasheva TA, Nikolaev AA, et al. Th1, Th17, and Th1Th17 Lymphocytes During Tuberculosis: Th1 Lymphocytes Predominate and Appear as Low-Differentiated CXCR3(+)CCR6(+) Cells in the Blood and Highly Differentiated CXCR3(+/-)CCR6(-) Cells in the Lungs. *J Immunol* (2018) 200(6):2090–103. doi: 10.4049/jimmunol.1701424
35. Lyadova IV, Panteleev AV. Th1 and Th17 Cells in Tuberculosis: Protection, Pathology, and Biomarkers. *Mediators Inflamm* (2015) 2015:854507. doi: 10.1155/2015/854507
36. Scriba TJ, Kalsdorf B, Abrahams DA, Isaacs F, Hofmeister J, Black G, et al. Distinct, Specific IL-17- and IL-22-Producing CD4+ T Cell Subsets Contribute to the Human Anti-Mycobacterial Immune Response. *J Immunol* (2008) 180(3):1962–70. doi: 10.4049/jimmunol.180.3.1962

37. Basile JI, Geffner LJ, Romero MM, Balboa L, Sabio YGC, Ritacco V, et al. Outbreaks of Mycobacterium Tuberculosis MDR Strains Induce High IL-17 T-Cell Response in Patients With MDR Tuberculosis That Is Closely Associated With High Antigen Load. *J Infect Dis* (2011) 204(7):1054–64. doi: 10.1093/infdis/jir460
38. Jurado JO, Pasquinelli V, Alvarez IB, Peña D, Rovetta AI, Tateosian NL, et al. IL-17 and IFN-γ Expression in Lymphocytes From Patients With Active Tuberculosis Correlates With the Severity of the Disease. *J Leukoc Biol* (2012) 91(6):991–1002. doi: 10.1189/jlb.1211619
39. Marín ND, Paris SC, Rojas M, García LF. Reduced Frequency of Memory T Cells and Increased Th17 Responses in Patients With Active Tuberculosis. *Clin Vaccine Immunol* (2012) 19(10):1667–76. doi: 10.1128/CVI.00390-12
40. Perreau M, Rozot V, Welles HC, Belluti-Enders F, Vigano S, Maillard M, et al. Lack of Mycobacterium Tuberculosis-Specific Interleukin-17A-Producing CD4+ T Cells in Active Disease. *Eur J Immunol* (2013) 43(4):939–48. doi: 10.1002/eji.201243090
41. Segueni N, Jacobs M, Ryffel B. Innate Type 1 Immune Response, But Not IL-17 Cells Control Tuberculosis Infection. *BioMed J* (2020) 207(8):1609–16. doi: 10.1016/j.bj.2020.06.011
42. Cruz A, Fraga AG, Fountain JJ, Rangel-Moreno J, Torrado E, Saraiva M, et al. Pathological Role of Interleukin 17 in Mice Subjected to Repeated BCG Vaccination After Infection With Mycobacterium Tuberculosis. *J Exp Med* (2010) 207(8):1609–16. doi: 10.1084/jem.20100265
43. Aguilo N, Alvarez-Arguedas S, Uranga S, Marinova D, Monzón M, Badiola J, et al. Pulmonary But Not Subcutaneous Delivery of BCG Vaccine Confers Protection to Tuberculosis-Susceptible Mice by an Interleukin 17-Dependent Mechanism. *J Infect Dis* (2016) 213(5):831–9. doi: 10.1093/infdis/jiv503
44. Counoupas C, Ferrell KC, Ashhurst A, Bhattacharyya ND, Nagalingam G, Stewart EL, et al. Mucosal Delivery of a Multistage Subunit Vaccine Promotes Development of Lung-Resident Memory T Cells and Affords Interleukin-17-Dependent Protection Against Pulmonary Tuberculosis. *NPJ Vaccines* (2020) 5(1):105. doi: 10.1038/s41541-020-00255-7

Conflict of Interest: The authors declare that the research was conducted in the absence of any commercial or financial relationships that could be construed as a potential conflict of interest.

Publisher's Note: All claims expressed in this article are solely those of the authors and do not necessarily represent those of their affiliated organizations, or those of the publisher, the editors and the reviewers. Any product that may be evaluated in this article, or claim that may be made by its manufacturer, is not guaranteed or endorsed by the publisher.

Copyright © 2021 Sharan, Singh, Rengarajan and Kaushal. This is an open-access article distributed under the terms of the Creative Commons Attribution License (CC BY). The use, distribution or reproduction in other forums is permitted, provided the original author(s) and the copyright owner(s) are credited and that the original publication in this journal is cited, in accordance with accepted academic practice. No use, distribution or reproduction is permitted which does not comply with these terms.

frontiers in Immunology

ORIGINAL RESEARCH
published: 30 August 2021
doi: 10.3389/fimmu.2021.712480

Mycobacterium tuberculosis-Specific T Cell Functional, Memory, and Activation Profiles in QuantiFERON-Reverters Are Consistent With Controlled Infection

Cheleka A. M. Mpande[1†], Pia Steigler[1,2†], Tessa Lloyd[1,3†], Virginie Rozot[1], Boitumelo Mosito[1], Constance Schreuder[1], Timothy D. Reid[1], Nicole Bilek[1], Morten Ruhwald[4,5], Jason R. Andrews[6], Mark Hatherill[1], Francesca Little[3], Thomas J. Scriba[1] and Elisa Nemes[1] on behalf of ACS Study Team[1]*

[1] South African Tuberculosis Vaccine Initiative, Institute of Infectious Disease and Molecular Medicine, Division of Immunology, Department of Pathology, University of Cape Town, Cape Town, South Africa, [2] Wellcome Centre for Infectious Diseases Research (CIDRI) in Africa, Institute of Infectious Disease and Molecular Medicine and Division of Immunology, Department of Medicine, University of Cape Town, Cape Town, South Africa, [3] Department of Statistical Sciences, University of Cape Town, Cape Town, South Africa, [4] Statens Serum Institut, Copenhagen, Denmark, [5] Foundation of Innovative New Diagnostics, Geneva, Switzerland, [6] Department of Medicine, Stanford University, Stanford, CA, United States

OPEN ACCESS

Edited by:
Julie G. Burel, La Jolla Institute for Immunology (LJI), United States

Reviewed by:
Jacqueline Margaret Cliff, University of London, United Kingdom
Delia Goletti, Istituto Nazionale per le Malattie Infettive Lazzaro Spallanzani (IRCCS), Italy

***Correspondence:**
Elisa Nemes
elisa.nemes@uct.ac.za

[†]These authors share first authorship

Specialty section:
This article was submitted to Microbial Immunology, a section of the journal Frontiers in Immunology

Received: *20 May 2021*
Accepted: *09 August 2021*
Published: *30 August 2021*

Citation:
Mpande CAM, Steigler P, Lloyd T, Rozot V, Mosito B, Schreuder C, Reid TD, Bilek N, Ruhwald M, Andrews JR, Hatherill M, Little F, Scriba TJ and Nemes E (2021) Mycobacterium tuberculosis-Specific T Cell Functional, Memory, and Activation Profiles in QuantiFERON-Reverters Are Consistent With Controlled Infection. Front. Immunol. 12:712480. doi: 10.3389/fimmu.2021.712480

Reversion of immune sensitization tests for *Mycobacterium tuberculosis* (M.tb) infection, such as interferon-gamma release assays or tuberculin skin test, has been reported in multiple studies. We hypothesized that QuantiFERON-TB Gold (QFT) reversion is associated with a decline of M.tb-specific functional T cell responses, and a distinct pattern of T cell and innate responses compared to persistent QFT+ and QFT- individuals. We compared groups of healthy adolescents (n=~30 each), defined by four, 6-monthly QFT tests: reverters (QFT+/+/-/-), non-converters (QFT-/-/-/-) and persistent positives (QFT+/+/+/+). We stimulated peripheral blood mononuclear cells with M.tb antigens (M.tb lysate; CFP-10/ESAT-6 and EspC/EspF/Rv2348 peptide pools) and measured M.tb-specific adaptive T cell memory, activation, and functional profiles; as well as functional innate (monocytes, natural killer cells), donor-unrestricted T cells (DURT: γδ T cells, mucosal-associated invariant T and natural killer T-like cells) and B cells by flow cytometry. Projection to latent space discriminant analysis was applied to determine features that best distinguished between QFT reverters, non-converters and persistent positives. No longitudinal changes in immune responses to M.tb were observed upon QFT reversion. M.tb-specific Th1 responses detected in reverters were of intermediate magnitude, higher than responses in QFT non-converters and lower than responses in persistent positives. About one third of reverters had a robust response to CFP-10/ESAT-6. Among those with measurable responses, lower proportions of T_{SCM} (CD45RA+CCR7+CD27+) and early differentiated (CD45RA-) IFN-γ-TNF+IL-2- M.tb lysate-specific CD4+ cells were observed in reverters compared with non-converters. Conversely, higher proportions of early differentiated and lower proportions of effector

(CD45RA-CCR7-) CFP10/ESAT6-specific Th1 cells were observed in reverters compared to persistent-positives. No differences in M.tb-specific innate, DURT or B cell functional responses were observed between the groups. Statistical modelling misclassified the majority of reverters as non-converters more frequently than they were correctly classified as reverters or misclassified as persistent positives. These findings suggest that QFT reversion occurs in a heterogeneous group of individuals with low M.tb-specific T cell responses. In some individuals QFT reversion may result from assay variability, while in others the magnitude and differentiation status of M.tb-specific Th1 cells are consistent with well-controlled M.tb infection.

Keywords: QuantiFERON reversion, memory T cell, donor unrestricted T cells, innate immune response, *Mycobacterium tuberculosis* infection

INTRODUCTION

Immunodiagnostics for *Mycobacterium tuberculosis* (M.tb) infection, such as tuberculin skin tests (TSTs) and IFN-γ release assays (IGRAs), were designed and are clinically interpreted based on the premise that detectable M.tb-specific immune responses are indicative of viable M.tb infection, i.e. bacterial persistence. Thus, asymptomatic M.tb infection in the absence of disease progression is commonly thought to be a chronic condition that may affect up to a quarter of the global population (1). However, longitudinal studies have demonstrated the dynamic nature of M.tb-specific immune responses, whereby TSTs and IGRAs revert from a positive to a negative test in some individuals.

Studies conducted during the pre-antibiotic era demonstrated that TST reversion was associated with a lower risk of disease progression. Detection of calcified lung lesions in some of these TST negative individuals, who had no recorded history of tuberculosis, was suggestive of contained or cleared disease (2). Guinea pigs that were infected with M.tb (defined by recent TST conversion upon experimental exposure) and then reverted to a negative TST had sterile lung lesions indicative of cured infection (3–5). These findings provide evidence that some individuals can spontaneously cure M.tb infection and gave rise to the hypothesis that reversion of immunodiagnostic test results may be associated with M.tb clearance. Reversion has been observed naturally (2, 6–14) and in association with antibiotic treatment (8, 13, 15, 16). Furthermore, a recent Bacille Calmette-Guerin (BCG) revaccination trial in M.tb-uninfected adolescents demonstrated vaccine efficacy against sustained M.tb infection, which was associated with transient IGRA conversion followed by reversion (IGRA- → IGRA+ → IGRA-) within a 6 month period (17). The phenomenon of IGRA reversions has posed challenges to clinicians making decisions about the need for preventive therapy, for which there is currently no guidance. Furthermore, as IGRA conversion is increasingly used as an outcome in vaccine trials, correctly interpreting reversions will be important to understanding vaccine efficacy.

IFN-γ, a T helper 1 (Th1) CD4 T cell associated cytokine, plays a critical role in the immune response to M.tb and is expressed by most M.tb-specific T cells (18, 19). Although many cell types have the capacity to produce IFN-γ, such as natural killer (NK) cells and donor-unrestricted T cells (DURT cells), including γδ T cells, mucosal-associated invariant T (MAIT) and natural killer T-like cells, IFN-γ expression by CD4 T cells is necessary for M.tb control (19, 20). Stimulation with M.tb CFP-10/ESAT-6 peptides in the IGRA primarily induces IFN-γ expression by MHC-class II restricted CD4 T cells (21), while DURT and NK cells contribute more significantly (approximately 50%) to IFN-γ production in response to whole mycobacteria, which also include non-protein antigens (22).

Functional and phenotypic characteristics of T cells, specifically CD4 T cells, are known to track antigen burden (23). We have recently demonstrated that relative proportions of M.tb lysate (cross-reactive with BCG)-specific IL-2+ and TNF+ stem cell memory (T_{SCM}) and central memory (T_{CM}) cells are higher in IGRA- compared to IGRA+ individuals, suggesting that low or no *in vivo* M.tb antigen exposure is associated with higher proportions of early differentiated mycobacteria-specific T cell subsets (24). These findings are supported by a study on resisters, tuberculosis household contacts (HHC) who remain TST and IGRA negative, showing that these individuals have detectable M.tb-specific antibodies and low levels of IFN-γ-independent (CD154+TNF+IL-2+) CD4 T cell responses (25). Expression of CD154, TNF and IL-2 is a hallmark of quiescent T_{SCM} and T_{CM} cells, which maintain long-lasting immunity in the absence of antigen exposure (23, 26). Further, we and others have demonstrated that high T cell activation, measured by CD38, HLA-DR or Ki-67 expression, is associated with recent M.tb infection, high risk to tuberculosis progression, or on-going tuberculosis disease (27–32). These data suggest that levels of M.tb-specific T cell activation are likely associated with M.tb antigen load, which in animal models peaks during primary infection, decreases to a plateau during established infection, and increases again during disease (33).

Acknowledging that measuring *in vivo* M.tb load in humans is not possible, we hypothesized that if reversion is associated with controlled infection this would be reflected in immune features associated with antigen load. Specifically, we would expect an increase in the relative proportions of M.tb-specific cells with T_{SCM} and T_{CM} phenotypes, IFN-γ-independent (CD154+, IL-2+ and/or TNF+) functional responses and lower

T cell activation in reverters compared to persistent QFT+ individuals. Since magnitude and functional profiles of antigen-specific T cells can be modulated by their interaction with innate cells, we further hypothesized that reverters would have reduced expression of pro-inflammatory cytokines (IFN-γ, IL-6 and/or TNF), increased expression of regulatory cytokines (IL-10) and/or reduced Th1 polarization (IL-12) by innate immune cells compared to persistently QFT+ individuals.

To test our hypotheses, we measured memory and functional profiles of M.tb-specific T cells, and functional features of myeloid, NK, DURT and B cells in persistent IGRA+ individuals, reverters and non-converters. We further integrated features from both adaptive and innate immune responses and applied statistical modelling to define the relationship between IGRA reverters, persistent IGRA+ individuals and non-converters.

METHODS

Study Design

South African adolescent participants were selected from a large epidemiological study conducted in the Worcester region of Western Cape, South Africa, between July 2005 and February 2009 [University of Cape Town Human Research Ethics Committee protocol references: 045/2005, 102/2017; (34)]. All adolescents were assumed to be BCG vaccinated at birth, according to the South African expanded program of immunization. M.tb infection status was determined using QuantiFERON-TB Gold In-Tube (QFT, Qiagen) and peripheral blood mononuclear cells (PBMC) were collected at enrolment and at 6-monthly intervals during 2 years of follow-up in a subset of the cohort. TST was also performed at yearly intervals. Adolescent participants provided written, informed assent and their parents or legal guardians provided written, informed consent. All participants were between 12-18 years old and enrolled at public high schools. Participants who were pregnant, lactating or who had chronic medical conditions at enrolment were excluded. We retrieved stored PBMC from healthy adolescents based on serial QFT test results, as defined below, and sample availability.

Definition of Study Groups

QFT reverters were defined as adolescents with two positive QFT tests followed by two negative QFT tests 6 months apart (**Supplementary Figure 1**). To reduce the likelihood of technical fluctuations around the assay cut-off, we selected reverters with at least one QFT positive and one negative test result outside the QFT uncertainty zone: 0.2-0.7 IU/mL [**Supplementary Figure 1**; (35)], wherever possible.

Persistent QFT+ individuals had 4 consecutive QFT positive tests, at least two of which with IFN-γ >0.7 IU/mL, 6 months apart over 18 months. This group has been described in detail in [(24, 36); **Supplementary Figure 1**].

QFT non-converter adolescents had 4 consecutive QFT negative tests (< 0.2 IU/mL) 6 months apart (**Supplementary Figure 1**). QFT non-converters were not selected based on TB exposure history, in this high transmission setting, and likely include a heterogeneous population of naïve participants, as well as previous TB exposed but uninfected individuals. Only 4 non-converters reported past TB exposure (all more than 1 year prior to study enrolment, **Supplementary Table 1**). We chose an upper limit of QFT response of 0.2 IU/mL, below the QFT uncertainty zone, to increase the likelihood that these individuals were truly M.tb "unsensitized" at the time of sampling, and could represent a meaningful negative control group.

Control groups (non-converters and persistent QFT+) were randomly selected from a pool of participants with available samples and matched to QFT reverters based on age at enrolment (± 1 years), gender, ethnicity and school [which relates to socio-economic and M.tb exposure status (37), **Supplementary Table 1**].

Measurement of M.tb-Reactive Adaptive and Innate Cells

M.tb-reactive adaptive (T cells) and innate cells [monocytes, NK, DURT and B cells (in their antigen-presenting cell capacity)] were detected using two different PBMC intracellular cytokine staining (ICS) and flow cytometry protocols.

The adaptive T cell protocol has been previously described in detail (24). Briefly, cryopreserved PBMC were stimulated with no antigen, peptide pools (15 mer peptides overlapping by ten amino-acids, 1μg/mL) spanning the full length of CFP-10/ESAT-6 (antigens in the QFT assay, GenScript Biotechnology) or Rv3615c (EspC) (33), Rv2348 and Rv3865 (EspF) (collectively referred to as EspC/EspF/Rv2348 peptide pool, GenScript Biotechnology), M.tb lysate (H37Rv, 10μg/mL, BEI resources) or Staphylococcus enterotoxin B [SEB (positive control), 1μg/mL, Sigma Aldrich] for 18 hours, with brefeldin A (5μg/mL, Sigma Aldrich) and monensin (2.5μg/mL, Sigma Aldrich) added after the first 3 hours of stimulation.

For the innate PBMC-ICS protocol, cryopreserved PBMC were stimulated with no antigen, M.tb lysate (H37Rv, 10μg/mL, BEI resources) or heat-killed Escherichia coli (*E.coli*, 10^7 bacteria per 10^6 PBMC, in-house preparation) for 6 hours, with brefeldin A (5μg/mL, Sigma Aldrich) and monensin (2.5μg/mL, Sigma Aldrich) added after the first 2 hours of stimulation (see **Supplementary Methods** for details).

Cells were then stained with fluorescent-labelled antibodies (**Supplementary Tables 2, 3**) and detected using flow cytometry to identify phenotypic marker and cytokine expression.

Data Analysis

Adaptive T Cell Analysis Pipeline

M.tb-specific lymphocytes, CD4 and CD8 T cells stimulated using the adaptive T cell protocol were identified using the gating strategy illustrated in **Supplementary Figure 2**. Most analyses from the adaptive T cell protocol focused on CD4 T cells because CD8 T cell responses were predominantly not different to background response in most individuals (data not shown). We then followed the analysis pipeline previously described (24): we utilized COMPASS (38), Pestle and SPICE (39) to

analyze expression of all antigen-specific cytokine combinations. We then identified individuals, referred to as responders, with total IFN-γ+ lymphocyte or Th1 cytokine+ CD4 T cell responses significantly [false discovery rate (FDR) ≤ 0.01] higher than background (unstimulated) using MIMOSA (40) and a fold-change over background ≥ 3. Since we had longitudinal samples, we applied the responder definition to each study visit for each participant. To prevent the introduction of bias, we first determined if frequencies of IFN-γ+ lymphocytes or Th1 cytokine+ CD4 T cells were significantly different between visits stratified by QFT status (detailed in Supplementary methods; **Supplementary Figure 3**). We then exported FCS files of IFN-γ+ lymphocytes or Th1 cytokine+ CD4 T cells from all visits that passed the responder criteria and concatenated FCS files based on QFT status to get a representative FCS file for each participant-QFT status combination (**Supplementary Figure 4**). Concatenated FCS files containing IFN-γ+ lymphocytes were used for tSNE analysis to identify cell clusters contributing to the total IFN-γ+ lymphocyte response (detailed in Supplementary Methods). Th1 cytokine+ CD4 T cells were used for CITRUS analysis to identify unique T cell features that could distinguish between two groups, *i.e.* persistent QFT+ *versus* pre-reverter, pre- *versus* post-reverter and post-reverter *versus* non-converter [**Supplementary Figure 5**; (41)]. We also used Th1 cytokine CD4 T cell responses to calculate functional differentiation score [**Supplementary Equation 1**; (42)].

Innate Cell Analysis Pipeline

M.tb-specific innate (monocytes and NK cells), DURT, B cells and T cells stimulated using the innate PBMC-ICS protocol were identified using the gating strategy illustrated in **Supplementary Figure 6**. Since spontaneous cytokine expression was detected in several innate cell subsets, as expected, analyses included responses measured in unstimulated samples, stimulated samples, as well as stimulated minus unstimulated samples. Since our flow cytometry panel included several functions that are known not to be expressed by all the cell subsets measured (i.e. are biologically irrelevant) we excluded variables that were not measurable in two-thirds of the samples [details about data filtering are provided in (43)]. Additional information about tSNE analyses of this dataset is provided in the **Supplementary Methods**.

Statistical Analysis

The adaptive T cell experimental protocol was performed on all study participant visits, where possible, while the innate protocol was performed on PBMC from all reverters visits, were possible, but on only two (consecutive) visits from persistent QFT+ individuals and non-converters. To prevent the introduction of bias due to repeated sampling from the same donor, we calculated a representative functional response based on QFT status for each individual. Firstly, to determine if functional responses (single cytokine, co-expression patterns, etc.) were significantly different between visits stratified by QFT status, we performed a Kruskal-Wallis test to compare responses detected at all 4 QFT negative and positive visits in non-converters and persistent QFT+, respectively (**Supplementary Figures 3A, B**). Wilcoxon signed-rank tests were used to compare functional responses detected at paired QFT negative and QFT positive visits in reverters (**Supplementary Figure 3C**). If none of the functional responses were significantly different ($p > 0.05$) between visits with the same QFT status, we calculated the median response for each participant based on QFT status. This resulted in a single value for each QFT non-converter and persistent QFT+ individual, and two values for QFT reverters according to QFT status (QFT+ = pre-reverter and QFT- = post-reverter), which were then used for inter- and intra-group comparisons: persistent QFT+ *vs* pre-reverter (Mann-Whitney test); pre- *vs* post-reverter (Wilcoxon signed-rank test) and post-reverter *vs* non-converter (Mann-Whitney test).

Bonferroni and Benjamini-Hochberg (FDR <0.05) methods were used to correct for multiple comparisons for up to 4 comparisons or more than 4 comparisons, respectively.

Projection to Latent Space Discriminant Analysis Modelling Pipeline

Several data pre-processing steps were applied prior to building the projection to latent space discriminant analysis (PLS-DA) (30) model, detailed in the **Supplementary Methods**.

Feature Selection

We tuned and built a least absolute shrinkage and selection operator (LASSO) model (44) to the integrated dataset in order to identify features that could stratify the two control groups (persistent QFT+ and non-converters) in the model. The model was therefore blinded to the differences between the reverters and the control cohorts. 10-fold cross-validation (CV) was repeated 500 times and the optimal shrinkage parameter, λ, was defined as the average λ across the 500 repeats. The final LASSO model was built using the optimal value of λ and the most stratifying features were identified as the non-zero coefficients in the final model.

PLS-DA

PLS-DA is a classification model that aims to classify samples into known groups and identify variables that drive the discrimination between the groups. The PLS-DA model (45) was built within the *ropls* R package (R package version 1.22.0. doi:10.18129/B9.bioc.ropls) to the vast standardized and MFA-imputed dataset containing the features selected by the LASSO model. The group status, namely persistent QFT positive, pre-reversion, post-reversion and non-converter, was defined as the response.

Model Validation

The performance of the PLS-DA model was assessed *via* a cross-validation procedure. For 1000 bootstrapped samples, 70% of the observations were set aside to make up the training set, and the remaining 30% the testing set. For each iteration, the data was split such that there were equal proportions of the four groups in the testing set (10 observations per group). The PLS-DA model was built to the training set of observations and the test set was used to assess the ability of the model to predict a new outcome based on

its training. The performance was reported as the average misclassification error across the 1000 bootstrapped iterations.

RESULTS

TST Dynamics

We defined M.tb infection using QFT only, but also had access to TST results, which were performed annually. We therefore determined the concordance between QFT and TST for each study group. We observed very good concordance of 95% and 88% between QFT and TST in persistent QFT+ individuals and non-converters, respectively (**Supplementary Figure 7**; **Supplementary Table 4**). However, the majority of QFT reverters were persistently TST+ throughout follow up, which resulted in a poor concordance between QFT and TST tests, with a 45% agreement between the two immuno-diagnostics (**Supplementary Figure 7**; **Supplementary Table 4**).

QFT Reversion Is Associated With Maintenance of Functional M.tb-Specific CD4+ T Cells

We utilized tSNE analysis to determine the cellular composition of CFP-10/ESAT-6- and M.tb lysate-specific IFN-γ+ lymphocytes in responders only. Too few reverters and non-converters had a robust IFN-γ+ lymphocyte response to CFP-10/ESAT-6 to be included in this analysis (**Supplementary Table 5**). tSNE analysis (and confirmatory flow cytometry gating) confirmed CD4 T cells as the major source of IFN-γ in persistent QFT+ individuals (regardless of stimuli) and (pre- and post-) reversion, while CD4 T cells accounted for <50% of M.tb lysate-specific IFN-γ+ lymphocytes in non-converters (**Supplementary Figure 8**). Based on these results, we decided to focus our T cell analysis on CD4 T cells.

Our experimental protocol detected CFP-10/ESAT-6-specific IFN-γ+ CD4 T cells that highly correlated with QFT responses (**Figure 1A**), confirming that PBMC-ICS and flow cytometry were suitable techniques to characterize M.tb-specific immune responses detected by QFT. However, CFP-10/ESAT-6-specific IFN-γ+ CD4 T cells did not decrease upon QFT reversion, and frequencies of these cells were maintained at similar levels throughout the study follow-up and did not correlate with quantitative QFT values (**Figures 1A, B**). Some QFT reverters (n=8) had either both pre-reversion or post-reversion QFT values within the uncertainty zone (**Supplementary Figure 1**). Regardless, the frequencies of their CFP-10/ESAT-6-specific IFN-γ+ CD4 T cells fell in the same dynamic range and showed no change over time as participants with at least one QFT positive value above 0.7 IU/mL and one QFT negative value below 0.2 IU/mL (data not shown). Since we did not observe a difference in frequencies of IFN-γ+ CD4 T cells across different visits, we calculated median responses for each participant stratified by QFT status. No significant differences in CFP-10/ESAT-6-specific IFN-γ+ CD4 T cells, nor IFN-γ+ CD8 T cells or IFN-γ+ lymphocytes, were observed pre- and post-reversion (**Figure 1C**).

We then determined whether recognition of other M.tb-specific immunodominant antigens or expression of IFN-γ-independent cytokines were also maintained in reverters. EspC/EspF/Rv2348- and M.tb lysate-specific IFN-γ+ CD4 T cells did not significantly decrease upon QFT reversion (**Figure 1D**). Frequencies of CFP-10/ESAT-6- and M.tb lysate-specific IFN-γ+ CD4 T cells detected pre-reversion were significantly lower than those in persistent QFT+ individuals, while those detected post-reversion were significantly higher than non-converters, respectively (**Figure 1D**). On the other hand, the magnitude of EspC/EspF/Rv2348-specific IFN-γ+ CD4 T cells observed pre- and post-QFT reversion was similar to persistent QFT+ individuals and non-converters, respectively (**Figure 1D**), probably due to high variability. Lastly, as observed for IFN-γ+ CD4 T cells, frequencies of TNF+ and IL-2+ CFP10-/ESAT-6-specific CD4 T cells did not decrease upon QFT reversion, and responses detected in reverters were of intermediate magnitude between non-converters and persistent QFT+ (**Supplementary Figure 9A**). The magnitude of CD154+ and CD107+ CFP10-/ESAT-6-specific CD4 T cells was not different between groups. (**Supplementary Figure 9A**).

Next, we investigated changes in M.tb-specific CD4 T cell cytokine co-expression profiles, and specifically whether QFT reversion was associated with preferential maintenance of IFN-γ-independent responses (observed in resisters) compared to persistent QFT+ individuals. The probability of detecting polyfunctional responses [polyfunctionality score calculated by COMPASS (38)] and frequencies of cytokine co-expressing CD4 T cell subsets were not significantly different pre- and post-reversion, with no enrichment of IFN-γ-CD154+TNF+IL-2+ CD4 T cells (**Figures 2A, B** and **Supplementary Figure 9B**). Group comparisons confirmed previous observations, where CFP-10/ESAT-6 polyfunctionality scores and the frequencies of IFN-γ+ co-expressing M.tb-specific cells in reverters were lower than persistent QFT+ individuals but higher than non-converters (**Figures 2A, B** and **Supplementary Figures 9B**). Exceptions to this were comparable M.tb lysate-specific polyfunctionality scores and frequencies of CFP-10/ESAT-6 IFN-γ- CD4 T cell subsets (including CD154+TNF+IL-2+) between persistent QFT+ individuals and pre-reverters (**Figures 2A, B** and **Supplementary Figure 9B**).

Further characterization of M.tb-specific CD4 T cells focused only on participants with robust Th1 responses (**Supplementary Table 6**), and only groups with at least one third of participants with a Th1 response were included. Definition of "responders" ignored expression of CD154 and CD107 because of their high background in unstimulated samples. Based on these arbitrary criteria, CFP-10/ESAT-6-specific responses in non-converters and EspC/EspF/Rv2348-specific responses in all groups were not further studied. Importantly, only 30-40% reverters had robust responses to CFP-10/ESAT-6, which were detectable in 97% of persistent QFT+ individuals.

Next, we compared proportions of Th1 cells expressing different combinations of IFN-γ, TNF and IL-2 in responders only. IFN-γ- CD4 T cells accounted for less than a quarter of M.tb lysate-specific CD4 T cells in persistent QFT+ individuals and reverters, compared to almost 40% of M.tb lysate-specific CD4 T cells in non-converters and only minor differences were observed across the study groups (**Supplementary Figure 10A**).

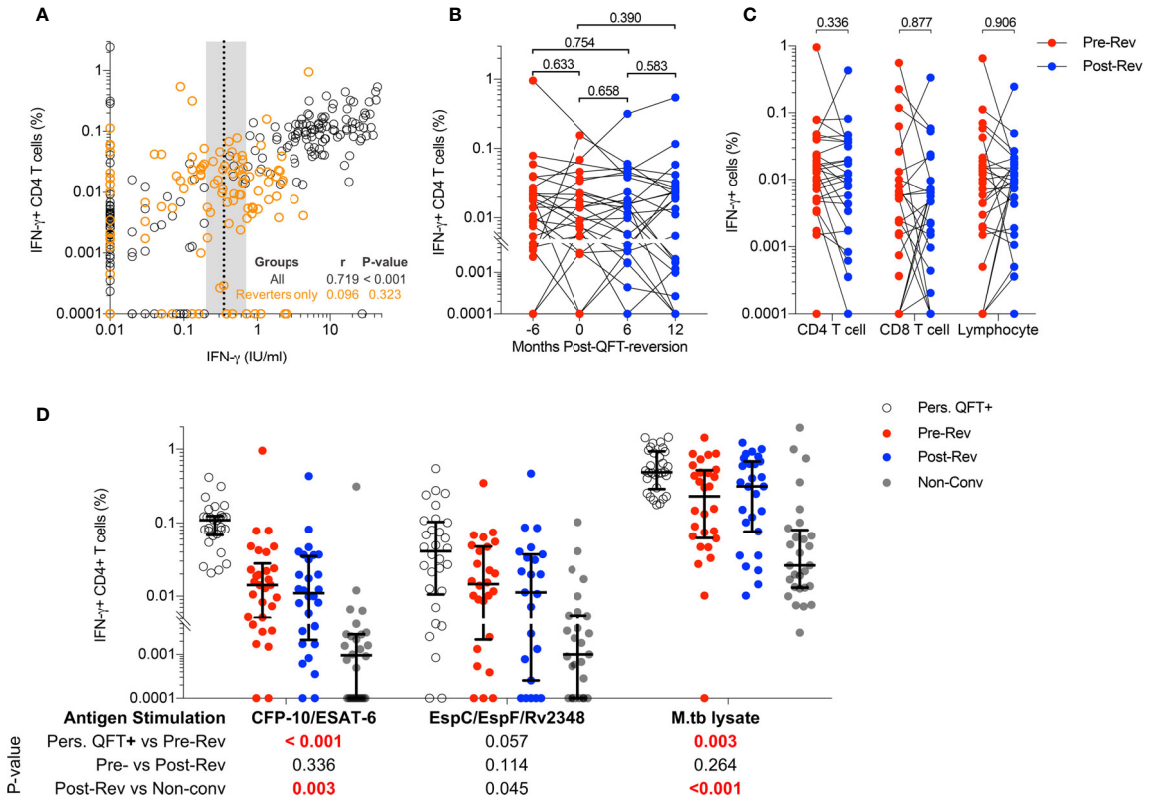

FIGURE 1 | Immunodominant M.tb-specific IFN-γ+ CD4 T cells are maintained during QFT reversion. **(A)** Immune responses detected by flow cytometry (% of CFP-10/ESAT-6-specific IFN-γ+ CD4 T cells) and QFT-ELISA (IFN-γ+ IU/mL). All participants and all visits are shown (n = 321). Dotted line and shaded area represent the QFT cut-off (0.35 IU/mL) and the uncertainty zone (0.2-0.7 IU/mL), respectively. The Spearman's correlation coefficient (r) was calculated on the entire cohort (black) and reverters only (orange). **(B)** Frequencies of background subtracted CFP-10/ESAT-6-specific IFN-γ+ CD4 T cells detected in QFT reverters at Month -6: n = 26 (QFT+, red symbol), Month 0: n = 25 (QFT+, red symbol), Month 6: n = 28 (QFT-, blue symbol) and Month 12: n = 26 (QFT-, blue symbol) post QFT reversions. **(C)** Median frequencies of CFP-10/ESAT-6-specific IFN-γ+ among CD4 and CD8 T cells and total lymphocytes, measured pre- (n = 30, red symbol) and post- (n = 28, blue symbol) QFT reversion. **(D)** CFP-10/ESAT-6- (P10-ES6), EspC/EspF/Rv2348- (Esp) and M.tb lysate- (M.tbL) specific IFN-γ+ CD4 T cells detected in persistent QFT+ individuals (P10-ES6: n = 29; Esp: n = 30; M.tbL: n = 30, white), pre-reversion (P10-ES6: n = 30; Esp: n = 26; M.tbL: n = 28, red), post-reversion (P10-ES6: n = 28; Esp: n = 23; M.tbL: n = 27, blue) and non-converters (P10-ES6: n = 28; Esp: n = 27; M.tbL: n = 28, grey). P-values were calculated using the Wilcoxon signed rank test for comparison of responses from reverters only, and Mann-Whitney test for persistent QFT+ *vs* pre-reversion and post-reversion *vs* non-converters. P-values < 0.05 for **(A)**, < 0.01 for **(B)** and < 0.0125 (for **C, D**) were considered significant after correction for multiple comparisons.

On the other hand, more than half of CFP-10/ESAT-6-specific responses in reverters were IFN-γ-, compared to less than 30% in persistent QFT+ individuals. Additionally, pre-reverters exhibited higher proportions of CFP-10/ESAT-6-specific IFN-γ-TNF+IL-2±, but lower proportions of IFN-γ+TNF+IL-2± compared with persistent QFT+ (**Supplementary Figure 10A**). Overall, reverters had a lower functional differentiation score compared to persistent QFT+ individuals in response to CFP-10/ESAT-6 and a higher functional differentiation score compared to non-converters in response to M.tb lysate (**Figure 2C**).

Taken together, these results suggest that although functional responses to diverse M.tb antigens are maintained even upon QFT reversion, reverters have intermediate magnitudes of M.tb-specific CD4 T cells responses and these cells are in intermediate states of functional differentiation compared to persistent QFT+ and non-converters.

QFT Reversion Is Not Associated With a Shift Towards a Less Differentiated T Cell Memory Phenotype

Less differentiated T cell memory and IFN-γ- functional phenotypes have been associated with lower antigen loads (23, 42). To determine if this is also true for M.tb-specific CD4 T cells during QFT reversion, we measured the proportions of M.tb-specific Th1 cells expressing different memory phenotypes in reverters and compared them to control groups. We defined memory subsets based on co-expression of CD45RA (RA), CCR7 (R7), CD27 (27) and KLRG-1 (G1). The predominant memory subsets in all groups, regardless of stimulation, were transitional (T_{TM}) and effector (T_E) memory T cells (**Supplementary Figure 10B**). We observed higher proportions of CFP-10/ESAT-6-specific T_{CM} cells in pre-reverters than in persistent QFT+ individuals, and lower proportions of M.tb lysate-specific

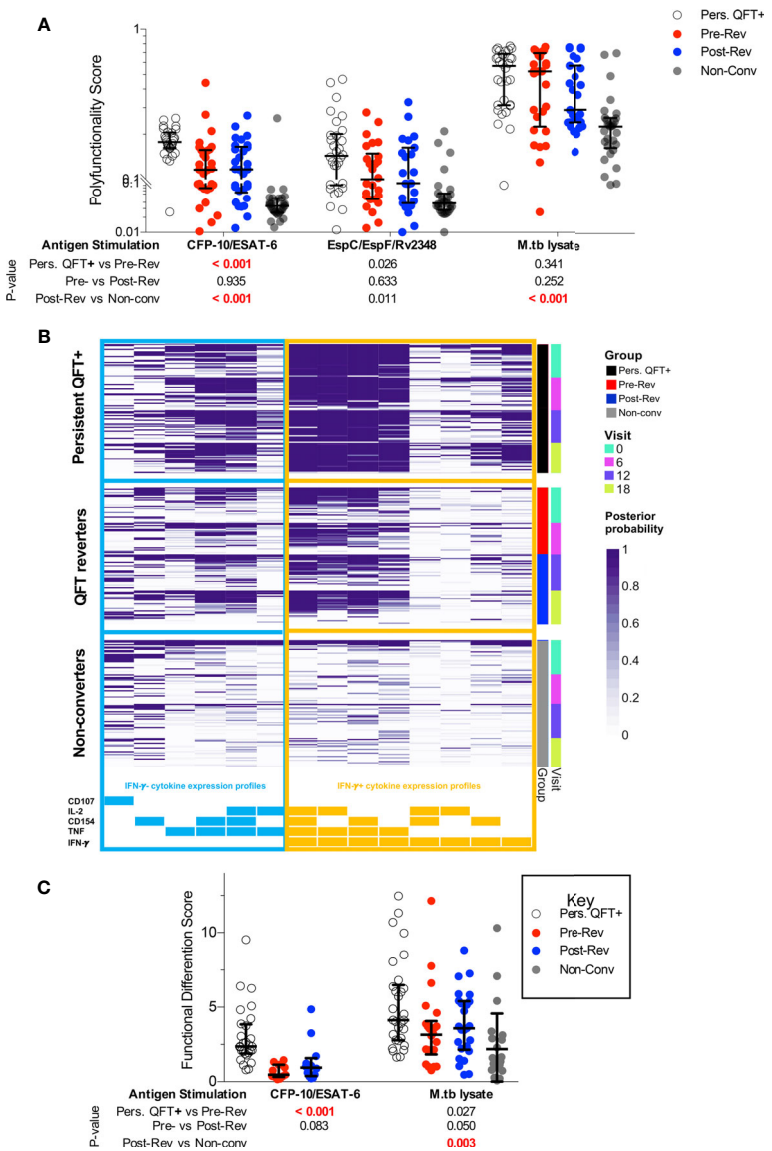

FIGURE 2 | Functional profiles of M.tb-specific CD4 T cells are maintained during QFT reversion. **(A)** CFP-10/ESAT-6-, EspC/EspF/Rv2348- and M.tb lysate-specific polyfunctionality scores calculated by COMPASS. **(B)** Posterior probabilities (purple shading) of detecting CFP-10/ESAT-6-specific CD4 T cells expressing different combinations of functional markers, as indicated at the bottom. Subsets including IFN-γ- cytokine expression profiles are grouped on the left (blue) and those including IFN-γ+ subsets are shown on the right (orange). All participants from all study groups and visits are shown. **(C)** Functional differentiation score (**Supplementary Equation 1**) of M.tb-specific CD4 T cells in persistent QFT+ (P10-ES6: n = 28; M.tbL: n = 30), pre-reversion (P10-ES6: n = 11; M.tbL: n = 22), post-reversion (P10-ES6: n = 12; M.tbL: n = 25) and non-converters (M.tbL: n = 24). Number of participants for **(A, B)**, and calculation of P-values are as in **Figure 1**. P-values highlighted in bold red were considered significant.

T_{SCM} cells post-reversion compared with non-converters (**Supplementary Figure 10B**).

To obtain more granular results, we next evaluated whether a combination of memory and functional markers could be used to identify subsets that were significantly different between groups using an unbiased approach, CITRUS [as described in (24)]. The composition of each differentially expressed T cell cluster (**Supplementary Table 7**) identified using CITRUS, was confirmed by manual gating on all responders (**Supplementary Figure 5B**).

In line with previous analyses, pre-reverters showed higher proportions of CFP-10/ESAT-6-specific early differentiated IFN-γ- Th1 cells, and lower proportions of more differentiated effector IFN-γ+ Th1 cells compared to persistent QFT+ individuals (**Figure 3A**).

Despite detecting differences in cellular composition using CITRUS, proportions of manually gated CFP-10/ESAT-6-specific early differentiated CD27+TNF+ Th1 cells (cluster 932) were not significantly different pre- *versus* post-reversion

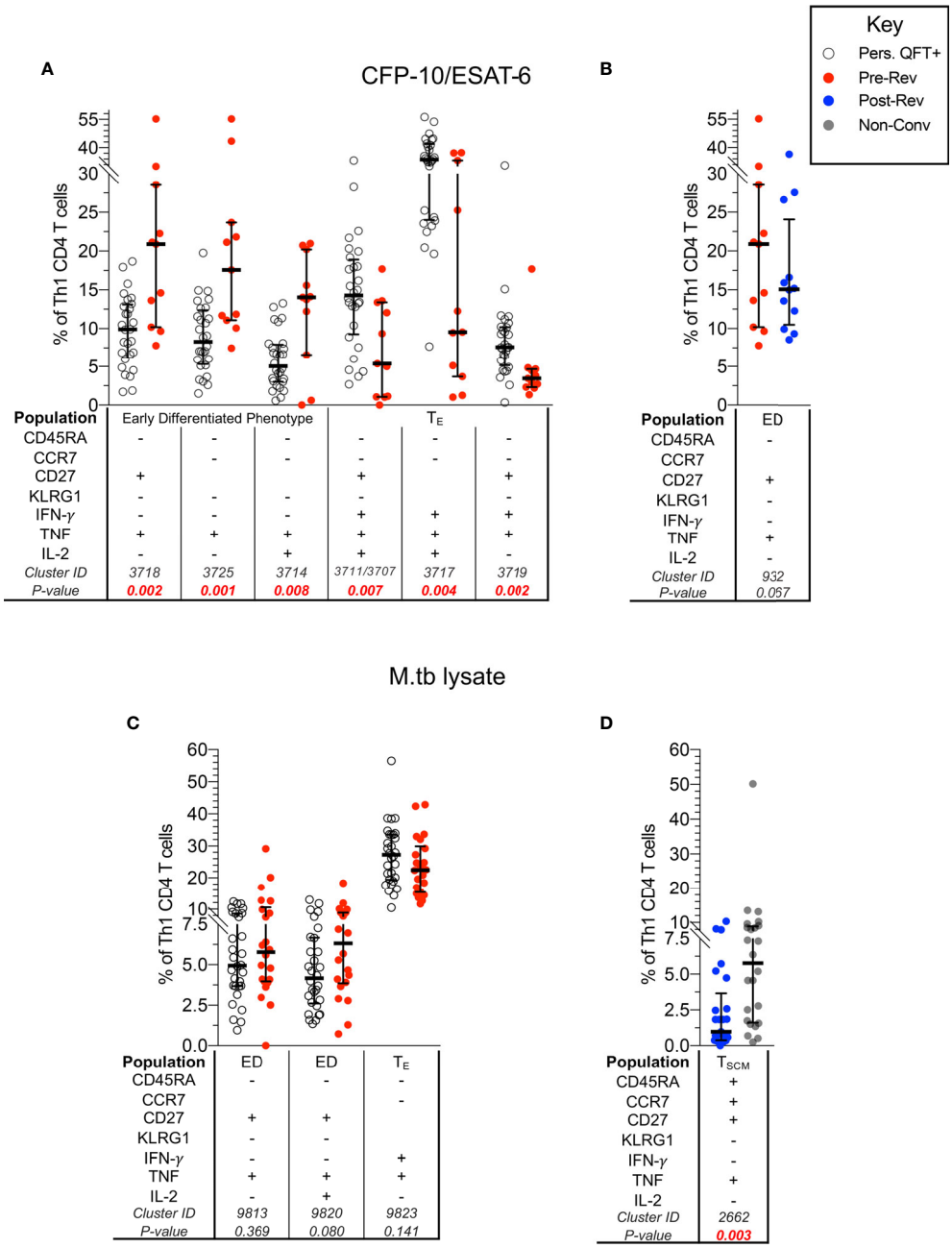

FIGURE 3 | CFP-10/ESAT-6-specific memory/functional co-expression patterns are different between persistent QFT+ and reverters. Scatter plots (with medians and inter-quartile ranges) of manually gated memory and functional markers combinations representing CITRUS clusters that were different between: CFP-10/ESAT-6-specific CD4 T cells in **(A)** persistent QFT+ *versus* pre-reverters and **(B)** pre- *versus* post-reverters, and M.tb lysate-specific CD4 T cells in **(C)** persistent QFT+ *versus* pre-reverters and **(D)** post-reverters *versus* non-converters. Number of participants, confirmatory statistical analysis and p-value calculations is as in **Figure 2C**.

(p = 0.067; **Figure 3B**). Similarly, the 3 M.tb lysate-specific clusters identified by CITRUS as differentially expressed in persistent QFT+ compared to pre-reverters were not different when gated manually (p > 0.05; **Figure 3C**). On the other hand, we confirmed lower proportions of M.tb lysate-specific TNF+ T_{SCM} (cluster 2662) cells in post-reverters compared to non-converters (**Figure 3D**), while no other differences were detected between these 2 groups.

Based on these results, we can conclude that M.tb-specific CD4+ T cells from QFT reverters are less differentiated compared to persistent QFT individuals, and are more similar to non-converters.

QFT Reversion Is Not Associated With a Decrease in T Cell Activation

Results described above suggest that QFT reversion was not associated with a decrease in functional activity nor a change in T cell memory subsets. Since we and others have shown that T cell activation may correlate with M.tb bacterial burden (29, 31, 36), we determined whether QFT reversion was associated with a decrease in T cell activation. Overall, no difference in proportions of activated (HLA-DR+) M.tb-specific (Th1 cytokine+) CD4 T cells, regardless of stimulation, were detected pre- and post-reversion, as well as compared to persistent QFT+ individual and non-converters (**Figure 4**).

QFT Reversion Is Not Associated With Modulation of Innate, DURT, and B Cell Responses

Since multiple cell types can contribute to IFN-γ production in response to mycobacteria, including NK and DURT cells, and innate cells can also modulate IFN-γ expression in classical T cells, we further explored the potential role of these cells in QFT reversion.

To confirm the capability of innate, DURT and B cell subsets to produce IFN-γ+ in response to *M.tb*, we utilized tSNE analysis (**Supplementary Figure 11**) (46, 47). NK cells, classical CD3+ T cells and MAIT cells were the main contributors to lymphocyte IFN-γ expression in response to M.tb lysate stimulation (**Supplementary Figures 11A, B**). As expected, spontaneous IFN-γ expression in unstimulated samples was mostly detected in NK cells, some T cell subsets and, surprisingly, B cells. NK and γδ T cells were the two major IFN-γ producers in response to *E. coli*.

We further used tSNE analysis to visualize which other cytokines innate, DURT and B cell subsets produce in response to M.tb lysate in all participants combined (**Supplementary Figure 12**) or reverters only (**Figure 5A**). Granzyme B in combination with IFN-γ and/or TNF was mostly expressed by NK cells; IFN-γ was expressed by NK and most T cell subsets; IL-6 was expressed by MAIT, some B cells and "ungated" cells (probably CD14- myeloid cells); TNF was expressed by NK cells, MAIT, classical T cells and B cells. The expression of IL-10 and IL-12 was very low and variable in all cell types in response to M.tb stimulation.

To compare innate, DURT and B cell responses longitudinally in reverters and cross-sectionally across study groups, frequencies of cytokine+ cells in unstimulated samples were subtracted from those in the M.tb lysate-stimulated samples. For cell types expressing multiple functional markers, co-expression profiles were also evaluated (data not shown). We found no statistical differences in innate, DURT and B cell responses over time in reverters, nor when reverters were compared with persistent QFT+ and non-converters (**Figure 5B** and data not shown). Except for monocytes, responses were generally low and variable, and unfortunately only half the number of participants in each group could be included in this analysis.

Overall, we confirmed that M.tb lysate induces cytokine production by innate, DURT and B cells, however, these functional responses did not differ upon QFT reversion or across study groups in the small subset of participants included in this analysis.

QFT Reverters Are More Similar to Non-Converters Than Persistent QFT+ Individuals

To further explore the relationship between QFT reverters and the control groups, the two (adaptive and innate) datasets were integrated and fitted to a PLS-DA model using LASSO selected features (**Figure 6**). The feature selection was based on persistent QFT+ and non-converters, then the model was applied to the reverters to evaluate whether they constituted a distinct population from the control groups. The LASSO model, blinded to the QFT reverters, identified seven stratifying features (all from the adaptive dataset) that could best distinguish persistent QFT+ and non-converters (**Figure 6B**, right). Using these seven features as exploratory variables and the four groups (persistent QFT+, pre-reverters, post-reverters

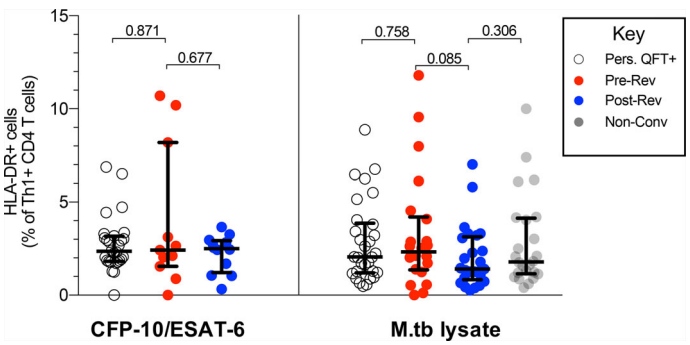

FIGURE 4 | QFT reversion is not associated with a decrease in T cell activation. Graphs depict proportions of HLA-DR+ CFP-10/ESAT-6- and M.tb lysate- specific Th1 cytokine+ CD4 T cells in persistent QFT+, pre-and post-reverters and non-converters. Number of participants in each group, confirmatory statistical analysis and p-value calculations is as in **Figure 2C**.

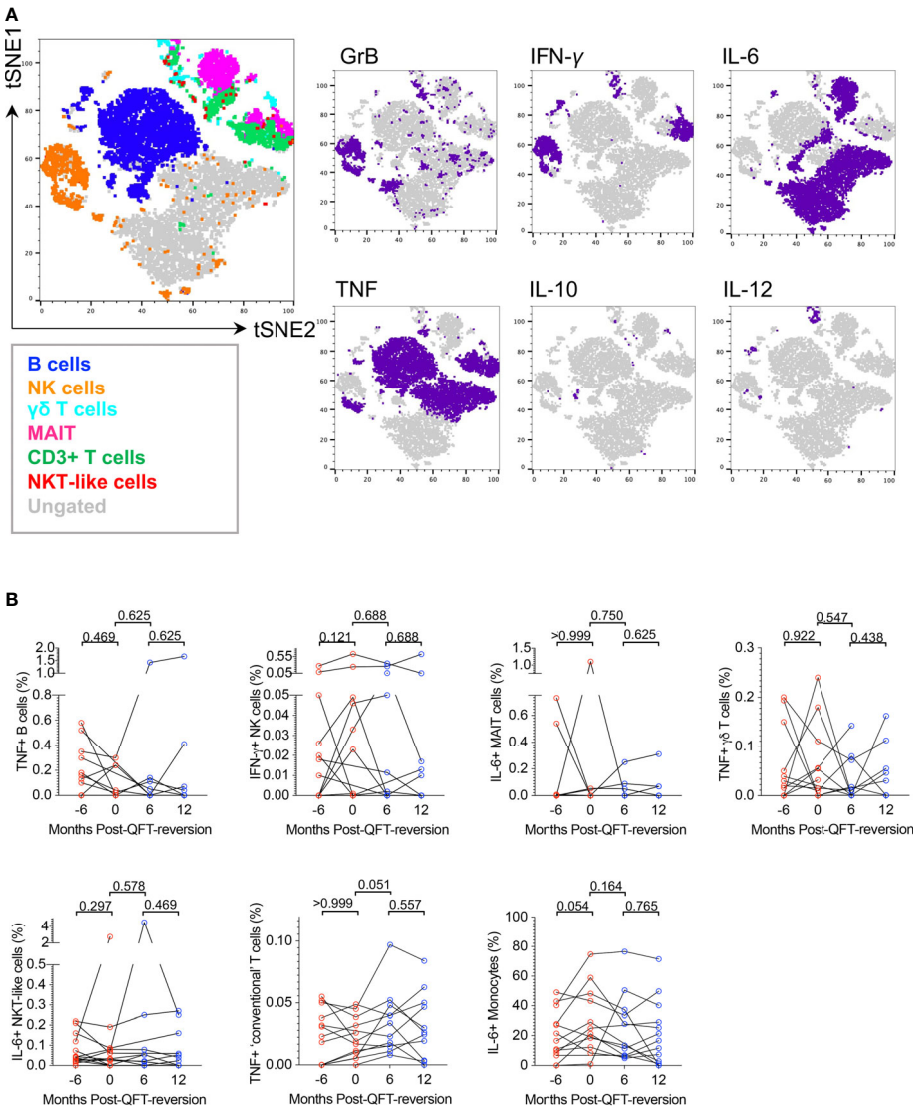

FIGURE 5 | M.tb lysate-reactive innate, DURT and B cell responses do not change upon QFT reversion. **(A)** tSNE visualization of M.tb-reactive lymphocyte cell subsets expressing any cytokine (Granzyme B (GrB), IL-6, IL-10, IL-12, IFN-γ, TNF) in QFT reverters (all visits included). **(B)** Background-subtracted frequencies of M.tb-reactive TNF+ B cells, IFN-γ+ NK cells, IL-6+ MAIT cells, TNF+ γδ T cells, IL-6+ NKT-like cells, TNF+ T cells and IL-6+ monocytes detected pre- and post-reversion. Month -6: n = 13 (QFT+, red symbol), Month 0: n = 11 (QFT+, red symbol), Month 6: n = 11 (QFT-, blue symbol) and Month 12: n = 11 (QFT-, blue symbol). P values were calculated by Wilcoxon signed rank test and $p < 0.017$ were considered significant.

and non-converters) as a response, a PLS-DA model was built to the vast scaled and MFA-imputed integrated dataset. In two dimensions, the model captured 71% of the total variability and was able to successfully separate persistent QFT+ and non-converter observations. The pre- and post-reversion groups greatly overlapped with each other and were positioned in between the controls (**Figure 6A**). The reverters, regardless of QFT status, had intermediate loading scores on latent component one, which were significantly different from both control groups (**Figure 6B**, left). The persistent QFT positives loaded negatively on the first component and the top variables that drove this were two CFP-10/ESAT-6-specific IFN-γ+ CD4+ T cell subsets. The non-converters, on the other hand, loaded positively on the first component and the expression of CCR7 on M.tb-lysate-specific total Th1 cells drove this separation (**Figure 6B**, right). The second latent component, which captured 21% of the total variability, could successfully separate the persistent QFT positives from the other three groups, but failed to differentiate the non-converters from the QFT reverters (**Supplementary Figure 13A**). The main features distinguishing reverters and non-converters from persistent QFT+ were M.tb lysate-specific IFN-γ- CD4 T cells (**Supplementary Figure 13B**).

The performance of this PLS-DA model was then assessed *via* a cross-validation procedure and the average misclassification error

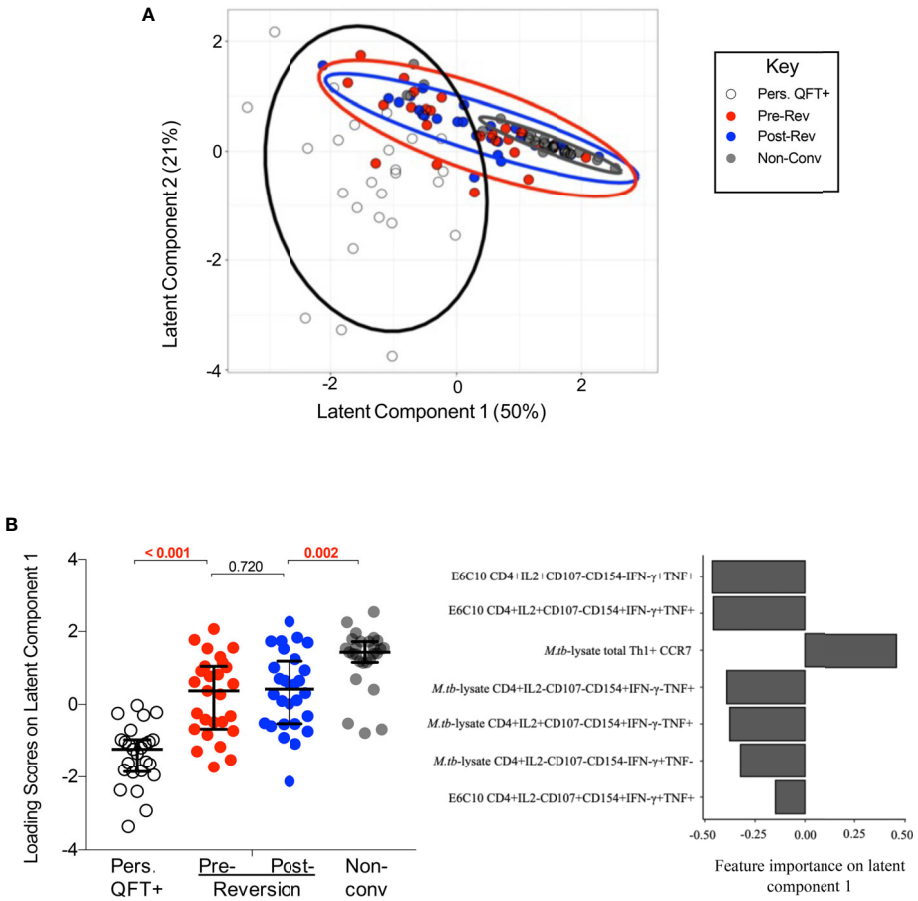

C

% correctly classified		PREDICTED			
		Pers. QFT+	Pre-Rev	Post-Rev	Non-conv
TRUE	Pers. QFT+	90	4	6	0
	Pre-Rev (QFT+)	20	8	25	47
	Post-Rev (QFT-)	11	12	28	29
	Non-conv	0	3	12	85

FIGURE 6 | Integrated analysis of classical T cell, innate, DURT and B cell responses to M.tb. **(A)** The PLS-DA biplot shows the first and second latent components from the model built on LASSO-selected features. Each dot represents a participant, all participants were included (n = 30 per group). The thick line curves denote the 95% confidence ellipses for each group. **(B)** Left: loading scores of each group on latent component one, where the pre- and post- reverter groups were compared using Wilcoxon's signed rank paired test and the other groups were compared using Mann Whitney's U test. Right: bar graph indicating feature importance in latent component one. **(C)** The average confusion matrix across 1000 bootstrapped samples after a cross-validation of the PLS-DA model. Each row represents the true outcome in the testing set and each column the outcome predicted by the model. Values in red represent the % of correctly classified observations.

after 1000 bootstrapped iterations was 0.48. The misclassification rate of persistent QFT positives and non-converters were 10% and 15%, respectively, while the misclassification rates of pre- and post-reverters were 92% and 72%, respectively. The average confusion matrix across the bootstrapped samples (**Figure 6C**) showed that about half of the observations from both reverter groups were misclassified as non-converters, which is twice as many as those that were classified as persistent QFT positives, or correctly classified as reverters.

Since reverters were not separated according to QFT status, a second PLS-DA model was built to assess whether the reverters could be stratified according to CFP-10/ESAT-6 responder status defined by MIMOSA (40). Responder and non-responder reverters were still not significantly different from each other and were significantly different from the control cohorts (**Supplementary Figure 13C**).

Finally, a LASSO model was built including all 3 groups (i.e. QFT reverters, persistent positives and negatives) as a class

outcome and similar variables to the LASSO model that was blinded to the reverters were identified. Consequently, the performance remained the same, with the reverters frequently misclassified (data not shown).

Taken together, statistical modelling performed on all available data confirmed that innate, DURT and B cell responses did not contribute to the stratification of the study groups, and that M.tb-specific CD4 T cell responses in reverters were overall more similar to those detected in non-converters compared to persistent QFT+.

DISCUSSION

Based on TST reversion studies in humans and guinea pig animal models, researchers hypothesize that QFT and/or TST reversion is associated with M.tb clearance or a reduction of bacterial burden (7). We found that QFT reversion was observed in a heterogenous group of individuals. In our cohort, none of the classical T cell, innate, DURT and B cell features we measured changed upon QFT reversion, suggesting that at least in some individuals reversion is due to QFT variability. However, reverters consistently displayed intermediate magnitude and differentiation status of M.tb-specific CD4 T cell responses compared to non-converters and persistent QFT+ individuals. Overall, reverters shared more similar features with non-converters compared to persistent QFT+ individuals, suggesting that reverters are generally exposed to very low or no antigen *in vivo*, which is consistent with well-controlled or previously cleared M.tb infection.

In our cohort of QFT reverters, functional and memory M.tb-specific CD4 T cell profiles did not change upon QFT reversion in response to a variety of M.tb immunodominant antigens. However, less than half of the reverters were classified as CD4 T cell responders to CFP-10/ESAT-6 stimulation both before and after reversion. This highlights the heterogeneity of QFT reverters, which include individuals who have low M.tb-specific immune responses which fluctuate around the QFT cut-off, as well as individuals who have low but detectable M.tb-specific responses despite falling below the QFT cut-off. M.tb-specific cytokine-producing CD4 T cells detected in reverters were of intermediate magnitude that fell between those observed in non-converters and persistent QFT+. These results are not consistent with findings by Jenum and colleagues, who reported that magnitude and cytokine co-expression profile of M.tb-specific Th1 CD4 T cells were not significantly different between IGRA reverters (n=6) and IGRA+ individuals [n=14, (9)]. M.tb-specific T cell activation (HLA-DR expression), which is likely associated with *in vivo* bacterial load during recent infection and active tuberculosis disease (29, 31, 32, 36), was very low and not significantly different across study groups. Based on these results, we found no clear evidence against the *reversion = clearance* hypothesis. In fact, the low level of activation in all groups suggests that even persistently QFT+ individuals are exposed to low bacterial burden *in vivo*, which does not trigger higher T cell activation than M.tb-uninfected individuals (non-converters).

We detected higher levels of CFP-10/ESAT-6-specific T_{TM} and early-differentiated IFN-γ-TNF+IL-2± memory subsets, but lower levels of IFN-γ+TNF+ T_E cells and functional differentiation in reverters compared with persistent QFT+. Further, with the exception of lower proportions of M.tb lysate-specific T_{SCM}, memory/functional subsets were not significantly different between reverters and non-converters. These findings suggest that reverters likely have a controlled, low-grade M.tb infection, or may have even had cleared infection, prior to detection of the QFT reversion. These results also highlight that once M.tb infection is established, immunological memory, consisting of both effector and T_{SCM}/T_{CM} cell subsets, is sustained even upon QFT reversion.

We hypothesized that distinct innate, DURT and B cell responses could contribute to controlling M.tb infection or modulate IFN-γ production resulting in QFT reversion. Overall, we observed no significant differences in these immune responses to M.tb lysate stimulation pre- and post-QFT-reversion for any of the functional molecules (IFN-γ, IL-6, TNF, IL-10, IL-12 and Granzyme B) expressed by different cell types (including monocytes, B, NK and DURT cells), nor differences between the groups. Unfortunately, this analysis was conducted on a small subset of participants, and therefore it was likely underpowered to detect small differences.

To evaluate whether a combination of features from the adaptive T cell as well as the innate, DURT and B cell datasets could better capture changes in the reverters, or classify them as distinct from persistent QFT+ and non-converters, we integrated and modelled all the outcomes generated in separate experiments. Performing LASSO feature selection prior to fitting the PLS-DA model improved the computational efficiency of the model and was used to identify the most differentiating features in the dataset that could discriminate between persistent QFT+ and non-converters. The LASSO model, and hence the PLS-DA model, were therefore blinded to the relationship between the reverters and the control cohorts. The model did not distinguish between QFT+ and QFT-reverters (*i.e.* pre- and post-reversion), nor between reverters who did or did not respond to CFP-10/ESAT-6 antigen stimulation, thereby confirming that overall there were no distinct immunological features that changed upon reversion. However, the model did not consistently identify the reverters as either one of the control cohorts, suggesting that the reverters are a biologically distinct but heterogeneous group of individuals with intermediate features between QFT+ and QFT- control groups. The initial PLS-DA model built to the integrated dataset was validated *via* a cross-validation procedure and yielded a poor average performance, with pre- and post-reverter observations that were more often misclassified than correctly classified. Specifically, the majority of the observations in the pre- and post-reverter groups were misclassified as non-converters more than they were correctly classified as reverters or misclassified as persistent QFT positives. This suggests that immune features measured in reverters are more similar to non-converters than persistent QFT positives, implying that the QFT reverters may have cleared, or at least controlled *M.tb* infection to a very low

load. However, given the small sample size of the dataset, using the misclassification error rate is a misleading performance metric and is difficult to draw definitive conclusions.

We acknowledge that this study has several other limitations, including discordance between QFT and TST responses in reverters; the majority of reverters were persistently TST positive during follow-up. This result suggests that TST may be a more sensitive test to detect less immunodominant or low mycobacteria-reactive responses than QFT. Purified protein derivative administered for TST consists of hundreds of antigens, in addition to the two antigens used in QFT. In addition, the long time frame (48-72 hours) between purified protein derivative injection and measurement of induration allows recruitment of lymphoid tissue-resident memory cells and for early differentiated cells to proliferate and induce a delayed-type hypersensitivity reaction, while QFT is a shorter *ex vivo* assay that detects circulating effector IFN-γ+ T cells. Our finding that early differentiated M.tb-specific CD4 T cells persisted in reverters is therefore consistent with their sustained TST reactivity even upon QFT reversion. Due to the limited amount of samples available, we could not perform long-term cell stimulations, which may have further confirmed higher proportions of early differentiated M.tb-specific CD4 T cells in reverters compared to persistent QFT positives (48).

We may have observed different M.tb-specific memory and functional kinetics if we had selected participants with concordant QFT and TST reversion. Unfortunately, not enough individuals with this phenotype in our larger adolescent cohort study had sufficient PBMC available.

We measured M.tb-specific responses to CFP-10/ESAT-6, other M.tb-specific immunodominant antigens EspC/EspF/Rv2348 (49); and to M.tb lysate, which includes antigens cross-reactive with BCG and environmental mycobacteria. We cannot exclude that T cell responses to other M.tb antigens expressed at varying abundance by M.tb bacilli with different metabolic states, such as the Ag85 complex or latency-associated proteins (50, 51), may be associated with reversion.

We did not measure expression of other cytokines or functions known to contribute to M.tb control, such as IL-17, which might be associated with protective immunity in non-human primates (46, 47). We did not include IL-17 in our panel because mycobacterial stimulation of human PBMC induces very low IL-17 production by T cells (52), which would have been insufficient to allow phenotyping of these cells.

Finally, we do not know when the cohort of reverters studied here acquired infection, as they were selected to be QFT+ for >6 months before reversion. Whether immune features associated with transient infection (QFT conversion followed by rapid reversion) or potential clearance of established infection (sustained remote QFT conversion followed by reversion) share similarities remains unknown.

We propose that QFT reverters represent a heterogenous grouping of individuals in the tuberculosis spectrum. This grouping includes individuals with detectable, pre-reversion levels of IFN-γ in the QFT assay, which are not robustly and universally detectable at a single cell level by flow cytometry, as well as post-reversion QFT- individuals with early differentiated T cell responses detected by flow cytometry and TST. In some individuals QFT reversion may therefore be simply due to technical variability of the assay. In other individuals, the low magnitude of M.tb-specific CD4 T cells responses and the memory and functional profiles observed in QFT reverters shared more characteristics with non-converters than persistently infected (QFT+) individuals, which is consistent with low or no *in vivo* antigen exposure and may indicate controlled or cleared M.tb infection.

DATA AVAILABILITY STATEMENT

The datasets presented in this study is accessible on ZivaHub (https://doi.org/10.25375/uct.14635503.v1).

ETHICS STATEMENT

The studies involving human participants were reviewed and approved by the University of Cape Town Human Research Ethics Committee, protocol references: 045/2005, 102/2017. Written informed consent to participate in this study was provided by the participants' legal guardian/next of kin.

AUTHOR CONTRIBUTIONS

EN, MH, and TS raised funding. EN, MH, TS, JA, and MR designed the study. CM, PS, CS, BM, TR, and NB generated the data. CM, PS, TL, and VR analyzed the data. FL supervised data analysis. CM, PS, TL, EN, TS, and FL interpreted the results. CM, PS, TL, and EN wrote the manuscript. All authors contributed to the article and approved the submitted version.

FUNDING

US NIH (R21AI127121 and BAA-NIAID-NIHAI201700104) funded the study. This work was also supported by Global Health Grant OPP1066265 from the Bill & Melinda Gates Foundation. The ACS study was supported by Aeras and BMGF GC12 (grant 37885) for QFT testing. The South African National Research Foundation and the University of Cape Town funded scholarships to CM. PS received a fellowship from the Wellcome Centre for Infectious Diseases Research (CIDRI) in Africa. TL received a bursary from the National Research Foundation (NRF) of South Africa.

ACKNOWLEDGMENTS

We are grateful to the study participants and their families; the Cape Winelands East district communities, the Department of

Education and the Department of Health; the SATVI clinical and laboratory teams; Thomas Hawn for critical input in the study design.

LIST OF ACS STUDY TEAM MEMBERS

ACS study team members: Hassan Mahomed, Willem A. Hanekom, Fazlin Kafaar, Leslie Workman, Humphrey Mulenga, Rodney Ehrlich, Mzwandile Erasmus, Deborah Abrahams, Anthony Hawkridge, E. Jane Hughes, Sizulu Moyo, Sebastian Gelderbloem, Ashley Veldsman, Michele Tameris, Hennie Geldenhuys, Gregory Hussey.

SUPPLEMENTARY MATERIAL

The Supplementary Material for this article can be found online at: https://www.frontiersin.org/articles/10.3389/fimmu.2021.712480/full#supplementary-material

REFERENCES

1. Organization GWH. *Global Tuberculosis Report 2020*. (2020). Available at: https://apps.who.int/iris/bitstream/handle/10665/336069/9789240013131-eng.pdf?ua=1.
2. Dahlstrom AW. The Instability of the Tuberculin Reaction Observations on Dispensary Patients, With Special Reference to the Existence of Demonstrable Tuberculous Lesions and the Degree of Exposure to Tubercle Bacilli. *Am Rev Tuberc Pulm Dis* (1940) 42:471–87. doi: 10.1164/art.1940.42.4.471
3. Riley RL, Mills CC, O'Grady F, Sultan LU, Wittstadt F, Shivpuri DN. Infectiousness of Air From a Tuberculosis Ward. *Am Rev Respir Dis* (1962) 85:511–25. doi: 10.1164/arrd.1962.85.4.511
4. Riley RL, Mills CC, Nyka W, Weinstock N, Storey Y PB, Sultan LU, et al. Aerial Dissemination of Pulmonary Tuberculosis A Two-Year Study of Contagion in a Tuberculosis Ward. *Am J Epidemiol* (1959) 70:185–96. doi: 10.1093/oxfordjournals.aje.a120069
5. Dharmadhikari AS, Basaraba RJ, Walt MLVD, Weyer K, Mphahlele M, Venter K, et al. Natural Infection of Guinea Pigs Exposed to Patients With Highly Drug-Resistant Tuberculosis. *Tuberculosis* (2011) 91:329 338. doi: 10.1016/j.tube.2011.03.002
6. Adams JM, Kalajan VA, Mork BO, Rosenblatt M, Rothrock WJ, O'Loughlin BJ. Reversal of Tuberculin Reaction in Early Tuberculosis. *Dis Chest* (1959) 35:348–56. doi: 10.1378/chest.35.4.348
7. Hawn TR, Day TA, Scriba TJ, Hatherill M, Hanekom WA, Evans TG, et al. Tuberculosis Vaccines and Prevention of Infection. *Microbiol Mol Biol R* (2014) 78:650–71. doi: 10.1128/mmbr.00021-14
8. Hill PC, Brookes RH, Fox A, Jackson-Sillah D, Jeffries DJ, Lugos MD, et al. Longitudinal Assessment of an ELISPOT Test for Mycobacterium Tuberculosis Infection. *PloS Med* (2007) 4:e192. doi: 10.1371/journal.pmed.0040192
9. Jenum S, Grewal HMS, Hokey DA, Kenneth J, Vaz M, Doherty TM, et al. The Frequencies of Ifnγ+Il2+Tnfα+ PPD-Specific CD4+CD45RO+ T-Cells Correlate With the Magnitude of the QuantiFERON® Gold In-Tube Response in a Prospective Study of Healthy Indian Adolescents. *PloS One* (2014) 9:e101224. doi: 10.1371/journal.pone.0101224
10. Medawar L, Tukiman HM, Mbayo G, Donkor S, Owolabi O, Sutherland JS. Analysis of Cellular and Soluble Profiles in QuantiFERON Nonconverters, Converters, and Reverters in the Gambia. *Immun Inflamm Dis* (2019) 7:260–70. doi: 10.1002/iid3.269
11. Pai M, Joshi R, Dogra S, Zwerling AA, Gajalakshmi D, Goswami K, et al. T-Cell Assay Conversions and Reversions Among Household Contacts of Tuberculosis Patients in Rural India. *Int J Tuberc Lung Dis* (2009) 13:84–92.
12. Xin H, Zhang H, Yang S, Liu J, Lu W, Bai L, et al. 5-Year Follow-Up of Active Tuberculosis Development From Latent Infection in Rural China. *Clin Infect Dis* (2019) 70(5):947–50. doi: 10.1093/cid/ciz581
13. Zhang H, Xin H, Wang D, Pan S, Liu Z, Cao X, et al. Serial Testing of Mycobacterium Tuberculosis Infection in Chinese Village Doctors by QuantiFERON-TB Gold Plus, QuantiFERON-TB Gold In-Tube and T-SPOT.TB. *J Infect* (2019) 78:305–10. doi: 10.1016/j.jinf.2019.01.008
14. van Zyl-Smit RN, Pai M, Peprah K, Meldau R, Kieck J, Juritz J, et al. Within-Subject Variability and Boosting of T-Cell Interferon-γ Responses After Tuberculin Skin Testing. *Am J Resp Crit Care* (2009) 180:49–58. doi: 10.1164/rccm.200811-1704oc
15. Ewer K, Millington KA, Deeks JJ, Alvarez L, Bryant G, Lalvani A. Dynamic Antigen-Specific T-Cell Responses After Point-Source Exposure to Mycobacterium Tuberculosis. *Am J Resp Crit Care* (2006) 174:831–9. doi: 10.1164/rccm.200511-1783oc
16. Johnson DF, Malone LL, Zalwango S, Oketcho JM, Chervenak KA, Thiel B, et al. Tuberculin Skin Test Reversion Following Isoniazid Preventive Therapy Reflects Diversity of Immune Response to Primary Mycobacterium Tuberculosis Infection. *PloS One* (2014) 9:e96613. doi: 10.1371/journal.pone.0096613
17. Nemes E, Geldenhuys H, Rozot V, Rutkowski KT, Ratangee F, Bilek N, et al. Prevention of M. Tuberculosis Infection With H4:IC31 Vaccine or BCG Revaccination. *N Engl J Med* (2018) 379:138–149. doi: 10.1056/nejmoa1714021
18. Domingo-Gonzalez R, Prince O, Cooper A, Khader SA. Cytokines and Chemokines in Mycobacterium Tuberculosis Infection. *Microbio Spectr* (2016) 4(5):TBTB2-0018–2016. doi: 10.1128/microbiolspec.tbtb2-0018-2016
19. North RJ, Jung Y-J. Immunity to Tuberculosis. *Immunology* (2004) 22:599–623. doi: 10.1146/annurev.immunol.22.012703.104635
20. Mogues T, Goodrich ME, Ryan L, LaCourse R, North RJ. The Relative Importance of T Cell Subsets in Immunity and Immunopathology of Airborne Mycobacterium Tuberculosis Infection in Mice. *J Exp Med* (2001) 193:271–80. doi: 10.1084/jem.193.3.271
21. Penn-Nicholson A, Nemes E, Hanekom WA, Hatherill M, Scriba TJ. Mycobacterium Tuberculosis-Specific CD4 T Cells Are the Principal Source of IFN-Γ in QuantiFERON Assays in Healthy Persons. *Tuberculosis* (2015) 95:350–1. doi: 10.1016/j.tube.2015.03.002
22. Suliman S, Geldenhuys H, Johnson JL, Hughes JE, Smit E, Murphy M, et al. Bacillus Calmette–Guérin (BCG) Revaccination of Adults With Latent Mycobacterium Tuberculosis Infection Induces Long-Lived BCG-Reactive NK Cell Responses. *J Immunol* (2016) 197:1100–10. doi: 10.4049/jimmunol.1501996
23. Seder RA, Darrah PA, Roederer M. T-Cell Quality in Memory and Protection: Implications for Vaccine Design. *Nat Rev Immunol* (2008) 8:nri2274. doi: 10.1038/nri2274
24. Mpande CAM, Rozot V, Mosito B, Musvosvi M, Dintwe OB, Bilek N, et al. Immune Profiling of Mycobacterium Tuberculosis-Specific T Cells in Recent and Remote Infection. *Ebiomedicine* (2021) 64:103233. doi: 10.1016/j.ebiom.2021.103233
25. Lu LL, Smith MT, Yu KKQ, Luedemann C, Suscovich TJ, Grace PS, et al. IFN-γ-Independent Immune Markers of Mycobacterium Tuberculosis Exposure. *Nat Med* (2019) 25:977–87. doi: 10.1038/s41591-019-0441-3
26. Lugli E, Dominguez MH, Gattinoni L, Chattopadhyay PK, Bolton DL, Song K, et al. Superior T Memory Stem Cell Persistence Supports Long-Lived T Cell Memory. *J Clin Invest* (2013) 123:594–9. doi: 10.1172/jci66327
27. Mpande CA, Musvosvi M, Rozot V, Mosito B, Reid TD, Schreuder C, et al. Antigen-Specific T-Cell Activation Distinguishes Between Recent and Remote Tuberculosis Infection. *Am J Respir Crit Care Med* (2021) 203:1556–65. doi: 10.1164/rccm.202007-2686OC
28. Musvosvi M, Duffy D, Filander E, Africa H, Mabwe S, Jaxa L, et al. T-Cell Biomarkers for Diagnosis of Tuberculosis: Candidate Evaluation by a Simple Whole Blood Assay for Clinical Translation. *Eur Respir J* (2018) 51:1800153. doi: 10.1183/13993003.00153-2018
29. Riou C, Bruyn ED, Ruzive S, Goliath RT, Arlehamn CSL, Sette A, et al. Disease Extent and Anti-Tubercular Treatment Response Correlates With

Mycobacterium Tuberculosis-Specific CD4 T-Cell Phenotype Regardless of HIV-1 Status. *Clin Transl Immunol* (2020) 9:e1176. doi: 10.1002/cti2.1176
30. Riou C, Berkowitz N, Goliath R, Burgers WA, Wilkinson RJ. Analysis of the Phenotype of Mycobacterium Tuberculosis-Specific CD4+ T Cells to Discriminate Latent From Active Tuberculosis in HIV-Uninfected and HIV-Infected Individuals. *Front Immunol* (2017) 8:968. doi: 10.3389/fimmu.2017.00968
31. Wilkinson KA, Oni T, Gideon HP, Goliath R, Wilkinson RJ, Riou C. Activation Profile of Mycobacterium Tuberculosis–Specific CD4+ T Cells Reflects Disease Activity Irrespective of HIV Status. *Am J Resp Crit Care* (2016) 193:1307–10. doi: 10.1164/rccm.201601-0116le
32. Adekambi T, Ibegbu CC, Cagle S, Kalokhe AS, Wang YF, Hu Y, et al. Biomarkers on Patient T Cells Diagnose Active Tuberculosis and Monitor Treatment Response. *J Clin Invest* (2015) 125:1827–38. doi: 10.1172/jci77990
33. Lin PL, Ford CB, Coleman MT, Myers AJ, Gawande R, Ioerger T, et al. Sterilization of Granulomas Is Common in Active and Latent Tuberculosis Despite Within-Host Variability in Bacterial Killing. *Nat Med* (2014) 20:75–79. doi: 10.1038/nm.3412
34. Mahomed H, Hawkridge T, Verver S, Abrahams D, Geiter L, Hatherill M, et al. The Tuberculin Skin Test Versus QuantiFERON TB Gold® in Predicting Tuberculosis Disease in an Adolescent Cohort Study in South Africa. *PloS One* (2011) 6:e17984. doi: 10.1371/journal.pone.0017984
35. Nemes E, Rozot V, Geldenhuys H, Bilek N, Mabwe S, Abrahams D, et al. Optimization and Interpretation of Serial QuantiFERON Testing to Measure Acquisition of Mycobacterium Tuberculosis Infection. *Am J Resp Crit Care* (2017) 196:638–48. doi: 10.1164/rccm.201704-0817oc
36. Mpande CAM, Musvosvi M, Rozot V, Mosito B, Reid TD, Schreuder C, et al. Antigen-Specific T Cell Activation Distinguishes Between Recent and Remote Tuberculosis Infection. *Am J Resp Crit Care* (2021) 148:1292–7. doi: 10.1164/rccm.202007-2686oc
37. Mahomed H, Hawkridge T, Verver S, Geiter L, Hatherill M, Abrahams D-A, et al. Predictive Factors for Latent Tuberculosis Infection Among Adolescents in a High-Burden Area in South Africa. *Int J Tuberc Lung Dis* (2011) 15:331–6.
38. Lin L, Finak G, Ushey K, Seshadri C, Hawn TR, Frahm N, et al. COMPASS Identifies T-Cell Subsets Correlated With Clinical Outcomes. *Nat Biotechnol* (2015) 33:610–6. doi: 10.1038/nbt.3187
39. Roederer M, Nozzi JL, Nason MC. SPICE: Exploration and Analysis of Post-Cytometric Complex Multivariate Datasets. *Cytom Part A* (2011) 79A:167–74. doi: 10.1002/cyto.a.21015
40. Finak G, McDavid A, Chattopadhyay P, Dominguez M, Rosa SD, Roederer M, et al. Mixture Models for Single-Cell Assays With Applications to Vaccine Studies. *Biostatistics* (2013) 15:87–101. doi: 10.1093/biostatistics/kxt024
41. Bruggner RV, Bodenmiller B, Dill DL, Tibshirani RJ, Nolan GP. Automated Identification of Stratifying Signatures in Cellular Subpopulations. *Proc Natl Acad Sci* (2014) 111:E2770–7. doi: 10.1073/pnas.1408792111
42. Moguche AO, Musvosvi M, Penn-Nicholson A, Plumlee CR, Mearns H, Geldenhuys H, et al. Antigen Availability Shapes T Cell Differentiation and Function During Tuberculosis. *Cell Host Microbe* (2017) 21:695–706.e5. doi: 10.1016/j.chom.2017.05.012
43. Lloyd T, Steigler P, Mpande CAM, Rozot V, Mosito B, Shreuder C, et al. Multidimensional Analysis of Immune Response Identified Biomarkers of Recent Mycobacterium Tuberculosis Infection. *PLoS Comput Biol* (2021) 17:e1009197. doi: 10.1371/journal.pcbi.1009197
44. Tibshirani R. Regression Shrinkage and Selection via the LASSO. *J R Stat Soc* (1996) 58:267–88. doi: 10.1111/j.2517-6161.1996.tb02080.x
45. Wold H. Partial Least Squared. *Encyclopedia Stat Sci* (1982) 1–53.
46. Darrah PA, Zeppa JJ, Maiello P, Hackney JA, Wadsworth MH, Hughes TK, et al. Prevention of Tuberculosis in Macaques After Intravenous BCG Immunization. *Nature* (2020) 577:95–102. doi: 10.1038/s41586-019-1817-8
47. Dijkman K, Sombroek CC, Vervenne RAW, Hofman SO, Boot C, Remarque EJ, et al. Prevention of Tuberculosis Infection and Disease by Local BCG in Repeatedly Exposed Rhesus Macaques. *Nat Med* (2019) 25:255–262. doi: 10.1038/s41591-018-0319-9
48. Butera O, Chiacchio T, Carrara S, Casetti R, Vanini V, Meraviglia, et al. New Tools for Detecting Latent Tuberculosis Infection: Evaluation of RD1-Specific Long-Term Response. *BMC Infect Dis* (2009) 9:182. doi: 10.1186/1471-2334-9-182
49. Ruhwald M, de Thurah L, Kuchaka D, Zaher MR, Salman AM, Abdel-Ghaffar A-R, et al. Introducing the ESAT-6 Free IGRA, A Companion Diagnostic for TB Vaccines Based on ESAT-6. *Sci Rep-uk* (2017) 7:45969. doi: 10.1038/srep45969
50. Rogerson BJ, Jung Y-J, LaCourse R, Ryan L, Enright N, North RJ. Expression Levels of Mycobacterium Tuberculosis Antigen-Encoding Genes Versus Production Levels of Antigen-Specific T Cells During Stationary Level Lung Infection in Mice. *Immunology* (2006) 118:195–201. doi: 10.1111/j.1365-2567.2006.02355.x
51. Shi L, Jung Y-J, Tyagi S, Gennaro ML, North RJ. Expression of Th1-Mediated Immunity in Mouse Lungs Induces a Mycobacterium Tuberculosis Transcription Pattern Characteristic of Nonreplicating Persistence. *Proc Natl Acad Sci* (2003) 100:241–6. doi: 10.1073/pnas.0136863100
52. Scriba TJ, Kalsdorf B, Abrahams D-A, Isaacs F, Hofmeister J, Black G, et al. Distinct, Specific IL-17- and IL-22-Producing CD4+ T Cell Subsets Contribute to the Human Anti-Mycobacterial Immune Response. *J Immunol* (2008) 180:1962–70. doi: 10.4049/jimmunol.180.3.1962

Conflict of Interest: The authors declare that the research was conducted in the absence of any commercial or financial relationships that could be construed as a potential conflict of interest.

Publisher's Note: All claims expressed in this article are solely those of the authors and do not necessarily represent those of their affiliated organizations, or those of the publisher, the editors and the reviewers. Any product that may be evaluated in this article, or claim that may be made by its manufacturer, is not guaranteed or endorsed by the publisher.

Copyright © 2021 Mpande, Steigler, Lloyd, Rozot, Mosito, Schreuder, Reid, Bilek, Ruhwald, Andrews, Hatherill, Little, Scriba and Nemes. This is an open-access article distributed under the terms of the Creative Commons Attribution License (CC BY). The use, distribution or reproduction in other forums is permitted, provided the original author(s) and the copyright owner(s) are credited and that the original publication in this journal is cited, in accordance with accepted academic practice. No use, distribution or reproduction is permitted which does not comply with these terms.

frontiers in Immunology

ORIGINAL RESEARCH
published: 23 November 2021
doi: 10.3389/fimmu.2021.727300

High Dimensional Immune Profiling Reveals Different Response Patterns in Active and Latent Tuberculosis Following Stimulation With Mycobacterial Glycolipids

Carolina S. Silva[1,2†], Christopher Sundling[3,4†], Elin Folkesson[3,4], Gabrielle Fröberg[3,4], Claudia Nobrega[1,2], João Canto-Gomes[1,2], Benedict J. Chambers[5], Tadepally Lakshmikanth[6], Petter Brodin[6,7], Judith Bruchfeld[3,4], Jérôme Nigou[8], Margarida Correia-Neves[1,2,3‡] and Gunilla Källenius[3‡]*

[1] Life and Health Sciences Research Institute, School of Medicine, University of Minho, Braga, Portugal, [2] ICVS/3B's, PT Government Associate Laboratory, Braga, Portugal, [3] Division of Infectious Diseases, Department of Medicine Solna, Center for Molecular Medicine, Karolinska Institutet, Stockholm, Sweden, [4] Department of Infectious Diseases, Karolinska University Hospital, Stockholm, Sweden, [5] Center for Infectious Medicine, Department of Medicine, Huddinge, Karolinska Institutet, Stockholm, Sweden, [6] Science for Life Laboratory, Department of Women's and Children's Health, Karolinska Institutet, Stockholm, Sweden, [7] Department of Immunology and Inflammation, Imperial College London, London, United Kingdom, [8] Institut de Pharmacologie et de Biologie Structurale, Université de Toulouse, Centre National de la Recherche Scientifique (CNRS), Université Paul Sabatier, Toulouse, France

Upon infection with *Mycobacterium tuberculosis* (Mtb) the host immune response might clear the bacteria, control its growth leading to latent tuberculosis (LTB), or fail to control its growth resulting in active TB (ATB). There is however no clear understanding of the features underlying a more or less effective response. Mtb glycolipids are abundant in the bacterial cell envelope and modulate the immune response to Mtb, but the patterns of response to glycolipids are still underexplored. To identify the $CD45^+$ leukocyte activation landscape induced by Mtb glycolipids in peripheral blood of ATB and LTB, we performed a detailed assessment of the immune response of PBMCs to the Mtb glycolipids lipoarabinomannan (LAM) and its biosynthetic precursor phosphatidyl-inositol mannoside (PIM), and purified-protein derivate (PPD). At 24 h of stimulation, cell profiling and secretome analysis was done using mass cytometry and high-multiplex immunoassay. PIM induced a diverse cytokine response, mainly affecting antigen-presenting cells to produce both pro-inflammatory and anti-inflammatory cytokines, but not IFN-γ, contrasting with PPD that was a strong inducer of IFN-γ. The effect of PIM on the antigen-presenting cells was partly TLR2-dependent. Expansion of monocyte subsets in response to PIM or LAM was reduced primarily in LTB as compared to healthy controls, suggesting a hyporesponsive/tolerance pattern derived from Mtb infection.

Keywords: tuberculosis, mycobacterial glycolipids, active tuberculosis (ATB), latent tuberculosis (LTB), hyporesponsiveness, lipoarabinomannan (LAM), phosphatidylinositol mannoside (PIM)

OPEN ACCESS

Edited by:
Julie G. Burel, La Jolla Institute for Immunology (LJI), United States

Reviewed by:
Alasdair Leslie, Africa Health Research Institute (AHRI), South Africa
Marco Pio La Manna, University of Palermo, Italy

***Correspondence:**
Christopher Sundling
christopher.sundling@ki.se

†*These authors have contributed equally to this work*

‡*These authors have contributed equally to this work*

Specialty section:
This article was submitted to Microbial Immunology, a section of the journal Frontiers in Immunology

Received: *18 June 2021*
Accepted: *18 October 2021*
Published: *23 November 2021*

Citation:
Silva CS, Sundling C, Folkesson E, Fröberg G, Nobrega C, Canto-Gomes J, Chambers BJ, Lakshmikanth T, Brodin P, Bruchfeld J, Nigou J, Correia-Neves M and Källenius G (2021) High Dimensional Immune Profiling Reveals Different Response Patterns in Active and Latent Tuberculosis Following Stimulation With Mycobacterial Glycolipids. Front. Immunol. 12:727300. doi: 10.3389/fimmu.2021.727300

INTRODUCTION

It is estimated that approximately 25% of the world population is latently infected with *Mycobacterium tuberculosis* (Mtb) (1). However, only about 10% of individuals with latent TB (LTB) are estimated to develop active TB (ATB) (2). It is clear therefore that in most cases Mtb infection is well controlled, but our understanding of what makes an effective immune response that controls and/or clears Mtb is limited.

Research on the host response to Mtb has so far mainly focused on protein-based antigens. However, the immune response to Mtb is initiated mainly through the interaction of Mtb cell envelope components, mostly glycolipids, with distinct cells of the innate immune system (3), which trigger activating or repressive responses in terms of cytokine production (4, 5). The ability of Mtb lipids to traffic outside infected cells (6–8) renders the direct contact of Mtb cell envelope glycolipids with distinct immune cells an important aspect of the immune response (9). Lipoarabinomannan (LAM) is a major glycolipid of the Mtb cell wall and has been studied quite extensively for its immunomodulatory properties (10, 11), compared to its biosynthetic precursors, the phosphatidyl-inositol mannosides (PIM_2 and PIM_6). Many host cell receptors take part in the initial interaction between mycobacteria and innate immune cells (12, 13). TLRs and C-type lectins are involved in this process, resulting in activation of several antimicrobial mechanisms by macrophages (Mφs) and dendritic cells (DCs) (14–17).

In addition to the extensive interaction with innate immune cells, PIM and LAM are also both recognized by CD1b-restricted T cells (9, 18–21). In fact, it was observed that purified-protein derivate (PPD) positive individuals respond through CD1-restricted T cells to several mycobacterial lipids, including PIM and LAM (18) and that this response may vary between individuals with ATB and LTB. Mtb whole lipid extract was shown to induce proliferation of CD1-restricted $CD4^+$ and, to a smaller extent, $CD8^+$ T cells in LTB. Interestingly, the same was observed for ATB patients only after the first two weeks of anti-TB treatment (22). A subset of LAM reactive CD1-restricted T cells co-expressing perforin, granulysin, and granzyme B (GrzB), mostly $CD8^+$, are more frequent in LTB than in individuals who developed ATB (evaluated after TB treatment) (22). Similarly, glycerol monomycolate-specific T cells are more frequent in LTB than ATB patients (18) and the response of these cells may vary between ATB and LTB individuals.

B cell-mediated immunity in Mtb infection has been less explored compared to monocyte- and T cell-mediated responses, although recent data strengthen the relevance of these cells in the immune response to Mtb. Recently it was shown that Mtb LAM induces IL-10 production by B cells and that these cells (B10) inhibit $CD4^+$ T_H1 polarization leading to increased Mtb susceptibility in mice (23). The response of B cells to LAM was shown to occur in a TLR2-dependent manner (23).

In the present study, we performed a detailed assessment and simultaneous comparison of the immune response to PIM, LAM and PPD from Mtb in peripheral blood mononuclear cells (PBMCs) from individuals with ATB or LTB and compared with healthy controls (HC). We performed immune profiling by secretome analysis and mass cytometry measuring simultaneously 37 cellular markers at the single-cell level to allow high-resolution of the cellular composition and secretion. We identified distinct subsets within memory T cells, NK cells, B cells and monocytes/DCs that were altered by PPD, PIM and LAM stimulation and further evaluated the role of TLR2 in this process.

MATERIALS AND METHODS

Study Participants

Participants were recruited in 2018 within an ongoing prospective cohort of adult (≥18 years) TB patients and contacts attending the TB Centre, Dept of Infectious Diseases Karolinska University Hospital Stockholm (**Supplemental Table 1**). ATB cases were defined upon microbiological (PCR and/or culture) verification. LTB participants were defined as asymptomatic, IGRA positive, close contacts to ATB cases. Healthy controls (HC) were defined as IGRA negative students and hospital staff without known previous Mtb exposure. Exclusion criteria were pregnancy, autoimmune diseases and HIV co-infection or other immunodeficiencies. ATB and LTB participants were screened with standard biochemical set-up and radiology.

Antigens

Tuberculin PPD (RT 50) was obtained from Statens Serum Institute, and PHA from *In vivo*gen. LAM and PIMs were prepared as previously described in detail (5). Briefly, heat-killed bacteria were frozen and thawed several times, sonicated and extracted in 40% hot phenol for 1 h at 70°C. ManLAM and PIM were obtained from the water and phenol phases respectively. The dialyzed water phase was submitted to affinity chromatography on Concanavalin A-Sepharose. After elution, bound material was subjected to hydrophobic interaction chromatography on Phenyl-Sepharose (Amersham, Sweden). Bound ManLAM was eluted and further separated from other glycolipids by gel filtration on Sephacryl S-100 (Amersham, Sweden). The phenol phase obtained above was washed 3 times with PBS and extracted with an equal volume of 2% SDS in PBS overnight at room temperature. The resulting water phase was precipitated with of ice-cold ethanol. PIMs contained in the precipitate were purified to homogeneity by gel filtration on Sephacryl S-100. PIM contains both PIM_2 and PIM_6 isoforms, differing in number of fatty acyl constituents (5).

PBMC Isolation

Venous blood from each participant was collected into EDTA tubes and PBMCs were purified through density gradient centrifugation using Lymphoprep™ (Stemcell) according to the manufacturer's instruction, with some modifications. The cell isolation primarily removes granulocytes and red blood cells. Briefly, white blood cells were counted using a HemoCue instrument and the blood was diluted to a maximum of

$240x10^6$ cells per 22.5 ml that were then layered onto 10 ml Lymphoprep. The cells were centrifuged at 400*g* for 30 min without any break. The mononuclear cell layer was collected into a new 50 ml tube and resuspended to 45 ml with PBS. The cells were spun at 300g for 10 min with break after which the cells were resuspended into 1-5 ml PBS and filtered using a 100 µm poor size cell strainer and counted on a Countess (ThermoFisher Scientific). The cells were centrifuged at 400*g* for 10 min with break and resuspended with freeze media (90% FBS supplemented with 10% DMSO) and placed in a CoolCell freezing container (Sigma) before moving to –80°C overnight followed by long-term storage in liquid nitrogen.

PBMC Stimulation

PBMCs from 5 patients with ATB, 5 with LTB and five HCs were thawed at 37°C followed by addition of 1 mL RPMI-1640 media supplemented with 10% fetal bovine serum (FBS), 1% penicillin/streptomycin (P/S) and 250 U/mL Benzonase (all from ThermoFisher). The cells were washed twice (300*g* for 5 min) in media followed by resuspension in RPMI-1640 culture media supplemented with 10% FBS, 1% P/S, 0.3 g/L L-Glutamine and 25 mM HEPES and counted. The cells were then plated in 24-well plates at $2x10^6$ PBMCs/mL in culture media containing either 5 µg/mL PHA, 10 µg/mL PPD, or 25 µg/mL LAM or PIM, or left untreated (PBS), for 24 h in a 37°C 5% CO_2 incubator. 4 h before collection, 5 µg/mL of brefeldin A and 2 µM Monensin (both ThermoFisher) were added to each well. PHA was used as positive control for PBMCs responsiveness (**Supplemental Figures 1**, **2**). The choice of concentration of LAM and PIM was based on titrations with cytokine secretion into supernatants as read-out (data not shown). The 24 h stimulation did not alter cell numbers between the conditions (**Supplemental Figure 3**).

Mass Cytometry Staining and Acquisition

After 24 h, cells were collected by centrifugation after a 15 min incubation with 2 mM EDTA. Supernatants were stored at –80°C and cells were fixed using the PBMCs fix kit (Cytodelics AB) and barcoded using Cell-ID™ 20-Plex Pd Barcoding Kit (Fluidigm Inc.), according to the manufacturer's recommendations. Samples were washed with CyFACS buffer (PBS with 0.1% BSA, 0.05% sodium azide and 2mM EDTA) and Fc receptors were blocked with 200 µL of blocking buffer (Cytodelics AB) for 10 min at RT. Cells were incubated with 200 µL of antibody cocktail (**Supplemental Table 2**) for 30 min at 4°C, washed with CyFACS buffer, and fixed with 1% formaldehyde. For intracellular staining, cells were permeabilized using an intracellular fixation and permeabilization kit (eBiosciences Inc.) according to the manufacturer's instructions. Subsequently, 200 µl of intracellular antibody cocktail (**Supplemental Table 3**) was added and incubated for 45 min at RT. Cells were washed, fixed in 4% formaldehyde at 4°C overnight, and stained with DNA intercalator (0.125 µM MaxPar® Intercalator-Ir, Fluidigm Inc.) on the following day. After that, cells were washed with CyFACS buffer, PBS and MiliQ water, counted and adjusted to 750,000 cells/mL. Samples were acquired in a CyTOF2 (Fluidigm) mass cytometer at a rate of 250-400 events/s using CyTOF software version 6.0.626 with noise reduction, a lower convolution threshold of 200, event length limits of 10-150 pushes, a sigma value of 3, and flow rate of 0.045 ml/min.

Analysis of Mass Cytometry Data

The mass cytometry FCS data files were gated for different cell subsets: $CD45^+$ leucocytes, $CD45^+CD3^+CD20^-$ T cells, $CD45^+CD3^-CD7^+$ NK cells, $CD45^+CD3^-HLA\text{-}DR^+$ antigen-presenting cells (APCs), and $CD45^+$ leukocytes producing IL-2, IL-4, IL-5, IL-6, IL-10, IL-17A, IFN-γ, TNF-α, GrzB, and GM-CSF using FlowJo™ v10.6.1. The gated populations were exported to new FCS files that were then analyzed using the R-package Cytofkit v1.12.0, which includes an integrated pipeline for mass cytometry analysis (24). Cytofkit was run in R-studio version 1.1.463 and R version 3.6.1. For analysis of total leukocytes, 5000 cells were used per sample. For analysis of gated T cells, NK cells, and APCs, 10000 cells were used per sample. For analysis of $cytokine^+$ cells, a ceiling of 5000 cells were included per sample. Dimensionality was reduced using Barnes-Hut tSNE with a perplexity of 30 with a maximum of 1000 iterations. Clustering was then performed using density-based machine learning with ClusterX (24) and cell subsets were identified by visual inspection of marker expression for each cluster. The Cytoftkit analysis was performed using PBS, PPD, PIM, and LAM FCS files together, whereas PHA stimulated cells were evaluated independently, using only PBS and PHA FCS files.

Secretome Analysis of Culture Supernatants

Cell culture supernatants (n=75) were randomized in a 96-well plate and analyzed with a multiplex proximity extension assay (PEA) (25), enabling simultaneous quantification of 92 inflammatory markers from the Olink inflammation panel (**Supplemental Table 4**). Markers where all samples were below the limit of detection of the assay were removed from subsequent analysis. The samples were run by the Translational Plasma Profile Facility at SciLifeLab, Stockholm, Sweden.

TLR2-Dependence of PBMCs Activation

To investigate TLR2-dependent PBMCs activation by the Mtb glycolipids PIM and LAM, frozen PBMCs from HC (n=5) were thawed in a 37°C water bath, washed 2 times in complete media (RPMI-1640 culture media supplemented with 10% FBS, 1% P/S, 1 mM sodium pyruvate and 10 mM HEPES) and plated as described for mass cytometry. Prior to stimulation, the cells were pre-incubated for 30 min at 37°C with 5 µg/mL of anti-TLR2 monoclonal antibody (clone T2.5, *In vivo*Gen) or with an isotype control (mIgG1, eBiosciences).

Flow Cytometry

Cells stimulated in the presence or absence of anti-TLR2 antibody for 24 h were collected after an additional 15 min incubation with 2 mM EDTA. The cells were then washed with FACS buffer (PBS with 0.3% BSA and 2 mM EDTA) and Fc receptors were blocked with 20 µL of blocking buffer Fc Receptor

Binding Inhibitor (eBiosciences) for 10 min at 4°C. The cells were incubated with 50 µL of antibody cocktail (**Supplemental Table 5**) for 30 min at RT, washed with PBS and incubated with Fixable Viability Dye eFluor™ 450 (eBiosciences) for 30 min at 4°C. For intracellular staining, the cells were permeabilized using the FoxP3 intracellular fixation and permeabilization kit (eBiosciences) according to the manufacturer's instructions. Subsequently, 50 µl of intracellular Ab cocktail (**Supplemental Table 5**) was added and incubated for 30 min at 4°C. Finally, the cells were washed, resuspended in PBS and kept at 4°C until acquisition on the next day. The cells were acquired on a 12-color LSRII flow cytometer using FACSDiva software (Becton Dickinson, Franklin Lakes, NJ); data analysis was performed using FlowJo™ v10.6.1. Gating strategies are represented in **Supplemental Figure 4**.

Statistical Analysis

Comparisons of a single variable for paired data for >2 groups were evaluated by Friedman's test followed by Dunnet's *post-hoc* test. Comparisons of a single variable for unpaired data for >2 groups were evaluated by using a Kruskal-Wallis test followed by Dunn's post-test. Comparisons of >1 variable for paired data were evaluated using repeated measures 2-way ANOVA followed by Dunnett's *post-hoc* test. Differences were considered significant when $p<0.05$. Statistical analyzes were performed using Prism9 (GraphPad Software, USA).

Study Approval

Written informed consent was received from all participants before inclusion in the study, whereby they were pseudoanonymized. The study was approved by the Regional Ethical Review Board at the Karolinska Institute in Stockholm (approval numbers 2013/1347-31/2 and 2013/2243-31/4) and by the Ethics Committee for Research in Life and Health Sciences of the University of Minho, Portugal (approval number SECVS 014/2015) and it is in accordance with the Declaration of Helsinki.

RESULTS

Effect of Stimulants on Cell Types and Cytokine Production

To investigate the effect of the Mtb glycolipids LAM and PIM on the immune response, PBMCs from individuals with ATB or LTB, and HC (**Supplemental Table 1**) were thawed and stimulated for 24 h; PPD was used as a control for responses to Mtb proteins, while mock stimulation (PBS) or phytohemagglutinin (PHA) were used as negative and positive culture controls, respectively. Proteins released into the culture supernatant were analyzed using the Olink proximity-extension assay (PEA), that allows for simultaneous measurement of 92 inflammatory markers. Cells were analyzed using mass cytometry for changes in the expression of 27 surface and 10 intracellular markers (**Figure 1** and **Supplemental Tables 2**, **3**).

To assess the effect of LAM, PIM, and PPD on secretion of cytokines and chemokines from stimulated PBMCs, we assessed the culture supernatant for relative levels of 92 different soluble inflammatory markers (**Figure 2**). Of these, we observed changes in protein levels for 58 proteins. LAM and PIM stimulation produced very similar marker profiles, with a slightly stronger effect from PIM, suggesting a similar mechanism of action. PPD induced a markedly different response, with considerably higher IFN-γ levels, but also several other inflammatory proteins, such as IL1α and CCL8, compared to LAM and PIM, suggesting a different mechanism of action (**Figure 2A**).

There were also some indications of different levels of secretion between the groups (ATB/LTB/HC), primarily with a greater effect observed for HC compared with ATB or LTB (**Figure 2B**). IL-1α, IL-10, IL-18, and VEGF were detected at higher levels in HC compared with LTB or ATB while CCL8 was significantly decreased in HC compared with ATB and/or LTB. CCL8 functions as a strong monocyte chemoattractant but has also been associated with multiple other effects on leukocyte behavior, suggesting that its lower levels could be due to its

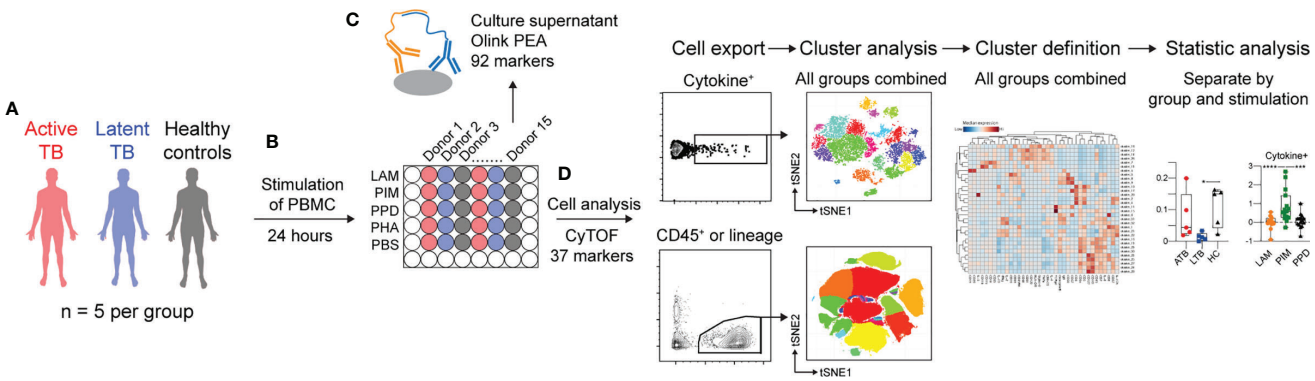

FIGURE 1 | Schematic of the study outline. **(A)** PBMCs from three groups, including active TB (ATB, red), latent TB (LTB, blue) and healthy controls (HC, black) were **(B)** stimulated for 24 h with the the mycobacterial glycolipids LAM or PIM. Control stimulations included PPD, or phytohemagglutinin (PHA), or mock stimulation (PBS). **(C)** Culture supernatants were analyzed by proximity extension assay (PEA), while **(D)** cells were analyzed by mass cytometry. Cells were either pre-gated for cytokine-secreting cells or different cell subsets prior to dimensionality reduction and cluster analysis. *p<0.05, ***p<0.001, ****p<0.0001.

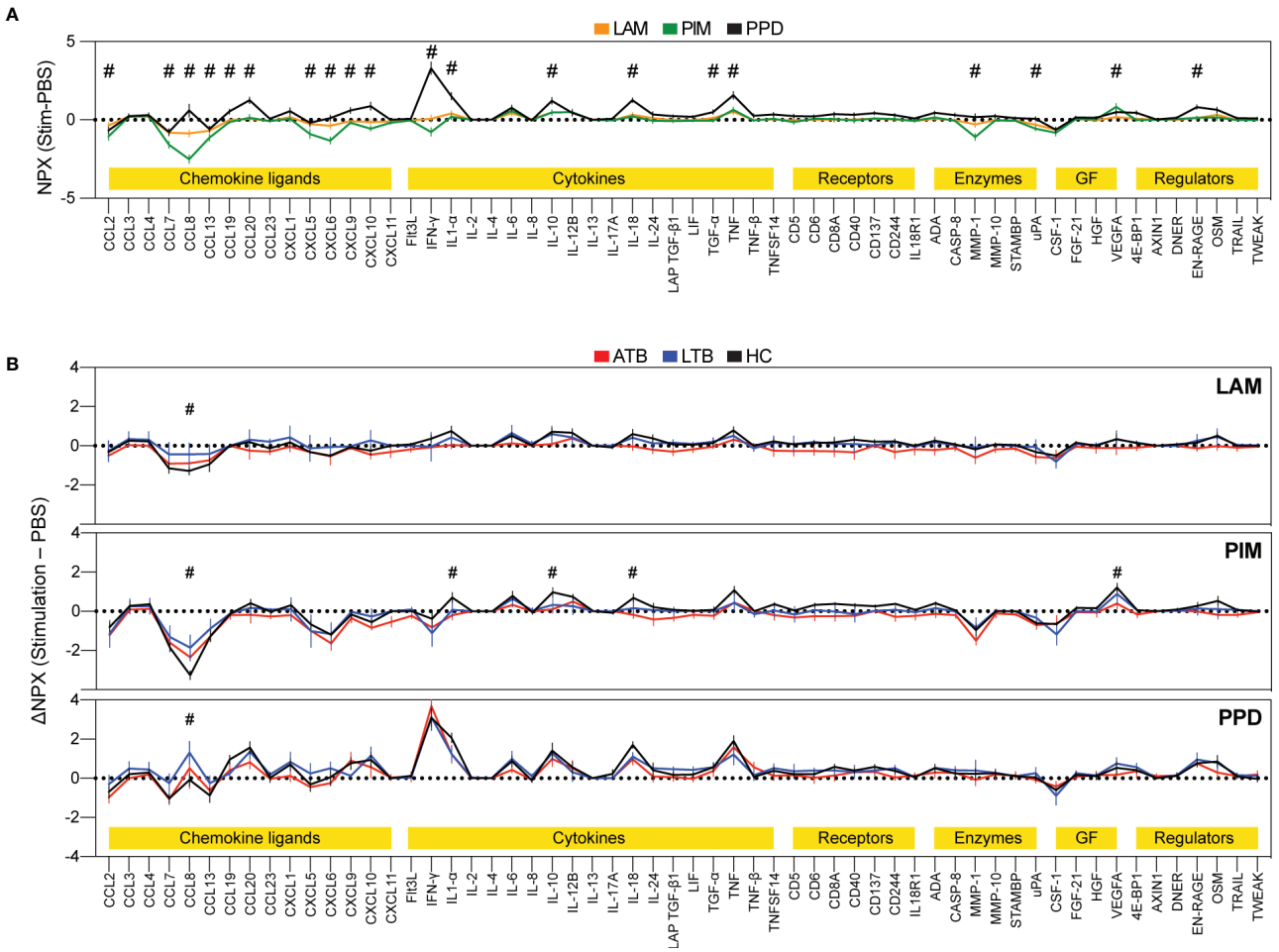

FIGURE 2 | Secretion of inflammatory proteins after stimulation with LAM, PIM, and PPD. Culture supernatants were assessed for 92 protein markers using the Olink inflammation panel after 24 h of culture. Only markers above background levels were included (n=58). The graphs show normalized protein expression (ΔNPX) for stimulated (LAM, PIM, or PPD) minus unstimulated (PBS) PBMCs (**A**, n=15/group) and separated into individuals with active TB (ATB; red), latent TB (LTB, blue), and healthy controls (HC, black) (**B**, n=5/group). The lines indicate the mean and error bars indicate SEM. The protein markers were grouped into different functional groups (yellow highlight), where GF correspond to growth factors. Statistics was evaluated using two-way ANOVA followed by Dunnet's posthoc test with significant differences between ATB or LTB against HC indicated by #, corresponding to a p-value < 0.05.

increased uptake from the culture supernatant by activated monocytes (26). Another possibility is that it is produced to a larger extent in PPD stimulated cultures, potentially *via* synergistic effects from IFN-γ and IL-1 as has been proposed previously (27).

Intracellular Cytokine Production in Response to Stimulation

To evaluate the effect of each stimulus on intracellular production of cytokines and GrzB, regardless of the experimental group, the cumulative frequency of cytokine$^+$ cells among CD45$^+$ leukocytes was compared to that of unstimulated cells (PBS; **Figures 3A, B**). As expected, PPD stimulation resulted in an increase in IFN-γ-producing cells, but also led to higher levels of IL-2, IL-6, IL-10, IL-17A, TNF-α and GrzB-producing cells. Unlike PPD, PIM did not stimulate production of IFN-γ but instead stimulated early production of IL-4 and GM-CSF. In addition, PIM stimulation led to increased levels of IL-2$^+$, IL-6$^+$, IL-10$^+$, IL17A$^+$ and TNF-α$^+$ cells (**Figure 3B**). To better understand if the cytokines were produced one their own or in combinations, we assessed polyfunctionality of the stimulated cells using the R-package COMPASS (28). Since GrzB is functionally distinct from the cytokines, it was excluded from the analysis. In total, 512 different combinations of cytokines, as defined by a Boolean gating strategy in FlowJo were included in the analysis. We observed that all stimulations resulted in polyfunctional cytokine production, although responses to LAM were significantly lower than to PIM and PPD (**Supplemental Figure 5**).

To get an overview of which cell types that were responsible for the cytokine production, we identified the cell subsets producing each cytokine, regardless of the group and stimuli. We observed that myeloid cells (identified through the

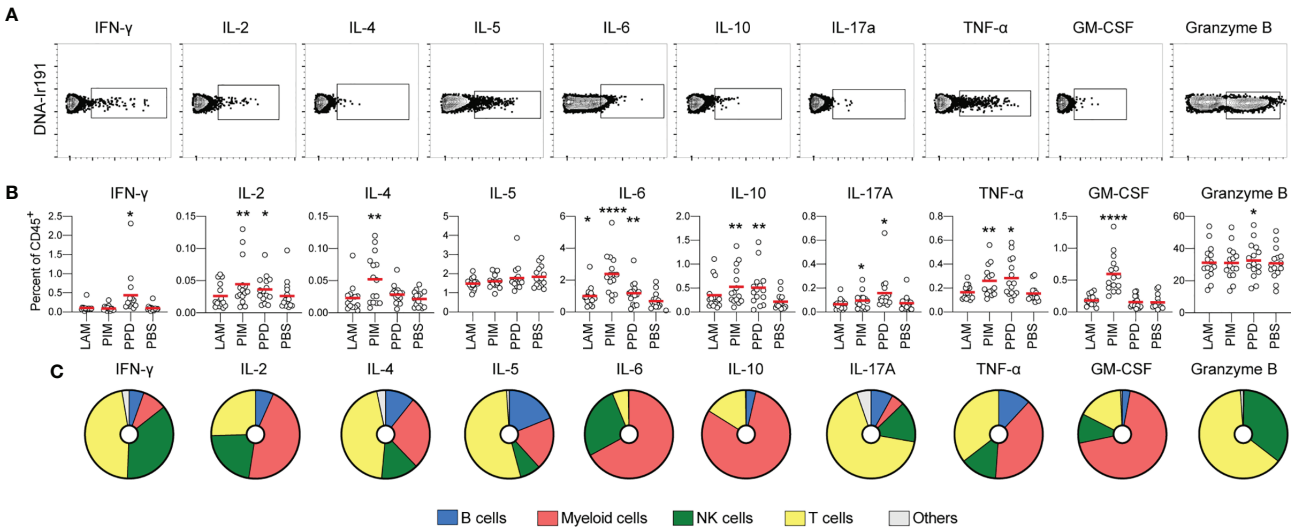

FIGURE 3 | Stimulation-induced cytokine production. **(A)** Representative gates for identification of cytokine producing CD45$^+$ cells *via* intracellular staining. **(B)** The frequency of cytokine positive cells out of CD45$^+$ cells for each stimulation at 24h. All donors merged (n=15/stimulation). Statistics was evaluated by Friedman's test with Dunnet's posttest where every group was compared with unstimulated cells (PBS). *p<0.05, **p<0.01, ****p<0.0001. **(C)** For each cytokine, the pie-charts indicate the frequency of cell type responsible for its production: B cells (blue), myeloid cells (red), NK cells (green), T cells (yellow), and others (grey).

expression of CD33) contributed strongly to the early production of IL-2, IL-6, IL-10, TNF-α, and GM-CSF. This is consistent with myeloid cells being the main source of pro-inflammatory cytokines such as IL-6 and TNF-α (29) (**Figure 3C**). This pattern largely overlapped with the cytokines stimulated by PIM, indicating that myeloid cells could be the main effector cells stimulated by Mtb glycolipids. T cells were the main cytokine producers of IFN-γ, IL-4, IL-5, IL-17A, and GrzB, while NK cells primarily produced IFN-γ, IL-2, IL-6, IL-17A, TNF-α, and GrzB. We also identified B cells, producing primarily IL-2, IL-4, IL-5, IL-17A, and TNF-α, although to a smaller extent compared with the other cell subsets (**Figure 3C**).

In summary, stimulation with Mtb glycolipids and PPD led to a polyfunctional cytokine response associated with production from multiple cell subsets.

Reduced Cytokine Production in Individuals With Active- or Latent TB

To investigate the overall cytokine response profile of the main cell populations in individuals with ATB, LTB and HC, we pooled all the cytokine-producing cells of each cell population after subtracting the number in unstimulated conditions for each donor and compared the cumulative production of cytokines within the different groups (**Figure 4**). For T cells, we observed a reduced cytokine production in individuals with ATB and LTB to PIM stimulation (**Figure 4A**). There was no overall significant effect on cytokine$^+$ NK cells associated with Mtb-infection (**Figure 4B**). For B cells, the overall cytokine production was reduced in individuals with ATB upon LAM and PIM stimulation compared with HC, primarily due to a reduced production of IL-5 (**Figure 4C**). For myeloid cells, a similar reduction of cytokine$^+$ cells was observed in individuals with LTB to LAM, PIM, and PPD stimulations. This effect was mainly attributed to a reduced production of IL-10 and IL-6. For ATB this effect was only observed in response to LAM (**Figure 4D**).

In summary, individuals with ATB or LTB responded with less cytokine production by especially myeloid cells and somewhat by B and T cells upon stimulation with Mtb antigens.

To further analyze the effect of LAM, PIM, and PPD on cytokine production by individual cell subsets between the three groups (ATB, LTB, and HC), we proceeded with dimensionality reduction using t-stochastic neighbour embedding (t-SNE) and cluster analysis. This was performed by pooling all PBS, PPD, PIM, and LAM mass cytometry data files together followed by analysis using Cytofkit (24). To allow a high level of resolution in the analysis, cytokine producing CD45$^+$ cells were gated for the individual cytokines (see gates in **Figure 3A**) which were then analyzed separately (**Supplemental Figure 6**, **7**).

Qualitatively Different T Cell Responses to PIM and PPD

Stimulation with PPD resulted in an increased number of T cells (identified as CD3$^+$) producing IFN-γ, IL-2, IL-5, IL-6, IL-17A, TNF-α, and GrzB compared with LAM and/or PIM. Stimulation with PIM contributed to higher numbers of IL-2$^+$, TNF-α$^+$, and GM-CSF$^+$ T cells compared with LAM stimulated cells (**Figure 5A**). Of all cells producing IFN-γ at 24 h, T cells represented 39%, comprising 11 different clusters (clusters 2, 3, 5, 8, 10, 11, 12, 14 15, 16, and 24) (**Figure 5B**). Four of these clusters (clusters 5, 11, 12, and 15) were significantly elevated by PPD stimulation compared to PIM and/or LAM (**Figure 5C**). These clusters corresponded to different CD4$^+$ and CD8$^+$ T cells subsets, including central memory (CD4$^+$CD45RA$^-$CD27$^+$, cluster 5), effector memory (CD45RA$^-$CD27$^-$, clusters 11 and

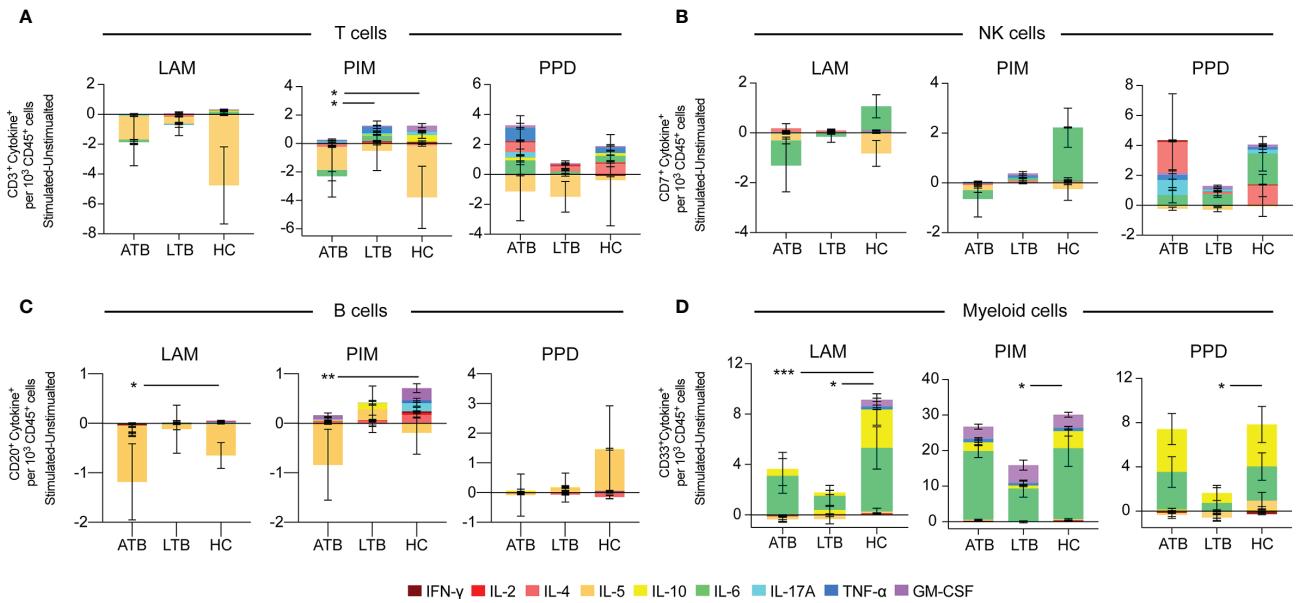

FIGURE 4 | Overall effect of stimulation on cytokine production from individuals with active- and latent TB and healthy controls. Average number of cytokine$^+$ cells following 24 h of stimulation with LAM, PIM, or PPD of PBMCs from individuals with active TB (ATB), latent TB (LTB), or healthy controls (HC) among **(A)** CD3$^+$ T cells, **(B)** CD3$^-$CD7$^+$ NK cells, **(C)** CD20$^+$ B cells, and **(D)** CD33$^+$ myeloid cells. The groups average number of cytokine-producing cells were compared using the Friedman test followed by Dunn's posttest. *p<0.05, **p<0.01, ***p<0.001.

15), and effector memory T cells re-expressing CD45RA (TEMRA - CD8$^+$CD45RA$^+$CD27$^-$, cluster 12; **Figure 5D**).

Approximately 23% of all IL-2 producing cells were identified as T cells (**Figure 5E**). These cells comprise six clusters, of which two (clusters 6 and 8) were significantly higher following PPD stimulation compared with LAM and/or PIM (**Figure 5F**). Cluster 6 corresponded to polyfunctional CD4$^+$ T cells, co-producing IFN-γ and TNF-α, while cluster 8 was composed of cells producing only IL-2 (**Figure 5G**).

Although the regulatory effect of IL-6 on T cells is well known (30), the literature on IL-6 producing T cells is limited. We identified one cluster of IL-6$^+$ T cells (cluster 5) corresponding to 5.3% of total IL-6$^+$ leukocytes after 24 h of stimulation (**Figure 5H**). This cluster was significantly elevated by PPD stimulation compared to LAM and was mainly attributed to ATB and HC, but not LTB individuals (**Figure 5I**). Cluster 5 was a mixed cluster consisting of cells expressing CD8$^+$, CD4$^+$, and double negative (DN) T cells (data not shown) with 36% of the cells co-producing GrzB (**Figure 5J**).

Approximately 14% of the GM-CSF$^+$ cells were T cells, represented by four different clusters (**Figure 5K**). Cluster 13 was significantly increased upon PIM stimulation compared to LAM and PPD (**Figure 5L**). The effect was more prominent in HC individuals compared to LTB. This cluster corresponded mostly to naïve (CD45RA$^+$CD27$^+$) CD8$^+$ T cells (**Figure 5M**).

T cells represented 62% of the IL-17A$^+$ cells (**Figure 5N**). Four out of 12 clusters (clusters 5, 14, 15, and 16) were increased by PPD compared with PIM and/or LAM stimulations, while clusters 1 and 2 were increased by PIM compared with PPD (**Figure 5O** left). In addition, the analysis of individual clusters showed that stimulation with LAM reduced cluster 1 in ATB, compared with HC individuals. Also, cluster 16 was higher in LTB compared with HC upon PIM stimulation (**Figure 5O** right). Three of these clusters corresponded to polyfunctional T cells (clusters 5, 14, and 15), with clusters 5 and 15 co-producing IFN-γ, and cluster 14 co-producing IFN-γ and TNF-α (**Figure 5P**).

In summary, T cell responses were mainly observed upon stimulation with PPD. The T cells producing IFN-γ, IL-2, IL-6, and IL-17A, some of those with a polyfunctional phenotype, were significantly increased with PPD compared with LAM and/or PIM. Interestingly, however, PIM stimulation led to an increase in GM-CSF-producing T cells, particularly in HC individuals, potentially indicating a different mechanism for GM-CSF induction also associated with disease status.

NK Cells Are Primarily Stimulated by PPD

As for T cells, the NK cells (identified as CD3$^-$CD7$^+$) showed minor responses to PIM and LAM, and were mainly affected by PPD stimulation, which resulted in significantly higher numbers of NK cells producing IFN-γ, IL-2, IL-6, IL-17A, and GM-CSF, compared to PIM and LAM (**Figure 6A**). Most of IFN-γ producing cells at 24 h of stimulation were NK cells. They represented 51% of all IFN-γ-producing cells and could be further divided into 9 clusters (clusters 1, 6, 7, 13, 19, 21, 22, 23, and 25) (**Figure 6B**). Of these, four clusters were significantly increased following PPD stimulation, compared with LAM and PIM (**Figure 6C**). All of these clusters were CD57$^-$ but expressed different levels of CD56 suggesting that they belonged to different NK subsets. Moreover, all clusters expressed GrzB while cluster 13 also expressed IL-17A (**Figure 6D**).

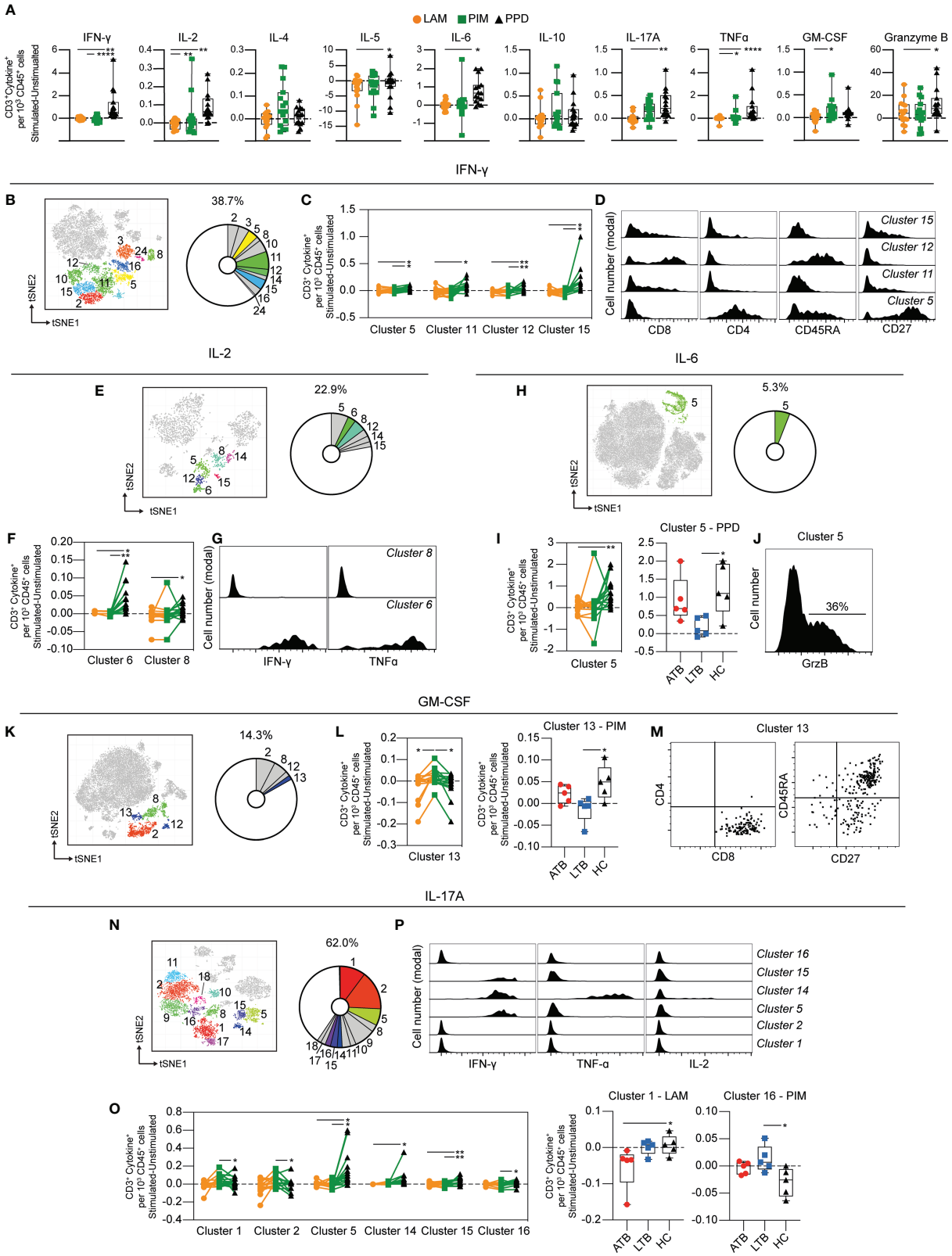

FIGURE 5 | Continued

FIGURE 5 | Cytokine production by stimulated T cells. **(A)** The number of cytokine-producing T cells per 1000 total $CD45^+$ cells for each stimulation at 24 h with the background (unstimulated) cytokine-production removed. **(B)** Cluster analysis of IFN-γ secreting cells with clusters 2, 3, 5, 8, 10, 11, 12, 14, 15, 16, and 24 corresponding to T cells. **(C)** Clusters significantly affected by stimulation with **(D)** cluster histograms indicating CD4, CD8, CD45RA, and CD27. **(E)** Cluster analysis of IL-2 secreting cells with clusters 5, 6, 8, 12, 14, and 15 corresponding to T cells. **(F)** Clusters significantly affected by stimulation with **(G)** cluster histograms indicating IFN-γ and TNF-α secretion. **(H)** Cluster analysis of IL-6 secreting cells with cluster 5 corresponding to T cells. **(I)** Cluster 5 is significantly affected by stimulation (left) and comparison of PPD stimulation on donors with active TB (ATB), latent TB (LTB) and healthy controls (HC) in cluster 5 (right). **(J)** Cluster histogram indicating GrzB secretion. **(K)** Cluster analysis of GM-CSF secreting cells with cluster 2, 8, 12, and 13 corresponding to T cells. **(L)** Cluster 13 is significantly affected by stimulation (left) and comparison of PIM stimulation on donors with ATB, LTB and HC in cluster 13 (right). **(M)** Cluster dot plots indicating CD4, CD8, CD45RA, and CD27 expression. **(N)** Cluster analysis of IL-17A secreting cells with cluster 1, 2, 5, 8, 9, 10, 11, 14, 15, 16, 17, and 18 corresponding to T cells. **(O)** Clusters significantly affected by stimulation (left) and comparison of PIM and LAM stimulation on donors with active ATB, LTB and HC in clusters 1 and 16, respectively (right) **(P)** Cluster histograms indicating IFN-γ, TNF-α, and IL-2. Statistical differences between stimulations in **(A, I, L)** were evaluated by Friedman's test with Dunnet's posttest, while comparisons within multiple clusters (**C, F, O** left panels) were evaluated by a matched-pair two-way ANOVA with Geissner-Greenhouse correction followed by Tukey's posttest (n=15/stimulation). Groups (ATB/LTB/HC) (**I, L, O** right panels) were compared using Kruskal-Wallis with Dunn's posttest (n=5/group) $^{*}p<0.05$, $^{**}p<0.01$, $^{***}p<0.001$, $^{****}p<0.0001$.

IL-2-producing NK cells constituted 24% of all $IL\text{-}2^+$ cells and represented two clusters (cluster 1 and 9) (**Figure 6E**). Cluster 1 was significantly increased by PPD, compared with LAM stimulation (**Figure 6F**). Both clusters were $CD57^-$ while cluster 1 expressed intermediate levels of CD56 and no CD27 while cluster 9 expressed high levels of CD56 and CD27 (**Figure 6G**). Both clusters co-produced IL-6 (**Figure 6G**). NK cells represent approximately 8% of all GM-CSF-producing cells at 24 h of stimulation (**Figure 6H**). The cytokine was produced by two clusters (4 and 16), one of which (cluster 16) was significantly higher in response to PPD compared with LAM and PIM stimulation (**Figure 6I**). Similar to PPD-mediated IL-2 secreting NK cells, GM-CSF was primarily produced by $CD57^-$ NK cells where >50% expressed intermediate CD56 levels while almost no cells expressed CD27 (**Figure 6J**). Cluster 16 cells were also co-producing IFN-γ (**Figure 6J**). Approximately 25% of all IL-6-producing cells at 24 h were identified as NK cells (**Figure 6K**), and two out of the six clusters (3 and 12) were significantly increased in numbers by PPD stimulation compared to LAM (**Figure 6L**). These two clusters belonged to different NK subsets with cluster 3 corresponding to $CD56^{high}CD57^-$ NK cells, of which 48% also expressed CD27, while cluster 12 was composed of $CD56^{int}CD57^+CD27^-$ NK cells (**Figure 6M**). The IL-17A producing NK cells were composed of two clusters at 24 h. However, they were not significantly different between the different stimulations (data not shown).

Thus, similar to T cells, NK cells were primarily induced to secrete cytokines through stimulation with PPD compared with the Mtb glycolipids LAM and PIM. The stimulation led to cytokine production by $CD56^{int}$ and $CD56^{bright}$ NK cells, independent on the expression of CD57. In summary, these results show that stimulation with PPD leads to rapid activation of different NK cell subsets with production of primarily pro-inflammatory cytokines.

Atypical B Cells Are a Major Source of Polyfunctional Cytokine Responses Following PIM Stimulation

Compared with T cells and myeloid cells, B cells (defined as $CD3^-$ $HLA\text{-}DR^+CD20^+$) were minor producers of the measured cytokines (**Figure 3**). There was however a primarily PIM-derived effect leading to significantly increased numbers of IL-4, IL-10, and GM-CSF producing B cells in comparison to LAM and/or PPD stimulation (**Figure 7A**). There were two B cell clusters producing IL-4 (cluster 6 and 12) (**Figure 7B**), but only cluster 6 was significantly increased by PIM stimulation, with PPD leading to the lowest numbers of cells in this cluster (**Figure 7C**). Cluster 6 was enriched for switched memory ($CD27^+IgD^-$) and double negative (DN; $CD27^-IgD^-$) B cells, while cluster 12 was enriched for naïve B cells ($CD27^-IgD^+$) (**Figure 7D**). Cluster 6 was further enriched for $CD11c^+$ B cells, which are associated with recent B cell activation and formation of atypical B cells during infection or inflammatory conditions (31).

B cells producing IL-10 and GM-CSF were also significantly expanded by PIM stimulation (**Figures 7E–J**). As B cells responding to PIM stimulation presented a highly homogenous phenotype, we further evaluated the cells for co-expression of the three cytokines (**Figure 7K**). We found that 42% of GM-CSF-producing B cells also produced IL-4 and IL-10. Compared with total B cell populations, the phenotype of the polyfunctional cells was highly enriched for double negative (DN - IgD^-CD27^-) B cells but also for unswitched and switched memory B cells ($CD27^+$) compared with total B cell populations (**Figure 7L**). The polyfunctional B cells were also approximately 10-fold enriched for $CD11c^+$ B cells compared with total B cells, suggesting that atypical B cells can respond to PIM stimulation (**Figure 7L**). We also quantified the levels of HLA-DR on the cell surface of the polyfunctional B cells and compared with the levels on total B cells and found an increased expression of HLA-DR on cells from cluster 7 (**Figure 7M**), consistent with previous reports on atypical B cells in mice and humans (32, 33).

Rapid Polyfunctional Response of Myeloid Cells to PIM Stimulation

The production of cytokines by $CD33^+$ myeloid cells was compared for each stimulation (**Figure 8A**). PIM stimulation led to a robust increase of cells producing IL-2, IL-4, IL-6, IL-10, TNF-α, compared to PPD, and of IL-6, IL-17A, TNF-α and GM-CSF in comparison to LAM (**Figure 8A**). Interestingly, IL-10 producing cells were induced by both PIM and PPD (**Figure 8A**), contrasting with the other cytokines that were primarily induced by PIM.

To understand if the effect of stimulation was associated with specific myeloid subsets, we further investigated the impact of

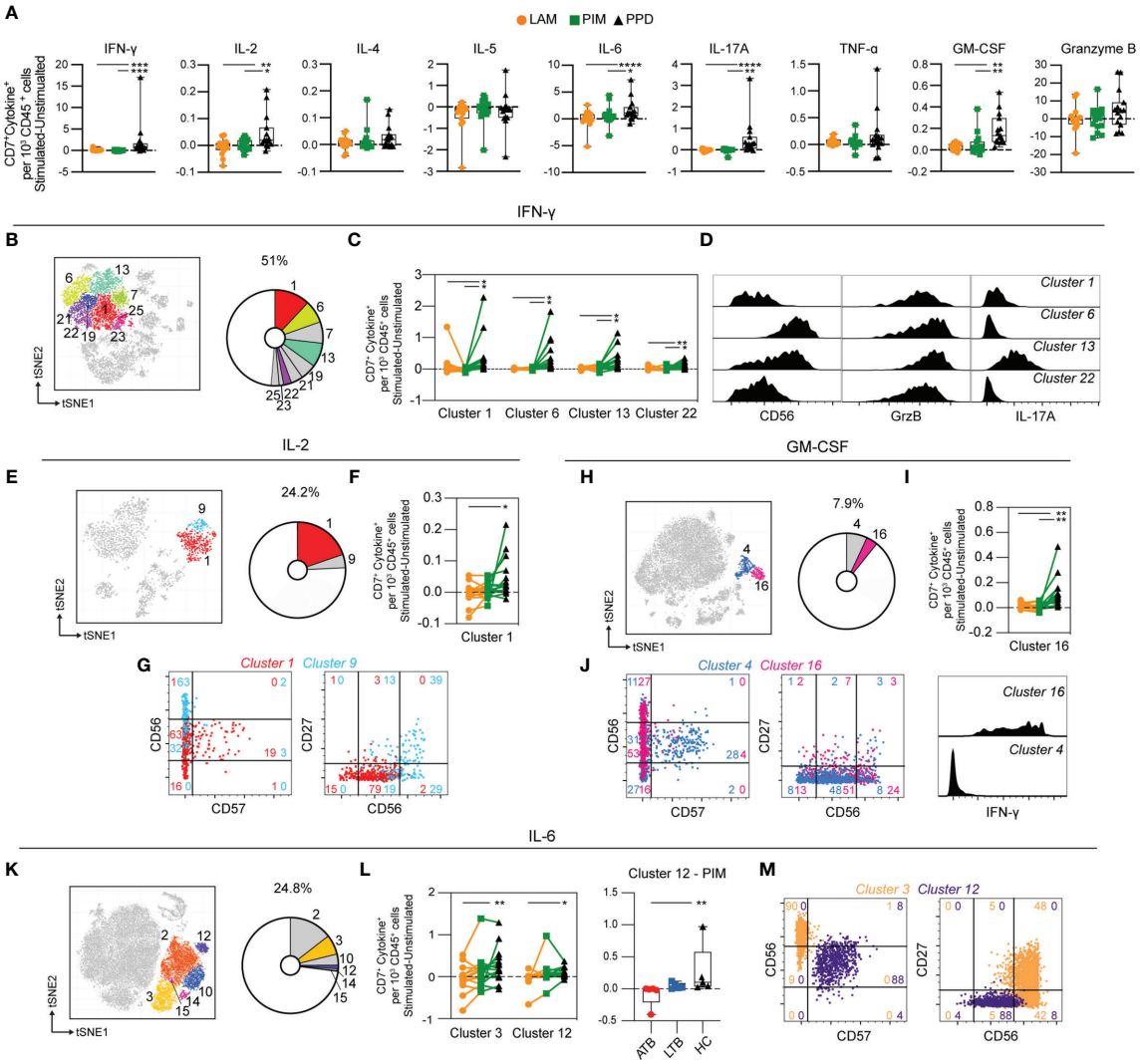

FIGURE 6 | Cytokine production by stimulated NK cells. **(A)** The number of cytokine-producing NK cells per 1000 total CD45$^+$ cells for each stimulation at 24 h with the background (unstimulated) cytokine-production removed. **(B)** Cluster analysis of IFN-γ secreting cells with clusters 1, 6, 7, 13, 19, 21, 22, 23, and 25 corresponding to NK cells. **(C)** Clusters significantly affected by stimulation with **(D)** cluster histograms indicating CD56 expression and GrzB and IL-17A secretion. **(E)** Cluster analysis of IL-2 secreting cells with cluster 1 and 9 corresponding to NK cells. **(F)** Clusters significantly affected by stimulation with **(G)** cluster dot plots showing CD56, CD57, and CD27 expression and histograms indicating IL-6 production. **(H)** Cluster analysis of GM-CSF secreting cells with cluster 4 and 16 corresponding to NK cells. **(I)** Cluster 16 significantly affected by stimulation. **(J)** Cluster's dot plots showing CD56, CD57, and CD27 expression and histogram indicating IFN-γ secretion. **(K)** Cluster analysis of IL-6 secreting cells with cluster 1 and 9 corresponding to NK cells. **(L)** Clusters significantly affected by stimulation (left) and comparison of PIM stimulation on donors with active TB (ATB), latent TB (LTB) and healthy controls (HC) in cluster 12 (right). **(M)** Cluster's dot plots showing CD56, CD57, and CD27 expression. Numbers in dot plots indicate the percentage within the cluster. Statistical differences between stimulations in **(A, F, I)** were evaluated by Friedman's test with Dunnet's posttest, comparisons within multiple clusters **(C, L** left**)** were evaluated by a matched-pair two-way ANOVA with Geissner-Greenhouse correction followed by Tukey's posttest (n=15/stimulation). Groups (ATB/LTB/HC) **(L,** right**)** were compared using Kruskal-Wallis with Dunn's posttest (n=5/group) *p<0.05, **p<0.01, ***p<0.001, ****p<0.0001.

stimulation on individual cell clusters. The IL-2 producing myeloid cells constituted 43.6% of all IL2-producing cells and were composed of four different clusters (cluster 3, 4, 7, and 13), of which three were differently affected by the stimuli (**Figure 8B**). For cluster 3 and 13, PIM stimulation led to significantly more IL-2$^+$ cells compared with PPD and/or LAM, while cluster 7 was higher in LAM compared to PPD (**Figure 8C**). Cluster 7 expressed CD14, while clusters 3 and 13 were mostly negative for CD14 (**Supplemental Figure 7**). Cluster 3 was associated with the co-production of IL-6 (**Figure 8C**).

Approximately 29% of all IL-4 producing cells after 24 h of stimulation expressed CD33. (**Figure 8D**). These cells were further distributed into three clusters (3, 7, and 11), of which cluster 7 and 11 were significantly higher in number following PIM stimulation compared with LAM and PPD stimulation. LAM stimulation also led to more IL-4 producing cells compared

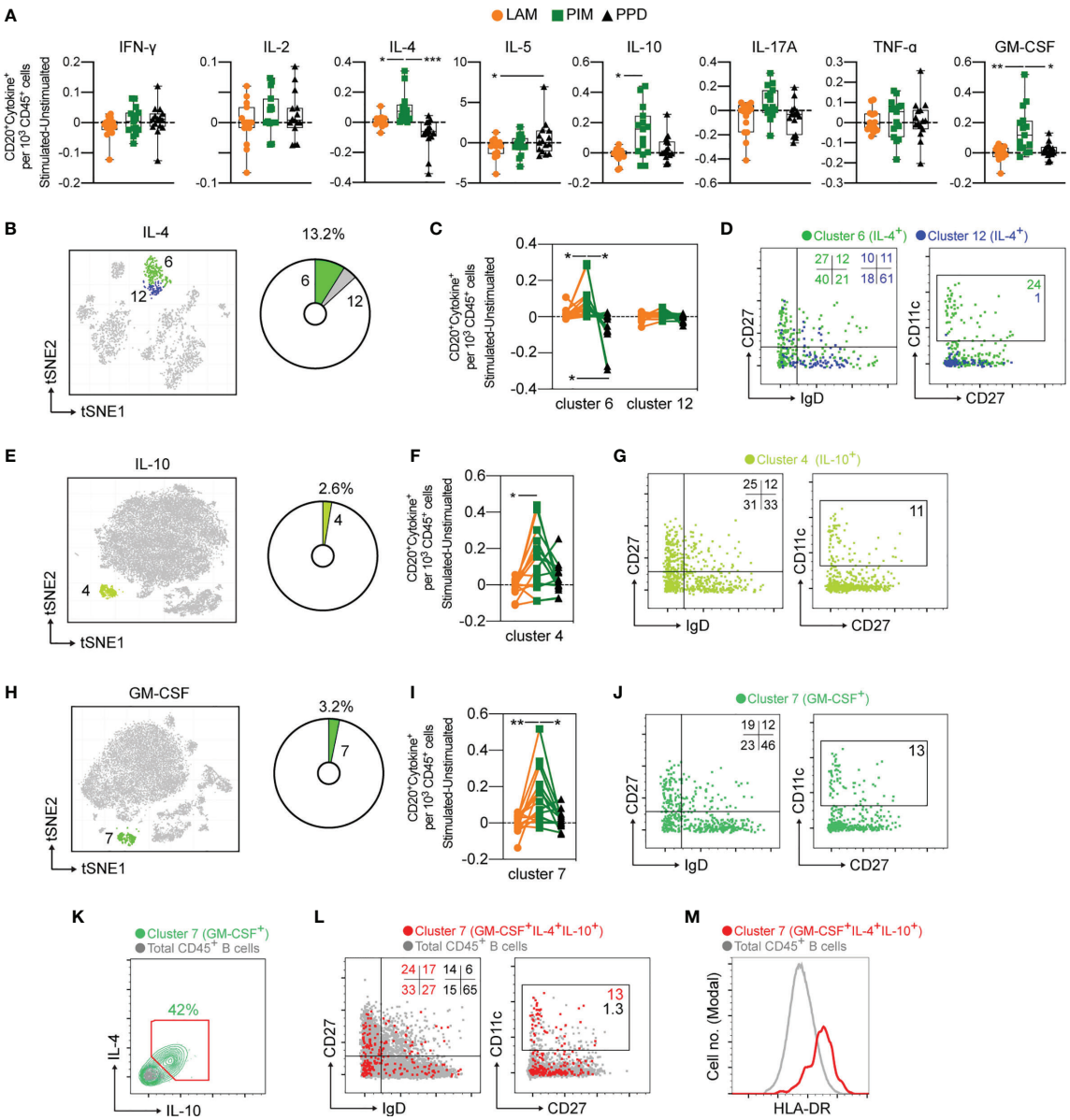

FIGURE 7 | Cytokine production by stimulated B cells. **(A)** The number of cytokine positive B cells per 1000 total CD45$^+$ cells for each stimulation at 24 h with the background (unstimulated) cytokine-production removed. **(B)** Cluster analysis of IL-4 secreting cells with cluster 6 and 12 corresponding to B cells. The pie-chart indicates cluster-specific and percent of total contribution to all IL-4 secreting cells. **(C)** Evaluation of the effect of LAM (orange circles), PIM (green boxes), or PPD (black triangles) stimulation on IL-4 secreting B cell clusters. **(D)** Overlay of concatenated IL-4 secreting B cells for cluster 6 (green) and cluster 12 (blue) assessing IgD and CD27 or CD11c and CD27 surface expression. **(E, G)** A similar analysis for IL-10 secreting cells and **(H–J)** GM-CSF secreting cells. **(K)** IL-4 and IL-10 co-expression among GM-CSF$^+$ B cells (green) and total B cells (grey). **(L)** Overlay scatter plot of GM-CSF$^+$IL-4$^+$IL-10$^+$ triple-secreting B cells (red) and total B cells (grey) assessing IgD and CD27 or CD11c and CD27 surface expression, with frequency of cells included in the gates indicated. **(M)** Overlay histogram indicating HLA-DR expression for GM-CSF$^+$IL-4$^+$IL-10$^+$ triple-secreting B cells (red) and total B cells (grey). Numbers in dot plots indicate the percentage within the cluster. Statistical differences between stimulations in individual groups **(A, F, I)** were evaluated by Friedman's test with Dunnet's posttest, while comparisons within multiple clusters **(C)** were evaluated by a matched-pair two-way ANOVA with Geissner-Greenhouse correction followed by Tukey's posttest (n=15/stimulation). *p<0.05, **p<0.01, ***p<0.001. n=15 for each group. Scatter and overlay plots show data concatenated from all samples and donors (n=60).

to PPD (**Figure 8E**). Both cluster 7 and 11 produced several other cytokines in addition to IL-4, with cluster 7 also producing IL-10, and cluster 11 producing IL-6, and IL-10 (**Figure 8E**). Interestingly, this effect of multiple cytokine production, was significantly reduced in individuals with LTB compared with ATB and HC (**Figure 8F**).

IL-6 was the most frequent cytokine produced following PIM stimulation (**Figure 8A**). Approximately 70% of all IL-6 secreting

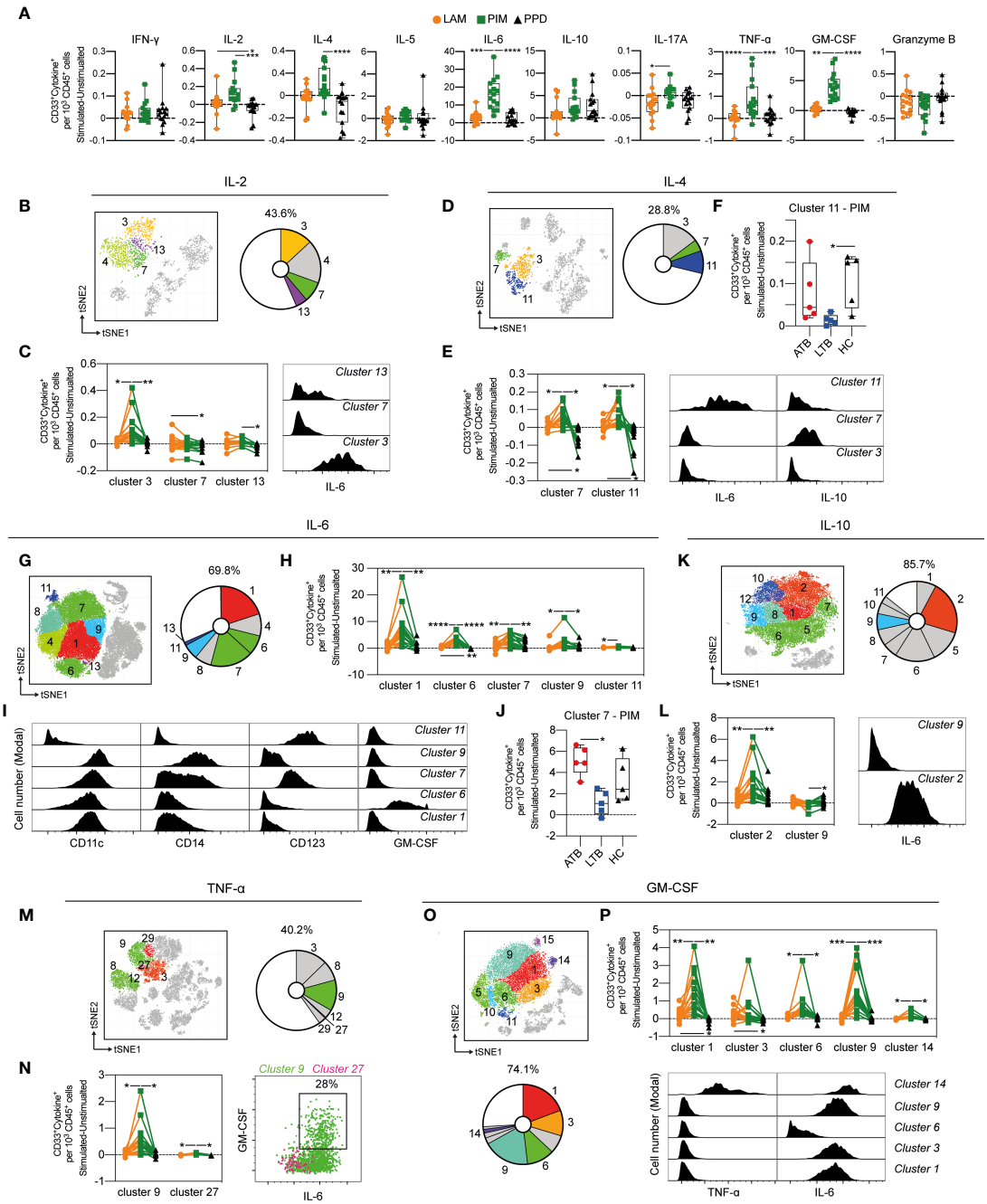

FIGURE 8 | Cytokine production by stimulated CD33$^+$ myeloid cells. **(A)** The number of cytokine positive CD33$^+$ myeloid cells per 1000 total CD45$^+$ cells for each stimulation at 24 h with the background (unstimulated) cytokine-production removed. **(B)** Cluster analysis of IL-2 secreting cells with cluster 3, 4, 7 and 13 corresponding to myeloid cells. **(C)** Clusters significantly affected by stimulation (left) with cluster histograms indicating co-secretion of IL-6. **(D)** Cluster analysis of IL-4 secreting with cluster 3, 7, and 11 corresponding to myeloid cells. **(E)** Clusters significantly affected by stimulation (left) and co-expression with IL-6 and IL-10 (right). **(F)** Comparison of PIM stimulation on donors with active TB (ATB), latent TB (LTB) and healthy controls (HC) in cluster 11. **(G)** Myeloid clusters secreting IL-6 **(H)** significantly affected by stimulation. **(I)** Cell surface phenotype of indicated cluster. **(J)** Differential effect of PIM stimulation on cluster 7 cells in ATB, LTB, and HC. **(K)** Myeloid clusters secreting IL-10 with **(L)** clusters significantly affected by stimulation (left panel) and histograms indicating IL-10 co-expression with IL-6. **(M)** Myeloid clusters secreting TNF-α **(N)** significantly affected by stimulation (left) with co-expression of GM-CSF and IL-6 (right). **(O)** Myeloid clusters secreting GM-CSF. **(P)** Clusters differently affected by stimulation (left) with co-expression of TNF-α and IL-6 (right). Statistical differences between stimulations in **(A)** were evaluated by Friedman's test with Dunnet's posttest, while comparisons within multiple clusters **(C, E, H, L, N, P)** were evaluated by a matched-pair two-way ANOVA with Geissner-Greenhouse correction followed by Tukey's posttest (n=15/stimulation). Groups (ATB/LTB/HC) **(F, J)** were compared using Kruskal-Wallis with Dunn's posttest (n=5/group) *p<0.05, **p<0.01, ***p<0.001, ****p<0.0001.

cells at 24 h were myeloid cells (**Figure 8G**) with 5 out of 7 clusters showing a significant increase following PIM stimulation compared with PPD and/or LAM (**Figure 8H**). Several subsets of myeloid cells responded with IL-6 production, including $CD11c^+CD14^-CD123^-$ DCs (cluster 1 and 6), intermediate/non-classical monocytes ($CD11c^+CD14^{int/-}CD123^+$, cluster 7), and classical monocytes ($CD11c^+CD14^+CD123^-$, cluster 9). Among these, the cluster 6 DCs also produced GM-CSF, in addition to IL-6 (**Figure 8I**). Similar to the $IL\text{-}4^+IL\text{-}6^+$ co-producing cluster 11 (**Figure 8F**), the intermediate/non-classical monocyte cluster 7 contracted in individuals with LTB, compared with those with ATB and HC (**Figure 8J**).

Myeloid cells were the main cell subset identified within IL-10, TNF-α and GM-CSF-producing cells, especially following stimulation with PIM (**Figures 8K, M, O**). One IL-10 cluster, two TNF-α clusters and five GM-CSF clusters were significantly increased compared with LAM and PPD (**Figures 8L, N, P**). Of these, parts of TNF-α cluster 9 and GM-CSF cluster 14 likely corresponded to the same polyfunctional cells as both clusters secreted TNF-α, GM-CSF, and IL-6 (**Figures 8L, N**). From the two IL-10 clusters that were affected by PIM, one only produced IL-10 while the other co-produced IL-6. GM-CSF cluster 1, 3, and 9 also co-produced IL-6, but not TNF-α, while cluster 6 only produced GM-CSF.

In summary, several myeloid cell subsets rapidly responded to stimulation by producing cytokines. The response was primarily induced by PIM and included phenotypes of cells producing both single and multiple cytokines. Among the most polyfunctional responses were cells producing IL-4, IL-6, and IL-10, or TNF-α, GM-CSF and IL-6.

Stimulation of Myeloid Cells With PIM Is Partially TLR2 Dependent

PIM and LAM stimulation induced a robust immune response in myeloid cells (**Figure 8A**). To investigate the mechanism responsible for this effect, and in particular the dependence on interaction with TLR2, PBMCs from HC were treated with anti-TLR2 blocking antibody before stimulation with PIM, LAM and PHA. Blocking TLR2 led to a reduction in the percentage of $CD33^+IL\text{-}6^+$ myeloid cells upon PIM stimulation, but not with LAM or PHA (**Figure 9**). We did not observe any significant effect of blocking TLR2 on IL-6 production from T cells, NK cells, or B cells (data not shown), although the frequency of $IL\text{-}6^+$ cells was very low on those cell subsets.

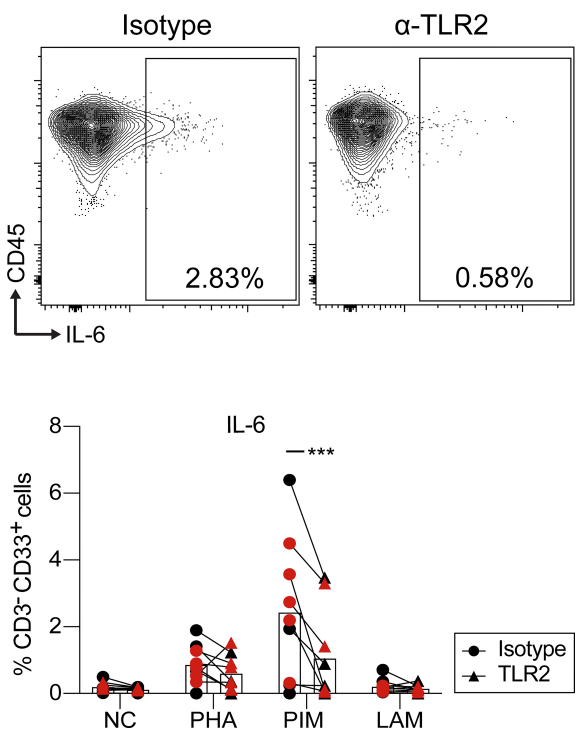

FIGURE 9 | IL-6 production by myeloid cells upon PIM stimulation is regulated *via* TLR2. Dot plots of IL-6 gating within myeloid cells (top) and percentage of cells producing IL-6 within myeloid cells (bottom). PBMCs were pre-treated with anti-TLR2 or isotype control and then stimulated with PIM, LAM, and PHA during 24 h. IL-6 production was evaluated by flow cytometry. Statistical differences between anti-TLR2 and isotype were evaluated by a paired t test (n=9) ***p<0.001. NC, negative control. The red and black colors correspond to two independent experiments.

DISCUSSION

In the present study, we show that LAM and PIM induce responses in PBMCs from Mtb-infected individuals that can be distinguished from those obtained from HC. In addition, we show that the responses to these glycolipids are clearly different from those elicited by PPD. The responses involve both expansion and contraction of particular cell subsets and production and secretion of distinct patterns of cytokines and chemokines.

When analyzing intracellular cytokine production, we found that PIM mainly induced antigen-presenting cells to produce a defined set of pro-inflammatory cytokines consisting of IL-2, IL-6, IL-17A, TNF-α and GM-CSF, the anti-inflammatory IL-10 as well as IL-4, but not IFN-γ. LAM triggered responses that tended to be similar to the ones generated by PIM, but weaker in most instances. Classical and intermediate monocytes are known to secrete high levels of pro-inflammatory cytokines in response to microbial products (34). In addition, compared to non-classical monocytes, they were previously shown to exhibit a greater polyfunctional pro-inflammatory response (IL1-α, IL1-β, IL-6, IL-8, IL-10, and TNF-α) to lipomannan from *Mycobacterium smegmatis*, a TLR-2 agonist (34). Here we show that PIM induced multifunctional monocytes producing cytokines in a combination of either pro-inflammatory IL-2, IL-6, GM-CSF and TNF-α, or IL-4 and the anti-inflammatory IL-10. In particular GM-CSF, which is increasingly recognized for its potential role in innate resistance to TB (35), was in our study mainly produced by myeloid cells upon PIM stimulation.

This response contrasted with the quite well-known immune response triggered by PPD, which was dominated primarily by T and NK cells. They produced predominantly the pro-inflammatory cytokines IFN-γ, IL-2, IL-6, IL-17A, TNF-α, and

GrzB, but also IL-10, although no IL-4. While T cells simultaneously producing combinations of cytokines have been extensively investigated in the context of the immune response in TB (36–38), we extended these findings to several other cell types. Our results reveal that multiple subsets of myeloid cells, NK, B and T cells respond to glycolipids and/or to PPD, with the production of different combinations of cytokines such as classical functional T cells producing IFN-γ, IL-2 and TNF-α, but also other combinations, such as IL6 and GrzB or IL-17A and TNF-α with or without IFN-γ.

B cells producing IL-10 and GM-CSF are known to be present at relatively low frequencies in human peripheral blood (39, 40). This is in agreement with our finding that B cells were minor producers of IL-10 and GM-CSF, even after stimulation. We did however identify subsets of polyfunctional B cells that produced a combination of GM-CSF, IL-4 and IL-10. These cells were enriched among DN ($CD27^{-}IgD^{-}$) B cells and unswitched and switched memory B cells ($CD27^{+}$). The polyfunctional B cells were also approximately 10-fold enriched among B cells expressing CD11c, which was recently associated with B cell activation and formation of atypical B cells (31), also known to expand during ATB (41). Human GM-CSF–expressing B cells are notable for being among the highest producers of both TNF-α and IL-6, and most *in vitro*-induced human $IL\text{-}10^{+}$ B cells are also reported to secrete TNF-α and/or IL-6 (42). However, human B cell subsets have been reported to show a near-mutually exclusive expression of GM-CSF and IL-10 (39). By contrast, in our study, B cells stimulated by PIM did not co-produce GM-CSF with TNF-α or IL-6, but rather with IL-4 and IL-10, indicating a different pathway of stimulation.

PIM and LAM did not trigger detectable polyfunctional T cells, although we identified several polyfunctional T cell subsets producing combinations of IFN-γ/IL-2/IL-6/TNF-α/IL-17A that were expanded by PPD stimulation, which is in agreement with previous reports of polyfunctional Mtb-specific T cells producing IFN-γ in combination with IL-2 and TNF-α (36, 37, 43).

One important observation in this study was that upon stimulation with PIM and LAM, cells and supernatants from individuals with ATB or LTB produced less cytokines than the cells from HC. This is obvious for myeloid cells and to a lesser extent for B and T cells. The hyporesponsive state in monocytes in response to PIM and LAM is compatible with trained immunity leading to a tolerogenic cellular response. Trained immunity is defined as a long-term adaptation of innate immune cells leading either to an enhanced responsiveness or a tolerance state to a subsequent challenge (44, 45). Chronic or repeated stimulation through TLRs can render immune cells unresponsive to subsequent challenges with the same or different TLR ligands (46–48) or other bacterial components (49). Our results support the hypothesis that continuous stimulation with LAM and PIM, in ATB and LTB individuals lead to a reduced response to these molecules compared with HC.

The response of myeloid cells to PPD was weaker in LTB compared to HC, indicating hyporesponsiveness also to PPD. This is in line with earlier observations of depression of PPD-induced proliferative responses by monocytes from TB patients (50, 51), where direct stimulation of monocytes primed during Mtb infection appear to be responsible for *in vitro* suppression of PPD responses (50). Interestingly we also found that T cells were somewhat hyporesponsive to PIM. The overall cytokine production was reduced in individuals with ATB upon PIM stimulation. These results are in agreement with the systematic review by Li et al. that found lower levels of IL-17 and IFN-γ in ATB when compared to LTB (52). An additional interesting observation in our study was that PIM expanded a cluster of $GMCSF^{+}$ $CD8^{+}$ T cells in HC but not in LTB patients. This hyporesponsiveness to PIM might be caused by T cell exhaustion or tolerance in Mtb infected individuals. Exhaustion of T cells represents a state of functional hyporesponsiveness due to persistent antigen exposure and inflammation reported for TB and other chronic infections (53–55). This effect can also be induced by repeated exposure to mycobacterial antigens (56), including direct exposure of T cells to LAM (57).

Antigen-specific $CD4^{+}$ T-cell activation can be directly inhibited by LAM (58–61) and PIM (59). By interfering with very early events in TCR signaling, LAM and PIM may drive cells to a state of anergy (59, 61), which could provide another explanation of the poor response of cells from ATB and LTB individuals to Mtb glycolipids. Alternatively, the hyporesponsiveness could be indirect, through upstream effects of hyporesponsive myeloid cells, since PIM and LAM also induce proliferation of specific T cells upon presentation by CD1 molecules on myeloid cells.

IL-6 is known to be strongly induced in monocytes and DCs upon TLR2 ligation (62). We observed that PIM stimulation induced IL-6 production mainly in myeloid cells (DCs and classical/nonclassical monocytes). Moreover, treatment with an anti-TLR2 antibody led to partial inhibition of PIM-induced IL-6 production in myeloid cells, suggesting that PIM induces IL-6 production through TLR2. This is in line with other studies where it was observed that PIMs and ManLAM from Mtb induce pro-inflammatory cytokine production in human and mouse Mφs *via* recognition by TLR2 (63–65). However, IL-6 production was not completely abolished suggesting that other mechanisms of PIM stimulation likely remain, or residual IL-6 production may be due to incomplete blocking rather than additional signaling pathways.

LAM and PIM had in general very similar effects, although LAM induced a weaker response than PIM. Presuming that LAM and PIM act through the same TLR2 pathway the different responses are potentially associated with structural differences, where a common active site may be partly masked in LAM compared to PIM. Nigou et al. showed that LAM induces a weaker signal through TLR2 compared to PIM_6, suggesting that the bulky arabinan domain may mask the mannan chain in such a way that they behave like molecules with a mannan restricted to a single mannosyl unit (65). This is also in line with observations by Shukla et al. that PIM_6 induces TLR2-mediated extracellular-signal-regulated kinase (ERK) activation and TNF-α secretion in Mφs, while LAM was not an effective functional activator of TLR2 signaling (66). The weaker effect of LAM compared to PIM may also in part depend on the fact that the LAM that was used in the present study has a higher molecular weight compared to PIM resulting in a lower molar concentration.

In contrast to the glycolipids, PPD displayed a markedly different response, mainly by inducing IFN-γ. PPD contains a complex mixture of proteins, including the antigens ESAT-6 and CFP10 that are the antigens used in the Mtb specific IFN-γ release assays. We did not identify which antigens in PPD that were responsible for the immune responses presented in this study. However, since PPD is still widely used in clinical testing, the high level of details presented here may be useful to better understand how individual immune cell subsets react with Mtb proteins.

The hyporesponsive state of monocytes observed in ATB and LTB in response to PIM was more prominent in LTB. The immune profile in LTB is thought to represent a more protective pattern than in ATB (67, 68). It is possible that during LTB a continuous level of stimulation maintains a pool of protective memory cells (18), while at the same time inducing tolerance in monocytes, which could indicate protection of the host from excessive production of pro-inflammatory cytokines and control of lung tissue damage (69).

In conclusion, the detailed high dimensional overview of the cellular source of cytokines produced in response to stimulation with the various antigens, suggesting several novel sources of important cytokines (NK cell and B-cell in particular), will provide a hypothesis- generating resource for future work.

DATA AVAILABILITY STATEMENT

The raw data supporting the conclusions of this article will be made available by the authors, without undue reservation.

ETHICS STATEMENT

The study was approved by the Regional Ethical Review Board at the Karolinska Institute in Stockholm (approval numbers 2013/1347-31/2 and 2013/2243-31/4) and by the Ethics Committee for Research in Life and Health Sciences of the University of Minho, Portugal (approval number SECVS 014/2015). The patients/participants provided their written informed consent to participate in this study.

AUTHOR CONTRIBUTIONS

GK, MC-N, and CS designed the study. CSS, CS, CN, JC-G, and TL performed experiments and/or analysis. EF, GF, and JB included patients and provided clinical data. CSS, CS, and EF generated the figures and tables. BC and PB provided key resources. CSS, CS, EF, JN, MC-N, and GK wrote the first draft and all authors contributed to manuscript revision. All authors contributed to the article and approved the submitted version.

FUNDING

The work presented was performed at Karolinska Institutet and Life and Health Sciences Research Institute (ICVS), University of Minho. Financial support was provided by grants from the Swedish Research Council (grant 2016-05683 and 2020-03602) and the Swedish Heart-Lung Foundation (grants 20160336, 20180386, and 20200194) to GK. Grants from Clas Groschinsky's memorial foundation (M2049), Åke Wiberg's foundation (M19-0559), the Swedish Medical Association (SLS-934363), and Magnus Bergvall's foundation (2019-03436) to CS. Grants from the Foundation for Science and Technology (FCT) - project UIDB/50026/2020 and UIDP/50026/2020 to MCN. CSS is supported by an FCT PhD grant, in the context of the Doctoral Program in Applied Health Sciences (PD/BDE/142976/2018). JC-G is supported by an FCT PhD grant, in the context of the Doctoral Program in Aging and Chronic Diseases (PD/BD/137433/2018). CN is a junior researcher under the scope of the FCT Transitional Rule DL57/2016. The funders had no role in study design, data collection and analysis, decision to publish, or preparation of the manuscript.

ACKNOWLEDGMENTS

We thank all study participants that were recruited into the study. We also thank Maximilian Julius Lautenbach for critically reading the manuscript. We would like to thank the team from the Translational Plasma Profile Facility at SciLifeLab for support and the generation of data for this project.

SUPPLEMENTARY MATERIAL

The Supplementary Material for this article can be found online at: https://www.frontiersin.org/articles/10.3389/fimmu.2021.727300/full#supplementary-material

REFERENCES

1. Houben RM, Dodd PJ. The Global Burden of Latent Tuberculosis Infection: A Re-Estimation Using Mathematical Modelling. *PLoS Med* (2016) 13(10): e1002152. doi: 10.1371/journal.pmed.1002152
2. Getahun H, Matteelli A, Chaisson RE, Raviglione M. Latent Mycobacterium Tuberculosis Infection. *N Engl J Med* (2015) 372(22):2127–35. doi: 10.1056/NEJMra1405427
3. Garcia-Vilanova A, Chan J, Torrelles JB. Underestimated Manipulative Roles of Mycobacterium Tuberculosis Cell Envelope Glycolipids During Infection. *Front Immunol* (2019) 10:2909. doi: 10.3389/fimmu.2019.02909
4. Kallenius G, Correia-Neves M, Buteme H, Hamasur B, Svenson SB. Lipoarabinomannan, and Its Related Glycolipids, Induce Divergent and Opposing Immune Responses to Mycobacterium Tuberculosis Depending on Structural Diversity and Experimental Variations. *Tuberc (Edinb)* (2016) 96:120–30. doi: 10.1016/j.tube.2015.09.005
5. Mazurek J, Ignatowicz L, Kallenius G, Svenson SB, Pawlowski A, Hamasur B. Divergent Effects of Mycobacterial Cell Wall Glycolipids on Maturation and Function of Human Monocyte-Derived Dendritic Cells. *PLoS One* (2012) 7 (8):e42515. doi: 10.1371/journal.pone.0042515
6. Beatty WL, Rhoades ER, Ullrich HJ, Chatterjee D, Heuser JE, Russell DG. Trafficking and Release of Mycobacterial Lipids From Infected

Macrophages. *Traffic* (2000) 1(3):235–47. doi: 10.1034/j.1600-0854.2000.010306.x
7. Brock M, Hanlon D, Zhao M, Pollock NR. Detection of Mycobacterial Lipoarabinomannan in Serum for Diagnosis of Active Tuberculosis. *Diagn Microbiol Infect Dis* (2019) 96(2):114937. doi: 10.1016/j.diagmicrobio.2019.114937
8. Sakamuri RM, Price DN, Lee M, Cho SN, Barry CE3rd, Via LE, et al. Association of Lipoarabinomannan With High Density Lipoprotein in Blood: Implications for Diagnostics. *Tuberc (Edinb)* (2013) 93(3):301–7. doi: 10.1016/j.tube.2013.02.015
9. Rodriguez ME, Loyd CM, Ding X, Karim AF, McDonald DJ, Canaday DH, et al. Mycobacterial Phosphatidylinositol Mannoside 6 (PIM6) Up-Regulates TCR-Triggered HIV-1 Replication in CD4+ T Cells. *PLoS One* (2013) 8(11):e80938. doi: 10.1371/journal.pone.0080938
10. Turner J, Torrelles JB. Mannose-Capped Lipoarabinomannan in Mycobacterium Tuberculosis Pathogenesis. *Pathog Dis* (2018) 76(4). doi: 10.1093/femspd/fty026
11. Vergne I, Gilleron M, Nigou J. Manipulation of the Endocytic Pathway and Phagocyte Functions by Mycobacterium Tuberculosis Lipoarabinomannan. *Front Cell Infect Microbiol* (2014) 4:187. doi: 10.3389/fcimb.2014.00187
12. Ernst JD. Macrophage Receptors for Mycobacterium Tuberculosis. *Infect Immun* (1998) 66(4):1277–81. doi: 10.1128/IAI.66.4.1277-1281.1998
13. Liu CH, Liu H, Ge B. Innate Immunity in Tuberculosis: Host Defense vs Pathogen Evasion. *Cell Mol Immunol* (2017) 14(12):963–75. doi: 10.1038/cmi.2017.88
14. Drummond RA, Brown GD. Signalling C-Type Lectins in Antimicrobial Immunity. *PLoS Pathog* (2013) 9(7):e1003417. doi: 10.1371/journal.ppat.1003417
15. Macauley MS, Crocker PR, Paulson JC. Siglec-Mediated Regulation of Immune Cell Function in Disease. *Nat Rev Immunol* (2014) 14(10):653–66. doi: 10.1038/nri3737
16. Drickamer K, Taylor ME. Recent Insights Into Structures and Functions of C-Type Lectins in the Immune System. *Curr Opin Struct Biol* (2015) 34:26–34. doi: 10.1016/j.sbi.2015.06.003
17. Toyonaga K, Torigoe S, Motomura Y, Kamichi T, Hayashi JM, Morita YS, et al. C-Type Lectin Receptor DCAR Recognizes Mycobacterial Phosphatidyl-Inositol Mannosides to Promote a Th1 Response During Infection. *Immunity* (2016) 45(6):1245–57. doi: 10.1016/j.immuni.2016.10.012
18. Busch M, Herzmann C, Kallert S, Zimmermann A, Hofer C, Mayer D, et al. Lipoarabinomannan-Responsive Polycytotoxic T Cells Are Associated With Protection in Human Tuberculosis. *Am J Respir Crit Care Med* (2016) 194(3):345–55. doi: 10.1164/rccm.201509-1746OC
19. Sieling PA, Chatterjee D, Porcelli SA, Prigozy TI, Mazzaccaro RJ, Soriano T, et al. CD1-Restricted T Cell Recognition of Microbial Lipoglycan Antigens. *Science* (1995) 269(5221):227–30. doi: 10.1126/science.7542404
20. Torrelles JB, Sieling PA, Zhang N, Keen MA, McNeil MR, Belisle JT, et al. Isolation of a Distinct Mycobacterium Tuberculosis Mannose-Capped Lipoarabinomannan Isoform Responsible for Recognition by CD1b-Restricted T Cells. *Glycobiology* (2012) 22(8):1118–27. doi: 10.1093/glycob/cws078
21. Fischer K, Scotet E, Niemeyer M, Koebernick H, Zerrahn J, Maillet S, et al. Mycobacterial Phosphatidylinositol Mannoside Is a Natural Antigen for CD1d-Restricted T Cells. *Proc Natl Acad Sci USA* (2004) 101(29):10685–90. doi: 10.1073/pnas.0403787101
22. Ulrichs T, Moody DB, Grant E, Kaufmann SH, Porcelli SA. T-Cell Responses to CD1-Presented Lipid Antigens in Humans With Mycobacterium Tuberculosis Infection. *Infect Immun* (2003) 71(6):3076–87. doi: 10.1128/IAI.71.6.3076-3087.2003
23. Yuan C, Qu ZL, Tang XL, Liu Q, Luo W, Huang C, et al. Mycobacterium Tuberculosis Mannose-Capped Lipoarabinomannan Induces IL-10-Producing B Cells and Hinders CD4(+)Th1 Immunity. *iScience* (2019) 11:13–30. doi: 10.1016/j.isci.2018.11.039
24. Chen H, Lau MC, Wong MT, Newell EW, Poidinger M, Chen J. Cytofkit: A Bioconductor Package for an Integrated Mass Cytometry Data Analysis Pipeline. *PLoS Comput Biol* (2016) 12(9):e1005112. doi: 10.1371/journal.pcbi.1005112
25. Lundberg M, Eriksson A, Tran B, Assarsson E, Fredriksson S. Homogeneous Antibody-Based Proximity Extension Assays Provide Sensitive and Specific Detection of Low-Abundant Proteins in Human Blood. *Nucleic Acids Res* (2011) 39(15):e102. doi: 10.1093/nar/gkr424
26. Gschwandtner M, Derler R, Midwood KS. More Than Just Attractive: How CCL2 Influences Myeloid Cell Behavior Beyond Chemotaxis. *Front Immunol* (2019) 10:2759. doi: 10.3389/fimmu.2019.02759
27. Struyf S, Proost P, Vandercappellen J, Dempe S, Noyens B, Nelissen S, et al. Synergistic Up-Regulation of MCP-2/CCL8 Activity Is Counteracted by Chemokine Cleavage, Limiting Its Inflammatory and Anti-Tumoral Effects. *Eur J Immunol* (2009) 39(3):843–57. doi: 10.1002/eji.200838660
28. Lin L, Finak G, Ushey K, Seshadri C, Hawn TR, Frahm N, et al. COMPASS Identifies T-Cell Subsets Correlated With Clinical Outcomes. *Nat Biotechnol* (2015) 33(6):610–6. doi: 10.1038/nbt.3187
29. Arango Duque G, Descoteaux A. Macrophage Cytokines: Involvement in Immunity and Infectious Diseases. *Front Immunol* (2014) 5:491. doi: 10.3389/fimmu.2014.00491
30. Li B, Jones LL, Geiger TL. IL-6 Promotes T Cell Proliferation and Expansion Under Inflammatory Conditions in Association With Low-Level RORgammat Expression. *J Immunol* (2018) 201(10):2934–46. doi: 10.4049/jimmunol.1800016
31. Karnell JL, Kumar V, Wang J, Wang S, Voynova E, Ettinger R. Role of CD11c (+) T-Bet(+) B Cells in Human Health and Disease. *Cell Immunol* (2017) 321:40–5. doi: 10.1016/j.cellimm.2017.05.008
32. Rubtsov AV, Rubtsova K, Kappler JW, Jacobelli J, Friedman RS, Marrack P. CD11c-Expressing B Cells Are Located at the T Cell/B Cell Border in Spleen and Are Potent APCs. *J Immunol* (2015) 195(1):71–9. doi: 10.4049/jimmunol.1500055
33. Reincke ME, Payne KJ, Harder I, Strohmeier V, Voll RE, Warnatz K, et al. The Antigen Presenting Potential of CD21(low) B Cells. *Front Immunol* (2020) 11:535784. doi: 10.3389/fimmu.2020.535784
34. de Pablo-Bernal RS, Canizares J, Rosado I, Galva MI, Alvarez-Rios AI, Carrillo-Vico A, et al. Monocyte Phenotype and Polyfunctionality Are Associated With Elevated Soluble Inflammatory Markers, Cytomegalovirus Infection, and Functional and Cognitive Decline in Elderly Adults. *J Gerontol A Biol Sci Med Sci* (2016) 71(5):610–8. doi: 10.1093/gerona/glv121
35. Mishra A, Singh VK, Actor JK, Hunter RL, Jagannath C, Subbian S, et al. GM-CSF Dependent Differential Control of Mycobacterium Tuberculosis Infection in Human and Mouse Macrophages: Is Macrophage Source of GM-CSF Critical to Tuberculosis Immunity? *Front Immunol* (2020) 11:1599. doi: 10.3389/fimmu.2020.01599
36. Beveridge NE, Price DA, Casazza JP, Pathan AA, Sander CR, Asher TE, et al. Immunisation With BCG and Recombinant MVA85A Induces Long-Lasting, Polyfunctional Mycobacterium Tuberculosis-Specific CD4+ Memory T Lymphocyte Populations. *Eur J Immunol* (2007) 37(11):3089–100. doi: 10.1002/eji.200737504
37. Scriba TJ, Tameris M, Mansoor N, Smit E, van der Merwe L, Isaacs F, et al. Modified Vaccinia Ankara-Expressing Ag85A, a Novel Tuberculosis Vaccine, Is Safe in Adolescents and Children, and Induces Polyfunctional CD4+ T Cells. *Eur J Immunol* (2010) 40(1):279–90. doi: 10.1002/eji.200939754
38. Wilkinson KA, Wilkinson RJ. Polyfunctional T Cells in Human Tuberculosis. *Eur J Immunol* (2010) 40(8):2139–42. doi: 10.1002/eji.201040731
39. Li R, Rezk A, Miyazaki Y, Hilgenberg E, Touil H, Shen P, et al. Proinflammatory GM-CSF-Producing B Cells in Multiple Sclerosis and B Cell Depletion Therapy. *Sci Transl Med* (2015) 7(310):310ra166. doi: 10.1126/scitranslmed.aab4176
40. Rezk A, Li R, Bar-Or A. Multiplexed Detection and Isolation of Viable Low-Frequency Cytokine-Secreting Human B Cells Using Cytokine Secretion Assay and Flow Cytometry (CSA-Flow). *Sci Rep* (2020) 10(1):14823. doi: 10.1038/s41598-020-71750-z
41. Joosten SA, van Meijgaarden KE, Del Nonno F, Baiocchini A, Petrone L, Vanini V, et al. Patients With Tuberculosis Have a Dysfunctional Circulating B-Cell Compartment, Which Normalizes Following Successful Treatment. *PLoS Pathog* (2016) 12(6):e1005687. doi: 10.1371/journal.ppat.1005687
42. Lighaam LC, Unger PA, Vredevoogd DW, Verhoeven D, Vermeulen E, Turksma AW, et al. *In Vitro*-Induced Human IL-10(+) B Cells Do Not Show a Subset-Defining Marker Signature and Plastically Co-Express IL-10 With Pro-Inflammatory Cytokines. *Front Immunol* (2018) 9:1913. doi: 10.3389/fimmu.2018.01913
43. Darrah PA, Patel DT, De Luca PM, Lindsay RW, Davey DF, Flynn BJ, et al. Multifunctional TH1 Cells Define a Correlate of Vaccine-Mediated

Protection Against Leishmania Major. *Nat Med* (2007) 13(7):843–50. doi: 10.1038/nm1592
44. Netea MG, Dominguez-Andres J, Barreiro LB, Chavakis T, Divangahi M, Fuchs E, et al. Defining Trained Immunity and Its Role in Health and Disease. *Nat Rev Immunol* (2020) 20(6):375–88. doi: 10.1038/s41577-020-0285-6
45. Divangahi M, Aaby P, Khader SA, Barreiro LB, Bekkering S, Chavakis T, et al. Trained Immunity, Tolerance, Priming and Differentiation: Distinct Immunological Processes. *Nat Immunol* (2021) 22(1):2–6. doi: 10.1038/s41590-020-00845-6
46. Cavaillon JM, Adib-Conquy M. Bench-To-Bedside Review: Endotoxin Tolerance as a Model of Leukocyte Reprogramming in Sepsis. *Crit Care* (2006) 10(5):233. doi: 10.1186/cc5055
47. Nomura F, Akashi S, Sakao Y, Sato S, Kawai T, Matsumoto M, et al. Cutting Edge: Endotoxin Tolerance in Mouse Peritoneal Macrophages Correlates With Down-Regulation of Surface Toll-Like Receptor 4 Expression. *J Immunol* (2000) 164(7):3476–9. doi: 10.4049/jimmunol.164.7.3476
48. Poovassery JS, Vanden Bush TJ, Bishop GA. Antigen Receptor Signals Rescue B Cells From TLR Tolerance. *J Immunol* (2009) 183(5):2974–83. doi: 10.4049/jimmunol.0900495
49. Ifrim DC, Quintin J, Joosten LA, Jacobs C, Jansen T, Jacobs L, et al. Trained Immunity or Tolerance: Opposing Functional Programs Induced in Human Monocytes After Engagement of Various Pattern Recognition Receptors. *Clin Vaccine Immunol* (2014) 21(4):534–45. doi: 10.1128/CVI.00688-13
50. Ellner JJ. Suppressor Adherent Cells in Human Tuberculosis. *J Immunol* (1978) 121(6):2573–9.
51. Ellner JJ. Regulation of the Human Cellular Immune Response to Mycobacterium Tuberculosis. The Mechanism of Selective Depression of the Response to PPD. *Bull Int Union Tuberc Lung Dis* (1991) 66(2-3):129–32.
52. Li Q, Li J, Tian J, Zhu B, Zhang Y, Yang K, et al. IL-17 and IFN-Gamma Production in Peripheral Blood Following BCG Vaccination and Mycobacterium Tuberculosis Infection in Human. *Eur Rev Med Pharmacol Sci* (2012) 16(14):2029–36.
53. Schietinger A, Greenberg PD. Tolerance and Exhaustion: Defining Mechanisms of T Cell Dysfunction. *Trends Immunol* (2014) 35(2):51–60. doi: 10.1016/j.it.2013.10.001
54. Blank CU, Haining WN, Held W, Hogan PG, Kallies A, Lugli E, et al. Defining 'T Cell Exhaustion'. *Nat Rev Immunol* (2019) 19(11):665–74. doi: 10.1038/s41577-019-0221-9
55. Khan N, Vidyarthi A, Amir M, Mushtaq K, Agrewala JN. T-Cell Exhaustion in Tuberculosis: Pitfalls and Prospects. *Crit Rev Microbiol* (2017) 43(2):133–41. doi: 10.1080/1040841X.2016.1185603
56. Liu X, Li F, Niu H, Ma L, Chen J, Zhang Y, et al. IL-2 Restores T-Cell Dysfunction Induced by Persistent Mycobacterium Tuberculosis Antigen Stimulation. *Front Immunol* (2019) 10:2350. doi: 10.3389/fimmu.2019.02350
57. Sande OJ, Karim AF, Li Q, Ding X, Harding CV, Rojas RE, et al. Mannose-Capped Lipoarabinomannan From Mycobacterium Tuberculosis Induces CD4+ T Cell Anergy *via* GRAIL. *J Immunol* (2016) 196(2):691–702. doi: 10.4049/jimmunol.1500710
58. Karim AF, Sande OJ, Tomechko SE, Ding X, Li M, Maxwell S, et al. Proteomics and Network Analyses Reveal Inhibition of Akt-mTOR Signaling in CD4(+) T Cells by Mycobacterium Tuberculosis Mannose-Capped Lipoarabinomannan. *Proteomics* (2017) 17(22). doi: 10.1002/pmic.201700233
59. Mahon RN, Rojas RE, Fulton SA, Franko JL, Harding CV, Boom WH. Mycobacterium Tuberculosis Cell Wall Glycolipids Directly Inhibit CD4+ T-Cell Activation by Interfering With Proximal T-Cell-Receptor Signaling. *Infect Immun* (2009) 77(10):4574–83. doi: 10.1128/IAI.00222-09
60. Athman JJ, Sande OJ, Groft SG, Reba SM, Nagy N, Wearsch PA, et al. Mycobacterium Tuberculosis Membrane Vesicles Inhibit T Cell Activation. *J Immunol* (2017) 198(5):2028–37. doi: 10.4049/jimmunol.1601199
61. Mahon RN, Sande OJ, Rojas RE, Levine AD, Harding CV, Boom WH. Mycobacterium Tuberculosis ManLAM Inhibits T-Cell-Receptor Signaling by Interference With ZAP-70, Lck and LAT Phosphorylation. *Cell Immunol* (2012) 275(1-2):98–105. doi: 10.1016/j.cellimm.2012.02.009
62. Flynn CM, Garbers Y, Lokau J, Wesch D, Schulte DM, Laudes M, et al. Activation of Toll-Like Receptor 2 (TLR2) Induces Interleukin-6 Trans-Signaling. *Sci Rep* (2019) 9(1):7306. doi: 10.1038/s41598-019-43617-5
63. Gilleron M, Quesniaux VF, Puzo G. Acylation State of the Phosphatidylinositol Hexamannosides From Mycobacterium Bovis Bacillus Calmette Guerin and Mycobacterium Tuberculosis H37Rv and Its Implication in Toll-Like Receptor Response. *J Biol Chem* (2003) 278(32):29880–9. doi: 10.1074/jbc.M303446200
64. Riedel DD, Kaufmann SH. Differential Tolerance Induction by Lipoarabinomannan and Lipopolysaccharide in Human Macrophages. *Microbes Infect* (2000) 2(5):463–71. doi: 10.1016/S1286-4579(00)00319-1
65. Nigou J, Vasselon T, Ray A, Constant P, Gilleron M, Besra GS, et al. Mannan Chain Length Controls Lipoglycans Signaling *via* and Binding to TLR2. *J Immunol* (2008) 180(10):6696–702. doi: 10.4049/jimmunol.180.10.6696
66. Shukla S, Richardson ET, Drage MG, Boom WH, Harding CV. Mycobacterium Tuberculosis Lipoprotein and Lipoglycan Binding to Toll-Like Receptor 2 Correlates With Agonist Activity and Functional Outcomes. *Infect Immun* (2018) 86(10):e00450-18. doi: 10.1128/IAI.00450-18
67. Roy Chowdhury R, Vallania F, Yang Q, Lopez Angel CJ, Darboe F, Penn-Nicholson A, et al. A Multi-Cohort Study of the Immune Factors Associated With M. Tuberculosis Infection Outcomes. *Nature* (2018) 560(7720):644–8. doi: 10.1038/s41586-018-0439-x
68. Lu LL, Chung AW, Rosebrock TR, Ghebremichael M, Yu WH, Grace PS, et al. A Functional Role for Antibodies in Tuberculosis. *Cell* (2016) 167(2):433–43.e14. doi: 10.1016/j.cell.2016.08.072
69. Divangahi M, Khan N, Kaufmann E. Beyond Killing Mycobacterium Tuberculosis: Disease Tolerance. *Front Immunol* (2018) 9:2976. doi: 10.3389/fimmu.2018.02976

Conflict of Interest: The authors declare that the research was conducted in the absence of any commercial or financial relationships that could be construed as a potential conflict of interest.

Publisher's Note: All claims expressed in this article are solely those of the authors and do not necessarily represent those of their affiliated organizations, or those of the publisher, the editors and the reviewers. Any product that may be evaluated in this article, or claim that may be made by its manufacturer, is not guaranteed or endorsed by the publisher.

Copyright © 2021 Silva, Sundling, Folkesson, Fröberg, Nobrega, Canto-Gomes, Chambers, Lakshmikanth, Brodin, Bruchfeld, Nigou, Correia-Neves and Källenius. This is an open-access article distributed under the terms of the Creative Commons Attribution License (CC BY). The use, distribution or reproduction in other forums is permitted, provided the original author(s) and the copyright owner(s) are credited and that the original publication in this journal is cited, in accordance with accepted academic practice. No use, distribution or reproduction is permitted which does not comply with these terms.

frontiers in Immunology

ORIGINAL RESEARCH
published: 26 November 2021
doi: 10.3389/fimmu.2021.712021

Pharmacological Poly (ADP-Ribose) Polymerase Inhibitors Decrease *Mycobacterium tuberculosis* Survival in Human Macrophages

Cassandra L. R. van Doorn, Sanne A. M. Steenbergen, Kimberley V. Walburg and Tom H. M. Ottenhoff†*

Department of Infectious Diseases, Leiden University Medical Center, Leiden, Netherlands

OPEN ACCESS

Edited by:
Jayne S. Sutherland, Medical Research Council The Gambia Unit (MRC), Gambia

Reviewed by:
Divya Tiwari, Queen Mary University of London, United Kingdom
Silvia Fernandez Villamil, Consejo Nacional de Investigaciones Científicas y Técnicas (CONICET), Argentina

***Correspondence:**
Cassandra L. R. van Doorn
clrvandoorn@mail.com

†ORCID:
Tom H. M. Ottenhoff
orcid.org/0000-0003-3706-3403

Specialty section:
This article was submitted to Microbial Immunology, a section of the journal Frontiers in Immunology

Received: *19 May 2021*
Accepted: *12 November 2021*
Published: *26 November 2021*

Citation:
van Doorn CLR, Steenbergen SAM, Walburg KV and Ottenhoff THM (2021) Pharmacological Poly (ADP-ribose) Polymerase Inhibitors Decrease Mycobacterium tuberculosis Survival in Human Macrophages. Front. Immunol. 12:712021. doi: 10.3389/fimmu.2021.712021

Diabetes mellites (DM) is correlated with increased susceptibility to and disease progression of tuberculosis (TB), and strongly impairs effective global TB control measures. To better control the TB-DM co-epidemic, unravelling the bidirectional interactivity between DM-associated molecular processes and immune responses to *Mycobacterium tuberculosis* (*Mtb*) is urgently required. Since poly (ADP-ribose) polymerase (PARP) activation has been associated with DM and with *Mtb* infection in mouse models, we have investigated whether PARP inhibition by pharmacological compounds can interfere with host protection against *Mtb* in human macrophage subsets, the predominant target cell of *Mtb*. Pharmacological inhibition of PARP decreased intracellular *Mtb* and MDR-*Mtb* levels in human macrophages, identifying PARP as a potential target for host-directed therapy against *Mtb*. PARP inhibition was associated with modified chemokine secretion and upregulation of cell surface activation markers by human macrophages. Targeting LDH, a secondary target of the PARP inhibitor rucaparib, resulted in decreased intracellular *Mtb*, suggesting a metabolic role in rucaparib-induced control of *Mtb*. We conclude that pharmacological inhibition of PARP is a potential novel strategy in developing innovative host-directed therapies against intracellular bacterial infections.

Keywords: tuberculosis, host-directed therapy, poly (ADP-ribose) polymerase, rucaparib, human macrophages

INTRODUCTION

Tuberculosis (TB) is an infectious disease caused by *Mycobacterium tuberculosis* (*Mtb*). Around 10 million new TB cases and 1.4 million deaths are reported annually and one quarter of the world's population is latently infected with *Mtb* (1). Different risk factors have been identified for progression of latent TB infection (LTBI) to active disease, including age, malnutrition, coinfection with human immunodeficiency virus (HIV) or cytomegalovirus (CMV), and diabetes mellitus (DM) (1–3). In addition, recent studies have shown that DM is also associated with poorer clinical TB outcome following anti-bacterial treatment. Current estimates are that 15% of the global TB burden is now associated with DM (4, 5). Host-directed therapy (HDT) offers the potential for

better treatment of Multi-Drug-Resistant (MDR)-TB, as well as shorten current standard (6-9 month) treatment regimens, thereby reducing toxicity, enhancing treatment compliance and as a result reducing emergence of *de novo* drug resistance. To better control the TB-DM co-epidemic, unravelling the bidirectional interactions between DM-dysregulated molecular processes and immune responses to *Mtb* is essential.

Macrophages (MFs) are known for their dual role in TB pathogenesis, as they provide a primary host niche for *Mtb* during infection while also being key host effector cells eliminating *Mtb*, and therefore represent key target cells in developing and evaluating novel therapeutic strategies for TB/DM, including innovative HDT. MFs are classically subdivided into pro-inflammatory macrophages (M1) and anti-inflammatory macrophages (M2), representing the polar ends of the macrophage spectrum. Both M1 and M2 have been reported in tuberculous granulomas, with M2 predominating in granulomas from patients with active TB (6).

Poly (ADP-ribose) polymerase (PARP) activation has been associated with cancer, diabetes and endothelial dysfunction in experimental mouse models and in humans (7–10). PARP-deficient mice and mice treated with PARP inhibitor PJ34 were resistant to streptozocin-induced diabetes, and pharmacological inhibition of PARP has been proposed for the treatment of DM (11–13). Interestingly, in addition, PARP inhibitors have recently been proposed as HDT compounds for reducing TB-induced inflammation (14), thereby providing a potential mechanistic link between the TB-DM co-morbidity at the molecular level. Several PARP inhibitors (PARPi) have been clinically approved for the treatment of cancer or are currently being evaluated in clinical trials for the treatment of advanced BRCA1/2 mutant ovarian and breast cancers, which can accelerate translation to HDTs against *Mtb*. PARP encompasses a family of enzymes involved in different cellular processes such as control of genomic stability, programmed cell death and DNA repair. When assisting in the repair of single-strand DNA nicks, PARP enzymes bind to single-stranded DNA breaks (SSB) or double-stranded DNA breaks (DSB) to generate PAR polymers on itself (auto-PARylation), histones and chromatin-associated proteins, which together leads to chromatin relaxation and recruitment of repair proteins. Inhibition of PARP results in accumulation of SSB due to delayed DNA repair. Given the dual role of PARP activation on diabetes and tuberculosis infection, we hypothesized that small molecule inhibitors that interfere with PARP activation at the cellular level may be able to redirect macrophage function in response to *Mtb* infection. Such chemical compounds could be valuable tools as part of immunomodulatory HDT regimens.

In the current study, we explore the potential of PARP inhibitors in the treatment of intracellular *Mtb* infections in human macrophages. We demonstrate that pharmacological inhibition of PARP decreases intracellular *Mtb* in human macrophages and modulates the immune response of *Mtb*-infected human macrophages. To our knowledge, the potential of targeting PARP for HDT in a human model of *Mtb*-infection has not been reported yet, and our work identifies PARPi as novel HDT compounds against *Mtb* and possibly other intracellular infectious diseases.

RESULTS

Pharmacological Inhibition of PARP Reduces *Mtb* Survival in Human Macrophages in a Host-Directed Manner

To study whether PARP may play a role during *Mtb* infections in human macrophages, we first evaluated intracellular *Mtb* survival after treatment with four clinically relevant PARPi (**Figures 1A, B**). We selected 10 μM as a relatively high PARPi concentration, which has been shown to target PARP *in vitro* (15–17) and which allowed us to directly compare drug efficacy of PARPi with each other and with control kinase inhibitor H-89 (18, 19). Rucaparib significantly decreased intracellular *Mtb* CFUs in M1 and M2 more efficiently than H-89 (**Figure 1C**, n=6). Additionally, niraparib and pamiparib decreased intracellular *Mtb* in M1 and A-966492 decreased intracellular *Mtb* in M2, suggesting cell-specific effects of PARP inhibition on bacterial load for these compounds. Furthermore, we assessed the effect of PARPi on cytotoxicity using uninfected macrophages from four different donors, to ascertain that PARPi was not detrimental to healthy human macrophages. PARPi did not affect host-cell integrity and was not cytotoxic (**Figure 1D**). Next, we used a flow cytometry-based method (18) to evaluate whether the inhibition of *Mtb* outgrowth by PARPi was accompanied by a decrease in the percentage of cells harboring Venus-expressing *Mtb*. Rucaparib, but not other PARPi, significantly reduced the percentage of *Mtb*-infected cells both in M1 and M2 (**Figure 1E**, n=8), further corroborating the *Mtb*-inhibiting effect of rucaparib in human macrophages. To exclude that PARPi had direct microbicidal effects, liquid *Mtb* cultures were treated with PARPi in the absence of macrophages in two independent experiments (**Figure 1F**). None of the PARPi limited bacterial growth directly, indicating that PARPi restrict intracellular outgrowth of *Mtb* by modulating host pathways.

To investigate whether PARPi-induced inhibition of intracellular bacterial growth was specific for *Mtb*, we evaluated whether pharmacological inhibition of PARP also restricted growth of other intracellular pathogenic bacteria, including *Mycobacterium avium* (*Mav*), *Salmonella enterica* serovar Typhimurium (*Stm*) and methicillin-resistant *Staphylococcus aureus* (MRSA). Interestingly, niraparib, but not other PARPi, significantly decreased *Stm* CFUs in M1 and M2 (**Figure 2A**, n=6) without exhibiting direct microbicidal effects in two independent experiments (**Figure 2B**). Rucaparib did not significantly diminish *Mav*, *Stm* or MRSA CFUs, suggesting that the effect of rucaparib is specific for *Mtb*. These results imply that both rucaparib and niraparib inhibit specific species of bacteria through modeling of host signaling pathways.

Taken together, these data suggest that PARP activity is involved in *Mtb* survival in human macrophages, and that although there is some difference in their efficacy against *Mtb*-infected M1 compared to *Mtb*-infected M2, pharmacological inhibition of PARP is a promising strategy to target intracellular *Mtb*. Moreover, the effects of different PARP inhibitors are highly specific to certain pathogen species.

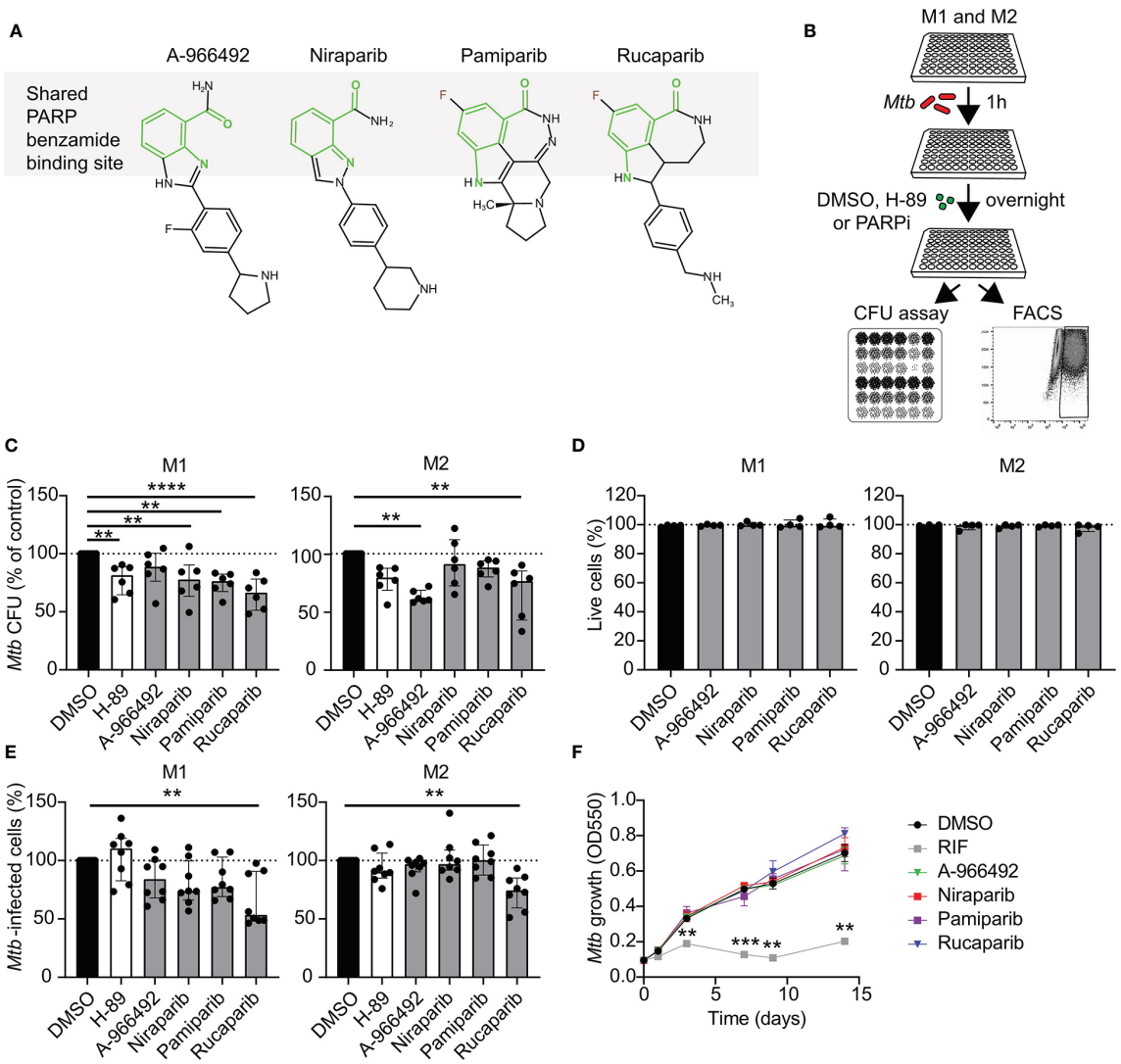

FIGURE 1 | Identification of PARP as potential host target during *Mtb* infections in human macrophages. **(A)** Chemical structures of the PARPi used in this study. The benzamide moiety that is shared between all PARP inhibitor structures is highlighted in light green. **(B)** Schematic representation of the experimental setup used in C and E. **(C)** *Mtb* H37Rv-infected M1 and M2 were treated overnight with PARPi (10 μM), H-89 (10 μM) or an equal volume of vehicle control DMSO (0.1% v/v). CFU data represent the median ± interquartile range of six different donors. Dots represent the mean from triplicate wells of a single donor. CFUs are expressed as percentage of vehicle control (i.e. DMSO). Differences were significant by RM one-way ANOVA with Dunnett's multiple test correction against DMSO. **(D)** Percentage of live M1 and M2 (i.e. PI-negative cells) after overnight treatment with PARPi (10 μM) or an equal volume of vehicle control DMSO (0.1% v/v). Data represent the median ± interquartile range from four different donors. Differences were tested by Friedman's test with Dunn's multiple test correction against DMSO. **(E)** Percentage of M1 and M2 infected with Venus-expressing *Mtb* H37Rv that were treated as in **(C)** Data represent the median ± interquartile range from eight different donors. Differences were significant by Friedman's test with Dunn's multiple test correction against DMSO. **(F)** Liquid *Mtb* H37Rv growth (in the absence of cells) was monitored for 14 days after addition of positive control RIF (20 μg/ml), PARPi (10 μM) or vehicle control DMSO (0.1% v/v). Data represent the means ± S.D. of triplicate wells from a representative experiment out of two independent experiments. Differences were significant by RM two-way ANOVA with Dunnett's multiple test correction against DMSO. $^{**}p < 0.01$.

The Translational Potential of PARPi for Clinical Application

To evaluate the translational potential of PARPi for the development of HDT, we first tested whether PARPi displayed activity against macrophages infected with two different multi-drug resistant (MDR)-*Mtb* strains: an MDR-*Mtb* strain belonging to the Beijing genotype (strain 16319) and an MDR-*Mtb* Dutch outbreak strain (strain 2003-1128), both resistant to rifampicin (RIF) and isoniazid (INH). Although drug-susceptible and MDR *Mtb* strains are expected to respond similarly to HDT compounds, previous experiments by our laboratory suggested that in selective cases compound efficacy may differ between *Mtb* strains (20). Here, rucaparib significantly decreased intracellular MDR-*Mtb* and A-966492 showed activity against the MDR-*Mtb*

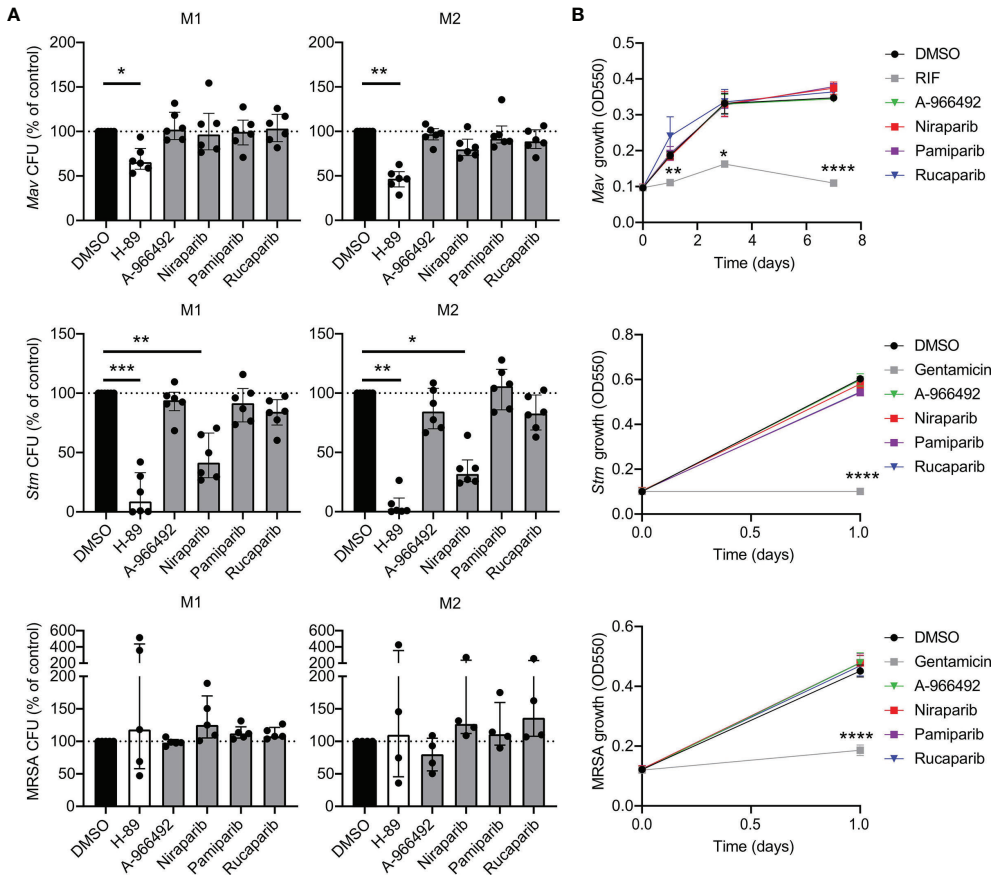

FIGURE 2 | PARPi niraparib decreases intracellular *Stm*. **(A)** *Mav, Stm* and MRSA CFUs after overnight treatment of infected M1 and M2 with PARPi (10 μM), H-89 (10 μM) or an equal volume of vehicle control DMSO (0.1% v/v). Data represent the median ± interquartile range from at least four different donors. Dots represent the mean from triplicate wells of a single donor. CFUs are expressed as percentage of vehicle control (i.e. DMSO). Differences were significant by Friedman's test with Dunn's multiple test correction against DMSO. **(B)** Liquid *Mav, Stm* and MRSA growth (in the absence of cells) was monitored during treatment with RIF (20 μg/ml; positive control for *Mav*), gentamicin (50 μg/ml; positive control for *Stm* and MRSA), PARPi (10 μM) or vehicle control DMSO (0.1% v/v). Data represent the means ± S.D. of triplicate wells from a representative experiment out of two independent experiments. Differences were significant by RM two-way ANOVA with Dunnett's multiple test correction against DMSO. *p < 0.05, **p < 0.01, ***, ****p < 0.0001.

Dutch outbreak strain (**Figures 3A, B**, n=6), highlighting the potential of PARPi to control intracellular outgrowth not only of drug-sensitive but also MDR-*Mtb* strains.

Next, the interaction of PARPi with first-line antibiotics was studied. Macrophages from five donors were infected with *Mtb* and treated with PARPi in the presence or absence of a non-toxic, suboptimal dose of RIF or INH (**Figure 3C**) (20, 21). As expected, PARPi significantly decreased *Mtb* CFUs in M1 (**Figure 3D**). In M2, however, several HDT compounds, including rucaparib, niraparib and positive control H-89 increased *Mtb* CFUs in two donors, illustrating the typically high variation in the response of donors to HDT compounds. Niraparib, pamiparib and rucaparib significantly enhanced the activity of INH against intracellular *Mtb* in M1. The coefficient of drug interaction (CID) of niraparib, pamiparib and rucaparib with RIF was close to 1 in M1, suggesting that these PARPi had an additive effect to the antibiotic treatment and not a synergistic effect (**Supplementary Table 1**). Furthermore, compared with other PARPi, pamiparib seemed to enhance the activity of RIF in M2 and of INH in M1 and M2, albeit not significant.

PARPi Induce Immunomodulatory Effects in *Mtb*-Infected Human M1 and M2

To investigate whether the effect of PARPi against *Mtb* correlated with macrophage activation during *Mtb* infection, cytokine and chemokine production was quantified in the supernatants of *Mtb*-infected macrophages that were treated with PARPi or vehicle control DMSO overnight. *Mtb*-infection induced cytokine and chemokine production in M1 and M2 and tended to induce tumor necrosis factor (TNF)-α, macrophage inflammatory protein (MIP)-1α,MIP-1β and IP-10 and fractalkine in M1 and M2 (**Figure 4A** and **Supplementary Table 2**, n=8). Exposure to PARPi altered the cytokine and chemokine response of M1 and M2 upon *Mtb* infection (**Figure 4B** and **Supplementary Table 2**, n=4): pamiparib and rucaparib both increased MIP-1α and MIP-1β secretion by M1

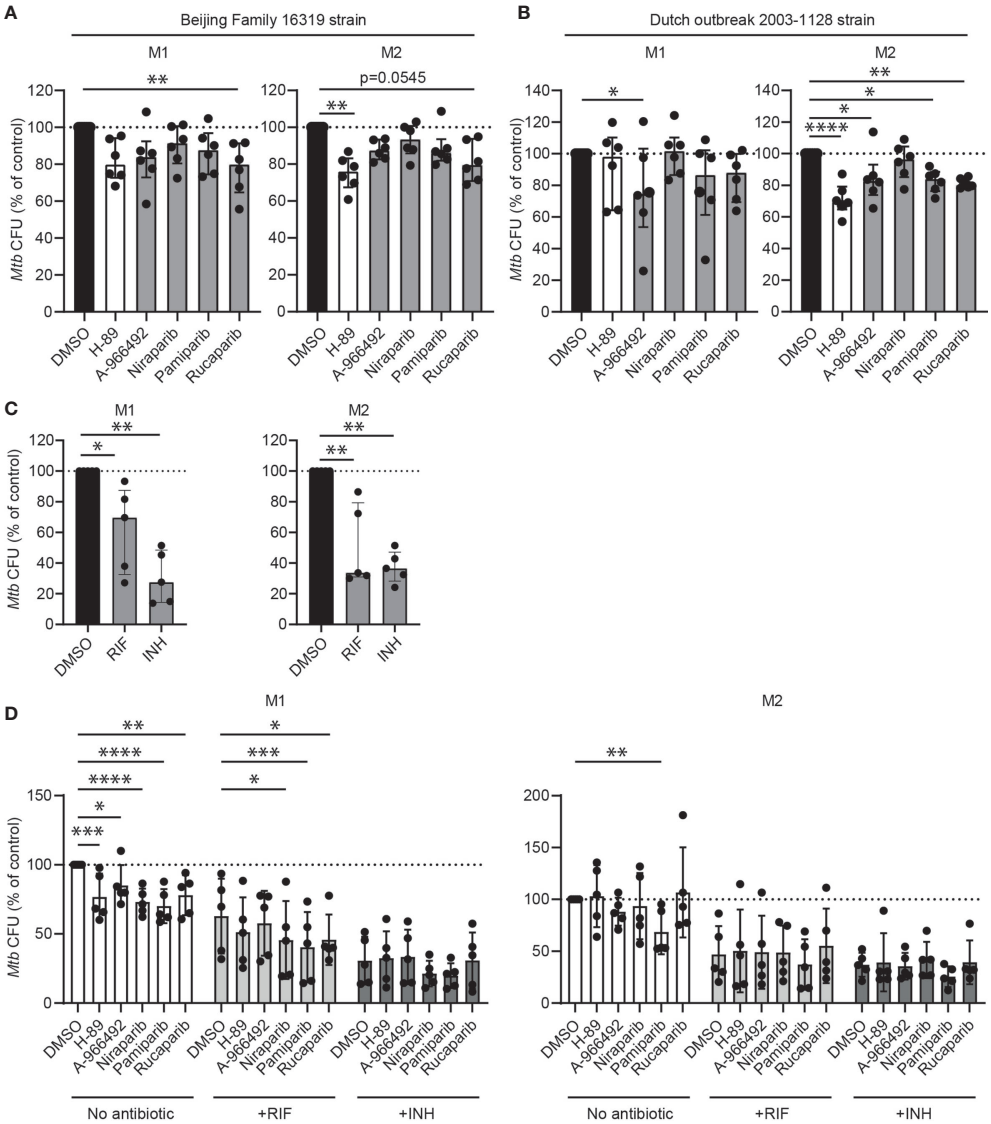

FIGURE 3 | The clinical potential of PARPi for host-directed therapy against *Mtb*. **(A)** Multidrug-resistant (MDR) *Mtb* CFUs after overnight treatment with PARPi (10 μM), H-89 (10 μM) or an equal volume of vehicle control DMSO (0.1% v/v) in M1 and M2. Data represent the median ± interquartile range from six different donors. Dots represent the mean from triplicate wells of a single donor. CFUs are expressed as percentage of control (i.e. DMSO). Differences were significant by Friedman's test with Dunn's multiple comparison test against DMSO. **(B)** MDR-*Mtb* CFUs after overnight treatment with PARPi (10 μM), H-89 (10 μM) or an equal volume of vehicle control DMSO (0.1% v/v) in M1 and M2. Differences were significant by RM one-way ANOVA with Dunnett's multiple comparison test against DMSO. **(C)** *Mtb* H37Rv CFUs after overnight treatment with RIF (0.05 μg/ml), INH (0.4 μg/ml) or an equal volume of vehicle control DMSO (0.1% v/v) in M1 and M2. Data represent the median ± interquartile range from five different donors. CFUs are expressed as percentage of control (i.e. DMSO). Differences were significant by RM one-way ANOVA with Dunnett's multiple comparison test against DMSO. **(D)** *Mtb* H37Rv CFUs after overnight treatment with PARPi (10 μM), H-89 (10 μM) or an equal volume of vehicle control DMSO (0.1% v/v) in the presence or absence of a suboptimal dose of RIF (0.05 μg/ml) or INH (0.4 μg/ml) in M1 and M2. Data represent the median ± interquartile range from five different donors. CFUs are expressed as percentage of DMSO in the absence of antibiotics. Differences were significant by RM two-way ANOVA with Dunnett's multiple comparison test against the DMSO controls in the presence or absence of antibiotics. *p < 0.05, **p < 0.01, ***p < 0.001, ****p < 0.001.

and significantly decreased IFN-α2 secretion by M2 compared to DMSO. Correlation plots between the cytokines and chemokines that were significantly modified by PARPi and *Mtb* CFUs did not identify a positive correlation between secretion profiles of macrophages and *Mtb* loads (**Supplemental Figure 1**). Collectively, these data suggest that pamiparib and rucaparib can modify the cytokine and chemokine response to *Mtb* infection.

Next, we investigated the expression levels of activation markers on the surface of *Mtb*-infected M1 and M2 that were treated with PARPi overnight. *Mtb*-infection tended to increase macrophage activation markers in M1 and M2 (**Figure 4C**, n=4). Surprisingly,

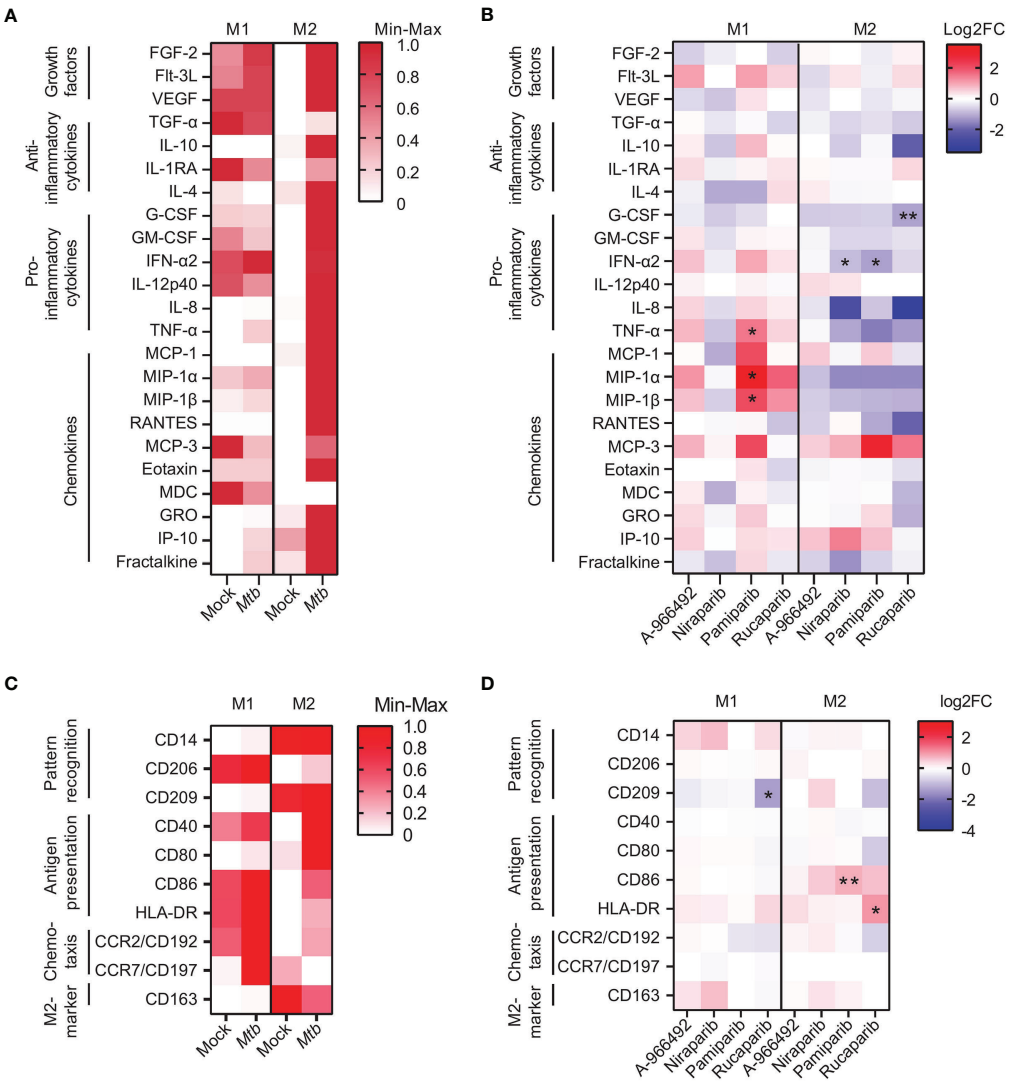

FIGURE 4 | PARP inhibitors induce immunomodulatory effects in human macrophages. **(A)** Heatmap displaying median cytokine/chemokine levels in the supernatants of *Mtb* H37Rv- or mock-infected M1 and M2 obtained from eight donors. Shown are the relative cytokine/chemokine secretion levels (>10 pg/ml) on a white to red color scale (min=0; max=1). Differences were tested using a Wilcoxon matched-pairs signed rank test. **(B)** Heatmap displaying median log2 fold change (FC) cytokine/chemokine levels relative to vehicle control DMSO in the supernatants of *Mtb* H37Rv-infected M1 and M2 obtained from four donors. *Mtb* H37Rv-infected macrophages were exposed to PARPi (10 μM) or an equal volume of DMSO (0.1% v/v) overnight. Differences were significant by Friedman's test with Dunn's multiple comparison test against DMSO. **(C)** Heatmap displaying relative geometric mean fluorescence intensity (gMFI) of proteins on the surface of Venus-expressing *Mtb* H37Rv-infected M1 and M2 obtained from four donors. Shown are the relative (geometric mean fluorescence intensity) gMFI levels on a white to red color scale (min=0; max=1). Differences were tested using a Wilcoxon matched-pairs signed rank test. **(D)** Heatmap displaying log2 FC gMFI of proteins on the surface of Venus-expressing *Mtb* H37Rv-infected M1 and M2 obtained from four donors relative to vehicle control DMSO. Macrophages were exposed to PARPi (10 μM) or an equal volume of DMSO (0.1% v/v) overnight. Differences were significant by Friedman's test with Dunn's multiple comparison test against DMSO. *$p < 0.05$, **$p < 0.01$.

rucaparib, but not other PARPi, tended to decrease expression of CD192 and CD209 and expression of human leucocyte antigen (HLA)-DR on the surface of *Mtb*-infected M1 and M2 (**Figure 4D** and **Supplemental Figure 2**, n=4). Furthermore, the expression of costimulatory molecule CD86 on the surface of M2 tended to be increased by rucaparib, and was significantly increased by pamiparib. These data suggest that rucaparib increases macrophage activation and possibly antigen presentation.

Given that several HDT compounds with demonstrated efficacy against intracellular *Mtb* in macrophages exert their activity by activating autophagy (22–25), we next assessed whether treatment with PARPi induced autophagy and lysosomal maturation. Accumulation of autophagic and lysosomal vesicles was quantified by confocal imaging on *Mtb*-infected and PARPi-treated macrophages from four donors that were stained with CYTO-ID or Lysotracker, respectively.

Formation of autophagic or lysosomal vesicles could not be detected after 4h treatment with PARPi compared to DMSO (**Supplemental Figures 3A, B**). To examine the effect of PARPi on the autophagic flux, macrophages from three donors were treated with PARPi in the presence or absence of bafilomycin A1 (Baf) which is an autophagy inhibitor that prevents fusion between autophagosomes and lysosomes. As expected, treatment with Baf induced microtubule-associated protein light chain 3 (LC3)-II accumulation in M1 and M2 (**Supplemental Figure 3C**). However, PARPi did not increase LC3-II protein levels, regardless of the presence of Baf. Also, PARPi did not increase LAMP1 protein levels, suggesting that PARPi do not act *via* induction of autophagic and/or lysosomal pathways to control intracellular *Mtb* in human macrophages.

Collectively, our data demonstrate that PARPi modulate the immune response of *Mtb*-infected human macrophages *via* cytokine/chemokine expression and surface markers, which play a role in antigen presentation and chemotaxis. Our data also suggest that a role of induction of autophagy and phagosome maturation in PARP-induced *Mtb* control is not likely mechanistically involved in the mode of action.

Lactate Dehydrogenase, a Secondary Target of Rucaparib, Induces *Mtb* Control in Human Macrophages

Hexose-6-phosphate dehydrogenase (H6PD) and lactate dehydrogenase (LDH) were recently identified as additional target molecules of rucaparib (26). We therefore hypothesized that these metabolic targets might play a role in the more profound inhibitory effect of rucaparib on *Mtb* survival compared to other PARPi (**Figures 1C, E**, **3A**, **5A**). Lactate levels were significantly decreased in the supernatants of *Mtb*-infected M1 and M2 that had been treated with rucaparib compared to DMSO, suggesting that rucaparib indeed impaired LDH activity (**Figure 5B**, n=4). Interestingly, none of the other selected PARPi significantly affected lactate levels, compatible with the fact that none of these have been reported to modulate LDH activity. To study whether inhibition of H6PD or LDH could have contributed to the effect of rucaparib on *Mtb* control, we treated *Mtb*-infected macrophages with the specific LDH-inhibitor FX-11 or the G6PD-inhibitor 6-aminonicotinamide (6-AN) and determined intracellular *Mtb* levels in a flow cytometry-based assay, which allows a more rapid quantification of intracellular *Mtb* levels compared to classical CFU assays and generally showed a greater effect window of rucaparib compared to CFU assay (**Figure 1C** versus **1E**). Interestingly, FX-11 significantly decreased the percentage of *Mtb*-infected M1 (n=7) and M2 (n=8), whereas no effect of 6-AN on intracellular *Mtb* could be detected (**Figure 5C**). FX-11 did not affect the percentage of live M1 cells (n=6), but did decrease the percentage of live cells in a subset of M2 cultures (n=5). Together, these data suggest that inhibition of LDH, but not G6PD, likely contributed to the *Mtb*-decreasing effect of rucaparib. Corroborating this hypothesis, FX-11 treatment significantly decreased lactate levels in the supernatant of *Mtb*-infected M1, corresponding with decreased LDH activity (**Figure 5E**, n=6). FX-11 treatment did not result in decreased lactate levels in M2, which is likely a result of cellular toxicity in M2 (**Figures 5D, E**). Collectively, these data suggest that LDH could be involved in rucaparib-induced inhibition of *Mtb* and identifies LDH as potential host target during *Mtb* infections.

DISCUSSION

In search of new potential treatments against TB, we have studied a series of PARPi, which are being considered for treatment of type 2 diabetes, for their ability to improve intracellular growth control by infected human M1 and M2 as novel candidate HDT therapeutics. Here, we showed that clinical compounds targeting PARP were able to decrease the intracellular survival of *Mtb*, suggesting that pharmacological inhibition of PARP can be a novel tool for TB treatment. PARPi had no direct antimycobacterial activity, suggesting that PARPi act in a HDT like fashion. In line with this, macrophage treatment with PARPi was associated with the modulation of macrophage function at the cytokine level and surface marker level. Lactate dehydrogenase (LDH) was identified as an additional target molecule for rucaparib's activity against intracellular *Mtb* which might explain the more profound inhibitory effect of rucaparib on *Mtb* survival compared to other PARPi. To our knowledge, the potential of PARPi as HDTs against *Mtb* has not been demonstrated before.

PARPs are host proteins involved in cellular processes acting *via* PARylation of their targets. It has recently been shown that PARP1 activation is triggered in mouse lungs upon *Mtb* infection (27). Importantly, genetic PARP1 depletion resulted in decreased lung bacterial burden in female mice. Here, we studied the role of PARP inhibition in a human and clinically relevant context. All clinical PARPi used in this study are known PARP1 and PARP2 inhibitors and have the ability to inhibit multiple proteins of the PARP family (28–31). Our data suggest that the efficacy of PARPi on bacterial clearance is specific for *Mtb* and does not translate to other intracellular bacteria, including the closely related species *Mav*. While not investigated here, this suggests that PARP is not a key target for MRSA, *Stm* and *Mav*, although the exact role of PARP during other bacterial infections remains to be resolved.

Several PARP inhibitors, such as olaparib and talazoparib, can be metabolized by the hepatic enzyme CYP3A4, which is induced by the first-line TB antibiotic RIF (32–34). Rucaparib, however, is less sensitive to metabolization by CYP3A4 and the sensitivity of other PARPi remains to be determined. In our *in vitro* infection model, pamiparib had a significant additive effect to RIF in M1 and seemed to have an additive effect to RIF in M2 and to INH in both M1 and M2. This possible additive effect of pamiparib to RIF and INH in M2 was unexpected, since pamiparib did not show activity against *Mtb* in the absence of antibiotics in these cells. Although we observed differences in the cellular response to pamiparib in M1 versus M2 based on cytokine/chemokine secretion, it remains currently undefined

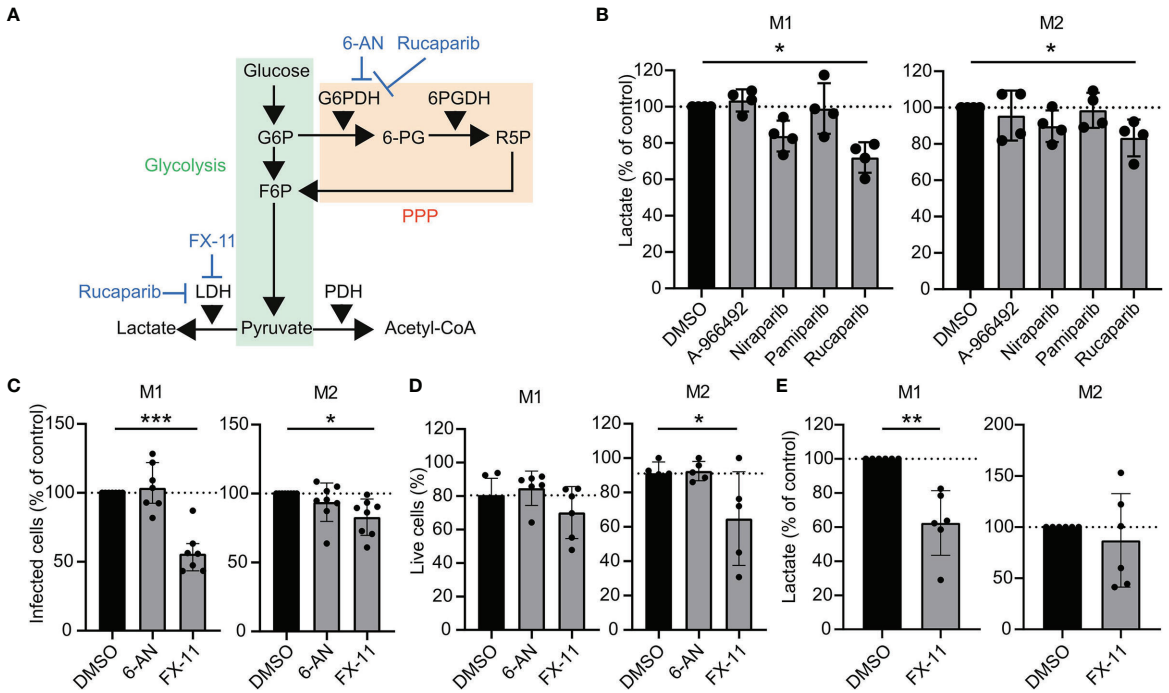

FIGURE 5 | Increased *Mtb* control by pharmacological inhibition of lactate dehydrogenase in human macrophages. **(A)** Schematic representation of metabolic pathway modulation by rucaparib, 6-AN and FX-11. Glycolysis is depicted in green; the pentose phosphate pathway (PPP) is depicted in orange. **(B)** Determination of lactate production in the supernatants of *Mtb* H37Rv-infected M1 and M2 that were treated with PARPi (10 μM) or an equal volume of vehicle control DMSO (0.1% v/v) overnight. Data represent the median ± interquartile range from four different donors. Dots represent the mean from duplicate wells of a single donor. Differences were significant by RM one-way ANOVA with Dunnett's multiple comparison test against DMSO. **(C)** Percentage of M1 and M2 infected with Venus-expressing *Mtb* H37Rv that were treated with G6PD-inhibitor 6-aminonicotinamide (6-AN, 100 μM) or LDH-inhibitor FX-11 (100 μM) or an equal volume of vehicle control DMSO (0.1% v/v) overnight. Data represent the median ± interquartile range from at least seven different donors. Differences were significant by RM one-way ANOVA with Dunnett's multiple comparison test against DMSO. **(D)** Percentage of live M1 and M2 (i.e. PI-negative cells) after overnight treatment with 6-AN (100 μM) or FX-11 (100 μM) or an equal volume of vehicle control DMSO (0.1% v/v). Data represent the median ± interquartile range from at least five different donors. Differences were significant by RM two-way ANOVA with Dunnett's multiple test correction against DMSO. **(E)** Determination of lactate production in the supernatants of *Mtb* H37Rv-infected M1 and M2 that were treated with FX-11 (100 μM) or an equal volume of vehicle control DMSO (0.1% v/v) overnight. Data represent the median ± interquartile range from six different donors. Differences were significant by RM one-way ANOVA with Dunnett's multiple comparison test against DMSO. *p < 0.05, **p < 0.01, ***p < 0.001.

which exact mechanisms were responsible for the difference in the efficacy of pamiparib against *Mtb* in M1 versus M2. This requires further investigation.

In addition to their role in DNA repair, mammalian PARPs display properties that are associated with and are likely to impact host-pathogen interactions. Firstly, PARPs are induced by the production of interferon-stimulated genes (ISGs), implicating a role during virus infection (35–38). The impact of PARP activity on virus replication remains controversial, as both promotion and reduction of viruses by PARP have both been described, which is likely dependent on the virus (as reviewed by (39). Moreover, an elevated type I IFN response correlates with progression to active TB in humans (40–42) and has been implicated in susceptibility to *Mtb* in mouse models (43, 44). Secondly, PARPs are involved in pro-inflammatory gene expression. Macrophages from PARP-deficient mice were unable to induce nuclear factor kappa B (NF-κB)-mediated activation in response to lipopolysaccharide (LPS), limiting inducible nitric oxide synthase (iNOS), tumor necrosis factor alpha (TNF-α) and interferon gamma (IFN-γ) levels (45, 46). Here, we show that the inflammatory response of *Mtb*-infected macrophages is modified by pharmacological inhibition of PARP. At the cytokine level, pamiparib and rucaparib induced expression of chemokines MIP-1α and MIP-1β in M1. We furthermore show that the higher MIP-1α and MIP-1β levels did not correlate directly with increased inhibition of intracellular *Mtb*, compatible with their primary role in chemotactic cellular recruitment. Decreased MIP-1α expression is associated with diabetes in *Mtb*-infected human monocyte-derived macrophages and in *Mtb*-infected diabetic mice (47–49). This suggests that macrophages obtained from diabetic patients or mice may be impaired in the recruitment of immune cells to *Mtb* sites of infection. Additionally, alveolar macrophages of diabetic mice feature decreased TNF-α secretion (47). Mice that have impaired TNF-α secretion and mice and humans treated with anti-TNF-α antibodies are more susceptible to *Mtb* infection, highlighting a direct protective effect of TNF-α against *Mtb* (50–52). Here, TNF-α was significantly induced by

pamiparib treatment and it tended to be induced by A-966492 and rucaparib in M1. However, like for MIP-1α, higher TNF-α levels did not correlate directly with decreased intracellular *Mtb* levels. Together, these data demonstrate that PARPi treatment alters the cytokine/chemokine response of human macrophages during infection with *Mtb*. These effects are not directly correlated with intracellular *Mtb* control by macrophages, but these cytokines/chemokines could exert effects *in vivo via* other cells such as recruitment of immune cells. The potential of PARPi to improve recruitment of immune cells to sites of infection remains to be elucidated and could play an important role in the *in vivo* activity of PARPi against *Mtb*.

When evaluating the activation status of *Mtb*-infected macrophages in response to PARPi treatment, rucaparib appeared to increase the expression of HLA-DR and CD86, in contrast to other PARPi. As previously published, monocyte-derived macrophages (MDMs) obtained from type 2 diabetes (T2D) patients displayed lower levels of HLA-DR and CD86 compared to MDMs obtained from healthy individuals upon *n vitro Mtb* infection (48). Collectively, these observations support the hypothesis that rucaparib is able to reverse diabetes-induced functional effects of macrophages and suggest that rucaparib could increase antigen presentation by human macrophages to specific T-cells.

Several studies have shown that diabetes was associated with a decrease in *Mtb* phagocytosis capacity in human and murine macrophages (47, 48, 53), possibly resulting from highly glycosylated proteins that impair recognition of bacterial components. Phagocytosis as mechanism of action of PARPi can be excluded in our current study, since PARPi were added well after phagocytosis, and further cell-to-cell exchange of *Mtb* bacteria was prevented by supplementing the culture medium with low dose gentamicin.

Multiple PARPi, including niraparib, rucaparib and talazoparib have recently been described to induce autophagy in cancer cell lines, as detected by increased LC3-I to LC3-II conversion on western blot analysis (54, 55). In our current study, induction of autophagy could not be detected, however, perhaps because non replicating primary cells (M1, M2) were used instead of cell lines.

Proteome and metabolome profiling have recently revealed additional targets for PARPi which could contribute to *Mtb* control in our human macrophage infection model. *In vitro* kinase profiling showed that olaparib and rucaparib have a relatively similar affinity for members of the PARP family, but differ substantially in their affinity for protein kinases (29, 56). Our observation that rucaparib performed significantly better against *Mtb* than other PARPi suggests that unique kinases targeted by rucaparib might contribute to its effect against *Mtb*. The reported unique additional targets of rucaparib include cyclin dependent kinase 1 and 16 (CDK1, CDK16), pim-3 oncogene (PIM3), hexose-6-phosphate dehydrogenase (H6PD) and lactate dehydrogenase (LDH) (26, 28, 56, 57). Here we show that rucaparib decreased lactate production in *Mtb*-infected M1 and M2. Moreover, the specific LDH inhibitor FX-11 had a similar effect as rucaparib on intracellular *Mtb* load. This suggests that LDH inhibition could be the major mechanism of action of rucaparib, and as such could be a promising target pathway in developing HDT against *Mtb*. In agreement with our findings, oral administration of FX-11 was recently described to decrease intracellular *Mtb* levels in mouse BMDM in a host-directed manner (58). Based on our data, we cannot exclude additional effects of rucaparib on further (secondary) targets during *Mtb* infection in human macrophages. Similarly, studying the potentially additive effects of the already described unique additional targets of niraparib are interesting in the development of novel HDT against *Mav* and *Stm*. Deoxynucleoside kinase (DCK) is a reported additional target of niraparib, and analysis of a published dataset of infected M2 showed that DCK is significantly upregulated 4h post *Stm*, but not *Mtb* infection (56, 59). Taken together, these data suggest that DCK is an interesting candidate for HDT against *Stm*.

There are several limitations of the current study. First, the current study has the limitation of small sample size. Although a small sample is common among studies with (primary) cells due to the laborious nature of these experiments, this could have resulted in insufficient statistical power between groups. Furthermore, we applied a single-dose administration of HDT compounds with a relatively short effect time (i.e. after overnight infection), which is an experimental setup that we generally use for the identification of novel HDT compounds (18, 20, 60). Although applying other compound concentrations, repeated doses or a longer treatment exposure could have resulted in a bigger effect size, the host targets (PARP and LDH) that we identified in our *in vitro* human macrophage model were recently published as host targets using *in vivo* mouse models as discussed above (27, 58). This agreeing set of independent findings underscores the power and validity of our approach, which aims to decipher novel pathways involved in host defense against intracellular bacterial infections in humans, and develop corresponding novel HDT.

In summary, we identified PARP as a host target for HDT during *Mtb* infections, and confirmed that PARP inhibition is a promising avenue in the development of HDT against *Mtb*. Furthermore, our data show that also off-target kinase pharmacology of PARP inhibitors may expand the current clinical scope of PARP inhibitors and that these molecules deserve serious consideration in the development of repurposed HDT against intracellular bacterial infections.

MATERIALS AND METHODS

Reagents and Antibodies

Dimethyl sulfoxide (DMSO), staurosporine solution from Streptomyces sp. (STSP), H-89 dihydrochloride hydrate (H-89), bafilomycin A1 (Baf), 6-aminonicotinamide (6-AN), lactate dehydrogenase A inhibitor (FX-11), rifampicin (RIF), gentamicin, tetracycline hydrochloride, ethylenediaminetetraacetic acid (EDTA) and Hoechst 33342 were obtained from Sigma-Aldrich (Zwijndrecht, The Netherlands). PARP inhibitors (A-966492,

niraparib, pamiparib and rucaparib) and isoniazid (INH) were purchased from SelleckChem.

PE anti-human CD209 (1:50, clone 9E9A8), PerCP/Cy5.5 anti-human CD192 (CCR2, 1:20, clone K036C2), PE/Cy7 anti-human CD40 (1:100, clone 5C3), Alexa Fluor® 647 anti-human CD163 (1:50, clone CHI/61), APC/Cy7 anti-human CD206 (1:50, clone 15-2) and BV785 anti-human CD14 (1:200, clone M5E2) were purchased from Biolegend (London, United Kingdom). APC-R700 anti-human CD80 (1:200, clone L307.4), V500 anti-human HLA-DR (1:100, clone G46-6) and BV711 anti-human CD86 (1:100, clone 2331) were purchased from BD Bioscience (Vianen, The Netherlands). BV605 anti-human CD197 (CCR7, 1:200, clone G043H7) was purchased from Sony Biotechnology (Weybridge, United Kingdom). Mouse monoclonal anti-human beta actin (1:2000, clone mAbcam 8226) and rabbit polyclonal anti-human LAMP1 (1:500) were purchased from Abcam (Amsterdam, The Netherlands). Rabbit polyclonal anti-human LC3-I/II (1:250) was purchased from Cell Signaling Technology (Leiden, The Netherlands). Secondary stabilized peroxidase conjugated antibodies goat anti-rabbit IgG (H+L) (1:10,000) and goat anti-mouse IgG (H+L) (1:10,000) were purchased from Thermo Fisher Scientific (Breda, The Netherlands).

Cell Culture

Human peripheral blood mononuclear cells (PBMCs) were isolated from buffy coats of healthy anonymous donors (Dutch, adults) after written informed consent (Sanquin Blood Bank, Amsterdam, The Netherlands) by density gradient centrifugation over Ficoll/amidotrizoaat as described earlier (61). The use of buffy coats for research purposes was approved by the Institutional Review Board of the Leiden University Medical Center, The Netherlands. Magnetic cell sorting using anti-CD14-coated microbeads (Miltenyi Biotec, Auburn, CA) was used to isolate CD14+ monocytes. CD14+ cells were cultured for six days at 37°C/5% CO_2 in Gibco Roswell Park Memorial Institute (RPMI) 1640 medium (Thermo Fisher Scientific) supplemented with 10% fetal bovine serum (FBS), 2 mM L-Alanyl-L-Glutamine (PAA, Linz, Austria), 100 units/ml penicillin (Thermo Fisher Scientific), 100 µg/ml streptomycin (Thermo Fisher Scientific) and either 5 ng/ml granulocyte-macrophage colony-stimulating factor (GM-CSF, Thermo Fisher Scientific) to promote M1 differentiation or 50 ng/ml macrophage colony-stimulating factor (M-CSF, R&D Systems, Abingdon, United Kingdom) to promote M2 differentiation. Cytokines were added again at day 3 of differentiation in equal concentrations. The M1 and M2 macrophage phenotypes were subsequently validated by flow cytometry based surface marker expression (M1: $CD14^{low}$, $CD163^{low}$, $CD11b^{high}$; M2: $CD14^{high}$, $CD163^{high}$, $CD11b^{low}$) and by quantifying IL-10 and IL-12p40 production by Enzyme-Linked Immuno Sorbent Assay (ELISA) following stimulation of cells in the presence or absence of 100 ng/ml lipopolysaccharide (LPS) for 24h (*In vivo*Gen, San Diego, United States) as described before (60).

Bacterial Culture

Mycobacterial strains were cultured at 37°C in Difco™ Middlebrook 7H9 Broth (BD Bioscience) containing 10% acid-albumin-dextrose-catalase (ADC, BD Bioscience), 0.5% Tween-80 (Sigma-Aldrich), 2% Glycerol (Sigma-Aldrich) and 50 µg/ml hygromycin B (Thermo Fisher Scientific) when appropriate. The following bacterial strains were used: *Mtb* H37Rv, Venus-expressing *Mtb* H37Rv (strain $mc^2$8120), DsRed-expressing *Mtb* H37Rv (18), MDR-*Mtb* Beijing family strain 16319 (62), MDR-*Mtb* Dutch outbreak strain 2003-1128 (62), *Mycobacterium avium* subsp. *avium* Chester strain 101 (ATCC, Wesel, Germany), DsRed-expressing *Salmonella enterica* serovar Typhimurium (*Stm*) strain SL1344 (18) and GFP-expressing methicillin-resistant *Staphylococcus aureus* (MRSA) strain USA300 JE2.

In Vitro Infection and Compound Treatment

Adherent cells were harvested by trypsinization and gentle scraping in FBS and seeded in RPMI 1640 medium supplemented with 10% FBS and 2 mM L-Alanyl-L-Glutamine on Costar 96-well flat bottom culture plates (30,000 cells/well) or on Costar 24-well flat bottom culture plates (300,000 cells/well) (Corning, Amsterdam, The Netherlands) and incubated overnight at 37°C/5% CO_2. Mycobacterial cultures were diluted to an early log-phase corresponding with an OD600 of 0.25 one day prior to infection in 7H9 broth containing 10% ADC, 0.5% Tween-80 and 2% Glycerol. DsRed-expressing *Stm* was recovered from frozen stock and cultured in Difco™ Luria-Bertani (LB) broth (BD Bioscience) containing 100 µg/ml ampicillin (Sigma-Aldrich) overnight at 37°C. Bacterial suspension was diluted 1:33 in LB broth and grown for 3-4h to reach a log-phase with an OD600 between 0.4-0.6. GFP-expressing MRSA was recovered from frozen stock and cultured in Tryptic Soy (TS) broth (BD Bioscience) containing 5 µg/ml tetracycline hydrochlorine overnight at 37°C. Bacterial suspension was diluted 1:33 in TS broth and grown for 2-3h to reach a log-phase with an OD600 between 0.4-0.6. MRSA was harvested by centrifugation and resuspended in cold PBS supplemented with 5 mM EDTA. The indicated bacteria were diluted in RPMI 1640 medium (10% FBS and 2 mM L-Alanyl-L-Glutamine) to reach a multiplicity of infection (MOI) of 10. Accuracy of the MOI was validated by plating a serial dilution of the mycobacterial inoculum on Difco™ Middlebrook 7H10 agar (BD Bioscience) plates containing 10% oleic acid-albumin-dextrose-catalase (OADC, BD Bioscience) and 5% glycerol, by plating *Stm* on Difco™ LB agar plates (BD Bioscience) or by plating MRSA on TS agar (BD Bioscience). For mock infections, 7H9 broth was diluted in RPMI 1640 medium (10% FBS and 2 mM L-Alanyl-L-Glutamine) in equal concentrations (v/v) as the infection inoculum. Cells in flat-bottom 96-well plates containing 100 µl RPMI 1640 medium (10% FBS and 2 mM L-Alanyl-L-Glutamine) per well were inoculated with 100 µl bacterial suspension or mock solution. Cells in flat-bottom 24-well plates containing 500 µl RPMI 1640 medium (10% FBS and 2 mM L-Alanyl-L-Glutamine) per well were inoculated with 500 µl bacterial suspension or mock solution. Plates were centrifuged for 3 min at 800 rpm to increase bacterial uptake and incubated for 1h for *Mtb, Mav* or MRSA infection or for 20 minutes for *Stm* infection at 37°C/5% CO_2. Extracellular bacteria were removed by washing with fresh RPMI 1640 medium supplemented with 10% FBS, 2 mM L-Alanyl-L-Glutamine and 30 µg/ml gentamicin sulphate for 10

min. Cells were incubated at 37°C/5% CO_2 in RPMI 1640 medium supplemented with 10% FBS and 2 mM L-Alanyl-L-Glutamine and 5 μg/ml gentamicin sulphate in the presence of H-89 (10 μM), A-966492 (10 μM), niraparib (10 μM), pamiparib (10 μM), rucaparib (10 μM), 6-AN (100 μM), FX-11 (100 μM), Baf (10 nM), INH (0.4 μg/ml), RIF (0.05 μg/ml) or an equal amount of vehicle control DMSO (0.1% v/v) until readout. To calculate the coefficient of drug interaction (CID) the following formula was used: CID = AB/(AxB), where A indicates the ratio between antibiotic to the control group (DMSO, without antibiotics), B indicates the ratio between HDT compound to the control group and AB indicates the ratio between the treatments combined to the control group (63). A CID of 1 indicates an additive effect, <1 a synergistic effect and >1 an antagonistic effect.

CFU Assay

Cells in 96-well flat bottom plates (30,000 cells/well) were washed with PBS and lysed in 0.05% sodium dodecyl sulfate (SDS) solution (Thermo Fisher Scientific). Serially diluted cell lysates were plated on 7H10 Agar containing 10% OADC and 5% Glycerol (*Mtb* and *Mav*), LB agar (*Stm*) or TS agar (MRSA) and incubated at 37°C. CFUs were determined from triplicate wells.

Cellular Toxicity Assay

The number and percentage of dead cells based on plasma membrane integrity of the adherent cell population was quantified by analysis of microscopy images. Cells in 96-well flat bottom plates (30,000 cells/well) were stained with 2 μg/ml propidium iodide (Sigma-Aldrich) and 2 μg/ml Hoechst 33342 (H3570, Sigma-Aldrich) in 40 μl/well phenol red-free RPMI (Sigma-Aldrich) supplemented with 10% FBS and 2 mM L-Alanyl-L-Glutamine and incubated for 5 min at room temperature (RT). Cells were imaged using a Leica AF6000 LC fluorescence microscope (Leica Microsystems, Wetzlar, Germany) combined with a 10x dry objective. Total and dead cell numbers were quantified by respectively counting the nuclei and the number of propidium iodide-positive cells using ImageJ software (64). STSP (2.5 μM) was included as a positive control for cell death (**Supplemental Figure 4**).

Extracellular Bacterial Growth Assay

Compounds were diluted in Difco™ Middlebrook 7H9 Broth (*Mtb*, *Mav*), Difco™ LB Broth (*Stm*) or TS Broth (MRSA) and were added to log-phase bacterial cultures in flat bottom 96-well plates (OD_{600} of 0.1). RIF (20 μg/ml) was added as positive control for reduction of *Mtb* and *Mav* growth and gentamicin (50 μg/ml) was added as positive control for reduction of *Stm* and *MRSA* growth. Bacterial plates were incubated at 37°C. Absorbance was measured directly after plating and at indicated times at a 550 nm wavelength on a Mithras LB 940 plate reader (Berthold Technologies, Bad Wildbad, Germany).

Western Immunoblot Analysis

Cells (300,000 cells/well in 24-wells plates) were lysed with 100 μl/well EBSB buffer (10% v/v glycerol, 3% SDS, 100 mM Tris-HCl, pH 6.8) supplemented with one tablet of cOmplete™ EDTA-free protease inhibitor cocktail (Sigma-Aldrich) and one tablet of phosphatase inhibitor cocktail (PhosSTOP EASYpack, Sigma-Aldrich) per 10 ml. Cell lysates were boiled for 10 minutes at 95°C and stored at -20°C until use. Total protein concentrations were determined using a Pierce™ BCA protein assay kit (Thermo Fisher Scientific) according to manufacturer' instructions and protein concentrations were equalized and diluted in Laemmli sample buffer (Biorad) containing β-mercaptoethanol (Sigma-Aldrich). Samples were loaded on a 15-well 4–20% Mini-PROTEAN® TGX™ Precast Protein Gel (Bio-Rad Laboratories, Veenendaal, the Netherlands) and Amersham ECL Rainbow Molecular Weight Marker was added as reference (Sigma-Aldrich). Proteins were transferred to methanol-activated Immun-Blot PVDF membranes (Biorad) in Tris-glycine buffer (25 mM Tris, 192 mM glycine and 20% methanol). Membranes were blocked for 1h in polysorbate 20 tris-buffered saline (TTBS) supplemented with 5% w/v non-fat dry milk and incubated with the indicated antibodies in 5% non-fat dry milk/TTBS overnight at 4°C. Membranes were washed thrice for 15 min in TTBS and stained with secondary antibodies in 5% non-fat dry milk/TTBS for 2h at RT. Membranes were washed for 30 min with TTBS prior to revelation using enhanced chemiluminescence (ECL)™ Prime Western Blotting System reagent (GE Healthcare, Hoevelaken, The Netherlands). Imaging was performed on ChemiDoc XRS+ (Bio-Rad) or on an iBright Imaging System (Invitrogen, Breda, The Netherlands). Protein bands were quantified using ImageJ/Fiji software (64) and normalized to actin.

Cytokine and Chemokine Secretion by Multiplex Beads Assay

Human cytokine/chemokine levels were determined using the MilliPlex Human Cytokine/Chemokine magnetic bead premixed 41-plex kit (Millipore Billerica, MA, USA) as described before (60). Culture supernatants were collected and sterilized by using a 96-well filter plate containing a 0.2 μm PVDF membrane (Corning) following centrifugation. The following analytes were measured on a Bio-Plex 100 with Bio-Plex ManagerTM software v6.1 (Biorad): sCD40L, EGF, FGF-2, Flt3 ligand, Fractalkine (CX3CL1), G-CSF, GM-CSF, GRO (CXCL1), IFN-γ, IFN-α2, IL-1α, IL-1β, IL-1RA, IL-2, IL-3, IL-4, IL-5, IL-6, IL-7, IL-8 (CXCL8), IL-9, IL-10, IL-12p40, IL-12p70, IL-13, IL-15, IL-17a, IP-10 (CXCL10), MCP-1 (CCL2), MCP-3 (CCL7), MDC (CCL22), MIP-1α (CCL3), MIP-1β (CCL4), PDGF-AB/BB, RANTES (CCL5), TGF-α, TNF-α, TNF-β, VEGF, Eotaxin (CCL11) and PDGF-AA.

Flow Cytometry

Adherent and floating cells (300,000 cells/well in 24-wells plates) were washed in PBS/0.1% BSA (Merck, Darmstadt, Germany) and Fc receptors were blocked with 5% human serum (HS) in PBS for 10 min at RT. Cells were washed in PBS/0.1% BSA and stained with antibodies diluted in PBS/0.1% BSA for 30 min at 4°C. Cells were washed in PBS/0.1% BSA and fixed with 1% paraformaldehyde for 1h at 4°C. Fluorescence minus one (FMO) control samples were included to define background fluorescence for each stain. Fluorescence staining was measured using a FACSLyric™ flow cytometer with FACSDiva software (BD Bioscience). Geometric mean fluorescence intensity (gMFIs) was recorded for each sample. Data were analyzed using FlowJo v10 software.

Lactate Assay

Cell culture supernatants were collected and sterilized by using a 96-well filter plate containing a 0.2 µm PVDF membrane (Corning) following centrifugation. Undiluted sodium l-lactate (Sigma-aldrich) standard (0-8 mM, 5 µl) or sample (5 µl) was added to a flat-bottom 96-well plate (Greiner Bio-One, Alphen a/d Rijn, The Netherlands). 200 µl of reaction mix (0.74 mM NAD, Roche Applied Science, Woerden, The Netherlands; 0.4 mM glycine, Sigma-Aldrich; 0.4 M hydrazine hydrate, Sigma-Aldrich) was added to allow conversion of lactate to pyruvate by lactate dehydrogenase (LDH): Lactate + NAD^+ <–> Pyruvate + NADH + H^+. Hydrazine hydrate was added to avoid conversion of the newly formed pyruvate back to lactate. Baseline NADH levels were measured using the SpectraMax i3x plate reader at OD340 before the addition of 2 µl of three times diluted LDH from rabbit muscle (Roche Applied Science) to each well to initiate the lactate to pyruvate conversion. Following the addition of LDH, plates were incubated on a shaker at RT for 90 mins and the OD340 was measured again using a SpectraMax i3x plate reader.

Immunostaining and Confocal Microscopy

For confocal microscopy, cells were cultured on pre-washed black glass bottom poly-d-lysine coated 96-well plates (no. 1.5, MatTek Corporation, Ashland, MA, USA) at a density of 30,000 cells/well in RPMI 1640 medium supplemented with 10% FBS and 2 mM L-Alanyl-L-Glutamine and incubated overnight at 37° C/5% CO_2. Cells were infected with DsRed-expressing *Mtb* H37Rv as described above and treated with compound (10 µM) or an equal volume of DMSO (0.1% v/v) for 4h. Culture medium was replaced with a solution of 75 nM LysoTracker® Deep Red (Thermo Fisher Scientific) and 1x CYTO-ID® Green 2.0 (1:500, Enzo Life Sciences, Bruxelles, Belgium) for 30 min at 37°C/5% CO_2 to stain lysosomal and autophagic vesicles, respectively. Cells were washed twice with PBS and fixed with Pierce™ 1% w/v formaldehyde (Thermo Fisher Scientific) for 1h at RT, washed twice with PBS and then stored at 4°C. Prior to imaging, plates were incubated with 2 µg/ml Hoechst 33342 for 5 min at RT and imaged using a SP8WLL confocal microscope (Leica) using a 63X oil immersion objective. Each treatment condition was performed in triplicate wells and three images were taken from each well. For image analysis, lysotracker and CYTO-ID channel background was subtracted using a rolling ball algorithm with a 10 pixel radius in Fiji/ImageJ (64). Lysotracker area and CYTO-ID area were specified for each image using Cellprofiler 3.1.9 (65) and were normalized to cell count based on Hoechst 33342 staining.

Statistical Analysis

All statistical analyses were carried out using GraphPad Prism 8 software (Graphpad Software, San Diego, CA, USA). Normal distribution of data sets was evaluated using the Shapiro-Wilk normality test. Correlation was evaluated with a Spearman's rank correlation test. Parametric paired data were tested with a paired t-test when comparing two groups and with RM one-way ANOVA or two-way ANOVA followed by Dunnett's multiple comparison test versus control when comparing three or more groups. Nonparametric paired data were tested with Wilcoxon matched-pairs signed rank test when comparing two groups and with Friedman's test followed by Dunn's multiple comparison test versus control when comparing three or more groups. Statistical tests were considered significant when $p<0.05$ at 95% confidence interval.

DATA AVAILABILITY STATEMENT

The original contributions presented in the study are included in the article/**Supplementary Material**. Further inquiries can be directed to the corresponding author.

ETHICS STATEMENT

The studies involving human participants were reviewed and approved by Institutional Review Board of the Leiden University Medical Center, The Netherlands. The patients/participants provided their written informed consent to participate in this study.

AUTHOR CONTRIBUTIONS

CD and TO designed the project and the main conceptual ideas. CD, SS, and KW performed the experiments and analyzed the experimental data. CD and TO wrote the manuscript. TO supervised the project. All authors contributed to the article and approved the submitted version.

FUNDING

This work received financial support from the Netherlands Organization for Health Research and Development (ZonMw-TOP grant 40-00812-98-14038). The funders had no role in study design, data collection and analysis, decision to publish, or preparation of the manuscript.

ACKNOWLEDGMENTS

We gratefully acknowledge Dr J. Bestebroer (VUMC, Amsterdam, The Netherlands) for mycobacterial reporter constructs and Dr. S. Joosten for proofreading this manuscript and helpful comments. DsRed-expressing *Stm* was kindly provided by Prof. dr. J. J. Neefjes (LUMC, Leiden, The Netherlands). GFP-expressing MRSA strain JE2 USA300 was kindly provided by Tomasz Prajsnar and Simon J. Foster (Department of Molecular Biology and Microbiology, University of Sheffield, Sheffield UK). Venus-expressing *Mtb*

was kindly provided by Prof. dr. William R. Jacobs (Albert Einstein College of Medicine, Yeshiva University, New York City, United States). MDR-*Mtb* strains were kindly provided by Dick van Soolingen and Kristin Kremer (Rijksinstituut voor Volksgezondheid en Milieu, RIVM).

SUPPLEMENTARY MATERIAL

The Supplementary Material for this article can be found online at: https://www.frontiersin.org/articles/10.3389/fimmu.2021.712021/full#supplementary-material

REFERENCES

1. World Health Organization. *Global Tuberculosis Report*. Geneva: World Health Organization (2020). Licence: CC BY-NC-SA 3.0 IGO.
2. Muller J, Tanner R, Matsumiya M, Snowden MA, Landry B, Satti I, et al. Cytomegalovirus Infection Is a Risk Factor for TB Disease in Infants. *JCI Insight* (2019) 4(23):e130090. doi: 10.1172/jci.insight.130090
3. Jeon CY, Murray MB. Diabetes Mellitus Increases the Risk of Active Tuberculosis: A Systematic Review of 13 Observational Studies. *PloS Med* (2008) 5(7):e152. doi: 10.1371/journal.pmed.0050152
4. Baker MA, Harries AD, Jeon CY, Hart JE, Kapur A, Lönnroth K, et al. The Impact of Diabetes on Tuberculosis Treatment Outcomes: A Systematic Review. *BMC Med* (2011) 9(1):81. doi: 10.1186/1741-7015-9-81
5. Lonnroth K, Roglic G, Harries AD. Improving Tuberculosis Prevention and Care Through Addressing the Global Diabetes Epidemic: From Evidence to Policy and Practice. *Lancet Diabetes Endocrinol* (2014) 2(9):730–9. doi: 10.1016/S2213-8587(14)70109-3
6. Huang Z, Luo Q, Guo Y, Chen J, Xiong G, Peng Y, et al. Mycobacterium Tuberculosis-Induced Polarization of Human Macrophage Orchestrates the Formation and Development of Tuberculous Granulomas *In Vitro*. *PloS One* (2015) 10(6):e0129744–e. doi: 10.1371/journal.pone.0129744
7. Soriano F, Virág L, Jagtap P, Szabó É, Mabley J, Liaudet L, et al. Diabetic Endothelial Dysfunction: The Role of Poly(ADP-Ribose) Polymerase Activation. *Nat Med* (2001) 7:108–13. doi: 10.1038/83241
8. Pacher P, Liaudet L, Soriano FG, Mabley JG, Szabo E, Szabo C. The Role of Poly(ADP-Ribose) Polymerase Activation in the Development of Myocardial and Endothelial Dysfunction in Diabetes. *Diabetes* (2002) 51(2):514–21. doi: 10.2337/diabetes.51.2.514
9. Szabo C, Zanchi A, Komjati K, Pacher P, Krolewski AS, Quist WC, et al. Poly (ADP-Ribose) Polymerase Is Activated in Subjects at Risk of Developing Type 2 Diabetes and Is Associated With Impaired Vascular Reactivity. *Circulation* (2002) 106(21):2680–6. doi: 10.1161/01.CIR.0000038365.78031.9C
10. Sachdev E, Tabatabai R, Roy V, Rimel B, Mita MM. PARP Inhibition in Cancer: An Update on Clinical Development. *J Targeted Oncol* (2019) 14 (6):657–79. doi: 10.1007/s11523-019-00680-2
11. Burkart V, Wang Z-Q, Radons J, Heller B, Herceg Z, Stingl L, et al. Mice Lacking the Poly (ADP-Ribose) Polymerase Gene Are Resistant to Beta-Cell Destruction and Diabetes Development Induced by Streptozocin. *Nat Med* (1999) 5:314–9. doi: 10.1038/6535
12. Pieper AA, Brat DJ, Krug DK, Watkins CC, Gupta A, Blackshaw S, et al. Poly (ADP-Ribose) Polymerase-Deficient Mice Are Protected From Streptozotocin-Induced Diabetes. *Proc Natl Acad Sci USA* (1999) 96(6):3059–64. doi: 10.1073/pnas.96.6.3059
13. Soriano FG, Pacher P, Mabley J, Liaudet L, Szabo C. Rapid Reversal of the Diabetic Endothelial Dysfunction by Pharmacological Inhibition of Poly (ADP-Ribose) Polymerase. *Circ Res* (2001) 89(8):684–91. doi: 10.1161/hh2001.097797
14. Krug S, Parveen S, Bishai WR. Host-Directed Therapies: Modulating Inflammation to Treat Tuberculosis. *Front Immunol* (2021) 12:1247. doi: 10.3389/fimmu.2021.660916
15. Nile DL, Rae C, Hyndman IJ, Gaze MN, Mairs RJ. An Evaluation *In Vitro* of PARP-1 Inhibitors, Rucaparib and Olaparib, as Radiosensitisers for the Treatment of Neuroblastoma. *BMC Cancer* (2016) 16:621. doi: 10.1186/s12885-016-2656-8
16. Cho H-y, Kim Y-B, Park W-h, No JH. Enhanced Efficacy of Combined Therapy With Checkpoint Kinase 1 Inhibitor and Rucaparib *via* Regulation of Rad51 Expression in BRCA Wild-Type Epithelial Ovarian Cancer Cells. *J Cancer Res Treat* (2021) 53(3):819–28. doi: 10.4143/crt.2020.1013
17. Smith HL, Prendergast L, Curtin NJ. Exploring the Synergy Between PARP and CHK1 Inhibition in Matched BRCA2 Mutant and Corrected Cells. *J Cancers* (2020) 12(4):878. doi: 10.3390/cancers12040878
18. Korbee CJ, Heemskerk MT, Kocev D, van Strijen E, Rabiee O, Franken KLMC, et al. Combined Chemical Genetics and Data-Driven Bioinformatics Approach Identifies Receptor Tyrosine Kinase Inhibitors as Host-Directed Antimicrobials. *Nat Commun* (2018) 9(1):358. doi: 10.1038/s41467-017-02777-6
19. Kuijl C, Savage NDL, Marsman M, Tuin AW, Janssen L, Egan DA, et al. Intracellular Bacterial Growth Is Controlled by a Kinase Network Around PKB/Akt1. *Nature* (2007) 450(7170):725–30. doi: 10.1038/nature06345
20. Heemskerk MT, Korbee CJ, Esselink J, dos Santos CC, van Veen S, Gordijn IF, et al. Repurposing Diphenylbutylpiperidine-Class Antipsychotic Drugs for Host-Directed Therapy of Mycobacterium Tuberculosis and Salmonella Enterica Infections. *bioRxiv* (2021) 11(1):19634. doi: 10.1038/s41598-021-98980-z
21. Singh M, Sasi P, Rai G, Gupta VH, Amarapurkar D, Wangikar PP. Studies on Toxicity of Antitubercular Drugs Namely Isoniazid, Rifampicin, and Pyrazinamide in an *In Vitro* Model of HepG2 Cell Line. *J Medicinal Chem Res* (2011) 20(9):1611–5. doi: 10.1007/s00044-010-9405-3
22. Rekha RS, Rao Muvva SSVJ, Wan M, Raqib R, Bergman P, Brighenti S, et al. Phenylbutyrate Induces LL-37-Dependent Autophagy and Intracellular Killing of Mycobacterium Tuberculosis in Human Macrophages. *Autophagy* (2015) 11(9):1688–99. doi: 10.1080/15548627.2015.1075110
23. Gutierrez MG, Master SS, Singh SB, Taylor GA, Colombo MI, Deretic V. Autophagy Is a Defense Mechanism Inhibiting BCG and Mycobacterium Tuberculosis Survival in Infected Macrophages. *Cell* (2004) 119(6):753–66. doi: 10.1016/j.cell.2004.11.038
24. Parihar SP, Guler R, Khutlang R, Lang DM, Hurdayal R, Mhlanga MM, et al. Statin Therapy Reduces the Mycobacterium Tuberculosis Burden in Human Macrophages and in Mice by Enhancing Autophagy and Phagosome Maturation. *J Infect Dis* (2013) 209(5):754–63. doi: 10.1093/infdis/jit550
25. Singhal A, Jie L, Kumar P, Hong GS, Leow MK-S, Paleja B, et al. Metformin as Adjunct Antituberculosis Therapy. *Sci Trans Med* (2014) 6(263):263ra159–263ra159. doi: 10.1126/scitranslmed.3009885
26. Nonomiya Y, Noguchi K, Katayama K, Sugimoto Y. Novel Pharmacological Effects of Poly (ADP-Ribose) Polymerase Inhibitor Rucaparib on the Lactate Dehydrogenase Pathway. *Biochem Biophys Res Commun* (2019) 510(4):501–7. doi: 10.1016/j.bbrc.2019.01.133
27. Krug S, Ordonez AA, Klunk M, Kang BG, Jain SK, Dawson TM, et al. Host Regulator PARP1 Contributes to Sex Differences and Immune Responses in a Mouse Model of Tuberculosis. *bioRxiv* (2021) 440820. doi: 10.1101/2021.04.21.440820
28. Antolin AA, Ameratunga M, Banerji U, Clarke PA, Workman P, Al-Lazikani B. The Kinase Polypharmacology Landscape of Clinical PARP Inhibitors. *Sci Rep* (2020) 10(1):2585. doi: 10.1038/s41598-020-59074-4
29. Carney B, Kossatz S, Lok BH, Schneeberger V, Gangangari KK, Pillarsetty NVK, et al. Target Engagement Imaging of PARP Inhibitors in Small-Cell Lung Cancer. *Nat Commun* (2018) 9(1):176. doi: 10.1038/s41467-017-02096-w
30. McGonigle S, Chen Z, Wu J, Chang P, Kolber-Simonds D, Ackermann K, et al. E7449: A Dual Inhibitor of PARP1/2 and Tankyrase1/2 Inhibits Growth of DNA Repair Deficient Tumors and Antagonizes Wnt Signaling. *Oncotarget* (2015) 6(38):41307–23. doi: 10.18632/oncotarget.5846
31. Thorsell A-G, Schüler H. Selectivity Profile of the Poly(ADP-Ribose) Polymerase (PARP) Inhibitor, A-966492. *bioRxiv* (2017) 119818. doi: 10.1101/119818
32. Ringley JT, Moore DC, Patel J, Rose MS. Poly (ADP-Ribose) Polymerase Inhibitors in the Management of Ovarian Cancer: A Drug Class Review. *P T* (2018) 43(9):549–56.

33. Glaeser H, Drescher S, Eichelbaum M, Fromm MF. Influence of Rifampicin on the Expression and Function of Human Intestinal Cytochrome P450 Enzymes. *Br J Clin Pharmacol* (2005) 59(2):199–206. doi: 10.1111/j.1365-2125.2004.02265.x
34. Attwa MW, Kadi AA, Abdelhameed AS, Alhazmi HA. Metabolic Stability Assessment of New PARP Inhibitor Talazoparib Using Validated LC-MS/MS Methodology: *In Silico* Metabolic Vulnerability and Toxicity Studies. *Drug Des Devel Ther* (2020) 14:783–93. doi: 10.2147/DDDT.S239458
35. Liu S-Y, Sanchez DJ, Aliyari R, Lu S, Cheng G. Systematic Identification of Type I and Type II Interferon-Induced Antiviral Factors. *Proc Natl Acad Sci* (2012) 109(11):4239. doi: 10.1073/pnas.1114981109
36. Atasheva S, Akhrymuk M, Frolova EI, Frolov I. New PARP Gene With an Anti-Alphavirus Function. *J Virol* (2012) 86(15):8147–60. doi: 10.1128/JVI.00733-12
37. Caprara G, Prosperini E, Piccolo V, Sigismondo G, Melacarne A, Cuomo A, et al. PARP14 Controls the Nuclear Accumulation of a Subset of Type I IFN–Inducible Proteins. *J Immunol* (2018) 200(7):2439. doi: 10.4049/jimmunol.1701117
38. Zhang Y, Mao D, Roswit WT, Jin X, Patel AC, Patel DA, et al. PARP9-DTX3L Ubiquitin Ligase Targets Host Histone H2BJ and Viral 3C Protease to Enhance Interferon Signaling and Control Viral Infection. *Nat Immunol* (2015) 16(12):1215–27. doi: 10.1038/ni.3279
39. Fehr AR, Singh SA, Kerr CM, Mukai S, Higashi H, Aikawa M. The Impact of PARPs and ADP-Ribosylation on Inflammation and Host-Pathogen Interactions. *Genes Dev* (2020) 34(5-6):341–59. doi: 10.1101/gad.334425.119
40. Zak DE, Penn-Nicholson A, Scriba TJ, Thompson E, Suliman S, Amon LM, et al. A Blood RNA Signature for Tuberculosis Disease Risk: A Prospective Cohort Study. *Lancet* (2016) 387(10035):2312–22. doi: 10.1016/S0140-6736(15)01316-1
41. Scriba TJ, Penn-Nicholson A, Shankar S, Hraha T, Thompson EG, Sterling D, et al. Sequential Inflammatory Processes Define Human Progression From M. Tuberculosis Infection to Tuberculosis Disease. *PloS Pathog* (2017) 13(11):e1006687. doi: 10.1371/journal.ppat.1006687
42. Ottenhoff TH, Dass RH, Yang N, Zhang MM, Wong HE, Sahiratmadja E, et al. Genome-Wide Expression Profiling Identifies Type 1 Interferon Response Pathways in Active Tuberculosis. *PloS One* (2012) 7(9):e45839. doi: 10.1371/journal.pone.0045839
43. Ji DX, Yamashiro LH, Chen KJ, Mukaida N, Kramnik I, Darwin KH, et al. Type I Interferon-Driven Susceptibility to Mycobacterium Tuberculosis Is Mediated by IL-1ra. *Nat Microbiol* (2019) 4(12):2128–35. doi: 10.1038/s41564-019-0578-3
44. Dorhoi A, Yeremeev V, Nouailles G, Weiner J3rd, Jörg S, Heinemann E, et al. Type I IFN Signaling Triggers Immunopathology in Tuberculosis-Susceptible Mice by Modulating Lung Phagocyte Dynamics. *Eur J Immunol* (2014) 44(8):2380–93. doi: 10.1002/eji.201344219
45. Oliver FJ, Ménissier-de Murcia J, Nacci C, Decker P, Andriantsitohaina R, Muller S, et al. Resistance to Endotoxic Shock as a Consequence of Defective NF-kappaB Activation in Poly (ADP-Ribose) Polymerase-1 Deficient Mice. *EMBO J* (1999) 18(16):4446–54. doi: 10.1093/emboj/18.16.4446
46. Hassa PO, Hottiger MO. A Role of Poly (ADP-Ribose) Polymerase in NF-kappaB Transcriptional Activation. *Biol Chem* (1999) 380(7-8):953–9. doi: 10.1515/BC.1999.118
47. Alim MA, Kupz A, Sikder S, Rush C, Govan B, Ketheesan N. Increased Susceptibility to Mycobacterium Tuberculosis Infection in a Diet-Induced Murine Model of Type 2 Diabetes. *Microbes infection* (2020) 22(8):303–11. doi: 10.1016/j.micinf.2020.03.004
48. Lopez-Lopez N, Martinez AGR, Garcia-Hernandez MH, Hernandez-Pando R, Castaneda-Delgado JE, Lugo-Villarino G, et al. Type-2 Diabetes Alters the Basal Phenotype of Human Macrophages and Diminishes Their Capacity to Respond, Internalise, and Control Mycobacterium Tuberculosis. *Memorias do Instituto Oswaldo Cruz* (2018) 113(4):e170326. doi: 10.1590/0074-02760170326
49. Vallerskog T, Martens GW, Kornfeld H. Diabetic Mice Display a Delayed Adaptive Immune Response to *Mycobacterium Tuberculosis*. *J Immunol* (2010) 184(11):6275. doi: 10.4049/jimmunol.1000304
50. Flynn JL, Goldstein MM, Chan J, Triebold KJ, Pfeffer K, Lowenstein CJ, et al. Tumor Necrosis Factor-Alpha Is Required in the Protective Immune Response Against Mycobacterium Tuberculosis in Mice. *Immunity* (1995) 2(6):561–72. doi: 10.1016/1074-7613(95)90001-2
51. Keane J, Gershon S, Wise RP, Mirabile-Levens E, Kasznica J, Schwieterman WD, et al. Tuberculosis Associated With Infliximab, a Tumor Necrosis Factor Alpha-Neutralizing Agent. *N Engl J Med* (2001) 345(15):1098–104. doi: 10.1056/NEJMoa011110
52. Mohan VP, Scanga CA, Yu K, Scott HM, Tanaka KE, Tsang E, et al. Effects of Tumor Necrosis Factor Alpha on Host Immune Response in Chronic Persistent Tuberculosis: Possible Role for Limiting Pathology. *Infection Immun* (2001) 69(3):1847. doi: 10.1128/IAI.69.3.1847-1855.2001
53. Martinez N, Ketheesan N, West K, Vallerskog T, Kornfeld H. Impaired Recognition of Mycobacterium Tuberculosis by Alveolar Macrophages From Diabetic Mice. *J Infect Dis* (2016) 214(11):1629–37. doi: 10.1093/infdis/jiw436
54. Santiago-O'Farrill JM, Weroha SJ, Hou X, Pang L, Rask P, Lu Z, et al. PARP Inhibitor-Induced Autophagy Provides an Adaptive Mechanism of Drug Resistance in Preclinical Models of Ovarian Cancer. *AACR* (2019) 126(4):894–907. doi: 10.1158/1538-7445.AM2019-4768
55. Liu Y, Song H, Song H, Feng X, Zhou C, Huo Z. Targeting Autophagy Potentiates the Anti-Tumor Effect of PARP Inhibitor in Pediatric Chronic Myeloid Leukemia. *AMB Express* (2019) 9(1):108. doi: 10.1186/s13568-019-0836-z
56. Antolín AA, Mestres J. Linking Off-Target Kinase Pharmacology to the Differential Cellular Effects Observed Among PARP Inhibitors. *Oncotarget* (2014) 5(10):3023–8. doi: 10.18632/oncotarget.1814
57. Knezevic CE, Wright G, Rix LLR, Kim W, Kuenzi BM, Luo Y, et al. Proteome-Wide Profiling of Clinical PARP Inhibitors Reveals Compound-Specific Secondary Targets. *Cell Chem Biol* (2016) 23(12):1490–503. doi: 10.1016/j.chembiol.2016.10.011
58. Krishnamoorthy G, Kaiser P, Abed UA, Weiner J3rd, Moura-Alves P, Brinkmann V, et al. FX11 Limits Mycobacterium Tuberculosis Growth and Potentiates Bactericidal Activity of Isoniazid Through Host-Directed Activity. *Dis Models Mech* (2020) 13(3):dmm041954. doi: 10.1242/dmm.041954
59. Blischak JD, Tailleux L, Mitrano A, Barreiro LB, Gilad Y. Mycobacterial Infection Induces a Specific Human Innate Immune Response. *Sci Rep* (2015) 5(1):16882. doi: 10.1038/srep16882
60. Moreira JD, Koch BE, van Veen S, Walburg KV, Vrieling F, Mara Pinto Dabés Guimarães T, et al. Functional Inhibition of Host Histone Deacetylases (HDACs) Enhances *In Vitro* and *In Vivo* Anti-Mycobacterial Activity in Human Macrophages and in Zebrafish. *Front Immunol* (2020) 11:36. doi: 10.3389/fimmu.2020.00036
61. Verreck FA, de Boer T, Langenberg DM, Hoeve MA, Kramer M, Vaisberg E, et al. Human IL-23-Producing Type 1 Macrophages Promote But IL-10-Producing Type 2 Macrophages Subvert Immunity to (Myco)Bacteria. *Proc Natl Acad Sci USA* (2004) 101(13):4560–5. doi: 10.1073/pnas.0400983101
62. Kremer K, van Soolingen D, Frothingham R, Haas WH, Hermans PWM, Martín C, et al. Comparison of Methods Based on Different Molecular Epidemiological Markers for Typing of Mycobacterium Tuberculosis Complex Strains: Interlaboratory Study of Discriminatory Power and Reproducibility. *J Clin Microbiol* (1999) 37(8):2607–18. doi: 10.1128/JCM.37.8.2607-2618.1999
63. Cao S-s, Zhen Y-s. Potentiation of Antimetabolite Antitumor Activity *In Vivo* by Dipyridamole and Amphotericin B. *Cancer Chemotherapy Pharmacol* (1989) 24(3):181–6. doi: 10.1007/BF00300240
64. Schindelin J, Arganda-Carreras I, Frise E, Kaynig V, Longair M, Pietzsch T, et al. Fiji: An Open-Source Platform for Biological-Image Analysis. *Nat Methods* (2012) 9(7):676–82. doi: 10.1038/nmeth.2019
65. Carpenter AE, Jones TR, Lamprecht MR, Clarke C, Kang IH, Friman O, et al. CellProfiler: Image Analysis Software for Identifying and Quantifying Cell Phenotypes. *Genome Biol* (2006) 7(10):R100. doi: 10.1186/gb-2006-7-10-r100

Conflict of Interest: The authors declare that the research was conducted in the absence of any commercial or financial relationships that could be construed as a potential conflict of interest.

Publisher's Note: All claims expressed in this article are solely those of the authors and do not necessarily represent those of their affiliated organizations, or those of the publisher, the editors and the reviewers. Any product that may be evaluated in

this article, or claim that may be made by its manufacturer, is not guaranteed or endorsed by the publisher.

Copyright © 2021 van Doorn, Steenbergen, Walburg and Ottenhoff. This is an open-access article distributed under the terms of the Creative Commons Attribution License (CC BY). The use, distribution or reproduction in other forums is permitted, provided the original author(s) and the copyright owner(s) are credited and that the original publication in this journal is cited, in accordance with accepted academic practice. No use, distribution or reproduction is permitted which does not comply with these terms.

Advantages of publishing in Frontiers

OPEN ACCESS
Articles are free to read for greatest visibility and readership

FAST PUBLICATION
Around 90 days from submission to decision

HIGH QUALITY PEER-REVIEW
Rigorous, collaborative, and constructive peer-review

TRANSPARENT PEER-REVIEW
Editors and reviewers acknowledged by name on published articles

Frontiers
Avenue du Tribunal-Fédéral 34
1005 Lausanne | Switzerland

Visit us: www.frontiersin.org
Contact us: frontiersin.org/about/contact

REPRODUCIBILITY OF RESEARCH
Support open data and methods to enhance research reproducibility

DIGITAL PUBLISHING
Articles designed for optimal readership across devices

FOLLOW US
@frontiersin

IMPACT METRICS
Advanced article metrics track visibility across digital media

EXTENSIVE PROMOTION
Marketing and promotion of impactful research

LOOP RESEARCH NETWORK
Our network increases your article's readership